The molecular basis for central nervous system primitive neuroectodermal tumour development

Dr James Timothy Hayden

Thesis submitted in partial fulfilment of the requirements

for the degree of Doctor of Philosophy

Newcastle University

Faculty of Medical Sciences

Northern Institute for Cancer Research

September 2011

Declaration

I certify that no part of the material documented in this thesis has previously been submitted for a degree or other qualification in this or any other university. I declare that this thesis represents my own unaided work, carried out by myself, except where it is acknowledged otherwise in the thesis text.

James Hayden

10th September 2011

Abstract

Central nervous system primitive neuroectodermal tumours (CNS-PNETs) are highly aggressive tumours with similar histopathological features to other intracranial PNETs (medulloblastomas). These two tumours have accordingly been treated using unified approaches, but CNS-PNETs have a dismal prognosis. Few studies have investigated the genetic features of CNS-PNETs. The molecular basis of CNS-PNET was therefore investigated in a cohort containing CNS-PNETs from children (n=33) and adults (n=5), to aid improvements in disease classification and treatment.

The common medulloblastoma molecular defects were investigated in CNS-PNETs, and showed *RASSF1A* promoter hypermethylation is a frequent event (18/22, 82%), and *MYC* family gene amplification occurs in a subgroup (*MYCN*: 3/25 (12%), *MYCC*: 0/25 (0%)). In contrast and in distinction to medulloblastoma, chromosome 17p loss is not a common feature (2/23, 9%), whilst p53 pathway signalling appears to play a major role (20/22, 91%), and associated with *TP53* mutations (4/22, 18%). Aberrant Wnt signalling was identified in 2 cases (2/22, 9%) and coupled with *CTNNB1* mutation in a single case. *IDH1* mutations (2/25, 8%) however, appear to occur in adult but not childhood CNS-PNETs or medulloblastoma. Subsequent genome-wide investigations of the CNS-PNET DNA methylome aimed at a wider characterisation of the molecular features of CNS-PNETs and its relationships to other childhood tumours identified CNS-PNETs as a heterogenous disease group without defined sub-clusters, which were predominantly distinct from medulloblastomas, but exhibited overlap with high-grade gliomas. A panel of 76 tumour-specific methylation events were identified as disease markers. The combination of either *RASSF1A* hypermethylation or *HLA-DPB1* hypomethylation discerned normal brain from CNS-PNET in 94% of cases (64/68). In addition, hypermethylation of *TAL1*, *MAP3K1* and *IGFBP1* is associated with non-infant disease.

In conclusion, this study has shown CNS-PNETs are a heterogenous group of tumours that are molecularly distinct from medulloblastomas, and has implicated developmental pathways and genetic events in their tumorigenesis. The associations between molecular events identified and clinical features warrant further investigation to aid classification and treatment advancements.

Table of Contents

Contents

Acknowledgements

First and foremost, I should like to thank the children and their families who have consented to participate in research and who have generously donated samples for this study to help future children diagnosed with this disease. I should also like to thank the North of England Children's Cancer Research Fund (NECCR), Clic Sargent and the Samantha Dickinson Brain Tumour Trust (SDBTT), as well as their supporters for providing the funding for this research.

I should like to express my sincere gratitude to my research supervisors, Professor Steve Clifford and Dr Simon Bailey, for their continued encouragement, enthusiasm and support during my PhD studies. I feel extremely privileged to have been a part of their group.

I would like to thank the superb group of scientists, clinicians and support staff of the Paediatric Brain Tumour Group at the NICR for the assistance they have provided and for the valuable discussions we have shared. I would like to offer special thanks to Drs Meryl Lusher and Janet Lindsey; for their patience and enthusiasm, and for the vast amount of laboratory expertise they have shared.

Thanks to Dr Sarra Ryan and Dr Matthew Allen for technical advice with qRT-PCR and MLPA experiments, and thanks also to Kieran O'Toole and Sarah Nicholson for help with the FISH and immunohistochemical techniques. In addition I would like to thank Dr Ed Schwalbe for his assistance with the methylation array data analysis and Mr Mike Cole for his input with some statistical analyses.

Finally, a special thank you is reserved for my friends and family. I am more grateful than they will ever know for their support, encouragement and kindness.

Dedication

I should like to dedicate this thesis to the young people in the North of England with cancer who I have had the privilege to serve over the last ten years.

Abbreviations

2HG	2-hydroxyglutarate
ADF	Alive and disease free
ADP	Adenosine diphosphate
ALL	Acute lymphoblastic leukaemia
AML	Acute meloid leukaemia
APC	Adenomatous polyposis coli
AQ	Absolute quantification
ARF	Aternative reading frame
ASO	Allele-specific oligoncleotide
ASO	Allele-specific oligonucleotide
ATM	Ataxia telangiectasia mutated
ATRT	Atypical teratoid rhabdoid tumour
AuSCR	Autologous stem cell rescue
AuSCT	Autologous stem cell transplant
AWD	Alive with disease
B2M	Beta-2-microglobulin
BAC	Bacterial artificial chromosome
BASH	BeadArray Subversion of Harshlight
BAX	BCL2-associated X protein
BCL2	B-cell CLL/ lymphoma 2
BCR-ABL	Philadelphia chromosome (fusion protein)
bd	Bis-die (twice daily)
bp	Base pair
BRCA1	Breast cancer associated gene 1
BRCA2	Breast cancer associated gene 2
CASP	Caspase, apoptosis-related cysteine peptidase
CCG	Childrens cancer group
CCLG	Children Cancer and Leukaemia Group
CCNU	Lomustine
CDH1	Cadherin 1, type 1, E-cadherin
CDKN2A	Cyclin-dependent kinase inhibitor 2A
CGH	Comparitive genome hybridisation
CGH	Comparative genomic hybridisation
CLL	Chronic lymphocytic leukaemia
CML	Chronic myelogenous leukaemia
CNS	Central Nervous System
COBRA	Combined bisulphite reaction analysis
CSF	Cerebrospinal fluid
CSI	Craniospinal irradiation
CSRT	Craniospinal radiotherapy

CT	Computerised tomography
Ct	Cycling threshold
CTNNB1	Beta catenin (cadherin -associated protein)
Cv	Coefficient of variation
DAB	Diaminobenzidine
DAPK1	Death-associated protein kinase 1
DBD	DNA binding domain
ddNTP	Dideoxy nucleoside triphosphates
DHFR	Dihdrofolate reductase
DLC-1	Deleted in liver cancer 1
DM	Double minute
DMSO	Dimethylsulphoxide
DNA	Deoxyribonucleic acid
DNMT	DNA methyltransferase
dNTP	Deoxynucleotide triphosphate
DOD	Died of disease
DTCS	Dye terminator cycle sequencing
EDTA	Ethylenediaminetetraacetic acid
EDV	Elevation detection value
EFS	Event free survival
EGFR	Epidermal growth factor receptor
EMA	Epithelial membrane antigen
EP300	E1A binding protein p300
ERH	Extended regions of homozygosity
ETANTR	Embryonal tumours with abundant neuropil and true rosettes
ETMR	Embryonal tumour with multilayered rosettes
FCS	Fetal calf serum
FFPE	Formalin fixed parrafin embedded
FHIT	Fragile histidine triad gene
FISH	Fluorescence *in situ* hybridisation
Fz	Frizzled
GBM	Glioblastoma muliforme
GCSF	Granulocyte colony stimulating factor
GFAP	Glial fibrillary acidic protein
Gli	Glioma-associated protein
GSK-3β	Glycogen synthase kinase-3β
Gy	Gray (unit of absorbed radiation)
H&E	Haematoxylin-eosin
HART	Hyperfractionated accelerated radiotherapy
hASH1	Achaete-scute complex homolog 1
HDAC	Histone deacetylase
HES	Hairy and enhancer of split
HGG	High grade glioma

HIF1α	hypoxia-inducible factor subunit 1α
HIT-SKK	Therapieprotokoll für Säuglinge und Kleinkinder mit Hirntumoren
hMLH1	Human MLH1 gene
hMSH2	Human MSH2 gene
HNPCC	hereditary non-polyposis colorectal carcinoma
HOMOD	Homozygous mapping of deletions
hPMS2	Human postmeiotic segregation increased 2 gene
HRAS	Harvey rat sarcoma viral oncogene homolog
HRP	Horseradish peroxidase
HSR	Homogenously stained region
HTA	Human Tissue Authority
icPNET	Intracranial primitive neuroectodermal tumour
IDH1	Isocitrate dehydrogenase-1
IDH2	Isocitrate dehydrogenase-2
IGF2	Insulin-like growth factor 2
IHC	Immunohistochemisty
INI1	SWI/SNF related, matrix associated, actin dependent regulator of chromatin, subfamily b, member 1
IQ	Intelligence quotient
Kb	Kilobase
KIT	v-kit Hardy-Zuckerman 4 feline sarcoma viral oncogene homolog
LCA	Large cell anaplastic
LEF	lymphoid enhancer factor
LFLS	Li-Fraumeni like syndrome
LFS	Li-Fraumeni syndrome
LHS	Left hybridising sequences
LOH	Loss of heterozygosity
LPO	Left probe oligonucleotide
LRP	Lipoprotein receptor-related protein
LSO	Ligand specific oligonucleotide
M stage	Metastatic stage
mAb	Monoclonal antibody
MB	Medulloblastoma
MBEN	Medulloblastoma with extended nodularity
MDM2	Mdm2, transformed 3T3 cell double minute 2, p53 binding protein
miR	Micro ribonucleic acid
ML1	Mucolipin 1
MLPA	Multiplex ligation-dependent probe amplification
MRI	Magnetic resonance imaging
mRNA	Messenger ribonucleic acid
MRS	Magnetic resonance spectroscopy
MSH2	MutS homolog 2

MS-MLPA	Methylation specific multiplex ligation-dependent probe amplification
MTX	Methotrexate
MYCC	V-myc myelocytomatosis viral oncogene homolog
MYCN	V-myc myelocytomatosis viral related oncogene, neuroblastoma derived
NADP	Nicotinamide adenine dinucleotide phosphate
NADPH	Reduced nicotinamide adenosine dinucleotide phosphate
NBCCS	Naevoid basal cell carcinoma syndrome
NCI	National Cancer Institute
NCID	Notch intracellular domain
NeuN	Neuronal nuclei
NF1	Neurofibromin 1
NF2	Neurofibromin 2
NHL	Non-Hodgkins lymphoma
NICR	Northern Institute for Cancer Research
NLS	Nuclear localization signals
OD	Optical density
ONS	Office for National Statistics
OS	Overall survival
PB	Pineoblastoma
PBS	Phosphate buffered saline
PDGFR	Platelet derived growth factor receptor
PFS	Progression free survival
PIG-3	Tumor protein p53 inducible protein 3
PNET	Primitive neuroectodermal tumour
PNET3	Primitive neuroectodermal tumour trial 3
PNET4	Primitive neuroectodermal tumour trial 4
POG	Pediatric Oncology Group
PTB	Primary tumour bed
PTCH	Patched homolog 1 gene
qRT	Quantitative real-time
RASSF1A	RAS- association domain 1
Rb	Retinoblastoma
RB1	Retinoblastoma gene
RHS	Right hybridising sequences
RICP	Raised intracranial pressure
RLGS	Restriction landmark genomic scanning
RNA	Ribonucleic acid
RPLPO	Acidic ribosomal protein P0
RPO	Right probe oligonucleotide
RQ	Relative quantification
RT	Radiotherapy

SAM	Sentrix Array Matrix
SD	Standard deviation
SFOP	Societè Française Oncologie Pèdiatrique
sFRP1	Secreted frizzled-related protein 1
Shh	Sonic hedgehog
SIOP	International Society of paediatric Oncology
SLS	Sample loading solution
SMO	Human smoothened gene
SOCS1	Suppressor of cytokine signalling 1
SPNET	Supratentorial primitive neuroectodermal tumour
SSC	Saline-sodium citrate buffer
SUFU	Suppressor of fused homolog
TAD	Transcriptional activation domain
TBE	Tris/Borate/EDTA
TBP	TATA-binding protein
TBS	Tris-buffered saline
TCF	T-cell –specific transcription factor
TIMP3	TIMP metallopeptidase inhibitor 3
Tm	Melting temperature
TP53	Tumour protein 53
TSG	Tumour suppressor gene
UK	United Kingdom
UKCCSG	United Kingdom Children's Cancer Study Group
USA	United States of America
USS	Unstained section
UV	Ultra violet
VEGF	Vascular epithelial growth factor
WHO	World Health Organisation
Wnt	Wingless
α-KG	α-ketoglutarate
β-catenin	Beta catenin (cadherin -associated protein)
β-TRCP	β-transducin repeat-containing protein

Table of Figures

Chapter 1

Chapter 2

Chapter 3

Chapter 4

Chapter 5

Table of Tables

Chapter 1

Chapter 2

Chapter 3

Chapter 4

Chapter 5

Chapter 1

Introduction

Table of contents

Chapter 1

1.1 Introduction to cancer

1.1.1 Cancer

The development and repair of normal tissue occurs through the highly regulated processes of cell growth (proliferation), differentiation and cell death (apoptosis). In health, response to different stimuli results in the transcription of genes to either promote or inhibit these processes. Tumour development ensues when abnormalities in gene expression result in aberrant regulation of cell cycle progression and cell death permitting increased cellular proliferation (Strachan and Read 2004). Tumours can be either benign or malignant. Benign tumours are contained within their local environment and do not invade adjacent tissues. Malignant tumours in contrast are more aggressive and may invade and cause damage to adjacent tissues. Malignant tumours may also spread to distant sites, and their ability to metastasise is facilitated by the lymphatic system and the bloodstream (Franks and Teich 1997).

1.1.2 The clonal origin of cancer

Cancer is a monoclonal disease and develops from a mutation in a single cell which provides it with a growth advantage over the surrounding cells. The mutated cell proliferates and creates a larger population of cells with the same genotype which increases the probability of further mutations, a process known as clonal evolution. Mutations may also render cells more susceptible to further mutational events by disrupting regulatory mechanisms including genes involved in DNA repair. Successive mutations confer additional growth advantages to the cancer cells which are clonally expanded until a tumour is formed from the different cancer clones. On average it has been proposed that six or seven successive mutations are required to convert a normal cell into an invasive carcinoma (Strachan and Read 2004)

The monoclonal origin of cancer has been confirmed in some tumours with chromosome X inactivation studies (Jones, Carr et al. 2005; Wang, Wang et al. 2009).

In these studies it has been demonstrated that tumour cells at different sites within an individual patient have the same inactive X chromosome, suggesting that they have arisen from the same cell. It has in contrast also been shown that in some cancers, cells may contain variable numbers of inactive X chromosomes suggesting a polyclonal origin in these tumours (Parsons 2008).

1.1.3 Cancer: A multistep process

As a cancer develops from successive aberrant genetic events a stepped divergence from a normal healthy tissue can occur. Initially morphological examination may show an excessive proliferation of normal cells (hyperplasia). As the process develops the proliferative cells can become immature (dysplasia), and become severely dysplastic but non-invasive (carcinoma *in situ*) before progressing to an invasive carcinoma (Strachan and Read 2004). This multistep process in the development of a cancer requires the acquisition of six key functional capabilities, illustrated in Figure 1.1. Cancers must develop (i) limitless replicative potential, (ii) self-sufficiency from growth signals, (iii) an insensitivity to growth inhibitory signals, (iv) an ability to evade apoptosis, (v) a sustained angiogenesis, and (vi) an ability to invade tissue and metastasise (Hanahan and Weinberg 2000).

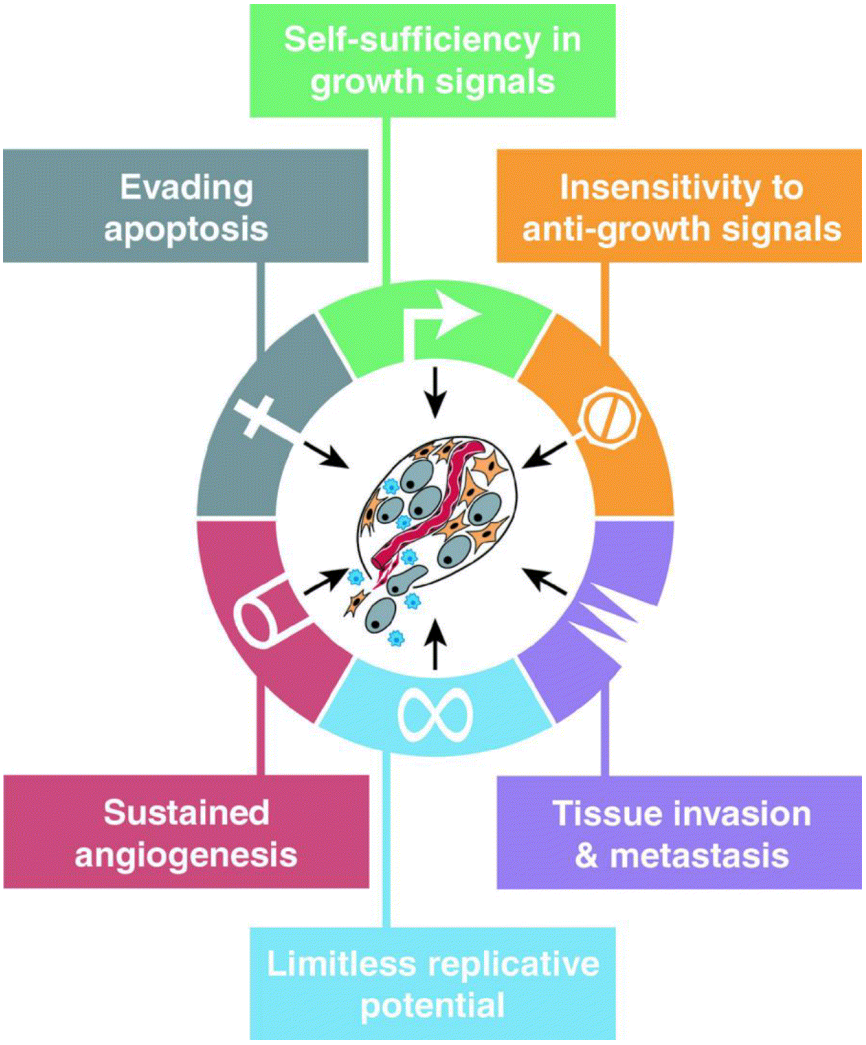

Figure 1.1. Acquired capabilities of cancer cells. Six essential capabilities of all cancers to facilitate tumour development. Figure taken from Hanahan and Weinberg (2000).

1.1.4 Cancer epidemiology

Cancer can affect any tissue within the body and in total more than 200 different types have been described in humans. One in three people will develop a cancer during their lifetime, and approximately one in every four people will die from this disease (www.info.cancerresearchuk.org). Cancer is responsible for 7.4 million worldwide deaths annually (13% of total), and this is expected to rise to 12 million by 2030 (WHO 2009). In the UK breast, lung, colorectal and prostate cancer are the four most

commonly diagnosed cancers, and together account for more than half of all cancers diagnosed each year (www.info.cancerresearchuk.org/cancerstats)(Figure 1.2).

The age at which people develop cancer varies significantly (Figure 1.3). As has been discussed (section 1.1.2), multiple genetic abnormalities are thought to be required to occur to promote the development of a cancer, and this may take a period of many years. This is reflected in the incidence of cancer development in which an exponential relationship is observed between age of diagnosis and incidence with cancer predominantly arising in people over the age of 60 years (Figure 1.3). Cancers in adults (over the age of 16 years) represent over 99% of all cancers (ONS 2010).

The current overall 5 year survival is 50% however there is significant variation in survival ranging from over 96% in testicular cancers to 3% in pancreatic cancers (Figure 1.4). The four most common cancers, (lung, breast, colorectal and prostate) are also responsible for almost half of all cancer-related mortality and are also a significant cause of morbidity (www.info.cancerresearchuk.org).

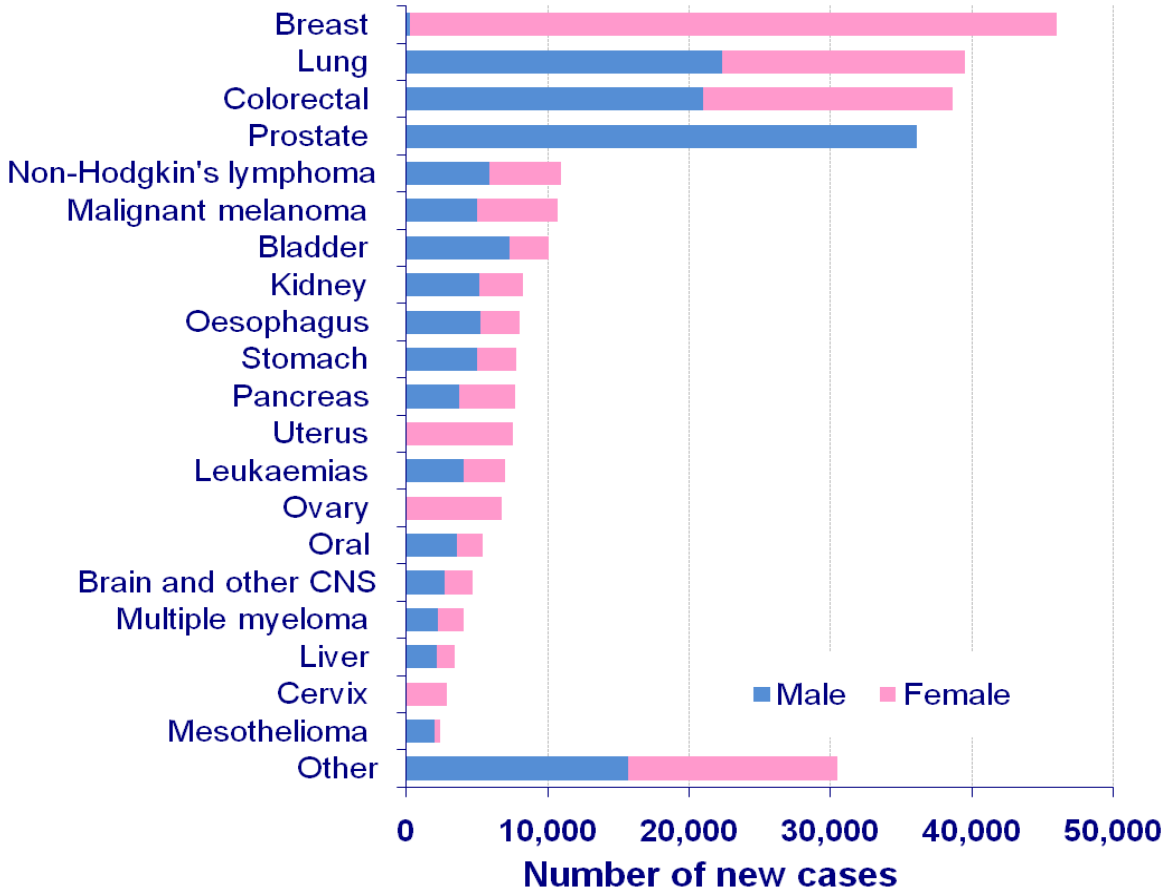

Figure 1.2. Incidence of the most common cancers diagnosed in the UK. The most commonly diagnosed cancers in the UK in 2007. CNS: Central Nervous System. Figure adapted from http://info.cancerresearchuk.org/cancerstats.

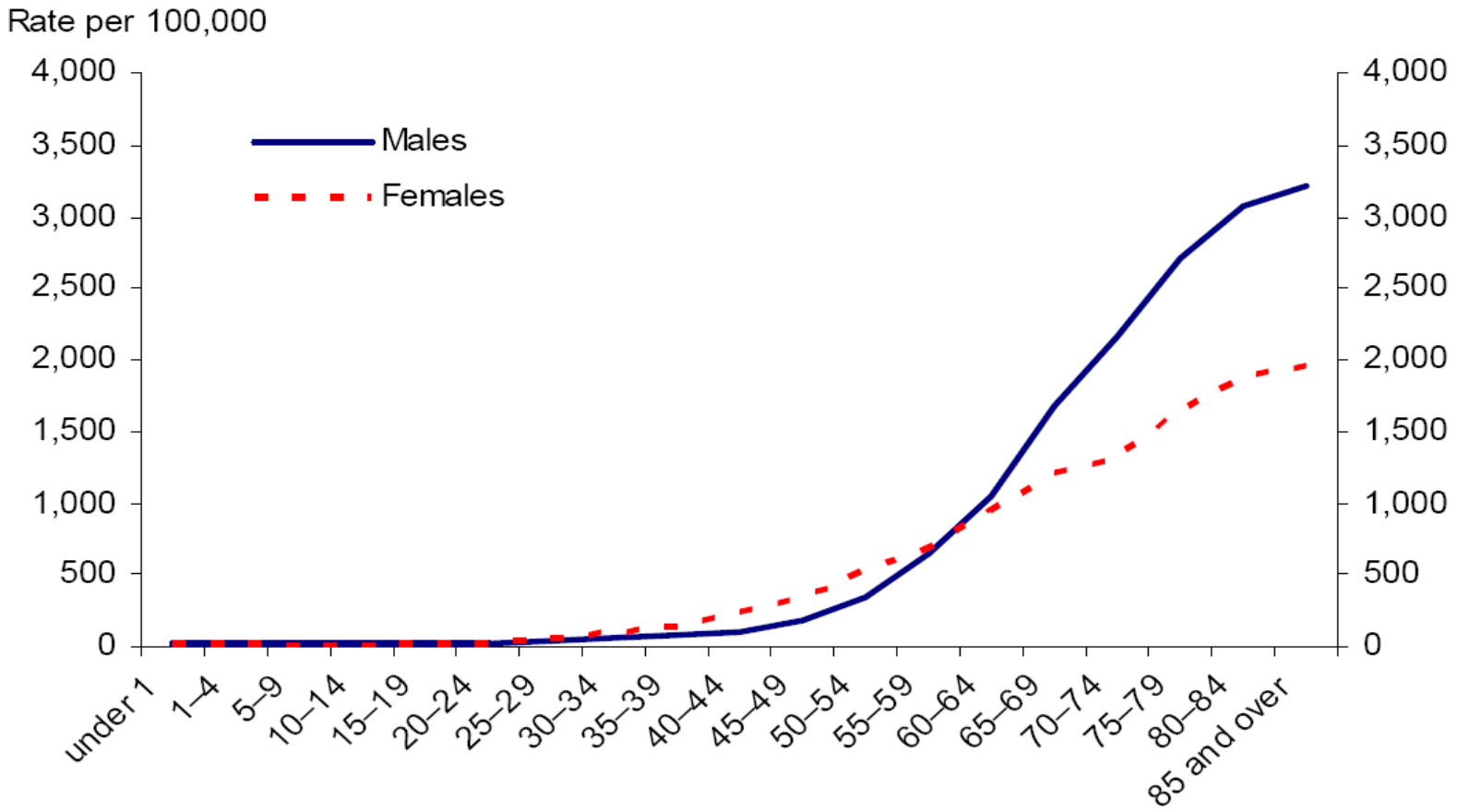

Figure 1.3. Incidence of cancer in people of different ages in England in 2007. Figures exclude non-melanomatous skin cancers. Cancers in those aged under 45 amounted to just over 5.4 per cent of the total for males and 9.2 per cent for females. Of the total of 245,327 malignancies, 1,147 (0.5 per cent) occurred in children aged under 15. Figure from(ONS 2010).

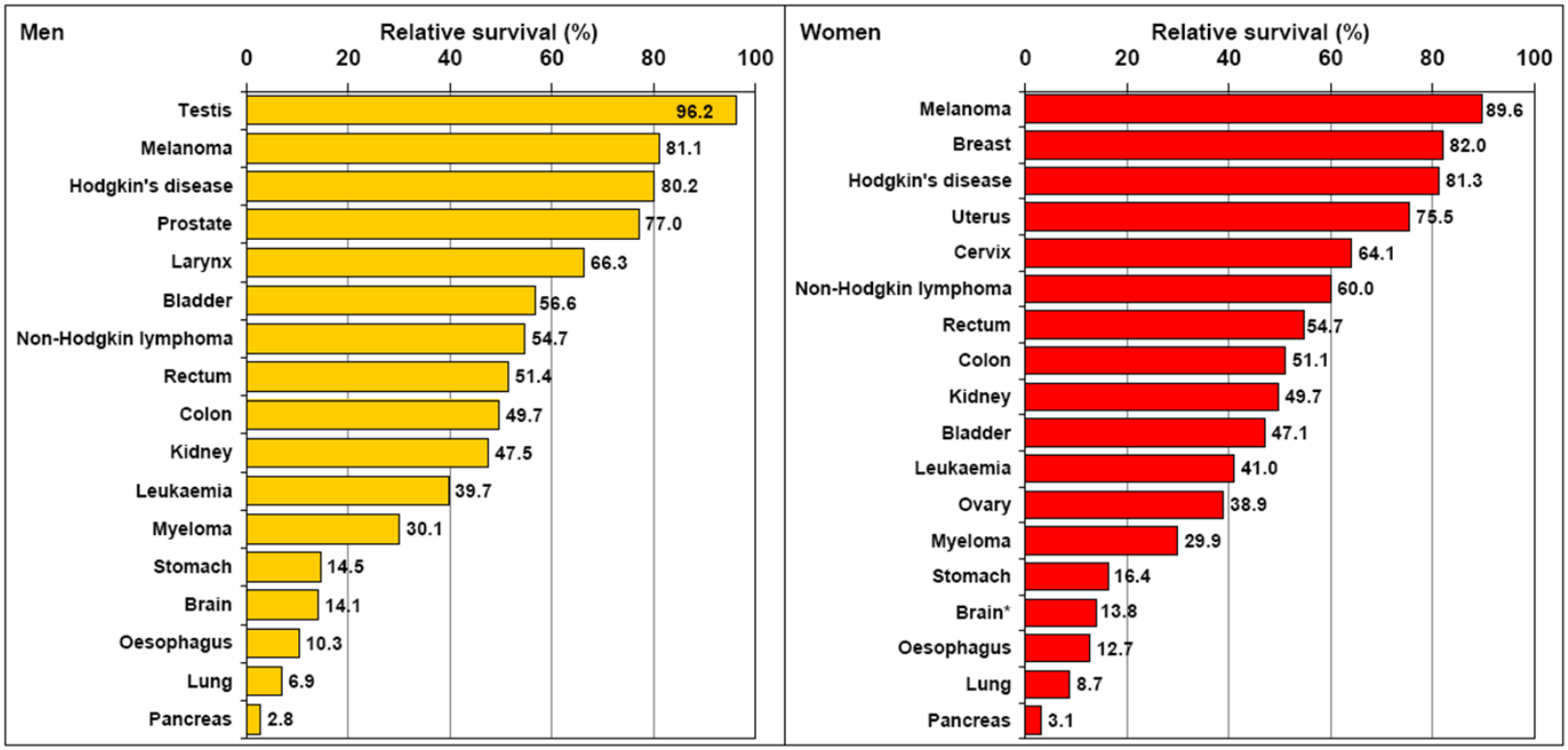

Figure 1.4. Survival from different types of cancer in men and women. Five year age standardised relative survival for the 21 most common cancers in adult men and women (15-99) diagnosed with cancer during 2001-2006 and followed up to 2007 in England. *Unadjusted survival rates given for women with brain tumours as age standardised rate could not be calculated due to the comparatively low incidence and poor survival for this group (ONS 2010).

1.1.5 Paediatric cancer epidemiology

Each year approximately 1200 new cases of cancer are diagnosed in children under the age of 15 in the UK, which represents 0.5-1% of all newly diagnosed cancers (www.info.cancerresearchuk.org). Overall, 1 in 500 children will develop a tumour before the age of 15. The risk of developing a leukaemia in childhood is 1 in 1600, 1 in 2200 for developing a CNS (brain and spinal cord) tumour, and 1 in 1100 for developing another form of cancer (www.info.cancerresearchuk.org). The risk of developing a cancer is 20% greater overall fora boy than that for a girl before the age of 15. Leukaemias are the most common form of cancer in children, and account for a third of all childhood cancers, whilst brain tumours account for 20-25% (Stiller 2004), and together they are responsible for more than half of all childhood cancers (Figure 1.5).

Survival rates, as with adult cancers, vary depending on the individual cancer type ranging from 96% with retinoblastoma or germ cell tumours to less than 5% with some forms of glioma (Figure 1.7). Overall the five year survival rate for children with cancer is 75%. In total however each year around 300 children with cancer will die from this disease, which account for 20% of all deaths in childhood (ONS 2010). Together, brain/ spinal cord tumours and leukaemias are responsible for almost two-thirds of childhood deaths from cancer (Figure 1.7).

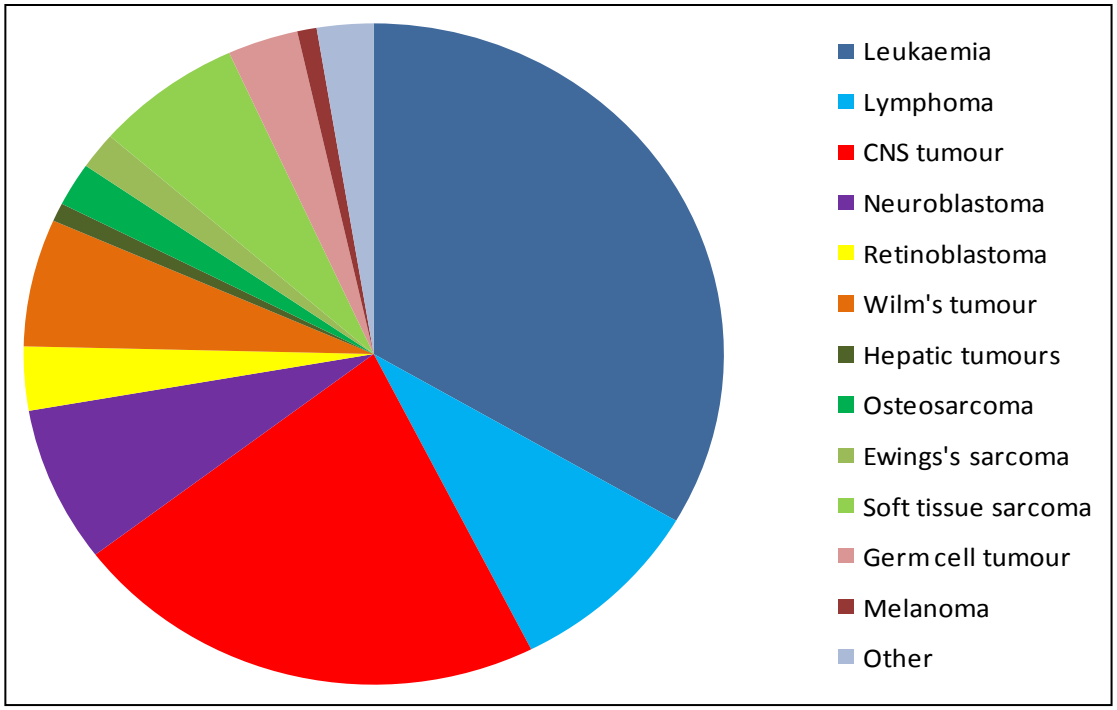

Figure 1.5. Incidence of childhood cancer in the UK. Age-standardised rates of childhood cancer (aged 0-14 years) in the UK. Data taken from (Stiller 2004).

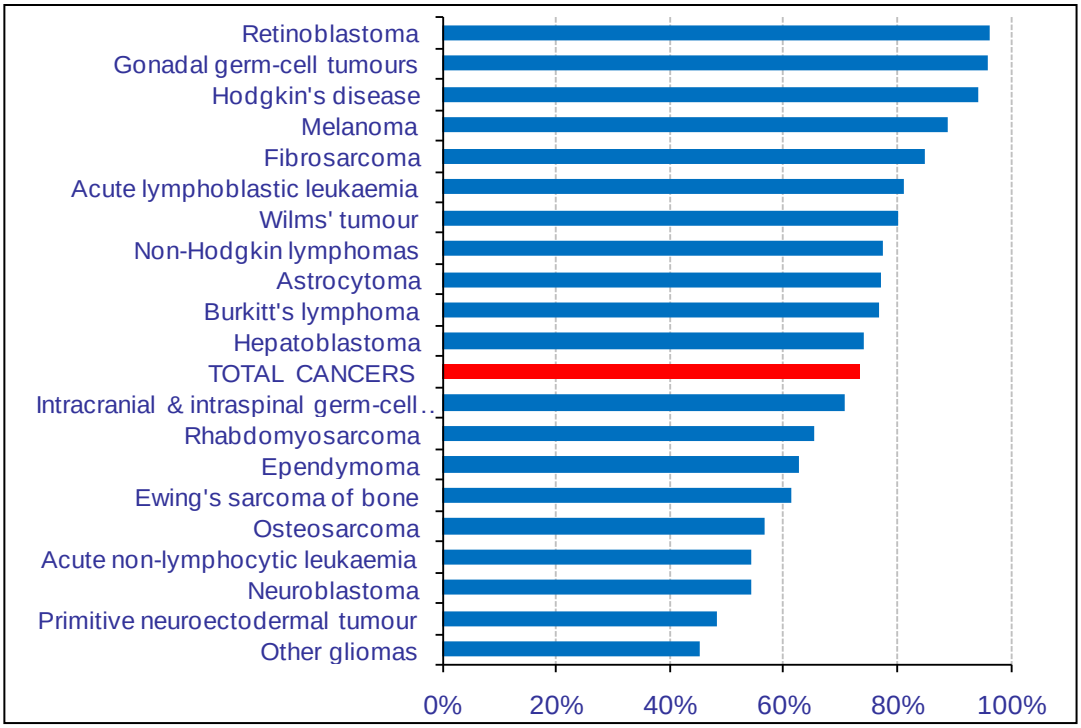

Figure 1.6. Survival rates at 5 years for children diagnosed with cancer in 1992-1996 in Great Britain. Figure adapted from http://info.cancerresearchuk.org/cancerstats.

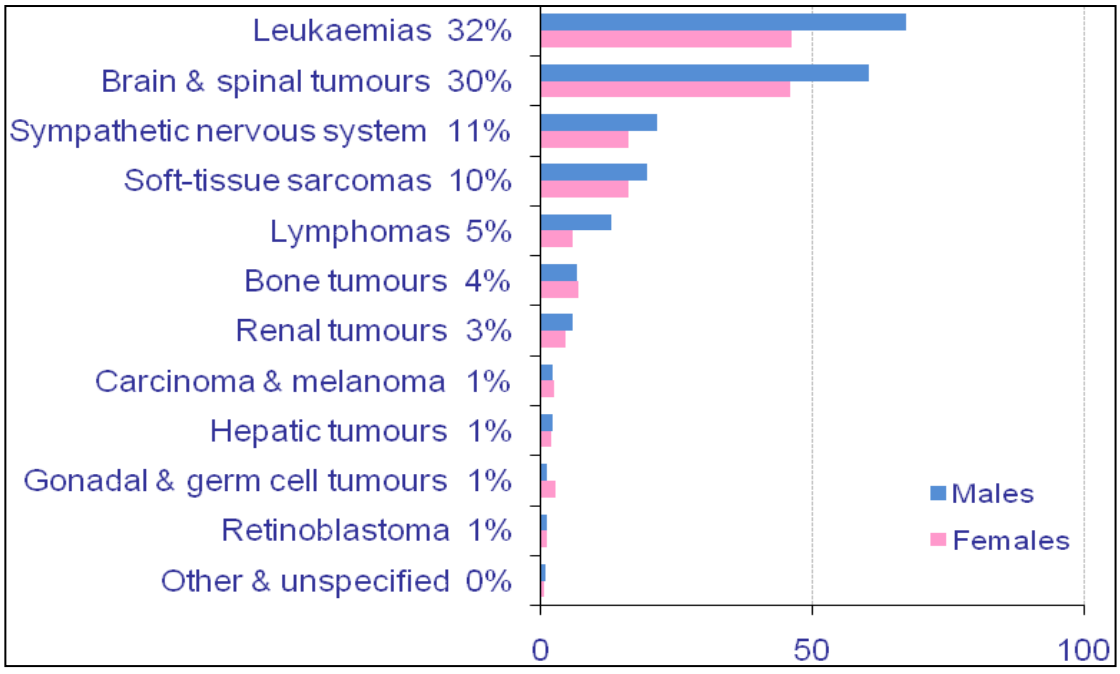

Figure 1.7. UK annual average number of deaths in children diagnosed with cancer under the age of 15 in 1997 - 2001. Figure adapted from http://info.cancerresearchuk.org/cancerstats.

1.2 Cancer: A genetic disease

1.2.1 Introduction

As has been discussed in section 1.1.3, multiple genetic anomalies are required to accumulate for a tumour to develop the characteristics required for tumorigenesis. These genetic anomalies may arise from environmental factors including exposure to ultraviolet light or ionizing radiation. The most common exposure, which results in almost a third (29%) of all cancer related deaths in the UK, is tobacco smoke (www.cancerresearch.org). Inherited genetic abnormalities, in which an individual inherits an abnormality in one allele of a gene rendering the individual susceptible to developing a cancer, are also implicated in a proportion of cancers. Individuals who inherit a *BRCA1* or *BRCA2* mutation, for example have an 85% chance of developing a breast cancer (Ford, Easton et al. 1998). Genes, such as *BRCA1* and *BRAC2* that may be implicated in the development of cancers are classified as being either oncogenes or tumour suppressor genes.

1.2.2 Oncogenes

An oncogene is a gene that when mutated or over-expressed is capable of dominantly promoting cancer by supporting the cellular processes required for tumour development (Figure 1.1). First discovered in the 1970's in viral induced cancers (leukaemias and lymphomas), over 100 oncogenes have now been described in human cancers and may be classified into five groups based on their function: (i) growth factors, (ii) growth factor receptors; (iii) signal transduction components; (iv) transcription factors; and (v) cell cycle/ apoptosis regulators (Strachan and Read 2004). Oncogenes, derived from mutated normal cellular genes are known as proto-oncogenes. The conversion to oncogenes may occur by a number of mechanisms including gene amplification, point mutation, translocation which incorporates a gene within a transcriptionally active region of chromatin, transcriptional activation by proteins upstream of the oncogene, or through a translocation which creates a novel

chimeric gene. These alterations (exemplified in Table 1.1) result in either an increased normal product or a new product with tumourigenic properties.

The targeting of oncogenic proteins by small molecules currently is an important area of both research in cancer therapeutics and clinical practice. Imatinib mesylate (Gleevec™, Novartis) for example was designed to target the chimeric BCR-ABL protein produced in chronic myeloid leukaemia (CML) and is now successfully used in the management of patients with this disease (Goldman and Melo 2001; Agrawal, Garg et al. 2010). It has also been shown to have activity both in other cancer types, and by operating on additional targets including PDGFR and KIT and has developed a broader clinical utility (Heinrich, Blanke et al. 2002; Casali, Messina et al. 2004)

Oncogene	Location	Function	Mechanisms of activation	Cancer association
PDGFB	22q13.1	Growth factor	Translocates to transcriptionally active region Point mutation	Dermatofibrosarcoma
EGFR	7p12	Growth factor receptor	Amplification Point mutation	Glioma Non-small cell lung cancer
HRAS	11p15.5	Signal transduction pathway component	Mutation Amplification	Colorectal carcinoma Rhabdomyosarcoma
MYCC	8q24.1	DNA binding transcription factor	Translocates to transcriptionally active region Amplification Point mutation Transcriptional activation	Burkitt lymphoma Breast and Prostate cancer B-CLL, Colorectal carcinoma
BCL2	18q21.3	Anti-apoptosis	Translocates to transcriptionally active region Transcriptional activation	NHL, CLL Melanoma
BCR-ABL	t(9;22)(q34;q11)	Tyrosine kinase	Translocation creating a novel chimeric gene	Breast prostate, lung cancer

Table 1.1. Function and activating mechanisms of common oncogenes. Examples of different oncogene functions and mechanisms of activation in different tumour types. CLL, chronic lymphocytic leukaemia; B-CLL, B-cell lineage CLL; NHL, Non-Hodgkin Lymphoma. Data collated from (Strachan and Read 2004; Croce 2008) and Wellcome Trust Sanger Institute Cancer Genome Project web site, http://www.sanger.ac.uk/genetics/CGP.

1.2.3 Gene amplification

The amplification of genes, as has been discussed in section 1.2.2, may result in the development of tumours by increasing mRNA and protein expression. Amplification of isolated genes may occur, but an amplicon may also comprise several genes an extend to several megabases (Storlazzi, Fioretos et al. 2004). Amplification, shown in Figure 1.8, may arise by a number of mechanisms. Repeated duplication of chromosomal regions may give rise to homogeneously staining regions (HSR) which may contain thousands of additional copies of a given gene. Extrachromosomal additional copies of a gene may also occur, and form "double minutes" (DMs). The definition of an amplified gene varies in different tumour types. In breast cancer for example, a two-fold increase in *EGFR* is considered amplified, whereas in neuroblastoma at least a four-fold increase in *MYCN* is necessary before this gene is considered to be amplified (Press, Finn et al. 2008; Theissen, Boensch et al. 2009). In addition to enabling tumour formation, cancer cells may also use gene amplification to develop chemotherapy resistance. It has been shown for example, that amplification of the dihydrofolate reductase gene (*DHFR*) can confer resistance to methotrexate (MTX) (Trask and Hamlin 1989), which would normally act to inhibit this enzyme, and is associated with an adverse clinical outcome (Goker, Waltham et al. 1995).

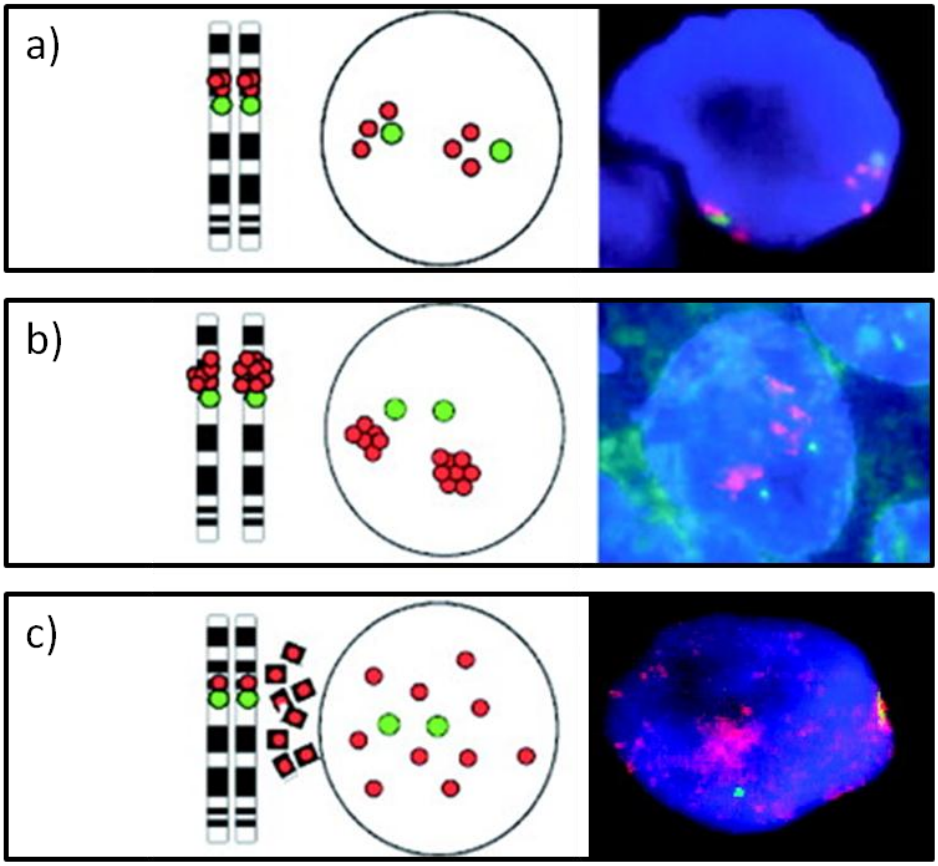

Figure 1.8. Schematic overview of gene amplification. Fluoresence *insitu* hybridisation (FISH) in a tumour cell using centromeric (green), and *MYCN* (red) probes. (a) Increased copy number of *MYCN* in a disomic cell, (b) *MYCN* amplification as part of a homogeneously staining region (HSR), (c) *MYCN* amplification with extra-chromosomal copies or double minutes (DM). Figure adapted from (Martin, Mazzucchelli et al. 2009).

1.2.4 Tumour suppressor genes

Tumour suppressor genes (TSGs) code for proteins which function as regulators of cellular processes by inhibiting cell proliferation, stabilising the genome by ensuring accurate DNA replication and repair, and promote apoptosis should the DNA become damaged and not repairable. Cancer may develop if the regulatory function of the TSGs is lost. Both TSG alleles are thus typically required to become inactivated for tumour development to occur, as was first hypothesised in a landmark study by Alfred Knudson in 1971. In a study of familial and sporadic retinoblastomas, and noticing that tumours developed earlier in the familial form, Knudson hypothesised that for retinoblastomas to develop, 2 mutational events are required ("the Knudson two-hit hypothesis") (Knudson 1971). In familial tumours it was postulated that one "hit" was inherited requiring only one mutational event or "hit" to occur, whilst for sporadic tumours to develop two mutational events or "hits" would be required to occur. This theorem was subsequently validated with the discovery of the retinoblastoma gene (*RB1*) and the observation that both alleles are inactivated in retinoblastomas (Friend, Bernards et al. 1986). Retinoblastomas in the familial form require only one "hit", occur at an earlier age and are bilateral, whilst additional time is required to accrue the two "hits" in a later onset (>2 years old) and unilateral tumour in the sporadic form.

Following the discovery of *RB1* as a TSG a number of additional genes have been found to be associated with familial cancers (Table 1.10) and in total over 100 TSGs have been identified (Yang and Fu 2003). The most common TSG implicated in the development of cancer is *TP53*, which has been found to be mutated or deleted in over 50% of all human cancers (Hollstein, Sidransky et al. 1991).

Gene	Location	Disease	Functions
APC	5q21	Familial adenomatous polyposis coli (FAP)	Nuclear signalling
MSH2, ML1	2p16, 3p21.3	Hereditary nonpolyposis colonic cancer (HNPCC)	DNA mismatch repair
BRCA1	17q21	Breast and ovarian cancer	Transcription regulator, DNA binding, DNA repair, homologous recombination, ubiquitination of proteins
BRCA2	13q12-q13	Early onset breast cancer	
TP53	17p13	Li-Fraumeni syndrome	Cell cycle regulation, apoptosis
PTCH	9q22-q31	Gorlin syndrome	Transmembrane receptor
ATM	11q22-q23	Ataxia telangiectasia	DNA repair
RB1	13q14	Retinoblastoma	Cell cycle regulation
NF1	17q12-q22	Neurofibromatosis type 1	RAS inactivation catalysis
NF2	22q12.2	Neurofibromatosis type 2	Cytoskeleton-membrane linkage
CDKN2A	9p21	Familial melanoma	p53 stabilizer
VHL	3p25-p26	von Hippel-Lindau disease	Transcription regulator

Table 1.2. Common tumour suppressor genes and associated familial cancer syndromes. Gorlin syndrome also known as basal cell naevus syndrome. Table adapted from (Strachan and Read 2004).

1.2.4.1 Inactivation of tumour suppressor genes

Loss of function of a TSG may occur by a variety of mechanisms (Figure 1.9). Chromosome loss, deletions, recombination, gene conversion and point mutations may all result in TSG loss of function (Reviewed in (Strachan and Read 2004)). Epigenetic modifications (reviewed in section 1.2.6) have also been shown to be involved in silencing TSG function by preventing the transcription of TSGs. Many of these mechanisms result in a loss of heterozygosity (LOH) of the TSG locus and therefore methods capable of detecting such LOH have been used to identify many loci harbouring candidate TSGs (Strachan and Read 2004).

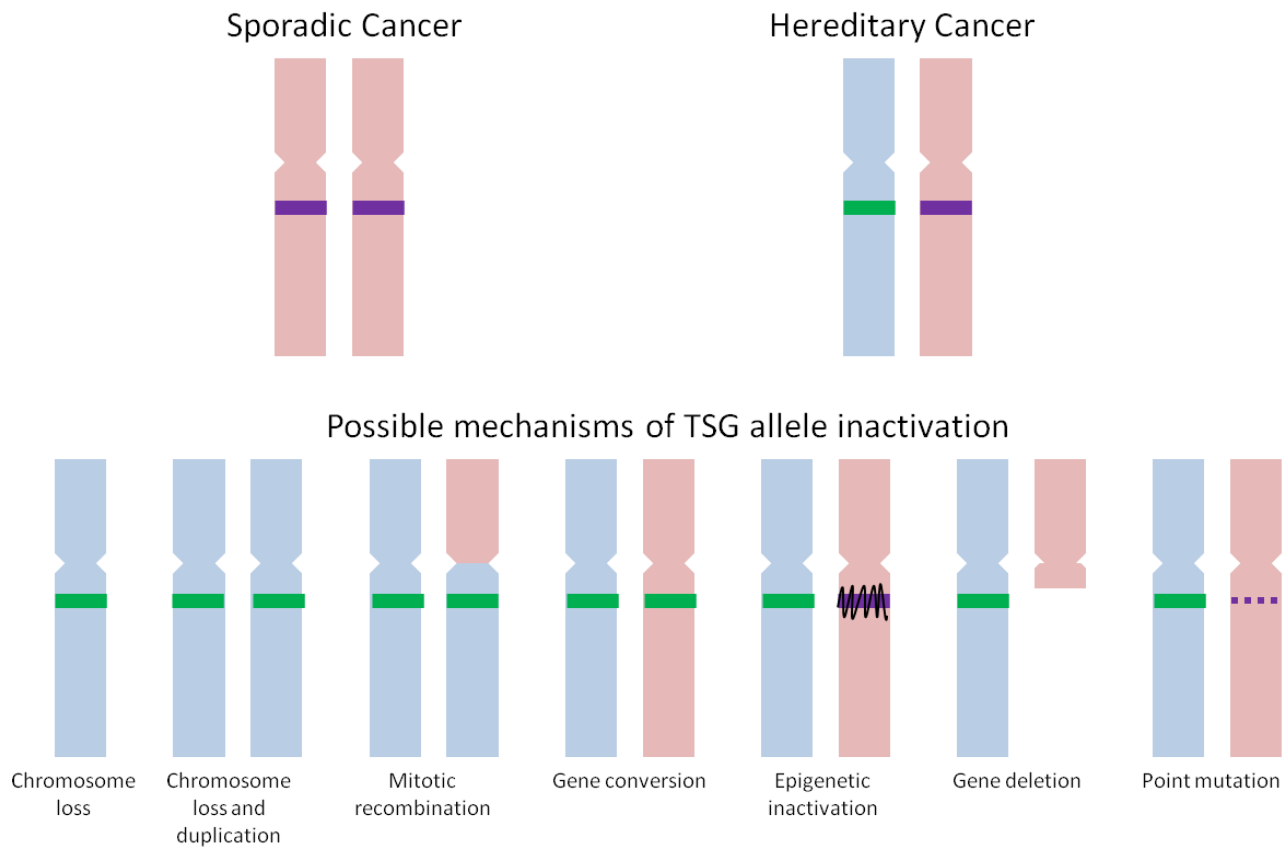

Figure 1.9. Mechanisms of inactivation of the normal allele of a tumour suppressor gene. In sporadic cancer (top left), both alleles must be inactivated (purple band) for tumour suppressor gene (TSG) loss of function. In hereditary or familial cancer (top right), an inactivated allele is inherited (green band) and the remaining wild type allele needs to be inactivated before tumour development may occur. The possible mechanisms that may give rise to inactivation of the normal allele ("second hit") are outlined in the bottom panel. Figure adapted from (Alberts, Johnson et al. 2002).

1.2.5 Cytogenetic abnormalities

Alterations in chromosomal structure and number, as illustrated in Figure 1.9, may result in tumorigenesis. These cytogenetic abnormalities, first detected in cancer cells in 1960, including the size and number of chromosomes are visualised by karyotyping, which requires analysis of the chromosomes of cells during cell cycle metaphase (Nowell and Hungerford 1960).

More recently, alterations in chromosomal structure may also be determined by comparative genomic hybridisation (CGH). This technique, first devised in 1992 and used to interrogate bladder tumours (Kallioniemi, Kallioniemi et al. 1992), requires an investigative sample of DNA to be processed simultaneously with a sample of normal control DNA. The two differentially labelled samples are then permitted to competitive hybridise with a normal metaphase spread on a slide, and the ratios of the two different signals along each chromosome is then recorded to determine whether there is a gain or loss at any given locus in the investigative sample. Unlike conventionally karyotyping which is limited both by the quality of the material being used and also the resolution at which defects can be determined (discussed in (Teyssier 1989)), CGH permits the use simply of fragments of DNA and yields an enhanced resolution, identifying smaller regions of chromosomal loss or gain which has aided in the identification of oncogenes and TSGs.

1.2.6 Epigenetic modification

In addition to genetic alterations, epigenetic modifications may also play a role in tumour development. Epigenetics is the study of heritable changes in gene expression that occur without a change in the DNA sequence. Epigenetic modification may occur by a number of mechanisms including DNA methylation, chromatin remodelling, histone modification and with micro ribonucleic acids (miRNAs).

1.2.6.1 Histone modification

Histones are basic proteins that form an octamer (H3/H4 tetramer and two H2A/H2B dimmers) with 147bp of DNA to form a chromatin nucleosome. Histone tails protrude outside of the nucleosome where they may be subjected to post-translational modification including acetylation, methylation, phosphorylation, ubiquitylation, sumoylation, glycosylation, ADP-ribosylation, biotinylation or carbonylation (Strahl and Allis 2000). The various histone tail domain modifications act in a sequential and combinatorial fashion to regulate chromatin structure, a concept known as the histone code, and exert their epigenetic control by either preventing or promoting the binding of proteins to the genome to activate or repress genetic transcription (Mizzen and Allis 2000).

Disruption of histone modifications including loss and gain of histone lysine acetylation and methylation has been reported to occur in cancerous cells (Fraga, Ballestar et al. 2005). The loss of lysine acetylation has been shown to be an early event in cancer development through gene silencing and also reducing a cell's DNA repair capability (Mutskov and Felsenfeld 2004; Masumoto, Hawke et al. 2005). Mutations in EP300, a histone acetyltransferase for example, have been associated with breast, colonic and pancreatic cancers (Gayther, Batley et al. 2000), and has subsequently stimulated interest in the therapeutic targeting of histone modification control and in particular inhibitors of histone deacetylases (HDACs)(Workman 2001).

1.2.6.2 Chromatin remodelling

DNA within the nucleus is highly folded, constrained and compressed by histones and other proteins to form chromatin. The repositioning of nucleosomes along the DNA can create nucleosome-free regions which permit gene transcription (Davis and Brackmann 2003). Alterations in chromatin structure may consequently be associated with cell cycle progression, DNA repair, DNA replication and chromosomal stability (Wolffe and Guschin 2000).

Chromosomal regions that become transcriptionally repressed appear highly condensed in interphase nuclei including the inactive X chromosome or "Barr body" in females (Brown 1966). Disorders of chromatin remodelling are implicated in a number of conditions including Rett, Rubinstein-Taybi and Coffin-Lowry syndromes (Ausio, Levin et al. 2003). Mutations in genes necessary for chromatin remodelling may also result in cancer development as occurs with mutations of *INI1* and the development of paediatric atypical teratoid rhabdoid tumours (ATRT) (Versteege, Sevenet et al. 1998).

1.2.6.3 DNA methylation

DNA methylation occurs with the addition of a methyl group to a cytosine residue 5' to a guanosine in a CpG dinucleotide. The CpG dinucleotide is under-represented in the genome apart from areas of approximately 0.5-4.0 Kb in length, with a high CpG content, located at the promoter region of almost half of all genes and known as "CpG islands". These islands are defined as being at least 500bp in length, with a combined guanosine and cytosine content greater than 50%, and an observed over expected frequency of the dinucleotide CG greater than 0.6 (Wang and Leung 2004).

Methylation of CpG dinucleotides is undertaken by DNA methyltransferases (DNMTs) which facilitates the replication of methylation patterns between parent and daughter cells. In normal somatic cells most promoter-associated CpG islands are unmethylated and associated with an open, transcriptionally active chromatin structure, whereas CpG dinucleotides elsewhere in the genome are generally methylated and therefore transcriptionally repressed (Figure 1.10) (Bestor 2000; Lindsey, Anderton et al. 2005). Epigenetic modification by DNA methylation is a dynamic process that facilitates variation in expression at different stages of development and in different tissue types and is therefore important in a range of processes including early development, tissue-specific gene expression, host defence, genomic stability and gene imprinting (reviewed in (Gopalakrishnan, Van Emburgh et al. 2008).

Aberrations in methylation may also occur and are implicated in a number of diseases (Robertson 2005). In addition to sex differences as a result from inheriting different X and Y chromosome combinations, sex specific differences in methylation patterns on other chromosomes may give rise to differential expression, in a process known as imprinting (Robertson 2005). The developmental disorders Prader-Willi (PWS) and Angelman syndrome (AS), for example may result from a loss of paternally or maternally expressed alleles respectively at the imprinting centre located at 15q11-q13 (Nicholls and Knepper 2001). Cancers have also been shown to occur as a result of genetic imprinting. The maternal allelic loss of expression on chromosome 11p15.5 of *H19* by imprinting for example, permits activation of the normally silent maternal *IGF2* gene which is associated with Wilms' tumour development (Steenman, Rainier et al. 1994).

Alterations in DNA methylation patterns are a hallmark of most human cancers (Baylin and Herman 2000). In cancer development, genome-wide hypomethylation of tumour cells compared to normal tissue has been shown predominate (Feinberg and Vogelstein 1983). This genome wide hypomethylation occurs as an early event in tumorigenesis and has been shown in some tumour types to correlate with both metastatic potential and disease severity (Widschwendter, Gattringer et al. 2004). Individual genes however may also become methylated in cancer. Methylation of *RB1* was the first gene to be associated with cancer (Ohtani-Fujita, Fujita et al. 1993), but DNA methylation has subsequently been shown to effect the expression of a plethora of genes involved in critical regulatory processes including those responsible for cell-cycle regulation, tumour invasion, apoptosis, transcription, DNA repair, cell signalling and chromatin remodelling (summarised in Table 1.3) (Robertson 2005).

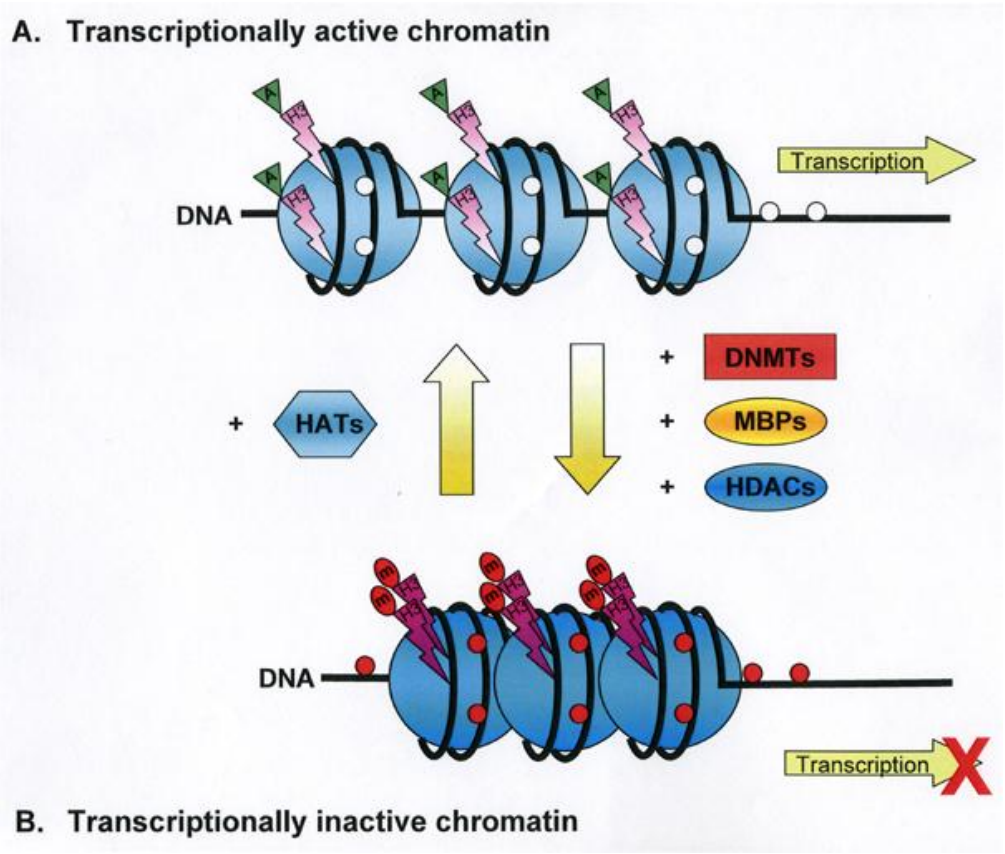

Figure 1.10. Epigenetic inactivation by promoter hypermethylation. (A) Transcriptionally active chromatin (euchromatin) is associated with widely spaced nucleosomes (light blue circles), unmethylated CpG residues (white circles), acetylation (green triangles) of histone H3 lysine residues (pink arrows) and an open chromatin structure. The open chromatin is easily accessible to transcription factors and enzymes involved in gene transcription including histone acetyl transferases (HATs). (B) The methylation of CpG residues (red circles), compacted nucleosomes (dark blue circles) and deacetylated histones (dark pink arrows) result in a compacted chromatin structure (heterochromatin) and repression of transcription. The establishment and maintenance of heterochromatin is performed by methyl-CpG binding proteins (MBPs), histone deacetylases (HDACs) and DNA methyltransferases (DNMTs). Figure taken from (Lindsey, Anderton et al. 2005).

Gene Function	Gene	Cancer type
Cell cycle regulation	*RB1*	Retinoblastoma
	CDKN2A	Colon, lung and others
Tumour cell invasion	*CDH1*	Breast, gastric, thyroid, leukaemia, liver
	CDH13	Lung, ovarian, pancreatic
	TIMP3	Brain, kidney
	VHL	Renal cell
DNA repair/ detoxification	*MLH1*	Colon, endometrial, gastric
	MGMT	Brain, colon, lung, breast
	BRCA1	Breast, ovarian
	GSTP1	Prostate, liver, colon, breast, kidney
Chromatin remodelling	*SMARCA3*	Colon, gastric
Cell signalling	*RASSF1A*	Lung, liver, brain
	SOCS3	Liver, colon, multiple myeloma
Transcription	*ESR1*	Colon, breast, lung, leukaemia
Apoptosis	*DAPK1*	Lymphoma

Table 1.3. Epigenetic silencing of genes by aberrant DNA methylation in cancer. *RB1*, retinoblastoma 1; *CDKN2A*, cyclin-dependent kinase inhibitor 2A; *CDH1*, cadherin 1 (E-cadherin); *CDH13*, cadherin 13 (H-cadherin); *TIMP3*, tissue inhibitor of metalloproteinase; *VHL*, von Hippel-Lindau; *MLH1*, mutL homolog; *MGMT*, methylguanine-DNA methyltransferase; *BRCA1*,breast cancer 1 ; *GSTP1*, glutathione S-transferase pi 1; *SMARCA3*, SWI/SNF related matrix associated actin dependent regulator of chromatin 3; *RASSF1A*, Ras association domain family member 1; *SOCS3*, suppressor of cytokine signaling 3; *ESR1*, oestrogen receptor 1; *DAPK1*, death-associated protein kinase 1 . Table adapted from (Robertson 2005).

1.2.6.4 MicroRNA

Discovered in 1993, miRNAs are single stranded RNA molecules comprised of 21-23 nucleotides which are not translated into a protein, but by complementing a number of messenger RNA (mRNA) molecules are able to down regulate gene expression (Lee, Feinbaum et al. 1993). In total more than 1000 miRNAs have been identified (http://microrna.sanger.ac.uk), and may be associated with cancer development by acting as oncogenes or tumour suppressor genes (Table 1.4). In chronic lymphocytic leukaemia (CLL) for example, down-regulation of anti-apoptotic *BCL2* by miR-15a and miR-16-1 can promote tumour development, whilst up-regulation of antiapoptotic miR-21 is implicated in glioblastoma development (Calin, Dumitru et al. 2002; Chan, Krichevsky et al. 2005; Ciafrè, Galardi et al. 2005).

Function	MicroRNA	Confirmed targets	Mechanism of action	Cancer Association
Tumour Suppressor miRNA	miR-15a, miR-16-1	*BCL2, WT1*	Induce apoptosis, reduce tumorigenicity	CLL
	let-7	*RAS, MYCC, HMGA2*	Induce apoptosis	Lung & breast cancer
	miR-29 (a,b,c)	*TCL1, MCL1, DNMT3*	Induce apoptosis, reduce tumorigenicity	CLL, AML, cholangiocarcinoma, lung & breast cancer
	miR-34 (a,b,c)	*CDK4, CDK6, cyclinE2, E2F3*	Induce apoptosis	Pancreatic, breast & colon cancer
Oncogenic miRNA	miR-155	c-maf	Induce lymphoproliferation	CLL, DLBCL, AML, Burkitt lymphoma, lung & breast cancer
	miR-17-92 cluster	*E2F1, PTEN*	Cooperate with c-myc to induce tumour development	Breast, lung, colon, stomach & pancreatic cancer. Lymphomas.
	miR-21	*PTEN, PDCD4, TPM1*	Blocks apoptosis, promotes tumorigenicity	Breast, colon, pancreatic, lung, prostate, liver & stomach cancers. AML, CML, Glioblastoma
	miR-372, miR-373	*LATS2*	Promote tumorigenesis in cooperation with RAS	Testicular tumours

Table 1.4. MiRNAs with tumour suppressor or oncogenic function in cancer. CLL, chronic lymphocytic leukaemia; AML, acute myeloid leukaemia; DLBCL, diffuse large B cell lymphoma. Table adapted from (Garzon, Calin et al. 2009)

1.3 Paediatric brain tumours

1.3.1 Introduction

Brain tumours are the most common solid tumours of childhood and in total account for 20% of all childhood malignant tumours. In the UK each year approximately 350-400 children are diagnosed with a brain tumour (CCLG 2010). Brain tumours are diagnosed in 3 per 100,000 children under the age of 15 each year and annually in 2 per 100,000 15-19 year olds (Capra, Hargrave et al. 2003; Peris-Bonet, Martinez-Garcia et al. 2006). The incidence of brain tumours increased in the 1970s to 1990s, as shown in Figure 1.11, and in children increased by 1.7% per annum between 1988 and 1997 (Peris-Bonet, Martinez-Garcia et al. 2006). This trend was recapitulated in a number of international studies during this period (Kaatsch, Steliarova-Foucher et al. 2006; Stiller 2007). More recently however it has been reported that this trend has reached a plateau (Linabery and Ross 2008; Peris-Bonet, Salmeron et al. 2010) and that the previously observed increases may have in fact been an artefact of changes in diagnostic and neurosurgical practice (Smith, Freidlin et al. 1998; Smith, Seibel et al. 2010).

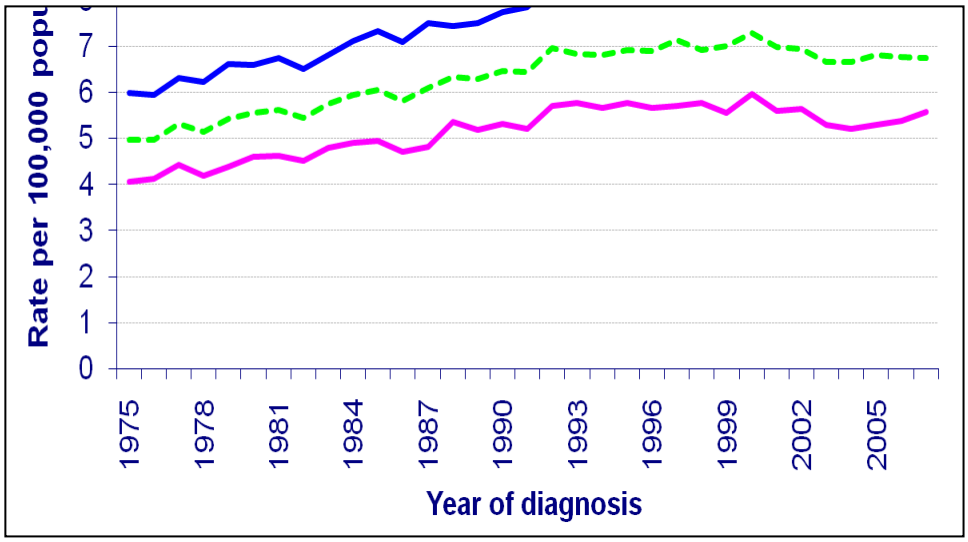

Figure 1.11. Age standardised European incidence rates of CNS tumours 1975 -2007. Figure taken from http://info.cancerresearchuk.org/cancerstats.

1.3.2 WHO classification

The World Health Organisation (WHO) first published a classification of human CNS tumours after a decade in development in 1979 (Zulch 1979). The aim of the WHO classification system was to establish a classification and grading system of human tumours that would be accepted worldwide and would facilitate the study of these tumours, but a consensus in classification has been difficult to establish (reviewed in (Scheithauer 2009)). The original classification was based on tumour site, grade and histology but developments in immunohistochemical techniques, clinical trial observations and molecular findings have resulted in 3 updated editions being produced in 1993, 2000 and 2007 respectively (Kleihues, Burger et al. 1993; Kleihues and Cavenee 2000; Louis, Ohgaki et al. 2007). The current fourth edition of the WHO classification of CNS tumours (summarised in Table 1.5.) includes eight new entities and additional histological variants.

The tumours are graded I to IV based on their aggressiveness (Louis, Ohgaki et al. 2007). Grade I tumours have a low proliferative potential and may be cured with surgical resection alone. Grade II tumours whilst also of low proliferative potential are infiltrative in nature and more likely to recur after surgical resection. Some of these grade II tumours also possess the ability to transform into higher grade tumours (eg diffuse astrocytomas, oligodendrogliomas, and oligoastrocytomas). Tumours which exhibit nuclear atypia and an increased mitotic index are classified as grade III. Patients with these tumours are usually treated with adjuvant therapy including radiotherapy and chemotherapy. The most aggressive tumours which are invasive and highly mitotically active are designated grade IV. Without successful multimodal therapy these tumours typically rapidly evolve and are fatal. The incidence of the different WHO brain tumour subtypes are shown in Figure 1.12.

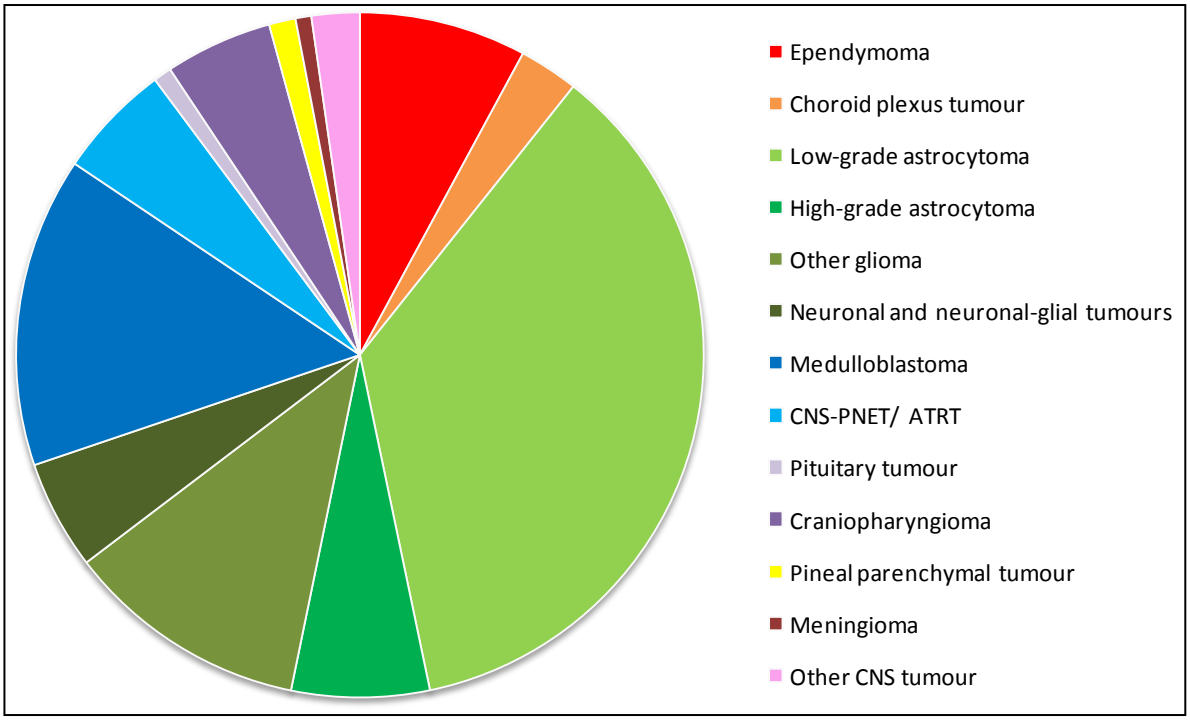

Figure 1.12. The incidence of CNS tumours of childhood. UK Children's Cancer registration data 1999-2008 (CCLG 2010).

	I	II	III	IV
Astrocytic tumours				
Subependymal giant cell astrocytoma	•			
Pilocytic astrocytoma	•			
Pilomyxoid astrocytoma		•		
Diffuse astrocytoma		•		
Pleomorphic xanthoastrocytoma		•		
Anaplastic astrocytoma			•	
Glioblastoma				•
Giant cell glioblastoma				•
Gliosarcoma				•
Oligodendroglial tumours				
Oligodendroglioma		•		
Anaplastic oligodendroglioma			•	
Oligoastrocytic tumours				
Oligoastrocytoma		•		
Anaplastic oligoastrocytoma			•	
Ependymal tumours				
Subependymoma	•			
Myxopapillary ependymoma	•			
Ependymoma		•		
Anaplastic ependymoma			•	
Choroid plexus tumours				
Choroid plexus papilloma	•			
Atypical choroid plexus papilloma		•		
Choroid plexus carcinoma			•	
Other neuroepithelial tumours				
Angiocentric glioma	•			
Chordoid glioma of the third ventricle		•		
Neuronal and mixed neuronal-glial tumours				
Gangliocytoma	•			
Ganglioglioma	•			
Anaplastic ganglioglioma			•	
Desmoplastic infantile astrocytoma and ganglioglioma	•			
Dysembryoplastic neuroepithelial tumour	•			

	I	II	III	IV
Central neurocytoma		•		
Extraventricular neurocytoma		•		
Cerebellar liponeurocytoma		•		
Paraganglioma of the spinal cord	•			
Papillary glioneuronal tumour	•			
Rosette-forming glioneuronal tumour of the fourth ventricle	•			
Pineal tumours				
Pineocytoma	•			
Pineal parenchymal tumour of intermediate differentiation		•	•	
Pineoblastoma				•
Papillary tumour of the pineal region		•	•	
Embryonal tumours				
Medulloblastoma				•
CNS primitive neuroectodermal tumour (PNET)				•
Atypical teratoid / rhabdoid tumour				•
Tumours of the cranial and paraspinal nerves				
Schwannoma	•			
Neurofibroma	•			
Perineurioma	•	•	•	
Malignant peripheral nerve sheath tumour (MPNST)		•	•	•
Meningeal tumours				
Meningioma	•			
Atypical meningioma		•		
Anaplastic / malignant meningioma			•	
Haemangiopericytoma		•		
Anaplastic haemangiopericytoma			•	
Haemangioblastoma	•			
Tumours of the sellar region				
Craniopharyngioma	•			
Granular cell tumour of the neurohypophysis	•			
Pituicytoma	•			
Spindle cell oncocytoma of the adenohypophysis	•			

Table 1.5. WHO Central Nervous System tumour classification. Tumours graded from benign to malignant (I to IV). Reproduced from (Louis, Ohgaki et al. 2007).

1.3.3 CNS Embryonal tumours

CNS embryonal tumours comprise a group of 5 highly aggressive, WHO grade IV tumours including medulloblastomas, atypical teratoid rhabdoid tumours (ATRT), medulloepitheliomas, ependymoblastomas and CNS-PNETs. The clinical features of these tumours are summarised in Table 1.6. The most common embryonal tumour is the medulloblastoma which arises in the cerebellum particularly in children (mean age 7 years) and accounts for a fifth of all brain tumours in childhood. The remaining 4 forms of embryonal tumours are comparatively uncommon and in total account for less than 5% of childhood brain tumours.

Recently, a new diagnostic category of "embryonal tumour with multilayered rosettes (ETMR) has been suggested to replace the ependymoblastoma sub-group (Paulus and Kleihues 2010), but this does not form part of the current WHO classification. Originally described by Eberhart et al in 2000, microscopically these tumours share classic features including ependymoblastic rosettes and neuronal differentiation and therefore have also been referred to as "embryonal tumours with abundant neuropil and true rosettes, (ETANTR)" (Eberhart, Brat et al. 2000; La Spina, Pizzolitto et al. 2006; Dunham, Sugo et al. 2007). Interestingly these tumours appear to only occur in young children and are associated with a poor outcome and with a focal amplification at 19q13.42 (Li, Lee et al. 2009; Pfister, Remke et al. 2009; Korshunov, Remke et al. 2010). It has been suggested that this amplification could be used as a genetic marker in clinical practice to augment the histopathological diagnosis, and promisingly describes for the first time a distinct biological entity within the CNS-PNET group (Korshunov, Remke et al. 2010).

	Medulloblastoma	CNS-PNET*	ATRT	Medulloepithelioma	Ependymoblastoma
Incidence	95%	1-2%	1-2%	<1%	<1%
Age	70% <16 years Mean: 7 years	80% < 10 years Mean: 5.5 years	94% < 5 years Mean: 17 months	< 5 years	< 5 years
Location	Cerebellum	Cerebrum, Suprasellar	Posterior fossa (52%) Supratentorial (40%) Pineal, Spinal	Periventricular Cerebral hemisphere	Supratentorial, Intraparenchymal
Histopathology	Undifferentiated cells ± neuronal/ glial differentiation 5 sub-types	Undifferentiated cells ± neuronal/ glial differentiation	Rhabdoid cells PNET, glial, epithelial and mesenchymal components	Resembles embryonic neural tube	Multilayered ependymoblastic rosettes
Immunohistochemistry	Synaptophysin + Vimentin + GFAP / NF ± INI1 +	Synaptophysin + GFAP / NF ± INI1 +	EMA and Vimentin + SMA, CK, GFAP, NF ± INI1 negative	Nestin and vimentin + INI1 +	Vimentin + GFAP, S100 negative EMA, NF negative INI1 +
Outcome	50-70% (5yr OS)	34% (5 year OS)	Mean: 1 year (<20%)	6 months - 1 year	6 months - 1 year

Table 1.6. Comparative profile of the clinical characteristics of CNS embryonal tumours. Five embryonal tumour/ PNET variants identified. CNS-PNET, central nervous system primitive neuroectodermal tumour; ATRT, atypical teratoid rhabdoid tumour; GFAP, glial fibrillary acidic protein; NF, neurofilament; EMA, epithelial membrane antigen; SMA, smooth muscle actin; CK, cytokeratin; wnt, wingless. Figure is adapted from (Sarkar, Deb et al. 2005), *updated using the current 2007 WHO classification (Louis, Ohgaki et al. 2007) with the term CNS-PNET replacing supratentorial PNET (SPNET) and the classification of pineoblastomas as a separate entity and not an CNS embryonal tumour.

1.3.4 The "PNET" concept and controversy

Embryonal primitive neuroectodermal tumours of the CNS have historically been classified using a plethora of terms based upon their histopathological characteristics. This has resulted in considerable controversy which persists today and affects contemporary management of these tumours.

Until 1837, these tumours were simply referred to as sarcomas after which time they were given a variety of names including spongioblastoma, neuroblastoma malignum, neurogliocytome embryonaire and medulloblastoma (Tola 1951). In 1925 Bailey and Cushing, as reviewed in Rorke et al 1997, named the undifferentiated ectodermal cells from which the tumours were considered to have arisen "medulloblasts", and the resultant tumour a "medulloblastoma cerebelli" (Rorke, Trojanowski et al. 1997). It was however noticed at this time that whilst most of the tumours arose in the posterior fossa around the fourth ventricle that they occasionally occurred in the cerebral hemispheres, and therefore the term "medulloblastoma cerebri" was later applied to these tumours.

Following a review of CNS tumours, in 1973 Hart and Earle established for the first time the term "primitive neuroectodermal tumour" (PNET), but applied this diagnostic category to cerebral neuroepithelial tumours only and specifically excluded pineal and cerebellar tumours (Hart and Earle 1973). The PNET diagnostic category was later adapted and expanded to include all poorly differentiated embryonal neuroepithelial tumours wherever they arose in the CNS, and the concept of the "PNET family" of tumours was established (Becker and Hinton 1983; Rorke 1983). The hypothesis that these histopathologically similar tumours may arise from a common precursor, and therefore would benefit from similar treatment approached, in turn facilitated the development of unifying "PNET" treatment strategies.

Pineoblastomas were later removed from the PNET family in the 2nd WHO CNS tumour classification (Kleihues, Burger et al. 1993) and co-classified with other pineal tumours, although they continued to be often included in studies with other non-cerebellar PNETs, and referred to as supratentorial PNETs (SPNETs). A discordance in outcome (as

will be discussed in 1.4.5.6) along with emerging molecular studies which suggest alternative origins for medulloblastomas and SPNETs has resulted more recently in further controversy of the "PNET" concept (Marino, Vooijs et al. 2000; Pomeroy, Tamayo et al. 2002; Pfister, Remke et al. 2007). In the current 4th edition of the WHO classification of CNS tumours therefore a new term "CNS PNET" was derived to apply to PNETs of the CNS that do not arise in the cerebellum (medulloblastoma) or in the pineal gland (pineoblastoma)(Louis, Ohgaki et al. 2007). This diagnostic category replaced the term "supratentorial PNET" or "SPNET" used in previous classifications and importantly included non-cerebellar and non-pineal PNETs located not only in the supratentorial compartment but also those that occur, albeit rarely, in the brain stem and spinal cord. Medulloblastomas in this classification are not considered PNETs at all, but represent a separate and distinct diagnostic entity.

The investigation and management of CNS-PNETs for over 30 years has been directed and moulded by advancements made predominantly in medulloblastoma as a result of the PNET concept. The suggestion that this hypothesis should be rejected and CNS-PNETs investigated and treated as a distinct entity provides a pivotal challenge: if not part of the medulloblastoma family of tumours, then what are these tumours and how should they best be treated?

1.4 CNS-PNET

1.4.1 Epidemiology

CNS-PNETs are the second most common CNS embryonal tumour and account for 2-3% of all paediatric brain tumours (Bruno, Rorke et al. 1981; Gaffney, Sloane et al. 1985; Dai, Backstrom et al. 2003). It is a disease of early childhood with a mean age of incidence of 5.5 years, and two-thirds of all CNS-PNETs occurring before the age of 5 (Jakacki, Zeltzer et al. 1995; Louis, Ohgaki et al. 2007). CNS-PNETs rarely arise in adulthood. A review in 2008 found only 57 reported cases worldwide of supratentorial PNETs in adults (Ohba, Yoshida et al. 2008).

1.4.2 Presentation features

Most frequently CNS-PNETs affect the frontal, temporal or parietal lobes of the cerebral cortex, however these tumours may also arise rarely in the suprasellar region. The presentation signs and symptoms that a patient presents with depends both on the site of the tumour and the age of the patient. Typically the child will present with non-specific symptoms as a result of the mass effect of their tumour and subsequent raised intracranial pressure (RICP) (Ashwal, Hinshaw et al. 1984). Such non-specific symptoms include headache, dizziness, nausea, vomiting, blurred vision, somnolence, seizures, weakness and occasionally hemiparesis (Behdad and Perry 2010). These tumours are particularly common in very young children who may therefore not be able to verbalise their symptoms. Vomiting, seizures and irritability were the most common presenting features of thirteen children under the age of 3 years who were diagnosed with a SPNET between 1986 and 1990 as part of a larger POG 8633 trial (Dai, Backstrom et al. 2003). Focal motor deficits were noted in 46% and in a quarter of patients an increased head circumference was noted. This latter sign is specific to the infants as it requires the skull bone plates to have non-ossified malleable cartilaginous connections which permit expansion of the cranium. Presentation features are

therefore characteristically non-specific and similar to those reported in other supratentorial tumours (Wilne, Collier et al. 2007).

1.4.3 Diagnostic investigations

1.4.3.1 Neuroimaging

MRI of the neuroaxis including the spinal cord is performed pre-operatively to avoid post-operative artefacts including subdural collections and contrast leakage into the subarachnoid and dural spaces from being misinterpreted as evidence of disease dissemination (Wiener, Boyko et al. 1990; Shaw, Weinberger et al. 1996). MRI scanning, as shown in Figure 1.13, reveal these tumours to be typically large, over 40% greater than 6cm in diameter at diagnosis (Albright, Wisoff et al. 1995) with heterogenous signals on both T1 and T2 weighted images due to the variable presence of calcification, cystic change and blood within the CNS-PNET tumour mass. Compared with glial tumours CNS-PNETs are typically hyperintense on diffusion weighted images (DWI), and fluid-attenuated inversion recovery (FLAIR) sequences may be used to differentiate necrotic areas (hyperintense) from cystic regions (hypointense). Whilst obstruction of CSF pathways resulting in hydrocephalus is a common finding, the presence of peritumoural oedema is typically absent (Dai, Backstrom et al. 2003). In accordance with other intracranial tumours, CNS-PNETs have been shown to exhibit high choline and low N-acetyl aspartate (NAA) on MR spectroscopy (MRS)(Chawla, Emmanuel et al. 2007).

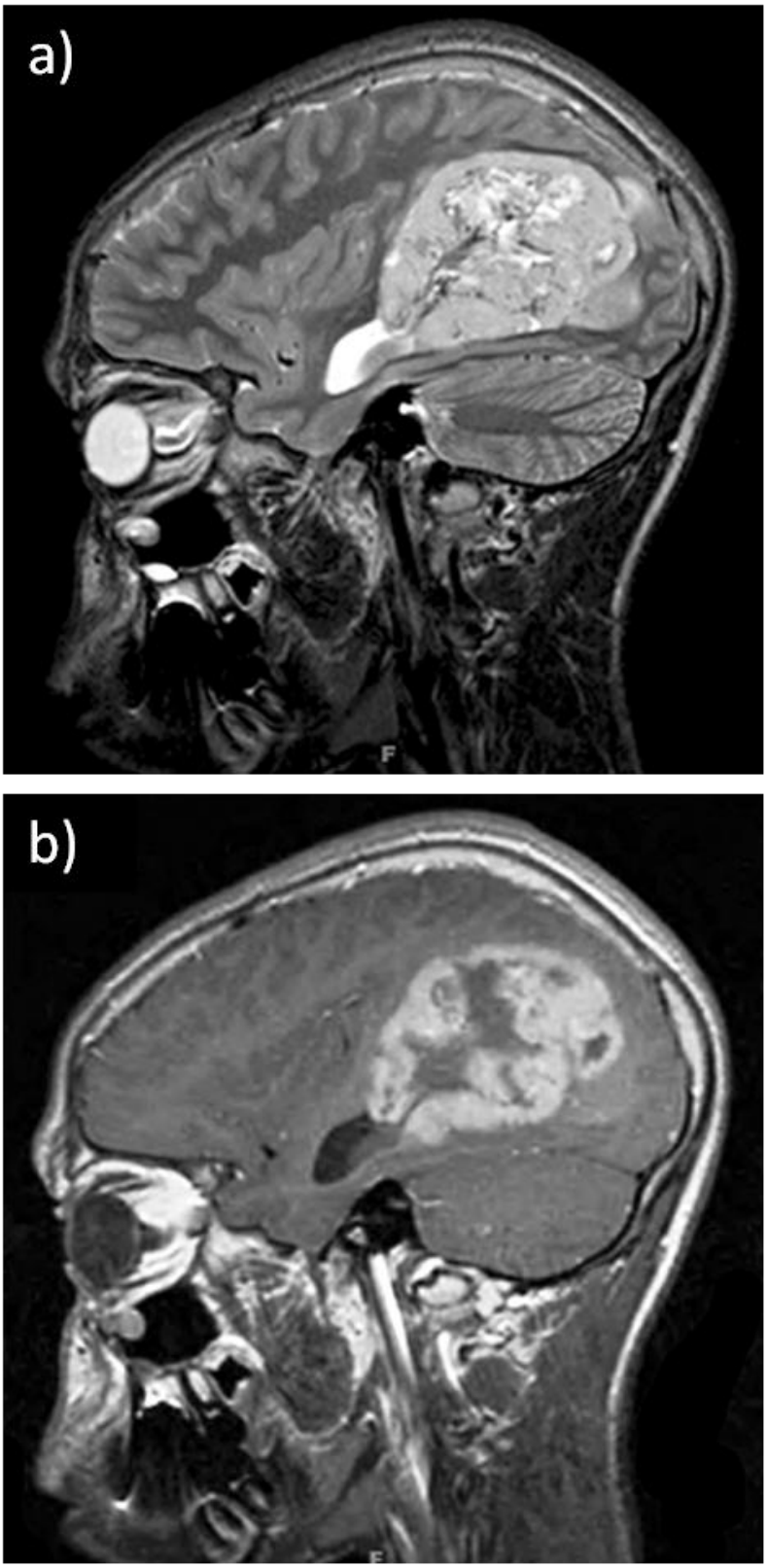

Figure 1.13. Saggital section magnetic resonance images (MRI) of a supratentorial CNS-PNET. (a) T2-weighted image showing a large heterogenous cerebral mass, (b) areas of hypodensity on T1-weighted imaging suggestive of necrosis within the tumor. Figure adapted from (Behdad and Perry 2010).

1.4.3.2 Neurohistopathology

CNS-PNETs, as described in the current WHO 2007 classification of CNS tumours (Louis, Ohgaki et al. 2007) appear as undifferentiated or poorly differentiated highly aggressive tumours composed of mitotically active cells, resulting in the proliferation index Ki67 antibody staining characteristically intensively, with high nuclear to cytoplasmic ratios. The nuclei are typically large and round although in some tumours the nuclei may be oval or elongated in shape. Homer-Wright rosettes (Figure 1.14) may also be present. The tumour cells may exhibit differentiation along neuronal, astrocytic, muscular or melanocytic lines. Neuronal markers such as synaptophysin and neurofilament are therefore characteristically positive, and markers such as glial fibrillary acidic protein (GFAP) may also be positive depending on the degree of astrocytic differentiation (Figure 1.15).

The diagnosis of a CNS-PNET frequently poses a diagnostic challenge for the neuropathologist. Depending on the degree of differentiation these tumours may resemble other brain tumours. In the SIOP PNET3 study, for example, 12% of CNS-PNET diagnoses were not confirmed at central pathological review and the diagnoses in these 6 patients changed to include anaplastic astrocytoma, atypical teratoid rhabdoid tumour (ATRT), anaplastic oligodendroglioma and anaplastic ependymoma (Pizer, Weston et al. 2006). Haberler *et al* have also reported a subset of previously diagnosed CNS-PNETs that were subsequently shown to have loss of INI1 nuclear expression (Haberler, Laggner et al. 2006). Whilst these tumours lacked the classical rhabdoid features of ATRT their aggressive phenotype and adverse outcome suggested that they should be reclassified as ATRT. Immunohistochemical testing for INI1, retained in CNS-PNETs and absent in ATRTs, now forms part of the mandatory diagnostic work up of these and all “PNET” tumours.

In the recently proposed ETANTR subgroup of CNS-PNETs (see section 1.3.3) primitive ependymoblastoma-like and Homer-Wright rosettes constructed of primitive hyperchromatic neurocytic cells and embedded within abundant neuropil are

prominent (Figure 1.16). CD99 staining also shows a characteristic dot-like pattern within the apical aspect of the rosette primitive cells (Dunham, Sugo et al. 2007).

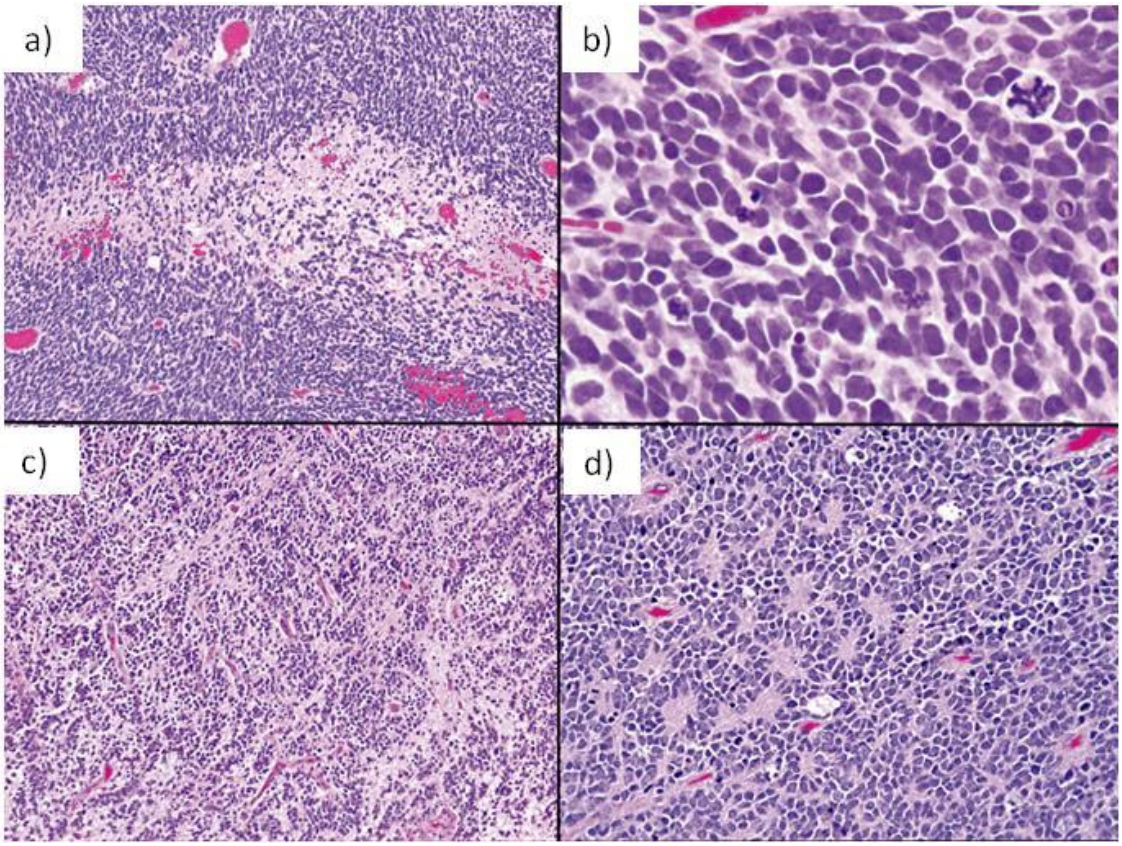

Figure 1.14. Classical CNS-PNET histopathological appearances. On haematoxylin and eosin staining (a) Hypercellularity with patchy necrosis is seen at low magnification (100x), (b) at higher magnification characteristic oval to carrot-shaped hyperchromatic nuclei with minimal cytoplasm is seen (400x). (c). Tumour-associated neuropil may be seen in a delicate fibrillary matrix (100x), (d) formation of Homer Wright neuroblastic rosettes (200x). Figure adapted from (Behdad and Perry 2010), no scale given in original paper, magnifications quoted are approximations.

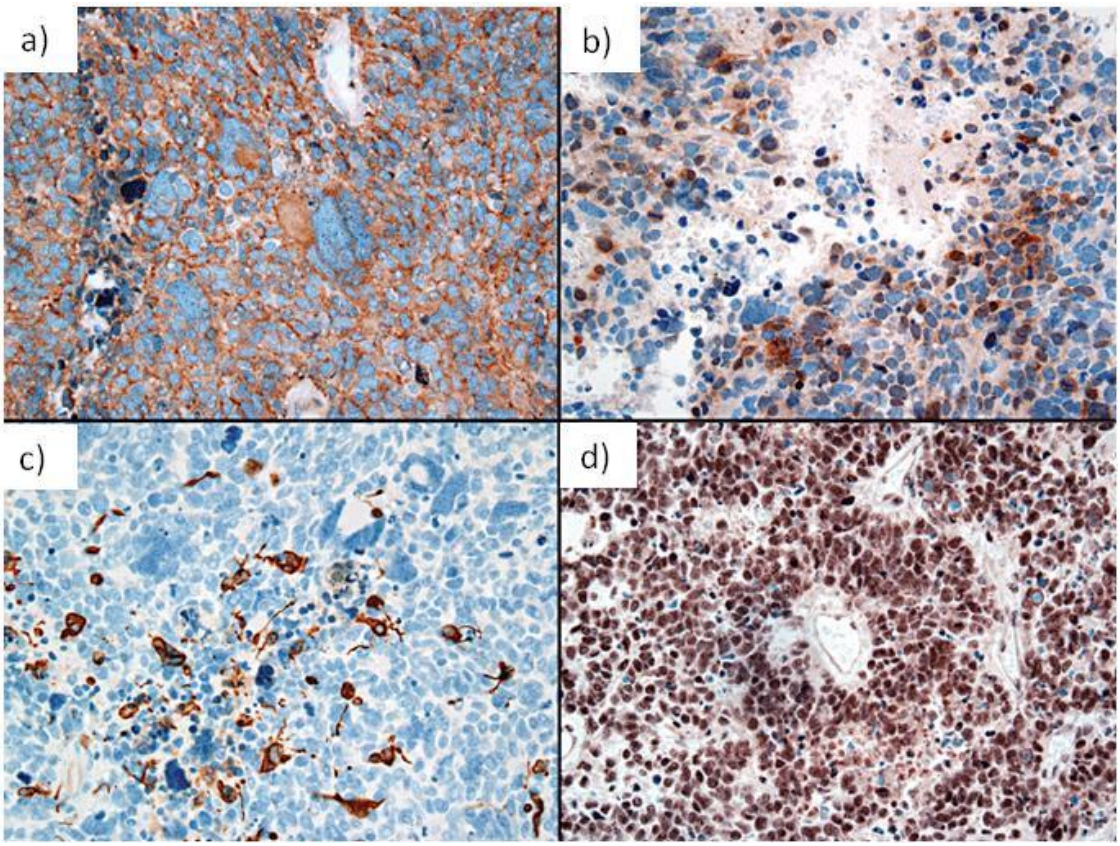

Figure 1.15. Immunohistochemical histopathological features of CNS-PNETs. (a) CNS-PNET with synaptophysin showing widespread presynaptic membranes (200x); (b) CNS-PNET with Neu-N. Neuronal marker showing patch uptake in areas of neuronal differentiation within the tumour (200x); (c) Glial-fibrillary acidic protein (GFAP) positivity in some tumour cells with glial features (200x); (d) retention of INI1 staining in the CNS-PNET, confirming that the tumour is not an atypical teratoid rhabdoid tumour (ATRT) in which this staining would be absent (200x). Figure adapted from (Behdad and Perry 2010), no scale given in original paper, magnifications quoted are approximations.

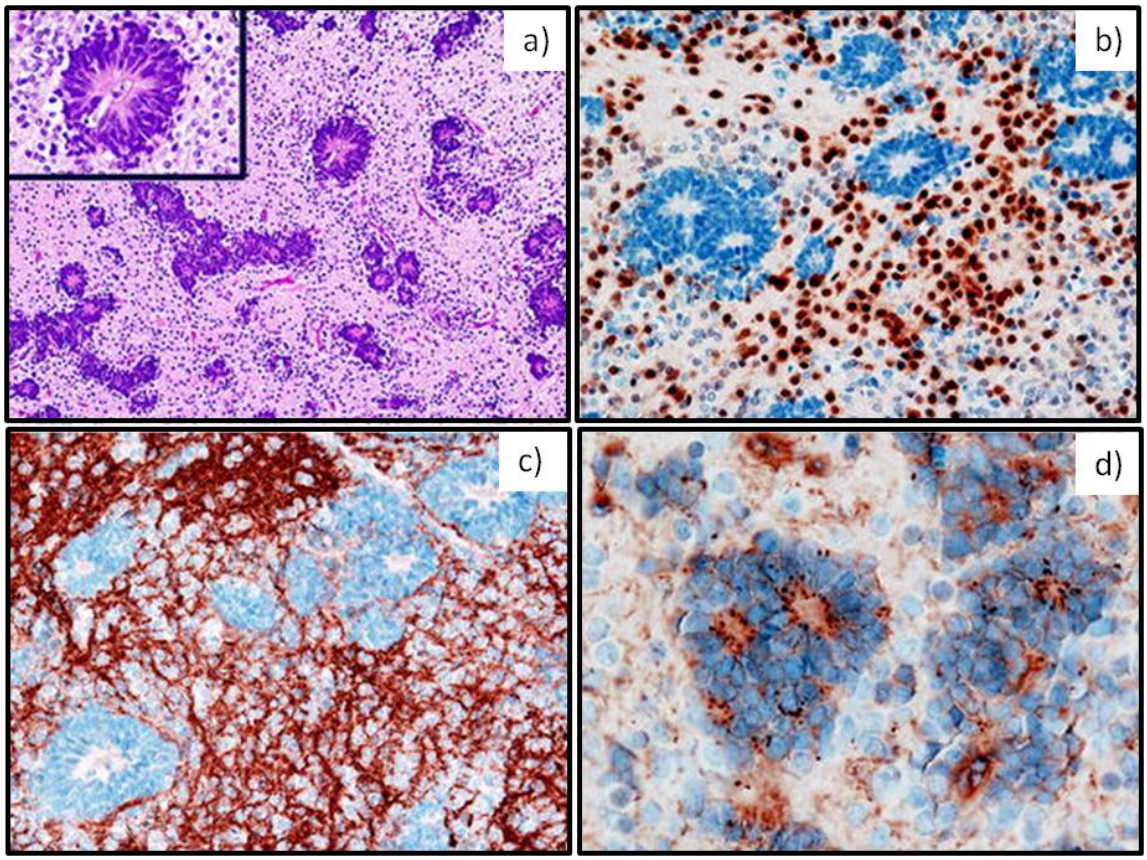

Figure 1.16. Histopathological features of ETANTR. Embryonal tumours with abundant neuropil and true rosettes (ETANTR) (a) show numerous ependymoblastic-like rosettes constructed of neurocytic cells and embedded within abundant neuropil (haematoxylin and eosin (H&E) staining, 200x). Inset shows an ependymoblastic-like rosette at higher magnification (400x). (b) NeuN staining of neurocytic cells (200x). (c) Synaptophysin stain highlighting the tumour cells (200x). (d) With CD99 staining a dot-like positivity can be observed within the apical aspect of the primitive tumour rosette (400x). Figure adapted from (Dunham, Sugo et al. 2007).

1.4.4 Disease risk stratification

There are no molecular or histopathological characteristics that are currently used to stratify CNS-PNET management. Treatment is based on the age of the patient, and is different in younger (age less than 3 years) and older (age greater than 3 years) patients, based on the need to avoid radiotherapy in young children (discussed in further detail in section 1.4.5.3). Staging is assigned using the modified Chang staging system originally designed for staging medulloblastomas which is based on a combination of MRI neuroaxis findings and morphological examination of cerebrospinal fluid (CSF) obtained through a lumbar puncture taken 10-14 days after surgery (Zeltzer, Boyett et al. 1999). In the same way that neuroaxis imaging is performed pre-operatively (section 1.4.3.1) to avoid misinterpretation of post-operative artefacts, delayed CSF sampling is performed to similarly avoid sampling tumour cells that have been deposited in the CSF at the time of surgery and misinterpreting this as evidence of metastasis.

Chang Stage	Classification criteria
M0	No evidence of metastasis
M1	Microscopic evidence of metastasis with tumour cells found in CSF
M2	Metastatic spread beyond the primary site, but remaining within the brain.
M3	Metastatic seeding into the spinal subarachnoid space
M4	Metastasis outside of the CNS

Table 1.7. Chang metastasis staging system. Classification of CNS-PNET metastasis based on the Chang staging system originally devised for medulloblastoma staging. Classification is based on cerebrospinal fluid (CSF) cytological examination and magnetic resonance imaging (MRI) scanning of the central nervous system (CNS) encompassing both brain and spinal cord. Table adapted from (Zeltzer, Boyett et al. 1999).

1.4.5 Treatment

1.4.5.1 Introduction

The management of children with CNS-PNETs requires multimodal therapy incorporating surgery, radiotherapy and chemotherapy as will be discussed in sections 1.4.5.2, 1.4.5.3 and 1.4.5.4 respectively. Currently there are no pathological or biological features that are used in treatment stratification. Age at diagnosis, with infants and young children under the age of 3-5 years depending on the series, remains the only parameter used to determine the treatment strategy. The management strategy employed in the UK currently is outlined in Figure 1.17.

In the UK, children under the age of 3 years are treated using guidelines that apply for children with either infratentorial or supratentorial PNETs. Current treatment requires

assessment of disease extent with MRI neuroaxis imaging and CSF cytology, and upfront surgery to resect as much of the tumour as possible. Following recovery from surgery, children receive 6 cycles of induction high-dose intensive chemotherapy with cyclophosphamide, carboplatin and vincristine with granulocyte colony stimulating factor (GCSF) support. The use of craniospinal radiotherapy after induction chemotherapy is, as will be discussed in 1.4.5.3, controversial but may be offered to some patients before a 6 month course of consolidation chemotherapy comprising 4 cycles of vincrsitine, lomustine (CCNU) and cisplatin ("Packer chemotherapy" (Packer, Sutton et al. 1994)).

For children diagnosed with a CNS-PNET over the age of 3 years in the UK since the discontinuation of the most recent UK CNS-PNET trial (UKCCSG HART SPNET) due to inadequate registration, the approaches used for children with high-risk medulloblastoma are employed. The recommended treatment in the UK follows the Milan approach (Massimino, Gandola et al. 2006) which is summarised in Table 1.8. Treatment involves surgery to remove the bulk of the tumour, followed by sandwich chemotherapy with methotrexate, cyclophosphamide, etoposide and carboplatin. Following recovery from the chemotherapy course the patient receives radiotherapy both to the tumour bed, and also to the entire craniospinal axis. In the UK conventional radiotherapy is used in preference to hyperfractionated accelerated radiotherapy (HART) as used in the Milan study and investigated in the UK HART SPNET study, at conventional doses with 20Gy to the tumour bed and 35Gy to the craniospinal axis that have been used in previous PNET studies (SIOP PNET 4) (Lannering and Kortmann 2004). Treatment is consolidated with 2 courses of high dose chemotherapy with thiotepa and peripheral blood autologous stem cell rescue (AuSCR). A few centres in the UK (personal communication Dr Barry Pizer, CCLG CNS division) may use the St Jude strategy (Chintagumpala, Hassall et al. 2009) which utilises a comparable radiotherapy strategy, does not include sandwich chemotherapy, and uses 4 cycles of cisplatin, cyclophosphamide and vincristine with peripheral blood AuSCR as part of a high dose consolidation strategy. The treatment strategies are summarised in Table 1.8.

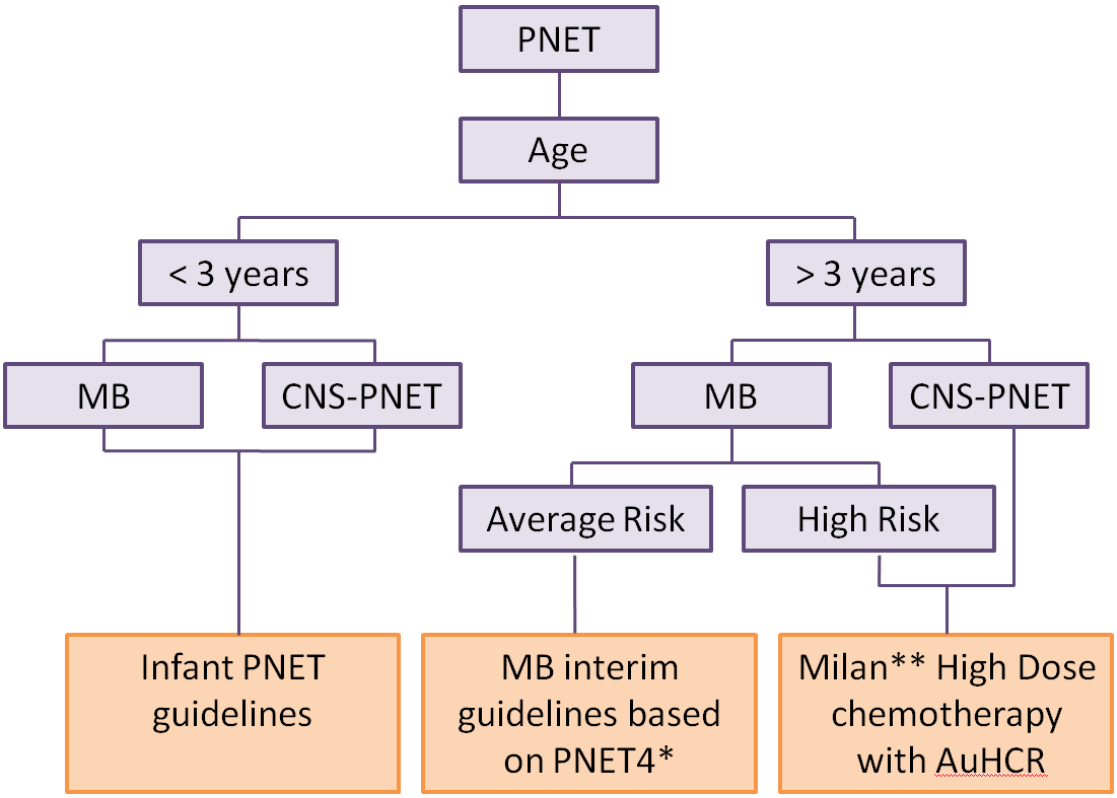

Figure 1.17. Current UK management recommendations for intracranial PNETs. *Average risk medulloblastoma patients treated suing conventional radiotherapy and Packer chemotherapy used in the SIOP/ CCLG PNET4 study. ** The UK CCLG CNS division recommendation for the management of high risk MB and CNS-PNET is to use high dose chemotherapy with autologous haematopoietic stem-cell rescue (AuHCR) as published by the Italian group (Massimino, Gandola et al. 2006)

Protocol	Milan	St Judes	UKCCSG HART SPNET	SIOP PNET4	
Sandwhich chemotherapy	Methotexate 8g/m^2 Etoposide 2.4g/m^2 Cyclophosphamide 4g/m^2 Carboplatin 800mg/m^2	Topotecan (Optional)	No	Weekly Vincristine 1.5mg/m^2 (x 8 doses) prior to, and during radiotherapy	
Radiotherapy	(Start 8 weeks after surgery if recovered from chemotherapy) **HART** 31.2 - 39 Gy CSI with 1.3 Gy fractions bd 21-29 Gy PTB (Max 60 Gy total) with 1.5 Gy fractions bd	(Start within 4-6 weeks from surgery) **Conventional** 36-39.6 Gy CSI PTB (55.8 Gy total)	(Start within 4-6 weeks from surgery) **HART** 39.7Gy CSI 22.3 Gy PTB 1.24 Gy fractions bd	(Start within 4-6 weeks from surgery) Randomisation	
				A **Conventional** 23.4 Gy CSI 30.6 Gy PTB 1.8 Gy fraction od	B **HART** 36 Gy CSI 32 Gy PTB 1 Gy fraction bd
Post-radiotherapy Chemotherapy	2 High dose cycles with PBSCT Thiotepa 300mg/m^2	4 High dose cycles with PBSCT Cisplatin 75mg/m^2 Cyclophosphamide 4g/m^2 Vincristine 1.5mg/m^2	"Packer Chemotherapy" 8 x 6 weekly cycles Lomustine 75mg/m^2 Cisplatin 70mg/m^2 Vincristine 1.5mg/m^2 x3	"Packer Chemotherapy" 8 x 6 weekly cycles Lomustine 75mg/m^2 Cisplatin 70mg/m^2 Vincristine 1.5mg/m^2 x3 doses	

Table 1.8. CNS PNET treatment following surgery in children over the age of 3 years. Protocols: Milan (Massimino, Gandola et al. 2006), St Judes (Chintagumpala, Hassall et al. 2009), UKCCSG HART SPNET (Saran, Taylor et al. 2004) and SIOP PNET 4 (Lannering and Kortmann 2004). Abbreviations: HART: hyperfractionated accelerated radiotherapy; Gy: Gray, od: once daily; bd: bis die (twice daily); CSI: cranial spinal radiotherapy; PTB: primary tumour boost; PBSCT: peripheral blood stem cell transplant. “Packer chemotherapy” as originally described in (Packer, Sutton et al. 1994).

1.4.5.2 Surgery

CNS-PNETs are often located close to the meningeal surface and may become firmly attached. Patients with meningeal involvement at the time of surgery are at a higher risk of developing progressive disease (Jakacki 1999). Gross total surgical resection is possible in only a minority of cases due to the large size of the tumours at presentation and their proximity or involvement of important structures. These tumours may also occur deep within the brain in thalamic, hypothalamic and paraventricular sites, which pose a significant challenge for their safe resection (Dai, Backstrom et al. 2003). It has been shown that with post operative residual disease measuring less than 1.5cm^2 (as judged by post operative imaging) that 4 year survival was 40% (± 22%), compared to 13% (± 8%) if residual tumour measuring more than 1.5cm^2 remains (Albright, Wisoff et al. 1995). The need for complete surgical resection does however remain controversial. In the HIT 88/89 German series patients with an incomplete resection fared as well as those who underwent macroscopically complete resection (Timmermann, Kortmann et al. 2002). Current surgical recommendations are therefore to attempt maximal surgical resection, aiming for a tumour residuum of less than 1.5cm^2, whilst minimising morbidity and mortality.

1.4.5.3 Radiotherapy

CNS-PNETs are radiosensitive tumours. Radiotherapy treatment targeted at the tumour bed is employed following surgery to improve local disease control. In the HIT 88/89 study for example, 60% of patients with a CNS-PNET relapsed, and of these in almost three-quarters (71%) disease recurred at the primary site only (Timmermann, Kortmann et al. 2002). These findings have been subsequently corroborated in the SIOP PNET 3 trial in which local failures occurred in 72% of relapsed patients (23/32) (Pizer, Weston et al. 2006), and in the CCG921 study where a local failure rate of 42% ± 8.5%, twice that seen in medulloblastomas, was reported (Hong, Mehta et al. 2004). These tumours do however also exhibit a propensity for leptomeningeal spread through the subarachnoid space and therefore irradiation of the entire craniospinal

axis (CSRT) in addition to the tumour bed is recommended (Timmermann, Kortmann et al. 2002). In the HIT 88/89 and 91 studies a significant 3year PFS advantage was observed in those receiving CSRT (43.7% v 14.3%, p=0.012) (Timmermann, Kortmann et al. 2002). The dose administered is important with a loss of local control observed with doses less than 54Gy (Hong, Mehta et al. 2004; Jakacki 2005). The use of radiotherapy, as reviewed in Saran 2004, in the treatment of this disease is however, determined by a number of factors including the patient's age, the anatomical location and extent of the tumour, availability of paediatric radiotherapy and allied supporting facilities, as well as patient, parental and physician attitudes towards and assent to treatment (Saran 2004).

Severe neurotoxicity, including profound deterioration in intelligence quotient (IQ) scores, have been shown to result from the use of radiotherapy in infants (Spunberg, Chang et al. 1981; Danoff, Cowchock et al. 1982; Jannoun and Bloom 1990; Mulhern, Kepner et al. 1998). In one large series that followed up 165 children under the age of 3 whose treatment for a brain tumour included radiotherapy found disabling long-term morbidity in 58%, and a poorer neurological outcome for those with supratentorial tumours ($p<0.001$)(Syndikus, Tait et al. 1994). The neurological toxicity observed is in particular related to the extent of white matter loss (Mulhern, Palmer et al. 2001). The use of radiotherapy in infants and very young children for these reasons in contemporary management is limited.

To avoid the devastating neurological consequences of delivering radiotherapy to the CNS of infants, strategies which delay or omit the use of radiotherapy have been developed. The use of intensive induction chemotherapy, as discussed in section 1.4.5.4 has been used in these strategies with some limited success (Marec-Berard, Jouvet et al. 2002; Timmermann, Kortmann et al. 2006).

1.4.5.4 Chemotherapy

The use of adjuvant chemotherapy in CNS-PNET management has arisen through "intracranial PNET" studies involving both medulloblastomas and supratentorial PNETs to eradicate minimal residual disease, and the observation that benefit is derived in those with high risk tumours. Whilst in medulloblastoma chemotherapy strategies have been shown to improve survival (Packer, Sutton et al. 1994; Taylor, Bailey et al. 2003), the effectiveness of a similar regimen in CNS-PNET is uncertain. In the SIOP/CCLG PNET3 trial no benefit was derived in either EFS or OS with the addition of chemotherapy (Pizer, Weston et al. 2006), raising doubt as to the effectiveness of Packer chemotherapy in this disease (Biswas, Burke et al. 2009). High dose chemotherapy has been employed in predominantly limited institutional series in this disease, but its role as discussed in 1.4.5.6, is currently under investigation.

In infants, chemotherapy has been used to delay or avoid the use of radiotherapy and its associated sequelae. In a paediatric oncology group (POG) study, 21 infants under the age of 3 years were treated with 2 cycles of vincristine and cyclophosphamide following surgery which resulted in a complete or partial response in 6 (29%), and stable disease in 9 (43%) (Duffner, Horowitz et al. 1993). Similar findings were observed in the Headstart I + II trials, in which 18/22 (82%) of patients treated with an intensive induction chemotherapy regimen comprising vincristine, etoposide, cyclophosphamide and (in Headstart II) methotrexate achieved a complete or partial response (Fangusaro, Finlay et al. 2008). In a further study, a 5 year EFS of 17 ± 6% was observed in a study of CNS-PNETs treated with surgery and induction chemotherapy only (Geyer, Sposto et al. 2005).

1.4.5.5 Recurrent or refractory disease

If tumours recur they tend to recur early, typically within 2 years of diagnosis. In 1955 Collins et al, proposed "Collins' Law" which states that these tumours recur within "*nine months plus the age at which they were diagnosed"* (Collins, Loeffler et al. 1956).

This has been largely supported in three subsequent studies by Paulino et al, Brown et al, Hong et al which showed that this law was upheld in between 93.3%, and 100% of cases (Brown, Tavare et al. 1995; Paulino and Melian 1999; Hong, Mehta et al. 2005). This law also supports the finding that relapses in younger children occur earlier as well as more frequently. In the largest study of CNS-PNETs (CCG 921) the median time to failure for children under the age of 3 was 0.38 years (range: 0.15 – 1.15 years) compared to 0.9 years (range: 0.4 - 5.8 years) for older children (Hong, Mehta et al. 2005). In the same study treatment failure also occurred earlier in those with metastatic disease (median age of 0.21 versus 0.41 years for those with metastatic and localised disease respectively).

The outcome for children with recurrent CNS-PNET is dismal. High dose chemotherapy has been used in this context, but with limited success. Studies treating patients with high dose chemotherapy for recurrent CNS-PNET have always to date been undertaken in combination with medulloblastomas, as reviewed in (Gajjar and Pizer 2010). High dose carboplatin, etoposide and thiotepa was used in two promising studies from the Memorial Sloan Kettering Cancer centre and Children's Cancer group incorporating 17 supratentorial PNETs including 9 CNS-PNETs (Broniscer, Nicolaides et al. 2004). In only one patient who had received upfront radiotherapy was a second durable remission attained (101 months), whilst in all 4 patients who had not received radiotherapy in first remission were alive at 40-123 months. Other studies however including the UK relapsed PNET and German HIT studies have not replicated these findings, and in total only 4.2% (5/118) patients treated with high dose chemotherapy have become event free survivors (Gajjar and Pizer 2010). In combination this suggests that second remission may be possible in a subgroup who has not received maximal initial therapy with aggressive surgery and radiotherapy, but relapsed patients who have received this as part of their upfront therapy continue to have a very poor outcome.

1.4.5.6 Clinical Studies of CNS-PNET

Recent reported clinical studies of CNS-PNETs are summarised in Table 1.9. These studies include a number of institutional reviews (Mason, Grovas et al. 1998; Yang, Nam et al. 1999; Reddy, Janss et al. 2000; Paulino, Cha et al. 2004; Massimino, Gandola et al. 2006; Chintagumpala, Hassall et al. 2009) in addition to clinical trials (Duffner, Horowitz et al. 1993; Albright, Wisoff et al. 1995; Cohen, Zeltzer et al. 1995; Marec-Berard, Jouvet et al. 2002; Timmermann, Kortmann et al. 2002; Hong, Mehta et al. 2004; Pizer, Weston et al. 2006; Timmermann, Kortmann et al. 2006; Fangusaro, Finlay et al. 2008; Grundy, Wilne et al. 2010). In all cases the reported results of CNS-PNETs were part of a larger study that incorporated previously classified other intracranial PNETs including medulloblastomas or pineoblastomas. The numbers of CNS-PNETs included in individual studies are typically small and the distinction in particular between pineoblastomas and CNS-PNETs historically is not always recorded.

The results for infants are consistently dismal and inferior to those achieved in older patients. The UKCCSG 9204 baby brain study reported a 0% event free survival (EFS) at 1 year (Grundy, Wilne et al. 2010), whilst the POG, Societè Française Oncologie Pèdiatrique (SFOP) and HIT SKK 87+92 studies resulted respectively in only a 19% progression free survival (PFS) at 2 years, 14% overall survival at 5 years, and a 17% PFS at 3 years (Duffner, Horowitz et al. 1993; Marec-Berard, Jouvet et al. 2002; Timmermann, Kortmann et al. 2002). An EFS of 43% at 2 years has been achieved in one study, but this was a single institutional study and included both pineoblastomas and CNS-PNETs and included children up to the age of 5 years (Mason, Grovas et al. 1998). Their approach however of using high dose chemotherapy with AuSCR following tumour resection forms the basis of current treatment in this age group.

In older children, CNS-PNET clinical studies combined with medulloblastomas using surgery, radiotherapy and chemotherapy have been undertaken, but yielded a consistently poorer outcome in those children with a CNS-PNET. In the UK for example, 54 patients with a CNS-PNET were treated on the PNET3 study. An inferior EFS of 41% at 5 years was achieved in this study, compared with 74% at 5 years in children treated

on the same protocol for medulloblastoma (Taylor, Bailey et al. 2003; Pizer, Weston et al. 2006). To date, the best reported results in children over the age of 3 years with CNS-PNET's were derived from a multi-institutional study using cycles of non-myeloablative chemotherapy and autologous stem cell rescue following tumour resection and radiotherapy (Chintagumpala, Hassall et al. 2009). An event free survival at 5 years of 78 ± 14% was reported. In this study, and for the first time patients were stratified as either being of "average" or "high" risk based on the presence of metastatic disease and degree of tumour resection. The craniospinal radiotherapy dose administered to those of average risk was lowered in this study. The 5 year EFS was 75% and 60% respectively for the average and high risk patients, suggesting that a reduction in CSI and its late effects may be achievable in this disease without compromising on survival. The series, however comprised of only 9 CNS-PNET cases and therefore needs to be replicated in a larger multi-institutional cohort.

Trial / series	Enrolment	Tumour	Cases	PFS (%)	Age (years)	Reference
POG	1986-1990	PB + CNS-PNET	36	19 ± 12 @ 2 yr	<3	(Duffner, Horowitz et al. 1993)
CCG 921	1986-1992	CNS-PNET	27	33 @ 3yrs	1.5 -19	(Albright, Wisoff et al. 1995; Cohen, Zeltzer et al. 1995; Hong, Mehta et al. 2004)
Memorial Sloan Kettering Cancer Center Institutional Study	1991-1995	PB	3	43 @ 2yr*	<5	(Mason, Grovas et al. 1998)
		CNS-PNET	11			
Institutional study (Seoul University)	1986-1995	PB	3	38 @ 5 yrs	<17	(Yang, Nam et al. 1999)
		CNS-PNET	25			
Institutional study (CNMC + CHP)	1981-1986	CNS-PNET	9	33 @ 5yrs	3-18	(Reddy, Janss et al. 2000)
HIT 88/89, 91	1988-1998	CNS-PNET	52	34 @ 3yrs	3-18	(Timmermann, Kortmann et al. 2002)
SFOP	1990-1997	PB	4	14 @ 5yrs**	<5	(Marec-Berard, Jouvet et al. 2002)
		CNS-PNET	21			
Institutional study (UoI + LUMC)	1980-2001	PB	7	36 @ 5yrs	1-32	(Paulino, Cha et al. 2004)
		CNS-PNET	18			
PNET3	1992-2000	CNS-PNET	54	41 @ 5 yrs	3 -16	(Pizer, Weston et al. 2006)
Milan	1997	PB	3	54 ± 14 @ 3yrs	3-18	(Massimino, Gandola et al. 2006)
		CNS-PNET	12			
HIT-SKK 87 +92	1987-1997	PB	2	17 @ 3yrs	< 3	(Timmermann, Kortmann et al. 2006)
		CNS-PNET	27			
Headstart I+II	1991-2002	CNS-PNET	30	48 ± 9 @ 5 yrs*	<10	(Fangusaro, Finlay et al. 2008)
Multi institutional study***	1996-2003	CNS-PNET	9	78 ± 14 @ 5yr*	3-21	(Chintagumpala, Hassall et al. 2009)
UKCCSG CNS 9204 (Baby Brain)	1993-2003	PB	3	0 @ 1yr*	<3	(Grundy, Wilne et al. 2010)
		CNS-PNET	8			

Table 1.9. Outcomes from clinical trials and studies of CNS-PNETs. POG, Pediatric Oncology Group; PB, pineoblastoma; CNS-PNET, central nervous system primitive neuroectodermal tumours; CCG, Children's Cancer Group; SFOP, Societè Française Oncologie Pèdiatrique; CNMC, Children's National Medical Center; CHP, Children's hospital of Philadelphia; UoI, University of Iowa; LUMC, Loyola University Medical Center; *event free survival (EFS); **overall survival (OS); ***Texas Children's hospital, USA; Melbourne Royal Children's hospital, Australia; Brisbane Royal Children's Hospital, Australia; St Jude Children's Research Hospital, Memphis, USA.

1.4.5.7 Treatment outcome

Survival from a CNS-PNET remains poor and inferior to that achieved for those with a medulloblastoma. An EFS of 78 ± 14% has been achieved in one pilot study involving children over the age of 3 years (Chintagumpala, Hassall et al. 2009), but larger studies have consistently shown a poorer outcome with a 3 year EFS of 33-54% (Yang, Nam et al. 1999; Reddy, Janss et al. 2000; Timmermann, Kortmann et al. 2002; Paulino, Cha et al. 2004; Massimino, Gandola et al. 2006; Pizer, Weston et al. 2006; Fangusaro, Finlay et al. 2008). The outcome for infants and children under the age of 3 remains bleak with a 3 year EFS of 0 - 19% (Duffner, Horowitz et al. 1993; Timmermann, Kortmann et al. 2006; Grundy, Wilne et al. 2010).

In addition to age, the presence of metastatic disease also affects outcome and may be present in up to a third of cases at diagnosis (Timmermann, Kortmann et al. 2002; Pizer, Weston et al. 2006; Fangusaro, Finlay et al. 2008). Five year EFS has been shown to fall from 64.3% to 36.4% in those with M0 or M1+ disease respectively (Pizer, Weston et al. 2006). Studies of large series of CNS-PNET are however required to investigate this relationship further.

1.4.5.7.1 Long-term therapy associated sequelae

Survival following a childhood brain tumour is known to be associated with a number of adverse sequalae. In a large survey of 342 survivors of childhood brain tumours with 479 sibling controls, survivors were found to be more than ten times less likely to be employed, and almost 30 times less likely to be able to drive a car (Mostow, Byrne et al. 1991). Young age at diagnosis, the use of cranial or CSI radiotherapy and a supratentorial location were all shown to be adverse factors. The association with a poorer outcome in those with a supratentorial compartment tumour has also been replicated in a recent study that followed 120 patients with a brain tumour (aged 2 – 24 years)(Kiehna, Mulhern et al. 2006). Increased cognitive dysfunction was observed in those with supratentorial tumours (p=0.035). Furthermore, tumours arising in the

dominant hemisphere (left sided cortical tumours, in right-handed people) are associated with increased cognitive dysfunction (Hahn, Dunn et al. 2003; Kiehna, Mulhern et al. 2006).

In a recent Childhood Cancer Survivor Study incorporating 818 adult survivors of childhood CNS tumours, radiation doses ≥ 30Gy to the temporal region were associated with a greater propensity for memory impairment, whilst radiotherapy to the frontal lobe was associated with physical performance limitations. (Armstrong, Jain et al. 2010). In addition survivors who had received temporal lobe radiotherapy reported dose dependent higher rates of poor general health and social functioning. Radiotherapy, and in particular CSI in addition to the cognitive and neurological deficits is also associated with hearing loss, neuroendocrine defects including hypothalamic axis, pituitary and thyroid dysfunction, pneumonitis, cardiotoxicity, scoliosis and secondary malignancies.(Schell, McHaney et al. 1989; Holm 1990; Silber, Littman et al. 1990; Constine, Woolf et al. 1993; Jakacki, Zeltzer et al. 1995; Bieri, Sklar et al. 1997; Adams, Lipshultz et al. 2003; Gleeson and Shalet 2004). The risk to benefit balance of the use of RT, particularly CSRT, is therefore the major determinant influencing treatments used in CNS-PNET.

Adjuvant chemotherapy may also cause late effects including peripheral neuropathy following cisplatin and vincristine administration; nephrotoxicity and subfertility following the use of cisplatin or CCNU; deafness with cisplatin; and an increased risk of secondary malignancies, and in particular leukaemias following lomustine (CCNU) or etoposide administration (Skinner, Wallace et al. 2005). Chemotherapy may also potentiate radiation induced defects including cardiac toxicity, growth retardation and hearing loss (Gleeson and Shalet 2004). The reduction of late effects arising from the surgery, radiotherapy, chemotherapy, or in combination therefore remains a key challenge in current management.

1.4.5.8 Emerging therapies

Whilst CNS-PNETs are radiosensitive tumours the late effects derived from the use of radiotherapy has limited its role in treatment strategies, particularly in infants and very young children under the age of 3 years. The use of conformal radiotherapy has enabled a reduction in such toxicities (Saran 2004), but to potentially avoid these risks further, proton beam radiotherapy, which enable radiation to be targeted to the tumour whilst delivering a reduced dose to surrounding normal structures, has been developed (Greco and Wolden 2007). Proton therapy has already become the "gold standard" for some tumours including base of skull chordoma and chondrosarcoma, and its use in paediatric and in particular childhood brain tumours is being investigated (St Clair, Adams et al. 2004; Bouyon-Monteau, Habrand et al. 2010).

The use of ifosfamide and temozolamide in CNS-PNET has been suggested, based on the hypothesis that as some of these tumours show similarities with glioblastoma which benefit from these therapies, a similar beneficial effect may be derived in patients with CNS-PNET (Biswas, Burke et al. 2009). In support of this, Temozolamide has been successfully used in an adult patient with a CNS-PNET (Terheggen, Troost et al. 2007).

1.4.6 CNS-PNET: The clinical challenge

Current therapeutic strategies for CNS-PNETs are derived from adjusted strategies for medulloblastomas based on the historical concept of an intracranial "PNET". These strategies result in a poorer prognosis for patients with CNS-PNET irrespective of disease spread or their age. In addition, survivors of this disease are frequently left with significant toxicities as a result of the treatment which confers further lifelong health and social disadvantages. There is therefore a very clear and urgent need to improve the outcomes for these patients, by improving the treatments they receive. Advancements could be made through the development of molecularly targeted therapies, or through the identification of disease sub-groups which may in turn permit

a stratified therapeutic approach. Both of these approaches have been successfully employed in the treatment of other cancers including the use of the tyrosine kinas inhibitor imatinib mesylate in the management of BCR-ABL chronic myeloid leukaemia(Baccarani, Dreyling et al. 2009), and in the management of childhood acute lymphoblastic leukaemia (ALL) a risk-adapted stratified approach is used based on a combination of clinical and molecular criteria (Moorman, Ensor et al. 2010). The fundamental clinical challenge of improving outcome is however itself restrained by the current poor understanding of the biological mechanisms involved in the development of a CNS-PNET as a result of a paucity of research into this tumour. To address the CNS-PNET challenge a programme of research into these tumours is therefore now required.

1.5 Molecular genetics of CNS-PNET

1.5.1 Introduction

To date, research into the biological basis of CNS-PNET tumorigenesis has been limited, and correspondingly our understanding of the molecular basis for these tumours is poor. Studies into the molecular characterisation specifically of CNS-PNETs, and the discovery of disease distinct events have rarely been undertaken. Insights into the development of these tumours have been derived from tumours developed in children with genetic predisposition syndromes (section 1.5.2), but have predominantly come from larger intracranial PNET studies, which have included only a limited number of CNS-PNETs, and comparison with defects observed in medulloblastomas.

1.5.2 Genetic predisposition to CNS-PNET

1.5.2.1 Introduction

A number of different familial conditions are associated with the development of brain tumours, summarised in Table 1.10. Li Fraumeni syndrome, Turcot syndrome, and Gorlin syndrome however are all associated with the development of intracranial PNETs.

Syndrome	Gene	Chromosome	CNS tumours
Neurofibromatosis type 1	*NF1*	17q11	Neurofibroma MPNST* Optic pathway glioma (OPG) Astrocytoma
Neurofibromatosis type 2	*NF2*	22q12	Bilateral vestibular schwannoma Meningioma Meningioangiomatosis Spinal ependymoma Astrocytoma
Von Hippel-Lindau	*VHL*	3p25	Hemangioblastoma
Tuberous sclerosis	*TSC1* *TSC2*	9p34 16p13	Subependymal giant cell astrocytoma
Li-Fraumeni	*TP53*	17p13	Primitive neuroectodermal tumour Astrocytoma
Turcot	*APC* *hMLH1* *hPSM2*	5q21 3p21 7p22	Medulloblastoma Glioblastoma
Cowden	*PTEN*	10q23	Dysplastic gangliocytoma of the cerebellum (Lhermitte-Duclos)
Gorlin**	*PTCH*	9q31	Medulloblastoma
Rhabdoid tumour predisposition syndrome	*INI1*	22q11.2	Atypical teratoid rhabdoid tumour

Table 1.10. Familial brain tumour predisposition syndromes. *MPNST: Malignant peripheral nerve sheath tumour, ** Gorlin syndrome, is also known as nevoid basal cell carcinoma syndrome (NBCCS). Table adapted from (Louis, Ohgaki et al. 2007)

1.5.2.2 Li Fraumeni Syndrome

Li Fraumeni syndrome (LFS) is an autosomal dominantly inherited disorder characterised by the development of multiple tumours in childhood and in adult life. Tumours that develop may include soft tissue sarcomas, osteosarcomas, breast cancer, leukaemia, adrenocortical tumours and brain tumours (Li, Fraumeni et al. 1988). The incidence of LFS ranges from 1 in 5000, to 1 in 20,000 live births (Lalloo, Varley et al. 2006; Gonzalez, Noltner et al. 2009). LFS families are defined as those where a patient develops a sarcoma before the age of 45 years, a first degree relative develops cancer

before the age of 45, and an additional first degree relative develops a cancer before the age of 45 or a sarcoma at any age (Li, Fraumeni et al. 1988). A Li-Fraumeni like syndrome (LFLS) has also been described where a childhood tumour, brain or adrenocortical tumour occur before the age of 45 in addition to a first or second degree relative developing any cancer before the age of 60 (Hottinger and Khakoo 2009). LFS results from mutation in the *TP53* gene (discussed in detail in section 1.5.5.1) in 70% of cases, whilst mutations in *TP53* (Kleihues, Schauble et al. 1997) are observed in only 20-40% of families with LFLS (Hottinger and Khakoo 2009). 46% of the mutations observed were missense and located at codons frequently mutated "hot-spot" codons in cancer 175, 213, 245, 248, 273, and 282 (Olivier, Goldgar et al. 2003).

Brain tumours occur in 10-15% of people with LFS, typically before the age of 45. The majority of these tumours are gliomas, but in up to a third medulloblastomas and CNS-PNETs develop (Taylor, Mainprize et al. 2000). Unfortunately almost half of all patients who are successfully treated for a cancer will develop a second cancer within 30 years (Birch, Alston et al. 2001). In patients with Li-Fraumeni Syndrome it is therefore recommended that ionising radiation therapy where possible is avoided to reduce the risk of further tumours (Evans, Birch et al. 2006).

1.5.2.3 Turcot syndrome

Turcot syndrome is an autosomal dominantly inherited condition characterised by adenomatous colorectal polyps or colonic carcinomas in addition to brain tumours. There are two forms of Turcot syndrome. In type 1 Turcot syndrome, glioblastomas occur in the presence of germline mutations of mismatch repair genes (*hPMS2*, *hMSH2* or *hMLH1*) or hereditary non-polyposis colorectal carcinoma (HNPCC). In type 2 Turcot syndrome medulloblastomas occur in patients with familial adenomatous polyposis (FAP) or with germ line mutations of *APC* (5q21). The risk of developing a brain tumour with Turcot syndrome is 92 times greater than in the general population (Hamilton, Liu et al. 1995). Turcot syndrome has also been described in children who develop CNS-

PNETs with mutations in germline *PMS2* and *MSH2* described (De Vos, Hayward et al. 2006; Jeans, Frayling et al. 2009).

1.5.2.4 Gorlin syndrome

Gorlin syndrome, or naevoid basal cell carcinoma syndrome (NBCCS) is an autosomal dominant disease characterised by a spectrum of developmental abnormalities and neoplasms, reviewed in (Lo Muzio 2008). It is caused by germline mutations of the *PTCH* gene, located on chromosome 9 (9q22.3) and in the UK affects 1 in 55,000 to 57,000 of the population (Farndon, Del Mastro et al. 1992; Evans, Ladusans et al. 1993). 90% of affected individuals develop multiple skin basal cell carcinomas in early childhood and also keratocysts of the jaw within the first three decades of life (Evans, Ladusans et al. 1993). Palmar and plantar dyskeratoses and congenital abnormalities including macrocephaly, cleft lip and/ or palate, and skeletal defects may also occur.

Within the CNS ectopic calcification and cyst development may occur (Stavrou, Dubovsky et al. 2000). The development of medulloblastoma in young children under the age of 2 years is also a feature of Gorlin syndrome. These tumours have been associated with desmoplasia and the medulloblastoma with extended nodularity (MBEN) subtype and a superior prognosis (Amlashi, Riffaud et al. 2003; Garre, Cama et al. 2009). In addition to the histopathological and prognostic associations, it has been suggested that the identification of patients with Gorlin syndrome may increasingly have a therapeutic significance (Choudry, Patel et al. 2007). Patients with Gorlin syndrome have an increased risk of radiation induced tumours and therefore it may be in the future that the judicious use of radiotherapy in the management of these “less aggressive” medulloblastomas may be warranted (Choudry, Patel et al. 2007).

1.5.3 Cytogenetic abnormalities in CNS-PNET

There have been very few studies to characterize cytogenetic abnormalities in CNS-PNET. As with nearly all genetic studies in this disease, when performed these studies have usually been as a part of an overarching "PNET" characterization study involving medulloblastomas and pineoblastomas, or as part of a paediatric brain tumour study. A series of studies have characterised the karyotype of 23 CNS-PNETs in total, (Chadduck, Boop et al. 1991; Fujii, Hongo et al. 1994; Bhattacharjee, Armstrong et al. 1997; Bigner, McLendon et al. 1997; Burnett, White et al. 1997; Bayani, Zielenska et al. 2000; Roberts, Chumas et al. 2001; Uematsu 2003), as summarised in Table 1.11. The most common abnormalities were found with chromosome 11 in 10/23 (43%) cases. These chromosome 11 cytogenetic abnormalities includes gains (1/23, 4%), losses (3/23, 13%), translocations (4/23, 17%) and other abnormalities (duplications, deletions and gain of additional material) in 4/23 (17%). A gain of chromosome 7 was observed in 4/23 (17%) and loss of chromosome 13 also in 4/23 (17%).

The most common cytogenetic abnormality seen in medulloblastoma is loss of the p-arm of chromosome 17 occurring in up to 40% of tumours (McDonald, Daneshvar et al. 1994; Burnett, White et al. 1997). This may occur in association with a gain of 17q and the formation of an isochromosome (i17q) or may arise as an isolated defect. 17p loss or i17q formation was not found in any of the CNS-PNET cases described, however chromosome 17 loss and a deletion of 17q21.3 were both observed in isolated cases (Bayani, Zielenska et al. 2000; Roberts, Chumas et al. 2001).

In a third of cases (8/23) a normal karyotype was found. Karyotyping may however not detect more subtle cytogenetic alterations, and therefore comparative genomic hybridization (CGH) studies have also been undertaken in a small number of cases. A study by Nicholson et al reported the cytogenetic features by CGH of 4 paediatric CNS-PNETs (Nicholson, Wickramasinghe et al. 2000). In one case no abnormality was detected, but in the other 3 cases a series of genetic losses and gains were observed, including in common with the previous karyotyping studies, frequent gains on chromosome 7 (2/4, 50%). Unfortunately in CGH studies by Russo et al, Avet-Loiseau et

al and Inda et al, involving 18 SPNETs the distinction between pineoblastomas and CNS-PNETs was not made, and therefore these findings cannot reliably be used to characterize CNS-PNET disease (Avet-Loiseau, Venuat et al. 1999; Russo, Pellarin et al. 1999; Inda, Perot et al. 2005).

More recently, three studies (summarised in Table 1.12 and Table 1.13) have interrogated CNS-PNETs by array-CGH, which has provided an enhanced resolution of genetic abnormalities observed in these tumours (Kagawa, Maruno et al. 2006; McCabe, Ichimura et al. 2006; Pfister, Remke et al. 2007). Even with the superior resolution that array CGH provides, in keeping with the previous karyotyping studies in 3 cases (3/20, 15%) no abnormality was observed suggesting that alternative tumourigenic mechanisms (see section 1.2) may be implicated in at least a sub-group in this disease. In total genetic gains were observed in 35% (7/20) involving chromosome 12, 30% (6/20) with chromosome 7q, and 20% (4/20) for both chromosomes 17q and 2p.

Interestingly, in the Pfister series loss of 17p was seen in 2 cases (2/10, 20%), and the region of loss (17p11.2-pter) occurred at the breakpoint similar to that which has been observed in medulloblastomas (Biegel, Janss et al. 1997; Scheurlen, Seranski et al. 1997). This finding was not observed however in either the McCabe et al, or Kagawa et al studies. In a recent large medulloblastoma study 25% (47/190) of medulloblastomas were shown to have loss of 17p (Ellison, Kocat et al. 2011). This finding, (as will be discussed in chapter 3 and summarised in table 3.28) has only rarely been observed in CNS-PNETs, but very limited small studies only have previously been performed and a dedicated study of 17p defects in CNS-PNETs has not previously been undertaken.

Finally, using a high resolution single nucleotide polymorphism (SNP) array on 39 CNS-PNETs, Li et al in common with the previous array CGH studies identified recurrent gains (8/39, 21%) on chromosome 2 incorporating the *MYCN* locus and also a novel amplicon on chromosome 19 (19q13.42) incorporating a micro RNA cluster (8/39, 21%) (Li, Lee et al. 2009). Amplification at this locus was shown to confer an adverse

prognosis (4 +/- 1.3 months in amplified cases versus 44 +/- 12.8 months in non-amplified cases; $p<0.0001$).

Reference	Age (Years)	Karyotype
(Chadduck, Boop et al. 1991)	<1	Normal
	<1	Normal
	<1	Normal
	<1	45, XY,-22
(Fujii, Hongo et al. 1994)	9	Normal
	11	43-44;XY;+2,-6;der(10)t(10;11)(q26;q21),del(11)(q21,-12,-13=mar,(8)/84/90,XXYY,der(10)t(10;11)(q26:21),der(10;11)(q26:q21),del(11)(q21),+2mar/(8)
	14	Normal
(Bhattacharjee, Armstrong et al. 1997)		46,XY,i(1)(q10);-9,t(9;11)(q34;q13)<8?/90; idemx2, -X,Y1/46;XY
(Bigner, McLendon et al. 1997)	2	46,XY,t(6:9)(q21;q13),del(10)(q22)2/34. idem, t(11;13)(q15;q11)-13
		Normal
		Normal
		Normal
(Burnett, White et al. 1997)	7	49,XX,add(3)(q23 or q24),+5,+8,dup(11)(q12q22.3 or q13q23),del(16)(q22q24),add(19)(p13),+21[8]/49.idem,add(13)(q34[1]
	16*	90,XX,add(X)(p22)x2,dic(1;9)(q42;p21)x2,dic(4;9)(q3?5;p2?2),6,add(6)(p24),9,add(11)(p15)x2,add(16)(q2?2),+mar1,+mar2[11]
(Bayani, Zielenska et al. 2000)	3	70-103 chromosomes, dmins and double rings
	3	55-75,XX,-X,del(1)(p22),i(4)(p10),-5,+6,+add(7)(q36),add(9)(p21),-11,-13,-17,add(18)(q23),-19,-19,+13mars+dmins
	4	46,X,?rea(X),?rea(10p),?rea(14q),add(19q),+?add(22q),22q
	6	46,XY,t(6;13)(q25;q14)
(Roberts, Chumas et al. 2001)		46,XX,del(2)(p22.2-2p23.1),del(5)(q33-q35)/46,idem,del(17)(q21.3q21.3)
		der(9:15)(q10;q10)x2,+11,+13,+18,+20,+56-59,Xc,+X<+1,+1,+1,add(1)(p?),add(1)(q?),+2,del(2)(p24),+7,+8,add(8)(q?)
		69~75XX,-X,add(10(q42)x2,-4,-4,add(4)(q3?),-10,-11,del(11)(q2?),-13,-16,-18,+7~13mar,dmin(cp7)dmins
(Uematsu, Takehara et al. 2002)	7	52,XX,+1x2,add(3)(q25)+7x2,add(11)(q25)x2,+21x2

Table 1.11. Reported karyotypes of CNS-PNETs. Karyotypes described using International System for Cytogenetic Nomenclature (ISCN) 1995 (Mitelman 1995), * relapse tumour sample.

Reference	Case	Age (years)	Gain	Loss
(Kagawa, Maruno et al. 2006)	1	<1	*MSH2* (2p22.3-p22.1), *ERBB2* (17q11.2-q12), *BCR* (22q11.23)	(none)
	2	2	Ch 7, *MYCN* (2p24.1), *MSH3* (5q11.2-q13.2), *EGFR* (7p12.3-p12.1), *RFC2* (7q11.23), *PTCH* (9q22.3), *DMBT1* (10q25.3-q26.1), *GLI* (12q13.2-q13.3), *ERBB2* (17q11.2-q12) , *TK1* (17q23.2-q25.3), *STK6* (20q13.2-q13.3)	Chr 6q, *MSH2* (2p22.3-p22.1)
	3	3	*MSH2* (2p22.3-p22.1), *EGFR* (7p12.3-p12.1), *RFC2* (7q11.23), *DBCCR1* (9q33.2), *CDK2* & *ERBB3* (12q13), *BRCA1* (17q21), *STK6* (20q13.2-q13.3)	*APC* (5q21-q22), *SNRPN* (15q12), *HRAS* (11p15.5), *GLI* (12q13.2-q13.3)
(McCabe, Ichimura et al. 2006)	4	-	*FIP1L1-CHIC2* (4q12)	13q14.11qter
	5	-	*FOXQ1-FOXF2* (6p25.3), *ALDH8A1-MYB* (6q23.3), *PHACTR2-SF3B5* (6q24.2)	*RASA3* (13q34)
	6	-	*CACNG8-LILRB5* (19q13.42)	*RASA3* (13q34)
	7	-	(none)	Chr 13q
	8	-	(none)	*CDKN2A/CDKN2B* (9p21.3)
	9	-	(none)	(none)
	10	-	(none)	(none)
(Pfister, Remke et al. 2007)	11	1	(none)	(none)
	12	1	*ADAM8* (10q26.3)	(none)
	13	2	*UNC5B/CDH23* (10q22.1)	(none)
	14	3	*PRDM16* (1p36.32), *CNTNAP2* (7q35), *NOS3* (7q36.1), *URP2* (11q13.1), *DACH1* (13q22), *TNFRSF6B* (20q13.33)	*UNC5C* (4q22.3)
	15	3	*TNFRSF6B* (20q13.33)	*AJAP* (1p36.13), *IGSF21* (1p36.13), *GRM2* (3p21.1), *TAF6L/HRASLS3* (11q13)
	16	6	*TMEM/MGC33556* (1p34.1), *MM-1* (12q13.13), NULL (12q23)	NULL (1q31.1), *UNC5C* (4q22.3), *GPR116* (6p12.3)
	17	7	*RHOB* (2p24.1), *MAP3K7* (6q16), *MM-1* (12q13.13), NULL (12q23), *DACH1* (13q22)	AJAP (1p36.13), IGSF21 (1p36.13), *HRG* (3q27.3), *DOK7* (4p16.2), *DUSP8* (11p15.5), *RHOG* (11p15.4), *JAM3* (11q25)
	18	7	*CNTNAP2* (7q35), *NOS3* (7q36.1)	*GPR116* (6p12.3), *MED4* (13q14.2)
	19	11	*LMO1/STK33* (11p15.4)	*MGMT* (10q26.3), *DUSP8* (11p15.5), *RHOG* (11p15.4), *TAF6L/HRASLS3* (11q13), *GRM5* (11q14.2), *JAM3* (11q25)
	20	12	*IGFB2/5* (2q35), *TNFRSF6B* (20q13.33), *PDGFB* (22q13.1)	*MED4* (13q14.2)

Table 1.12. Losses and gains in CNS-PNET tumour samples by array CGH. Genes names in italics: www.ensembl.org/Homo_sapiens. NULL: Gene unspecified. Regions of gains or losses <3MB only are shown for cases 11-20 from the Pfister et al study.

Chromosome	Loss or Gain	Number	Frequency (%)
13q	Gain	5	25
20q	Loss	5	25
2p	Gain	4	20
7q	Gain	4	20
12q	Gain	4	20
10q	Gain	3	15
11p	Loss	3	15
11q	Loss	3	15
17q	Gain	3	15

Table 1.13. Summary of the most frequent chromosomal abnormailities by array CGH in CNS-PNETs. The most frequent nine abnormalities observed in 20 CNS-PNETs investigated by array CGH in three studies (Kagawa, Maruno et al 2006; McCabe, Ichimura et al 2006; and Pfister, Remke et al 2007).

1.5.3.1 19q13.42 amplification and ETMR

In 2009, Pfister et al reported the results of an array CGH performed on the tumour sample taken from a 2 year old girl with a CNS-PNET(Pfister, Remke et al. 2009). An amplification at 19q13.42 was detected which has been subsequently been identified from two further studies in an additional 48 cases (Li, Lee et al. 2009; Korshunov, Remke et al. 2010). This amplification appears to be specific to CNS-PNETs, and did not occur in an additional 300 paediatric brain tumours screened for this amplicon (Korshunov, Remke et al. 2010). The histopathological feature of the original case and 72% (8/11) of the Li et al, series were consistent with the proposed embryonal tumour with multilayered rosettes (ETMR) subtype (see section 1.3.3), whilst all of the tumours investigated by Korshunov et al, were of the ETMR subtype, and the 19q13.42 amplicon was present in 93% (37/40). In addition to the histopathological correlation, these tumours also appear to occur in children under the age of 3 and associated with an inferior outcome compared with other children with CNS-PNETs.

1.5.4 Gene specific defects in CNS-PNET

The development of CNS-PNETs in those with cancer predisposition syndromes has suggested a role of a number of cell signalling pathways, including wnt/wingless, p53, sonic hedgehog and Notch, in CNS-PNET tumorigenesis. Aberrations of components of these pathways have subsequently been shown to be implicated in this disease, as is discussed in section 1.5.5. Cytogenetic studies, as discussed in section 1.5.3, have also identified a number of loci associated with CNS-PNET development including *CDKN2A* (section 1.5.5.1) and the *MYCC* and *MYCN* (section 1.5.4.1).

1.5.4.1 *MYC* family genes

The *MYC* family of oncogenes comprises 3 genes (*MYCN*, *MYCC* and *MYCL*) which are involved in cell growth, proliferation, differentiation and apoptosis (Pelengaris, Khan et

al. 2002). In humans *MYCC, MYCN* and *MYCL* are mapped to 8q24.1, 2p24 and 1p34 respectively, and have similar gene structures (Ryan and Birnie 1996).

1.5.4.1.1 The functional role of MYC

The *MYC* genes are essential for normal development. In murine models knockdown of either *c-myc* or *n-myc* is lethal within 10.5 and 12.5 days respectively (Charron, Malynn et al. 1992; Davis, Wims et al. 1993). Germ-line mutation and deletions of *MYCN* have also been shown to be associated with a number of developmental defects including oesophageal atresia, duodenal atresia, congenital cardiac defects, macrocephaly and learning difficulties as part of Feingold syndrome (FES) (van Bokhoven, Celli et al. 2005).

In cancer, MYC is implicated in promoting cell growth, vasculogenesis, reducing cell adhesion, increasing genomic instability and promoting metastasis (summarised in Figure 1.18) (Adhikary and Eilers 2005; Vita and Henriksson 2006). Cell growth is promoted through the role of MYC enabling G0/1 to S phase cell cycle progression (Meyer and Penn 2008). MYC messenger RNA (mRNA) and protein levels increase during cellular proliferation, but are absent in differentiated quiescent cells. Sustained up-regulation of MYC expression conversely has been shown to be associated with an inhibition of cellular differentiation and the promotion of tumour development including tumours that resemble human PNETs (Su, Gopalakrishnan et al. 2006). Genomic instability has been shown to result from up-regulated MYC expression (Mai, Hanley-Hyde et al. 1996), occurring through a variety of mechanisms including alteration in chromosomal structure, the promotion of DNA strand breaks with increased levels of reactive oxygen species, and bypassing the p53 checkpoint through repression of p53 (Prochownik and Li 2007). The role of MYC in angiogenesis has also been demonstrated in cell line and murine models (Ngo, Gee et al. 2000; Prochownik and Li 2007). In addition to its effect on growth, MYC family members may also promote apoptosis through p53 dependent and independent pathways (Prochownik and Li 2007; Meyer and Penn 2008).

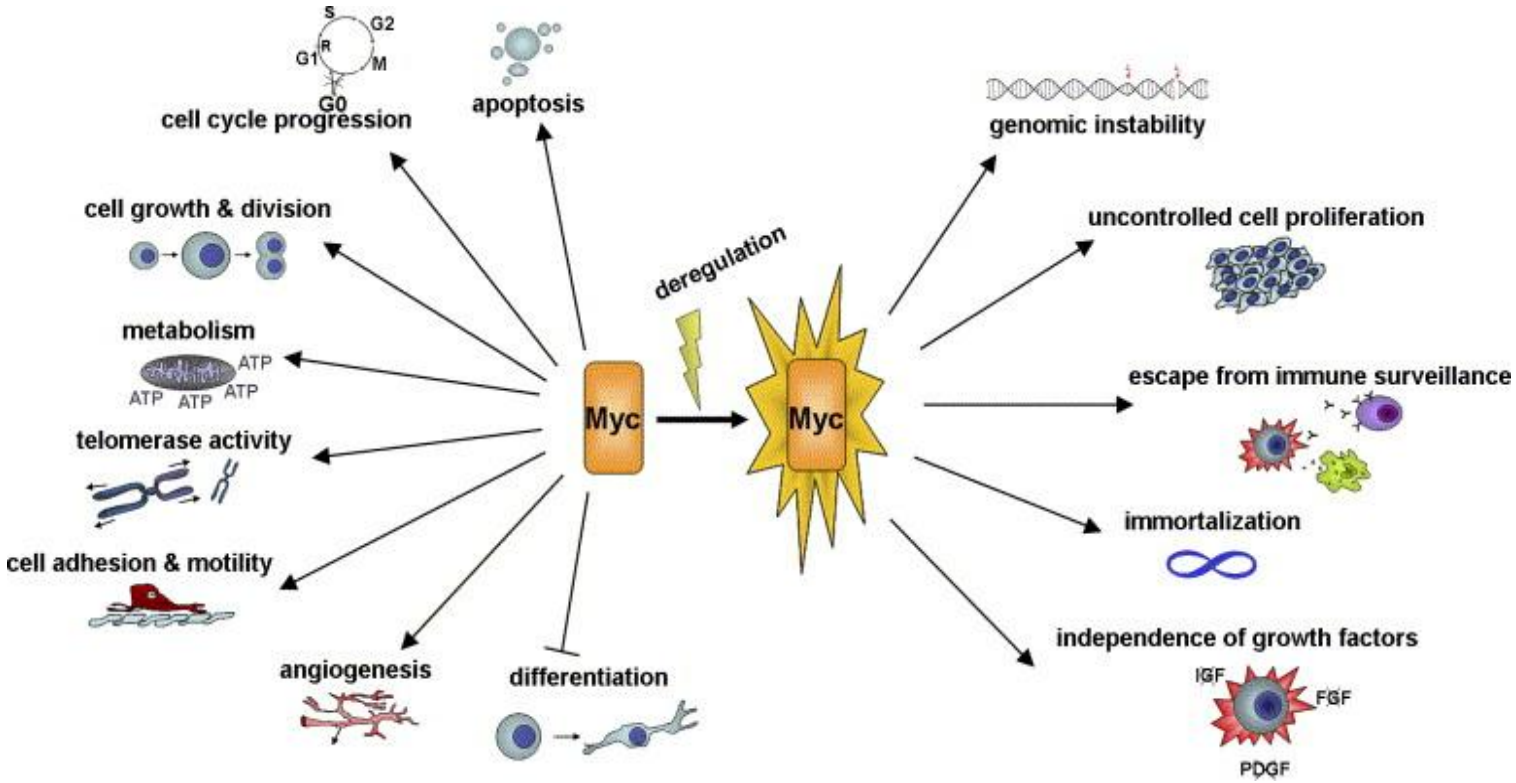

Figure 1.18. Cellular control by MYC during normal conditions and tumorigenesis. Myc is a key regulator of many biological activities and the deregulation of Myc may result in apoptosis, genomic instability, uncontrolled cell proliferation, escape from immune surveillance, growth factor independence, and immortalization. Figure taken from (Vita and Henriksson 2006).

1.5.4.1.2 MYC genes in human cancers

The involvement of *MYCC*, *MYCN* and *MYCL* have are all implicated in human cancer development. MYCC is up-regulated in approximately 70% of all human tumours (reviewed in (Vita and Henriksson 2006) but most frequently occurs in Burkitt's lymphomas which is characterized by a translocation incorporating the *MYCC* locus which results in MYCC over-expression in 91% of cases (Vita and Henriksson 2006). *MYCC* amplification may also occur in many human tumours including osteosarcomas, melanoma and ovarian, beast, bladder, prostate, cervical, colonic, lung, gastric and hepatocellular carcinomas (Vita and Henriksson 2006). Amplification, particularly at a high level, is frequently associated with a poorer prognosis (Nesbit, Tersak et al. 1999; Takei, Nguyen et al. 2009). *MYCN* amplification in contrast with *MYCC* amplification is associated with predominantly paediatric tumours including neuroblastoma, rhabdomyosarcoma, medulloblastoma and retinoblastoma (Nesbit, Tersak et al. 1999). It is however also associated with a more aggressive phenotype and a poorer prognosis. *MYCN* amplification was the first genetic marker used in the management of neuroblastoma which is associated with a reduced 5 year overall survival from 98% to 36% in *MYCN* amplified cases (Lu, Pearson et al. 2003; Vasudevan, Nuchtern et al. 2005). The *MYCL* gene has been less commonly associated with tumours in humans compared to the *MYCC* and *MYCN* homologues, but has been seen in ovarian carcinoma and small cell lung carcinoma (Vita and Henriksson 2006). The impact of *MYCL* amplification on clinical outcome has however not been established.

1.5.4.1.3 *MYC* genes in medulloblastoma and CNS-PNET

MYCC and *MYCN* amplification occur in 15-25% of medulloblastomas, are associated with large cell anaplastic subtype and an unfavourable outcome (Leonard, Cai et al. 2001; Lamont, McManamy et al. 2004; Vita and Henriksson 2006; Pfister, Remke et al. 2009). Few studies however have investigated MYC family amplification in CNS-PNETs. In murine models CNS-PNETs have been shown to develop with increased *c-myc* expression. In a study involving 43 p53 deficient mice, CNS-PNETs developed in 35%

(15/43) of cases, located in the periventricular region in 53% (Momota, Shih et al. 2008). In human studies 54 CNS-PNET tumour samples analysed across three clinical cohorts revealed *MYCC* and *MYCN* amplification in 5% cases (*MYCN* amplification 1/54, *MYCC* amplification 5/54) (Fruhwald, O'Dorisio et al. 2000; Pfister, Remke et al. 2007; Behdad and Perry 2010). However in CNS-PNETs unlike in medulloblastomas, no clinicopathological correlation with MYC expression has been derived. In summary, the previous studies in CNS-PNET show that the *MYC* family genes are implicated in CNS-PNET development, and demands further investigation.

1.5.5 Developmental pathways disrupted in CNS-PNET

1.5.5.1 The p53 pathway

Located on chromosome 17 at 17p13.1, *TP53* was one of the first tumour suppressor genes discovered four decades ago (Linzer and Levine 1979). *TP53* codes for a 393 amino acid phosphoprotein transcription factor found at low levels in all healthy tissues, and has a number of critical roles that has lead to it being referred to as "*the guardian of the genome*" (Lane 1992). Cellular stresses including DNA damage, hypoxia, growth factor depletion, oncogenic activation and microtubule disruption result in the stabilisation and nuclear accumulation of activated p53 (Figure 1.19). Activated p53 is then able to induce a number of responses including cell cycle arrest and apoptosis (Vousden and Lu 2002).

During embryogenesis up to 50% of neurones undergo apoptosis under the control of p53 as they fail to differentiate correctly (Oppenheim 1991). The pro-apoptotic functions of p53 are however potentially lethal and are therefore tightly regulated (Figure 1.19). MDM2, an E3 ubiquitin ligase, is a critical negative regulator of p53. MDM2 itself is induced in response to p53 activation and therefore forms a tightly regulated negative feedback loop. Deletion of mdm2 in the mouse model is lethal in early embryonic development (Marine, Francoz et al. 2006). In addition the tumour suppressor $p14^{ARF}$, both negatively regulates MDM2 and inhibits the p53-MDM2

interaction by binding to MDM2 within the nucleolus facilitating p53 accumulation and enabling p53 induced transcriptional activity (Sionov, Coen et al. 2001). P53 levels are highest in G1 phase, and accumulate in the nucleus in S phase (Shaulsky, Goldfinger et al. 1990)

Post translation modifications of p53 may arise in response to stress and may include the addition of a functional group to p53 by phosphorylation, ubiquitylation, acetylation, sumolyation, glycosylation, ribosylation and methylation and direct whether apoptotic genes or those involved in cell cycle arrest are transactivated (Vousden and Lu 2002). Subcellular location is another important component of p53 regulation. Whilst p53 may readily shuttle in a cell cycle dependent manner between the nucleus and cytoplasm, translocation to the nucleus is essential for it to undertake its transcriptional activity (Jimenez, Khan et al. 1999; Sionov, Coen et al. 2001).

Targets of p53 may inhibit cell cycle progression leading to G1 or G2 arrest and include $p21^{WAF1}$ and GADD45. $p21^{WAF1}$ is an inhibitor of cyclin dependent kinases (CDKs) and by binding to cyclin-CDK complexes blocks cell cycle progression from G1 to S phase (Levine 1997; Vogelstein, Lane et al. 2000). GADD45 directly inhibits G2M transition through binding with B1-Cdc" complexes (Zhan, Antinore et al. 1999).

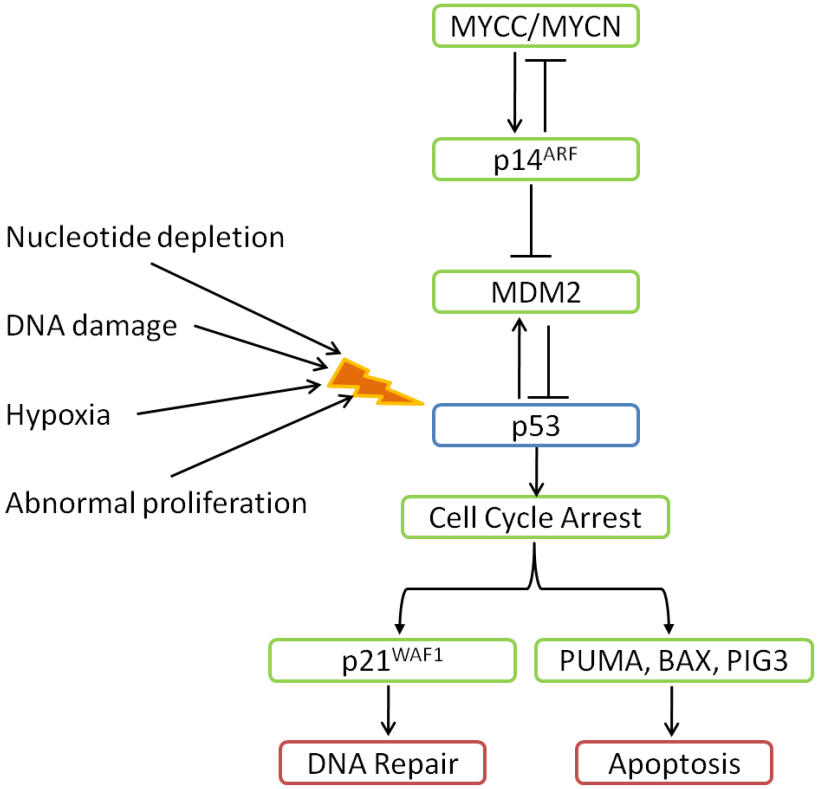

Figure 1.19. Overview of the p53 pathway. The cellular response of p53 to DNA damage and stresses includes cell cycle arrest enabling either apoptosis or DNA repair. Control of the pathway is influenced by MDM2 by negative feedback inhibition. Levels of MDM2 are themselves controlled by $p14^{ARF}$ and both MYCC and MYCN**.** Figure adapted from (Carr, Bell et al. 2006).

1.5.5.1.1 The *TP53* gene and cancer

The *TP53* gene encodes a 393 amino acid phosphoprotein and is comprised of five functional domains (Vousden and Lu 2002). Amino acid residues 1-42 at the N-terminus form the transcriptional activation domain (TAD) where interaction with basal transcriptional machinery results in transactivation of downstream target genes. It is at this site where negative regulators such as MDM2 bind to inhibit p53 mediated transcriptional activity. A second domain is located at codons 40-92 and contains a series of repeated proline residues and a second transactivation domain. The amino acid residues 101-306 constitute the (central) DNA binding domain (DBD). DNA binds to p53 at this site, and it is within the DBD where *TP53* is commonly mutated. An oligomerization domain at codons 307-355 is involved in the formation of p53 dimers.

The final carboxy-terminus of p53 (amino acid residues 356-393) contains 3 nuclear localization signals (NLS) and a non-specific DNA binding domain that binds to damaged DNA. This region is also involved in downregulation of DNA binding to the central domain (DBD).

TP53 is frequently mutated in human cancers, and occurs in over a third of non-melanomatous skin (80%), lung (70%), head and neck (60%), colonic (60%), ovarian (60%), bladder (60%), gastric (45%) and oesophageal (40%) cancers (data from http://p53.free.fr/p53). *TP53* mutation most commonly occurs at residues R175, G245, R248, R249, R273 and R282, accounting for 30% of all *TP53* mutations (Figure 1.20) and result in damage to the structural integrity of the DBD (Greenblatt, Bennett et al. 1994; Levine 1997). The majority of *TP53* mutations result in a single amino acid substitution; 75% are missense and 7% nonsense (http://www-p53.iarc.fr/). Mutation results in the accumulation of an inactive mutant protein although in some cases a gain of function has been demonstrated (Lang, Iwakuma et al. 2004; Olive, Tuveson et al. 2004; Soussi and Lozano 2005). Germline mutations of *TP53* result in the Li Fraumeni cancer predisposition syndrome (see section 1.5.2.2).

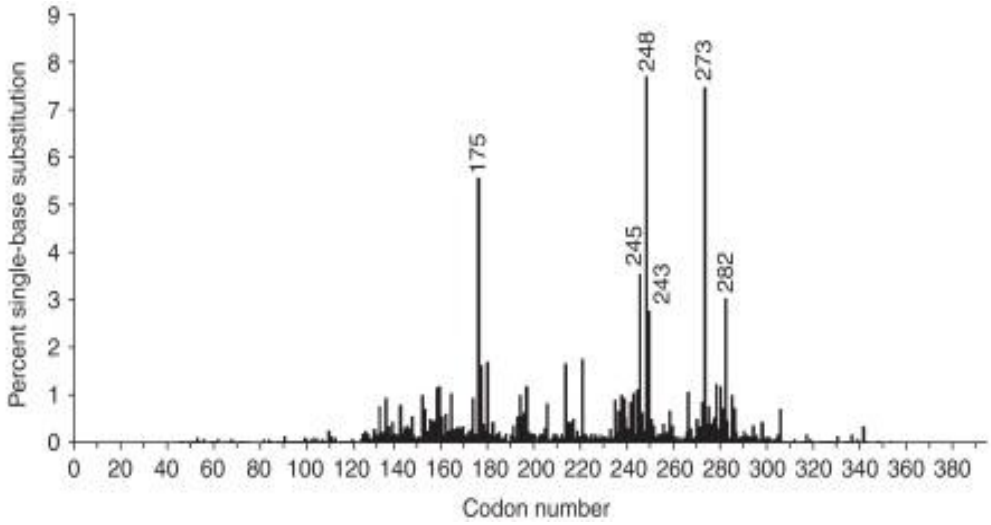

Figure 1.20. Genetic location of *TP53* mutations in human cancers. In 30% of tumours mutations arise in the DNA binding region at 6 codons (175, 245, 248, 273 and 282). 75% of these mutations are missense substitutions, 9% frameshift and deletions, 7% are nonsense mutations and in 5% mutations are silent. Data and figure adapted from the IARC *TP53* Database (http://www-p53.iarc.fr/, R13, November 2008) and (Petitjean, Mathe et al. 2007)

1.5.5.1.2 The p53 pathway in cancer

The importance of the p53 pathway in cancer development was demonstrated in murine models where a high incidence of tumours developed in mice deficient in *p53* (Donehower, Harvey et al. 1992). Mutations of *TP53* are the most common cause of p53 pathway dysregulation, but the pathway may be disrupted through a variety of other mechanisms. The aberrant accumulation of the MDM2 protein for example, occurs in many tumours (Onel and Cordon-Cardo 2004). This accumulation may arise as a result of amplification of the *MDM2* gene, which occurs in 7% of all cancers, or increased genetic transcription (Momand, Jung et al. 1998; Michael and Oren 2002). Aberrant expression of $p14^{ARF}$ may also result in tumour development. Alternative splicing of *CDKN2A* at 9p21 produces both $p16^{INK4A}$ and $p14^{ARF}$and the homozygous deletion of *CDKN2A* has been shown to occur in a number of tumours including in up to 40% of glioblastomas (Schmidt, Ichimura et al. 1994) including paediatric cases (Newcomb, Alonso et al. 2000). The MYC family of genes also play a role in the regiulation of p53, as shown in Figure 1.19, the role of the MYC genes in cancer development is described in further detail in section 1.5.4.1.

1.5.5.1.3 The role of the p53 pathway in CNS-PNET

Germ line mutations in *TP53* resulting in Li-Fraumeni syndrome are known to be associated with an array of tumours including CNS-PNETs (Malkin, Li et al. 1990; Orellana, Martinez et al. 1998; Reifenberger, Janssen et al. 1998). In addition mice models have provided further evidence for the importance of p53 in CNS-PNET tumorigenesis with the development of CNS-PNETs as well as medulloblastomas in $p53^{-/-}$ mice (Tong, Ohgaki et al. 2003). CNS-PNETs have also been shown to develop within 3 months in p53 deficient murine models with *c-myc* and/ or *β-catenin* (Momota, Shih et al. 2008).

Reviewed in Ellison 2002, mutations in *TP53* have been shown to occur in less than 10% of medulloblastomas (Ellison 2002)(Ellison 2002)(Ellison 2002)(Ellison 2002)(Ellison

2002)(Ellison 2002)(Ellison 2002)(Ellison 2002)(Ellison 2002)(Ellison 2002) which was confirmed recently in a large study investigating 310 medulloblastomas in which *TP53* mutations were observed in 6.8% (21/310) (Pfaff, Remke et al. 2010). The clinical significance of *TP53* mutations has not been established. In a recent study mutation was associated with a universally poor outcome ($p<0.001$) (Tabori, Baskin et al. 2010), but in the Pfaff et al 2010 study no correlation with survival was observed ($p=0.63$) (Pfaff, Remke et al. 2010). To date, few CNS-PNET tumours have been investigated for *TP53* mutations. In five studies a total of 46 CNS-PNET tumour samples were screened for *TP53* mutations, and identified in 7 cases (Table 3.30)(Ho, Hsieh et al. 1996; Burnett, White et al. 1997; Zagzag, Miller et al. 2000; Kraus, Felsberg et al. 2002; Zakrzewska, Rieske et al. 2004). Evidence of p53 pathway dysregulation appears however to be a common event in CNS-PNET and appears to occur significantly more frequently than in medulloblastomas (Eberhart, Chaudhry et al. 2005). In the Eberhart et al study, p53 dysregulation, assumed with the immunohistochemical accumulation of p53, occurred in 88% (7/8) CNS-PNETs, but only 18% (8/44) classic medulloblastomas ($p<0.001$).

The involvement of MDM2 in CNS-PNET has been investigated in one study. Kraus et al 2002, reported the results of 12 CNS-PNETs, and found no evidence of *MDM2* amplification (Kraus, Felsberg et al. 2002). In the same study evidence of *CDKN2A* ($p14^{ARF}$) deletion was also investigated, and not found to be a feature. However more recently a series of studies have reported a role of *CDKN2A* in CNS-PNET disease. Array CGH studies identified loss of the *CDKN2A* locus at 9p21.3 in 3 tumours (McCabe, Ichimura et al. 2006; Pfister, Remke et al. 2007). Using fluorescence *in situ* hybridisation (FISH) in a second cohort Pfister et al showed loss of *CDKN2A* in a total of 7/21 (33%) of CNS-PNETs, and reported an associated trend with metastatic disease ($p=0.07$). An investigation of the role of p53 pathway dysregulation, *TP53* mutations, *MDM2* amplification and *CDKN2A* loss in a large series of CNS-PNETs is required to determine the role of this pathway in CNS-PNET tumorigenesis.

1.5.5.2 Wingless signalling pathway

1.5.5.2.1 Overview of Wingless (WNT) signalling

The wingless (WNT) pathway is a critical developmental signal transduction pathway involving a group of lipid-modified signaling proteins, collectively known as Wnt proteins, in the proliferation, fate specification, polarity, and migration of cells (Willert, Brown et al. 2003; Logan and Nusse 2004). Signal transduction may occur via either a β-catenin dependent (canonical) or an independent pathway.

Under normal conditions cytoplasmic β-catenin is degraded by a protein complex comprising axin, APC and glycogen synthase kinase-3β (Axin-APC-GSK3β complex). GSK-3β phosphorylates β-catenin which is then available for proteosomal degradation. β-catenin, through its degradation, is prevented from translocating into the nucleus to replace Groucho to permit Wnt target gene expression and therefore expression is repressed (Kalderon 2002).

In the canonical Wnt signalling pathway, Wnt signalling (Figure 1.21) is initiated through the binding of Wnt proteins to a transmembrane receptor complex. The transmembrane receptor complex comprises one of the seven Frizzled (Fz) proteins and the low density lipoprotein receptor-related protein (LRP). The binding results in phosphorylative activation of LRP and the cytoplasmic recruitment of Axin in addition to phosphorylation of Dishevelled (Dsh) by (Fz). The resulting Axin-APC-GSK-3β complex inhibits the phosphorylation of β-catenin by GSK-3β. The hypophosphorylated β-catenin is unsuitable for proteosomal degradation in this state which results in its cytoslic accumulation and translocation into the nucleus. In the nucleus it replaces Groucho and in a partnership with T-cell –specific transcription factor (TCF) and lymphoid enhancer factor (LEF) activates gene expression including cmyc, cyclin D1 and Axin 2 (He, Sparks et al. 1998; Shtutman, Zhurinsky et al. 1999; Tetsu and McCormick 1999; Jho, Zhang et al. 2002; Lustig, Jerchow et al. 2002).

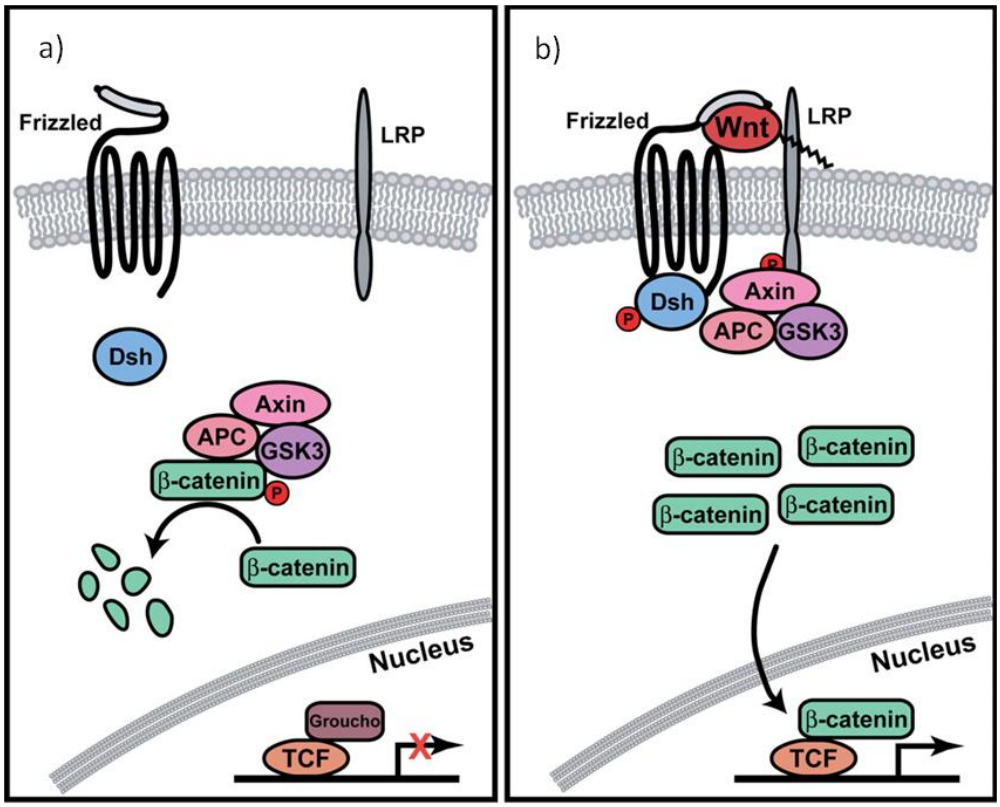

Figure 1.21. Overview of canonical WNT signalling. (a) In cells not exposed to Wnt, β-catenin associates with a complex comprising Axin, APC, and GSK-3. Phosphorylation of β-catenin occurs which targets it for degradation. Wnt target genes are in this state are repressed by the association of TCF with Groucho. (b) Wnt binds to the Fz and LRP receptors which induces phosphorylation of LRP and recruitment of Axin. Dsh is also phosphorylated, and the Axin·APC·GSK-3 complex is inhibited, leading to accumulation of cytosolic β-catenin. Accumulated β-catenin then translocates to the nucleus, replaces Groucho from TCF, and activates target genes. Abbreviations: APC, adenomatous polyposis coli; GSK3, glycogen synthase kinase 3β; TCF, T-cell specific transcription factors; Fz, Frizelled; LRH, lipoprotein receptor related protein; Dsh, Dishevelled (Figure adapted from (Gordon and Nusse 2006)).

1.5.5.2.2 WNT signalling in medulloblastoma and CNS-PNET

Aberrant Wnt signalling resulting from germ line defects in the Wnt signalling pathway may give rise to medulloblastoma or CNS-PNET development, as has been described in Turcot syndrome (see section 1.5.2.3). In clinical trials, aberrant Wnt signalling, identified by β-catenin accumulation has been shown to occur in 16% of patients with medulloblastomas (Ellison, Kocat et al. 2011). In this study, mutations in exon 3 at codons 33,34 and 41 in *CTNNB1,* that affect the binding site for the β-transducin

repeat-containing protein (β-TRCP) which promotes the degradation of β-catenin in the proteosome (Gilbertson 2004), were found to occur in 10% of medulloblastomas. There have however only been two previous small studies in which Wnt pathway disruption has been investigated in CNS-PNETs, and in total 16 tumours were screened for *CTNNB1* mutations and 33 for β-catenin nuclear accumulation by immunohistochemistry (Koch, Waha et al. 2001; Rogers, Miller et al. 2009). In these studies only a single case of *CTNNB1* mutation was observed. Unlike in medulloblastoma where a favourable prognostic phenotype has been repeatedly and convincingly demonstrated with Wnt pathway disruption (Ellison, Onilude et al. 2005; Gajjar, Chintagumpala et al. 2006; Fattet, Haberler et al. 2009; Ellison, Kocat et al. 2011), the effect of *CTNNB1* mutations and β-catenin accumulation in CNS-PNET has not been determined. Further study of this pathway is now required in this disease to clarify its role in CNS-PNET development and to establish whether it may be exploited in the future for treatment stratification, as is being proposed currently for the management of children with medulloblastomas (Pizer and Clifford 2009).

1.5.5.3 Sonic hedgehog pathway

The sonic hedgehog signalling (shh) pathway is involved in the development of the brain and in particular the external granular layer of the cerebellum. The SHH gene is located at 7q36 and produces a ligand that binds to the patched receptor to initiate shh pathway signalling (Figure 1.22). The patched gene (*PTCH1)* is situated on chromosome 9q22.3 and is responsible for medulloblastoma tumour development as part of the Gorlin syndrome when mutant (section 1.5.2.4).

Activation of the SHH ligand results in dissociation of PTCH from SMO, releasing SMO to activate Gli which, following nuclear translocation, induces target gene expression, including those that are involved in angiogenesis (components of the platelet derived growth factor (PDGF) and vascular epithelial growth factor (VEGF) pathways), and in controlling cell proliferation (cyclin D, cyclin E, and *MYC)* (di Magliano and Hebrok 2003).

Mouse models have shown that transgenic *Ptc*$^{+/-}$ mice and a transgenic mouse model with mutant SmoA1 both develop medulloblastoma tumours (Goodrich, Milenkovic et al. 1997; Hallahan, Pritchard et al. 2004). Mutations in the PTCH, SMO and SUFU genes, have been shown to be important in the development of medulloblastomas and in particular the nodular desmoplastic subtype (Xie, Murone et al. 1998; Taylor, Liu et al. 2002). In murine models, downstream effectors of Shh signalling (Gli 1-3) have been identified in the cerebral cortex and midbrain in addition to the cerebellum, suggesting that Shh signalling may also be implicated in brain development outside of the infratentorial compartment (Dahmane, Sanchez et al. 2001). The role of the shh pathway in CNS-PNET pathogenesis has however not been extensively investigated, but in a series of 3 CNS-PNET tumours all were shown to express the downstream target of the Shh-Gli pathway, MYCN (Moriuchi, Shimizu et al. 1996). In an additional study 3 out of 8 CNS-PNETs harboured mutations at the PTCH gene locus, at 9q22.3, Vorechovsky, Tingby et al. 1997), suggesting that aberrant shh signalling could be a feature in a small subset of CNS-PNETs.

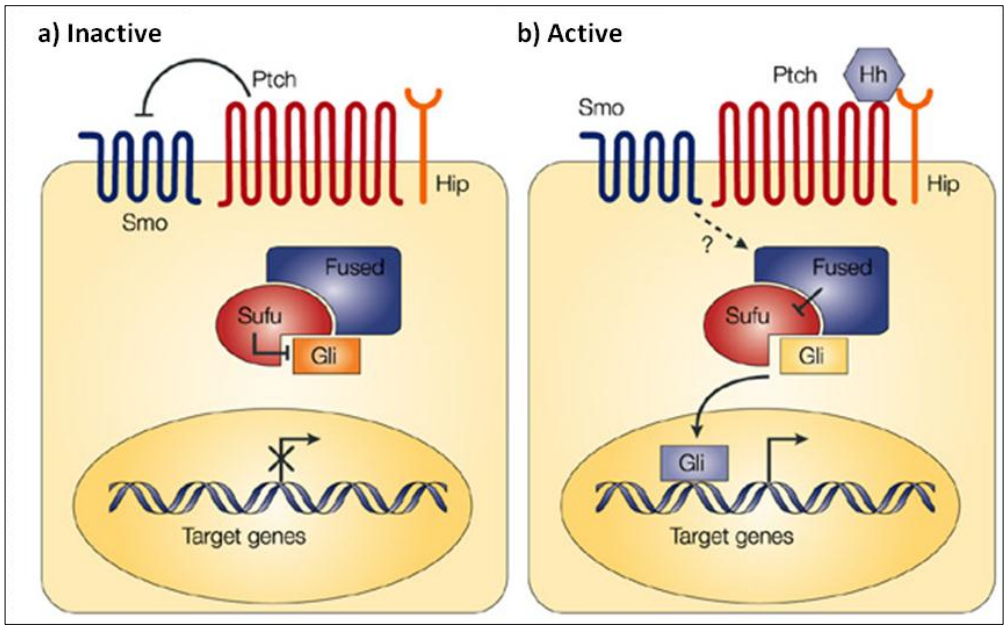

Figure 1.22. The sonic hedgehog signalling pathway. (a) In the absence of ligand, the sonic hedgehog signaling pathway (shh) is inactive. The transmembrane protein receptor Patched (Ptch) inhibits the activity of Smoothened (Smo) and the downstream transcription factor Gli is prevented from entering the nucleus to activate transcription through interactions with cytoplasmic proteins Fused and Suppressor of fused (Sufu). (b) Pathway activation. Binding of the hedgehog ligand (Hh) to Ptch results in the removal of Smo repression and activation of a cascade that leads to the translocation of activated Gli to the nucleus. Nuclear Gli activates target gene expression, including those that are involved in angiogenesis (components of the platelet-derived-growth-factor (PDGF) and vascular-epithelial-growth-factor (VEGF) pathways), and in controlling cell proliferation (cyclin D, cyclin E, and *MYC)*. Figure taken from (di Magliano and Hebrok 2003).

1.5.5.4 The Notch signalling pathway

The Notch signalling pathway is involved in the regulation of mechanisms that control multiple cell differentiation processes during both embryonic and adult life using cell to cell communication. Large transmembrane proteins (Notch 1-4) are encoded by the NOTCH genes which act as receptors for ligands expressed by neighbouring cells and activation of this pathway results in the release of the notch intracellular domain (NICD) and activation of the Hes(1-3) target genes (Kume 2009) as illustrated in Figure 1.23. Signalling plays an important role in the normal development of many tissues effects cellular differentiation, survival, and proliferation. The pathway has also been

shown to be involved in the regulation of normal neurogenesis (Ishibashi, Ang et al. 1995; Gaiano and Fishell 2002).

Aberrant Notch signalling, first observed in T-cell leukaemias with a translocation involving the *NOTCH1* locus on chromosome 9 (t(7;9)) (Reynolds, Smith et al. 1987), has been shown to be involved in many cancers including small cell lung cancer, basal cell skin cancer, prostate cancer, neuroblastoma and cervical cancer (reviewed in (Allenspach, Maillard et al. 2002). To date there has been limited research on the NOTCH signalling pathway in intracranial PNET development but activation of this pathway has been shown in two studies suggesting that it may play a role in CNS-PNET development (Rostomily, Bermingham-McDonogh et al. 1997; Fan, Mikolaenko et al. 2004). Rostomily et al, demonstrated differential expression of hASH1, a basic helix-loop-helix protein inhibited by NOTCH signalling, in CNS-PNETs. In the subsequent Fan et al study, differential expression of NOTCH 1 and 2 was interestingly shown in CNS-PNET and MB with high levels of NOTCH 2 detectable in CNS-PNETs. Inactivation and associated cell growth retardation in the CNS-PNET cell line PFSK, provided further support for the role of NOTCH 2 in CNS-PNET tumorigenesis (Fan, Mikolaenko et al. 2004).

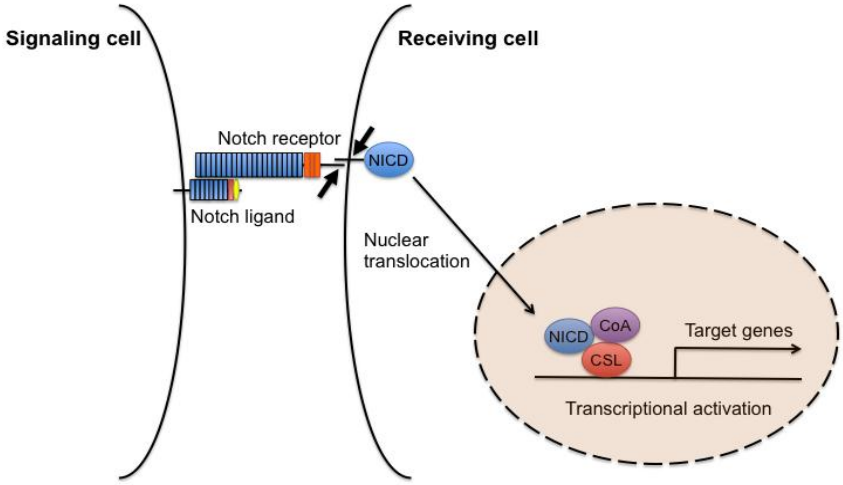

Figure 1.23. Overview of the Notch signalling pathway. Upon Notch ligand binding, a two-step proteolysis cleavage process (small arrows) is catalyzed by a member of the disintegrin and metalloproteases (ADAMS) family and the γ-secretase containing complex. Notch intracellular domain (NICD) is then released from the membrane and translocates to the nucleus, where it forms a transcriptional activation complex with CSL and coactivators (CoA), and induces transcription of target genes. Figure taken from (Kume 2009).

1.5.6 Epigenetic events in CNS-PNET

The role and mechanisms of epigenetic modification in CNS-PNET are currently poorly understood. A number of recent studies investigating micro RNAs in CNS-PNET have however provided significant insights into CNS-PNET tumourigeneis and have supported the hypothesis that this disease may in fact consist of a number of entities. In a case report in 2009, Pfister et al, reported the molecular features of a 2 year old girl with an ETANTR CNS-PNET (Pfister, Remke et al. 2009). Molecular analysis revealed a 19q13.42 amplicon containing C19MC, a known microRNA cluster. In a subsequent study by Li et al, 45 CNS-PNET tumours were investigated and a similar amplification of C19MC within the 19q13.41 amplicon was identified in 24% (11/45) (Li, Lee et al. 2009). Expression of miR-520g and miR-517c from within this cluster were found to be significantly elevated in the amplified cases, and in both *in vivo* and *in vitro* models associated with oncogenic effects including promoting cell survival.

Changes in DNA methylation patterns appear also to be a significant feature of intracranial PNETs, and studies have estimated that aberrant hypermethylation occurs in up to 1% of CpG islands in primary PNET tumours (Fruhwald, O'Dorisio et al. 2001). To date there have however been few studies investigating DNA methylation epigenetic modification in CNS-PNET. Reported DNA methylation events in CNS-PNET, in common with genetic aberrations, have been identified as a part of wider brain tumour or intracranial PNET cohorts, rather than specific CNS-PNET studies. These studies have investigated a selected group of genes and reported evidence of aberrant methylation in a subset, as summarised in Table 1.14.

Methylation of the $p14^{ARF}$ promoter has been shown to be a feature of supratentorial PNETs in one study, occurring in 50% (3/6) of analysed tumours (Inda, Munoz et al. 2006) . In contrast, in this study $p14^{ARF}$ promoter hypermethylation was seen in only 14% (3/21) of medulloblastomas. A subsequent study however did not corroborate this finding (Muhlisch, Bajanowski et al. 2007). Promoter hypermethylation of *CASP8* has been observed in a third of CNS-PNETs (8/24) (Muhlisch, Schwering et al. 2006), and in a further study by Chang et al, promoter hypermethylation of *FHIT* and *sFRP1* was detectable in 22% (2/9) and 11% (1/9) of cases respectively (Chang, Pang et al. 2005). Promoter hypermethylation of the tumour suppressor *DLC-1* was identified in a single CNS-PNET case (9%, 1/11) (Jesse Chung-Sean, Qing et al. 2005). In a study that screened the largest number of genes in CNS-PNET, only *CDH1* was found to be frequently methylated in 60%, but the investigative cohort only comprised of 5 CNS-PNET tumours (Muhlisch, Bajanowski et al. 2007). In this study evidence of methylation for *DAPK1, DUTTI1, p16INK4A, P15INK4B* and *SOCS1* was not seen in any of the primary CNS-PNET tumours.

The most commonly methylated gene identified in CNS-PNET to date is *RASSF1A*. In total, 39 CNS-PNETs have been investigated in three small studies for hypermethylation of the *RASSF1A* promoter (Chang, Pang et al. 2005; Muhlisch, Schwering et al. 2006; Inda and Castresana 2007). Overall, *RASSF1A* promoter hypermethylation was shown to occur in 77% (30/39) of cases, but these findings require validation in larger series.

Gene	Hypermethylation Frequency	Reference
CASP8	8/24 (33%)	(Muhlisch, Schwering et al. 2006)
CDH1	3/5 (60%)	(Muhlisch, Bajanowski et al. 2007)
DAPK1	0/5 (0%)	(Muhlisch, Bajanowski et al. 2007)
DLC-1	1/11 (9%)	(Jesse Chung-Sean, Qing et al. 2005)
DUTTI	0/5 (0%)	(Muhlisch, Bajanowski et al. 2007)
FHIT	2/9 (22%)	(Chang, Pang et al. 2005)
$p14^{ARF}$	0/4 (0%)	(Muhlisch, Bajanowski et al. 2007)
	3/6 (50%)	(Inda, Munoz et al. 2006)
$p15^{INK4B}$	0/2 (0%)	(Muhlisch, Bajanowski et al. 2007)
$p16^{INK4a}$	0/5 (0%)	(Muhlisch, Bajanowski et al. 2007)
	1/6 (17%)	(Inda, Munoz et al. 2006)
RASSF1A	6/9 (67%)	(Chang, Pang et al. 2005)
	19/24 (79%)	(Muhlisch, Schwering et al. 2006)
	5/6 (83%)	(Inda and Castresana 2007)
sFRP1	1/9 (11%)	(Chang, Pang et al. 2005)
SOCS1	0/3 (0%)	(Muhlisch, Bajanowski et al. 2007)
TIMP3	1/5 (20%)	(Muhlisch, Bajanowski et al. 2007)

Table 1.14 Promoter hypermethylation in CNS-PNET primary tumours.

1.5.6.1 RASSF1A

The *RASSF1* (Ras Association Domain Family Protein 1) gene is located on chromosome 3p21.3 and encodes a protein of 38.8kD which is expressed in all tissues. It contains 2 promoters and produces 7 different transcripts (*RASSF1A-G*) using different combinations of alternative splicing and promoters. The *RASSF1* locus has CpG islands associated with its two promoter regions, and the first CpG island includes the promoter region for *RASSF1A* (Pfeifer and Dammann 2005).

RASSF1A is a tumour suppressor gene which promotes cell cycle arrest, apoptosis, microtubule stability and proliferation (Agathanggelou, Cooper et al. 2005). Expression of RASSF1 proteins has been shown to promote cell cycle arrest and apoptosis (Feig and Buchsbaum 2002), and the discovery that *RASSF1A* -/- cells are more sensitive to depolymerization and induced microtubule damage by nocodazole has provided evidence for its role in microtubule stability (Liu, Tommasi et al. 2003).

1.5.6.1.1 *RASSF1A* in cancer

Evidence supporting epigenetic suppression of *RASSF1A* leading to tumorigenesis originates from mouse models. The first mice developed lacking *rassf1α* were engineered by Smith et al, (Smith, Xian et al. 2002). Tommasi and colleagues later engineered a knockout mouse model, deleting exon 1α and thus *Rassf1α,* and tumours developed in the mice included lymphomas, lung adenomas and a breast adenocarcinoma (Tommasi, Dammann et al. 2005). *RASSF1A* promoter methylation has subsequently been observed in multiple tumour types including a range of paediatric malignancies, summarised in Table 1.15 (Agathanggelou, Cooper et al. 2005).

Tumour Type	*RASSF1A* Methylation	
	%	Tumours
Ewings Sarcoma	0	0/8
Hepatoblastoma	19	5/7
Medulloblastoma	79	27/34
Neuroblastoma	55	37/67
Osteosarcoma	0	0/11
Rhabdomyosarcoma	61	11/18
Retinoblastoma	59	10/17
Wilm's tumour	71	22/31

Table 1.15. *RASSF1A* promoter methylation in primary paediatric tumours.
Summarised from data in the review by (Agathanggelou, Cooper et al. 2005).

1.5.6.1.2 *RASSF1A* promoter methylation in PNET

RASSF1A promoter methylation has been shown to be a prominent feature in intracranial PNETs. In six studies incorporating 129 medulloblastoma tumour samples *RASSF1A* methylation occurred in 79-100% of cases (Table 1.16)(Harada, Toyooka et al. 2002; Lusher, Lindsey et al. 2002; Horiguchi, Tomizawa et al. 2003; Lindsey, Lusher et al. 2004; Chang, Pang et al. 2005; Inda and Castresana 2007). Methylation of the *RASSF1A* promoter is not known however to confer a survival bias or be associated with any clinicopathological feature (Harada, Toyooka et al. 2002; Lindsey, Lusher et al. 2004). Three small studies have investigated *RASSF1A* promoter methylation in CNS-PNET, and determined rates of methylation of 67% (6/9), 79% (19/247) and 83% (5/6)(Chang, Pang et al. 2005; Muhlisch, Schwering et al. 2006; Inda and Castresana 2007). In limited series, *RASSF1A* methylation is therefore the most common epigenetic event detected in CNS-PNET to date, but both validation of this finding and the determination of any clinic-pathological correlates needs to be established. Taken together, these data also suggest a role for methylation events in CNS-PNET, which now requires further investigation.

Reference	Cohort size		Methylation
	Size	Age (yrs)	Freq
(Lusher, Lindsey et al. 2002)	34	1-11	27/34 (79%)
(Harada, Toyooka et al. 2002)	16	<16	14/16 (88%)
(Horiguchi, Tomizawa et al. 2003)	5	-	5/5 (100%)
(Lindsey, Lusher et al. 2004)	28	0-68	27/28 (96%)
(Chang, Pang et al. 2005)	25	3-69	25/25 (100%)
(Inda and Castresana 2007)	21	2-87	19/21 (91%)

Table 1.16. *RASSF1A* promoter hypermethylation in medulloblastoma tumours.

1.6 Project summary and aims

CNS-PNETs are embryonal malignant brain tumours that arise particularly in young children. The tumours are treated aggressively according to their age with multi-modal therapy including surgery, radiotherapy and chemotherapy. However, whilst there has been an improvement in the outcome for children with cancer as a whole over the last few decades, with over 75% of all children now surviving beyond 5 years (ONS 2010), the outcome for children with a CNS-PNET remains dismal. Fewer than half of the children who develop this tumour survive. Improving the chance of cure remains the most critical goal in the clinical management of patients with this disease.

Establishing the diagnosis of a CNS-PNET remains both a significant challenge and controversial. Whilst the introduction of routine INI1 staining has aided in the differentiation between ATRTs and other CNS tumours including CNS-PNETs, no specific test is currently available to confidently classify a tumour as a CNS-PNET. On histopathological examination, a CNS-PNET appears as a highly malignant tumour but may exhibit a diverse array of non-specific features which frequently overlap with, and may be misclassified as other diagnoses, and in particular high grade gliomas. New approaches are therefore essential to assist in the diagnosis of this tumour.

The PNET concept, devised by Harte and Earle in 1973, classified together tumours throughout the CNS with similar histopathological features. The hypothesis that histopathologically similar tumours would respond to a similarly unified treatment approach has directed international management in these tumours for over three decades. The consistent disparity in outcome however, between intracranial PNETs arising from the cerebellum (medulloblastoma), and those arising elsewhere in the CNS has led to renewed controversy in the PNET concept. The contemporary hypothesis is that despite histopathological similarities, the differences in outcome seen in children with intracranial PNETs at different sites reflect diversity at the molecular genetic level.

A well characterised series of molecular events have now been shown to be implicated in medulloblastoma development. The most frequent aberration in this disease is *RASSF1A* promoter methylation, which has been shown to occur in 79-100% of cases. The development of medulloblastomas in patients with cancer predisposition syndromes including Li-Fraumeni, Turcot and Gorlin syndromes, suggested that aberrant p53, Wnt and sonic hedgehog signalling respectively is involved in the pathogenesis of this disease, and dysregulation of these pathways are frequently observed in tumour samples. In addition, large clinical trial based cohorts in this disease have more recently revealed the prognostic impact of some of these events which are now being exploited clinically to provide stratified treatment regimens.

To date, research into CNS-PNET has been very limited. The few studies that have been undertaken typically have arisen as part of either a paediatric brain tumour or intracranial PNET study and have shown extensive molecular heterogeneity in the CNS-PNETs. Consequently, studies have commonly lacked sufficient power or specific focus to detect novel insights into the pathogenesis of CNS-PNETs. Investigation of molecular events frequently observed in other intracranial PNETs in a large and well characterised CNS-PNET cohort is required to determine the role of these events in this disease, and to define the relationship with medulloblastomas.

The overall objective of this project was to investigate in comparison with medulloblastomas the molecular mechanisms that may be involved in the development of a CNS-PNET and to determine their clinical and histopathological significance, by attending to the following specific aims:

1. To investigate in a large cohort of primary CNS-PNET tumour samples and cell lines the role of common genetic features associated with medulloblastomas, and to identify clinical and histopathological correlates (Chapter 3).

2. To follow up the findings of recent large-scale genome-wide genetic studies in brain tumours in which novel candidate genes have been identified to determine their role in CNS-PNET (Chapter 4).

3. Undertake a systematic investigation of the CNS-PNET methylome in a cohort of primary tumours, to investigate the role of DNA methylation epigenetic modification in CNS-PNETs, to identify new genetic markers in CNS-PNET and their clinico-pathological significance, and also to compare and contrast the CNS-PNET methylome with medulloblastomas and other paediatric brain tumours (Chapter 5).

Chapter 2

Materials & methods

Table of contents

Chapter 2

2.1 Clinical cohort

2.1.1 Primary CNS-PNET tumour samples

The cohort of primary CNS-PNET samples for this study was collected in the Northern Institute for Cancer Research (NICR) tumour bank at Newcastle University. Tissue was stored in accordance with the Human Tissue Act 2004 (Human Tissue Act, 2004) and the Human Tissue Authority (HTA) code of practice (Human Tissue Authority, 2009). Ethical approval for the registration, storage, access and study of samples was obtained from the Newcastle and North Tyneside Local Research Ethics Committee. All clinical data was anonymised.

The cohort consisted of 39 primary CNS-PNETs. The samples (frozen tumour material in 21 cases and formalin fixed and paraffin embedded in a further 18) were kindly provided from local, national and international sources including the Newcastle Upon Tyne NHS Trust pathology archive, the Children Cancer and Leukaemia Group (CCLG) tumour bank, Professor Richard Grundy (Nottingham University, UK), Professor Michael Fruhwald and Dr Martin Hasselblatt (University Hospital of Munster, Germany), and Dr Peter Hauser (Semmelweis University, Budapest, Hungary). All cases underwent a central pathological review. Cases were reviewed in three review sessions by UK neuropathologists involved in providing central pathological review for the UK Children Cancer and Leukaemia Group (CCLG) brain tumour studies, and included Professor David Ellison (formerly Northern Institute Cancer Research, Newcastle University, UK and now, St Judes Children's Research Hospital, Memphis, USA), Dr Keith Robson and Dr Jim Lowe (University of Nottingham, UK), and Dr Tom Jacques (Great Ormond Street Hospital, London, UK).

The characteristics of the cohort are summarised in Table 2.1. The metastatic stage for each tumour is given using the Chang staging system score (see section 1.4.4). Tumours in the cohort collected prior to the routine clinical assessment of CSF to ascertain evidence of microscopic metastatic disease and therefore where no CSF results is available are classified by convention as stage M0/1, and are considered as

being non-metastatic (Pizer, Weston et al. 2006). Additional details of the tumour samples used in each study will be given in the methods section of each results chapter.

Tumour sample ID	Diagnosis	Site	Sex	Age at diagnosis (Months)	Metastasis Stage (Chang)	Status	Follow up (months)	Investigated in studies in chapter		
								3	4	5
SP3	CNS-PNET	Parieto-occipital lobes	Male	48	M0/1	Dead	17			
SP4	CNS-PNET	Parietal lobe	Female	78	M0/1	Alive	121			
SP7	CNS-PNET	Intraventricular	Female	75	M0	Dead	7			
SP10	CNS-PNET	3rd Ventricle	Male	158	M0/1	Alive	112			
SP13	CNS-PNET	Cerebral	Male	106	M0/1	Dead	71			
SP14	CNS-PNET	Parietal lobe	Female	105	-	Alive	100			
SP21	CNS-PNET	Left tempoparietal lobes	Male	65		Dead	25			
SP23	CNS-PNET	Cerebral	Male	126	M0/1	Alive	108			
SP24	CNS-PNET	Cerebral	Male	31	-	Dead	7			
SP28	CNS-PNET	Right frontal lobe	Female	23	M0/1	Dead	9			
SP40	CNS-PNET	Right parietal lobe	Female	348	M0/1	-	-			
SP41	CNS-PNET	Left Fronto-temporal lobes	Male	56	M0/1	Dead	24			
SP42	CNS-PNET	Right temporal lobe	Female	288	M0/1	Alive	24			
SP43	CNS-PNET	Left parietal lobe	Male	-	M0/1	-	-			
SP45	CNS-PNET	Right parietal lobe.	Female	11	M0/1	-	-			
SP46	CNS-PNET	Left frontal lobe	Female	312	M0/1	Dead	36			
SP47	CNS-PNET	Left frontal lobe	Female	87	M0/1	Alive	132			
SP49	CNS-PNET	Right temporal lobe	Female	15	M2	Alive	36			
SP50	CNS-PNET	Left tempoparietal lobes	Female	36	M0/1	Dead	15			

SP51	CNS-PNET	Cerebral	Female	360	-	Dead	55			
SP52	CNS-PNET	Left parietal lobe	Male	127	M0/1	Alive	43			
SP54	CNS-PNET	Infra + Supratentorial	Female	26	M0/1	Dead	3			
SP55	CNS-PNET	Temporal lobe	Male	77	M0/1	Dead	15			
SP57	CNS-PNET	Frontal + temporal lobes	Male	21	M0/1	Alive	39			
SP58	CNS-PNET	Right (superficial) parietal lobe	Female	223	M0	Alive	17			
SP101	CNS-PNET	Right parietal lobe	Female	10	M2	Dead	41			
SP103	CNS-PNET	Right frontal lobe	Female	20	M0	Dead	0			
SP104	CNS-PNET	Right parietal lobe	Male	122	M0	Alive	52			
SP106	CNS-PNET	Right frontal lobe	Male	141	M3	Dead	30			
SP108	CNS-PNET	Left cerebral hemisphere	Male	107	M2	Dead	71			
SP110	CNS-PNET	Right temporal Lobe	Male	37	M4	Dead	6			
SP111	CNS-PNET	Right frontal, temporal & parietal lobes	Female	53	M0	Alive	36			
SP113	CNS-PNET	Sub thalamic, left lateral & 3rd ventricle	Male	142	M0	Dead	0			
SP115	CNS-PNET	Right frontoparietal Lobes	Female	71	M0	Dead	5			
SP116	CNS-PNET	Left frontal lobe	Male	61	M0	Dead	21			
SP117	CNS-PNET	Midline frontal region	Male	59	M2	Dead	9			
SP124	CNS-PNET	Suprasellar	Female	14	M2	Alive	24			
SP125	CNS-PNET	Suprasellar	Female	144	M0	Alive	3			
SP126	CNS-PNET	Right parietal lobe	Male	84	M1	Dead	1.6			

Table 2.1. Clinical characteristics of CNS-PNETs used in studies. Highlighted boxes indicate cases investigated in studies described in specific chapters of this thesis.

2.1.2 Normal brain tissue cohort

A panel of normal brain tissue samples were also investigated (Table 2.2) which was derived from Newcastle Upon Tyne NHS Trust post-mortem specimens. The conditions in which the samples were collected and stored were as described in section 2.1.1 for the tumour cohort assembly.

ID	Site	Age	Sex
cbll17	Cerebellum	prenatal*	male
cbll18	Cerebellum	prenatal*	male
cbll19	Cerebellum	-	-
cbll20	Cerebellum	67 years	male
cbll21	Cerebellum	newborn	female
cbll22	Cerebellum	60 years	male
cbll23	Cerebellum	prenatal*	female
cbll24	Cerebellum	prenatal*	male

Table 2.2. **Clinical characteristics of normal brain samples used in this study.**
*Prentatal samples from foetuses as 18-22 weeks gestation.

2.1.3 CNS-PNET cell lines

Two immortalised cell lines of CNS-PNETs were investigated (PFSK and CHP707m), and these were both kindly donated by Dr Michael Grotzer (University Children's Hospital, Zurich, Switzerland) and cultured for experiments. PFSK was derived from a 22 month old boy with a right frontal lobe CNS-PNET. He underwent a subtotal resection and received postoperative chemotherapy, but died within 4 months of diagnosis from extensive disease. (Fults, Pedone et al. 1992). The second cell line, CHP707m, was derived from a 33 year old man with a right frontal lobe CNS-PNET. He also underwent a subtotal resection and this was followed by radiotherapy to the tumour bed and the

craniospinal axis. He relapsed at 11 months and the cell line was derived from a bone marrow metastatic deposit at this time. (Baker, Reddy et al. 1990). The clinical and cytogenetic features of PFSK and CHP707m are summarised in Table 2.3.

The CHP707m cell line contains a t(11;22) translocation. This is however a characteristic feature of Ewing's sarcomas and peripheral PNETs (Nagao, Ito et al. 1997) and is not observed in CNS-PNETs. Indeed, the presence of a t(11;22) has been used to distinguish peripheral PNETs from CNS-PNETs when these tumours may rarely arise in the central nervous system (Dedeurwaerdere, Giannini et al. 2002; Ohba, Yoshida et al. 2008). There is therefore some doubt as to the true nature of the CHP707m cell-line and caution with interpreting results based on experiments using this, as it may in fact have arisen from a peripheral PNET/ Ewings rather than a CNS-PNET.

	PFSK	CHP707m
Sex	Male	Male
Patient age	22 months	33 years
Location	Right Frontal lobe	Right Frontal lobe
Surgery	Subtotal	Subtotal
Radiotherapy	No	Tumour bed + C/S axis
Chemotherapy	Vincrisine, Cyclophosphamide, Methylprednisolone	No
Relapsed	At 3 months, metastasising into both cerebral hemispheres	At 11 months, metastatic to bone marrow
Died	At 4 months from diagnosis	At 21 months after diagnosis
Cell line	From primary tumour at diagnosis	From metastatic deposit at relapse
Cytogenetics	81,XXYY,t(Xp;8q), del(1)(p22), -2, -3, del(4)(p14), -5, -8, -9, -9, -13, -13, -14, -14, -16, -20, -22	n52XY,+Y, -1,-3,+8,-11,+13, -14, +17, -20, -22, +i(1q), +der(3), del(5)(q31), del(7)(q21q32), +del(7)(q11.2), t(9;18)(q13;q11.2), +der(11ins) t(11,22)

Table 2.3. Clinical and cytogenetic features summary of supratentorial CNS-PNET cell lines.

2.1 CNS-PNET cell line *in vitro* culture

2.1.1 Principles of *in vitro* cell culture

Cell culture is the culture of dispersed cells taken from the original tissue and was first devised in 1902 by Haberlandt (Freshney 2000). Tissue culture is used as a means of studying the behaviour of cells at relatively low cost whilst the physicochemical environment is controlled. A primary cell culture is started from cells taken directly from an organism and may be propagated into a cell line. A continuous cell line has the capacity for infinite survival and is therefore also referred to as being "established" or "immortalised" as described by George Gey, in 1952, with the production of the first continuous human (uterine cervix cancer) cell line, HeLa(Jones, McKusick et al. 1971).

All tissue culture experiments were performed in a Class II tissue culture hood (Streamline lab) using standard sterile techniques and pipettes.

2.1.2 Resurrection of cells from liquid nitrogen

Cryopreservation tubes (Nunc, Denmark) containing the frozen cells were removed from liquid nitrogen and placed on ice. Tubes were thawed rapidly in a 37°C water bath. The thawed cells were then transferred to pre-cooled 25ml universal tubes kept on ice. Ice-cold Fetal Calf Serum (FCS) (Sigma-Aldrich, UK) was added drop-wise to the cells; the cell suspension was mixed gently and left on ice for 20 minutes to allow the dimethylsulphoxide (DMSO) to diffuse out of the cells. The universal tube was then centrifuged for 5 minutes at 1000g in a MSE Mistral 2000R centrifuge (MSE Incorporation, USA) and the supernatant was discarded. The cell pellet was resuspended in fresh medium containing 10% (v/v) FCS and transferred to a sterile tissue culture flask (Corning, USA) and placed in a humid incubator (SANYO) to culture.

2.1.3 Cell line maintenance and sub culture

Cells were grown in optimal growth conditions at 37°C with air containing 5% carbon dioxide within a humid incubator (SANYO). The cells growing in culture were passaged twice weekly to optimise growth potential and nutrient availability. The flasks were first inspected for contamination and growth status assessed by cell density under a phase contrast inverted light microscope (Nikon E400) at x100 magnification. The colour of the medium was used as an additional guide as to when replenishment of medium was necessary since it contained phenol red which becomes progressively more yellow with a fall in pH, seen with the accumulation of metabolic waste products (Sambrook and Russell 2001).

2.1.3.1 Maintenance and subculture of PFSK

Cells were grown in RPMI 1640 media (Sigma) containing 10% (v/v) FCS and 1% (v/v) sodium pyruvate (Sigma-Aldrich). 1% (v/v) streptomycin / penicillin (sigma-Aldrich, UK) was also added to protect against bacterial contamination. To passage cells excess media was gently aspirated off the cells, which were then washed with 5-15ml of sterile phosphate buffered saline (PBS) at 37°C to remove traces of FCS. PBS was then drawn off the cells and 1-3ml of 1xEDTA- trypsin solution (Sigma-Aldrich, UK) was added to detach cells from the flask. Cells were incubated for 5 minutes at 37°C, and microscopy was used to gauge detachment. An equal volume of prepared media was used to neutralise the trypsin and then the cells were transferred to a 25ml universal tube. The universal tube was centrifuged at 1000g for 5 minutes in a MSE Mistral 2000R centrifuge (MSE Incorporation, USA) and the supernatant was discarded. The cell pellet was resuspended in 10ml fresh media pre-warmed to 37°C, before being split into 3-4 aliquots. Each aliquot was transferred using sterile pipettes into a separate sterile flask and made up to 25ml with fresh media at 37°C.

2.1.3.2 Maintenance and subculture of CHP707m

Cells were again grown in RPMI 1640 media (Sigma-Aldrich, UK)) containing 10% (v/v) FCS, 1% Sodium pyruvate, and 1% (v/v) streptomycin / penicillin. CHP707m grows as a non-adherent culture and so to passage the cells the contents of the flask were centrifuged at 1000g in a MSE Mistral 2000R centrifuge (MSE Incorporation, USA) for 5 minutes in a 25ml sterile universal container. The supernatant was discarded and the cells pelleted at the bottom were washed in 20ml sterile PBS at 37°C. The PBS was removed by centrifugation at 1000g for 5 minutes. The resulting cell pellet was resuspended in 10ml fresh media pre-warmed to 37°C, before being split into 3-4 aliquots. Each aliquot was transferred using sterile pipettes into a separate sterile flask and made up to 25ml with fresh media at 37°C.

Cell line	**CHP707m**	**PFSK**
Growth characteristics	Non- adherent	Adherent
Media	RPMI 1640 R8758 + 10% Fetal Calf Serum + 1% Sodium Pyruvate + 1% Penicillin/ streptomycin	RPMI 1640 R8758 + 10% Fetal Calf Serum + 1% Sodium Pyruvate + 1% Penicillin/ streptomycin

Table 2.4. Supratentorial CNS-PNET cell lines growth characteristics and media requirements.

2.1.3.3 Mycoplasma testing

Unlike bacterial and fungal contamination, infection with *mycoplasma* is not readily identified by the naked eye. Cultures were tested every 2 months for *mycoplasma* infection using the MycoAlert® mycoplasma detection kit (Lonza, UK) following the manufacturer's instructions, by DR E Matheson in the Northern Institute for Cancer Research. Any *mycoplasma* positive cultures identified would be discarded.

2.1.3.4 Cell number assessment

To determine the concentration of cells, the suspension was firstly gently pipetted to remove clumping and to generate a suspension containing single cells. A 10µl aliquot of suspension was then drawn under the cover-slip on a haemocytometer (Sigma-Aldrich, UK) by capillary action. The haemocytometer had 2 chambers each comprising 9 large grids of 25 squares. The area of each grid was $1mm^2$ with depth of 0.1mm with a resultant volume of $0.1mm^3$ ($1x10^{-4}$ml). Using a light microscope cells contained in four large grids were counted, including those cells on the top and left borders only, to avoid counting the same cell twice. The number of cells was subsequently divided by four to produce an average number of cells in each grid, and finally multiplied by 10^4 to ascertain the total number of cells/ ml in suspension.

2.1.4 Harvesting cells for DNA extraction

Cell suspensions were generated and removed from the tissue culture flask into 25ml universal tubes as previously described (section2.1.3). Cell numbers were assessed as described in section 2.1.3.4. The cell suspension was centrifuged at 1000g in a MSE Mistral 2000R centrifuge (MSE Incorporation, USA). The supernatant produced was discarded and the resulting cell pellet was resuspended in 20ml of ice-cold PBS. The suspension was again centrifuged at 1000g for 5 minutes before the supernatant was gently aspirated away from the cell pellet which was resuspended in PBS to yield a final concentration of $5x10^6$ cells/ ml. Aliquots contacting 1ml of cell suspension were transferred into 1.5ml microfuge tubes and centrifuged at 12000g using an Eppendorf 5147R centrifuge (eppendorf). The supernatant was gently aspirated from the tubes without dislodging the cell pellet which was snap-frozen with liquid nitrogen and stored until DNA extraction, at -80°C.

2.1.5 Long-term cryopreservation of cell lines

The cell suspension from the tissue culture flask was transferred into a 25ml universal tube and centrifuged at 1000rpm for 5 minutes. The supernatant was discarded and the cells were resuspended at a concentration of 5-6x10^6 cells/ml in ice cold FCS and left on ice for 10 minutes. Pre-cooled FCS containing 20% DMSO was added drop wise to minimise shock to the cells in an equal volume to the cell suspension. To allow the DMSO to permeate the cells, the universal tube was left on ice for 30 minutes. The cell suspension was transferred to pre-cooled cryopreservation tubes and stored overnight at -80°C, before being transferred into liquid nitrogen for long-term storage.

2.2 DNA extraction

2.2.1 Primary tumour DNA extraction

DNA from formalin fixed-paraffin embedded material (FFPE) was extracted using the QIAamp DNA FFPE Tissue Kit (Qiagen, UK). The FFPE tissue was first dewaxed and digested using 1-2x25µm curls according to the manufacturer's instructions. For samples where frozen material was available the DNeasy kit (Qiagen, UK) was employed, and extraction was achieved following the manufacturer's instructions.

2.2.2 Cell line DNA extraction

DNA from cell line pellets was extracted using the DNeasy kit (Qiagen, UK) according to the manufacturer's instructions and stored in the EB elution buffer provided.

2.2.3 Quantification of extracted DNA

The concentration and quality of extracted DNA was evaluated using the NanoDrop™ Spectrophotometer (Thermo scientific). Using 1µl of sample the spectrophotometer assessed the UV light absorbency (optical density (OD)) at OD_{260} and OD_{280}. DNA molecules show maximum UV light absorbance at OD_{260} and therefore the amount of light absorbed at OD_{260} reflects the concentration of DNA in a sample, and the ratio with OD_{280} give an indication of the DNA quality. Using spectrophotometry to estimate DNA concentration is reviewed by Sambrook et al (Sambrook and Russell 2001). Working stocks of 25ng/µl were prepared and stored at -20°C, and concentrated stocks were stored at -80°C.

2.3 Polymerase chain reaction (PCR)

2.3.1 Introduction

The polymerase chain reaction (PCR) was devised by Mullis and colleagues in 1984, and is a method for the *in vitro* amplification of DNA fragments (Mullis and Faloona 1987). A sample containing DNA is first heated to 95^{o}C so that 2 single strands are produced (denaturation step). The reaction mixture is then cooled so that short amplimers (oligonucleotides of 15-30 bases) hybridise to the target sequence (annealing step). The optimal temperature for the primer annealing depends on the melting temperature of the primers used (50-65^{o}C). The next step (extension step) utilises a thermostable DNA polymerase to catalyse the addition of deoxynucleotides (dNTPs) to the new double strand DNA in a 5' to 3' direction at a rate of 1000 bases per second at 72^{o}C. This cycle yields 2 copies of the targeted DNA, a further cycle will result in 4 double stranded copies. The process is repeated for 30- 40 cycles resulting in an exponential accumulation of PCR product.

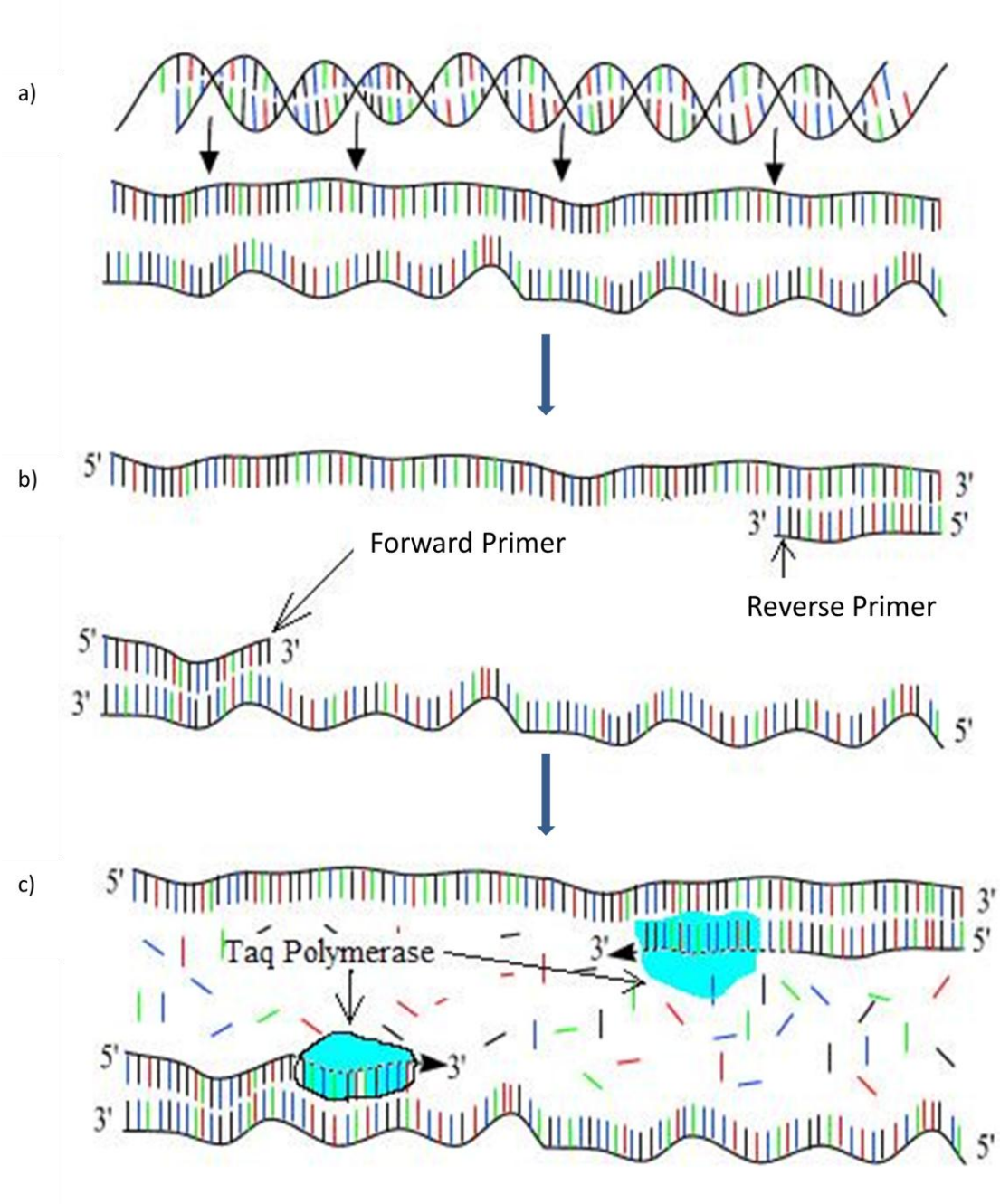

Figure 2.1. The three steps of a PCR reaction. During the first step a) the double stranded DNA is denatured by the reaction being heated to 95°C**.** The temperature is then lowered b) to enable specific primers to anneal to either strand of the single stranded DNA. In the final extension step c) the temperature is raised to 72°C and the DNA polymerase adds complementary dNTPs to synthetise new DNA strands. Figure is adapted from (http://commons.wikimedia.org/wiki/File:PCR_Steps.JPG)

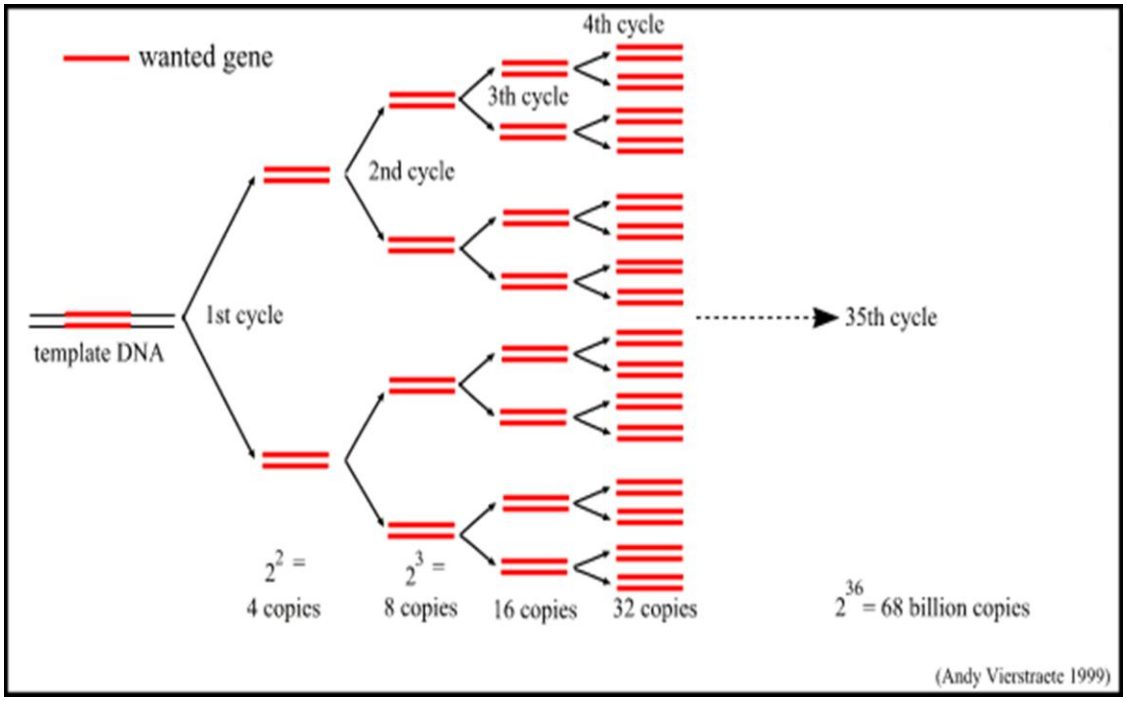

Figure 2.2. The exponential amplification of PCR. From a single starting template after 35 cycles of a PCR reaction 68 billion copies are produced (adapted from: users.ugent.be/~avierstr/principles/pcrsteps.gif).

2.3.2 Primer design

A set of two primers were designed for each PCR reaction which contained complimentary sequences to the region of DNA to be amplified. One primer was designed to bind to the forward DNA strand, and another to the reverse to which DNA polymerase would attach to promote the synthesis of new complimentary DNA strands in the 5' to 3' direction.

Primers were optimised considering the following factors to contain a G/C content of approximately 50%, be of 20-25 nucleotides in length, to avoid complementary regions between the primer pair, and to avoid repetitive sequences to prevent the formation of hairpin loops. All designed primers were reviewed using BLAST (http://blast.ncbi.nlm.nih.gov) and BLAT (http://genome.ucsc.edu) searches to ensure that the resultant amplified PCR products would contain only the correct and unique

sequence. Details of primers used in particular studies are given in the methods of the relevant chapter (see sections 3.2, 4.2 and 5.2).

2.3.3 Standard PCR protocol

For each sample to be tested, 25µl reactions mixtures were set up and volumes were doubled if sequencing was to be performed in PCR tubes containing 2.5µl each of 10µM Forward and Reverse Primer (Invitrogen), 2.5µl of Amplitaq Gold 10 x PCR Buffer (Applied Biosystems), 1.0µl of 5mM dNTPs (Amersham Biosciences), 1.5µl of 25mM MgCl2 (Applied Biosystems), 0.3µl Amplitaq Gold (Applied Biosystems) and 12.7µl of sterile water to a final volume of 22µl. Two microlitres of each cell line or tumour DNA (25ng/µl) were added to individual tubes as outlined in Table 2.5. The tubes were then placed in a GeneAmp PCR System 9700 machine (Applied Biosystems) programmed to perform automated cycles using parameters optimised for each reaction as shown in Table 2.6.

Reagent	**Volume (µl)**	**Final Concentration**	**Source**
Forward primer (10µM)	2.5	1µM	Invitrogen
Reverse primer (10µM)	2.5	1µM	Invitrogen
10 PCR buffer	2.5	-	Applied Biosystems
Magnesium chloride (25mM)	1.5	1.5mM	Applied Biosystems
dNTP (5mM)	1	0.2mM	Amersham Biosciences
Distilled water	12.7	-	ELGA, UK
AmpliTaq Gold (5U/µl)	0.3	0.06U/µl	Applied Biosystems
Genomic DNA (25ng/µl)	2	2ng/µl	-
Total	25		

Table 2.5. Standard PCR reaction reagents. Reagents were added as listed to make a final volume of 25µl.

	Stage 1	Stage 2			Stage 3
		Step 1	Step 2	Step 3	
Process	Denaturation	Denaturation	Annealing	Extension	Elongation
Temperature	95°C	95°C	50-65°C	72°C	72°C
Duration (mins)	5-10	0.5 -1	0.5-1	0.5-1	7
No. Of cycles	1	30-40			1

Table 2.6. Standard PCR conditions. The PCR reactions can be divided into 3 main stages. During the first stage the double stranded DNA is denatured and the *Taq* polymerase activated. The second stage consists of three steps (denaturation, annealing and extension) which are repeated in 30- 40 cycles. In stage 3 the extension step is elongated to enable the completion of all newly synthesised single stands. Following the completion of the PCR the product is cooled for storage to 4°C.

2.3.4 Fast-PCR protocol

Some PCR reactions were performed using a contemporary rapid methodology. The GeneAmp® Fast PCR system (Applied Biosystems) uses a hot start polymerase system that has been optimised to reduce the overall amplification time, reducing the time taken to perform a PCR from 2-3 hours to 20 -30 minutes. For a standard reaction , 10µl of GeneAmp® Fast PCR Mix (2X) was added to 2µl of both 10µM forward and reverse oligonucleotide primers, 50ng DNA template and made up to 20µl with water (Elga). The samples were placed in a GeneAmp PCR System 9800 machine (Applied Biosystems) and the PCR reaction run using the settings shown in Table 2.7. During cycling there is a combined annealing and extension step. The temperature for this step is dependent on the melting temperature of the primers but must be set between 62-72°C for the optimal performance of the GeneAmp Fast PCR Master Mix. The duration of this step is determined by the PCR product length and is set at 25 seconds for every 1000 bases. Details of primers and cycling conditions for each experiment are given in the method sections of chapters 3,4 and 5.

Step	1	2		3	4
	Denaturation & *Taq* activation	PCR Amplification (30-40 cycles)		Elongation	HOLD
		Denature	Annealing & Extension		
Temp	95°C	94°C	62-72°C	72°C	4°C
Time	10-60 sec	0 sec	25 seconds / Kb	10-60 sec	∞

Table 2.7. Fast PCR standard conditions. Conditions programmed into a GeneAmp PCR System 9800 machine (Applied Biosystems). A combined annealing and denaturation step is set at a temperature in between a conventional PCR extension temperature of 72 °C and an annealing temperature based on the melting point of the oligonucleotide primers and is set to continue for a period based on the predicted amplification product size.

2.3.5 PCR product purification

The products obtained after a PCR reaction contain not only the desired amplified sequence but also some low molecular weight sequences including primer excess and additional primer dimer structures. These sequences may impede subsequent sequence analysis and were removed using the PureLink™ PCR Purification Kit (Invitrogen, UK) according to the manufacturer's instructions. The purified PCR products were stored at -20°C before processing.

2.4 Agarose gel electrophoresis

2.4.1 Introduction

Agarose gel electrophoresis is a technique used to separates the product of a PCR reaction, DNA fragments, according to their size. The negatively charged DNA molecules are transported across the agarose gel by the application of an electric current. The migration of larger fragments is reduced by the gel's polysaccharide matrix resulting in separation based on molecular size which may be referenced against DNA ladders producing bands of known sizes. The DNA is visualised by adding ethidium bromide to the gel which intercalates between the bases of the DNA and fluoresces under ultraviolet light illumination.

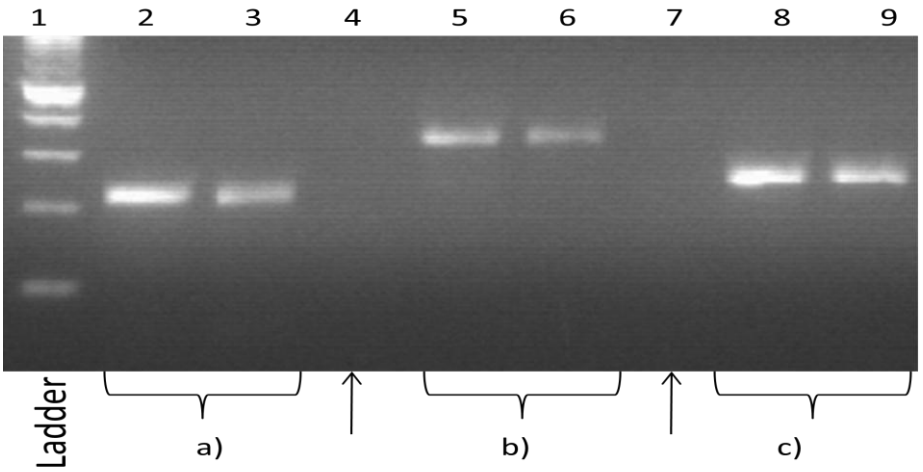

Figure 2.3. Image of a electrophoresis gel stained with ethidium bromide under UV light. Comparing the size of the bands against the standard size marker ladder (Invitrogen, UK) in lane 1 shows the products in lanes a) i 2 and 3 to be 210 base pairs, b) 5 and 6 to be 336 base pairs and c) 8 and 9 260 base pairs. No PCR product is seen in lanes 4 and 7 (arrows).

2.4.2 Standard protocol

Agarose gels were produced at a 2% (w/v) concentration in 1 x TBE buffer. 150ml of 0.1mM Tris, 1M Boric acid, 10mM EDTA buffer (1 x TBE buffer) was added to 3g of agarose (Invitrogen), this solution was heated in a microwave. Two drops of ethidium bromide was added to the molten agarose when cooling which was then set in a gel-casting tray (Gibco) with combs in position to produce wells once the gel set. The PCR product was mixed (4 parts to 1) with Orange G loading buffer (800µl Glycerol, 40µl 0.5M EDTA pH 8.0, 1160µl water and a pinch of Orange G (Sigma)) before being loaded into an individual well on the gel. A Power Pac 3000 (Bio-Rad) was used to run the gel, immersed in a gel tank containing 1 x TBE (see appendix), at 100 volts. Band sizes were determined using a 100bp marker (125µl of 1µg/µl 100bp marker (Invitrogen), 250µl of bromophenol blue loading dye and 875µl 1 x Tris EDTA (TE)) and the gels were photographed using a Bio Vision UV trans-illuminator (Biogene Limited).

2.5 Direct sequencing

2.5.1 Introduction

This method of sequencing, illustrated in Figure 2.4, was devised by Frederick Sanger in 1974 (Sanger, Nicklen et al. 1977). A short oligonucleotide primer first attaches to the DNA template. DNA polymerase and dNTPs are added to the mix so that complementary strands can be produced. In addition however dideoxynucleoside triphosphates (ddNTPs) are added which are dideoxy analogues that lack the 3'OH group necessary for chain elongation.

The new strand synthesis continues until it is terminated by the incorporation of a ddNTP lacking the necessary hydroxyl group for chain elongation. Using the 4 different dideoxy analogues the new strands formed will terminate at all the possible nucleotide positions. The resultant mix will contain new strands of every length. For automated DNA sequencing the ddNTPs are labelled using different fluorescent probes. The sample is passed across a gel and separated according to size by electrophoresis. The samples pass across a laser detector which interprets the fluorescence wavelength and assigns a base at that position.

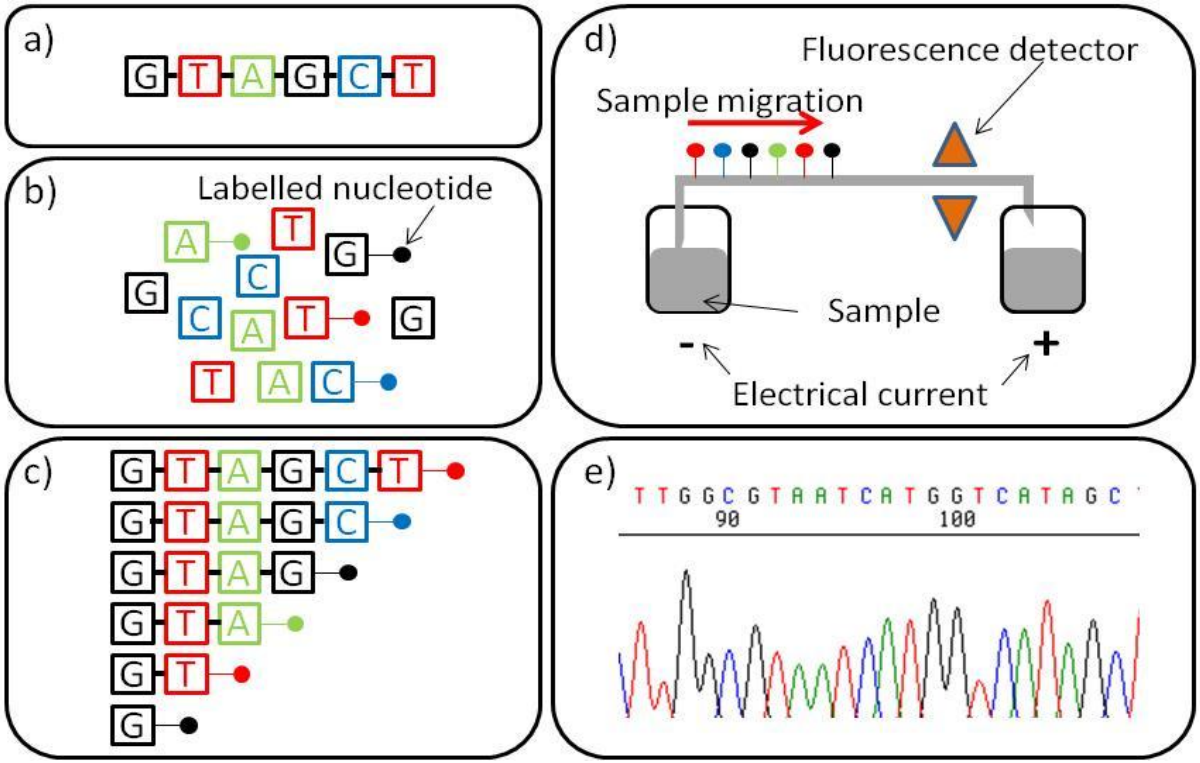

Figure 2.4. Sanger sequencing. The steps involved in sequencing are shown. (a) DNA sequence to be analysed. (b) A mixture of nucleotides are added including labelled dideoxynuceoside triphosphates (ddNTPs) which lack a hydroxyl group necessary for chain elongation so that (c) when incorporated in to the sequence result in sequence termination. The pool of sequences of various lengths, are then (d) passed across an electrical current. Smaller chains pass across first and the terminal labelled ddNTP is detected by a fluorescence detector and (e) an electrophoregram of the sequence is generated.

2.5.2 Standard protocol

PCR reactions were carried out and purified as detailed above (section 2.3). Sequencing reactions were carried out using CEQ 2000 Dye Terminator Cycle Sequencing (DTCS) with Quick Start Kit (Beckman Coulter). The following reagents were added to 0.2ml thin-walled PCR tubes (Abgene): 8μl of DTCS Quick Start Master Mix, 0.5μl of 8μM forward or reverse primer (as used for the original PCR reaction), and 11.5μl of DNA purified using the QIAquick® Gel Extraction Kit. The tubes were run on the following cycle using a GeneAmp PCR System 9700 machine:

96°C for 20 seconds, 50°C for 20 seconds and 60°C for 4 minutes, for a total of 30 cycles, followed by a holding step of 4°C.

The sequencing products were precipitated using the CEQ 2000 DTCS Kit. Four microlitres of stop solution (1.5M NaOAc and 50mM EDTA, prepared by adding equal volumes of 3M NaOAc and 100mM EDTA (Sigma-Aldrich)) and 1μl of 20mg/ml glycogen (Beckman Coulter) were added to 1.5ml eppendorph tubes. The sequencing reactions were transferred to the appropriately labelled tubes and vortexed. Sixty microlitres of ice-cold 95% (v/v) ethanol was added to the tubes, which were immediately centrifuged at 10000g 4°C for 20 minutes in an Eppendorf 5417R Centrifuge. The supernatant removed and the pellets were rinsed twice with 200μl of 70% ice-cold ethanol. The samples were centrifuged at 12000g for 3 minutes and the supernatant carefully removed in between each washing. The pellets were vacuum dried for approximately 40 minutes, to remove all remaining ethanol. Each sample was resuspended in 30μl of sample loading solution (SLS, Beckman Coulter).

Samples were loaded into the appropriate wells on the CEQ sample plates (Beckman Coulter). One drop of light mineral oil (Beckman Coulter) was added to the surface of each sample on the plate. The plate was loaded into the CEQ 8000 Genetic Analysis System™ and processed using the appropriate method program for the size of the PCR product. Sequence traces were analysed using the CEQ analysis software.

2.6 Quantitative real-time PCR (qRT-PCR)

2.6.1 Introduction

A PCR reaction goes through three phases: exponential, rate-limiting and plateau. Quantitative real-time PCR (qRT-PCR) was devised in 1992 to take advantage of these properties to enable the simultaneous amplification and quantification of PCR products (Higuchi, Dollinger et al. 1992). At the start of a PCR reaction reagents are plentiful and the DNA template is at a low concentration so as not to interfere with primer binding, and therefore the PCR amplification proceeds at an exponential rate (the exponential phase). Eventually, when reagents become limited and the concentration of DNA template inhibits primer binding and further template synthesis, the reaction enters a rate-limiting phase. The point at which the reaction exits the exponential phase and enters the rate limiting phase is variable. Finally the formation of product stops and the reaction enters the terminal plateau phase. Analysis of PCR products in the plateau phase can identify the presence or absence of a particular product as in conventional PCR (see section 2.4), but cannot determine the quantity of starting template. Measurement however of the amount of product during the exponential phase of a PCR reaction permits the estimation of the template quantity.

Higushi et al first demonstrated that a PCR method could both simultaneously amplify and quantify PCR products exploiting the characteristics of the exponential phase of a PCR reaction with the addition of ethidium bromide to the reaction reagents (Higuchi, Dollinger et al. 1992). Ethidium bromide intercalates into double-stranded DNA so that the intensity of fluorescence emitted is proportional to the quality of double stranded DNA produced. The fluorescence emitted at the end of every PCR cycle is plotted and a graph plotted which identifies the exponential, rate-limiting and plateau phases, as illustrated by Figure 2.5. If a threshold is set in the exponential phase, then the number of cycles taken to reach a given threshold will be less in samples with a higher concentration of template DNA. The number of cycles required to achieve this threshold is defined as the Ct (cycle threshold). Modern quantitative real-time PCR (qRT-PCR) protocols in preference to ethidium bromide use less toxic chemistries such

as TaqMan™ probes (Applied Biosystems) and SYBR™ green (Molecular Probes) to intercalate with double stranded DNA. Computerised automated platforms also now exist to systematically calculate the level of fluorescence after each cycle. For reviews of qRT-PCR, see (Valasek and Repa 2005; Kubista, Andrade et al. 2006).

2.6.2 Absolute quantification (AQ)

qRT-PCR can be employed to determine the absolute quantity (copy numbers, ng, mRNA) of specific genes within a particular sample using an absolute quantification (AQ) , or standard curve method (reviewed in Bustin 2000). For this approach a sample of known concentration is first serially diluted to produce a series of samples of known concentration. A standard curve is then generated for each target gene and endogenous control by plotting the initial concentration of each sample against the qRT-PCR cycle number at which the Ct is reached (Figure 2.6). The quantity of a specific gene in an unknown sample can then be calculated by interpolation of the standard curve using the Ct value of the target gene and endogenous control in the unknown sample. The target gene is normalised to the endogenous control to account for sampling issues and then determine the absolute quantity of the target gene in the unknown sample.

The slope of the standard curve can be used to measure the efficiency of the reaction primers. If the primers are 100% efficient the amount of PCR product should double with every cycle in the exponential phase. If then the results from a 10-fold serial dilution are plotted, as on a standard curve, the individual Ct values should differ by 3.32 cycles. The slope of a standard curve from -3.2 to -3.6 therefore represents primer efficiencies in the range of 90-100%.

Following the PCR reaction the AQ method performs a dissociation step which can be used to assess primer specificity (Figure 2.7). During this step the PCR products are heated from 60°C by 1°C every 15 seconds up to 95°C and the amount of fluorescence recorded. When the new double stranded molecules become denatured

the fluorescence intensity falls and a bell shaped dissociation plot produced. Due to the unique biochemical properties of individual sequences each PCR product has a specific dissociation temperature (Tm). Using non-specific primers will therefore result in multiple dissociation curves for each product produced rather than the single curve seen when primers bind to a single specific template region.

2.6.3 qRT-PCR primer design

Primers were designed with Dr Sarra Ryan (Northern Institute Cancer Research) to cover all transcript variants of a specific gene found using the NCBI and Ensembl genomic databases (www.ncbi.nlm.nih.gov, www.ensemble.org). PrimerExpress® software (Applied Biosystems, UK) was used to design the qRT-PCR primers with amplicons of 50-150 base pair, a Tm of 58-60°C, and have a G/C content of 30-80%. The primers were then checked using BLAST (www.ncbi.nlm.nih.gov) and BLAT (www.genome.ucsc.edu) searches to determine their uniqueness. Concentrated primer stocks (Sigma, UK) were made up to 100nmol with Purelab Ultra water (ELGA, UK) and stored at -80°C, and 10nmol working solutions aliquots were stored at -20°C. Primer specificity was initially assessed by performing a conventional PCR (section 2.3.3) and identifying products on an electrophoretic gel (section 2.4.2). A dissociation curve was subsequently generated using the AQ method (section 2.6.2) to test for non-specific products. Nucleic acid sequences of primers used in this study will be provided in the relevant methods sections.

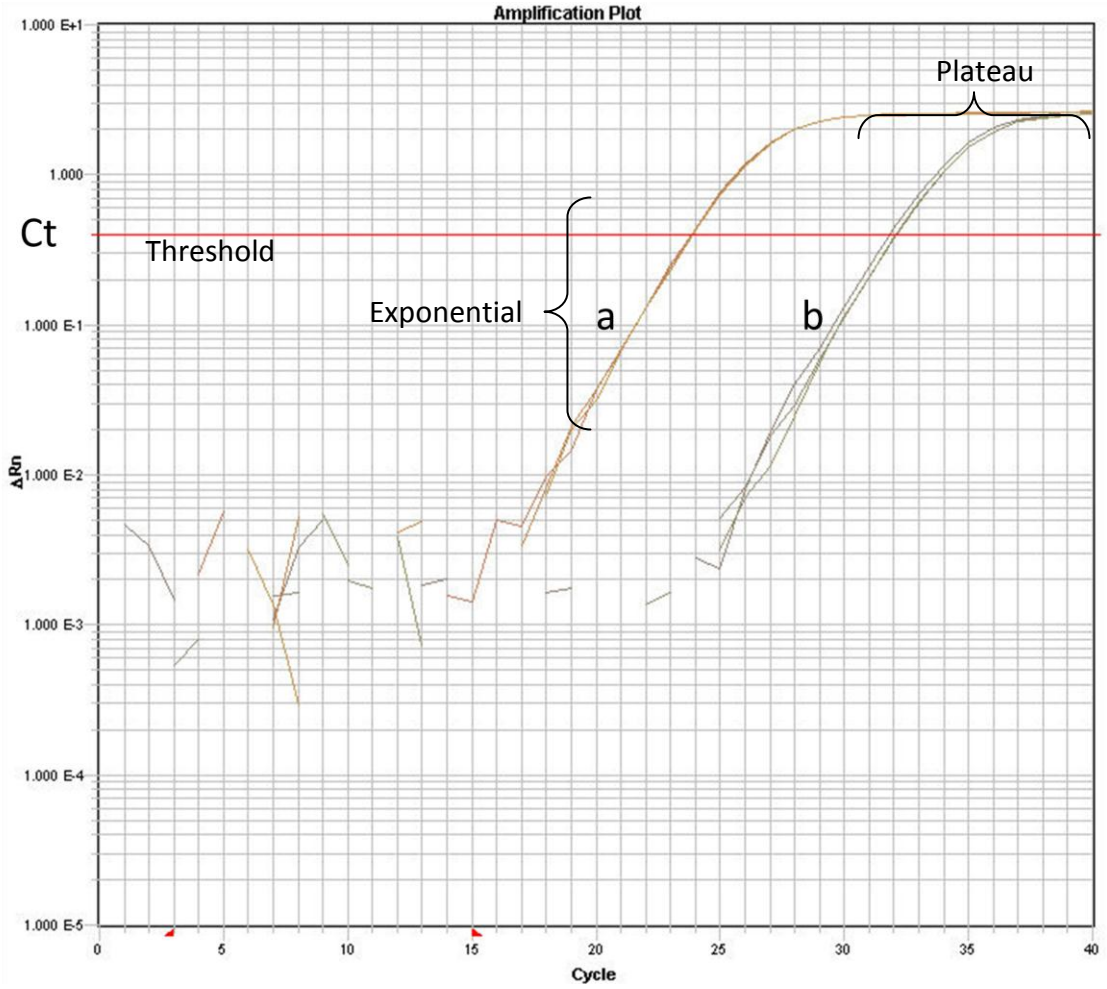

Figure 2.5. An amplification plot produced from a qRT-PCR assay. The number of cycles required to achieve the cycle threshold (Ct) for samples (a) and (b) repeated in triplicate is shown. The Ct is set during the exponential phase of product amplification. Sample (a) consistently requires fewer cycles to achieve Ct compared to (b) which suggests an elevated initial sample template.

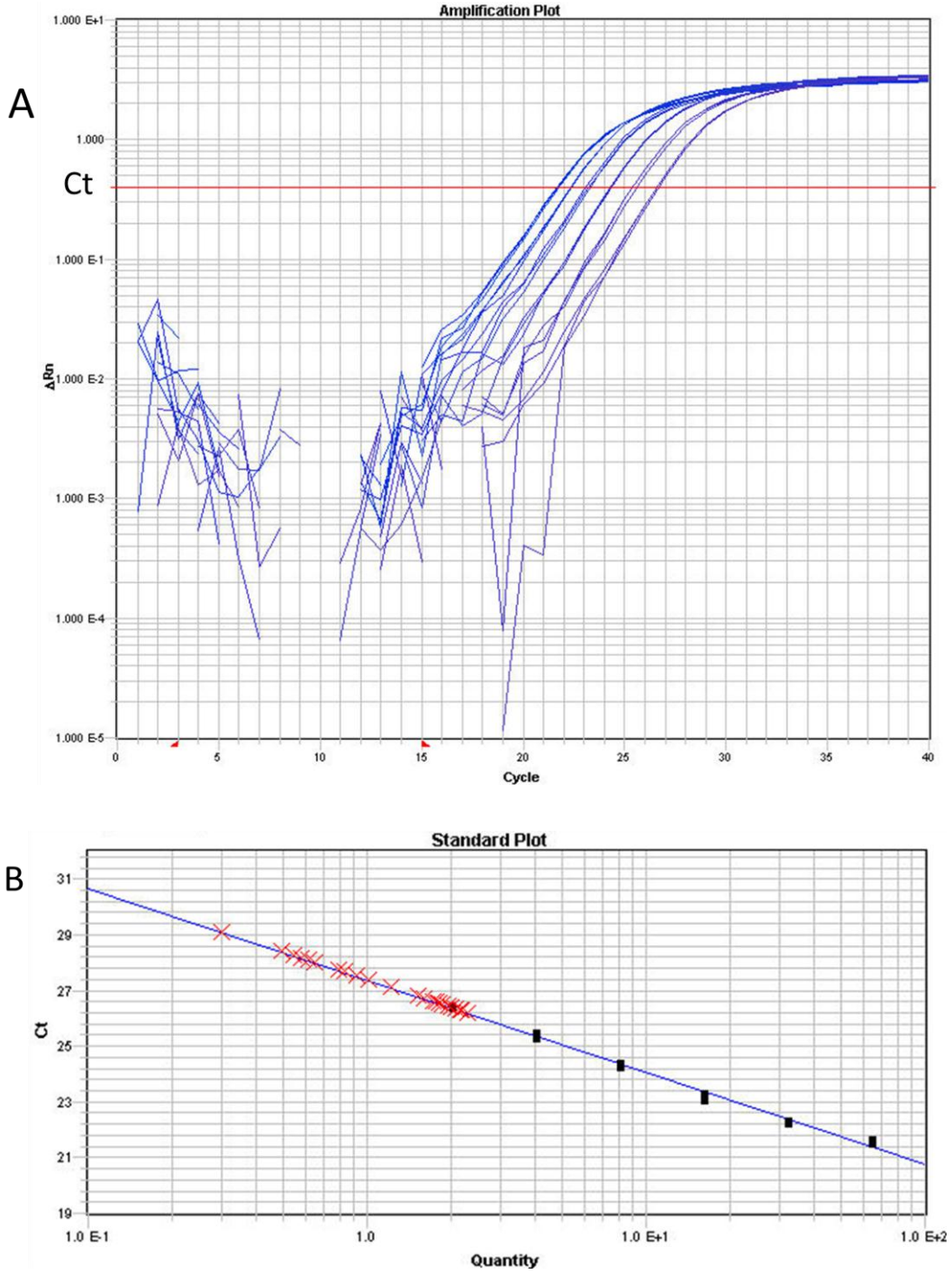

Figure 2.6. The development of a standard curve in a qRT-PCR assay. (A) qRT-PCR is performed on a serial dilution of a control sample at a known concentration which results in the samples with a higher-fold initial template achieving the cycle threshold (Ct) with fewer PCR cycles. (B) A standard curve for the primer set shown in (A). The slope coefficient is -3.2 showing the PCR efficiency to be almost 100%. The number of cycles required to achieve the Ct value is plotted on the y-axis and the amount of template DNA on the x-axis. Plots in red record the results of test samples with an unknown starting template concentration which can now be calculated by interpolating the standard curve.

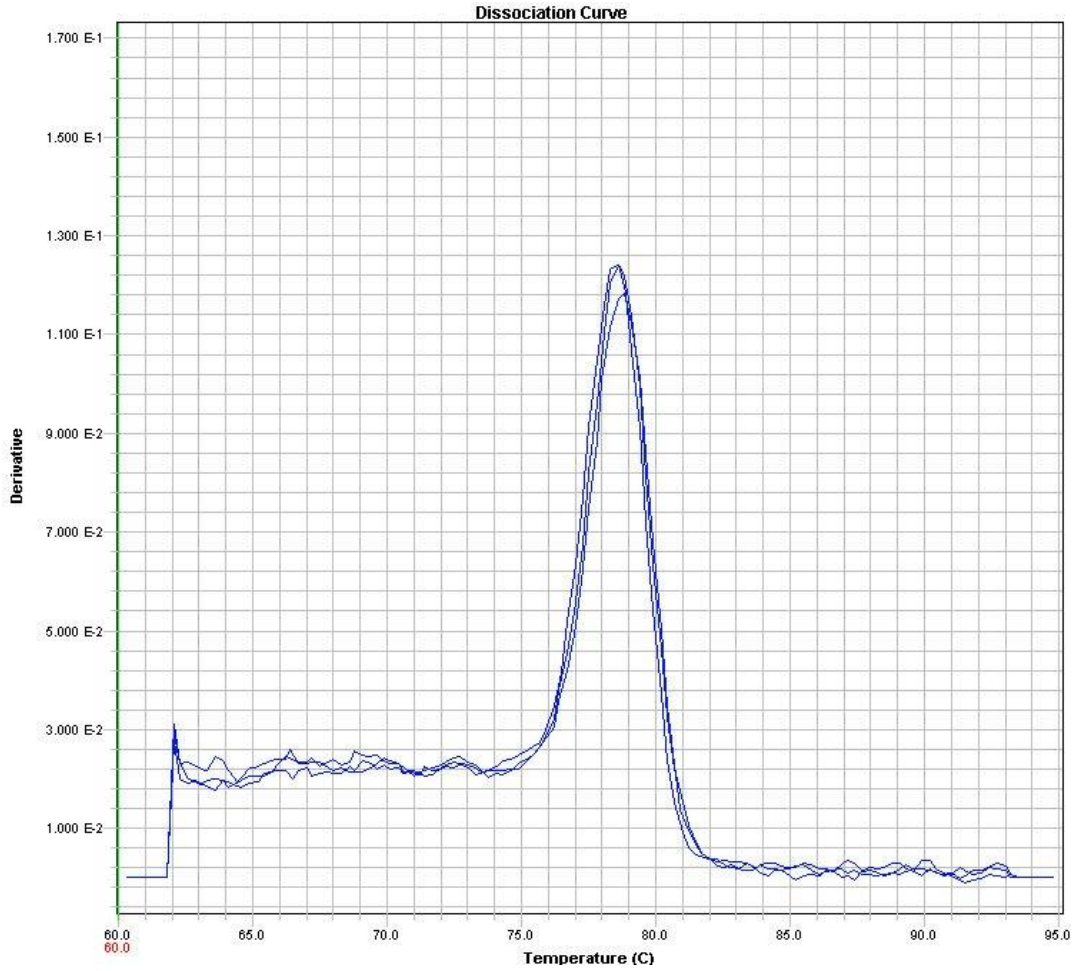

Figure 2.7. A dissociation curve produced from a qRT-PCR assay. The dissociation curve for a single gene repeated in triplicate on one sample is shown. A single product is produced with a Tm of 78°C.

2.6.4 Standard protocol

QRT-PCR was performed on an ABI PRISM 7900HT instrument (Applied Biosystems, UK) using the reagents and reagent concentrations shown in Table 2.8. The assays were performed in 384-well plates (Applied Biosystems, UK) which were covered with adhesive lids (Applied Biosystems, UK). All samples were assessed in triplicate in a single experiment, and where copy number alterations were observed the experiment was repeated on two further occasions to corroborate the finding. On each plate a

negative control containing Purelab Ultra water (ELGA, UK) and a cell-line DNA positive control was added. Standard cycling conditions were as outlined in Table 2.9. The data generated was analysed using SDS version 2.2 (Applied Biosystems) and converted into Excel®2007 (Microsoft) format for normalisation and further analysis.

Reagent	Volume (µl)	Final Concentration	Source
SYBR green (+Rox)	5.1	-	Invitrogen, UK
Forward primer	0.2	-	VhBio, UK
Reverse primer	0.2	0.2µM	VhBio, UK
Purelab Ultra Water	0.5	0.2µM	ELGA, UK
Genomic DNA	4	variable ng/µl	-
Total	10		

Table 2.8. Standard qRT-PCR reaction reagents. The addition of the Rox reference dye reduces the background noise by normalising non-PCR fluorescent fluctuations

	Stage 1	Stage 2	Stage 3		Stage 4		
			Step 1	Step 2			
Process	UDG Activation	Denaturation & *Taq* activation	Denaturation	Annealing & Extension	Dissociation		
Temperature	50°C	95°C	95°C	60˚C	95°C	60˚C	95˚C
Duration	2 min	10 min	15 sec	1min	15sec	20 sec	15 sec
No. Of cycles	1	1	40		1		

Table 2.9. Standard qRT-PCR conditions.

2.7 Loss of heterozygosity (LOH) assessment

2.7.1 Introduction to LOH

Loss of heterozygosity (LOH) is a frequent finding in tumours and indicates the loss of one of the two alleles of a gene in a cell. By screening paired blood and tumour samples and identifying differences, genome-wide scanning techniques which identify regions of LOH have been used to identify narrow regions of chromosomal loss for further investigation which in turn may harbour tumour suppressor genes (Strachan and Read 2004). The identification of LOH can be undertaken using polymorphic microsatellite markers. Microsatellites are short polymorphic nucleotide repeat sequences consisting of di-, tri-, or tetra- nucleotide repeats (eg; CACACACA, or CAGCAGCAGCAG, or CAGTCAGTCAGTCAGT). The number of repeats present is polymorphic and therefore for a given microsatellite the number of repeats inherited on each allele is likely to be different. If this region were amplified by using flanking primers in a PCR reaction, yielding two products would suggest the retention of both alleles, whilst the production of a single product in a tumour sample where two are seen in the constitutive DNA, would indicate a loss of heterozygosity.

2.7.2 The HOMOD method

Homozygous mapping of deletions (HOMOD) is a technique used to identify LOH without using constitutive DNA as a comparator. HOMOD uses a statistical approach to identify extended regions of homozygosity (ERH) with polymorphic satellite markers. The frequency of heterozygosity for each marker in the general population is known and details may be obtained from databases including the Marshfield Clinic Research Foundation (http://research.marshfieldclinic.org/genetics/GeneticResearch/). The probability of a number of consecutive markers being homozygous is calculated by multiplying the homozyosity scores (1 - heterozygous probability) of each marker together. LOH is recorded when the probability of homozygosity at contiguous markers

is ≤0.001, which is typically equivalent to ≥5 adjacent homozygous markers (Goldberg, Glendening et al. 2000).

2.7.3 Primer design

Polymorphic markers covering the chromosomal region to be investigated were identified from the Marshfield Research Foundation website (http://research.marshfieldclinic.org/genetics/GeneticResearch/). The markers were then entered into the National Center for Biotechnology Information (NCBI) Uni-STS database from which details of the nucleotide primer sequences and PCR product sizes for each marker were derived. The forward oligonucleotide primer of each set was labelled with a fluorescent dye, WeLLRED, at the 5' end (Sigma-Proligo, France). Further details of the primers used in HOMOD studies are described in (section 3.2.6)

2.7.4 Standard protocol

PCR products for each marker were generated using primers described in section 3.2.6 and methods described in section 2.3.3. Products were subsequently analysed using the CEQ 8000 Genetic Analysis System (Beckman Coulter) by loading 0.5µl PCR product onto a 96 well plate (Beckman Coulter) and adding 40µl sample loading solution (SLS, Bekman Coulter), and 0.5µl 400 size standard (Beckman Coulter). A fragment analysis installed programme was run (Frag-4) according to the manufacturer's instructions. As described in paragraph 2.5.2 and illustrated on Figure 2.4, this system involved the PCR products travelling across a fluorescent sensor during electrophoresis. Smaller products labelled with the WeLLRED dye were detected by the sensor at an earlier stage, resulting in a peak in fluorescent intensity. By labelling different PCR primers of different sizes with altering coloured WeLLRED tags up to 3 samples were loaded into the same well of a plate and analysed together (Figure 2.8). A fragment analysis

programme was subsequently run on the CEQ8000 Analysis System (Beckman Coulter) to convert the raw data into interpretable traces.

2.7.5 Interpretation of results

The results are interpreted by recognising the specific pattern that each polymorphic microsatellite produces as shown in Figure 2.9, In addition the pattern of nucleotide repeats for each microsatellite (mono, di, tri, tetra) is also considered. The presence of a single major peak suggests homozygosity at that marker. More than one peak may however still be interpreted as homozygous, if it is the characteristic pattern of a particular marker to produce a number of minor peaks to represent a major peak. Minor peaks always occur within 2, 3 or 4 base-pairs of the major peak of a mono, di, tri, or tetra nucleotide repeat marker respectively. In addition, a second peak is only considered to be a major peak if it is at least 30% of the size of the main peak. Taken together samples are assigned as being homozygous for a particular marker if there is a single peak, or if additional peaks are less than 30% of the size of the major peak. Heterozygosity is assigned if two peaks whose height measure within 50% of each other are observed. Where the peak heights fall between 30 and 50% of each other a non-informative assignment is made, and the experiment for that sample repeated.

Details of the polymorphic microsatellite markers used in this study are described in section 3.2.6.

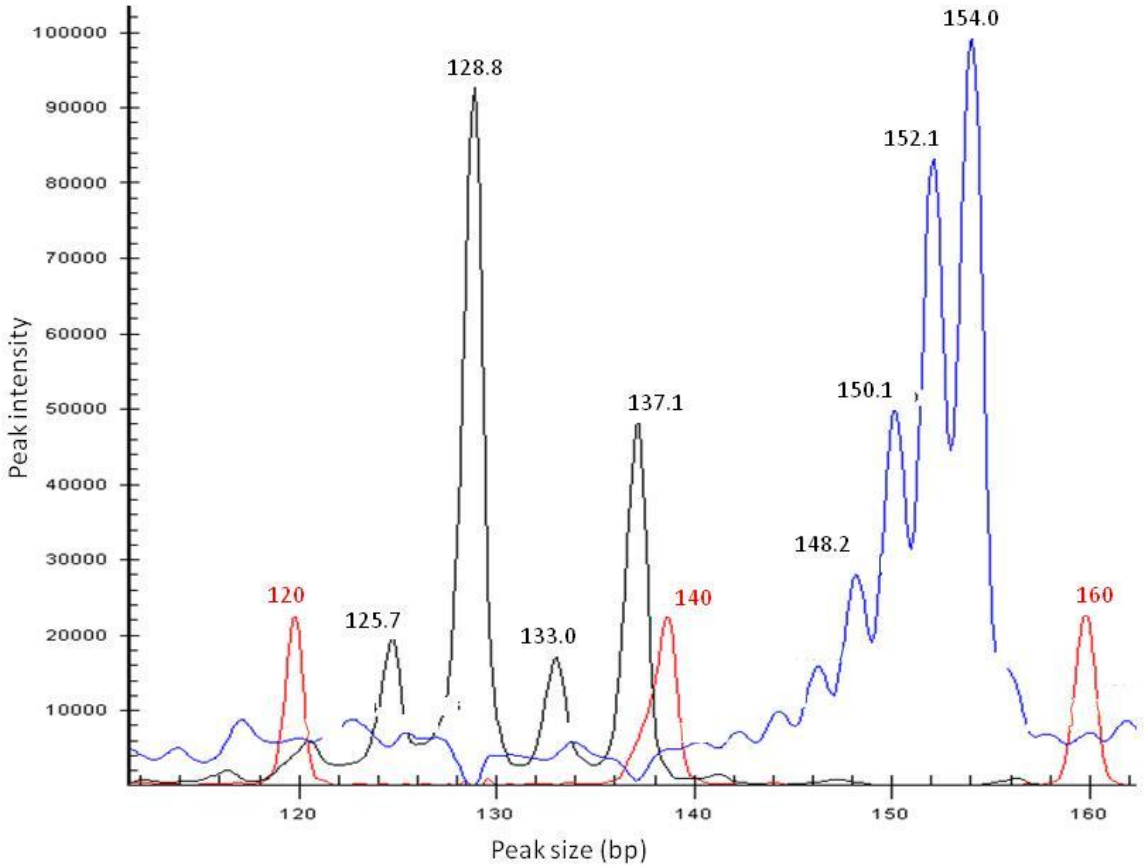

Figure 2.8. HOMOD trace. For this sample two different polymorphic microsatellite markers have been analysed simultaneously. D17S969 (black) shows 2 major peaks (128.8 and 137.1) more than 3 base pairs apart indicating a retention of heterozygosity at this locus. The trace in blue shows the result for the tetra-nucleotide marker D17S1866. This marker produces a characteristic pattern of 4 minor peaks. These minor peaks constitute a single major peak suggesting homozygosity at this locus. Standard size markers are shown in red.

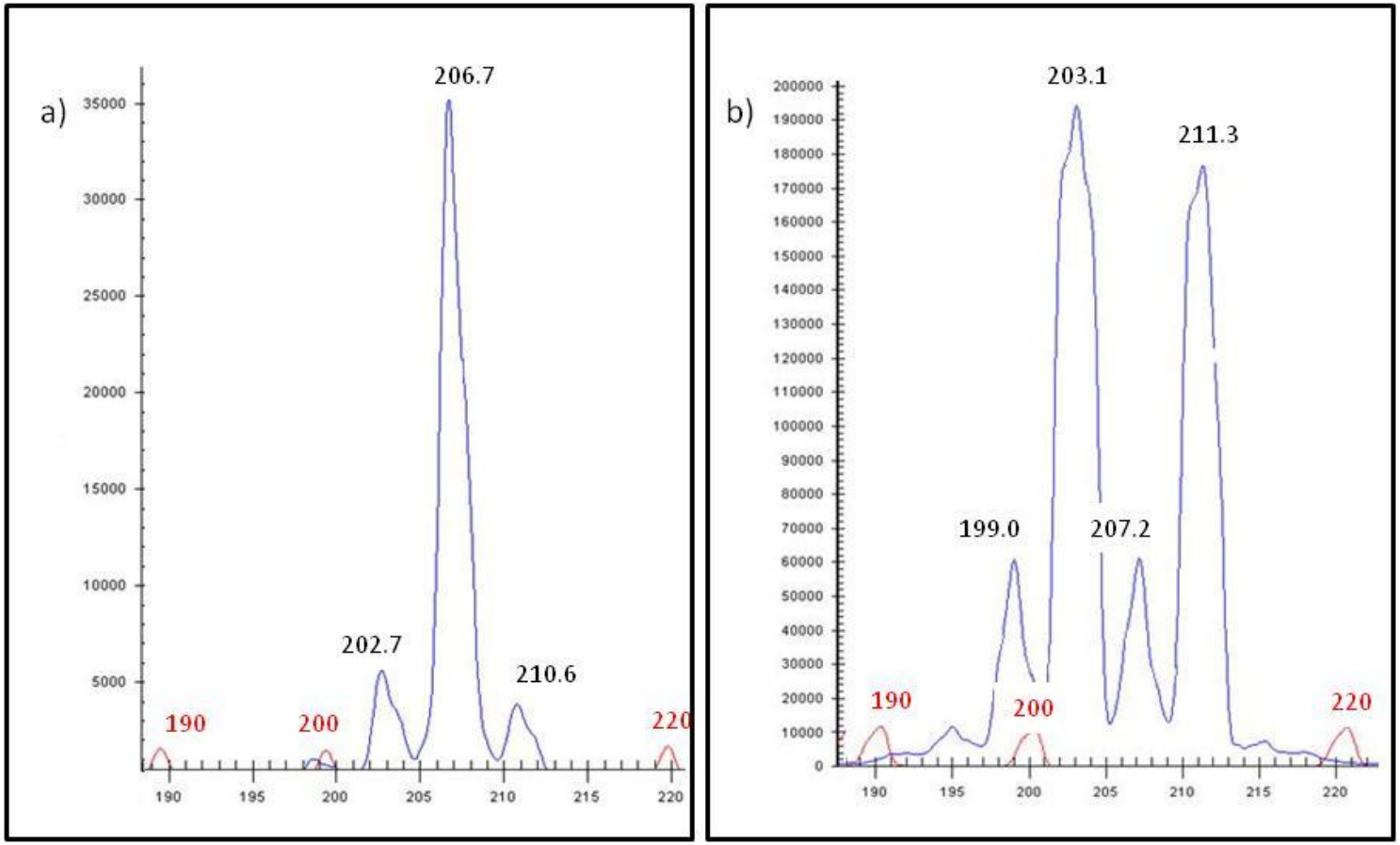

Figure 2.9. Fragment analysis traces at a polymorphic microsatellite site. Analysis using dinucleotide polymorphic microsatellite marker D17S974.(a) A single major peak (206.7) is produced suggesting homozygosity at this locus. (b) Heterozygous trace. The marker produces a major peak for each allele positioned more than 3 base pairs apart (203.1 and 211.3). Standard size markers are shown in red.

2.8 Multiplex ligation-dependent probe amplification (MLPA)

2.8.1 Introduction

Multiplex ligation-dependent probe amplification (MLPA) is a multiplex PCR based method first described in 2002 that can be employed to detect abnormalities in genomic DNA or RNA copy number (Schouten, McElgunn et al. 2002). Probes can also be designed to incorporate known mutation sites and epigenetic methylation changes using methylation-specific MLPA (MS-MLPA)(Eldering, Spek et al. 2003). Crucially because it is a multiplex technique up to 50 different sequences may be interrogated within a single reaction with only 20-100ng DNA or RNA template.

The MLPA reaction is divided into five steps: (1) DNA denaturation and hybridisation of MLPA probes, (2) ligation reaction, (3) PCR reaction, (4) separation of amplification products by electrophoresis, and (5) data analysis, as shown in Figure 2.10. The DNA is first denatured and hybridized with two separate oligonucleotide MLPA probes. The two oligonucleotide probes are designed to hybridize at immediately adjacent regions on the template DNA and also contain one of the PCR primer sequences. A ligation reaction is then performed. Crucially only ligated sequences will contain both PCR primer sequences, and therefore only these will be amplified and produce a signal in the subsequent PCR reaction (see section 2.3).

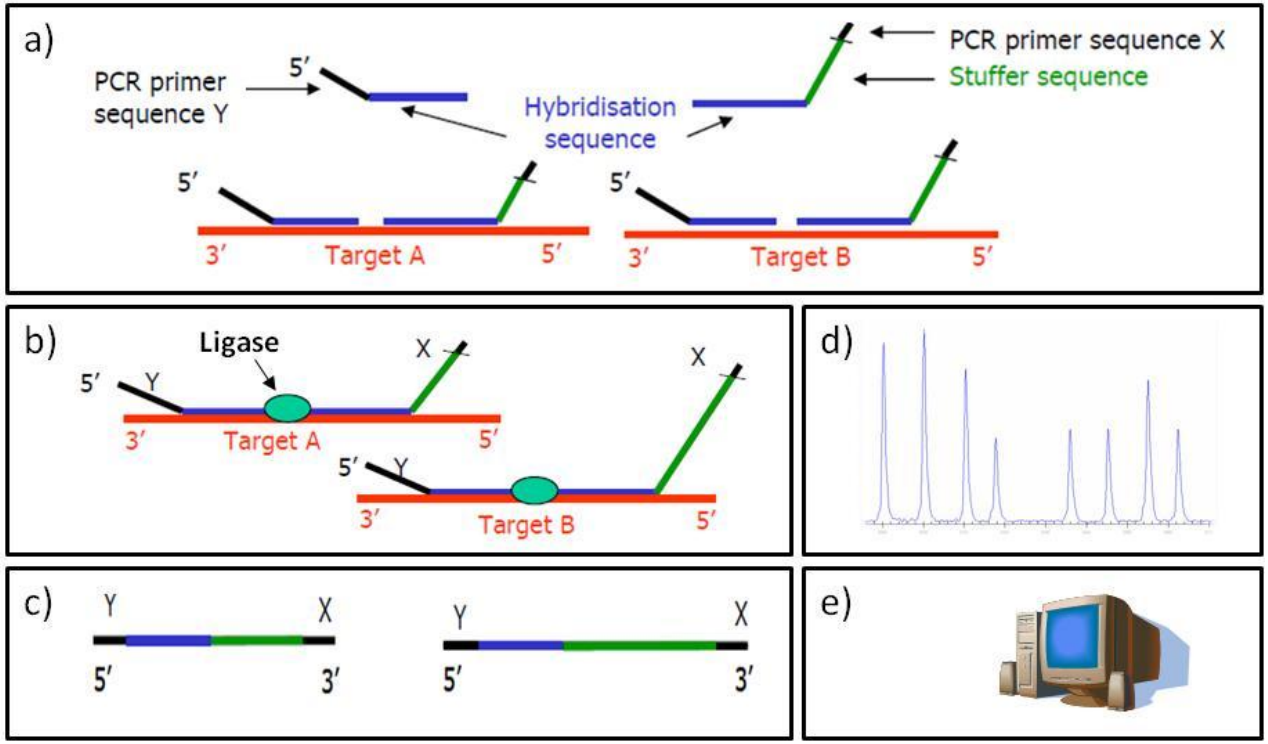

Figure 2.10. The 5 stages of MLPA. (a)DNA denaturation and hybridisation of MLPA probes: Two probes with a complementary sequence to the target DNA hybridise adjacent to each other. Attached towards the 3' end of the probe is a non-hybridising stuffer sequence which elongates the final product to a pre-determined length. At the 5' and 3' ends are common MLPA primers; (b) Ligation: The adjacent probes are joined together (c) PCR amplification: The ligated sequence is the amplified using the common PCR primers (X and Y), (d) Electrophoresis: The MLPA product is run on a Beckman-Coulter Genetic analysis system and each product length is determined using a fragment analysis programme. (e) Data analysis: The results are subsequently analysed in comparison to normal controls using GeneMarker®software to determine copy number changes. (Figure adapted from (Schouten, McElgunn et al. 2002))

2.8.2 Primer design

The sequences of genes to be investigated were obtained from http://www.ncbi.nlm.nih.gov/sites/entrez?db=gene. Probes were designed with Dr Matthew Allan (Northern Institute for Cancer Research) following the guidance provided by MRC-Holland (MRC-Holland 2009) and manufactured by Metabion (Germany). Each MLPA probe consisted of a left probe oligonucleotide (LPO) and a right probe oligonucleotide (RPO). The MLPA probes were designed to be 100-140 nucleotides in length, with the length of each probe being at least 4 nucleotides different from any other probe to facilitate distinct fragment separation and avoiding lengths of probes already contained in the normalisation probe mix. Each MLPA probe contained PCR primers comprising 42 base pairs and therefore the left and right hybridising sequences (LHS and RHS) combined with a stuffer sequence were designed to be 58-98 base pairs in length (optimal MLPA probe length – PCR primer length) . The structure of an MLPA probe is outlined in Figure 2.11. The LHS and RHS sequences were reviewed using BLAST (http://blast.ncbi.nlm.nih.gov) and BLAT (http://genome.ucsc.edu) searches to ensure that following hybridisation and subsequent PCR amplification that the resultant products would comprise only the correct and unique sequence. Details of the MLPA probes designed and used in the study are given in (sections 3.2.7.4 and 3.2.8.5).

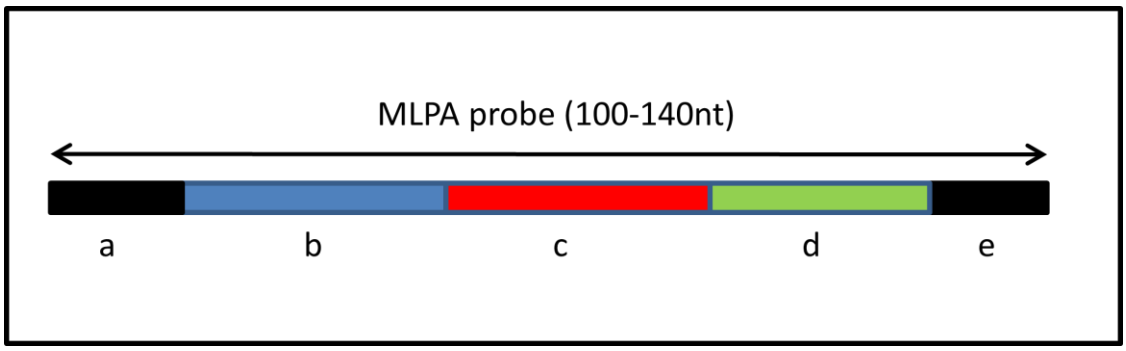

Figure 2.11. Schematic representation of a MLPA probe. An optimal MLPA probe following ligation is between 100 and 140 nucleotides in length. It comprises two standard PCR primers (a) and (e) of 42 nucleotide in length. The combination of the (b) left hybridising sequence (LHS), with the (c) right hybridising sequence (RHS), and a stuffer sequence (d) must measure between 58 and 98 nucleotides.

2.8.3 Standard protocol

All probes and reagents used in the MLPA reactions were supplied by MRC-Holland. The probes were provided at a concentration of 20nM and were diluted with 200µl TE (see Appendix) to make 100µM stock solutions which were stored at -20°C. Working aliquots of 1 µM of each probe were made by diluting 10µl stock solution with 1ml TE and stored at -20°C.

In the first step, 50-200ng (5µl) sample DNA was first denatured by heating aliquots in PCR tubes in a GeneAmp PCR System 9700 thermal cycler (Applied Biosystems) to 98°C for 5 minutes. This was then left to cool to room temperature before the MLPA SALSA probe mix was added (detailed in Table 2.10). In a GeneAmp PCR System 9700 thermal cycler (Applied Biosystems) the mix was incubated at 95°C for 1 minute, and then heated at 60°C for 16 hours to enable hybridisation to occur. Following hybridisation the temperature of the thermal cycler was reduced to 54°C and 32µl of ligation mix (Table 2.10) was added which was then incubated at 54°C for 15 minutes followed by 98°C for 5 minutes in the thermal cycler. In a separate PCR tube a mix containing 4µl SALSA PCR buffer and 26µl of PureLab Ultra water (ELGA, UK) was prepared to which 10µl of the ligation reaction product was added. The tubes were

incubated in a GeneAmp PCR System 9700 thermal cycler at 60°C to which 10µl of a polymerase mix (Table 2.10) was added before proceeding with the MLPA PCR programme (Table 2.11). Samples containing 40µl sample loading solution (Beckman Coulter), 0.5µl 400 size marker (Beckman Coulter) and 1µl PCR product were subsequently loaded into the appropriate wells on the CEQ sample plates (Beckman Coulter). One drop of light mineral oil (Beckman Coulter) was added to the surface of each sample on the plate. The plate was loaded into the CEQ 8000 Genetic Analysis System™ and processed using the MLPA installed software programme (MLPA). The data generated was downloaded and analysed initially using GeneMarker® version 1.75 (Softgenetics). The peak intensity of all probes including the control probes within a sample was derived. This data was then transferred to an Excel® 2007 (Microsoft) format and the intensities of the test probes relative to a series of control probes calculated. Details of the probes used can be found in (sections 3.2.7.4 and 3.2.8.5).

a)

Reagent	Volume (µl)	Source
P200	1	MRC-Holland
Synthetic Probemix	0.5	MRC-Holland
MLPA Buffer	1.5	MRC-Holland

b)

Reagent	Volume (µl)	Source
Ligase-65 buffer A	3	MRC-Holland
Ligase-65 Buffer B	3	MRC-Holland
PureLab Ultra Water	25	Elga, UK
Ligase-65	1	MRC-Holland

c)

Reagent	Volume (µl)	Source
SALSA PCR primers	2	MRC-Holland
SALSA Enzyme dilution buffer	2	MRC-Holland
PureLab Ultra water	5.5	Elga, UK
SALSA Polymerase	0.5	MRC-Holland

Table 2.10. Reaction reagents prepared on ice in a standard MLPA experiment. (a) Constituents of a hybridisation reaction to which 5µl denatured DNA template is added. Following hybridisation a ligation reaction is performed to which the (b) ligation mix is added. After ligation a PCR step is performed requiring a 10µl ligation reaction product aliquot to be combined with (c) a polymerase mix.

	Stage 1			Stage 2	Stage 3
	Step 1	**Step 2**	**Step 3**		
Process	Denaturation	Annealing	Extension	Elongation	Hold
Temperature	95°C	60°C	72°C	72°C	15°C
Duration	30 seconds	30 seconds	1 minute	20 minutes	∞
No. Of cycles	35			1	∞

Table 2.11. MLPA PCR program conditions. Prior to commencing the PCR program samples were kept at 60°C whilst a polymerase mix was added.

2.9 Fluorescence *in situ* hybridisation (FISH)

2.9.1 Introduction

Fluorescence *in situ* hybridisation (FISH) is a cytogenetic technique employed to detect the presence or absence of chromosomal abnormalities including changes in copy number and structural rearrangements which affect the DNA sequence. Probes are designed to be complimentary to the specific region under investigation. The technique then involves hybridizing, either directly or indirectly the fluorescently labelled DNA probes to interphase nuclei or metaphase chromosomes. Using a fluorescence microscope the detection of genetic sequences may then be viewed within a cellular context.

Probes may be labelled directly or indirectly with fluorophores by a variety of methods. In a technique referred to as nick translation some of the nucleotides from a DNA sequence are replaced using DNA Polymerase I with fluorescently labelled analogues. In addition to direct labelling techniques which involve the attachment of fluorophores to a nucleic acid probe indirect techniques may be employed where the nucleic acid probe binds to a non-fluorescent molecule such as biotin and digoxigenin. With indirect techniques following *in situ* hybridisation of non-fluorescent probes to cells, a fluorophore-labelled antibody or avidin is applied which provides the fluorescent signal.

The steps involved in a typical FISH experiment are illustrated in Figure 2.12. For a detailed review of FISH, see (Fan 2002; Gorczyca 2008).

Bacterial artificial chromosomes (BACs) are vectors derived from *E.coli* bacteria which are often used to develop probes for FISH studies. The BACs contain foreign DNA fragments of 100-200kb into which probe DNA sequences can be incorporated and subsequently inserted into *E.coli* bacteria by electroporation. The advantage of this system is that with growth the transformed bacteria will produce a large amount of cells containing the probe in a short period which can be harvested when the cells are lysed and the DNA content purified. For a detailed review of BAC cloning, see (Birren, Green et al. 1999)

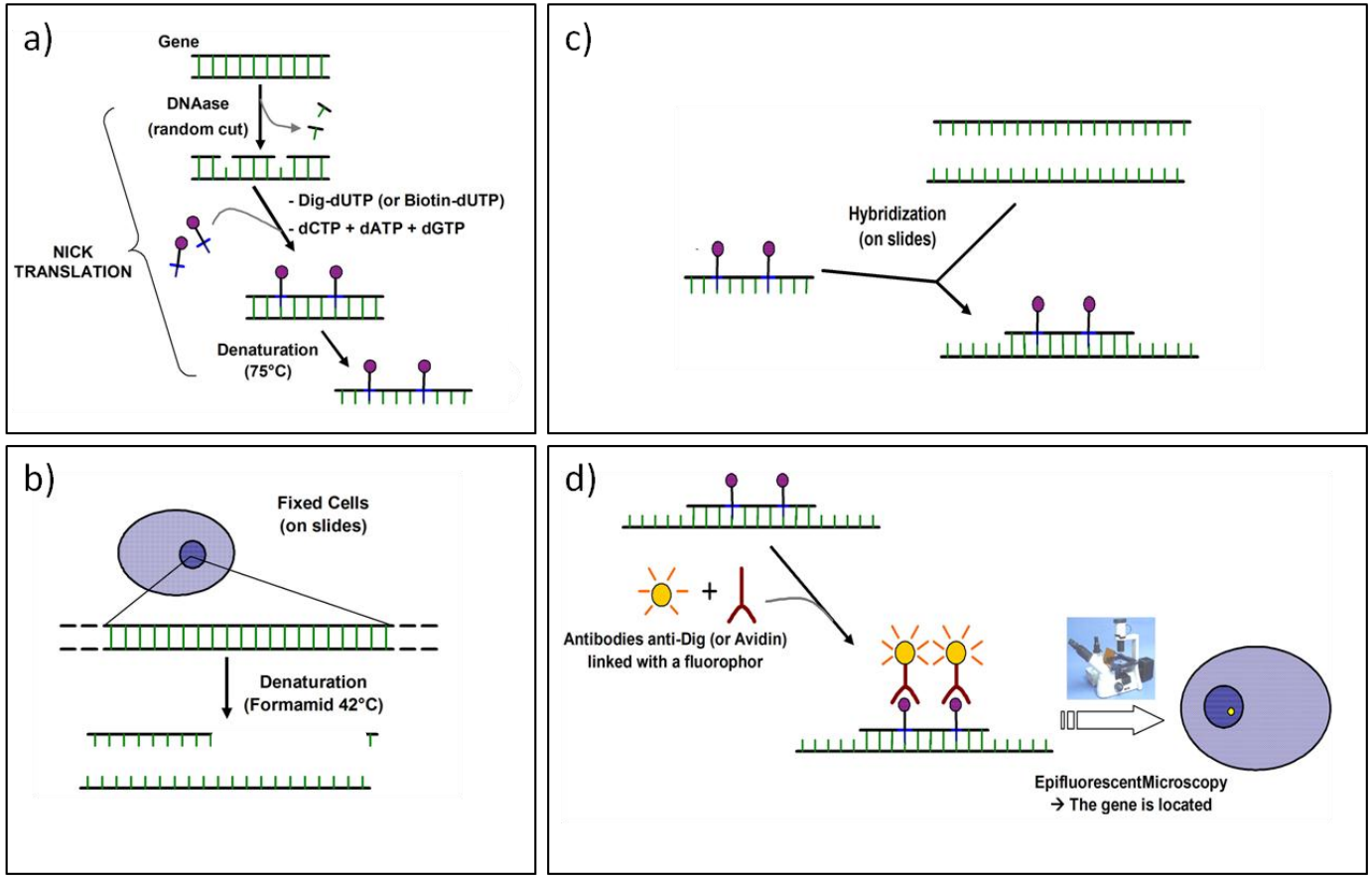

Figure 2.12. Scheme showing the principle of indirect FISH. a) A DNA probe is labelled with a non-fluorescent molecules preparation and a slide is prepared b) with fixed cells, to which c) the probe hybridizes. Antibodies to the probe are then applied d) which are linked to fluorescent molecules which allows the material to be viewed under a fluorescent microscope. (Adapted from www.en.wikipedia.org/wiki/fluorescent_in_situ_hybridization).

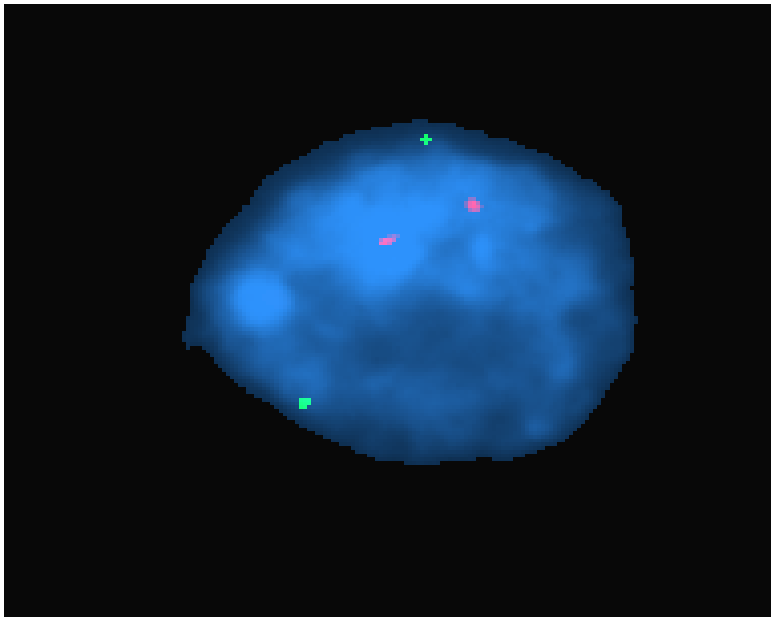

Figure 2.13. Fluorescence in situ hybridisation composite image showing a normal cellular diploid copy number of *MYCN*. Image captured using a fluorescence microscope with a excitation wavelength of 540nm to capture the Texas red labelled centromeric probe, and a 490nm to capture the *MYCN* Fluorecein isothiocyanate labelled (green) probe.

2.9.2 Slide preparation

All FISH studies were performed using FFPE material. Where available 10µm sections were cut from a FFPE tissue block and fixed to microscope slides (Nunc) by baking at 60°C for 5 minutes. Before using in the FISH studies the fixed sections were dewaxed by placing them in xylene for 5 minutes and rehydrating them through an alcohol graded series of ethanol baths (100% (v/v), 80% (v/v), 70% (v/v), 50% (v/v)) for a minute each. To each slide 400µl of 0.5% pepsin (Sigma-Aldrich, UK) in 0.1M HCl was applied. The slides were then incubated in a humidified chamber for 2 hours at 37°C before being washed in 37°C water and immersed in PBS (see Appendix) for 5 minutes at 37°C. The slides were then rehydrated by descending through a series of ethanol baths (95% (v/v), 85% (v/v) and 75% (v/v)) and left to dry for 5 minutes before applying the probe.

To perform FISH on isolated nuclei a single 25µm section curl of FFPE tissue was placed in a 1.5ml microfuge tube containing xylene to dewax. The xylene was then aspirated and the tissue resuspended in ethanol before being centrifuged at 12000g for 5 minutes in an Eppendorf 5147R centrifuge (Eppendorf). This process was repeated to facilitate the removal of all xylene from the suspension. The cycle was repeated a third time with the tissue resuspended in PBS before being passed through a 70µm mesh cell strainer (Fisher) at 1000g in a pre-cooled to 4°C Eppendorf 5147R centrifuge (Eppendorf) for 10 minutes. The resultant isolated nuclei were then centrifuged at 1000g for 10 minutes onto microscope slides (Nunc) using a Cytospin 2 centrifuge (Thermal Scientific). The slides were stored at -20°C until used at which time they were warmed in a 37°C water bath for 10 minutes before 100-200µl of pepsin (Sigma-Aldrich) solution (4mg/ml HCl) was applied and incubated in a 37°C humidified chamber for 16 minutes. The slides were then washed in 37°C water and placed in PBS (see Appendix) for 5 minutes at 37°C before finally being rehydrated with passage through a series of ethanol baths (95% (v/v), 85% (v/v), and 75% (v/v)) and left to dry.

2.9.3 Standard protocol

The labelled probe was placed in a water bath at 37°C for 20 minutes and then 2.5µl was pipette onto the pre-prepared slides (section 2.9.2). A small cover slip (Nunc, Denmark) was placed over the top which was then sealed to the slide with a rubber cement (Marabo, Germany). Slides were placed onto a hot plate and heated to 75°C for 5 minutes to denature the genomic and probe DNA before being left overnight in a humidified incubator at 37°C. The following morning, the cover slips were taken off by removing the rubber seal and then gently agitating the slides in 2x saline-sodium citrate buffer (SSC, Becton Dickinson) at 37°C. To remove any unbound DNA molecules the slides were then washed twice in 30% (v/v) formamide (Sigma-Aldrich) in 1xSSC at 43°C for 5 minutes. The slides were then placed in 2xSSC at 37°C for 5 minutes, followed by incubation in 4xSSC (see Appendix) in a humidified chamber at 37°C for 15 minutes. The slides were then incubated at 37°C for 20 minutes in a

humidified chamber with 50-100µl of six different antibodies washed twice in 4xSSC for 5 minutes in between each antibody exposure. The antibodies were added in the following order:

1) 1:20 anti-digoxigenin fluorescence fab fragments (FITC, (Roche))

2) 1:50 rabbit anti-sheep IgM (DAKO)

3) 1:40 anti-rabbit FITC (DAKO)

4) 1:500 Texas red avidin (Vector)

5) 1:100 goat biotinalated anti-avidins (Vector)

6) 1:500 Texas red avidin (Vector)

The slides were subsequently washed for 4 minutes with 2xSSC twice and with PBS for 2 minutes once before being rehydrated through an ethanol gradient series (95%, 85%, and 75%). The slides were then left to dry in the dark for 15 minutes before being counterstained with a drop of DAPI (Vector) and protected with a cover slip (Nunc) sealed with nail varnish. The probes were then visualised with a DM300 Fluorescence Microscope (Leica) using the appropriate probe excitation wavelengths as shown in Table 2.12.

	Wavelenth (nm)	
Probe	**Excitation**	**Fluorescent emission**
Fluorecein isothiocyanate (FITC)	490	520
Texas red	590	620

Table 2.12. FISH probe excitation and fluorescent emission wavelengths.

2.10 Immunohistochemistry (IHC)

2.10.1 Introduction

Immunohistochemisty (IHC) is an established process which identifies cellular proteins or antigens in tissues by using labelled antibodies and observing antigen-antibody interactions with marker fluorescent dyes or enzymes. The visualisation of an antigen-antibody interaction may use a fluorophore, as first described in 1941 by Albert Coons (Coons, Creech et al. 1941), or by conjugation of an antibody to an enzyme that catalyses a colour producing reaction (Nakane and Pierce 1966). IHC enables the distribution and location of specific cellular components to be identified within intact cells. Specific molecular markers may be associated with particular cellular process or disease states and therefore this technique is widely used to discern normal from abnormal cells, and in particular the demonstration of cancerous cells.

2.10.2 Antibodies for antigen detection in IHC

Antibodies used in IHC can be either polyclonal or monoclonal (mAb). Typically polyclonal antibodies are generated by injecting an animal with an antigen and then harvesting the antibodies that are produced in response. Polyclonal antibodies therefore comprise a hetergenous mix of antibodies to a variety of epitopes. Monoclonal antibodies differ as they are monospecific, created by the overproduction of a unique immunoglobulin against a particular antigen. This method was first devised in 1975 with the creation of a hybridoma using a mouse myeloma to produce an antibody from an immunised donor (Kohler and Milstein 1975). This approach can now be used to selectively produce specific antibodies to defined antigens.

Antibodies may be further sub-classified as being primary or secondary. Primary antibodies are raised against an antigen of interest and are usually unlabelled (unconjugated), while secondary antibodies are raised against primary antibodies and identify immunoglobulins of a particular species.

Antigens may be detected through either a direct or indirect method (see Figure 2.14). In the direct method a single labelled antibody reacts directly with the antigen. Whilst simple this method has the disadvantage of poor signal amplification and is comparatively expensive. More commonly an indirect approach is used. In this method the primary antibody again reacts with a specific antigen but is unlabelled. A secondary labelled antibody is then applied which reacts with the primary antibody. Importantly, the same labelled secondary antibody may be used with many different primary antibodies derived from the same species which makes this a particularly economical approach.

To facilitate visualisation the secondary antibody is conjugated to biotin, or a reporter enzyme, or fluorescent dyes such as alkaline phosphatase or horseradish peroxidase (HRP). Commonly a biotinylated secondary antibody is coupled with a streptavidin tagged horseradish peroxidase enzyme which is reacted with diaminobenzidine (DAB) to produce colorimetric reaction. The resultant brown staining identifies and localises the antigen under investigation and the signal intensity is typically amplified as the secondary antibody is able to react with a number of epitopes on the primary antibody.

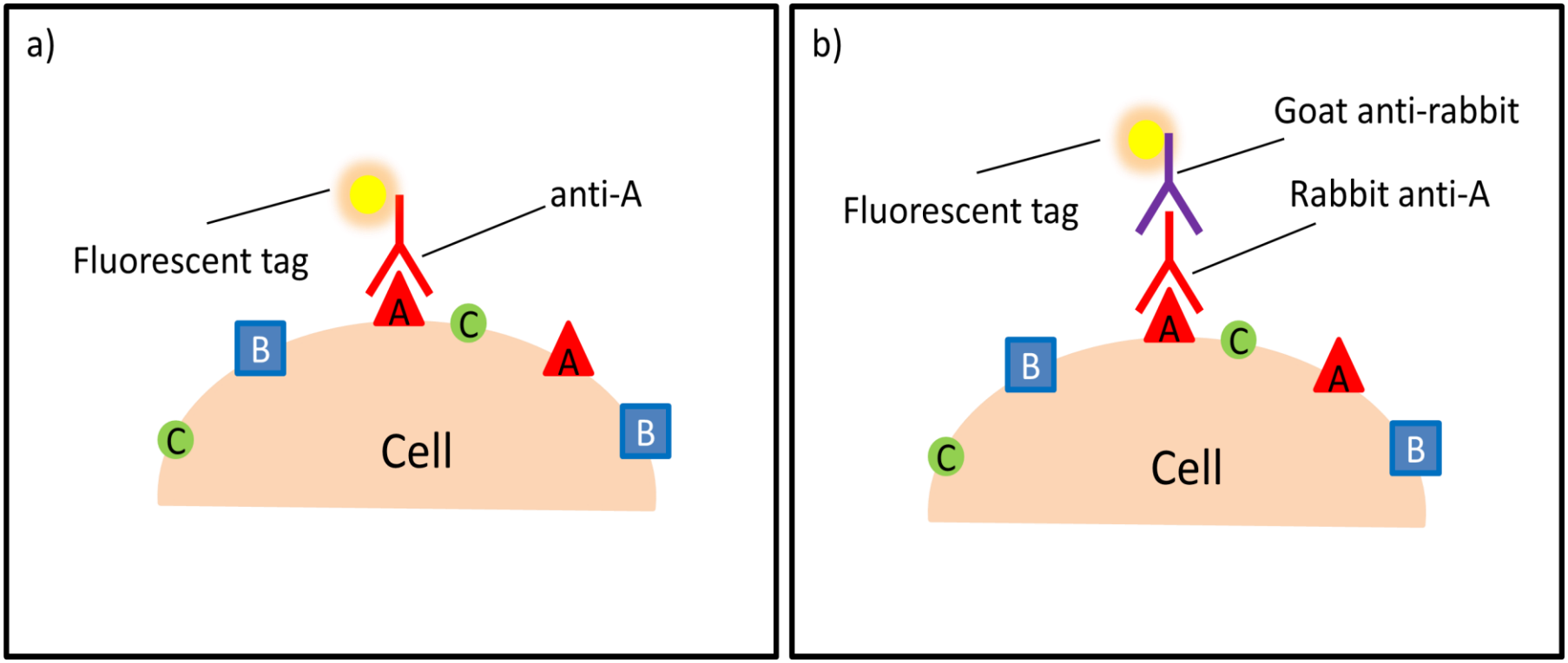

Figure 2.14. Immunohistochemical (IHC) approaches. (a) The direct method: A single labelled antibody (red inverted Y) binds to a specific cell antigen (A), and not to other cellular proteins (B and C). (b) The Indirect Approach: A primary antibody is applied which binds to a specific cellular antigen. A second antibody (purple inverted Y) is then applied which is labelled and reacts with the primary antibody. (redrawn from: http://en.wikipedia.org/wiki/Immunohistochemistry).

2.10.3 Standard protocol

Slides were placed in an oven at 60°C for 30 minutes before being transferred into a xylene bath for 10 minutes to dewax. The slides were then passed through a descending ethanol gradient to rehydrate for 30 seconds in each bath (100% (v/v), 100% (v/v), 95% (v/v), 95% (v/v), 75% (v/v), water). The slides were placed in a non metallic polyacetal slide rack trough (Thermo Scientific) and submerged in a citrate buffer pH6 (see Appendix) before being microwaved at full energy for 5 minutes. The slides were then inspected to ensure that they continued to be submerged in citrate buffer which was replenished as necessary before being microwaved at full energy for a further 5 minutes. The slides and buffer were then left to cool for 20 minutes before being rinsed in water. The slides were then placed into a coplin jar (Fisher Scientific) for 20 minutes containing 100ml 6% hydrogen peroxide (Sigma-Aldrich). The slides were then rinsed initially in water and then using 10x TBS-Tween (see Appendix). The slides were then placed on a slide hydration tray (Fisher Scientific) containing 1ml of water in each lane and 100-200µl of the antibody solution depending on the area of the section was applied. The tray was covered and left to incubate at room temperature for 1 hour.

After an hour excess antibody was rinsed off using 0.05M TBS (see Appendix). To ensure the complete removal of all free antibody the slides were then placed in a coplin jar containing TBS and rinsed. This was repeated a second time with TBS before the slides were placed in 10x TBS-Tween. To enable antibody detection the Menapath™polymer-HRP detection kit (Menarini Diagnostics) was used according to the manufacturer's instructions. 1-2 drops of the Menapath™ universal probe was applied to cover the tissue on each slide and left in a hydration tray for 30 minutes. The slides were then rinsed with TBS to remove any excess which was repeated twice further in a coplin jars containing TBS. Excess solution was removed and then 1-2 drops of Menapath™ HRP-polymer was applied and left in a hydration tray for 20 minutes. Excess solution was removed by rinsing the slides in running water for 20 minutes. A solution containing 1ml DAB dilutent and 1 drop of chromagen liquid DAB was prepared and 1-2 drops were dropped on each slide and left for 3-4 minutes. The slides were then rinsed in water before being counterstained with haematoxylin for 30

seconds, rinsed again in water, and dipped into an acid/ alcohol bath. The slides were then rinsed again in water before being placed in a solution of Scott's water for 10 seconds and then re-ascending a gradient of ethanol baths (75% (v/v), 95% (v/v), 100% (v/v)). The tissue was finally fixed with xylene, mounted in DPX and protected with a cover slip (Nunc) before placing at 4 °C for storage. Details on the preparation of the counterstains may be found in the Appendix.

2.11 DNA methylation analysis

2.11.1 Introduction

DNA methylation is an enzyme-mediated chemical modification that adds methyl (CH_3) groups to the carbon-5 position of the cytosine base (C) and occurs in approximately 3-5% of the cytosine residues in genomic DNA (Ehrlich et al, 1982). Almost 60% of genes contain regions of DNA with a high content of cytosine and guanosine (G+C) nucleotides and a high frequency of the CpG dinculeotide, known as CpG islands. These CpG islands frequently arise upstream to transcriptional start sites or promoter regions and methylation may result in chromatin remodelling into a transcriptionally repressive structure, and therefore act as an epigenetic modification by altering transcription without affecting the nucleotide sequence, as discussed in section 1.2.6. Methods to assess DNA methylation often require an initial modification to reveal the methylation status at a particular locus, including bisulphite modification.

2.11.2 Bisulphite modification of DNA

Bisulphite modification is a technique employed to detect whether methylation of CpG diucleotides is present by introducing a sequence alteration between methylated and hypomethylated states. In this process all unmethylated cytosines are deaminated and sulphonated by the sodium bisulphite treatment which converts them to uracils. Methylated cytosines are resistant to this treatment, and therefore the sequence at

this residue remains unaltered. In subsequent PCR amplification the uracils are replaced by thymines as outlined in Figure 2.15 and Figure 2.16.

2.11.3 Sequencing of bisulphited DNA

Following bisulphite treatment the DNA sequence is transformed to produce altered sequences for both methylated and unmethylated DNA. To determine these sequences PCR amplification is performed. Oligonucleotide primers are generated to amplify the converted sequences, and are therefore different to those that would be employed to amplify the same locus in the original untreated DNA template. Primers need to be able to amplify both unmethylated and methylated sequences and therefore the primers are designed not to contain any CpG dinucleotides. Primer design is undertaken using MethPrimer (http://www.urogene.org/methprimer/index1.html), an online tool that initially *in silico* bisulphite converts a genomic sequence, and then computes appropriate primer pairs. The details of oligonucleotide primers are provided in sections 3.2.5 and 5.2, and were synthesised by Invitrogen.

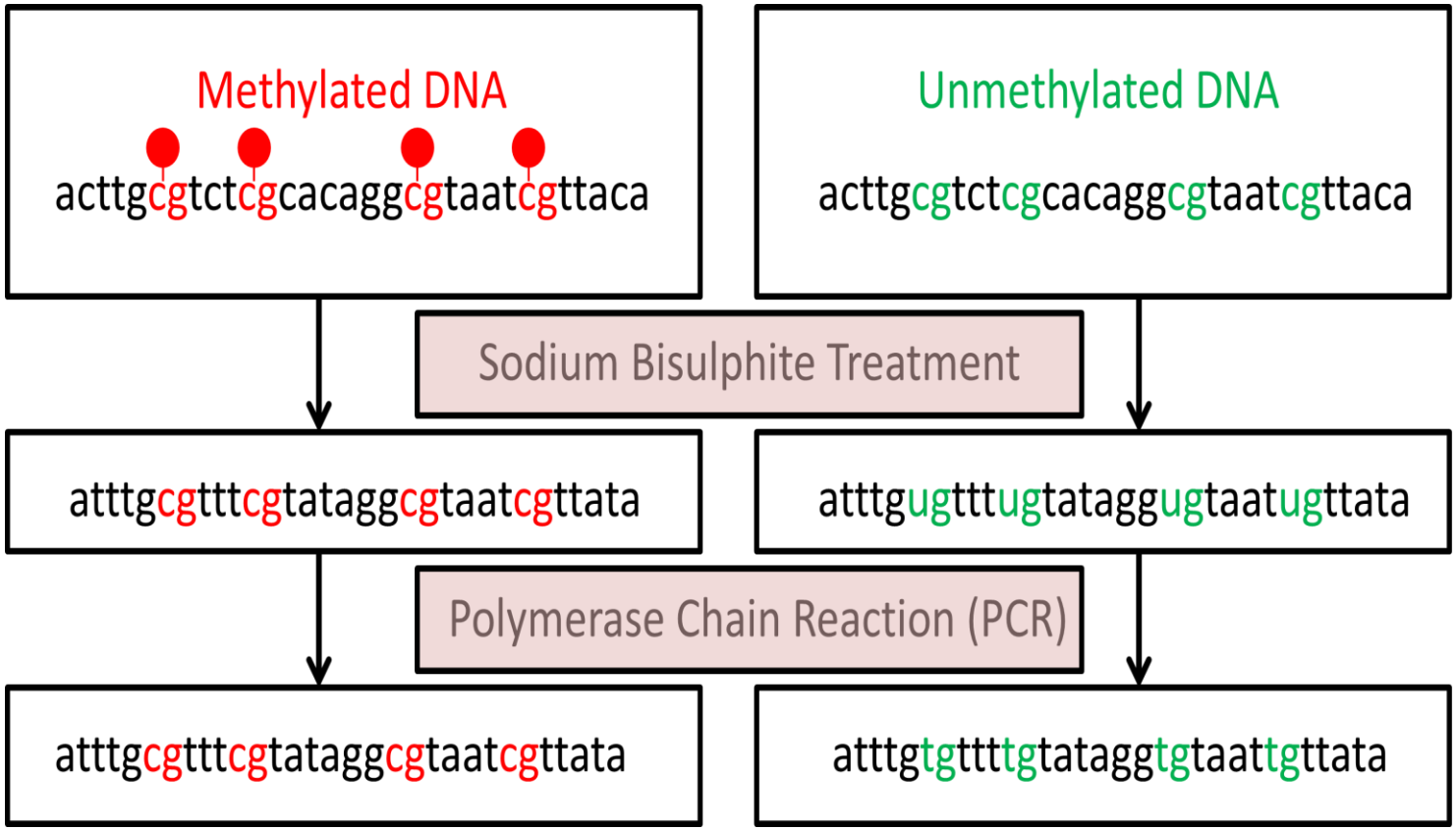

Figure 2.15. Sodium bisulphite modification of DNA. Treatment of DNA with sodium bisulphite selectively deaminates unmethylated cytosine (C) residues (green) converting them to uracil (U). When methylated (closed red circle) methylcytosine residues (red) remain unaffected by the bisulphite modification. The modified DNA sequences can then be analysed for sequence variation using PCR techniques.

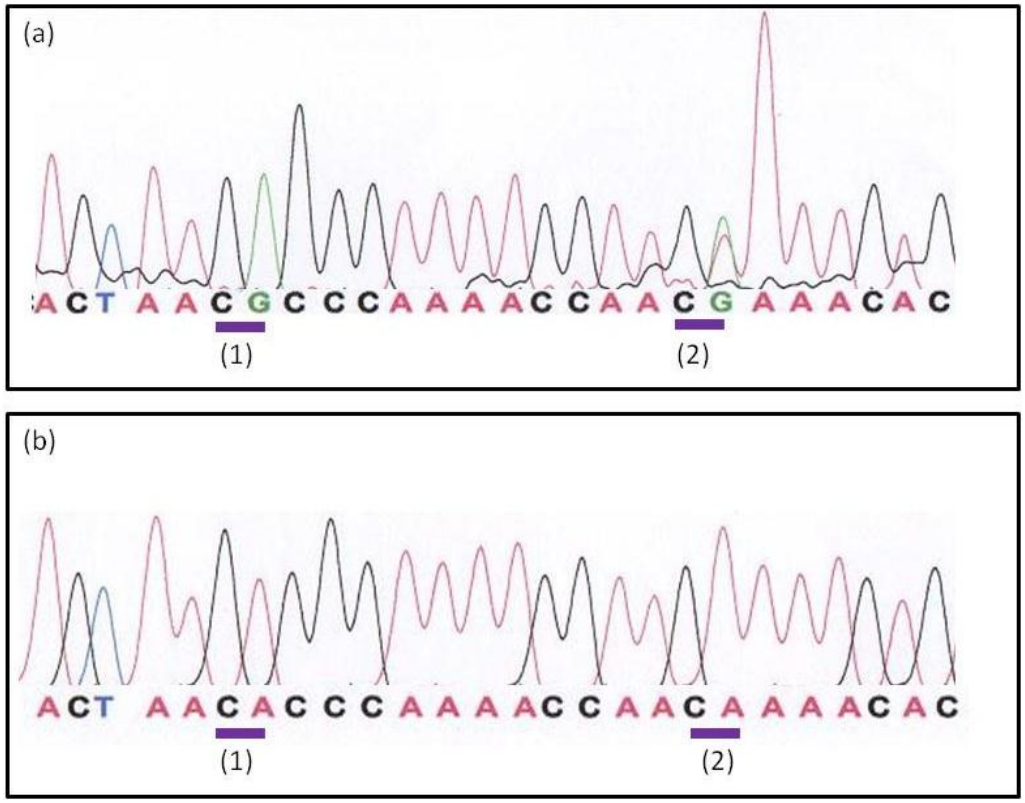

Figure 2.16. Electrophoregrams demonstrating the effect of methylation following bisulphite modification. Reverse trace sequences for *RASSF1A* on two samples are shown. (a) Methylated sequence, showing the preservation of CG dinucleotides following bisulphite treatment. The first CpG (1) is shown to be fully methylated, but the 2nd CpG (2) shows evidence of partial methylation with an adenine peak in addition to the guanine in this reverse sequence. (b) Unmethylated sequence. Bisulphite conversion has deaminated all non-methylated cytosines resulting in CA dinucleodide at both CpG sites.

2.11.4 Standard protocol

Bisulphite conversion was performed on 500ng of genomic DNA using the EpiTect® (Qiagen) kit, following the manufacturer's instructions. Converted DNA was eluted in EB buffer (Qiagen) and stored in two 20µl aliquots at -80°C until used. PCR reactions were performed as described in section 2.3.3, visualised by gel electrophoresis as described in section 2.4.2 and purified using the PureLink® (Invitrogen) system (section 2.3.5). Purified products were subsequently sequenced as previously outlined in section 2.5.2and the methylation status assigned by interrogating each CpG dinucleotide on the electrophotegrams and scoring as being either methylated, partially methylated or hypomethylated.

2.12 Illumina GoldenGate methylation array

2.12.1 Introduction

The GoldenGate® methylation array (Illumina) platform is a high-throughput method that enables the methylation status of up to 96 samples to be simultaneously evaluated (Bibikova, Lin et al. 2006; Fan, Gunderson et al. 2006). Using the GoldenGate® Methylation Cancer Panel I 1505 CpG sites across 807 genes are assessed. The genes incorporated in this panel have been selected as they are either tumour suppressor genes, oncogenes, genes involved in DNA repair, or genes that regulate cell cycle control or apoptosis or cell differentiation. In the panel 28.6% of the genes are represented by a single CpG on the array, 57.3% with 2 CpGs and 14.1% by 3 or more CpG dinucleotides.

An outline of the Illumina GoldenGate methylation array process is shown in Figure 2.17. Genomic DNA is first bisulphite treated to deaminate non-methylated cytosines and has been previously described (section 2.11.2). The transformed sequences are then hybridised with probe pairs designed for unmethylated and methylated sequences. Each probe pair contains an allele-specific oligonucleotide (ASO) and locus-

specific oligonucleotide (LSO). The probes anneal to the modified target DNA at the ASO and LSO. A ligation reaction is then performed which extends the ASO to the corresponding LSO, to form a PCR template. Universal PCR primers attached to both the 5’ and 3’ the ends of the probes are used to amplify the resulting sequence. The PCR primers also contain fluorophores, different for methylated and unmethylated sequences. Following PCR amplification the sequence are hybridised to a bead with a complementary sequence and the fluorescence intensity of both fluorophores generated at each bead recorded by the BeadArray reader (Illumina). Each of the 1505 sites is represented up to 30 times on different beads on the Sentrix Array Matrix (SAM). The intensity of the 2 wavelengths for each bead is registered and an average (mean) value for each CpG generated (average delta beta). The average delta beta scores range from 0 (fully unmethylated) to 1 (fully methylated).

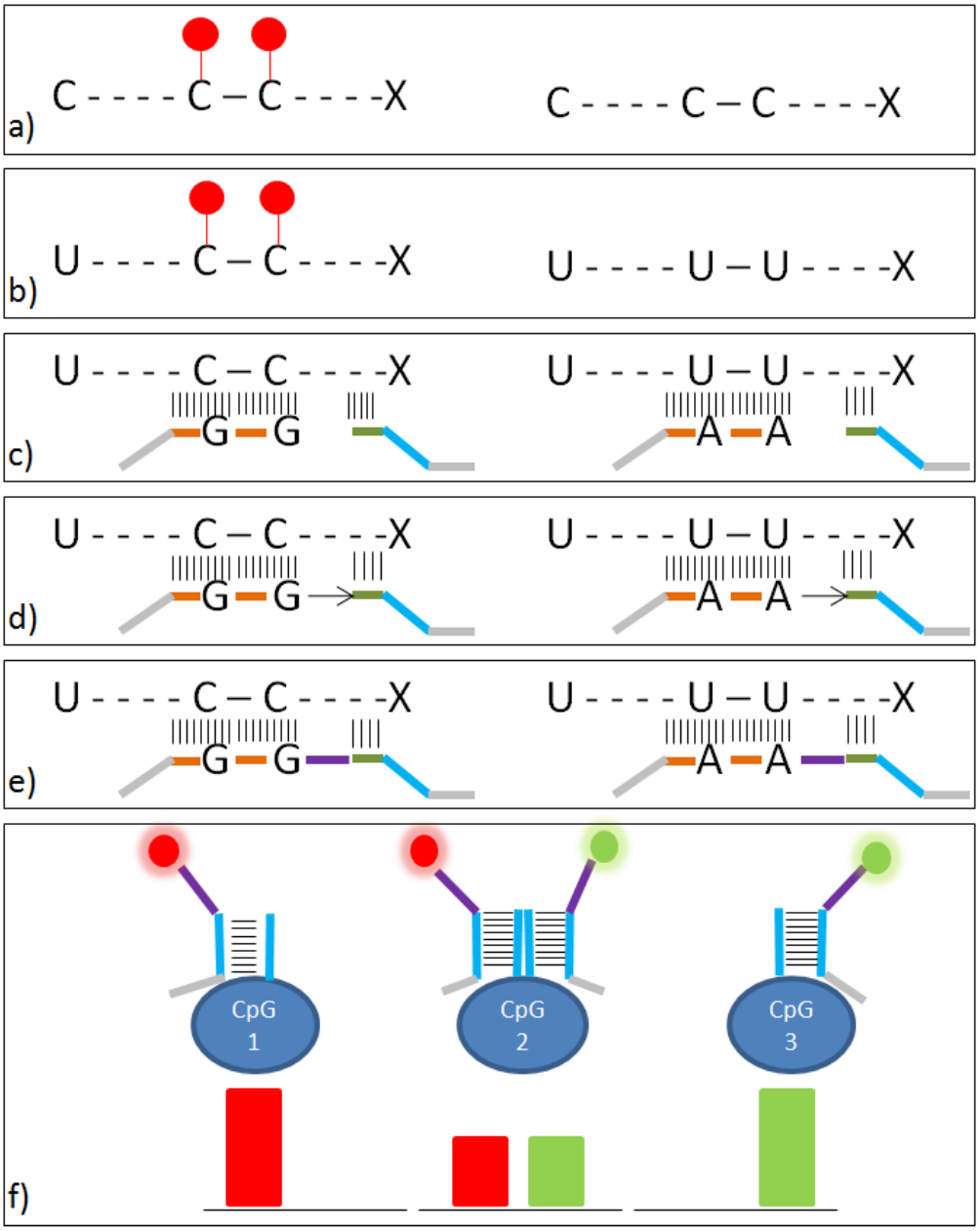

Figure 2.17. GoldenGate methylation array flow process. The steps involved in the Illumina GoldenGate methylation array for methylated (left) and unmethylated (right) sequences are shown. (a) Genomic sequences showing methylation (closed red circle) at CpG dinucleotides. (b) Sequence transformation following bisulphite treatment.(c) For each CpG site two pairs of probes are designed: an allele-specific oligonucleotide (ASO (orange)) and locus-specific oligonucleotide (LSO (green)) probe pair for the methylated and unmethylated states. The pooled oligonucleotides anneal to the target DNA. (d) Extension in the LSO direction. (e) Ligation (purple) of the extended ASO to the corresponding LSO to create a PCR template. The ligated products are then PCR amplified using fluorescently labelled common primers (grey) and (f) hybridise to a bead array bearing the complementary sequence (blue). Two fluorophores are then used to distinguish methylated and unmethylatyed loci. (redrawn from: www.illumina.com/technology/goldengate_methylation_assay.ilmn)

2.12.2 Sample plate preparation

Methylation analysis on the Illumina GoldenGate Methylation array platform was performed by the Wellcome Trust Centre for Human Genetics (Oxford, UK). For each sample to be analysed 750ng of genomic DNA was prepared. The clinical details of tumours and controls used in this study are given in section 5.2)

2.12.3 Quality control assessment

2.12.3.1 BeadStudio Methylation Module quality control assessment

The raw data was first subjected to a quality control assessment using BeadStudio Methylation Module, version 3.0 (Illumina). A control summary graph was produced to evaluate each step of the methylation process. These steps included a quality control assessment of bisulphite conversion, a determinant of gender specific methylation, allele specific extension, contamination, hybridisation to the DNA template, secondary hybrisdaiation to the array beads and negative controls following the manufacturer's instructions (Illumina) and illustrated in Figure 2.18 and Figure 2.19. Samples that failed these quality control steps were excluded from subsequent analyses.

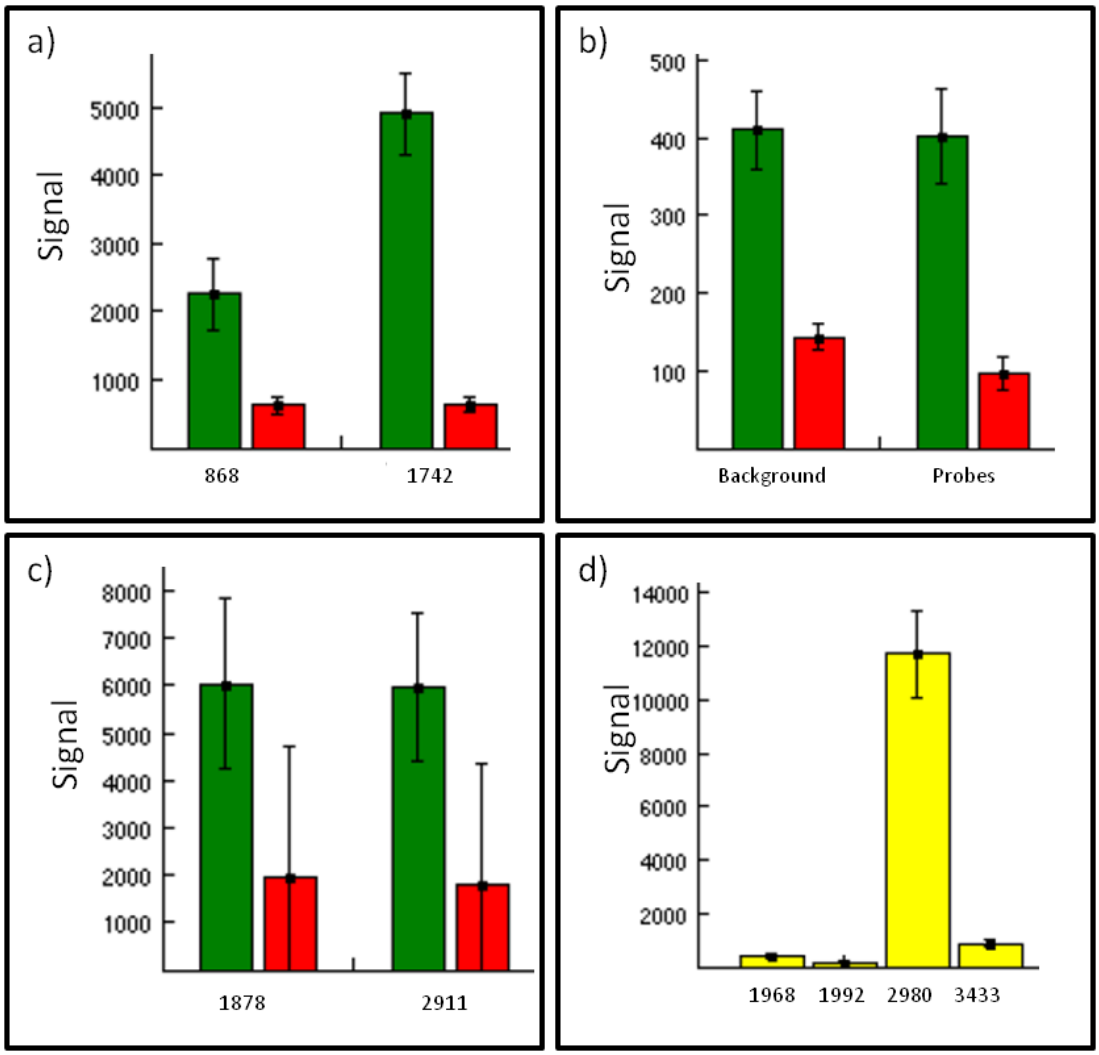

Figure 2.18. Illumina GoldenGate Methlyation array control panel (A) summary. (a) Bisulphite conversion: The efficiency of bisulphite conversion is verified by checking for the presence of genomic DNA (red) compared to bisulphite converted DNA (green) in the assay using two primers (868 and 1742) designed to amplify genomic DNA at the same locus**.** (b) Negative controls: A panel of 22 negative control probes are included in the oligonucleotide pool which target bisulphite converted sequences but should not produce a signal as they do not contain an ASO and will not be PCR amplify. Any signal produced therefore represented a background signal resulting from cross-hybridisation, or non-specific binding of dye. (Note the intensity scale is 10-fold lower with minimal signals detected). (c) Gender specific methyaltion: The sex of the samples was verified using two X-linked genes (G6PD (1878) and ELK1 (2911)). These genes are known to exhibit DNA dose compensation by becoming partially methylated when two X chromosomes are present. Only a Cy3 (green) signal in males and both Cy3 and Cy5 (red) signals in females should be observed. (d) Contamination: PCR contamination was detected using four control oligonucleotides (1968, 1992, 2980, 3433). Only one was added to each oligonucleotide pool and so the presence of more than one suggests contamination. 2980 was added to the pool shown which shows no evidence of contamination.

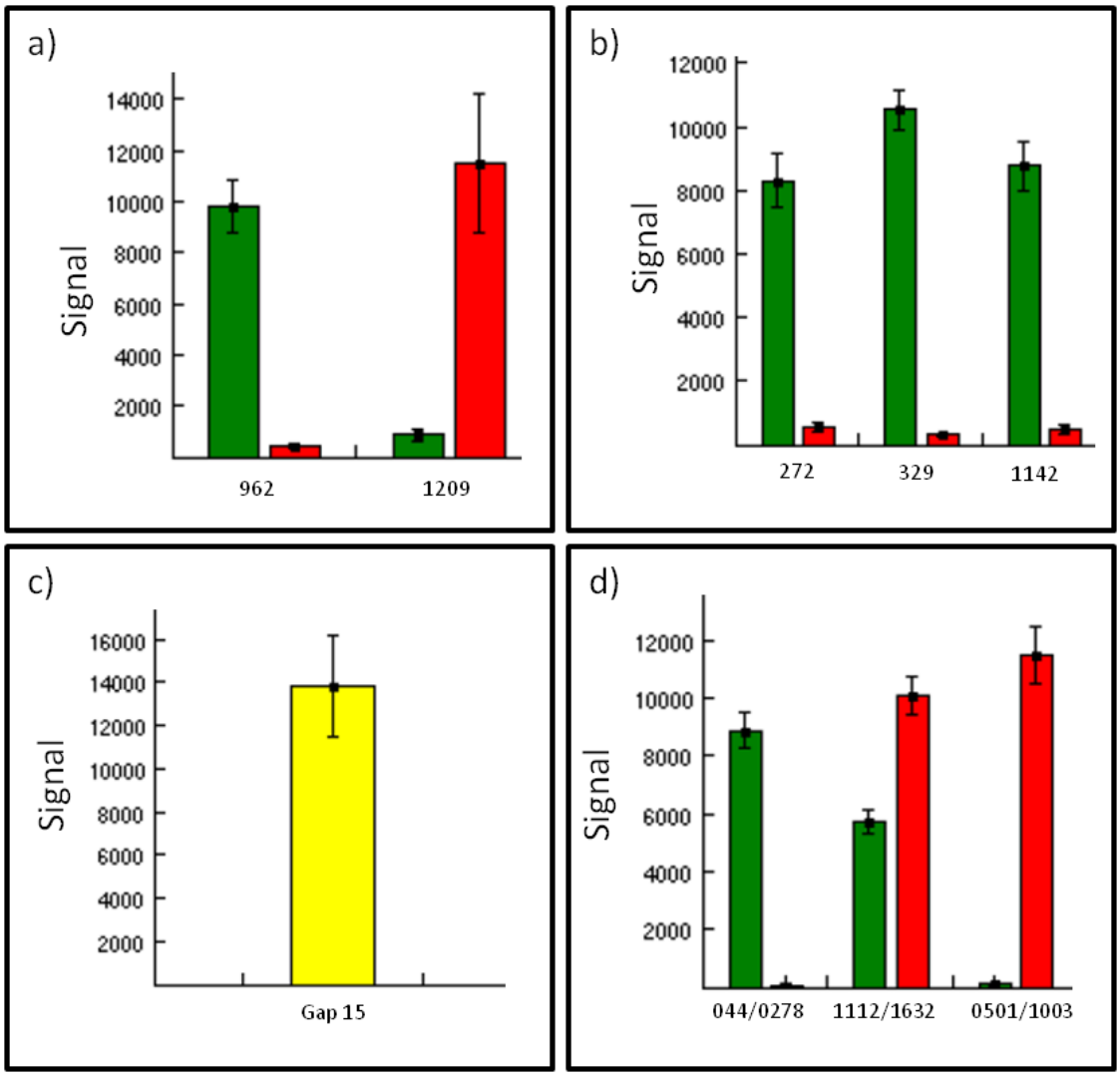

Figure 2.19. Illumina GoldenGate Methylation array control panel (B) summary. Cy3 unmethylated signals are shown in green, Cy5 methylated signals in red. (a) First hybridisation: Hybridisation of the allele-specific oligonucleotide (ASO) to the DNA template specificity is assessed using 2 different control probes. 962 should provide only a Cy3 and 1209 a Cy5 signal if hybridisation has occurred successfully. (b) Allele-specific extension: The allele-specific extension control test uses 3 sequences (272, 329 and 1142) to ensure that a Cy5 methylation signal is observed only when a specific ASO is applied and that methylation is not being non-specifically detected. Only a Cy3 signal should be observed. (c) Extension gap: Tests the efficiency of extending 15 bases from the ASO to the locus-specific oligonucleotide (LSO) to produce an intense (yellow) signal. (d) Second hybridisation: Hybridisation of generated products to the array beads was tested with a panel of known methylated (044/0278), partially methylated (1112/1632) and unmethylated (0501/1003) control sequences that should produce Cy5 only, Cy5 and Cy3, and CY3 only signals respectively.

2.12.3.2 BASH analysis quality control assessment

Following the BeadStudio quality control analysis the raw data from the BeadArray reader (Illumina) was then input into "beadarray"((Dunning, Smith et al. 2007), downloaded from Bioconductor (www.bioconductor.org/). Using this package the fluorescent intensities of both wavelengths (red and green) for each bead and their geographical location on the SAM were analysed to detect any spatial artefacts. Artefacts may result because of a damaged chip or from a speck of dust which distorts the fluorescent intensities from being read by the BeadArray reader (Illumina). Due to the random placement of up to 30 multiple beads for each CpG on the array the effect of an erroneous reading from a single bead on the average delta beta methylation value will be negligible. Larger defects affecting a number of beads may however make the result unreliable.

Three types of defect have been described: Extended, compact and diffuse ((Cairns, Dunning et al. 2008). Extended defects occur where a significant variation in intensities between different chips is observed, suggesting a chip fault; compact defects occur when small connected clusters of outlying values are seen; and diffuse defects contain small regions where more outliers than expected are observed.

The BeadArray Subversion of Harshlight (BASH) programme within the beadarray package was used to produce an "error image" for each sample and discover any spatial artefacts. Small (<20%) defects were "masked" from inclusion in the generation of average delta beta values for each probe and compared with the raw data values as illustrated in Figure 2.20. These corrected values were used in subsequent studies.

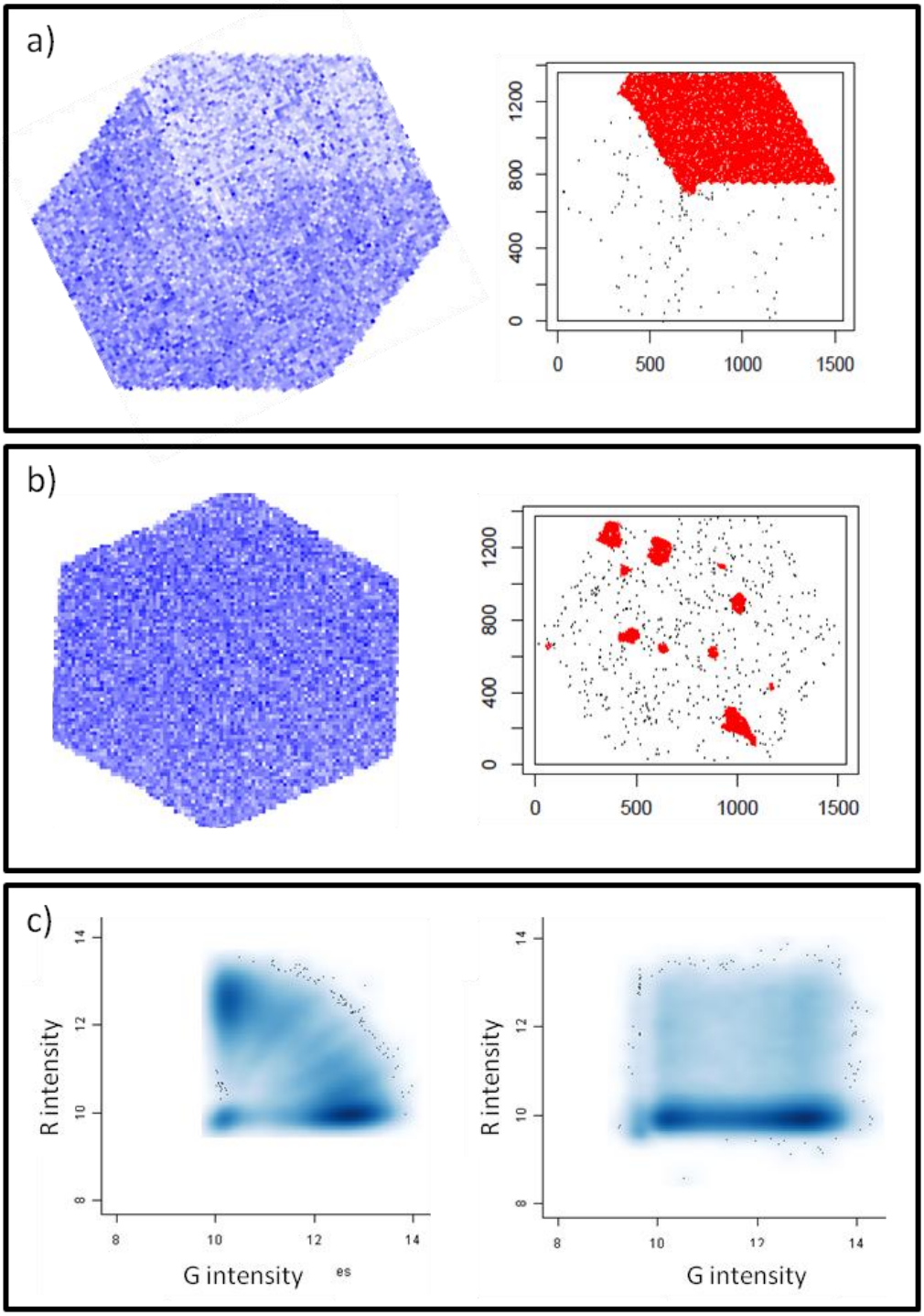

Figure 2.20. BASH analysis plots. (a) BeadArray reader scan (Left) of a sample with a segmental defect, with (right) area identified and masked (red) in BASH analysis. (b) Normal read and BASH analysis plots with small focal defects. (c) Plot of unmethylated (G, green) and methylated (R, red) intensities across all 1505 CpG dimnucleotides for a sample. Left: Normal result with a bimodal distribution (results are methylated or unmethylated at most loci with partial methylation occurring at few loci). Right: Sample failure, as a paucity of methylation (R) signal detected.

2.12.4 Bioinformatic analyses

BASH adjusted data were analysed in a series of *in-silico* experiments using the R project for statistical computing (http://www.r-project.org/). To describe the variation and recognise patterns within this dataset unsupervised analysis using cluster and principal component analysis (PCA) was undertaken. Details of the programming scripts used in these analyses may be found in the Appendix.

2.12.4.1 Principal component analysis (PCA)

Principal component analysis reduces the number of characters within a dataset by producing new characters that are a combination of contributions from the original characters. In this way the relationship between objects with complex characterisations comprising more than 3 components, and therefore cannot normally be visualised, may be reduced to form data that can be plotted and inspected in 2 or 3 dimensions. PCA analysis of the methylation dataset was undertaken within R using the *stats* package within the *gplots* (version 2.8.0) package and the *rgl* (version 0.92.798) package to create 3 dimensional plots downloaded from Comprehensive R Archive Network (CRAN) (http://cran.r-project.org/).

2.12.4.2 Cluster analysis

In contrast to PCA, in cluster analysis complex data is managed to facilitate pattern recognition by reducing the number of objects rather than characters. In cluster analysis objects are grouped by their relatedness (Kapetonovik IM 2004). In the methylation analysis hierarchical clustering was employed which uses a 'bottom up' method of clustering in which each sample begins in its own cluster before successive agglomeration of similar pairs resolves all of the samples into a single cluster. In order to determine the extent of sample relatedness in clusters, the Euclidean distance between them was measured (Quackenbush 2001). Cluster analysis was performed

within R using the *pvclust* (version 1.2-2) package downloaded from CRAN (http://cran.r-project.org/).

2.13 Statistical analysis

Statistical analyses were performed using Prism 4 (GraphPad software). Significance was tested using Fisher Exact tests, t-tests, and chi-squared tests where appropriate. Survival analyses were measured using Kaplan-Meier survival curves, and tested using univariate (log-rank) and multivariate (Cox proportional hazard tests). The p-value was used as a threshold for determining significance and Benjamini-Hochberg corrections applied with multivariate testing. Further details of the statistical analyses employed are given in the relevant results chapters.

Chapter 3

Investigation of frequent medulloblastoma molecular defects in CNS-PNET

Table of contents

Chapter 3

3.1 Introduction

The CNS-PNET is an aggressive embryonal tumour predominantly affecting young children. These tumours, in contrast with medulloblastoma, arise at sites outside of the cerebellum within the CNS. Their similar immunohistochemical appearance to medulloblastoma has resulted in the suggestion that these tumours share a common origin and the term "PNET" applied to refer to both groups of tumours (Rorke 1983). Patients with intracranial "PNETs" have been treated along parallel lines as it has been assumed that the mechanisms underlying their development, in view of their similar morphological phenotype, are likely to be correspondingly analogous. The results from a series of international clinical studies have consistently shown an adverse outcome with an extra-cerebellar intracranial PNET and raised doubt as to whether the fundamental concept of a "PNET" entity remains valid (discussed in detail in chapter 1).

There have been few studies investigating the molecular basis of CNS-PNETs. Where investigation has occurred, this has typically been in the context of a combined study with medulloblastoma, in which a few cases of CNS-PNET have been analysed in addition, but seldom are the focus of the study. This has meant that the molecular characterisation of CNS-PNETs and the extent to which they may share similar features with their cerebellar counterparts remains yet to be clearly characterised.

The frequent molecular events in medulloblastoma that characterise this disease are summarised in Table 3.1. Promoter methylation of *RASSF1A* (section 1.5.6) is the most frequent event in medulloblastoma (Lindsey, Lusher et al. 2004), whilst loss of the p-arm on chromosome 17 (section 1.5.3) is the most common karyotypic abnormality (McDonald, Daneshvar et al. 1994; Burnett, White et al. 1997). The most common biological pathways demonstrated to be involved in tumourigenisis are the *TP53* and Wnt pathways (discussed in detail in section 1.5.5), with disruption associated with an aggressive and favourable phenotype respectively (Eberhart, Chaudhry et al. 2005; Tabori, Baskin et al. 2010; Ellison, Kocat et al. 2011). In addition amplification of the *MYC* family of oncogenes (see section 1.5.4) are frequently observed (Ellison, Kocat et

al. 2011). The involvement of these defects in CNS-PNET is however unclear and needs investigation.

Defect	Manifestation	Medulloblastoma		Reference
		Frequency*	Significance	
RASSF1A methylation	Promoter hypermethylation	54/62 (87%)	Most common medulloblastoma tumour specific event.	(Lindsey, Lusher et al. 2004)
MYC family gene amplification	*MYCC* amplification	6/292 (2%)	Associated with a more aggressive phenotype.	(Ellison, Kocat et al. 2011)
	MYCN amplification	16/292 (5%)	Associated with a more aggressive phenotype.	
Chromosome 17 defects	17p loss	47/190 (25%)	Associated with a more aggressive phenotype.	(Megahed 2010)
TP53 pathway disruption	Nuclear p53 immunopositivity by immunohistochemistry	17/64 (27%)** 15/49 (30%)**	Associated with a more aggressive phenotype.	(Eberhart, Chaudhry et al. 2005; Tabori, Baskin et al. 2010)
	TP53 mutation	8/49 (16%)**	Associated with a more aggressive phenotype.	(Tabori, Baskin et al. 2010)
Wnt signalling disruption	β-catenin nuclear immunopositivity by immunohistochemistry	33/206 (16%)	Favourable prognosis	(Ellison, Kocat et al. 2011)
	CTNNB1 mutations	20/195 (10%)	Favourable prognosis	

Table 3.1. Summary of medulloblastoma molecular defects to be investigated in CNS-PNET. *Based on equivalent studies in local Newcastle (Northern Institute for Cancer Research) cohorts. **Based on studies reported in the literature.

The overall aim of studies reported in this chapter was to determine whether the significant medulloblastoma defects outlined in Table 3.1 are features of CNS-PNET disease.

The following specific aims were investigated.

1. Investigation of *RASSF1A* promoter methylation status in CNS-PNET primary tumours and cell lines.

2. Analysis of the frequency of *MYCC* and *MYCN* amplification in CNS-PNET primary tumours by qRT-PCR, using MLPA and FISH validation.

3. Determine whether loss of the short of chromosome 17 is a feature of CNS-PNET disease.

4. Investigate whether defects in the *TP53* pathway are observed in CNS-PNET primary tumour samples. Defects studies included abnormal nuclear p53 protein accumulation, mutation analysis of *TP53*, *MDM2* amplification and homozygous loss of *CDKN2A.*

5. To investigate whether aberrant Wnt signalling is a feature of CNS-PNETs.

6. Determine any clinicopathological correlations with identified defects.

7. Compare and contrast the genetics of CNS-PNET with medulloblastoma.

3.2 Materials and methods

3.2.1 CNS-PNET cell lines

Two CNS-PNET cell lines (PFSK and CHP707m) were investigated in this study. Further details regarding these cell lines and their culture may be found in sections 2.1.2 and 2.2 . Genomic DNA was extracted from the cell lines as described previously in section 2.3.2.

3.2.2 Control cell lines

Two medulloblastoma and a neuroblastoma cell line were used in this study to provide control DNA. The medulloblastoma cell line DNA was generously provided by Dr Sara Ryan (Northern Institute Cancer Research, Newcastle University, UK), and that from the neuroblastoma cell line from Dr Jane Carr (Northern Institute Cancer Research, Newcastle University, UK). Details of these cell lines are given in Table 3.2. The medulloblastoma cell lines were cultured as reported by Langdon et al (Langdon, Lamont et al. 2006). The establishment of IMR-32 is described (Tumilowicz, Nichols et al. 1970).

Cell line	Derivation	Source	Reference
D341 Med	Medulloblastoma	American Type Culture collection	(Friedman, Burger et al. 1988)
MHH-MED1	Medulloblastoma metastatic cells present in the CSF.	Dr T Pietsch. (University of Bonn Medical centre, Bonn Germany).	(Pietsch, Scharmann et al. 1994)
IMR-32	Neuroblastoma	American Type Culture collection	(Tumilowicz, Nichols et al. 1970)

Table 3.2. Control cell lines used in this study.

3.2.3 Normal brain control cohort

To provide reference DNA a cohort of 6 normal brain samples was used. Clinical details of these samples is given in Table 3.3.

Sample ID	Location	Age	Material
N3	Cerebral cortex	4 years	FFPE
N9	Right temporal lobe	14 years	FFPE
N18	Temporal lobe	34 years	FFPE
N21	Cerebral cortex	Adult	FFPE
N26	Frontal lobe	14 years	FFPE
CB3	Cerebellum	-	FFPE

Table 3.3. Normal brain samples cohort. FFPE: Formalin fixed paraffin embedded material

3.2.4 CNS-PNET primary tumour cohort

A total of 25 primary CNS-PNETs were investigated in this study. All samples had undergone a central pathological review as described in section 2.1.1. Clinical details of these tumours are given in Table 3.4. The cohort included material from 11 male and 14 female cases enrolled on a number of different studies who underwent different treatment strategies. The patients were aged 11 – 360 months (0.92 – 30 years), with a median age of 77.5 months (6.5 years) at diagnosis. A single case had evidence of metastatic disease on neuroimaging at diagnosis. Genomic DNA was extracted as described in section 2.3.1.

Tumour ID	Diagnosis	Site	Sex	Age at diagnosis (Months)	Metastasis Stage (Chang)	Status	Follow up (months)
SP3	CNS-PNET	Parieto-occipital lobes	M	48	M0/1	Dead	17
SP4	CNS-PNET	Parietal lobe	F	78	M0/1	Alive	121
SP7	CNS-PNET	Intraventricular	F	75	M0	Dead	7
SP10	CNS-PNET	3rd Ventricle	M	158	M0/1	Alive	112
SP13	CNS-PNET	Cerebral	M	106	M0/1	Dead	71
SP14	CNS-PNET	Parietal lobe	F	105	-	Alive	100
SP21	CNS-PNET	Left temporo-parietal lobes	M	65	-	Dead	25
SP23	CNS-PNET	Cerebral	M	126	M0/1	Alive	108
SP24	CNS-PNET	Cerebral	M	31	-	Dead	7
SP28	CNS-PNET	Right frontal lobe	F	23	M0/1	Dead	9
SP40	CNS-PNET	Right parietal lobe	F	348	M0/1	-	-
SP41	CNS-PNET	Left fronto-temporal lobes	M	56	M0/1	Dead	24
SP42	CNS-PNET	Right temporal lobe	F	288	M0/1	Alive	24
SP43	CNS-PNET	Left parietal lobe	M	-	M0/1	-	-
SP45	CNS-PNET	Right parietal lobe.	F	11	M0/1	-	-
SP46	CNS-PNET	Left frontal lobe	F	312	M0/1	Dead	36
SP47	CNS-PNET	Left frontal lobe	F	87	M0/1	Alive	132
SP49	CNS-PNET	Right temporal lobe	F	15	M2	Alive	36
SP50	CNS-PNET	Left temporo-parietal lobes	F	36	M0/1	Dead	15
SP51	CNS-PNET	Cerebral	F	360	-	Dead	55
SP52	CNS-PNET	Left parietal lobe	M	127	M0/1	Alive	43
SP54	CNS-PNET	Infra + Supratentorial	F	26	M0/1	Dead	3
SP55	CNS-PNET	Temporal lobe	M	77	M0/1	Dead	15
SP57	CNS-PNET	Frontal + temporal lobes	M	21	M0/1	Alive	39
SP58	CNS-PNET	Right parietal lobe	F	223	M0	Alive	17

Table 3.4. Clinical details of CNS-PNET primary tumour samples used in medulloblastoma defect comparison study. M: Male, F: female.

3.2.5 Analysis of *RASSF1A* methylation status

3.2.5.1 Bisulphite conversion of genomic DNA

To determine *RASSF1A* methylation status 500ng of genomic DNA of each tumour sample was bisulphite treated as described in section 2.12.2.

3.2.5.2 PCR amplification of *RASSF1A* promoter

To determine *RASSF1A* methylation status primers were designed in the *RASSF1A* promoter region, using the CpG plot program (http://www.ebi.ac.uk/emboss/cpgplot/) to determine the promoter region and MethPrimer (http://www.urogene.org/methprimer/index1.html) to design primers, as described in section 2.12.3 and shown in Figure 3.1. The PCRs were performed using the standard method and conditions described in section 2.4.3. Details of the primers used and annealing temperature are given in Table 3.5.

3.2.5.3 Sequencing of *RASSF1A* products

PCR products were purified prior to further analysis as described in section 2.4.5. *RASSF1A* purified products were sequenced using methods described in section 2.6, and the methylation status at each CpG dinucleotide assessed as either being methylated, partially methylated or hypomethylated as discussed in section 2.12.3.

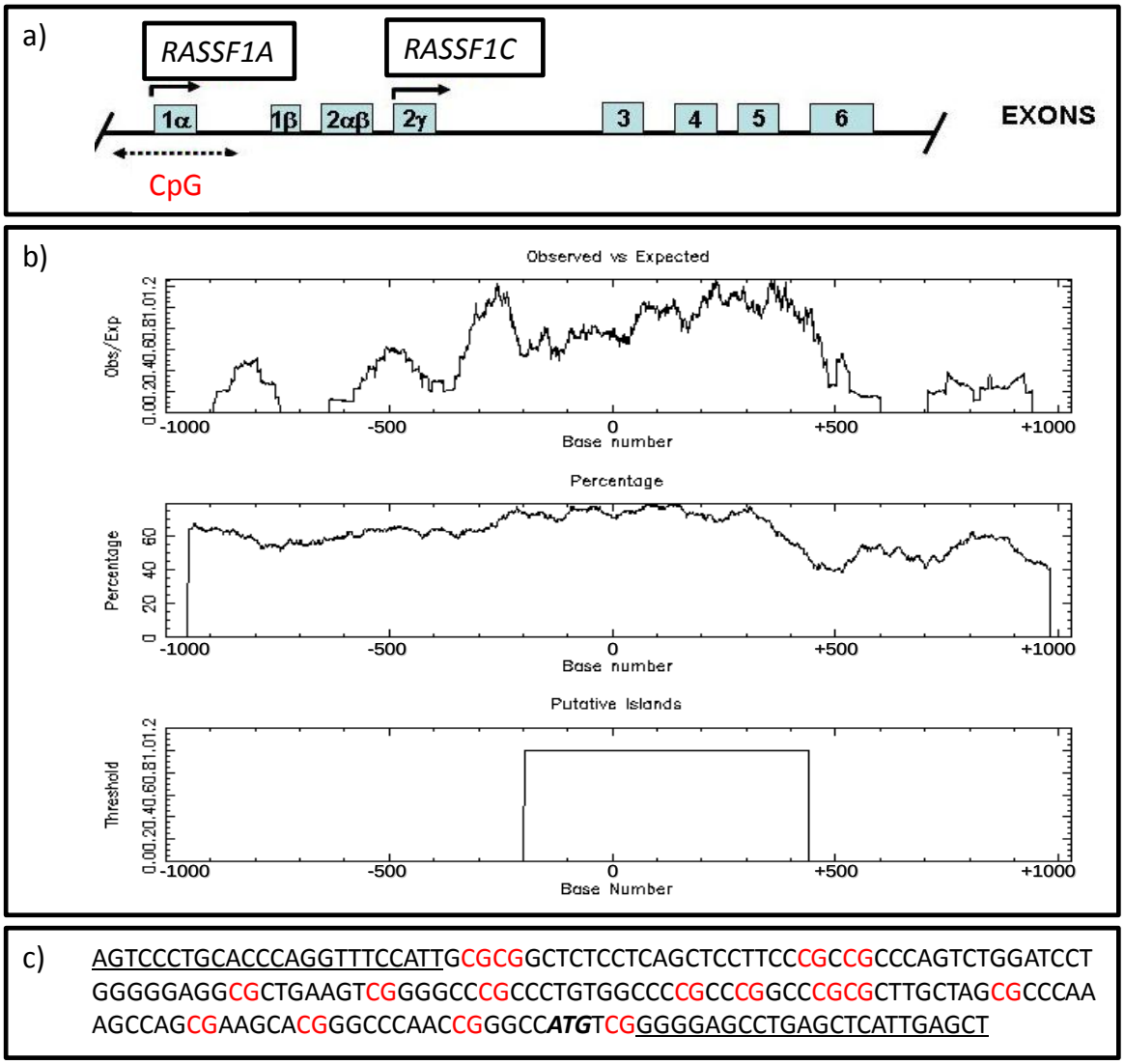

Figure 3.1. Identification of *RASSF1A* promoter associated CpG island and bisulphite sequencing primers. a) Section of chromosome 3 containing the *RASSF1* gene (ensemble gene ID ENSG00000068028). Blue boxes denote exons, the promoter regions and CpG islands marked. b). *In silico* identification of the *RASSF1A* CpG island using the CpG plot program (http://www.ebi.ac.uk/emboss/cpgplot/). The observed vs expected (obs/exp) ratio of the frequency of the CpG dinucleotide, percentage G/C content and CpG islands predicted by this program. The first 100bp of the gene and 1000bp upstream flanking sequence are shown and the base pairs relative to the transcriptional start site are recorded. (c). Section of *RASSF1A* CpG island between -162 to +29 bps relative to the transcriptional start site. Methylated bisulphite converted sequence is shown. Primers were designed using MethPrimer (http://www.urogene.org/methprimer/index1.html), and are shown underlined, CpG sites shown in red type, and the transcriptional start site in bold italic.

Gene	Primer location	Forward sequence	Reverse sequence	Product size (bp)	Annealing temperature (°C)	PCR method
RASSF1A	Promoter*	5'-GTTTTATAGTTTTTGTATTTAGGTTTTTAT-3'	5'-AACTCAATAAACTCAAACTCCCC-3'	191	56	Standard

Table 3.5. Primers used in the PCR analysis of *RASSF1A* methylation status. DNA was amplified using a standard 40 cycle PCR reaction using the annealing temperatures given. *The promoter location between -162 to +29 bps relative to the transcriptional start site was identified using the CpG plot program (http://www.ebi.ac.uk/emboss/cpgplot/).

3.2.6 HOMOD assessment of the p-arm of chromosome 17 status

3.2.6.1 PCR amplification of 17p microsatelites

PCR primers to amplify polymorphic microsatellite sites on the short arm of chromosome 17 were designed as described in section 2.8.3. The location of the regions that were amplified by the seven primer sets are shown in Figure 3.2. PCRs were performed using the "fast" method as described in section 2.4.4, using a combined annealing/ extension temperature of 62 °C. The primer sequences, location and product sizes are given in Table 3.6.

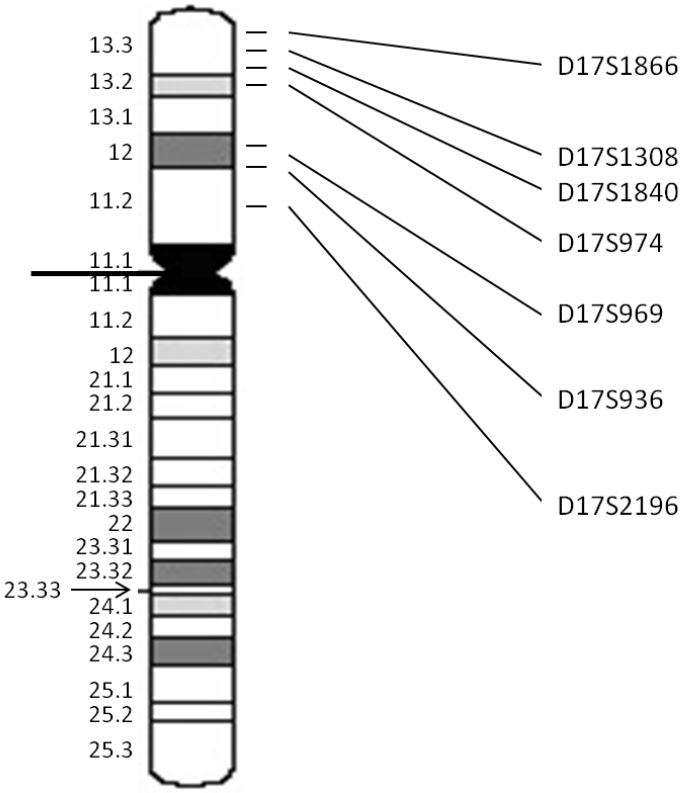

Figure 3.2. Chromosome 17 ideogram showing the location of 7 polymorphic microsatelite markers. Markers were designed and location ascertained using Marshfield Research Foundation website (http://research.marshfieldclinic.org/genetics/GeneticResearch/).

Marker	Chromosome location	NCBI-STS map location (bp)	Forward sequence	Reverse sequence	Product size (bp)	Annealing temperature (°C)	PCR method
D17S2196	17p11.2	17016698 - 17016842	5'-CCAACATCTAGAATTAATCAGAATC-3'	5'-ATATTTCAATATTGTAACCAGTCCC-3'	139-163	62	Fast
D17S936	17p12-p11.2	13328455 - 13328553	5'-ATTTGAAACCACAACAGCA-3'	5'-AGGTATATGCCCACCCC-3'	93-103	62	Fast
D17S969	17p12	11746071 - 11746198	5'-ATCTAATCTGTCATTCATCTATCCA-3'	5'-AACTGCAGTGCTGCATCATA-3'	116-140	62	Fast
D17S974	17p13.2	10418376 - 10418583	5'-AGACCCTGTCTCAGATAGATGG-3'	5'-TAAAATAGAAAGTGCCCCTCC-3'	201-217	62	Fast
D17S1840	17p13.3	867416 - 867610	5'-GCCTGGGCGACAGAGTGA-3'	5'-TGGGGCAGACTTGGTCCTT-3'	173-225	62	Fast
D17S1308	17p13.3	533715 - 534016	5'-TGTGAAACTTTGTCATCACTATACC-3'	5'-TTGGTGACAAAGAAAGTCTCC-3'	304-318	62	Fast
D17S1866	17p13.3	102127 - 102307	5'-TGGATTCTGTAGTCCCAGG-3'	5'-GGTTCAAAGACAACTCCCC-3'	154-185	62	Fast

Table 3.6. PCR primers used to investigate chromosome 17p polymorphic microsatelites. For each polymorphic microsatellite marker the primer pair nucleotide sequence, PCR product size range and amplification settings are given. The location on chromosome 17 for each marker is shown using the National Center for Biotechnology Information sequence Tagged Sites (NCBI-STS) database as recorded in the Marshfield Research Foundation website (http://research.marshfieldclinic.org/genetics/GeneticResearch/).

3.2.6.2 Fragment analysis of 17p products

PCR products were analysed on a CEQ 8000 Genetic Analysis System (Beckman Coulter) as previously described (section 2.8.4). Traces were assessed as being homozygous, heterozygous or indeterminate at each locus in all samples and the presence of an extended region of homozygosity (ERH) determined as outlined in section 2.8.5 using the homozygous probability values from the Marshfield Research Foundation (http://research.marshfieldclinic.org/genetics/GeneticResearch/data/info/info17.txt) and given in Table 3.7. The probabilities returned from the Marsfield Reserach Foundation maps have been constructed on the basis of nearly 1 million genotypes and incorporated over 8,000 short tandem-repeat polymorphisms (Broman, Murray et al. 1998).

Marker	Probability	
	Heterozygous	Homozygous
D17S936	0.6	0.4
D17S974	0.64	0.36
D17S969	0.64	0.36
D17S2196	0.81	0.19
D17S1866	0.79	0.21
D17S1308	0.62	0.38
D17S1840	0.83	0.17

Table 3.7. Chromosome 17 p-arm polymorphic microsatellite markers population probability scores. The probability of a heterozygous or homozygous result for each marker locus as given in the Marshfield Research Foundation (http://research.marshfieldclinic.org/genetics/GeneticResearch/data/info/info17.txt)

3.2.7 Investigation of *MYCC* and *MYCN* amplification

3.2.7.1 Polymerase chain reaction validation of real-time PCR primers

Primers to be used in subsequent real-time PCR (RT-PCR) studies were designed as previously described in section 2.7.3. In addition to *MYCC* and *MYCN* primers a further three primer sets were designed to be used as endogenous controls. These primers were designed to amplify chromosome regions which rarely harbour copy number aberrations in either medulloblastomas (Bayani, Zielenska et al. 2000; Eberhart, Kratz et al. 2002; Rossi, Conroy et al. 2006) or CNS-PNET (Li, Bouffet et al. 2005). The three endogenous controls comprised *TBP* (chromosome 6), *RPLPO* (chromosome 12) and *B2M* (chromosome 15). Validation PCRs were performed using standard conditions as described previously in section 2.7.4. The PCR annealing temperature was set at 60 °C to correspond with the annealing temperature that would be used in subsequent RT-PCR experiments. Nucleotide sequences of the RT-PCR primers, location and the resultant product length are summarised in Table 3.8 for each analysed gene. PCR products were initially analysed by agarose gel electrophoresis as described in section 2.5 and the size of the bands determined by comparison with a 100bp DNA ladder (Invitrogen, UK).

3.2.7.2 Quantitative real-time PCR

Quantitative real-time PCR (qRT-PCR), described in section 2.7, was used to validate the copy number determination produced from the MLPA screen of CNS-PNET tumours and cell lines for *MYCC* and *MYCN.* All samples were analysed in triplicate. A standard curve was derived using a panel of six dilutions (100ng, 50ng, 10ng, 5ng, 1ng and 0.5ng) of a medulloblastoma cell line DNA (MHH-Med1), which has previously been shown to have a diploid copy number of both *MYCC* and *MYCN* (Langdon, Lamont et al. 2006). The cycle threshold (Ct) was determined during the exponential phase of the PCR reaction as previously discussed (section 2.7.2). For each gene investigated a negative control was added (Ultrapure water (Elga, UK)) in addition to two additional

medulloblastoma cell line positive controls (IMR-32 (*MYCN* amplified;(Carr, Bown et al. 2007)) and D341-MED (*MYCC* amplified; (Bigner, Friedman et al. 1990)). 4ng of Genomic DNA (1ng/µl) from the unknown samples to be tested was added to each reaction as previously described (section 2.7.4). The results for *MYCC* and *MYCN* for each sample processed in triplicate were first averaged and then measured relative to the three endogenous controls (*TBP, RPLPO, B2M*) to generate an average copy number for both *MYCC* and *MYCN* for each unknown sample. Samples that showed an elevation in copy number relative to two or three of the control genes were reanalysed on a further two separate replicates to corroborate the finding.

3.2.7.3 Determining elevated *MYCC* or *MYCN* copy number by qRT-PCR

The values derived from section 3.2.7.2 were compared with a reference cohort to determine whether a tumour sample had an elevated *MYCC* or *MYCN* copy number. A reference cohort comprising of 6 normal brain samples (section 3.2.3) which had been processed equivalently to the tumour samples was used. Each reference sample was investigated as previously described (section 2.7.2). The average copy number of *MYCC* and *MYCN* for this reference panel was derived and designated to represent a copy number of one to which the value for each test sample would be normalised to. The elevation detection value (EDV) was defined as the reference panel mean + 3 standard deviations. Tumour samples with a *MYCC* or *MYCN* copy number greater than the EDV measured relative to at least 2 of the endogenous controls in all 3 independent replicates were classified as showing an elevated copy number.

Gene	Location	Forward sequence	Reverse sequence	Product size (bp)	Annealing temperature (°C)	PCR method
MYCC	Intron 1-2	5'-CTTTCGAGATTTCTGCCTTATGAAT-3'	5'-CCCAAAACCCAGAGAGCAATT-3'	95	60	Standard
MYCN	Intron 2-3	5'-AAACTTGGTGATAAGCCTCCAGT-3'	5'-AAGTGCTTCCTCACCAAAAGCT-3'	83	60	Standard
TBP	Intron5-6	5'-TCTCTCTGACCATTGTAGCGGTT-3'	5'-CCGTGGTTCGTGGCTCTCT-3'	64	60	Standard
B2M	Intron 1-2	5'-TCTAGGCGCCCGCTAAGTT-3'	5'-TCGCGTGCTGTTTCCTCC-3'	81	60	Standard
RPLPO	Intron 2-3	5'-ATAAACGGGCTCAGGCAAGTT-3'	5'-CGCGCTCTTTTAGAAGCCAG-3'	81	60	Standard

Table 3.8. Primers used in the RT-PCR assessment of *MYCC* and *MYCN.*

3.2.7.4 Multiplex ligation-dependent probe amplification (MLPA)

MLPA, which has been previously described in section 2.9, was used to determine the copy number of *MYCC* and *MYCN* genes in the cohort of CNS-PNET primary tumour samples and cell lines. Probes for 2 control genes (*TBP* and *B2M*), *MYCC* and *MYCN* were designed to produce products of different sizes as described in section 2.9.2. The nucleotide sequences and product lengths for the MLPA probes are given in Table 3.9. MLPA was undertaken on all tumour samples as described in section 2.9.3. The results for *MYCC* and *MYCN* for each sample were measured relative to two of the endogenous control genes used in the qRT-PCR study (*TBP* and *B2M*) in addition to a further 2 control probes (Table 3.10) supplied in the MLPA P200 (MRC Holland) reaction mix to generate an average copy number for both *MYCC* and *MYCN* for each unknown sample. Samples that showed an elevation in copy number relative to three or four of the control genes were reanalysed to corroborate the finding.

3.2.7.5 Determining elevated *MYCC* or *MYCN* copy number by MLPA

The values derived from 3.2.7.4 were compared with the normal brain reference cohort (Table 3.3) to determine whether a tumour sample had an elevated *MYCC* or *MYCN* copy number. The average copy number of *MYCC* and *MYCN* for this reference panel was derived and designated to represent a copy number of one to which the value for each test sample would be normalised to. The elevation detection value (EDV) was defined as the reference panel mean + 3 standard deviations. Tumour samples with a *MYCC* or *MYCN* copy number greater than the EDV measured relative to at least 2 of the endogenous controls in all 3 independent replicates were classified as showing an elevated copy number.

Gene	Stuffer Length (nt)	Probe Length (nt)	Left hybridising sequence	Right hybridising sequence
B2M	7	90	5'-CTGACAGCATTCGGGCCGA-3'	5'-GATGTCTCGCTCCGTGGCCTTA-3'
TBP	4	96	5'-TCATGGATCAGAACAACAGCCTGCCAC-3'	5'-CTTACGCTCAGGGCTTGGCCTCC-3'
MYCN	24	110	5'-GAGCTGGGTCACGGAGATGCT-3'	5'-GCTTGAGAACGAGCTGTGGGGCA-3'
MYCC	25	116	5'-GTGCCACGTCTCCACACATCAGCACAA-3'	5'-CTACGCAGCGCCTCCCTCCACT-3'

Table 3.9. Primers used in the MLPA analysis of *MYCC* and *MYCC.*

Name	Probe	Probe length (nt)	Location
Ctrl 1	3578-L02939	172	7q31
Ctrl 2	3139-L02607	178	14q22

Table 3.10. Control MLPA probes supplied in the P200 kit (MRC Holland).

3.2.7.6 Fluorescence *in situ* hybridisation (FISH)

Where material was available FISH was performed on cases showing an elevated copy number of *MYCN*. Nuclear preparations and unstained sections were prepared and used as described in sections 2.12.2 and 2.12.3. A probe to chromosome 2p24.3 corresponding to the *MYCN* locus (*MYCN*, bA355H10) was compared with a probe to the centromere of the same chromosome (pBSD4D). Both probes were kindly provided by Dr Kieran O'Toole (Northern Institute for Cancer Research, Newcastle University UK) from DNA isolated from BAC clones as previously described and validated by Lamont et al (Lamont, McManamy et al. 2004).

The genetic status of each cell was assigned based on the ENQUA recommended criteria (Ambros, Benard et al. 2003) which is summarised in Table 3.11. Tumour samples were considered as showing *MYCN* amplification if the test probe to centromeric probe ratio was equal or greater than 4. The presence of either speckling or clumping within the cells consistent with double minute (DM) or homogenously staining region (HSR) formation respectively was also considered to show evidence of amplification as has been previously described (Bown 2001; Mathew, Valentine et al. 2001; Lamont, McManamy et al. 2004; Yoshimoto, Bayani et al. 2006).

Status	Test probe copy number	Test probe: Centromeric control ratio
Monosomy	1	1
Diploid	2	1
Trisomy	3	1
Tetrasomy	4	1
Ploidy	>4	1
Gain	>4	>1 to <4
Amplification	>4	≥4

Table 3.11. Criteria to define genetic status of cells by FISH. In this study a probe to the centromere of chromosome 2 was used as a control and that to *MYCN* as the test probe.

3.2.8 Investigation of *TP53* pathway defects

3.2.8.1 Immunohistochemistry

Slides were prepared from FFPE material as has been previously described (section 2.11.3) using Dako High pH Target Retrieval Buffer (Dako, USA) (see appendix A). Disruption of the p53 pathway was assessed using the M7001 clone D-07 antibody (Dako, USA) used in previous medulloblastoma and CNS-PNET studies (Jaros, Lunec et al. 1993; McLendon, Friedman et al. 1999; Eberhart, Chaudhry et al. 2005; Tabori, Baskin et al. 2010). A 1/2000 dilution of the M7001 clone D-07 p53 antibody was applied and detected using the methods previously detailed (section 2.11.3). Slides were viewed under a light microscope and scored according to nuclear staining according to previously described scoring system (Ng, Lo et al. 1994) with three categories of positive results and a negative score with the absence of nuclear staining as shown in Table 3.12.

Score	p53 nuclear positive cells (%)
0	0
+	1-25
++	26-50
+++	>50

Table 3.12. Scoring of p53 immunohistochemical slides.

3.2.8.2 Polymerase chain reaction

PCR primers were designed as described previously (section 2.4.2) to amplify the commonly mutated *TP53* exons 4-9. To investigate the presence of a homozygous deletion of *CDKN2A* (p14) primers were designed to amplify exon 1β of this gene. The *CDKN2A* primer pair were amplified in a duplex PCR reaction with the addition of a

previously described control primer pair to *SCN4A* (Frank, Hernan et al. 2004; Carr, Bell et al. 2006). Details of the primers and PCR reactions are given in Table 3.13. The *TP53* exons were amplified using reaction mixes, given previously in section 2.4.4. For the *CDKN2A* duplex PCR 2µl of each of the 4 primers (10µM) was added to 10µl of the GeneAmp® Fast PCR Master Mix and 50ng of DNA template to yield a final volume of 20µl. PCR amplification was performed using a 40 cycle reaction using the fast method (section 2.4.4) with an annealing and extension step of 10 seconds.

3.2.8.3 Sequencing of *TP53* products

PCR products were purified prior to further analysis as described in section 2.4.5. prior to sequencing on an ABI 3730 (Applied Biosystems) by DBS genomics (Durham University, Durham, UK). Raw data was returned for subsequent mutational analysis.

3.2.8.4 Agarose gel electrophoresis

The PCR products from the p14 duplex PCRs were separated on an agarose gel by electrophoresis as has been previously described (section 2.5). Evidence of p14 loss was determined by the absence of a *CDKN2A-1β* band in the presence of a band generated from the control gene (*SCN4A*). Abnormal results were repeated to confirm the finding.

Gene	Location (Exon)	Forward sequence	Reverse sequence	Product size (bp)	Annealing temperature (°C)	PCR method
TP53	4	5'-GGCTGAGGACCTGGTCCTCTGA-3'	5'-GCCAGGCATTGAAGTCTCATGG-3'	371	64	Fast
TP53	5	5'-ATCTGTTCACTTGTGCCCTG-3'	5'-CAACCAGCCCTGTCGTCTCTC-3'	275	64	Fast
TP53	6	5'-GCCTCTGATTCCTCACTGAT-3'	5'-GGAGGGCCACTGACAACCA-3'	203	64	Fast
TP53	7	5'-AAGGCGCACTGGCCTCATCTT-3'	5'-CAGGGGTCAGAGGCAAGCAGA-3'	220	64	Fast
TP53	8	5'-GAGCCTGGTTTTTTAAATGG-3'	5'-TTTGGCTGGGGAGAGGAGCT-3'	344	64	Fast
TP53	9	5'-AGCGAGGTAAGCAAGCAGG-3'	5'-GCCCCAATTGCAGGTAAAACAG-3'	267	64	Fast
CDKN2A	1β	5'-CTGTGGCCCTCGTGCTGATGCTAC-3'	5'-AATGCGCCCCGGACTTTTC-3'	103	64	Fast
SCN4A	24	5'-TCGGCATCTGCTTCTTCTGCA-3'	5'-TCGAACTTCTCCCATGTCTCG-3'	166	64	Fast

Table 3.13. *TP53* pathway studies PCR primers

3.2.8.5 MLPA assessment of *MDM2* amplification

To determine the copy number of the *MDM2* gene in the cohort of CNS-PNET primary tumour samples and cell lines, MLPA was used as detailed in section 2.9.3. Four reference control probes were used (as discussed in 3.2.7.5) in addition to a probe set for *MDM2* (Table 3.10 and Table 3.14). Samples that showed an elevation in copy number relative to three or four of the control genes were reanalysed to corroborate the finding.

Gene	*MDM2*
Stuffer Length (nt)	1
Probe Length (nt)	123
Left hybridising sequence	5'-GATCAGTTTAGTGTAGAATTTGAAGTTGAATCTCTCGACT-3'
Right hybridising sequence	5'-CAGAAGATTATAGCCTTAGTGAAGAAGGACAAGAACTCTC-3'

Table 3.14. MLPA probe for *MDM2* copy number ascertainment. nt: nucleotides.

3.2.8.6 Determining elevated *MDM2* copy number by MLPA

The values derived from 3.2.8.4 were compared with the normal brain reference cohort as has been described for the *MYC* genes in section 3.2.7.5. The elevation detection value (EDV) was defined as the reference panel mean + 3 standard deviations. Tumour samples with a *MDM2* copy number greater than the EDV measured relative to 3 or 4 of the endogenous controls were classified as showing an elevated copy number.

3.2.9 Wnt pathway defects investigation

3.2.9.1 Immunohistochemistry

Slides were prepared from FFPE material as has been previously described (section 2.11.3) using freshly prepared citrate Buffer see appendix A). Disruption of the Wnt pathway was assessed using β-catenin antibody (610514, BD Transduction labs, USA) as described in section 2.11.3 and used in previous medulloblastoma studies (Ellison, Onilude et al. 2005; Clifford, Lusher et al. 2006; Ellison, Kocat et al. 2011). Slides were viewed under a light microscope and scored according to nuclear accumulation of β-catenin. Nuclear immunohistochemical status was scored using the same criteria as used in the aforementioned studies, summarised in Table 3.15.

β-catenin nuclear immunohistochemistry		
Description	**Score**	**Classification**
No nuclear staining	0	Negative
<10% nuclear staining	+	Negative
Widespread nuclear staining	++	Positive
Patchy nuclear staining >10%	++	Positive

Table 3.15. β-catenin immunohistochemistry scoring system.

3.2.9.2 Polymerase chain reaction (PCR) amplification of *CTNNB1*

PCR products spanning the GSK-3β phosphorylation domain of β-catenin (see section 1.5.5.2) were generated for subsequent sequencing and mutational screening. PCRs were performed using a standard 40 cycle reaction as described in section 2.4.3 using the previously described *CTNNB1* primers (Ellison, Onilude et al. 2005). Primer details and PCR conditions are given in Table 3.16.

Gene	*CTNNB1*
Primer location	Exon 3
Forward sequence	5'-TCCAATCTACTAATGCTAATACTG-3'
Reverse sequence	5'-TAAGGCAATGAAAAATAATACTC-3'
Product size (bp)	293
Annealing temperature (˚C)	53
PCR method	Standard

Table 3.16. *CTNNB1* mutation analysis PCR primers.

3.2.9.3 Sequencing of *CTNNB1*

All PCR products were purified prior to further analysis as described in section 2.4.5. prior to sequencing on an ABI 3730 (Applied Biosystems) by DBS genomics (Durham University, Durham, UK). Raw data were returned for subsequent mutational analysis

3.3 Results

3.3.1 *RASSF1A* promoter methylation in CNS-PNET

3.3.1.1 Investigation of *RASSF1A* promoter methylation in CNS-PNET cell lines and primary tumours

Methylation of the *RASSF1A* promoter was determined in 2 control samples, 2 CNS-PNET cell lines and in 25 primary CNS-PNET tumour samples. Illustrative electropherograms from the methylated DNA and unmethylated DNA control samples are shown in Figure 3.3 and Figure 3.4 respectively. Within each amplicon, 15 CpG dinucleotides were analysed. The methylation status at each CpG dinucleotide within the amplified sequence for the CNS-PNET cell lines and tumour samples is shown in Figure 3.3.

Both CNS-PNET cell lines (PFSK and CHP707) investigated were found to exhibit *RASSF1A* promoter methylation. *RASSF1A* methylation results were not obtained in 3 samples (SP7, SP10 and SP13). In the remaining 22 samples, 18 (82%) exhibited promoter methylation and 4 (18%) were hypomethylated.

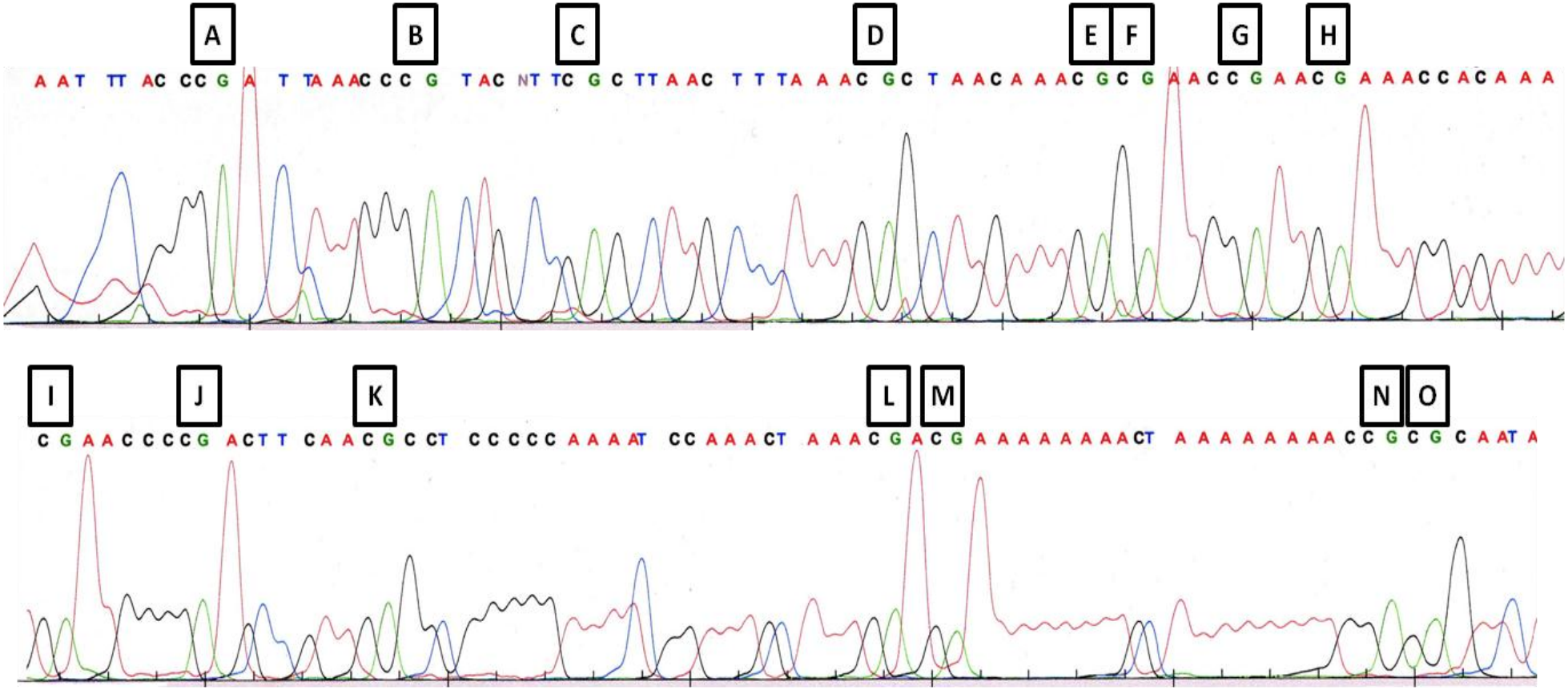

Figure 3.3. Methylated control electrophoregram of *RASSF1A* promoter amplified sequence. Antisense sequence following bisulphite conversion shown. CpG dinucleotides are marked A to O.

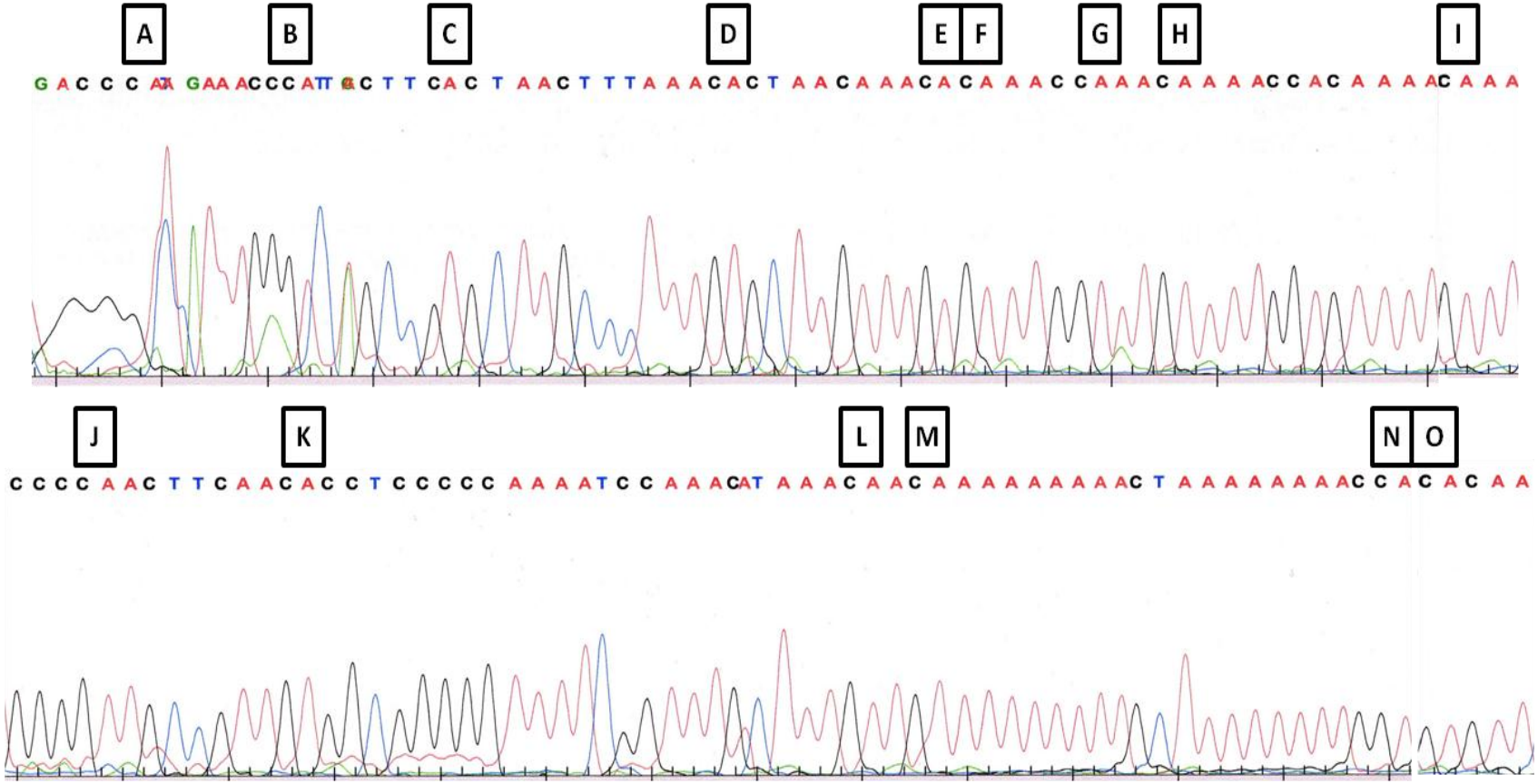

Figure 3.4. Unmethylated control electrophoregram of *RASSF1A* promoter amplified sequence. Antisense sequence following bisulphite conversion shown. CpG dinucleotides are marked A to O. The unmethylated cytosines are converted to uracils with bisulphite treatment, seen as an adenine substitution when sequenced using the *RASSF1A* antisense primer.

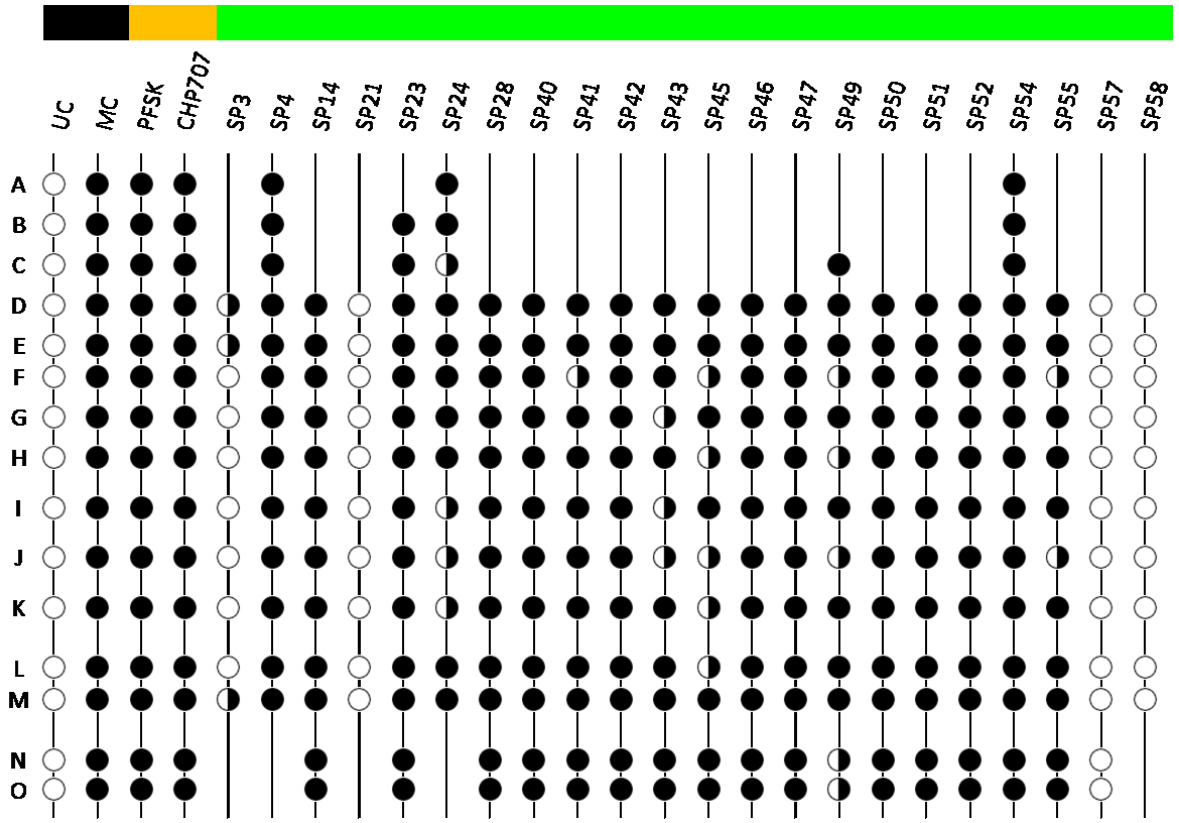

Figure 3.5. *RASSF1A* promoter methylation in CNS-PNET primary tumours and cell lines. The methylation status at each CpG dinucleotide (A to O) of 2 control samples (black bar), including an unmethylated control (UC) and a methylated control (MC), 2 CNS-PNET cell lines (orange bar) and samples from 22 primary CNS-PNETs (green bar). Methylation status at each CpG dinucleotide is given as hypomethylated (open circle), partially methylated (half closed circle) and methylated (closed circle).

3.3.1.2 Comparison of CNS-PNET and medulloblastoma *RASSF1A* promoter methylation.

Lindsey et al observed a frequency of methylation in a total cohort of 62 primary medulloblastoma samples of 87% (54/62) using equivalent methods (Lindsey, Lusher et al. 2004). Methylation of the *RASSF1A* promoter occurred at a similar rate (82%, 18/22) in this cohort of CNS-PNET primary tumour samples (p=0.50, Fisher's exact test).

3.3.2 Investigation into chromosome 17p loss in CNS-PNET

3.3.2.1 HOMOD investigation of 17p loss

Investigations to determine the status of the p-arm of chromosome 17 were undertaken in 2 CNS-PNET cell lines and the panel of tumours shown in Table 3.1. The 7 polymorphic microsatellite markers were amplified and assessed as showing homozygous or heterozygous state at each locus as shown in Figure 3.6. Retention of heterozygosity was observed for both CNS-PNET cell lines as shown in Figure 3.7. The results for 23/25 primary tumour samples are given in Figure 3.8. Results are not available for samples SP3 or SP7. No evidence of entire chromosome 17p loss was seen in any of the primary tumour samples or cell lines. However, in 2 cases (SP46 and SP55) an extended region of homozygosity (ERH) was observed with the identification a loss of heterozygosity (homozygous state) at 6 consecutive polymorphic markers (p=0.00064) consistent with segmental loss of chromosome 17p.

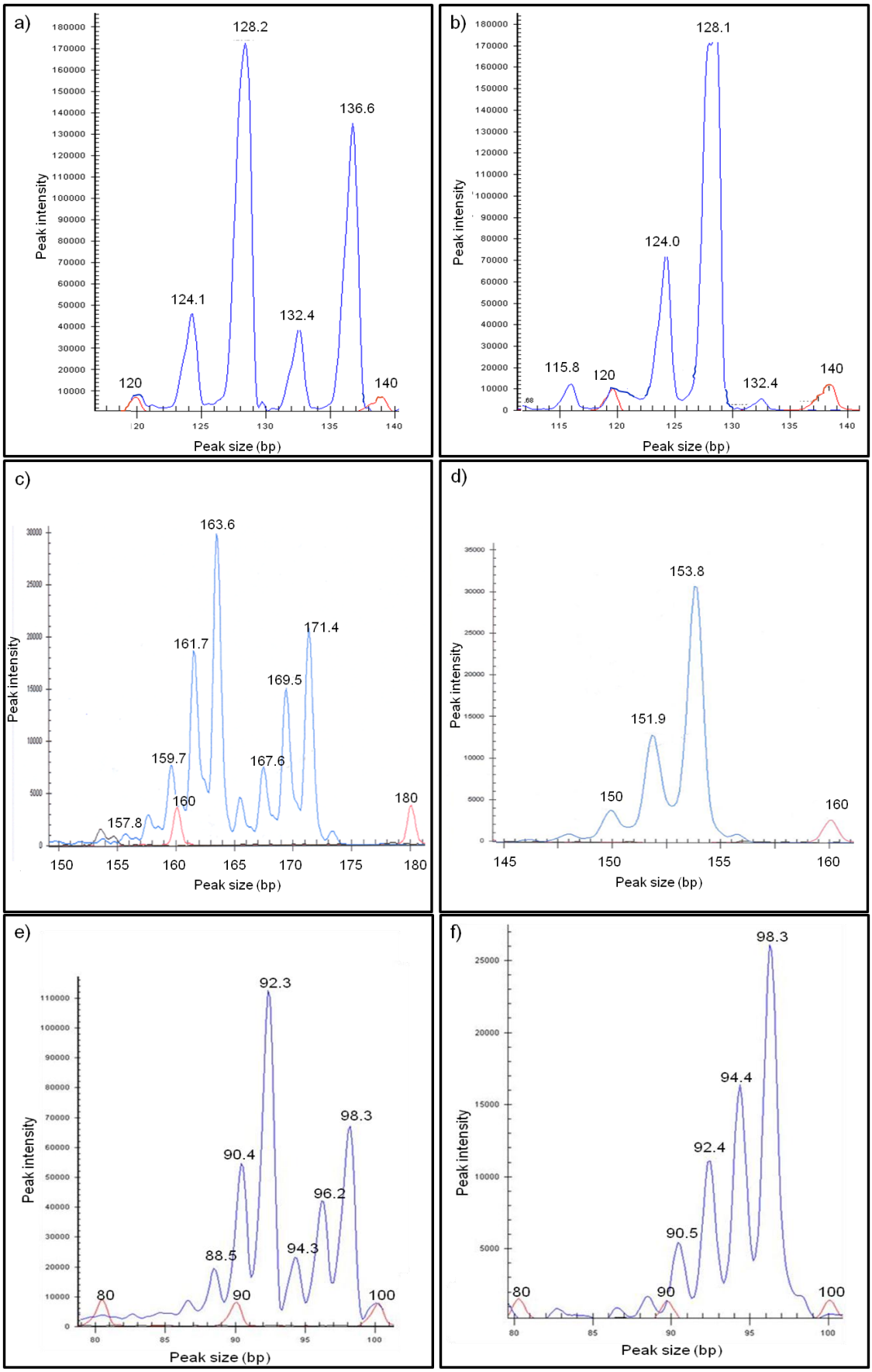
a)
Peak intensity
Peak size (bp)
128.2
136.6
124.1
132.4
120
140
b)
Peak intensity
Peak size (bp)
128.1
124.0
115.8
120
132.4
140
c)
Peak intensity
Peak size (bp)
163.6
161.7
171.4
169.5
159.7
167.6
160
180
157.8
d)
Peak intensity
Peak size (bp)
153.8
151.9
150
160
e)
Peak intensity
Peak size (bp)
92.3
98.3
90.4
96.2
88.5
94.3
80
90
100
f)
Peak intensity
Peak size (bp)
98.3
94.4
92.4
90.5
80
90
100

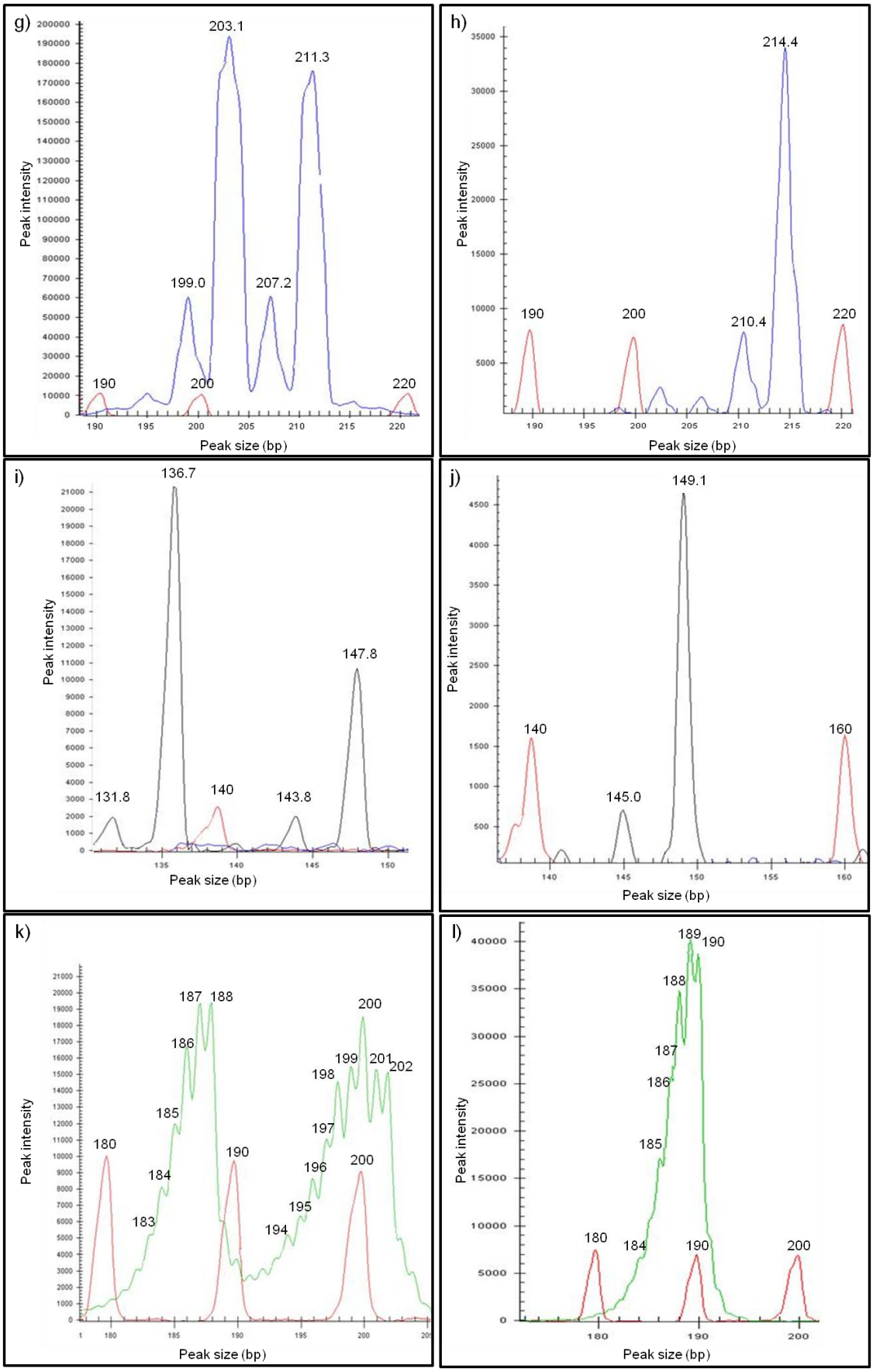
g)
Peak intensity
Peak size (bp)
203.1
211.3
199.0
207.2
190
200
220
h)
Peak intensity
Peak size (bp)
214.4
190
200
210.4
220
i)
Peak intensity
Peak size (bp)
136.7
147.8
131.8
140
143.8
j)
Peak intensity
Peak size (bp)
149.1
140
145.0
160
k)
Peak intensity
Peak size (bp)
187
188
186
200
199
201
202
198
185
197
180
190
184
196
200
183
195
194
l)
Peak intensity
Peak size (bp)
189
190
188
187
186
185
180
184
190
200

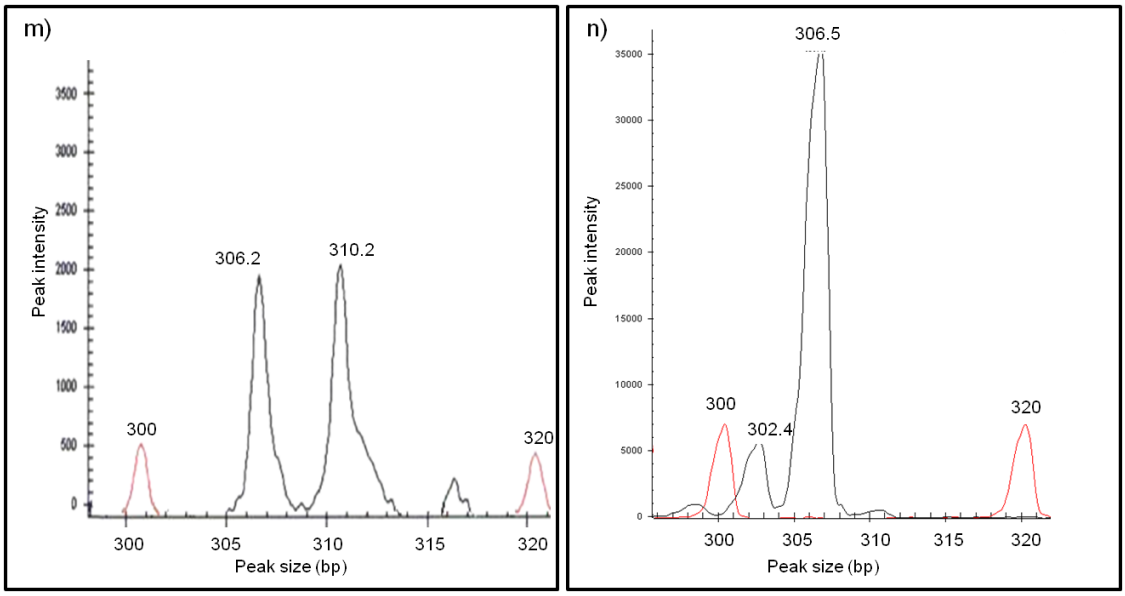

Figure 3.6. Chromosome 17p polymorphic microsatelite marker CEQ traces. Standard size markers are shown in red. (a) and (b): Fragment analysis traces for tetra-nucleotide repeat marker D17S969; (a) Two sets of two minor peaks 4 base pairs apart constitute two major peak indicating a heterozygous trace, (b) Homozygous trace with a single major peaks. (c) and (d): Fragment analysis traces for di-nucleotide repeat marker D17S1866 and (e) and (f) fragment analysis traces for di-nucleotide repeat marker D17S936. (c) and (e) Three minor peaks 2 base pairs apart are shown to constitute a major peak in these heterozygous traces, (d) and (f) homozygous traces. (g) and (h): Heterozygous and homozygous traces respectively for tetra-nucleotide repeat polymorphic microsatellite marker D17S974. (i) and (j): Heterozygous and homozygous traces respectively for D17S2196. (K) and (l). Mono-nucleotide repeat marker D17S1840 using green fluorescence to enable to discern this result from the simultaneous assessment of other markers. (K) example of a heterozygous trace, (l) homozygous status. (m) and (n): Traces for D17S1308 producing the largest product size (304-318 base pairs) of all the markers used. (m) heterozygous and (n) homozygous status.

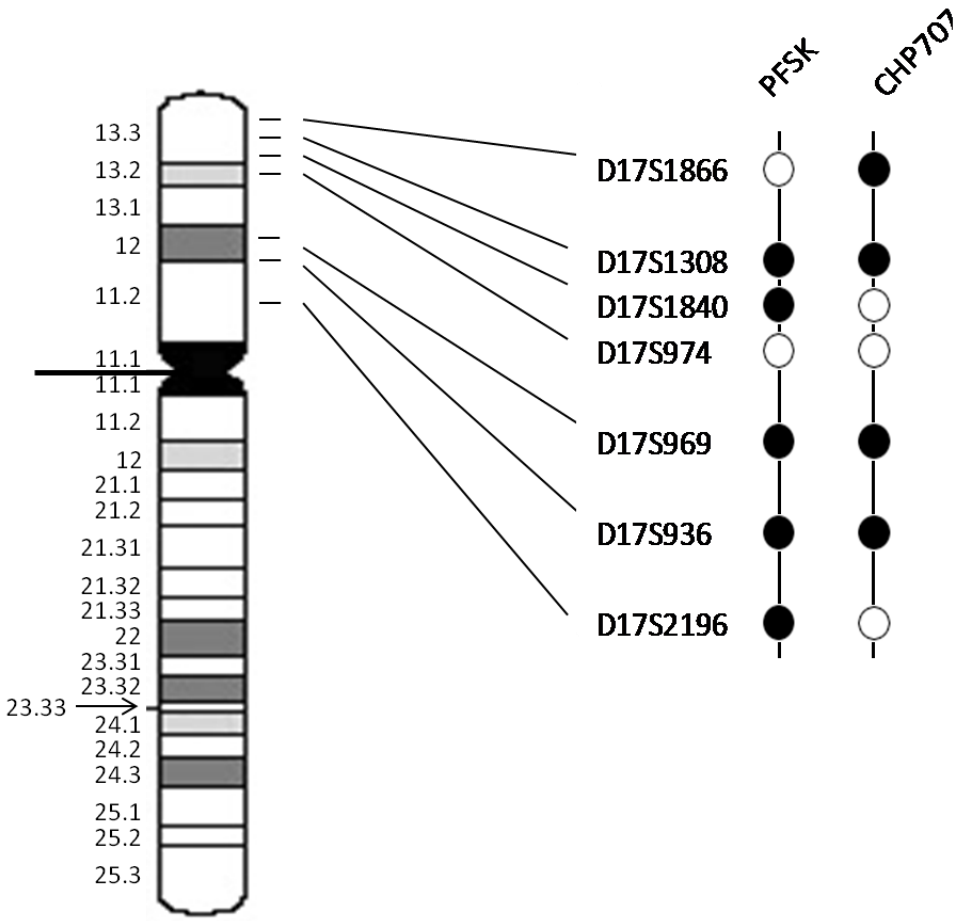

Figure 3.7. CNS-PNET cell line results from chromosome 17 p-arm homozygosity of deletion (HOMOD) mapping. The location of each of the 7 polymorphic microsatelite markers on the p-arm of chromosme 17 is shown with the result for both CNS-PNET cell lines (PFSK and CHP707). Closed circle: Homozygous, open circle: heterozygous.

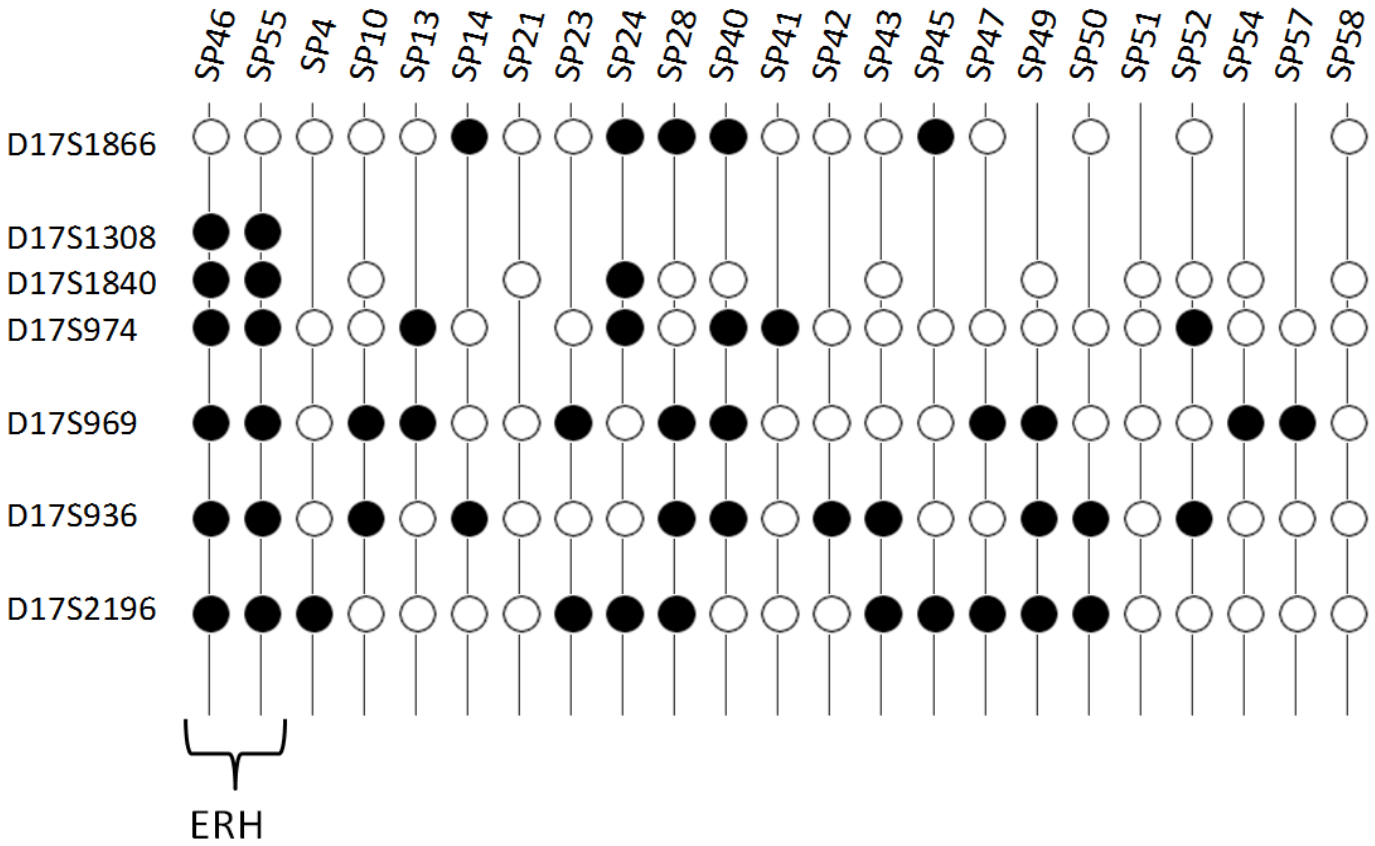

Figure 3.8. Chromosome 17p Homozygosity mapping of deletions (HOMOD) in primary CNS-PNET. The results for 23 primary CNS-PNET samples are shown for each marker - homozygous (closed circle), and heterozygous (open circle). An extended region of homozygosity (ERH) with more than 5 consecutive markers displaying a homozygous status was observed in both SP46 and SP55.

3.3.2.2 Comparison of chromosome 17p loss in CNS-PNET and medulloblastoma.

In a large study by Megahed (Megahed 2010), who undertook an identical approach to investigate chromosome 17 status in 190 primary medulloblastoma samples, 25% (47/190) were found to have lost the p-arm of chromosome 17 (data not shown). This result however does not differ statistically significantly with these results in the CNS-PNET study where 17p loss was observed in 2/23 of the primary tumour samples (p=0.08, Fisher's exact test).

3.3.3 Investigation of *MYCC* and *MYCN* gene amplification

3.3.3.1 Development of the qRT-PCR assay

Primers designed to amplify *B2M*, *RLPO*, *TBP, MYCC* and *MYCN* genes were tested using a standard PCR reaction and assessed on an agarose gel to confirm that single products of the correct size were produced as given in Table 3.8. Dissociation plots for each primer pair were generated by qRT-PCR to confirm that the qRT-PCR reaction resulted in a single product with a specific melting temperature (Tm) as shown in Figure 3.9.

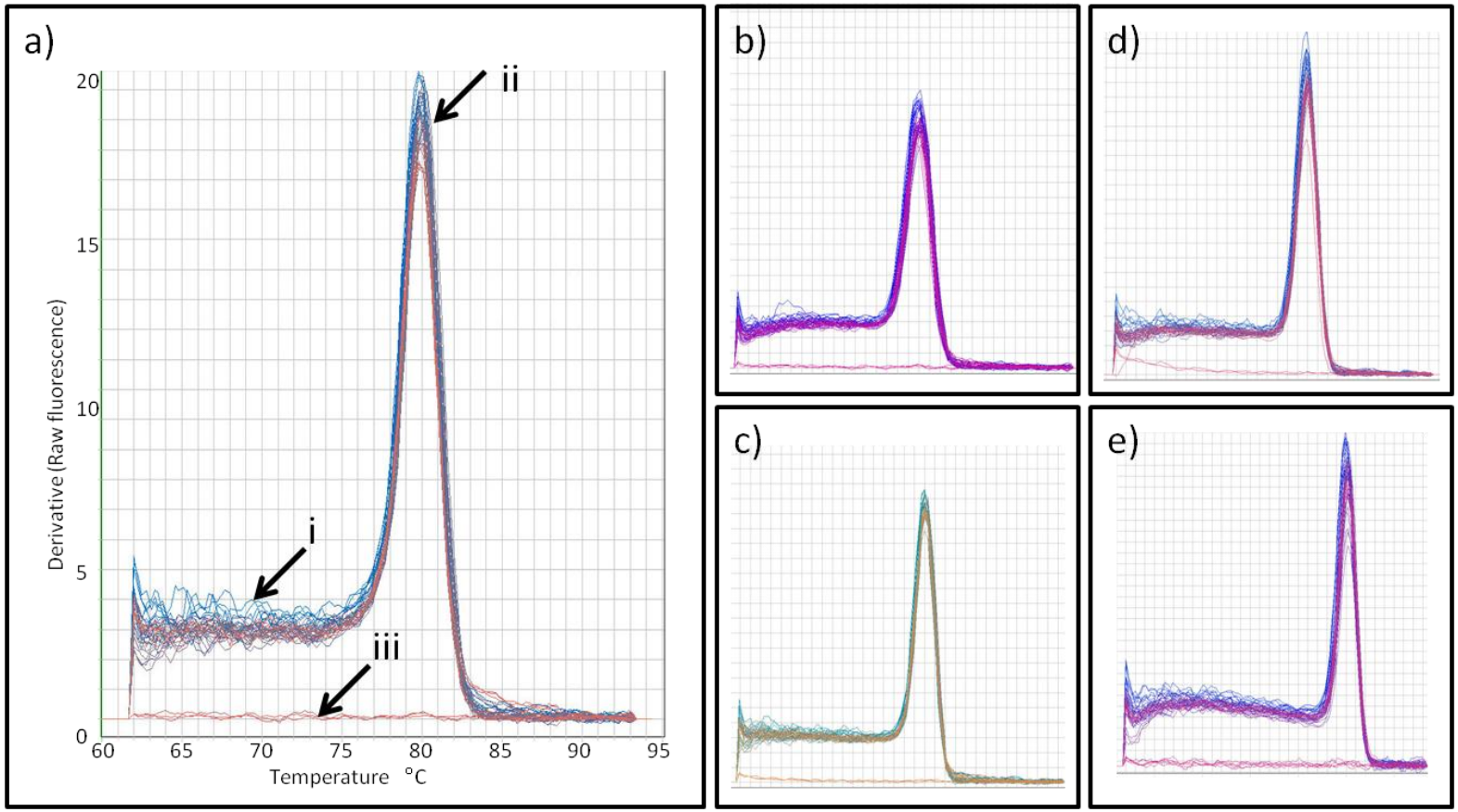

Figure 3.9. Dissociation curves for genes used in qRT-PCR *MYC* family study. (a) Dissociation curve generated using the *MYCC* primers. i) multiple replicates resulting in ii) a single PCR product following denaturation, without any products being produced using iii) negative controls (water). (b-e) Unique products produced for all the genes used in the qRT-PCR study, (b) *B2M*, (c) *MYCN*, (d) *TBP*, (e) *RPLPO*.

3.3.3.2 Development of elevated copy number thresholds for *MYCN* and *MYCC* by qRT-PCR using a reference cohort

The results from qRT-PCR of a panel comprising of the DNA extracted from FFPE material from 6 normal brain samples was used as a reference cohort as described in 3.2.7.3. The copy numbers of *MYCC* and *MYCN* were measured relative to the three internal control genes (*TBP*, *B2M* and *RPLPO*). The average copy number of *MYCC* and *MYCN* was measured in three independent replicates and the mean, standard deviation (SD) and coefficient of variation (Cv) determined as shown in Table 3.17. The elevation detection value (EDV) determined by calculating the mean +3SD for *MYCC* and *MYCN* of the reference cohort was used as a cut-off to identify samples in the test series with an elevated copy number. Details of the EDV for *MYCC* and *MYCN* compared to each of the reference genes in the reference cohort are shown in Table 3.17.

	MYCC			***MYCN***		
	TBP	***B2M***	***RPLPO***	***TBP***	***B2M***	***RPLPO***
Mean	0.8097	1.0775	0.7342	3.8287	5.1932	3.5703
SD	0.2234	0.2270	0.1482	0.7000	0.9258	0.7966
EDV	1.4799	1.7587	1.1788	5.9288	7.9705	5.9600
Log_{10} EDV	0.1702	0.2452	0.0715	0.7730	0.9015	0.7752

Table 3.17. qRT-PCR of *MYCN* and *MYCC* copy number in the reference cohort and derivative values. Mean, standard deviation (SD) and elevation detection values (EDV) for both *MYCC* and *MYCN* compared to three reference genes (*TBP, B2M* and *RPLPO*).The EDV was set at mean + 3SD.

The capacity for the qRT-PCR assay to detect *MYCC* or *MYCN* copy number changes was confirmed as discussed in section 3.2.7.2 with the inclusion of 2 cell lines known to exhibit *MYCN* (IMR-32) and *MYCC* (D384) amplification and shown in Figure 3.10.

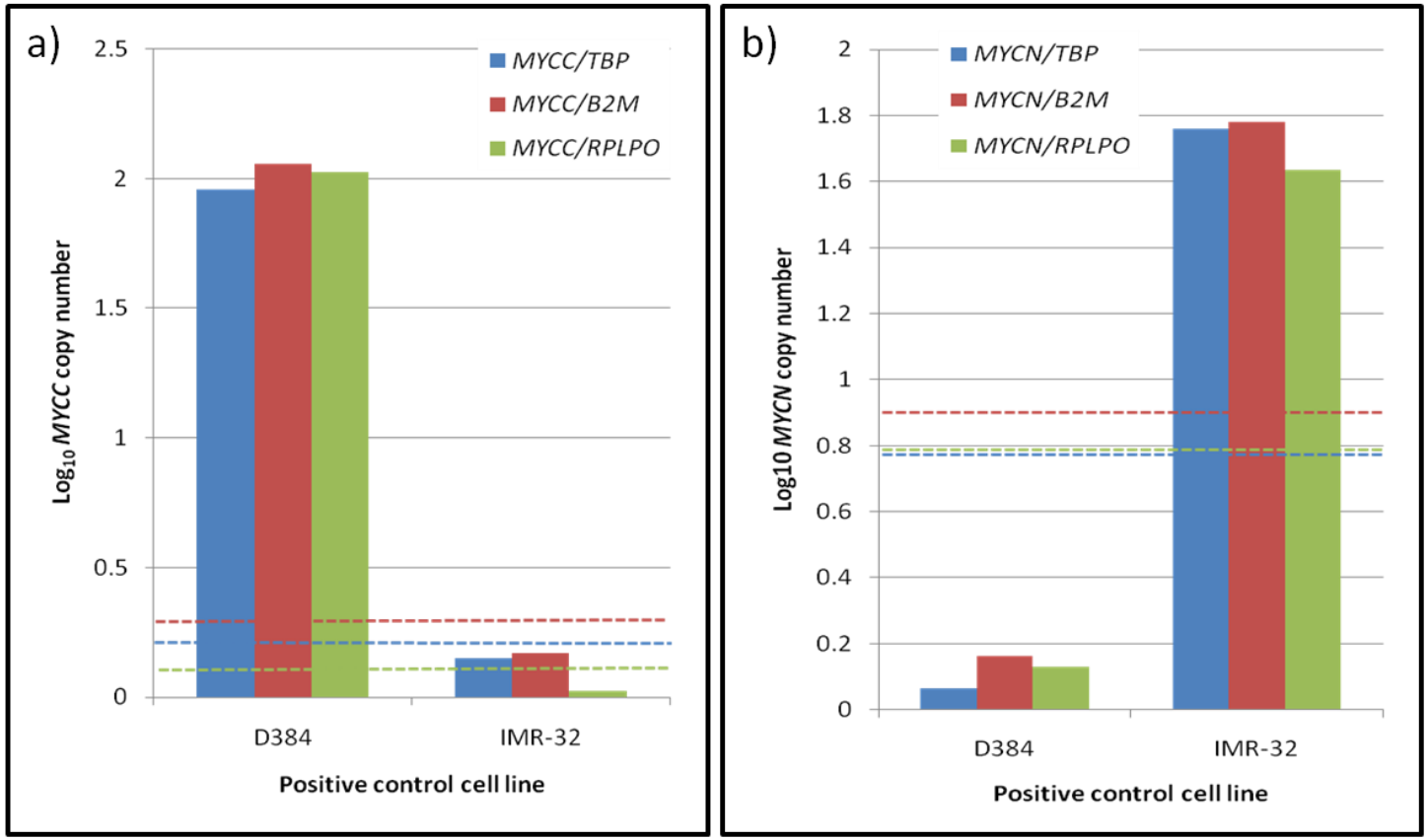

Figure 3.10. *MYCC* and *MYCN* amplification in qRT-PCR positive control cell lines. (a) *MYCC* amplification in medulloblastoma cell line D384. (b) *MYCN* amplification in neuroblastoma cell line IMR-32. A copy number greater than the elevation detection value (EDV) when compared with at least 2 control genes (*TBP*, *B2M* or *RPLPO*) denotes a gain. The EDV for *TBP*, *B2M* and *RPLPO* are shown by the blue, red and green dotted lines respectively.

3.3.3.3 Assessment of *MYCC* and *MYCN* copy number in CNS-PNET cell lines and primary tumour samples.

Two CNS-PNET cell lines and 25 primary CNS-PNET samples were investigated for copy number changes of the *MYC* family genes by qRT-PCR. PFSK and CHP707 were both found to have a raised copy number of *MYCC* when compared relative to the three internal control genes (*TBP, B2M* and *RPLPO*) and were validated in three independent replicates. This finding was not observed in any of the primary tumour samples (0/25) as shown in Figure 3.11. A gain in *MYCN* copy number was not present in either cell line. In 3/25 (12%) primary tumours investigated, a gain in *MYCN* copy number was observed in comparison to the control genes, which was validated in three independent replicates Figure 3.12.

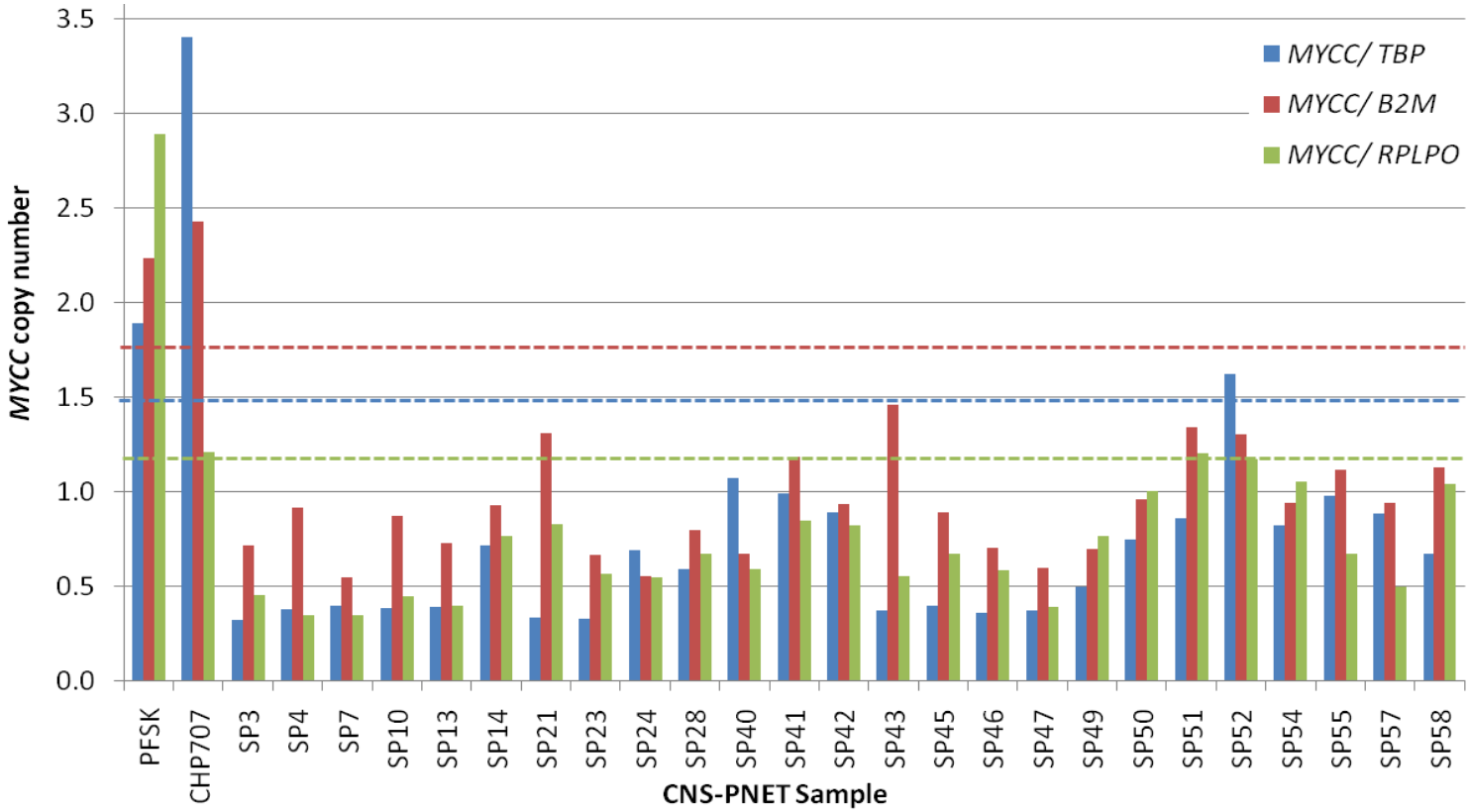

Figure 3.11. *MYCC* copy number in CNS-PNET by qRT-PCR. *MYCC* copy number in 2 CNS-PNET cell lines and 25 primary CNS-PNET tumours measured relative to 3 internal control genes (*TBP, B2M* and *RPLPO*). Copy number elevation in both CNS-PNET cell lines (PFSK and CHP707) as denoted by values above the elevation detection values (EDV) for all 3 control genes (*TBP*, blue dotted line; *B2M*, red dotted line; and *RPLPO*, green dotted line). A normal copy number was observed in all primary tumours (relative copy number <EDV when compared with 1> control gene).

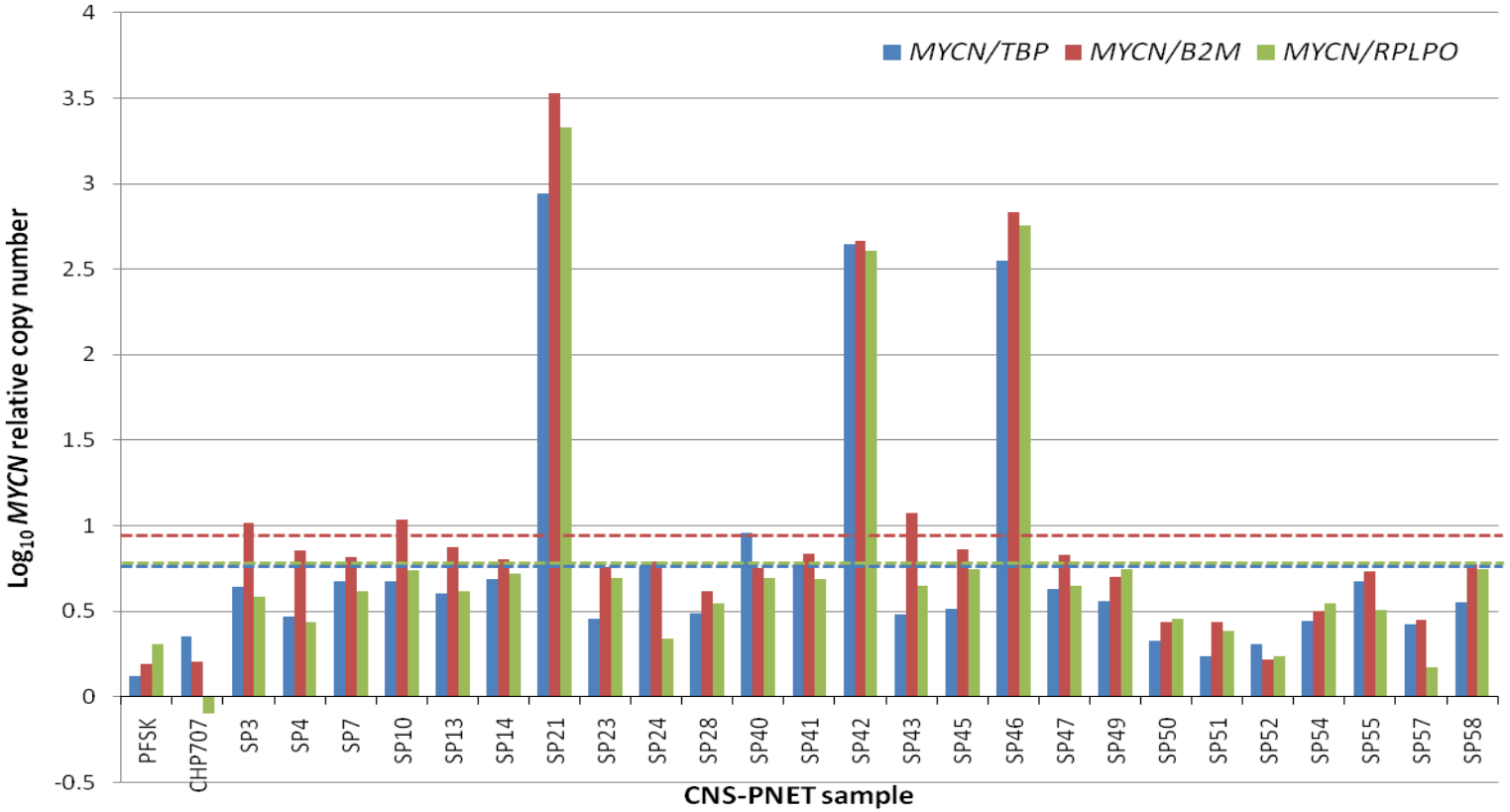

Figure 3.12. Log10 *MYCN* copy number in CNS-PNET by qRT-PCR. Log_{10} *MYCN* copy number is shown in 2 CNS-PNET cell lines and 25 primary CNS-PNET tumours measured relative to 3 internal control genes (*TBP, B2M* and *RPLPO*). A normal copy number was observed in both CNS-PNET cell lines (PFSK and CHP707) as denoted by values below the elevation detection values (EDV) for 2 or 3 control genes (*TBP*, blue dotted line; *B2M*, red dotted line; and *RPLPO*, green dotted line). A *MYCN* copy number elevation was observed in 3 primary CNS-PNET tumour samples (SP21, SP42 and SP46).

3.3.3.4 Development of the elevated copy number thresholds to be used for the MLPA validation of the qRT-PCR results

The reference cohort used in determining the qRT-PCR EDV for both *MYCC* and *MYCN* was used to determine the EDV for the MLPA analysis. The copy numbers of *MYCC* and *MYCN* were measured relative to four internal control genes (*TBP*, *B2M* Ctrl and *Ctrl2*). *TBP* and *B2M* as previously described (section 3.2.7.5) had product lengths smaller than the test genes, whilst Ctrl1 and Ctrl2 produced products greater than the *MYC* products (as shown in Figure 3.13). The elevation detection value (EDV) was determined by calculating the mean +3 SDs for *MYCC* and *MYCN* as shown in Table 3.18.

Gene ratio	Mean	SD	EDV	Log_{10} EDV
MYCN*/*B2M	1.2023	0.3306	2.1942	0.3413
MYCN*/*TBP	1.2812	0.4155	2.5277	0.4027
***MYCN*/Ctrl1**	1.0857	0.1636	1.5766	0.1977
***MYCN*/Ctrl2**	1.4050	0.3263	2.3838	0.3773
MYCC*/*B2M	1.1936	0.1535	1.6540	0.2185
MYCC*/*TBP	1.2454	0.1915	1.8198	0.2600
***MYCC*/Ctrl1**	1.1109	0.1919	1.6866	0.2270
***MYCC*/Ctrl2**	1.4056	0.2063	2.0244	0.3063

Table 3.18. MLPA reference cohort *MYCC* and *MYCN* copy number derived values. Mean, standard deviation (SD) and elevation detection values (EDV) for both *MYCC* and *MYCN* compared to four reference genes (*TBP, B2M*, Ctrl1 and Ctrl2).The EDV was set at mean + 3SD.

The capacity for the MLPA assay to detect *MYCC* or *MYCN* copy number changes was confirmed as discussed in section 3.2.7.2 with the inclusion of 2 cell lines known to exhibit *MYCN* (IMR-32) and *MYCC* (D384) amplification and shown in Figure 3.14.

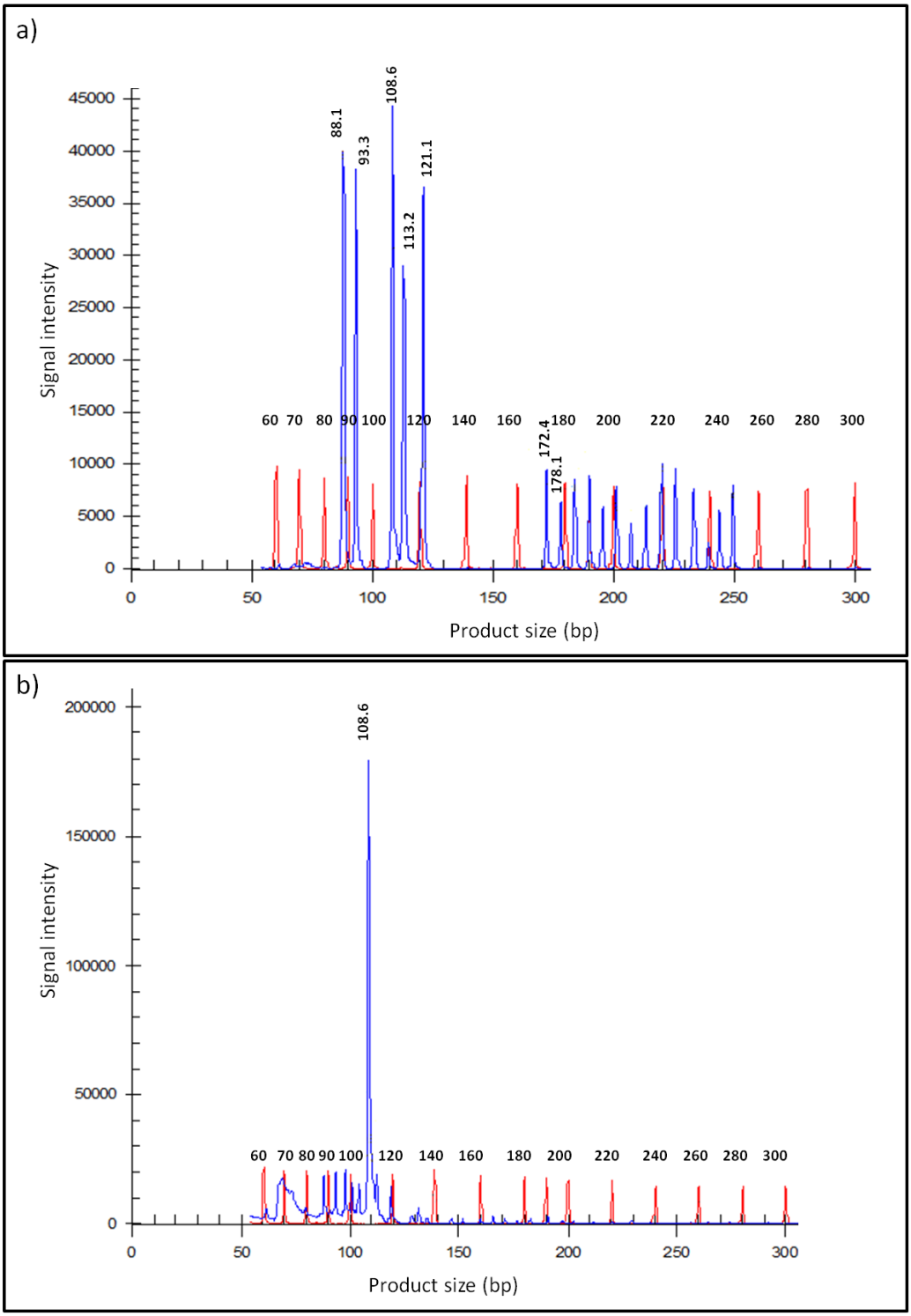

Figure 3.13. MLPA analysis raw traces. (a) Raw trace from control sample N9. Normal size control peaks (blue) for *B2M* (88.1bp), *TBP* (99.3bp), Ctrl1 (172.4bp) and Ctrl2 (178.1bp). In between these peaks are three test peaks for *MYCN* (108.6bp), *MYCC* (113.2bp) and *MDM2* (121.1bp). Additional peaks of molecular size greater than Ctrl2 reflect redundant additional probes in the MRC-Holland P200 probemix. Reference size marker (red). (b) *MYCN* amplification in SP42. Signal intensity for the *MYCN* probe (108.6bp) is ten-fold greater than the panel of reference and other test probes.

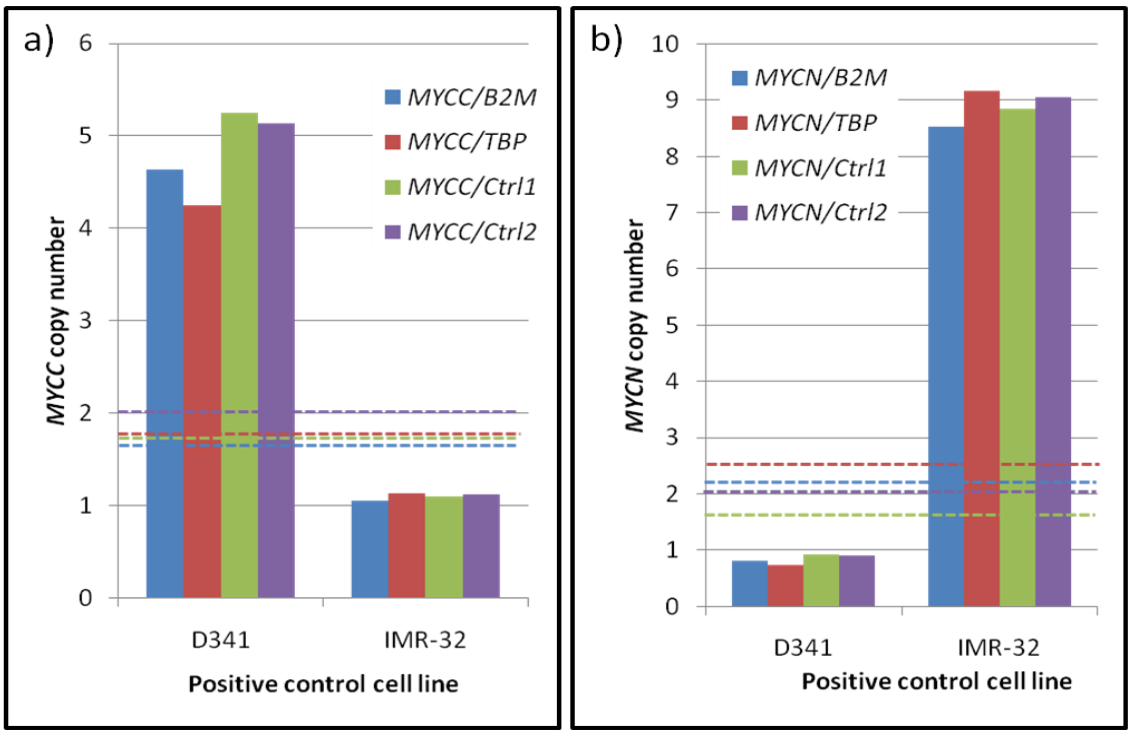

Figure 3.14. *MYCC* and *MYCN* amplification in MLPA positive control cell lines. (a) *MYCC* amplification in medulloblastoma cell line D384. (b) *MYCN* amplification in neuroblastoma cell line IMR-32. A copy number greater than the elevation detection value (EDV) when compared with at least 3 control genes (*TBP*, *B2M*, Ctrl1 or Ctrl2) denotes a copy number elevation. The EDV for *B2M*, *TBP*, Ctrl1 and Ctrl2 are shown by the blue, red, green and purple dotted lines respectively.

3.3.3.5 Assessment of *MYCC* and *MYCN* copy number in CNS-PNET cell lines and primary tumour samples by MLPA.

The reference cohort EDV was used as a cut-off to identify samples in the test series with an elevated copy number. The qRT-PCR cohort comprising two CNS-PNET cell lines and 25 primary CNS-PNET samples were investigated for copy number changes of the MYC family genes by MLPA. CHP707 was found to have a raised copy number of *MYCC* (1/2 CNS-PNET cell lines) when compared relative to the control genes. This finding was not observed in any of the primary tumour samples (0/25) as shown in Figure 3.15. A gain in *MYCN* copy number was not present in either cell line. In 3/25 (12%) primary tumours investigated a gain in *MYCN* copy number was observed (Figure 3.16).

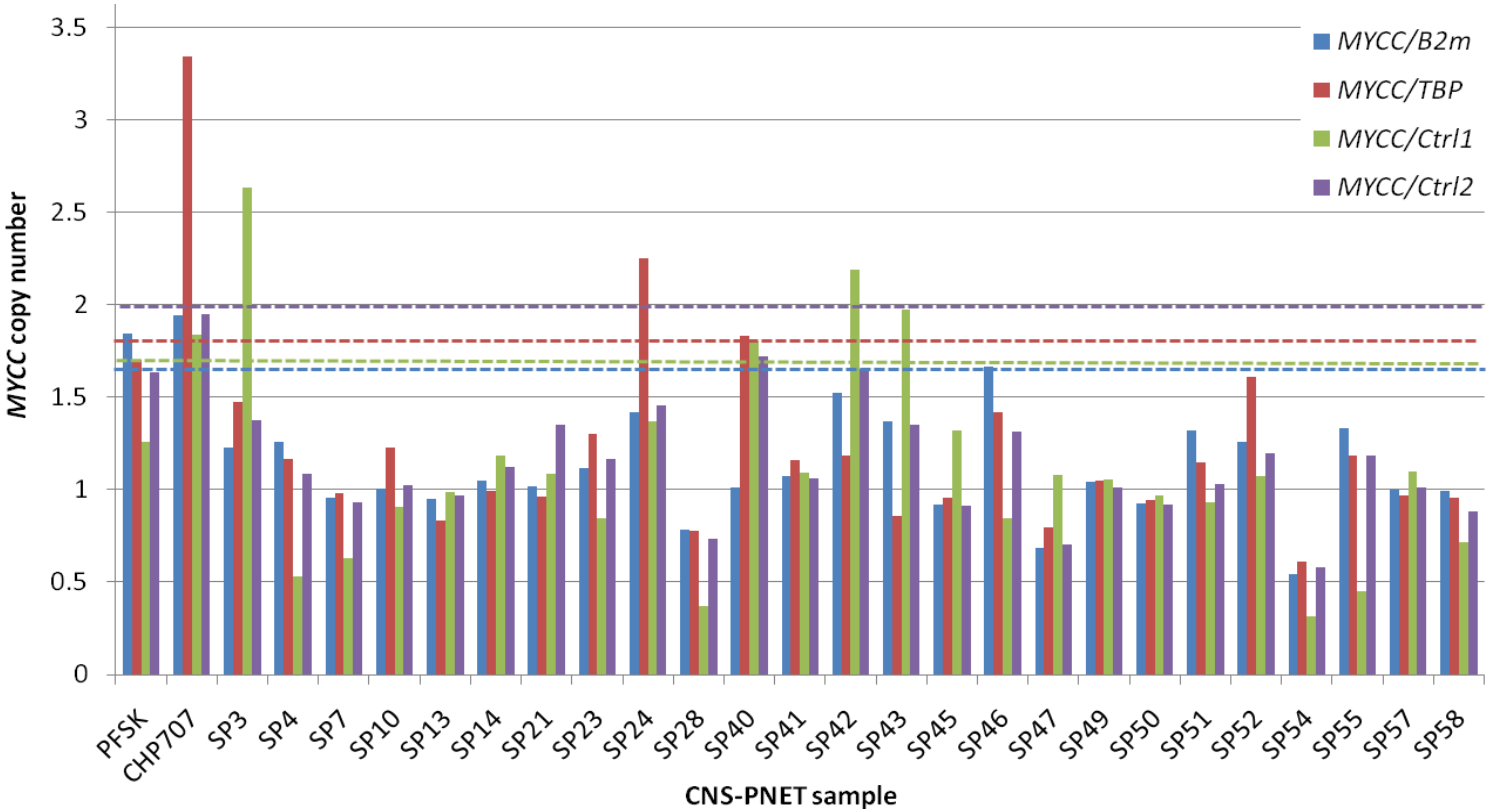

Figure 3.15. *MYCC* copy number in CNS-PNET by MLPA. *MYCC* copy number in 2 CNS-PNET cell lines and 25 primary CNS-PNET tumours measured relative to 4 internal control genes (*TBP, B2M*, *Ctrl1* and *Ctrl2*). Copy number elevation was observed in CHP707 as denoted by values above the elevation detection values (EDV) for all 4 control genes (*B2M*, blue dotted line; *TBP*, red dotted line; and *Ctrl1*, green dotted line; and *Ctrl2*, purple dotted line). A normal copy number was observed in all primary tumours (relative copy number <EDV when compared with 1> control gene).

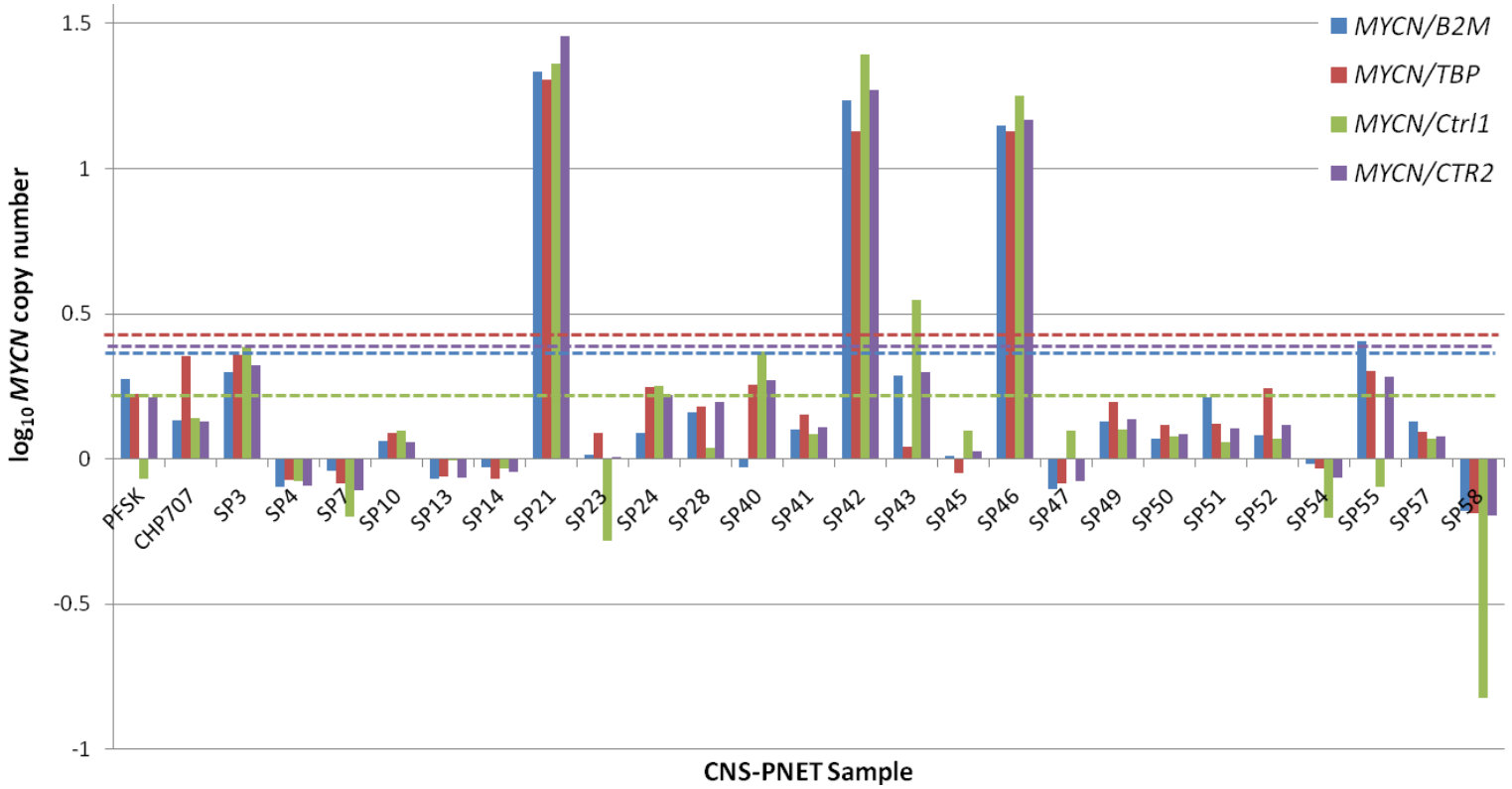

Figure 3.16. Log10 *MYCN* copy number in CNS-PNET by MLPA. Log_{10} *MYCN* copy numbers are shown in 2 CNS-PNET cell lines and 25 primary CNS-PNET tumours measured relative to 4 internal control genes (*TBP, B2M*, *Ctrl1* and *Ctrl2*). Normal copy numbers were observed in both CNS-PNET cell lines (PFSK and CHP707) as denoted by values below the elevation detection values (EDV) for 3 or 4 control genes (*B2M*, blue dotted line; *TBP*, red dotted line; *Ctrl1*, green dotted line and; *Ctrl2*, purple dotted line). *MYCN* copy number elevation was observed in 3 primary CNS-PNET tumour samples (SP21, SP42 and SP46).

3.3.3.6 FISH validation of *MYCN* amplification

Material was available in two of the cases with evidence of *MYCN* copy number elevation (SP21 and SP46), to be used for FISH validation in addition to a reference cohort diploid sample (N9) which was used as a diploid normal copy number reference control. A normal diploid signal for both the centromeric and *MYCN* probes was observed in the reference sample. *MYCN* signals for both SP21 and SP46 demonstrated clumps of varying sizes consistent with HSR formation and confirming *MYCN* amplification (*MYCN* probe: control centromeric probe ratio ≥4) in these cases, as shown in Figure 3.17. Based on these results, and the equivalent copy numbers observed for the three cases with evidence of *MYCN* copy number elevation, it may be inferred that the copy numbers observed for sample SP42, for which suitable material for FISH analysis was not available, are consistent with gene amplification.

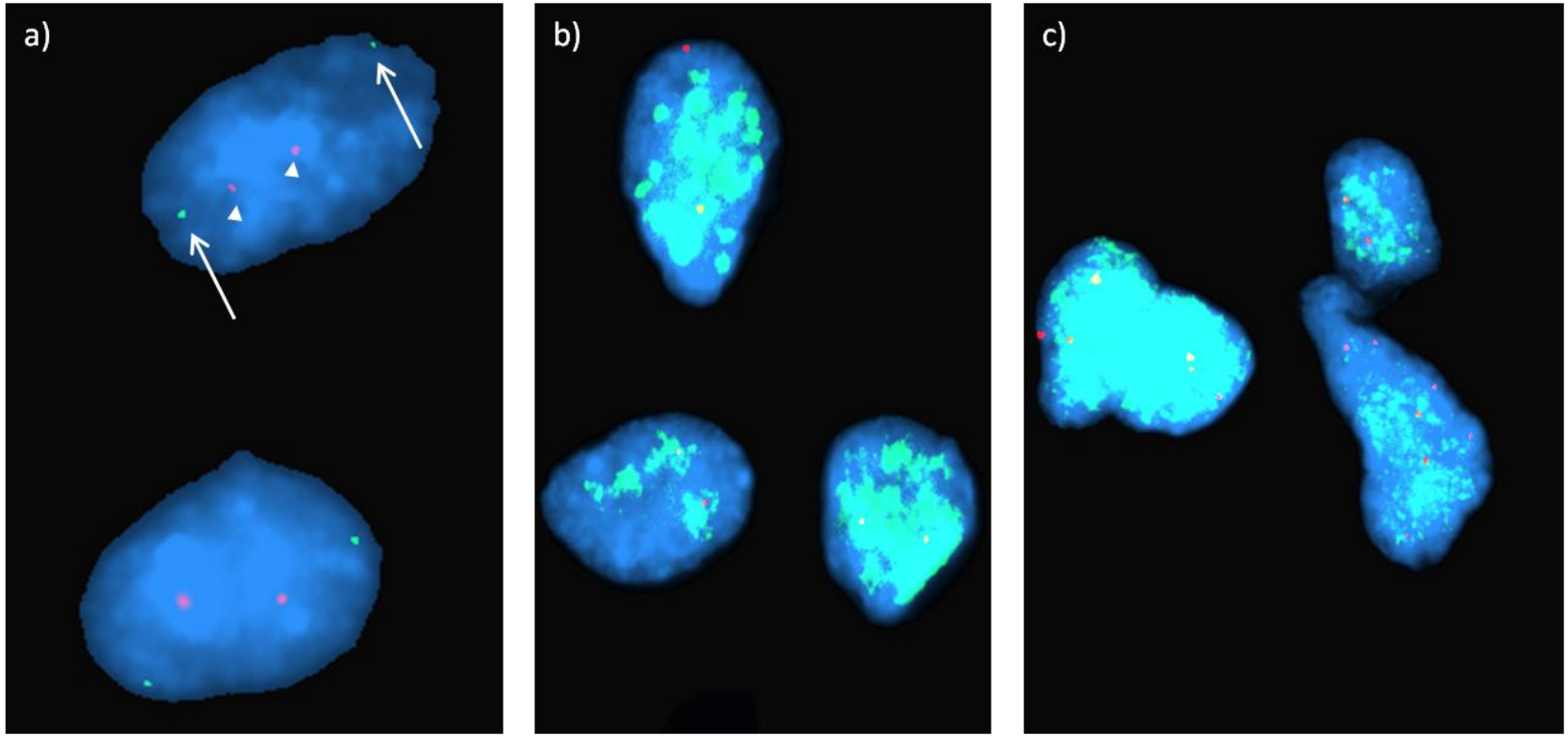

Figure 3.17. *MYCN* amplification by fluorescence in situ hybridisation. (a) N9: Normal diploid status. Two (red) centromeric signals are seen in each cell (closed arrow head), and two *MYCN* (green) signals (arrow). (b) SP21: Two centromeric signals are seen indicating that the cells contatin 2 copies of chromosome 2, but innumerable additional green signals are also observed indicating *MYCN* amplification. (c) *MYCN* amplification in SP46. Some cells have additional copies of chromosome 2 with up to 6 centromeric signals in each cell. The *MYCN* signal exceeds 6 copies, again confirming *MYCN* amplification.

3.3.3.7 Summary of *MYCN* and *MYCC* amplification findings in CNS-PNET primary tumour samples

An elevation of MYCC copy number was not observed in any of the primary CNS-PNET tumour samples (0/25, 0%). This finding was confirmed by both qRT-PCR and MLPA. An elevation in copy number (>5) consistent with amplification was observed in 3/25 (12%) primary tumour samples by both qRT-PCR and MLPA with 100% concordance. In two of these cases appropriate material was available to confirm this finding by FISH. A summary of these results is given in Table 3.19.

3.3.3.8 *MYCN* and *MYCC* amplification in CNS-PNET in comparison with medulloblastoma

The results from a large study by (Ryan 2009) undertaken using a qRT-PCR approach to investigate *MYC* family gene amplification in 292 primary medulloblastoma samples showed *MYCC* amplification in 2% (6/292) and *MYCN* amplification in 5.5% (16/292) of cases. These findings are consistent with those identified in the current CNS-PNET study (p=0.53 and 0.23 respectively, Fisher's exact test).

ID	*MYCN* copy number		
	qRT-PCR	MLPA	FISH
SP3	Diploid	Diploid	-
SP4	Diploid	Diploid	-
SP7	Diploid	Diploid	-
SP10	Diploid	Diploid	-
SP13	Diploid	Diploid	-
SP14	Diploid	Diploid	-
SP21	Amplified	Amplified	Amplified (HSR)
SP23	Diploid	Diploid	-
SP24	Diploid	Diploid	-
SP28	Diploid	Diploid	-
SP40	Diploid	Diploid	-
SP41	Diploid	Diploid	-
SP42	Amplified	Amplified	-
SP43	Diploid	Diploid	-
SP45	Diploid	Diploid	-
SP46	Amplified	Amplified	Amplified (HSR)
SP47	Diploid	Diploid	-
SP49	Diploid	Diploid	-
SP50	Diploid	Diploid	-
SP51	Diploid	Diploid	-
SP52	Diploid	Diploid	-
SP54	Diploid	Diploid	-
SP55	Diploid	Diploid	-
SP57	Diploid	Diploid	-
SP58	Diploid	Diploid	-

Table 3.19. Summary of *MYCN* copy number elevation determined by different molecular techniques summary. Copy number results derived from quantitative real-time PCR (qRT-PCR), multiplex ligation dependent probe amplification (MLPA) and fluorescence *insitu* hybridisation (FISH) are shown. An amplified result by qRT-PCR or MLPA denotes a relative copy number ≥5. HSR: homogenously staining region.

3.3.4 Investigation of *TP53* pathway defects in CNS-PNET

3.3.4.1 Assessment of p53 nuclear accumulation in CNS-PNET cell lines and primary tumour samples.

Assessment of p53 nuclear accumulation was made in 22 primary CNS-PNET tumours where suitable material was available (Not performed on SP3, SP21 or SP51). No evidence of p53 accumulation was observed in 2 cases (2/22, 9%), low level accumulation (1-25% of cells) in 23% (5/22), moderate accumulation in 32% (7/22) and evidence of nuclear accumulation in more than 50% nuclei in 36% (8/22). These results are summarised in Table 3.20, Figure 3.18, Figure 3.19 and Table 3.20.

ID	p53 nuclear immunohistochemistry score
SP4	+
SP7	++
SP10	0
SP13	0
SP14	++
SP23	+
SP24	+
SP28	++
SP40	+
SP41	++
SP42	+++
SP43	+++
SP45	++
SP46	+++
SP47	+++
SP49	+++
SP50	+++
SP52	+++
SP54	++
SP55	+++
SP57	++
SP58	+

Table 3.20. p53 nuclear accumulation in primary CNS-PNET tumours.

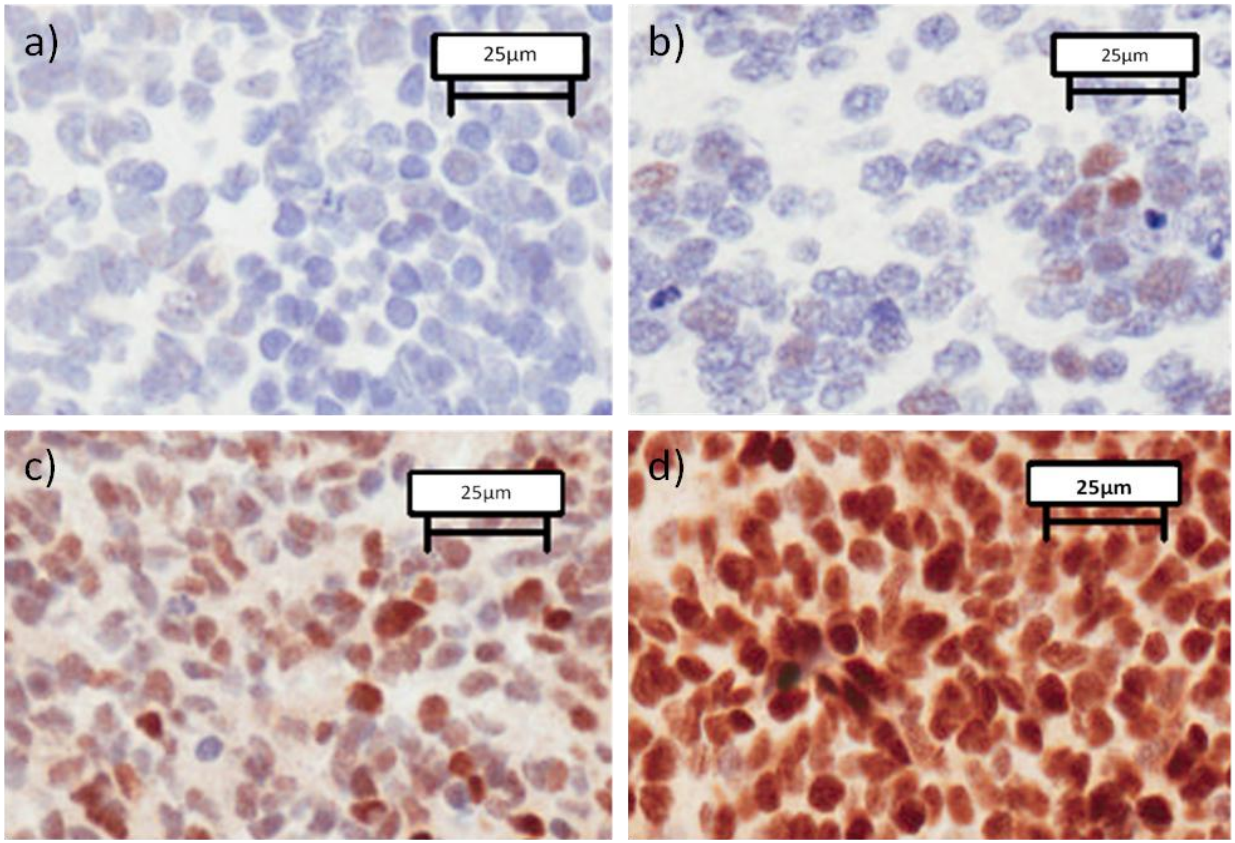

Figure 3.18.Immunohistochemical analysis of p53 pathway activation. (a) Score: 0. No evidence of pathway activation. (b) Score: +. 1-25% of cells show evidence of nuclear accumulation. (c) Score: ++. 25-50% of cells show nuclear accumulation. (d) Score: +++. Intense staining of greater than 50% nuclear accumulation.

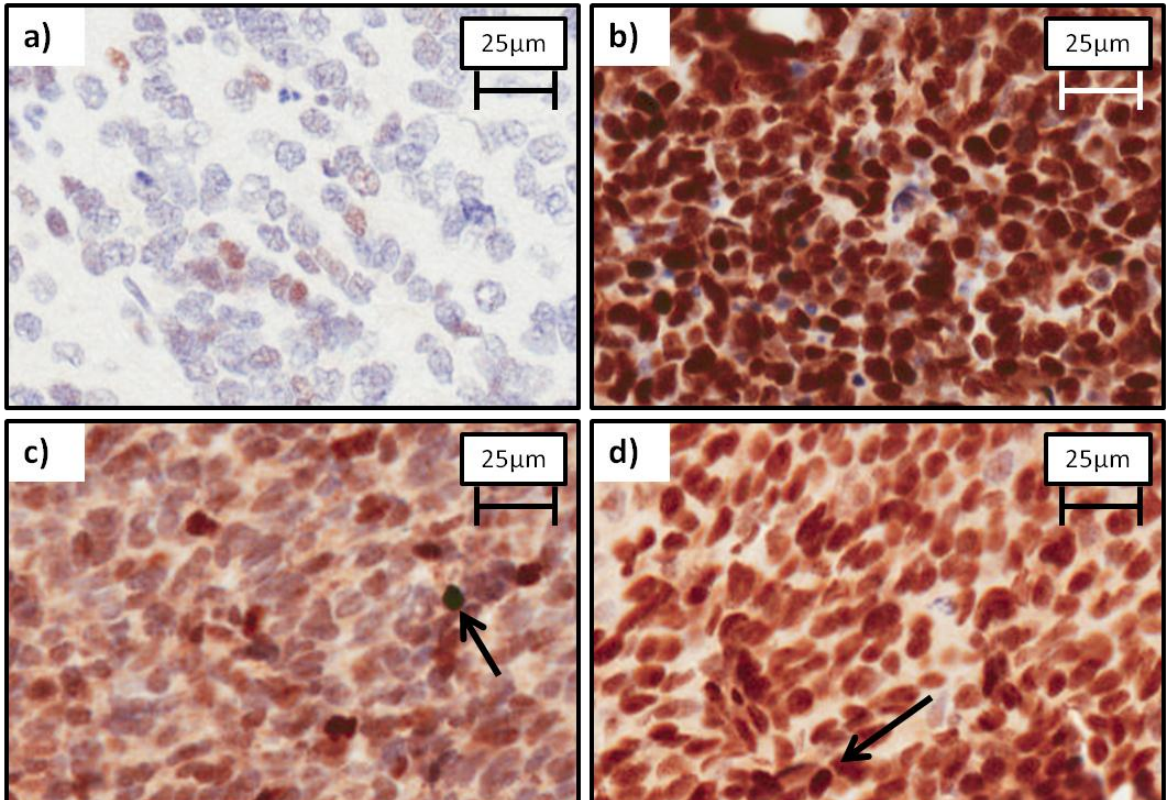

Figure 3.19. p53 nuclear accumulation in TP53 mutant CNS-PNET primary tumours. (a)SP4: Showing 10-15% positive cells; (b) SP46: Intense nuclear staining in all tumour cells; (c) SP47: Widespread accumulation with intense staining in some nuclei (arrow); (d) SP55. Widespread accumulation with intense staining in some nuclei (arrow).

3.3.4.2 CNS-PNET *TP53* mutation analysis

TP53 mutation analysis of exons 4-9 was successfully performed on 2 CNS-PNET cell lines (PFSK and CHP707) and 22 primary CNS-PNET tumour samples. A total of 5 non-synonymous point mutations were discovered in 4 tumour samples (4/22, 18%). No mutation was seen in either cell line. In SP47 a substitution mutation was detected in exon 5 (471G>T, V157F), a substitution (823T>G, C275G) in exon 8 of SP4 and a further substitution mutation in exon 8 of SP46 (817C>T, R273C) as shown in Figure 3.20, Figure 3.22 and Figure 3.23. In SP55 homozygous substitutions in both exons 5 and 8 are observed (460G>A (G154S) and 847C>T, (R283C)), shown in Figure 3.21 and Figure 3.24. All identified mutations were confirmed on independent repeat sequencing and, were cross-correlated with the International Agency for Research in Cancer (IARC) TP53 database and p53 Mutation Manual, and were confirmed to have been previously described in cancer (Petitjean, Mathe et al. 2007; Hjortsberg L, Rubio-Nevado J.M et al. 2010).

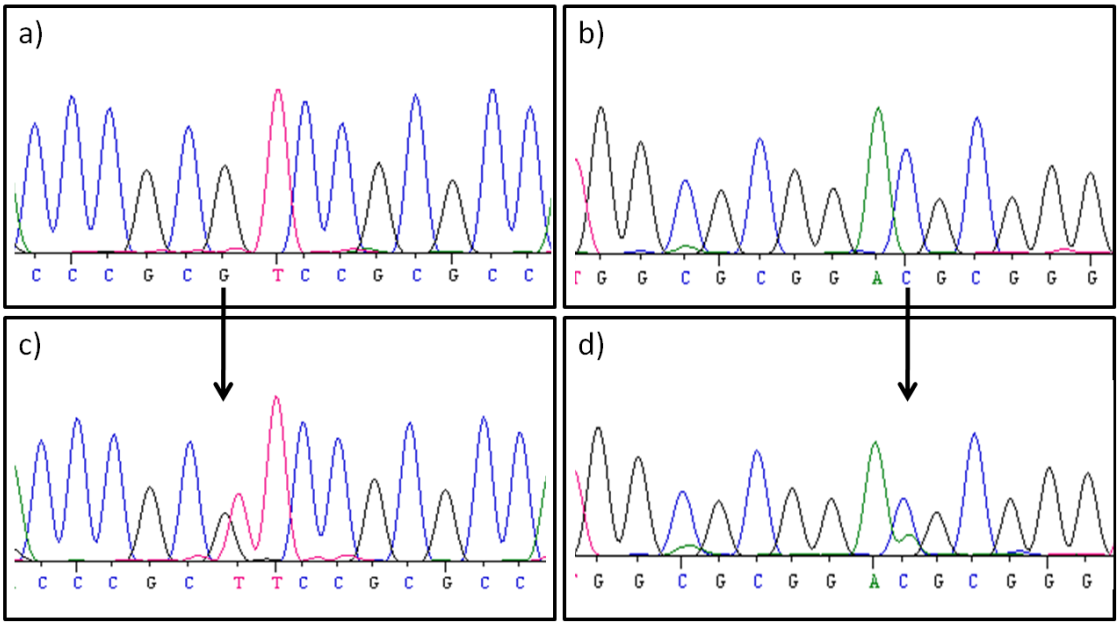

Figure 3.20. Electrophoregrams of *TP53* exon 5 showing a mutation in SP47 in comparison with a wild type sequence. (a) and (b) wild type sequences in sense and anti-sense direction respectively. (c) and (d) Corresponding region in SP47 in both sense and antisense directions respectively showing a non-synonymous heterozygous codon 157 GTC to TTC point mutation (arrow).

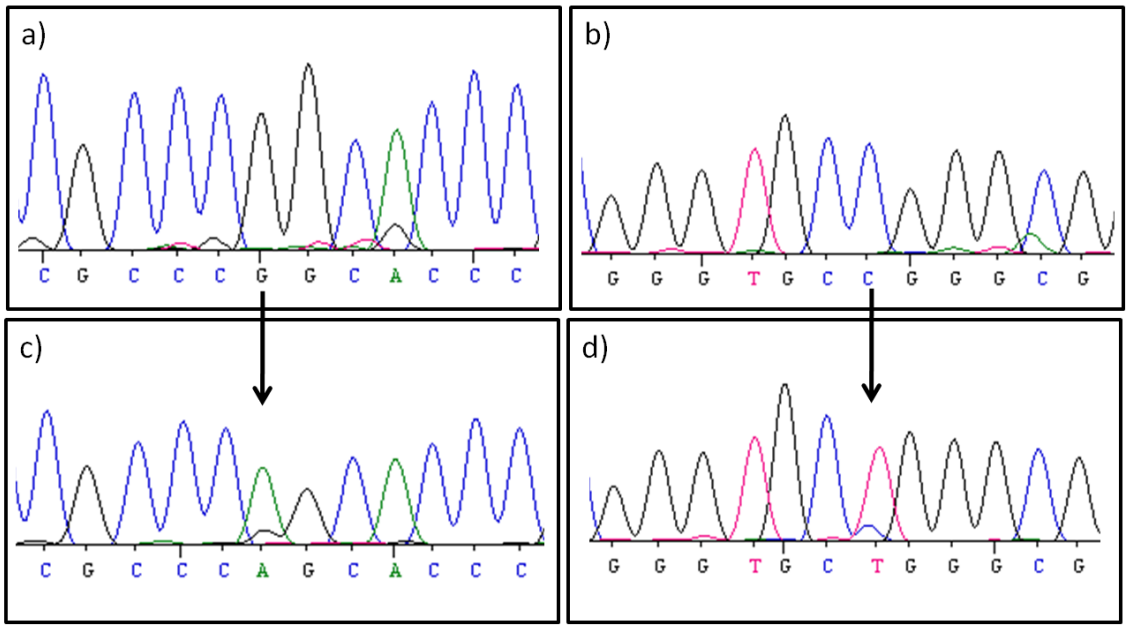

Figure 3.21. Electrophoregrams of *TP53* exon 5 showing a mutation in SP55 in comparison with a wild type sequence. (a) and (b) wild type sequences in sense and anti-sense direction respectively. (c) and (d) Corresponding region in SP55 in both sense and antisense directions respectively showing a non-synonomous homozygous codon 154 GGC to AGC point mutation (arrow).

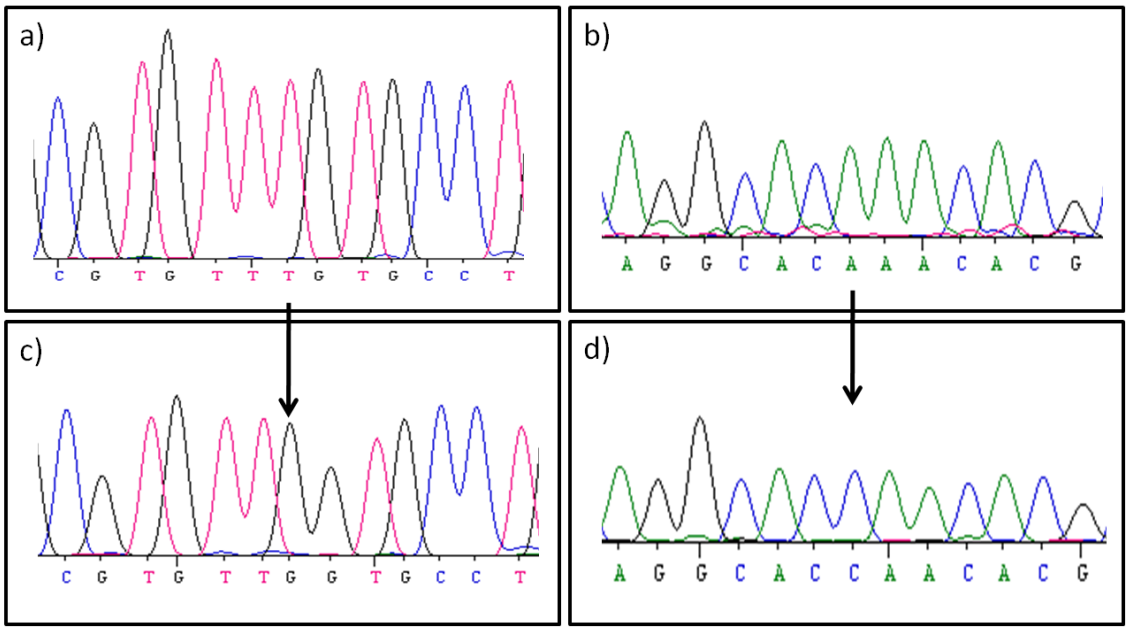

Figure 3.22. Electrophoregrams of *TP53* exon 8 showing a mutation in SP4 in comparison with a wild type sequence. (a) and (b) wild type sequences in sense and anti-sense direction respectively. (c) and (d) Corresponding region in SP4 in both sense and antisense directions respectively showing a non-synonomous homozygous codon 275 TGT to GGT point mutation (arrow).

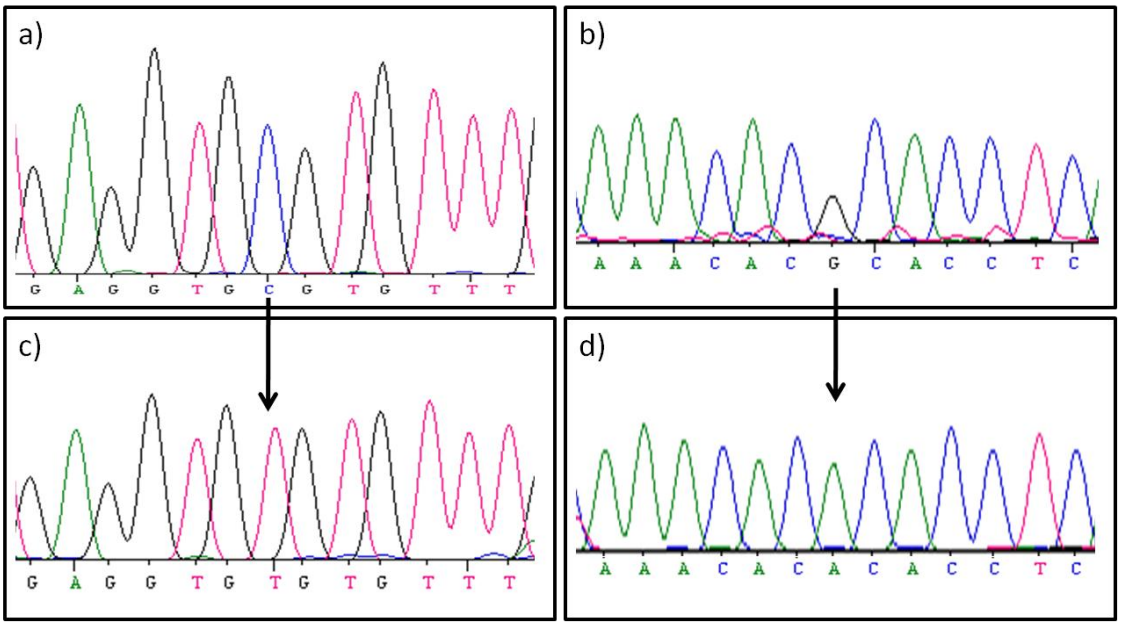

Figure 3.23. Electrophoregrams of *TP53* exon 8 showing a mutation in SP46 in comparison with a wild type sequence. (a) and (b) wild type sequences in sense and anti-sense direction respectively. (c) and (d) Corresponding region in SP46 in both sense and antisense directions respectively showing a non-synonomous homozygous codon 273 CGT to TGT point mutation (arrow).

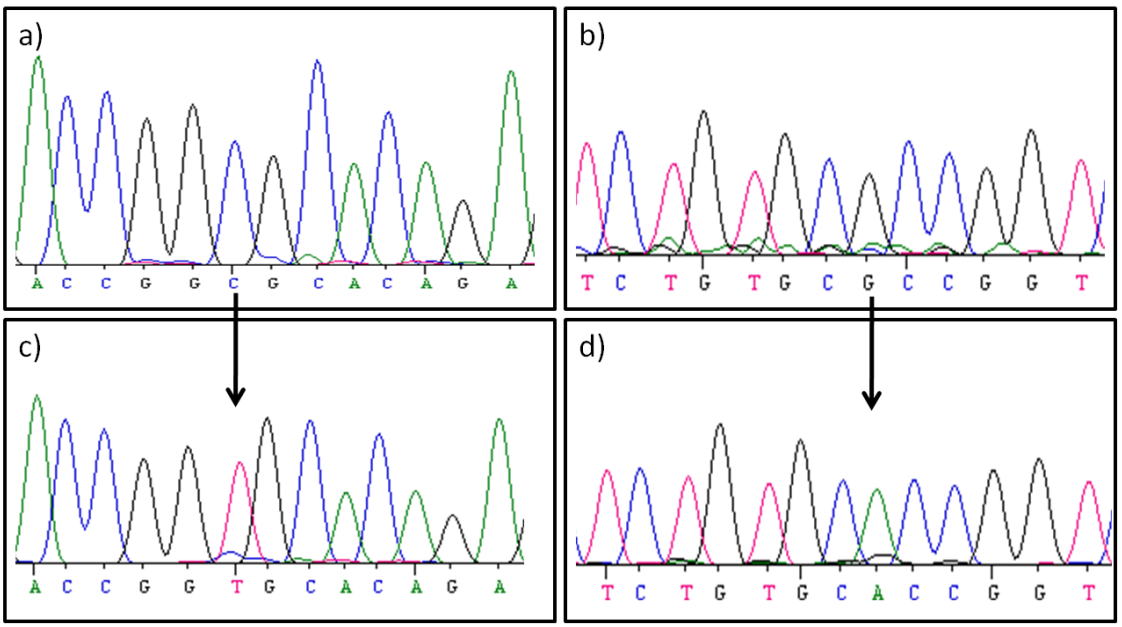

Figure 3.24. Electrophoregrams of *TP53* exon 8 showing a mutation in SP55 in comparison with a wild type sequence. (a) and (b) wild type sequences in sense and anti-sense direction respectively. (c) and (d) Corresponding region in SP55 in both sense and antisense directions respectively showing a non-synonomous homozygous codon 283 CGC to TGC point mutation (arrow).

3.3.4.3 *MDM2* amplification in CNS-PNET

A reference cohort comprising the same samples used in the *MYC* study was used in a study to determine the EDV for an MLPA analysis investigating *MDM2* amplification. The copy number of *MDM2* was measured relative to four internal control genes (*TBP*, *B2M,* Ctrl and *Ctrl2*). *TBP* and *B2M* as previously described (section 3.2.7.5) had product lengths smaller than the test genes, whilst Ctrl1 and Ctrl2 produced products greater than the *MDM2* products (as shown in Figure 3.13a). The elevation detection value (EDV) was determined by calculating the mean +3 SDs for *MDM2* as shown in Table 3.21.

	MDM2/B2M	***MDM2/TBP***	***MDM2/Ctrl1***	***MDM2/Ctrl2***
Mean	1.6471	1.7155	1.5518	1.9351
SD	0.1859	0.2308	0.3652	0.2145
EDV	2.2048	2.4079	2.6475	2.5787
Log_{10} EDV	0.3434	0.3816	0.4228	0.4114

Table 3.21. MLPA reference cohort *MDM2* derived copy number values. Mean, standard deviation (SD) and elevation detection values (EDV) for *MDM2* relative to four reference genes (*TBP, B2M*, Ctrl1 and Ctrl2).The EDV was set at mean + 3SD.

Two CNS-PNET cell lines and 25 primary CNS-PNET samples were examined for evidence of *MDM2* amplification. A normal *MDM2* copy number was detected for both PFSK and CHP707. A copy number elevation of *MDM2* was observed in a single (SP40) CNS-PNET primary tumour sample (1/25, 4%) as shown in Figure 3.25.

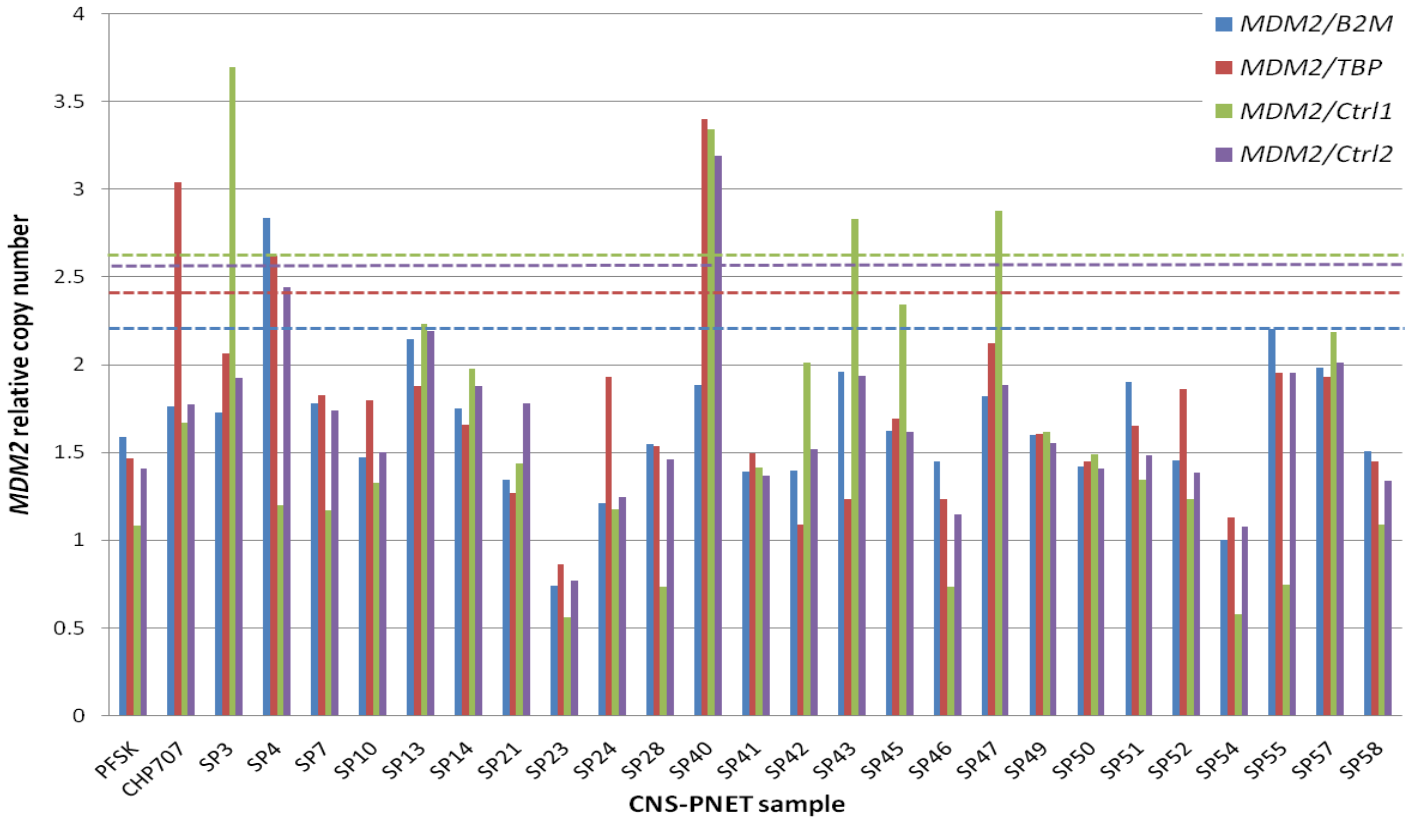

Figure 3.25. *MDM2* copy number in CNS-PNET by MLPA. *MDM2* copy number in 2 CNS-PNET cell lines and 25 primary CNS-PNET tumours measured relative to 4 internal control genes (*TBP, B2M*, *Ctrl1* and *Ctrl2*). Normal copy numbers were observed in both CNS-PNET cell lines (PFSK and CHP707) as denoted by values below the elevation detection values (EDV) for 3 or 4 control genes (*B2M*, blue dotted line; *TBP*, red dotted line; *Ctrl1*, green dotted line and; *Ctrl2*, purple dotted line). A *MDM2* copy number elevation was observed in a single primary CNS-PNET tumour samples (SP40).

3.3.4.4 Investigation of *CDKN2A* homozygous deletion in CNS-PNET

Results were obtained for both CNS-PNET cell lines and CNS-PNET primary tumour samples examined (25/25). Evidence of homozygous deletion of *CDKN2A* was found in one of the cell lines was observed (CHP707). PFSK and CHP707 were both subsequently used when investigating the primary tumour cohort for *CDKN2A* deletion as positive controls, as shown in Figure 3.26. There was no evidence of a homozygous deletion of *CDKN2A* in any of the primary tumours investigated (0/25, 0%).

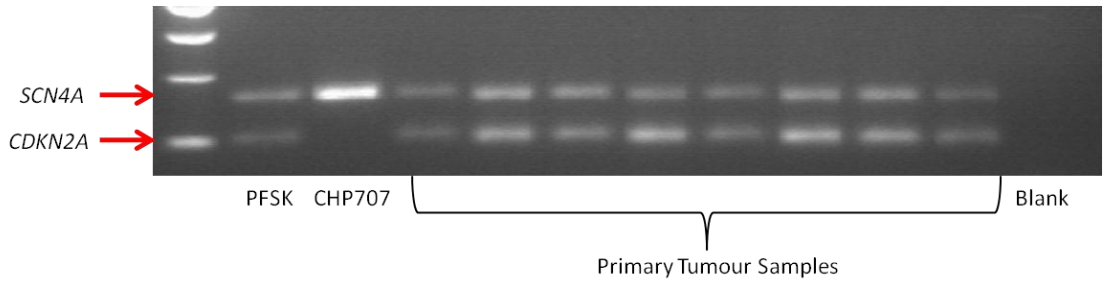

Figure 3.26. *CDKN2A* homozygous deletion analysis in CNS-PNET by duplex PCR. Primers to both *CDKN2A* and control gene *SCN4A* were amplified in a duplex PCR reaction and run on an agarose electrophoretic gel. Duplex bands for both *SCN4A* and *CDKN2A* using PFSK and a single band for SCN4A with CHP707 indicates a retention and a homozygous loss of *CDKN2A* in these 2 cell line samples, respectively. *CDKN2A* homozygous loss was not observed in any of the CNS-PNET primary tumour samples.

3.3.4.5 Summary of *TP53* pathway defects in CNS-PNET and comparison with medulloblastoma

The results of the investigation into *TP53* pathway in CNS-PNET are summarised in Table 3.22. Nuclear accumulation of p53 was identified in 20/22 (91%) primary CNS-PNET samples. In medulloblastoma cohorts, p53 nuclear accumulation have been reported to occur at rates of ranging from 9-31% in previous studies (Eberhart, Chaudhry et al. 2005; Pfaff, Remke et al. 2010; Tabori, Baskin et al. 2010). In these previous studies p53 nuclear accumulation has been assumed to indicate pathway dysfunction. The frequency of p53 nuclear accumulation in CNS-PNET primary tumour

samples is thus significantly greater than in medulloblastoma (p=0.0001, Fisher's exact test), and may be associated with a higher prevalence of pathway dysfunction. In 53% of cases in the Tabori et al study, p53 nuclear accumulation in medulloblastoma was associated with a *TP53* mutation (Tabori, Baskin et al. 2010), and Pfaff et al reported p53 nuclear accumulation in 82% of those with *TP53* mutations (Pfaff, Remke et al. 2010). In the current study of CNS-PNET, mutations occurred in a lower frequency of 4/20 (20%) of cases with p53 nuclear accumulation (p=0.071, Fisher's exact test). *TP53* mutations were not observed in cases without p53 nuclear accumulation..

To identify alternative mechanisms resulting in disruption of *TP53* pathway both *MDM2* amplification and homozygous loss of *CDKN2A* ($p14^{ARF}$) were investigated. There was no evidence of homozygous loss of *CDKN2A* in the cohort studied, and *MDM2* amplification was observed in only a single case. *MDM2* amplification occurred in the presence of p53 nuclear accumulation, but unfortunately suitable material was not available to permit FISH validation of the *MDM2* status in this case. These findings suggest that MDM2 amplification may play a role in p53 pathway disruption in a subset of CNS-PNETs, but that additional alternative mechanisms are responsible for the frequency of p53 nuclear accumulation and possible *TP53* pathway disruption in CNS-PNET, which requires further investigation.

ID	*TP53* mutation	p53 nuclear immunohistochemistry score	*MDM2* copy number	*CDKN2A homozygous deletion*
SP4	Homozygous mutation: 275 TGT>GGT	+	Diploid	No
SP7	wt	++	Diploid	No
SP10	wt	0	Diploid	No
SP13	wt	0	Diploid	No
SP14	wt	++	Diploid	No
SP23	-	+	Diploid	No
SP24	wt	+	Diploid	No
SP28	wt	++	Diploid	No
SP40	wt	+	Elevated	No
SP41	wt	++	Diploid	No
SP42	wt	+++	Diploid	No
SP43	wt	+++	Diploid	No
SP45	wt	++	Diploid	No
SP46	Homozygous mutation: 273 CGT>TGT	+++	Diploid	No
SP47	Heterozygous mutation: 157 GTC>TTC	+++	Diploid	No
SP49	wt	+++	Diploid	No
SP50	wt	+++	Diploid	No
SP51	wt	-	Diploid	No
SP52	wt	+++	Diploid	No
SP54	wt	++	Diploid	No
SP55	Homozygous mutations: 154 GGC>AGC 283 CGC>TGC	+++	Diploid	No
SP57	wt	++	Diploid	No
SP58	wt	+	Diploid	No

Table 3.22. Summary of *TP53* pathway defects in CNS-PNET primary tumour samples.

3.3.5 Investigation of defects in the Wnt signalling pathway in CNS-PNET.

3.3.5.1 Accumulation of nuclear β-catenin in CNS-PNET primary tumour samples.

Assessment of β-catenin nuclear accumulation was made in 22 primary CNS-PNET tumours where suitable material was available. No evidence of β-catenin accumulation was observed in 18 cases (18/22, 72%), low level accumulation (1-10% of cells) in 9% (2/22), and evidence of intense nuclear accumulation in more than 10% nuclei in two cases, SP10 and SP13 (2/22, 9%). These results are summarised in Table 3.23 and Figure 3.27 and Figure 3.28.

ID	β-catenin nuclear immunohistochemistry	
	Description	Score
SP4	Negative Staining	0
SP7	Negative Staining	0
SP10	Widespread (100%) & strong intensity staining	++
SP13	Patchy (50%) & strong intensity staining	++
SP14	Negative Staining	0
SP23	Negative Staining	0
SP24	Negative Staining	0
SP28	Negative Staining	0
SP40	Negative Staining	0
SP41	Negative Staining	0
SP42	Negative Staining	0
SP43	Negative Staining	0
SP45	Negative Staining	0
SP46	Negative Staining	0
SP47	Negative Staining	0
SP49	Negative Staining	0
SP50	5% Weak intensity staining	+
SP52	Negative Staining	0
SP54	Negative Staining	0
SP55	Negative Staining	0
SP57	5% weak intensity staining	+
SP58	Negative Staining	0

Table 3.23. Nuclear β-catenin accumulation in primary CNS-PNET tumours. Scoring: Nuclear accumulation in 0% cells, 0 (negative); 1-10%, + (weakly positive); and >10% of cells, ++ (strongly positive).

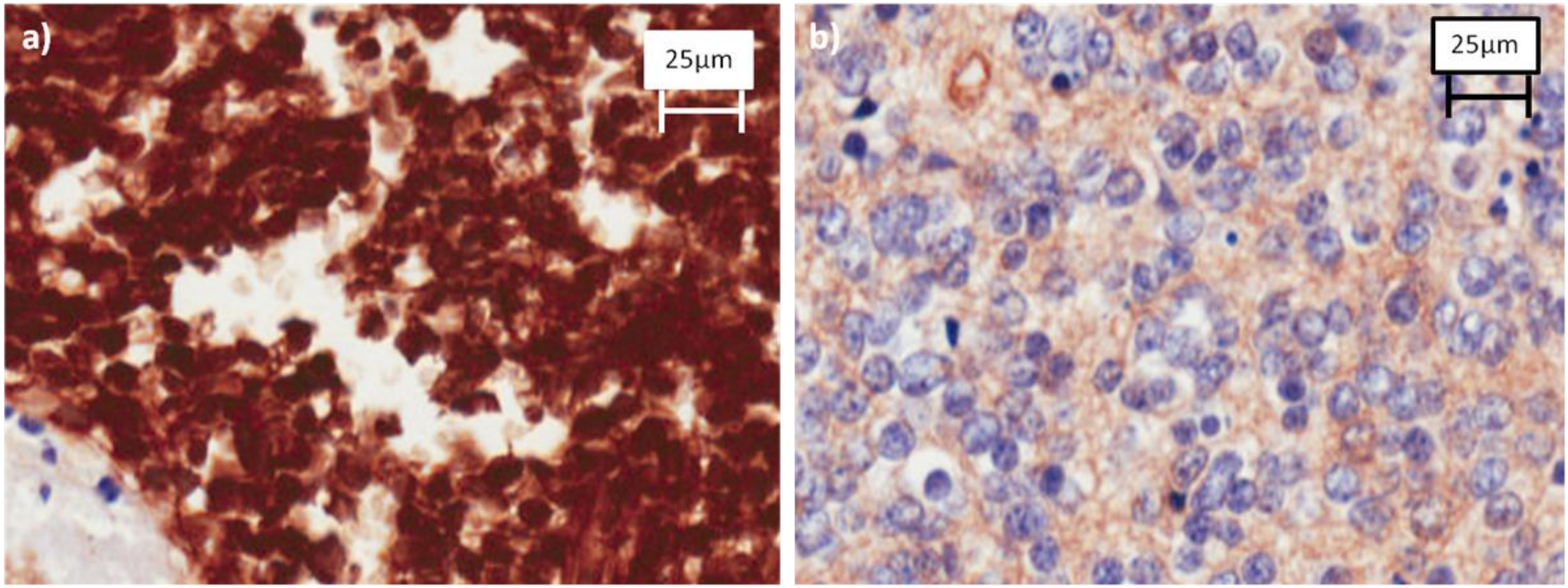

Figure 3.27. Immunohistochemistry analysis of β-catenin nuclear accumulation and Wnt pathway activation. (a) Positive: Nuclear staining in all cells in SP10, (b) Negative staining in SP40. Some cytoplasmic staining but absent β-catenin nuclear accumulation.

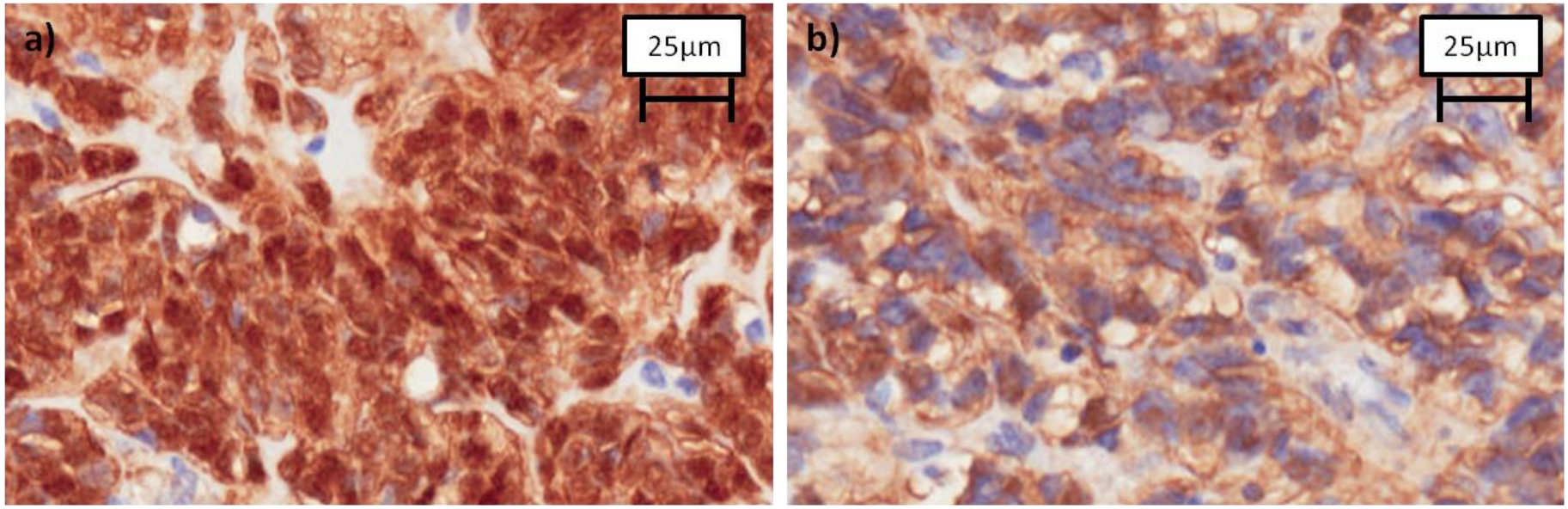

Figure 3.28. β-catenin immunohistochemical analysis of SP13. Sample contained regions with evidence of differential Wnt pathway activation (a) nuclear accumulation, and (b) normal status with only β-catenin antibody cytoplasmic staining.

3.3.5.2 *CTNNB1* mutation analysis in CNS-PNET cell lines and primary tumour samples.

CTNNB1 exon 3 mutation analysis was performed on both CNS-PNET cell lines (PFSK and CHP707) in addition to 25 CNS-PNET primary tumour samples. Both cell lines exhibited a wild type sequence. A heterozygous point mutation in codon 34 (100G>C, (G34R)) was detected in a single primary tumour sample (1/25, 4%) resulting in an amino acid change from glycine to arginine (Figure 3.29). This mutation was observed in SP13 which also exhibited immunohistochemical β-catenin nuclear accumulation. No mutation of *CTNNB1* was however detected in the only other case in the CNS-PNET cohort that exhibited β-catenin nuclear accumulation (SP10).

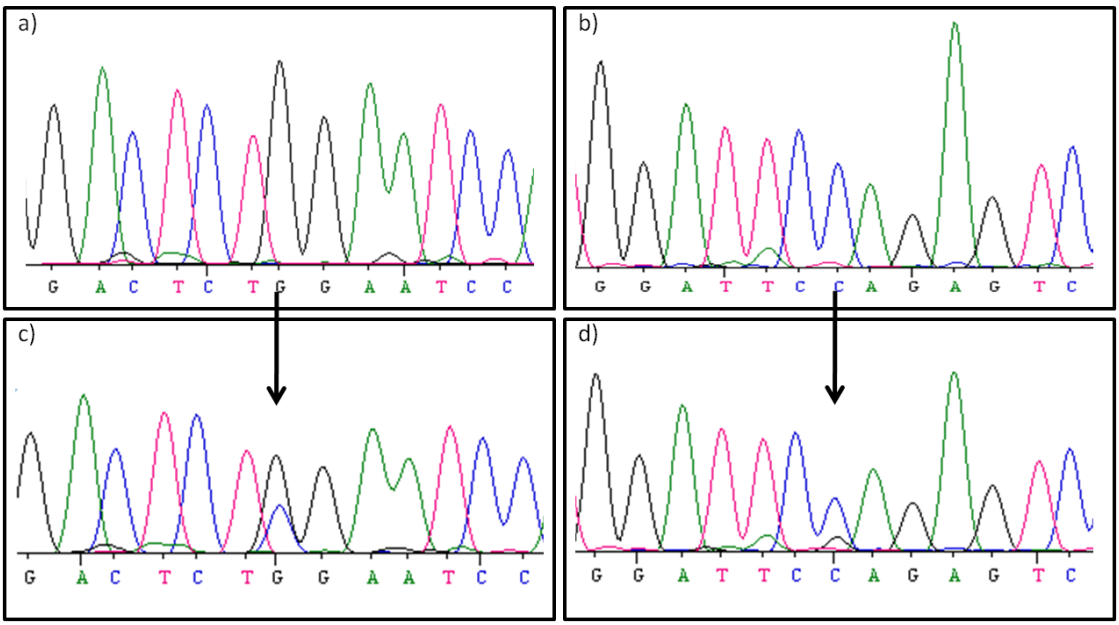

Figure 3.29. Electrophoregrams of *CTNNB1* showing a mutation in SP13 compared with a wild-type sequence. (a) and (b) wild type sequences in sense and anti-sense direction respectively. (c) and (d) Corresponding region in SP13 in both sense and antisense directions respectively showing a non-synonomous heterozygous codon 34 GGA to CGA point mutation (arrow).

3.3.5.3 CNS-PNET Wnt pathway defects in comparison with medulloblastoma.

Defects in the Wnt pathway were detected in 2/22 primary CNS-PNETs. The frequency of β-catenin nuclear accumulation was comparable (p=0.542, Fisher's exact test) with that reported in medulloblastoma (33/206, 16%, (Ellison, Kocat et al. 2011)). No mutation in *CTNNB1* was observed in the absence of nuclear β-catenin accumulation, but this finding did not reach statistical significance (p=0.09, Fisher's exact test).

3.3.6 Analysis of clinical features of investigated medulloblastoma defects in CNS-PNET

A series of defects frequently observed in medulloblastoma cohorts were investigated in CNS-PNET primary tumour samples. The results of these investigations are summarised in Table 3.24.

ID	*RASSF1A* meth[1]	17p loss[2]	Amplification		*TP53* Pathway defect				Wnt pathway defect	
			MYCC	*MYCN*	p53 IHC[3]	*TP53* mutation	*MDM2* elev[4]	*CDKN2A* deletion	β-catenin IHC[5]	*CTNNB1* mutation
SP3	No	-	No	No	-	-	No	No	No	No
SP4	Yes	No	No	No	Yes	Yes	No	No	No	No
SP7	-	-	No	No	Yes	No	No	No	No	No
SP10	-	No	No	No	No	No	No	No	Yes	No
SP13	-	No	No	No	No	No	No	No	Yes	Yes
SP14	Yes	No	No	No	Yes	No	No	No	No	No
SP21	No	No	No	Yes	-	-	No	No	-	No
SP23	Yes	No	No	No	Yes	-	No	No	No	No
SP24	Yes	No	No	No	Yes	No	No	No	No	No
SP28	Yes	No	No	No	Yes	No	No	No	No	No
SP40	Yes	No	No	No	Yes	No	Yes	No	No	No
SP41	Yes	No	No	No	Yes	No	No	No	No	No
SP42	Yes	No	No	Yes	Yes	No	No	No	No	No
SP43	Yes	No	No	No	Yes	No	No	No	No	No
SP45	Yes	No	No	No	Yes	No	No	No	No	No
SP46	Yes	ERH	No	Yes	Yes	Yes	No	No	No	No
SP47	Yes	No	No	No	Yes	Yes	No	No	No	No
SP49	Yes	No	No	No	Yes	No	No	No	No	No
SP50	Yes	No	No	No	Yes	No	No	No	No	No
SP51	Yes	No	No	No	-	No	No	No	-	No
SP52	Yes	No	No	No	Yes	No	No	No	No	No
SP54	Yes	No	No	No	Yes	No	No	No	No	No
SP55	Yes	ERH	No	No	Yes	Yes	No	No	No	No
SP57	No	No	No	No	Yes	No	No	No	No	No
SP58	No	No	No	No	Yes	No	No	No	No	No
Total	**18/22 (81%)**	**2/23 (9%)**	**0/25 (0%)**	**3/25 (12%)**	**20/22 (91%)**	**4/22 (18%)**	**1/25 (4%)**	**0/25 (0%)**	**2/23 (9%)**	**1/25 (4%)**

Table 3.24. Summary of common medulloblastoma defects investigated in CNS-PNET.
Cohort comprises 25 primary CNS-PNET samples. [1] *RASSF1A* promoter methylation, [2] Loss of the p-arm of chromosome 17, [3] p53 immunohistochemistry nuclear accumulation, [4] *MDM2* copy number elevation, and [5] β-catenin nuclear positivity in >10% cells.

An initial analysis of survival in relation to the presence of identified medulloblastoma defects in CNS-PNET showed no survival correlations with any of the identified defects (Table 3.25).

Molecular defect	Frequency	Survival statistical analysis	Significance (pval)
RASSF1A methyaltion	18/22	Log-rank	0.664
Chromosome 17p loss	2/23	Log-rank	0.526
MYCN amplification	3/25	Log-rank	0.624
MYCC amplification	0/25	-	-
p53 nuclear immunohistochemistry	(0) 2/22, (+) 5/22, (++) 7/22, (+++) 8/22	Cox regression	0.525
TP53 mutation	4/22	Log-rank	0.580
MDM2 amplification	0/23	-	-
CDKN2A homozygous deletion	0/23	-	-
β-catenin nuclear immunohistochemistry	(0) 2/22, (+) 2/22, (++) 18/22	Cox regression	0.691
CTNNB1 mutation	1/25	Log-rank	0.940

Table 3.25. Summary of investigated medulloblastoma defects in primary CNS-PNET survival analyses.

The presence of metastatic disease and age at diagnosis are the two clinical features known to be associated with outcome in CNS-PNET disease. The study cohort comprised of only a single case with metastatic disease (SP49), whilst in 4 cases the metastatic status was unknown (Table 3.4). An analysis of association between detected medulloblastoma defects and metastatic status was therefore not feasible using this cohort. In the cohort, 6 of the patients were diagnosed as infants (age<3yrs), 13 as children (3-18 years old) and 5 as adults (age >18 years). Information on age at diagnosis was not available for SP43 and therefore was excluded from the age related analyses. The relative frequencies of the investigated

medulloblastoma defects which occurred in more than one case at different ages are given in Table 3.26. No statistically significant association was found between age at diagnosis and the presence of *RASSF1A* promoter methylation (p=0.83), *MYCN* amplification (p=0.16), positive p53 nuclear accumulation (p=0.69), chromosome 17p loss (p=0.45), *TP53* mutation (p=0.41), or β-catenin nuclear accumulation (p=0.69). There was however a tendency towards significance when considering *MYCN* amplification in adults compared with all paediatric cases (1/18 v 2/5, p=0.10 Fisher's exact test).

Molecular defect	Age			Significance (pval)
	Infant (<3yrs)	Child (3-18 yrs)	Adult >18yrs	
RASSF1A methylation	5/6 (83%)	8/10 (80%)	4/5 (80%)	0.83
MYCN amplification	0/6 (0%)	1/13 (8%)	2/5 (40%)	0.16
Chromosome 17p loss	0/6 (0%)	1/12 (8%)	1/5 (40%)	0.45
Positive p53 nuclear immunohistochemistry	6/6 (100%)	9/11 (72%)	4/4 (100%)	0.69
TP53 mutation	0/6 (0%)	3/13 (23%)	1/5 (20%)	0.41
Positive β-catenin nuclear immunohistochemistry	0/6 (0%)	2/11 (18%)	0/4 (0%)	0.69

Table 3.26. Common medulloblastoma defects in CNS-PNET patients at different ages. Information on the age at diagnosis was available in 24 cases. Positive β-catenin immunohistochemistry includes cases where β-catenin nuclear accumulation was present in >10% cells. Statistical significance was determined by Fisher's exact test using the multitest package (Pollard, Gilbert et al. 2010) in the R statistical software program.

3.4 Discussion

3.4.1 *RASSF1A* methylation in CNS-PNET

Methylation of the *RASSF1A* promoter was identified in 81% of primary CNS-PNETs which represents one of the most frequent molecular defects detected in this disease. Few studies have previously investigated *RASSF1A* methylation in CNS-PNET (Chang, Pang et al. 2005; Muhlisch, Schwering et al. 2006; Inda and Castresana 2007) and have found comparable rates of methylation in these series as shown in Table 3.27. In the Chang et al study the *RASSF1A* methylation status of 25 medulloblastomas was compared with that of 9 CNS-PNETs. All of the medulloblastomas were methylated in this series and a statistically significant difference between the 2 tumour groups reported (p=0.014, Fisher's exact test). In this current larger study *RASSF1A* promoter methylation in 22 CNS-PNETs compared with a large cohort of medulloblastomas (n=62) does not corroborate this finding.

Reference	Cohort		*RASSF1A* methylation	
	Number	Age (yrs)	Frequency	Method
Chang et al, 2005	9	1-26	6/9 (67%)	MSP
Muhlisch et al, 2006	24	1-40	19/24 (79%)	MSP & BS
Inda et al, 2007	6	4-49	5/6 (83%)	MSP

Table 3.27. *RASSF1A* methylation in published CNS-PNET series. *RASSF1A* promoter methylation ascertained using methylation specific PCR (MSP) and direct bisulphite sequencing (BS).

In some tumour groups, *RASSF1A* methylation has been shown to be associated with clinical correlates including poorer survival (Astuti, Agathanggelou et al. 2001; Burbee, Forgacs et al. 2001; Harada, Toyooka et al. 2002; Tomizawa, Iijima et al. 2004; Yang, Zage et al. 2004; Banelli, Gelvi et al. 2005; Michalowski, de Fraipont et al. 2008). However in common with previous studies including medulloblastoma (Lindsey, Lusher et al. 2004; Muhlisch,

Schwering et al. 2006) and general paediatric malignancy studies (Wong, Chan et al. 2004) no such correlation in CNS-PNET was identified. The cohort size in this investigation was however limited, and the study was not powered to determine whether a lack of correlation was statistically significant, and therefore further study is required to determine whether *RASSF1A* methylation is associated with clinical correlates.

3.4.2 *RASSF1A* methylation as a diagnostic marker

Studies have shown that *RASSF1A* promoter methylation is a tumour specific event and not seen in the normal brain cerebral or cerebellar tissue (Lusher, Lindsey et al. 2002; Chang, Pang et al. 2005; Muhlisch, Schwering et al. 2006). The tumour specific nature and frequency of *RASSF1A* methylation make it an ideal candidate to be used as a tumour marker. *RASSF1A* promoter methylation has however been identified as a frequent event in a range of malignant and benign brain tumours including glioma (Horiguchi, Tomizawa et al. 2003; Gao, Guan et al. 2004; Hesson, Krex et al. 2008), glioblastoma (Piperi, Themistocleous et al. 2010) , medulloblastoma (Lusher, Lindsey et al. 2002; Horiguchi, Tomizawa et al. 2003; Chang, Pang et al. 2005; Lindsey, Anderton et al. 2005; Inda and Castresana 2007), meningioma (Horiguchi, Tomizawa et al. 2003) and ependymoma (Hamilton, Lusher et al. 2005; Michalowski, de Fraipont et al. 2006) and therefore its role as a novel marker is limited to being a non-specific tumour marker.

In addition to assaying methylation profiles within tumour specimens, *RASSF1A* has also been investigated in non-invasive clinical material and has suggested a role for *RASSF1A* as a screening tool for tumours. In non-small cell lung cancer (NSCLC) *RASSF1A* methylated DNA can be found in broncheoalveolar lavage fluid (Topaloglu, Hoque et al. 2004; Grote, Schmiemann et al. 2006), and in sputum (Honorio, Agathanggelou et al. 2003) . Methylated *RASSF1A* can also be found in nipple fluid in patients with breast adenocarcinoma (Krassenstein, Sauter et al. 2004), and urine in patients with kidney(Battagli, Uzzo et al. 2003), bladder (Chan, Chan et al. 2003; Dulaimi, Uzzo et al. 2004) and prostate cancers (Roupret, Hupertan et al. 2007). *RASSF1A* methylation in CSF samples potentially could therefore be used to detect brain tumours including CNS-PNET.

Patients with cancer have increased levels of circulating free DNA within their blood serum (Leon, Shapiro et al. 1977; Stroun, Anker et al. 1989). Methylated tumour DNA can also be detected in serum samples (Muller, Fiegl et al. 2004; Hauser, Zahalka et al. 2010) and may be used to detect disease and potentially to identify those with high risk neoplasms. More recently *RASSF1A* methylation has been used in models to detect papillary thyroid carcinoma (Mohammadi-Asl, Larijani et al. 2010), non-familial breast cancer(Jing, Yuping et al. 2010) and prostate cancer (Ahmed 2010). The persistence of methylation markers may also be used to assess treatment response. In a breast cancer study *RASSF1A* was used as a surrogate marker for response to Tamoxifen®, with the persistence or resolution of *RASSF1A* methylation in blood sera indicating treatment resistance or a good response respectively (Fiegl, Millinger et al. 2005).

The precedent for the potential to use methylation markers in the management of brain tumours has recently been reported in a study in glioma (Liu, Cheng et al. 2010). In this study the methylation profile of a combination of 4 genes (*MGMT*, *P16^{INK4a}*, *TIMP-3* and *THβS1*) from CSF and serum samples was used to predict prognosis, and was found to be 100% specific in this series. However the limitation of using non-invasive rather than tumour material is exemplified by two recent studies. Firstly, in a case-control study involving *RASSF1A* in combination with three other markers (*GSTP1*, *APC* and *RARβ2*), the test failed to distinguish breast carcinoma from normal tissue using pre-diagnostic serum samples (Brooks, Cairns et al. 2010). In a second study in prostate cancer in which the specificity of using *RASSF1A* as a serum marker was found to be 100%, the test however was only 28% sensitive (Sunami, Shinozaki et al. 2009) again limiting its potential clinical utility.

This study has shown that *RASSF1A* is a highly frequent event in CNS-PNET development. Further studies are however now required to determine the role of *RASSF1A* methylation in CNS tumorigeneis and whether this may be exploited therapeutically, potentially as a disease marker. Moreover the role of epigenetics in CNS-PNET development as discussed in (section 1.5.6) is currently poorly understood. This current study however highlights the potential for identifying events to further advance our understanding of these tumours and may provide novel clinical application opportunities. A study to investigate epigenetic methylation events and determine the "CNS-PNET methylome" is now required.

3.4.3 Loss of chromosome 17p in CNS-PNET

The most common cytogenetic abnormality seen in medulloblastoma is loss of the p-arm of chromosome 17, occurring in up to 40% of tumours (McDonald, Daneshvar et al. 1994; Burnett, White et al. 1997). This may occur in association with a gain of 17q and the formation of an isochromosome (i17q) or may arise as an isolated defect. The absence of 17p loss in both CNS-PNET cell lines is consistent with previously reported karyotpe and FISH studies of these cell lines (Cohen, Betts et al. 2004). Investigation of 17p loss in CNS-PNET has not previously been performed in a large cohort of CNS-PNET tumours. In the current study, 17p loss, as evidenced by an extended region of homozygosity, was observed in 9% (2/23) primary CNS-PNETs, compared with a rate of 17p loss of 25% (47/190) in a panel of medulloblastomas analysed using an identical approach (Megahed 2010). This result whilst not statistically significant (p=0.08, Fisher's exact test) is in keeping with the findings of a number of published small studies incorporating 49 cases in total where 17p status has been investigated, summarised in Table 3.28. Chromosome 17p loss was identified in only a single isolated case (Bayani, Zielenska et al. 2000) amongst these 49 CNS-PNETs. The findings from this current comprehensive study and their consistency with previous reports suggest that unlike in medulloblastoma chromosome 17p loss is not a frequent feature of CNS-PNET disease. Accordingly, tumour suppressor genes thought to be located at 17p13.1, telomeric to the *TP53* locus, and important in the development of medulloblastomas (Biegel, Burk et al. 1992; Giangaspero, Bigner et al. 2000), may only be a feature in the development of CNS-PNETs in a small subset. The HOMOD method however, can only detect comparatively large chromosomal losses and therefore may not detect a localised regional loss confined to 17p13.1.

Whilst this study has confirmed that 17p loss is an infrequent feature of CNS-PNET the role of 17q still requires evaluation. Moreover the frequency, nature and clinical correlates of cytogenetic aberrations in CNS-PNET still need to be determined. As discussed in (section 1.5.3) those studies published to date have been in small series and produced inconsistent findings. Studies of large cohorts of pathologically reviewed CNS-PNETs, as used in this study, are necessarily required.

Reference	Cohort		Chromosome 17p loss	
	Number	Age (yrs)	Frequency	Method
(Thomas and Raffel 1991)	n=5	1-12	0/5	RFLP
(Burnett, White et al. 1997)	n=8	0-16	0/8	RFLP
(Scheurlen, Schwabe et al. 1998)	n=2	6-12	1/2	LOH
(Russo, Pellarin et al. 1999)	n=7	1-31	0/7	CGH
(Bayani, Zielenska et al. 2000)	n=5	2-6	1/5	CGH
(Kraus, Felsberg et al. 2002)	n=12	2-9	0/12	LOH
(Kagawa, Maruno et al. 2006)	n=3	0.6-3	0/3	aCGH
(McCabe, Ichimura et al. 2006)	n=7	2.7-23	0/7	aCGH
(Pfister, Remke et al 2007)	n=10	0.6-13	2/10	aCGH

Table 3.28. Loss of chromosome 17 p-arm in CNS-PNET. Chromosome 17p loss detected using different methodologies. Restriction fragment length polymorphism (RFLP), loss of heterozygosity (LOH), comparative (or chromosomal) genomic hybridisation (CGH), array CGH (aCGH).

3.4.4 Regional deletion on chromosome 17p is a feature of CNS-PNET

Whilst a complete loss of chromosome 17p was not demonstrated, a deletion of a region in a subset is suggested by the resultsusing the HOMOD method in this study. In two tumours, SP46 and SP55, an extended region of homozygosity (ERH) not extending to the telomere was observed. FISH or CGH studies for validation to confirm the presence and map the extent of this regional loss were not part of this current study as unfortunately further suitable material to undertake these studies was not available. The *TP53* locus (17p13.1) however is situated within this ERH and, in both cases, homozygous mutations of *TP53,* were identified which are consistent with an allelic partial loss on 17p. In a third case (SP4) a *TP53* homozygous mutation was also identified without evidence of an ERH. Interestingly the polymorphic microsatellite markers either side of the *TP53* locus in this case revealed retention of heterozygousity (D17S974, (17p13.2) and D17S969 (17p12)) suggesting that

regional loss was not an initiating feature in this case, although cannot exclude a restrictive deletion incorporating the *TP53* locus. Array-CGH studies in larger cohorts of CNS-PNETs would be helpful in determining whether smaller restrictive losses rather than complete 17p11.2-17pter deletions are a consistent feature in a subset of CNS-PNETs. The 17p11.2 breakpoint, as described in medulloblastoma (Biegel, Janss et al. 1997; Scheurlen, Seranski et al. 1997), may therefore play a role in CNS-PNET.

3.4.5 Involvement of *MYC* family gene amplification in CNS-PNET

MYCC and *MYCN* amplification was not observed in either of the two CNS-PNET cell lines, PFSK or CHP707, studied. This finding is consistent with the previously reported molecular characterisation of these cell lines (Cohen, Betts et al. 2004). The analysis in primary tumours showed no evidence of *MYCC* amplification but amplification of *MYCN* in 12% (3/25). These findings were not statistically significantly different to a comparable study in medulloblastoma (Ryan 2009), or in relation to previous studies in CNS-PNET as summarised in Table 3.29. In a study by Fruhwald et al profiling 5 CNS-PNET samples, a single case of both *MYCN* and *MYCC* amplification was observed (Fruhwald, O'Dorisio et al. 2000). Of note, the *MYCC* and *MYCN* amplification was observed within the same sample which was taken at relapse 2 years after the original treatment. In a further recently published study (Behdad and Perry 2010) assessment of *MYCC* and *MYCN* in a cohort of both paediatric and adult CNS-PNETs observed amplifications of both *MYCC* (3/28) and *MYCN* (9/28) by FISH. 41% of the paediatric samples were found to exhibit *MYCN* amplification. The frequency of *MYCC* and *MYCN* amplification do not differ significantly from the current study (p=0.24 and p=0.11 Fisher's exact tests respectively) but a real difference may nonetheless exist as a result of the different methodological approaches employed.

The qRT-PCR and MLPA approaches taken in the current study are not able to determine the copy number of a gene in a given cell, but instead return an average result from the amplified DNA extracted from many cells within a tumour sample. If, as has been shown in a study by Lamont et al with *MYCC* gene amplification, there is heterogeneity of copy number amongst the tumour cells in a sample(Lamont, McManamy et al. 2004), qRT-PCR and MLPA

may fail to detect this, but would be identified using FISH. This observation has been previously reported with respect to *MYCC* and *MYCN* amplification in medulloblastoma (McManamy, Lamont et al. 2003) . In the current study therefore there may have been cases where *MYCC* or *MYCN* amplification occurred in sub-populations of tumour cells but not sufficiently frequently to alter the overall "average" result. The potential importance of identifying *MYC* gene amplification in tumour subpopulations is exemplified in a neuroblastoma case report where amplification of *MYCN* was identified within a metastatic deposit but only gain within the primary tumour (Noguera, Canete et al. 2003). This suggests that *MYCN* amplification was present in a minority of primary tumour cells from which the metastic depost was derived. Suitable material was not available in the current study to validate the copy number results in all samples using FISH based methods and so the presence of small populations of undetected *MYCN* or *MYCC* amplification may have been present in some of these tumours.

Finally, determining the downstream effects of *MYC* gene amplification in the three amplified cases needs to be determined to elucidate its role in CNS-PNET development. However, as has been shown in medulloblastoma studies, the biological effect of up-regulation may be dependent on the activating mechanism with Myc expression resulting from Wnt pathway activation associated with a favourable phenotype, whilst Myc expression resulting from *MYCC* amplification is often associated with a large cell anaplastic and more aggressive phenotype (Ellison, Onilude et al. 2005; Takei, Nguyen et al. 2009). This is an area for further study.

Reference	Analysis Method	Cohort		Amplification	
		Number	Age (years)	*MYCC*	*MYCN*
(Fruhwald, O'Dorisio et al. 2000)	RLGS + CGH	5	3-6	1/5	1/5
(Pfister, Remke et al. 2007)	FISH + aCGH	21	0.6 - 18	1/21	0/21
(Behdad and Perry 2010)	FISH	6	20-61	1/6	0/6
		22	0.5-18	2/22	9/22

Table 3.29. *MYC* family gene amplification in CNS-PNET. Abbreviations: Restriction landmark genomic scanning (RLGS), fluorescence *in situ* hybridisation (FISH), comparative genomic hybridisation (CGH) and array CGH (aCGH).

3.4.6 Disruption of the *TP53* signalling pathway in CNS-PNET

3.4.6.1 Frequent p53 pathway disruption and p53 accumulation in CNS-PNETs.

In 91% of primary tumour samples there was evidence of p53 nuclear accumulation by IHC. The frequency of accumulation in CNS-PNET was shown to be higher than in previous medulloblastoma series (Eberhart, Chaudhry et al. 2005; Tabori, Baskin et al. 2010). However, whilst these studies all used the same p53 antibody, the scoring of p53 positivity differed. In the Eberhart et al study, as with the current study, cases with positive staining nuclei within tumour cells were classified as positive. In the Tabori et al study, however, cases were only scored as positive if p53 staining was both intense and present in at least 50% of nuclei which has also been used in another medulloblastoma study (Ray, Ho et al. 2004). Using this approach, Tabori et al found that p53 IHC positivity correlated with an adverse outcome. If in the present study this scoring system were applied 8 cases (SP42, SP43, SP46, SP47, SP49, SP50, SP52, SP55) would be found to be positive, but the association with survival remains not significant (p=0.87, Logrank test) (Figure 3.30). This study does not however exclude the possibility that a significant association between an adverse outcome and p53 nuclear accumulation in CNS-PNET exists. Whilst this is a comparatively large CNS-PNET study the

nevertheless low sample numbers and high frequency of censored events resulting from a relatively short follow up increases the possibility of a type 1 error, that a real association is rejected.

The high frequency of nuclear p53 accumulation suggests that either the pathway is highly active in this disease, or frequently disrupted resulting in an abnormal accumulation. To identify whether the pathway is dysfunctional in up to 91% of CNS-PNETs further investigation of downstream targets, including p21 (cyclin dependent kinase inhibitor), (Shariat, Kim et al. 2003) is required.

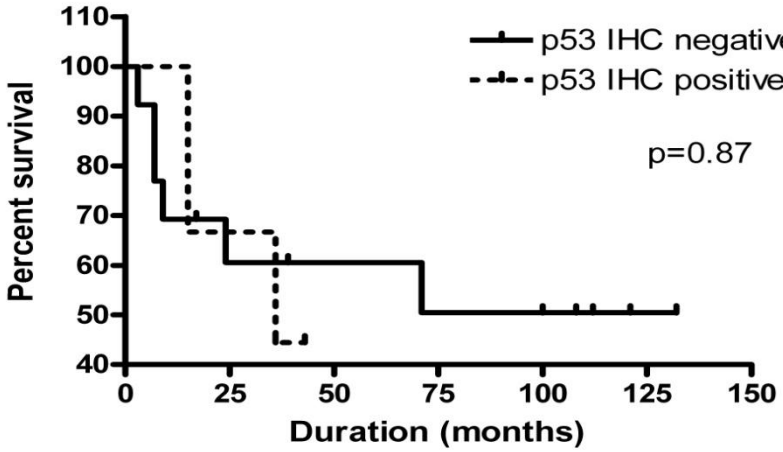

Figure 3.30. Kaplan-meier curve of CNS-PNET survival in relation to p53 immunohistochemical nuclear staining. Positive scores obtained only in cases with intense nuclear staining in >50% of cells.

3.4.6.2 *TP53* mutations in pathway disruption

TP53 mutations were detected in 18% (4/22) of cases (SP4, SP46, SP47, SP55). All were missense mutations and were associated with p53 nuclear positivity on IHC suggesting the accumulation of a mutant protein (Figure 3.19). In three of these tumours (SP46, SP47 and SP55) mutation was associated with intense and widespread nuclear accumulation. In SP4 however there was faint staining in a minority of cells suggesting that accumulation of

mutant p53 protein was occurring to a lesser degree than in the other mutated cases. Variation in p53 accumulation in mutated cases is known to occur (Horiuchi, Kawamata et al. 2004). In a study of 99 colorectal *TP53* mutated tumours, 28% did not show any evidence of p53 accumulation on immunohistochemical testing (Kressner, Inganas et al. 1999). In this colorectal study, in some cases nonsense mutations predicted the production of a truncated protein which may not be detected by the anti-p53 antibody, 18% (15/84) of missense mutations were also negative on immunohistochemical testing. Whilst in the current study p53 IHC identified all the cases with mutation, the scoring approach used by Tabori et al and Ray et al would have not detected ¼ of the cases with defects in the *TP53* pathway. Together this suggests that p53 IHC cannot be used reliably as a sensitive screening test for defects in the *TP53* pathway.

The current study however represents the largest CNS-PNET cohort screened for *TP53* mutations to date. *TP53* mutations have previously been identified in CNS-PNET in a number of small studies (Table 3.30). Interestingly in the study by Ho et al, 43% (6/14) of adult CNS-PNET were found to have mutations of the DNA biding domain (Ho, Hsieh et al. 1996). In contrast in paediatric studies few mutant cases have been identified (Burnett, White et al. 1997; Zagzag, Miller et al. 2000; Kraus, Felsberg et al. 2002; Zakrzewska, Rieske et al. 2004). In the current study mutations occurred in patients aged 6.4, 6.5, 7.3 and 26 years and was not significantly associated with age (p=0.41, Fisher's exact test).

Mutations outside of the DNA binding domain as discussed in (section 1.5.5) may occur but the frequency of these mutations may have been underestimated as studies usually screen only for mutations in the binding domain exons (5-8). A case of such a *TP53* mutation outside the DNA binding domain has been reported in a CNS-PNET in a study that investigated predominantly gliomas but contained a single CNS-PNET case (Kato, Kato et al. 2000). A nonsense mutation in exon 10 was discovered (1043T>A, L348X). It is possible therefore that *TP53* mutation may be responsible for additional cases of *TP53* pathway dysfunction and may be identified if subsequent studies of CNS-PNET incorporated sequencing of all exons.

Finally, constitutional DNA was not available for a paired parallel analysis for any of the cases in the investigated cohort. In addition the clinical details available were not sufficiently comprehensive to exclude a family history of cancer and in the context of *TP53* mutations in a CNS-PNET, to exclude the possibility that tumours arose in individuals with Li-Fraumeni Syndrome (LFS). The outcome for patients with LFS who develop a CNS-PNET (or medulloblastoma) is not however known to be different but determining LFS status may confer other clinical benefits (discussed in section 1.5.2)

Reference	Exons	Cohort		Mutation frequency
		Size	Age (years)	
(Ho, Hsieh et al. 1996)	5-9	n=14	19-77	6/14 (43%)
(Burnett, White et al. 1997)	4-9	n=8	0-16	0/8 (0%)
(Zagzag, Miller et al. 2000)	5-9	n=7	1-8	0/7 (0%)
(Kraus, Felsberg et al. 2002)	5-8	n=12	2-9	1/12 (8%)
(Zakrzewska, Rieske et al. 2004)	4	n=5	1-13	0/5 (0%)

Table 3.30. *TP53* mutations in published series of CNS-PNET.

3.4.6.3 Alternative mechanisms of *TP53* pathway disruption: *MDM2* and *CDKN2A*

The prevalence of p53 expression in the current study, could not be accounted for by *TP53* mutation in the majority of cases. Alternative mechanisms for pathway disruption (discussed in section 1.5.5.1), *MDM2* amplification and deletion of *CDKN2A* were therefore investigated. Increased expression of Mdm2 can be observed in the presence of p53 over-expression (Barak, Juven et al. 1993) which has been shown to occur through *MDM2* amplification in many cancer types and in 7% of all cancers (Momand, Jung et al. 1998). Mdm2 binds to p53 to promote its degradation and therefore prevent it from promoting apoptosis or inhibiting the cell cycle and therefore in excess may lead to cancer development. In the current study there was evidence of *MDM2* copy number elevation in a single case (SP40) out of the 23 primary CNS-PNETs investigated (1/23, 4%). These findings are in keeping with a previous study in which no evidence of *MDM2* amplification was observed in a cohort of 12 CNS-PNETs (Kraus, Felsberg et al. 2002). To determine whether this was indeed an *MDM2* allelic gain rather than a gain of part of chromosome 12 containing the *MDM2* locus (12q13-q14) FISH probes to *MDM2* and chromosome 12 would have ideally been applied, but this was unfortunately not possible due to a lack of appropriate material. The effect of copy number changes on Mdm2 expression did not form part of the present study, but should be investigated further.

As discussed in section 1.5.5.1, alternative splicing of *CDKN2A* encodes for 2 different proteins including $p14^{ARF}$ which is involved in the regulation of p53 through inhibition of Mdm2. Inhibition of $p14^{ARF}$ permits the unchecked expression of Mdm2, subsequent proteosomal degradation of p53 and tumour development. Homozygous deletion of *CDKN2A* has been shown to occur in a number of tumours including in up to 40% of glioblastomas (Schmidt, Ichimura et al. 1994) including paediatric cases (Newcomb, Alonso et al. 2000). In the current study there was no evidence of homozygous deletion of *CDKN2A* being responsible for *TP53* pathway disruption which supports the combined findings (0/21) of two smaller previous studies in CNS-PNETs (Kraus, Felsberg et al. 2002; Inda, Munoz et al. 2006). However a previous CGH study (McCabe,

Ichimura et al. 2006) homozygous deletion of the *CDKN2A* locus was observed in a single CNS-PNET (1/7 studied) and in a second study by Pfister et al homozygous deletion of 9p21 was observed using FISH in 2/11 CNS-PNETs (Pfister, Remke et al. 2007). Heterozygous deletion was found in an additional 3 cases in this study and both homozygous and heterozygous deletions were associated with reduced "CDKN2A protein" expression and a more aggressive phenotype. In the current study suitable material was unfortunately not available to ascertain using FISH whether heterozygous deletion of the *CDKN2A* locus was present in any of the CNS_PNETs in this series. Finally Inda et al have shown that epigenetic regulation of *CDKN2A* in CNS-PNET may also be implicated in pathway disruption, (Inda, Munoz et al. 2006) but this needs further evaluation in larger series.

3.4.7 Therapeutic targeting of the *TP53* pathway in CNS-PNET

91% of tumours in this study were shown to exhibit nuclear p53 accumulation which may indicate *TP53* pathway dysfunction. Apart from tumour development, mutant p53 protein may therefore also significantly contribute to the dismal prognosis in this disease by conferring resistance to vincristine and cisplatin which are used as part of current treatment protocols (Hamada, Fujiwara et al. 1996; Shelling 1997; Giannakakou, Sackett et al. 2000). On the other hand the prevalence of pathway disruption may enable therapeutic exploitation of the aberrant *TP53* pathway function to provide significant opportunities in CNS-PNET. Currently, as reviewed by Lu et al, a number of new agents have been developed as possible new treatments in cancers with *TP53* pathway disruption (Lu and El-Deiry 2009). Treatments include the reintroduction of wild-type p53 using an adenovirus vector; elimination of mutant p53 by selective adenovirus lysis; p53 degradation inhibition and stabilisation using nutlins to displace p53 from Mdm2; activation of other components of the pathway including p63 and p73 to substitute for the aberrant p53; and a number of agents designed to restore wild-type function. Such therapeutic approaches have not been used in CNS-

PNET to date, but the current study suggests that such approaches may have a role in this disease.

3.4.8 Disruption of Wnt signalling pathway in CNS-PNET

Disruption of the canonical Wnt signalling pathway as identified with nuclear accumulation of β-catenin was determined in 2/22 (9%) primary CNS-PNET cases. In one of these cases β-catenin accumulation was associated with a *CTNNB1* mutation. These findings are not significantly different to those observed in medulloblastoma in which nuclear β-catenin immunopositivity and *CTNNB1* mutations have been shown to occur in 33/206 (16%) and 20/195 (10%) cases respectively (Ellison, Kocat et al. 2011). In two previous studies which have investigated wnt pathway disruption in CNS-PNETs a total of 16 tumours were screened for *CTNNB1* mutations and 33 for β-catenin nuclear accumulation by immunohistochemistry (Koch, Waha et al. 2001; Rogers, Miller et al. 2009). In these studies, as summarised in Table 3.31, only a single case of *CTNNB1* mutation was observed. As in the current study a non-synonomous mutation in codon 34 was identified, resulting in a valine substitution at this position (GGA>GTA, G34V) rather than an arginine as in the current study. Both of these mutations have been identified in previous studies in medulloblastoma (Fattet, Haberler et al. 2009; Ellison, Kocat et al. 2011) and are known to affect the β-transducin repeat-containing protein (β-TRCP) which promotes the degradation of β-catenin in the proteosome (Gilbertson 2004).

Reference	Cohort		*CTNNB1* mutation frequency	β-catenin nuclear IHC positivity
	Number	Age (years)		
(Koch, Waha et al. 2001)	4	0.1-59	1/4	1/4*
(Rogers, Miller et al. 2009)	29	0.4-15.5	0/12	9/29**

Table 3.31. Wnt pathway defects in CNS-PNET. Mutation in *CTNNB1* exon 3 studied. (*) A *CTNNB1* mutation in addition to β-catenin nuclear accumulation was observed. (**) 9/29 cases showed strong β-catenin nuclear accumulation in >10% of cells, and in an additional 3/29 samples low level accumulation (1-10%) was reported.

3.4.9 Targeting Wnt pathway in CNS-PNET

This study has confirmed that disrupted canonical Wnt signalling is involved in a subset of CNS-PNETs. The role this disruption has on tumourignesis now needs detailed characterisation and further investigation. In similar studies in medulloblastoma (Thompson, Fuller et al. 2006; Kool, Koster et al. 2008) canonical Wnt pathway disruption with nuclear β-catenin accumulation has been associated with an up-regulation of Wnt effector gene expression, and associated with a favourable prognostic phenotype (Ellison, Onilude et al. 2005; Gajjar, Chintagumpala et al. 2006; Fattet, Haberler et al. 2009; Ellison, Kocat et al. 2011). The effect of *CTNNB1* mutations and β-catenin accumulation in CNS-PNET however is currently unknown and the total numbers of reported Wnt pathway disrupted cases are too few currently to determine whether this defect is associated with a favourable phenotype in CNS-PNET.

Identifying CNS-PNETs with Wnt pathway disruption may lead to the use of novel treatment strategies which exploit this pathway in these cases. This approach is currently being explored in a number of different tumours including colonic carcinoma in which aberrant Wnt signalling is observed in 90% of cases (Barker and Clevers 2006). In contrast to medulloblastoma and CNS-PNET, in 80% this is attributable to mutant *APC* (Miyaki 1994; Korinek 1997), and mutations in *CTNNB1* or Axin-2 in a small group (Morin 1997; Polakis 2000). In a number of other tumours however, including

hepatocelluar carcinoma; hepatoblastoma; endometrial carcinoma; ovarian carcinoma; prostate cancer; melanoma and wilm's tumour, disruption of Wnt signalling results from frequent mutations in *CTNNB1* (Polakis 2000). The range of therapeutic approaches currently being investigated to exploit Wnt signalling disruption includes the use of aspirin and similarly acting drugs (Non-steroidal anti-inflammatory drugs (NSAIDs)). Aspirin has been shown to be protective in familial colonic cancer (Thun 1997; Thun, Henley et al. 2002) and other NSAIDs have been shown to have a similar effect(Giardiello 1993; Phillips 2002; Koehne and Dubois 2004). These agents however are limited by their toxicity profile. Modified NSAIDS including aspirin which donate nitric oxide and induce oxidatitive stress within the tumour cell (Rigas and Williams 2002; Rigas 2007) have been developed which result in a more potent reduction in gene expression by disruption of the β-catenin/TCF complex (Williamson, Lu et al. 2005), have fewer side effects and have been shown to be effective in a number of tumours including colonic carcinoma (Rigas and Williams 2002; Gao, Liu et al. 2005), breast cancer (Nath, Vassell et al. 2009) and prostate cancer (Lu, Tinsley et al. 2009). Antibody therapies to the Wnt and Fz proteins have also been developed. In many tumours these proteins are over-expressed (Katoh, Kirikoshi et al. 2001; Holcombe, Marsh et al. 2002; Rhee, Sen et al. 2002; Milovanovic 2004; You, He et al. 2004; You, He et al. 2004a), and have been found to be effective in *in-vitro* models (You, He et al. 2004; You, He et al. 2004a). Of particular note a recently published study using a small molecule inhibitor (OSU03012) resulted in growth inhibition with reduced nuclear β-catenin and a consequent reduction in both cyclin-D1 and c-myc through repression of TCF/LEF transcription in a series of medulloblastoma and CNS-PNET cell lines (Baryawno, Sveinbjornsson et al. 2010). Targeting of the Wnt pathway may therefore provide a therapeutic option for a subgroup of patients with CNS-PNET and merits further investigation.

3.4.10 Medulloblastoma molecular defects in CNS-PNET: Implications for the "PNET" concept

In this study a series of molecular events frequently observed in medulloblastomas have been investigated in a CNS-PNET cohort. This approach has shown that CNS-PNETs are a heterogenous group of tumours which may possess a range of molecular defects, but important differences with medulloblastomas are observed.

In common with many other tumour types *RASSF1A* promoter methylation is a highly frequent event in CNS-PNET. This finding suggests that understanding epigenetic modification by methylation in CNS-PNET may provide novel insights into the tumour development in this disease. Our current understanding of the CNS-PNET methylome is however very limited and only populated by the results of a few small studies in which candidate markers in other brain tumours are investigated in a few CNS-PNET in addition. A systematic study to investigate the CNS-PNET methylome in a large cohort of such tumours is now required, and forms the basis of the study reported in chapter 5.

As discussed in section 1.3.4, the PNET concept suggests that tumours that have a similar histological phenotype share a common origin and despite their diverse location within the CNS is a unified entity. The current study of a range of frequent medulloblastoma defects does not support this hypothesis. Whilst some defects are seen in subgroups of tumours (*MYCN* amplification and Wnt pathway disruption), both the frequency of chromosome 17p loss and *TP53* pathway activation or dyrsregulation, suggests that different mechanisms underlie the development of CNS-PNET compared with medulloblastomas. This study has however investigated only a limited number of defects. Further genome-wide studies are now needed to investigate and characterise the similarities and differences between these two tumour groups in greater detail.

This study suggests that progress in our understanding of the molecular basis for this group of tumours will be derived from future biological studies and programmes investigating CNS-PNET as a distinct entity in addition to studies with

medulloblastomas. The benefits of such an approach are illustrated with the elucidation of a novel gene identified in CNS-PNET and not in medulloblastoma in chapter 4. Adequate material and corresponding clinical data to undertake these studies is crucial and as a consequence of their relative rarity the need for further international collaboration to achieve this, as will be discussed in further detail in chapter 7, is both necessary and provides exciting opportunities.

Chapter 4

A study of *IDH1* mutations in CNS-PNET

Table of contents

Chapter 4

4.1 Introduction

4.1.1 *IDH1* mutations in cancer

Research into the genetic events involved in CNS-PNET tumorigenesis have evolved primarily by extending studies into MB, as has been discussed in detail in section 1.5. New genome-wide techniques however provide a different approach and potentially novel opportunities to identify critical genetic events. A genome wide screen incorporating 20,661 protein coding genes from 22 human glioblastoma multiforme (GBM) samples in 2008 identified recurrent mutations in a gene not previously known to be associated with GBM tumorigenesis (Parsons, Jones et al. 2008). In this study, mutations in isocitrate dehydrogenase-1 (*IDH1*) were discovered in 5 of an initial panel of 22 tumours, which was then expanded to include 149 GBMs, in which a total of 18 (12%) had *IDH1* mutations. The mutation discovered in all cases was a point mutation in exon 4 resulting in the substitution of guanine to adenine at position 395, leading to arginine being replaced by histidine at residue 132.

Located on chromosome 2q33.3, *IDH1* encodes isocitrate dehydrogenase-1, an enzyme that catalyses the rate-limiting step in the citric acid (Kreb's) cycle converting isocitrate to α-ketoglutarate (α-KG) with the production of nicotinamide adenine dinucleotide phosphate (NADPH) (Barnes, Kuehn et al. 1971). It is located in the cytoplasm, peroxisomes and endoplasmic reticulum (Geisbrecht and Gould 1999; Margittai and Banhegyi 2008) and plays a central role in tissue energy metabolism and through the production of NADPH, a role in the cellular control of oxidative damage (Lee, Koh et al. 2002).

Subsequent to the Parsons et al study (Parsons, Jones et al. 2008), there have been a number of studies designed to investigate the presence of *IDH1* mutations in a series of brain tumours (Balss, Meyer et al. 2008; Parsons, Jones et al. 2008; Bleeker, Lamba et al. 2009; Watanabe, Nobusawa et al. 2009; Yan, Parsons et al. 2009). In total, 1603 brain tumours (at the time of undertaking this study) had been assessed, and mutations discovered in 37%, as summarised in Table 4.1. Research into this novel

event in tumours originating outside of the brain was also undertaken by a number of investigators (Bleeker, Lamba et al. 2009; Yan, Parsons et al. 2009). These studies included 1053 tumours from a variety locations and histopathological subtypes, but did not reveal any *IDH1* mutations, suggesting that these mutations may be implicated exclusively in the tumorigenesis of CNS tumours.

4.1.2 *IDH1* mutations in CNS-PNET

In the study by Balss et al (Balss, Meyer et al. 2008), a panel of embryonal tumours were screened for *IDH1* mutations. In addition to MB samples, this panel included 9 CNS-PNETs and discovered G395A mutations in a third (3/9). No mutations were seen in any of the medulloblastoma samples, which corroborated findings by Yan et al in their panel of MB samples (Yan, Parsons et al. 2009). Taken together, 113 MB samples have been analysed in addition to 9 CNS-PNETs and *IDH1* mutation occurs only in CNS-PNET embryonal tumours (p=0.0003, Fisher's exact test). Investigation in a larger cohort of CNS-PNET is therefore now required.

4.1.3 Aims

The aim of this chapter was to investigate the role of *IDH1* mutations in CNS-PNET tumorigenesis, and determine any correlation with clinicopathological features.

The specific aims were:

1. To screen a CNS-PNET cohort for *IDH1* mutations

2. To correlate findings with clinicopathological features

CNS tumour type		Number of tumours analysed	IDH1 Mutation		References
			Number	Frequency (%)	
Astrocytic tumours		917	307	33	(Parsons, Jones et al. 2008; Bleeker, Lamba et al. 2009; Nobusawa, Watanabe et al. 2009; Watanabe, Nobusawa et al. 2009; Yan, Parsons et al. 2009)
Oligodendroglial tumours		241	182	76	(Balss, Meyer et al. 2008; Bleeker, Lamba et al. 2009; Watanabe, Nobusawa et al. 2009; Yan, Parsons et al. 2009)
Oligoastrocytic tumours		124	101	81	(Balss, Meyer et al. 2008; Watanabe, Nobusawa et al. 2009; Yan, Parsons et al. 2009)
Embryonal	CNS-PNET	9	3	33	(Balss, Meyer et al. 2008)
	Medulloblastoma	113	0	0	(Balss, Meyer et al. 2008; Yan, Parsons et al. 2009)
Ependymal tumours		87	0	0	(Balss, Meyer et al. 2008; Watanabe, Nobusawa et al. 2009; Yan, Parsons et al. 2009)
Sellar region tumour		23	0	0	(Balss, Meyer et al. 2008)
Cranial & paraspinal nerve tumour		17	0	0	(Balss, Meyer et al. 2008)
Meningothelial cell tumours		72	0	0	(Balss, Meyer et al. 2008)

Table 4.1. Summary of *IDH1* mutations identified in brain tumours.

Tumour type	Number of tumours analysed	*IDH1* Mutation		References
		Number	Frequency (%)	
Leukaemia	63	0	0	(Yan, Parsons et al. 2009)
Bladder	34	0	0	(Bleeker, Lamba et al. 2009)
Breast	223	0	0	(Bleeker, Lamba et al. 2009; Yan, Parsons et al. 2009)
Gastric	57	0	0	(Yan, Parsons et al. 2009)
Colorectal	267	0	0	(Bleeker, Lamba et al. 2009; Yan, Parsons et al. 2009)
Lung	142	0	0	(Bleeker, Lamba et al. 2009; Yan, Parsons et al. 2009)
Melanoma	23	0	0	Bleeker, Lamba et al. 2009)
Thyroid	42	0	0	Bleeker, Lamba et al. 2009)
Ovary	73	0	0	(Bleeker, Lamba et al. 2009; Yan, Parsons et al. 2009)
Pancreas	118	0	0	(Bleeker, Lamba et al. 2009; Yan, Parsons et al. 2009)
Prostate	11	0	0	(Bleeker, Lamba et al. 2009; Yan, Parsons et al. 2009)

Table 4.2. Summary of *IDH1* mutations identified in non- central nervous tissue (CNS) tumours.

4.2 Materials and methods

4.2.1 CNS-PNET cell lines

Two CNS-PNET cell lines (PFSK and CHP707m) were investigated in this study. Further details regarding these cell lines and their culture may be found in section 2.1.2. Genomic DNA was extracted from the cell lines as described in section 2.3.2.

4.2.2 CNS-PNET primary tumours

A total of 25 primary CNS-PNETs were investigated in this study. All samples had undergone a central pathological review as described in section 2.1.1. Clinical details of these tumours are given in Table 4.3. The cohort included material from 11 male and 14 female cases enrolled on a number of different clinical studies who underwent different treatment strategies. The patients were aged 11 – 360 months (0.92 – 30 years), with a median age of 77.5 months (6.5 years) at diagnosis. A single case had evidence of metastatic disease on neuroimaging at diagnosis. Genomic DNA was extracted as described in section 1.3.1.

ID	Diagnosis	Site	Sex	Age at diagnosis (Months)	Metastasis Stage (Chang)	Status	Follow up (months)
SP3	CNS-PNET	Parieto-occipital lobes	M	48	M0/1	Dead	17
SP4	CNS-PNET	Parietal lobe	F	78	M0/1	Alive	121
SP7	CNS-PNET	Intraventricular	F	75	M0	Dead	7
SP10	CNS-PNET	3rd Ventricle	M	158	M0/1	Alive	112
SP13	CNS-PNET	Cerebral	M	106	M0/1	Dead	71
SP14	CNS-PNET	Parietal lobe	F	105	-	Alive	100
SP21	CNS-PNET	Left tempoparietal lobes	M	65	-	Dead	25
SP23	CNS-PNET	Cerebral	M	126	M0/1	Alive	108
SP24	CNS-PNET	Cerebral	M	31	-	Dead	7
SP28	CNS-PNET	Right frontal lobe	F	23	M0/1	Dead	9
SP40	CNS-PNET	Right parietal lobe	F	348	M0/1	-	-
SP41	CNS-PNET	Left fronto-temporal lobes	M	56	M0/1	Dead	24
SP42	CNS-PNET	Right temporal lobe	F	288	M0/1	Alive	24
SP43	CNS-PNET	Left parietal lobe	M	-	M0/1	-	-
SP45	CNS-PNET	Right parietal lobe.	F	11	M0/1	-	-
SP46	CNS-PNET	Left frontal lobe	F	312	M0/1	Dead	36
SP47	CNS-PNET	Left frontal lobe	F	87	M0/1	Alive	132
SP49	CNS-PNET	Right temporal lobe	F	15	M2	Alive	36
SP50	CNS-PNET	Left tempoparietal lobes	F	36	M0/1	Dead	15
SP51	CNS-PNET	Cerebral	F	360	-	Dead	55
SP52	CNS-PNET	Left parietal lobe	M	127	M0/1	Alive	43
SP54	CNS-PNET	Infra + supratentorial	F	26	M0/1	Dead	3
SP55	CNS-PNET	Temporal lobe	M	77	M0/1	Dead	15
SP57	CNS-PNET	Frontal + temporal lobes	M	21	M0/1	Alive	39
SP58	CNS-PNET	Right parietal lobe	F	223	M0	Alive	17

Table 4.3. Clinical characteristics of CNS-PNET tumour samples used in *IDH1* study.

4.2.3 Polymerase chain reaction

PCRs were performed on both cell line and tumour material suing the Fast PCR method as described in section 2.4.4, using a combined annealing and extension temperature of 64°C for 10 seconds and cycled 40 times. The primer sequences used were as previously described (Balss, Meyer et al. 2008) and are given in Table 4.4. Primer sequences were verified using BLAST (http://blast.ncbi.nlm.nih.gov) and BLAT (http://genome.ucsc.edu) searches as described in section 2.4.2. PCR products were analysed by gel electrophoresis and their size approximated using a 100bp DNA ladder (as described in section 2.5.2).

Gene Name	Forward primer sequence	Reverse primer sequence	Product length (bp)	Location
IDH1	5'-CGGTCTTCAGAGAAGCCATT-3'	5'-GCAAAATCACATTATTGCCAAC-3'	129	Exon 4

Table 4.4. *IDH1* PCR primers.

4.2.4 Direct sequencing of *IDH1*

PCR products were purified as described in section 2.4.5, before being sent to DBS genomics (Durham University) for sequence analysis using an ABI 3730 analyser (Applied Biosystems) as described in section 2.6.2. Products were sequenced in both forward and reverse directions using the PCR primer set in Table 4.4**.** The sequence data generated was imported and analysed in DNASTAR (DNASTAR Inc, USA). Samples showing evidence of *IDH1* mutation were repeated to corroborate this finding.

4.3 Results

4.3.1 *IDH1* sequence analysis

Twenty-five tumour samples were screened for mutations of *IDH1* in exon 4. The results of the sequence analysis are summarised in Table 4.5. *IDH1* mutations were identified in 2 cases (8%), and confirmed on repeating the PCR amplification and sequencing of products. In both cases a non-synonymous point mutation was observed in codon 132 with the substitution of guanine for adenine (G395A) as shown in Figure 4.1 and a corresponding change to the amino acid residue (R132H).

ID	*IDH1* sequence analysis result
SP3	wt
SP4	wt
SP7	wt
SP10	wt
SP13	wt
SP14	wt
SP21	wt
SP23	wt
SP24	wt
SP28	wt
SP40	G391A (heterozygous mutation)
SP41	wt
SP42	wt
SP43	wt
SP45	wt
SP46	G391A (heterozygous mutation)
SP47	wt
SP49	wt
SP50	wt
SP51	wt
SP52	wt
SP54	wt
SP55	wt
SP57	wt
SP58	wt

Table 4.5. *IDH1* exon 4 sequence analysis results. (wt = wild type sequence)

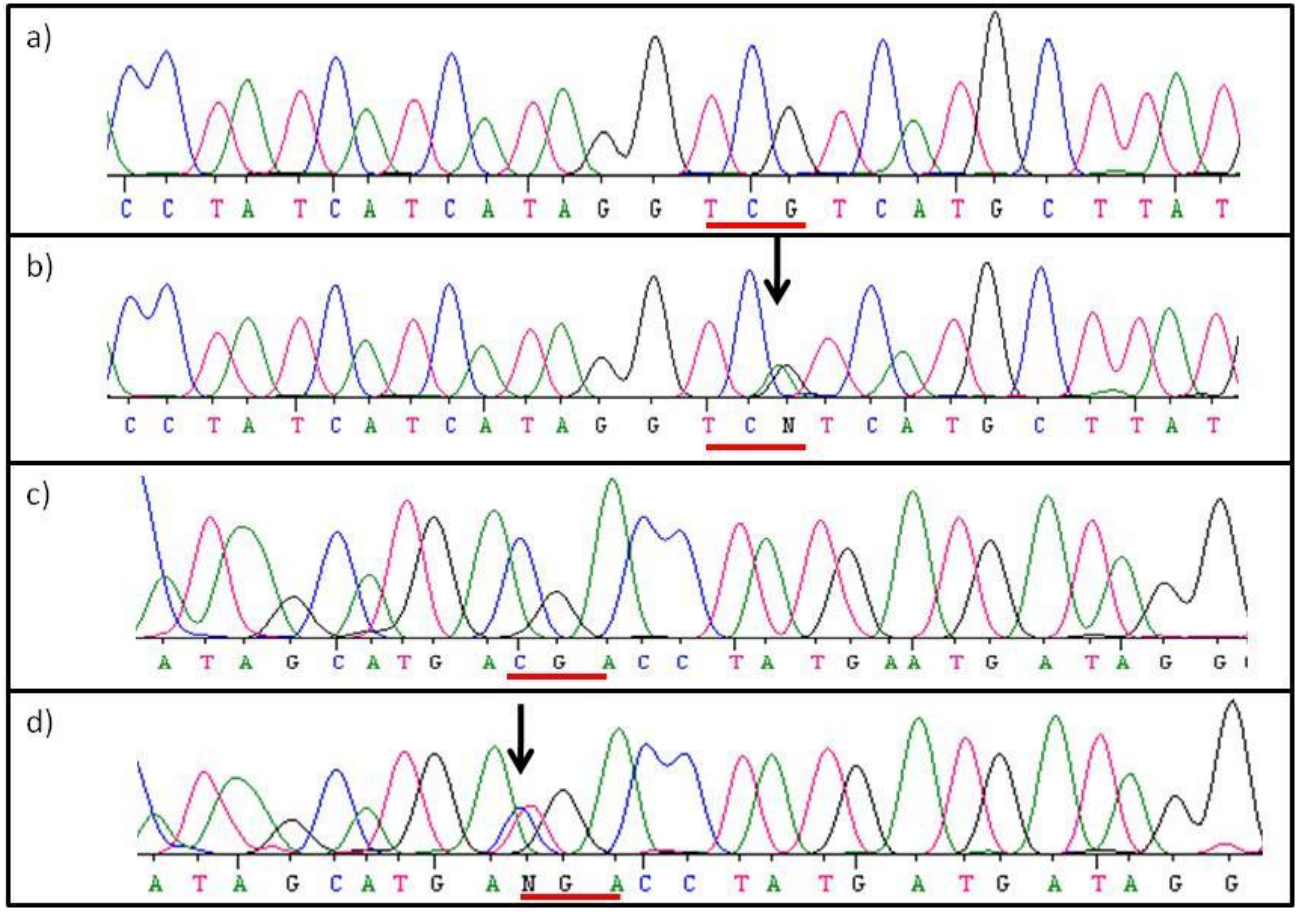

Figure 4.1. *IDH1* exon 4 sequence traces. (a) Normal forward sequence in PFSK, (b) Point substitution (G→A) mutation in codon 132 (red bar) in SP40. (c) PFSK wild type sequence confirmed in reverse, and (d) reverse trace confirms mutation in SP40 (arrow).

4.3.2 Association of *IDH1* mutation with clinical characteristics

The outcome data for one of the cases found to contain an *IDH1* mutation are not known and therefore it was not possible to correlate mutation status with survival. As discussed in section 1.4.4, there are 2 clinical characteristics, age at diagnosis and Chang stage, which are known to affect prognosis. Both cases with a G395A mutation were recorded as having a Chang metastatic stage of M0/1. The *IDH1* cohort however contained only 1 case (SP49) with metastatic disease confirmed on imaging at diagnosis, and so correlation cannot be made. No case of *IDH1* mutation occurred in infants or in children. The 2 events were seen in adults cases only (26 and 29 years of age). The finding that *IDH1* mutation occurred solely in adult cases is significant (2/5 adult cases (>16years) vs 0/19 child cases (<16years), p = 0.04, Fisher's exact test).

4.4 Discussion

4.4.1 *IDH1* mutations exclusivity to brain tumours

The original papers that described *IDH1* mutations (discussed in section 4.1.1) suggested that these events occurred exclusively in tumours of the central nervous system. It has however subsequently been discovered that whilst these events have been found to be most prevalent in CNS tumours, in particular occurring in 70-80% of secondary GBM (Balss, Meyer et al. 2008; Parsons, Jones et al. 2008; Bleeker, Lamba et al. 2009; Hartmann, Meyer et al. 2009; Ichimura, Pearson et al. 2009; Nobusawa, Watanabe et al. 2009) and other tumours of glial origin (Ichimura, Pearson et al. 2009), that these aberrations may also be detected in extracranial disease. *IDH1* mutations have been observed in myeloproliferative neoplasms including acute myeloid leukaemia (AML) (Pardanani, Lasho et al. 2010; Patnaik, Lasho et al. 2010; Tefferi, Lasho et al. 2010; Thol, Weissinger et al. 2010). Interestingly, when in conjunction with AML, different mutations at the same locus are seen with up to half associated with a R132C mutation (Mardis, Ding et al. 2009; Chou, Hou et al. 2010). *IDH1* mutations have also been identified in a minority of prostate tumours (2/75, 2.7%) in a screen of 1186

cancers from various sites including 1161 extracranial tumours (Kang, Kim et al. 2009). They do not appear however to play a pivitol role in the development of cerebral metastases from an extracranial solid tumours (Holdhoff, Parsons et al. 2009). Overall, extracranial *IDH1* mutations remain an infrequent finding.

4.4.2 *IDH1* mutations occur solely in adult CNS-PNET disease

This study has shown *IDH1* mutations to be correlated with the development of CNS-PNETs in adults. Clinical data pertaining to the CNS-PNET samples from the original brain tumour screening series which also identified *IDH1* mutations in CNS-PNET (Balss, Meyer et al. 2008) are shown in Table 4.6 (kindly supplied by Professor Andreas Deimling). R132H mutations were observed in 3 cases in this other, and all were in adults (26.8, 27 and 32 years old). These data in combination with the results of this study confirm the finding that *IDH1* mutations appear to occur solely in adult cases (combined data: 5/12 adults (>16 years) vs 0/21 childhood tumours (<16years), p=0.003, Fisher's exact test) and represents the only biological aberration to date to be associated specifically with the adult CNS-PNET phenotype. This in turn suggests for the first time that tumorigenesis mechanisms within the spectrum of CNS-PNET disease may be different at different ages. *IDH1* mutations appear also to be one of the most common mutational events discovered in CNS-PNET development to date.

ID	Age (Months)	*IDH1* Sequence analysis
D1	322	G395A (heterozygous mutation)
D2	676	wt
D3	664	wt
D4	40	wt
D5	325	G395A (heterozygous mutation)
D6	209	wt
D7	384	G395A (heterozygous mutation)
D8	84	wt
D9	562	wt

Table 4.6. Details of CNS-PNETs from Balss et al study, 2008. Wt: wild type. (Personal communication, data kindly provided by Professor Andreas van Deimling)

4.4.3 *IDH1* role in tumorigenesis

The identification of mutations in *IDH* genes has resulted in a series of investigations into its functional role in cancer development. It has been postulated that *IDH1* may act as a tumour suppressor rather than oncogene (Zhao, Lin et al. 2009) and is implicated in cancer development by establishing a cellular environment in which carcinogenic events may arise (illustrated in Figure 4.2).

The first postulated effect of an *IDH1* mutation is loss of function (Yan, Parsons et al. 2009), by approximately 2 –fold (Bleeker, Atai et al. 2010), in the catalysis of isocitrate to α-KG. The mutant *IDH1* (mIDH1) also however derives a gain of function to produce 2-hydroxyglutarate (2-HG) by an NADPH-dependent reduction of α-KG (Bleeker, Atai et al. 2010) which has been shown to occur in all analysed tumours with an *IDH1* mutation (Dang, White et al. 2010). The reduction of α-KG and accumulation of 2-HG

has three main effects. Firstly, the process requires NADPH and therefore in addition to this not being produced through the IDH1 conversion of isocitrate, the cell becomes further depleted. The reduction of NADPH increases the risk of oxidative stress associated with increased reactive oxygen species (ROS), which in turn may increase the risk of cancer development (Kolker, Pawlak et al. 2002; Latini, Scussiato et al. 2003). Secondly, the α-KG control on the hypoxia-inducible factor subunit 1α *(HIF1α)* " master switch" of cellular adaptation is impaired by the reduction of cytoplasmic α-KG (Zhao, Lin et al. 2009), resulting in the transcription of genes which may promote tumorigenesis by aiding cell mobility, invasion and energy metabolism (Hughes, Groot et al. 2010). Thirdly, accumulation of 2-HG is known to be associated with cancer development. 2HG is known to accumulate in 2-hydroxyglutaric aciduria, an autosomal recessive inherited metabolic disorder characterized by psychomotor retardation and progressive ataxia. This inborn error of metabolism occurs due to the deficiency of 2-hydroxyglutarate dehydrogenase which converts 2-HG to α-KG (Struys, Salomons et al. 2005) and is associated with the development of brain tumours (Wajner, Latini et al. ; Kolker, Mayatepek et al. 2002; Aghili, Zahedi et al. 2009). mIDH1 has been shown to gain the function of catalysing α-KG to 2-HG (Zhao, Lin et al. 2009; Bleeker, Atai et al. 2010) and, as CNS tissues are uniquely able to uptake glutamate and convert it to α-KG (Tsacopoulos 2002) an abundant substrate for mIDH1 is available, thus potentially increasing the risk of future tumour development.

Additional studies to improve our understanding of the role *IDH1* plays in tumour development are now required. Drugs to inhibit the mIDH1 expression, or that inhibit 2HG (Sonoda and Tominaga 2010), and drugs currently being developed to target HIF1α (Semenza 2003), could have a potential role in the management of this disease.

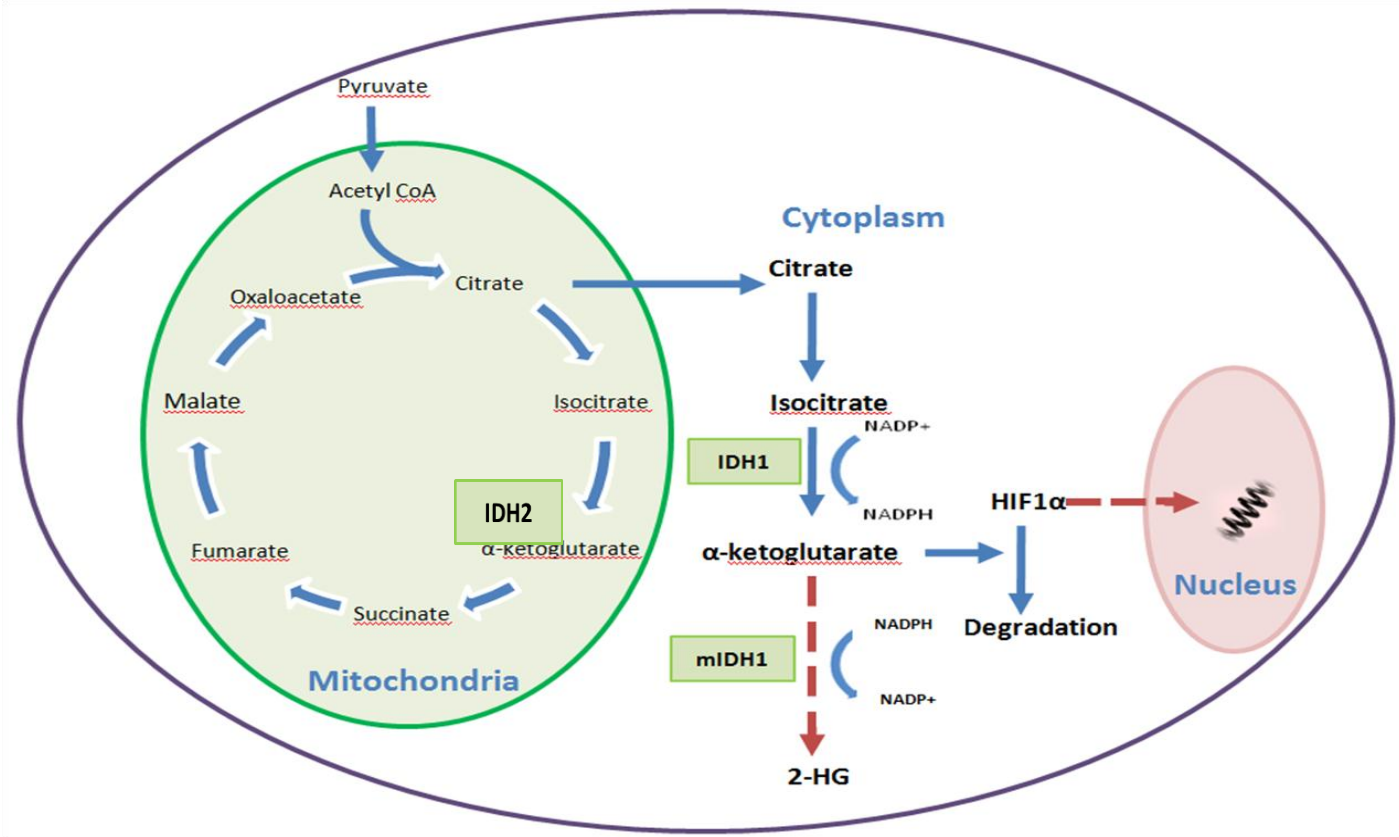

Figure 4.2. The cellular roles of IDH1 and IDH2. Isocitrate dehydrogenase (IDH) enzymes catalyse the conversion of isocitrate to α-ketoglutarate (α-KG) in the cytoplasm (IDH1) and mitochondria (IDH2). This results in the reduction of nicotinamide adenine dinucleotide phosphate (NADP+) and degradation of hypoxia-inducible factor 1α (HIF1α). Mutation of IDH1 results in a reduction of α-KG and the transcription of HIF1α genes, a depletion of NADPH and an accumulation of carcinogenic 2-hydroxyglutarate (2-HG).

4.4.4 Emergence of *IDH2* mutations

The isocitrate dehydrogenase family comprises 5 members. *IDH1* is the only one to be located in the cytoplasm, the other isoforms exert their catalytic properties in the mitochondria (Geisbrecht and Gould 1999). No mutational events have ever been described in the IDH3, IDH4 or IDH5 isoforms but mutations in *IDH2*, located on 15q26.1, have now been described in gliomas (Hartmann, Meyer et al. 2009; Sonoda, Kumabe et al. 2009; Yan, Parsons et al. 2009) and also myeloproliferative disorders (Tefferi, Lasho et al. 2010). In common with *IDH1* mutations, these involve an arginine residue in the substrate binding site, usually affecting codon 172 (Hughes, Groot et al. 2010; Tefferi, Lasho et al. 2010). To date, the role of *IDH2* mutations in CNS-PNET disease has not been investigated, which in light of these recent findings should now be considered.

4.4.5 The role of *IDH1/2* mutations as biological markers

IDH1 mutation in low grade oligoastroctytomas and oligodendrogliomas occurs at a higher frequency than in grade III tumours (79% and 79% vs 60% and 49% $p<0.05$) (Gravendeel, Kloosterhof et al. 2010) and have been confirmed on review of previous series (Hartmann, Meyer et al. 2009; Watanabe, Nobusawa et al. 2009). Unusually the presence of mutation is more characteristic of a lower grade tumour. The high frequency of mutation in these tumours and the development of a monoclonal antibody to detect R132H (Capper, Zentgraf et al. 2009) has led to the suggestion that this may be used in the diagnostic clinical setting (Paulus 2009). In particular an IDH1 antibody could be employed to aid diagnostic challenges which arise, as current techniques can fail to distinguish diffuse from pilocytic astrocytoma and differentiate simple reactive gliosis from diffuse astrocytoma invasion.

IDH1 mutation has also been associated with prognosis. Improved survival in gliomas is seen (Parsons, Jones et al. 2008; Sanson, Marie et al. 2009; Gravendeel, Kloosterhof et al. 2010) and is associated with increased survival by 1 year on average for patients

with GBM (Bleeker, Atai et al. 2010). In contrast, in myelodysplastic syndromes, mutation is associated with an increased rate of transformation to AML and poorer survival (Tefferi, Lasho et al. 2010; Thol, Weissinger et al. 2010).

Studies in CNS-PNET disease now need to be expanded to include a larger cohort before survival analyses have sufficient power to determine any difference in outcome.

4.4.6 Summary

The investigation of *IDH1* mutational status in CNS-PNET disease has identified *IDH1* mutations to be one of the most common mutational events in this disease and a novel mechanism involved in tumorigenesis in a subgroup of cases. For the first time, a molecular event has been shown to be associated with patient age. The identification of *IDH1* mutation in adults also supports the hypothesis that CNS-PNET disease is different in patients of varying ages. The consequences of this mutation may also be exploited to aid classification and provides new targets for novel therapeutic approaches.

Chapter 5

DNA methylation profiling of CNS-PNET

Table of contents

Chapter 5

5.1 Introduction

Epigenetic modifications involving alterations in DNA methylation patterns are a hallmark of most human cancers (Baylin and Herman 2000). In cancer development, genome-wide hypomethylation outside of CpG islands of tumour DNA compared to normal tissue DNA has been shown to predominate (Feinberg and Vogelstein 1983). Against this background, changes in DNA methylation may also potentially affect any of the estimated 45,000 CpG islands (section 1.2.6.3) present in the genome (Antequera and Bird 1993). Changes in methylation of CpG islands associated with the promoter region may result in aberrant transcriptional silencing of tumour suppressor genes or activation of oncogenes, or lead to genomic instability and facilitate tumour development and progression (Esteller 2006; Irizarry, Ladd-Acosta et al. 2009). As discussed in section 1.2.6.3, DNA methylation alterations of genes involved in critical regulatory processes including those responsible for cell-cycle regulation, tumour invasion, apoptosis, transcription, DNA repair, cell signalling and chromatin remodelling, have been implicated in tumour development.

Aberrant DNA hypermethylation has been estimated to occur in up to 1% of CpG islands in CNS-PNETs (Fruhwald, O'Dorisio et al. 2001). Current understanding of methylation patterns in this disease, including which CpG islands are affected and specifically which genes are epigenetically modified, however, is limited. The results from a series of small studies which have investigated a number of candidate genes (table 1.12) have demonstrated aberrant methylation in CNS-PNETs, and support the importance of alterations in DNA methylation being implicated in this disease (Chang, Pang et al. 2005; Muhlisch, Schwering et al. 2006; Inda and Castresana 2007; Muhlisch, Bajanowski et al. 2007). In addition, in chapter 3, methylation of the *RASSF1A* promoter was identified in 81% of primary CNS-PNETs. To date, aberrant methylation of the *RASSF1A* promoter is therefore one of the most frequent molecular events identified in this disease. Studies to describe and interpret the CNS-PNET DNA methylome in detail and potentially identify additional genes that are implicated in the epigenetic development of these tumours are now required.

5.1.1 DNA methylation assessment technologies

Significant progress has been made in the last decade in deciphering the DNA methylome with the development of a spectrum of new techniques and technological advancements (reviewed in (Laird 2010)). The methodologies used to determine DNA methylation can be broadly divided in two categories based on the process used to pre-treat the DNA: segregation and bisulphite conversion. Segregation techniques can be further subdivided into those which utilise methylation specific restriction enzymes or those that employ processes which enrich and separate out the methylated DNA fraction. Methylation patterns of individual CpG dinucleotides are typically determined using locus-specific or gel-based analyses. These techniques however can only be employed to determine the methylation status of a limited number of CpG dinucleotides. The development of array-based technologies and, more recently, next-generation sequencing has enabled the automated assessment of large numbers of CpG dinucleotides. Whilst each technique has merits and disadvantages, which can be exploited in different experimental contexts, the gold standard for determining DNA methylation remains methods which use bisulphite-based DNA sequencing (Clark, Statham et al. 2006). A summary of the spectrum of approaches that may be used in DNA methylation studies is given in Table 5.1.

Pretreatment	Analytical step			
	Locus-specific analysis	**Gel-based analysis**	**Array-based analysis**	**NGS-based analysis**
Enzyme digestion	*Hpall*-PCR	Southern blot RLGS MS-AP-PCR AIMS	DMH MCAM HELP MethylScope CHARM MMASS	Methyl-seq MCA-seq HELP-seq MSCC
Affinity enrichment	MeDIP-PCR		MeDIP mDIP mCIP MIRA	MeDIP-seq MIRA-seq
Sodium bisulphite	MethylLight EpiTYPER Pyrosequencing	Sanger BS MSP MS-SNuPE COBRA	BiMP GoldenGate Infinium	RRBS BC-seq BSPP WGSBS

Table 5.1. DNA methylation analyses. AIMS, amplification of inter-methylated sites; BC-seq, bisulphite conversion followed by capture and sequencing; BiMP, bisulphite methylation array profiling; BS, bisulphite sequencing; BSPP, bisulphite padlock probes; CHARM, comprehensive high-throughput arrays for relative methylation; COBRA, combined bisulphite restriction analysis; DMH, differential methylation hybridisation; HELP, *Hpall* tiny fragment enrichment by ligation PCR; MCA, methylation CpG island amplification; MCAM, MCA with microarray hybridisation; MeDIP, mDIP and mCIP, methylated DNA immunoprecipitation; MIRA, methylated CpG island recovery assay; MMASS, microarray-based methylation assessment of single samples; MS-AP-PCR, methylation-sensitive arbitrarily primed PCR; MSCC, methylation-sensitive cut counting; MSP, methylation specific PCR; MS-SNuPE, methylation-sensitive single nucleotide primer extension; NGS, next generation sequencing; RLGS, restriction landmark genome scanning; RRBS, reduced representation bisulphite sequencing; WGSBS, whole-genome shotgun bisulphite sequencing. Table taken from (Laird 2010).

5.1.1.1 DNA methylation analysis using segregation techniques

DNA methylation may be identified using segregation techniques that rely on either restriction endonucleases or methods which can select for “enrichment” of methylated loci.

5.1.1.1.1 Segregation by endonuclease digestion

Commonly employed restriction enzymes include the isoschizomers *HpaII* / *MspI* and *SmaI* / *XmaI. HpaII* and *MspI* recognise the nucleotide sequences CCGG, whilst CCCGGG is the target sequence for *SmaI* and *XmaI. HpaII* and *SmaI* cannot however cut when the internal cytosine in the recognition sequence is methylated and therefore in combination with their respective isoschizomers can be used to determine the relative frequency of methylation at a CpG site. The combination of both *HpaII* and *MspI* can be used to assess up to 98.5% of CpG islands in the human genome (Oda, Glass et al. 2009).

Originally, methylation-sensitive restriction enzymes were used to differentially digest methylated and unmethylated DNA which produced fragments of different sizes which could be visualised, following PCR amplification, using gel electrophoresis. Methods included methylation sensitive arbitrarily primed PCR (MS-AP-PCR), amplification of inter-methylated sites (AIMS), restriction landmark genomic scanning (RLGS) and Southern blots. These methods are labour intensive and false positive results may arise if there is inadequate digestion by the restriction enzyme which limits the use of these techniques (Kaput and Sneider 1979; Frigola, Ribas et al. 2002; Liang, Gonzalgo et al. 2002; Allegrucci 2007).

A number of array-based technologies which reduce labour costs also use endonclease digestion in determining methylation profiles, but still require relatively large quantities of high quality DNA (reviewed in (Laird 2010)). These technologies include: methylated CpG island amplification and array hybridisation (MCAM) in which the differential cutting properties of *SmaI* and *XmaI* are exploited; differential methylation

hybridisation (DMH) where the relative intensities of digested (using *MseI*) and undigested fluorescently labelled DNA at different loci on the array are measured; a modification of DMH, MethylScope, in which the methylation-dependent endonuclease *McrBC* is used to improve the sensitivity within methylated regions; comprehensive high-throughput arrays for relative methylation (CHARM) which again uses the same principle as DMH but, with the optimised workflow, permits a greater performance; microarray-based methylation assessment of single samples (MMASS) where a cocktail of restriction enzymes are used; and *HpaII* tiny fragment enrichment by ligation-mediated PCR (HELP), which uses a ligation-mediated PCR to amplify digested fragments prior to array hybridisation.

More recently, next generation sequencing (NGS) techniques that exploit endonuclease digestion have been developed. The main advantages of these methods are that they do not require an appropriately designed array, less DNA is needed and they permit allele-specific analysis. These techniques include Methyl-seq and MSCC (methylation-sensitive cut counting) which employ NGS following digestion with *HpaII* or *MspI* compared with randomly sheared products in the former and *HpaII* and *MmeI* digestion with adaptor ligation in the latter, and an adaption of the HELP assay in which the output is analysed by NGS (HELP-seq) (Berman, Weisenberger et al. 2009; Brunner, Johnson et al. 2009; Oda, Glass et al. 2009).

5.1.1.1.2 Segregation by enrichment

Methylated cytosines (5mC) and the proteins that specifically recognize and bind to these molecules may be identified using specific antibodies. This has permitted the development of immunoprecipitation-based methods for DNA methylation analysis which have been used to identify DNA methylation markers in cancer (Weber, Davies et al. 2005; Koga, Pelizzola et al. 2009). Hybridisation to an array following enrichment by immunoprecipitation forms the basis of a number of techniques (MeDIP, mCIP, mDIP and MIRA) which have enabled the methylation profiling on a larger scale (Rauch

and Pfeifer 2005; Weber, Davies et al. 2005; Keshet, Schlesinger et al. 2006; Zhang, Yazaki et al. 2006).

Finally, enrichment techniques have recently been combined with next generation sequencing, including MeDIP-seq and MIRA-seq. These novel techniques enable rapid genome-wide DNA methylation assessment to be made, but unlike the bisulphite based methods (section 5.1.1.2) cannot resolve the sequence structure at the individual CpG dinucleotide level (Down, Rakyan et al. 2008).

5.1.1.2 DNA methylation analysis using bisulphite treated DNA

In addition to the segregation methods outlined in section 5.1.1.1, DNA methylation analyses may also be undertaken using bisulphite treated DNA. As has been discussed in detail in section 2.12, sodium bisulphite treatment, first described by Frommer et al in 1992, causes the deamination of unmethylated cytosines whilst methylated cytosine residues are unaffected and therefore results in the production of differing sequences dependent on the methylation status (Frommer, McDonald et al. 1992). The change in sequence may then be identified using sequencing technologies, including Sanger sequencing as previously described (section 2.6).

Mass spectrometry of bisulphite converted DNA has been used in a technique known as EpiTYPER to determine methylation status at a given CpG dinucleotide. This technique utilises the different size and charge properties of methylated and unmethylated CpG DNA to determine the methylation status, and can be combined with an array format to assess the methylation status of a series of CpG dinucleotides within an amplicon (Coolen, Statham et al. 2007). The methylation status at a particular locus may also be ascertained using MethyLight or pyrosequencing. In the former process, differentially fluorescently labelled PCR probes are generated for unmethylated and methylated sequences for a given locus. A real-time PCR reaction is then performed and the quantity of methylation estimated by analysis of the fluorescent signal generated (Eads, Danenberg et al. 2000). In pyrosequencing in

contrast, four enzymes are used including Luciferase for the sequence structure to be identified using a bioluminescence real-time approach (Reviewed in (Ahmadian, Ehn et al. 2006)).

DNA methylation may be analysed using bisulphite converted DNA in gel-based systems. In methylation-specific PCR (MSP) primers to unmethylated or methylated sequences are designed and the methylation status at a locus determined with the presence of bands on gel electrophoresis. Gel electrophoreisis is also employed in combined bisulphite restriction analysis (COBRA) to distinguish methylation status based on product size following the application of a methylation sensitive restriction enzyme. The methylation status at a given CpG dinucleotide may also be determined by methylation-sensitive single nucleotide primer extension (MS-SNuPE). The MS-SNuPE technique uses internal primers which anneal immediately adjacent to the nucleotide to be analysed in an amplified PCR product and the methylation status is determined with the inclusion of differently labelled dNTPs (Gonzalgo and Jones 1997). Finally, Sanger sequencing, described in section 2.6, utilises a gel based method to determine the nucleotide sequence identity.

Array and next generation sequencing-based platforms have also been developed in sodium bisulphite pre-treated methylation detection strategies. These permit both higher throughput and automation of processing and therefore have the advantage of being more cost-effective when large numbers of samples and CpG sites require investigation. Methylation analysis of small genomes containing methylation dense regions maybe investigated by hybridisation to oligonucleotide arrays in bisulphite methylation profiling (BiMP) (Reinders, Delucinge Vivier et al. 2008). Discussed in section 2.13.1, Bibikova et al in 2006 reported the development of a high throughput DNA-methylation profiling technique using an Illumina bead array (Bibikova, Lin et al. 2006). In this study 1536 CpG dinucleotides were assessed in 371 selected cancer related genes, with each gene represented by 1-9 CpG sites. Subsequently a panel incorporating 807 known cancer causing genes, and including 1505 CpG sites was developed (Cancer Panel I, Illumina) to be used to investigate the methylation profiles of different cancers. Most recently this approach has been further modified with the

development of the Illumina Infinium platform, which can profile 27,578 CpG dinucleotides using less than 1 microgram of DNA including DNA extracted from FFPE material (Bibikova, Le et al. 2009; Thirlwell, Eymard et al. 2010).

Lately a number of techniques have also been developed which combine next generation sequencing with bisulphite treated DNA which enable detailed assessment of methylation status within a sample, known as “sequencing based methylation profiling” (Zhang and Jeltsch 2010). These technologies include reduced representation bisulphite sequencing (RRBS); bisulphite conversion followed by capture and sequencing (BC-seq); bisulphite padlock probes (BSPP); and whole genome shotgun bisulphite sequencing (WGSBS). Cost however currently limits the use of these technologies in screening the methylome in multiple samples (Laird 2010).

5.1.2 Illumina Goldengate methylation arrays in cancer

As has been described in section 5.1.1, methylation arrays permit the interrogation and elucidation of tumour epigenetic characteristics. In the construction of global methylation profiles new candidate genes may be discovered that could be utilised to predict therapeutic outcomes (Shen, Kondo et al. 2007) and patient survival in cancer (Rosenbaum, Hoque et al. 2005). Methylation arrays also facilitate a genetic study where adequate material may not be available for expression arrays. In particular the Illumina Goldengate methylation array may be employed using DNA extracted from FFPE tumour material. The Illumina Goldengate methylation array has been successfully used to investigate a series of adult cancers which have been reported in recent years. These have included; mesothelioma, glioma, AML, lymphoma, and gastric, renal cell, colorectal, ovarian, breast, hepatocellular, pancreatic and urothelial cancers (Aik Choon, Antonio et al. 2009; Hinoue, Weisenberger et al. 2009; McRonald, Morris et al. 2009; O'Riain, O'Shea et al. 2009; Alvarez, Suela et al. 2010; Christensen, Houseman et al. 2010; Christensen, Kelsey et al. 2010; Houshdaran, Hawley et al. 2010; Loh, Liem et al. 2010; Milani, Lundmark et al. 2010; Noushmehr, Weisenberger et al. 2010; Shin, Kim et al. 2010; Wolff, Chihara et al. 2010). Apart from investigation into

haematological malignancies including childhood ALL (Milani, Lundmark et al. 2010), to date there have been no publications that have specifically investigated paediatric malignancies.

5.1.3 Genetic profiling in paediatric embryonal brain tumours

In recent years, the establishment of array technology has provided critical insights into both the molecular development of paediatric brain tumours and how these tumours may be sub-classified. In 2002, Pomeroy et al reported the results of an expression array of CNS embryonal tumours (Pomeroy, Tamayo et al. 2002). This study included 60 children with medulloblastomas, 10 children with ATRTs, 10 young adults with malignant gliomas and 8 children with supratentorial PNETs. Overall the embryonal tumours were shown to comprise of a heterogeneous group, with the medulloblastomas clustering separately from the CNS-PNETs. A sub-analysis of the medulloblastoma cohort however identified correlations between the tumour expression profiles with clinical features including subtype and outcome. This study though was limited by the availability of suitable genetic material, and in particular high quality RNA extracted from frozen samples.

A series of studies in medulloblastoma have now been performed showing that between 4 and 6 molecular subtypes exist (Thompson, Fuller et al. 2006; Kool, Koster et al. 2008; Cho, Tsherniak et al. 2010; Northcott, Korshunov et al. 2010). In the study by Thompson et al in 2006, the gene profiles of 46 medulloblastomas were investigated and 5 subgroups identified. Two of these subgroups were associated with known genetic events in medulloblastoma development, namely Wnt pathway and sonic hedgehog (SHH) pathway disruption (Thompson, Fuller et al. 2006). Kool et al investigated the expression profiles of 62 primary medulloblastomas and combined this with genomic data in 52 cases. A subgroup containing tumours expressing genes associated with Wnt pathway disruption (“group A” or “Wnt group”) and a second group comprising those with SHH pathway disruption (“group B” or “SHH group”) were again identified. In addition 3 other groups were identified, which were associated

with metastatic disease and a poorer outcome. Expression and molecular features of neuronal differentiation were observed in “group C”, photoreceptor differentiation in “group E”, and a mixture of both neuronal and photoreceptor differentiation in the final group (“group D”).

Northcott et al combined the DNA copy number and expression data of 103 primary medulloblastomas and identified 4 distinct genetic subgroups (Northcott, Korshunov et al. 2010). The four groups again comprised both a Wnt and a SHH group in addition to 2 non-wnt and non-SHH groups referred to as “group C” “group D”, the former associated with high MYC levels, CSF dissemination and an inferior outcome. Finally, in the largest study to date investigating the expression profiles of medulloblastomas, Cho et al reported the expression profiles of 194 primary medulloblastomas and identified 6 subgroups (Cho, Tsherniak et al. 2010). In addition to a Wnt and SHH group, 2 groups of medulloblastomas incorporating genes associated with photoreceptor and GABAergic expression, and another 2 groups with tumours with neuronal and glutamategic expression were identified. Taken together, these studies have consistently identified subgroups associated with Wnt and SHH signalling. The number of non-wnt and non-SHH subgroups and their precise definition and characterisation has yet to be fully elucidated.

Currently unpublished work undertaken by Dr Ed Schwalbe at the Northern Institute for Cancer Research at Newcastle University has compared the expression profiles of primary medulloblastoma tumours with their methylomic profiles. These data, summarised in Figure 5.1, have shown that using methylation profiling a number of distinct subgroups can be determined, which correlate with the groups identified by expression profiling. In particular, a cluster of samples with aberrant Wnt pathway activation (Wnt group), a second cluster with aberrant sonic hedgehog signalling (SHH group), and a third cluster without Wnt or sonic hedgehog pathway activation (non-Wnt, non-SHH) can be identified as distinct entities, in addition to a few outlying samples that do cluster with any of three groups.

The relationship between molecular events and methylomic profiling has not previously been investigated in CNS-PNET disease and to date, no stratification or sub-classification based on clinical or molecular features has been identified in this disease. Methylomic profiling may, as has been demonstrated with medulloblastomas, facilitate the discovery of subgroups within this otherwise heterogenous group of tumours and provide both critical insights into the genetic development of these tumours and a rationale for the development of stratified and potentially targeted therapeutic approaches.

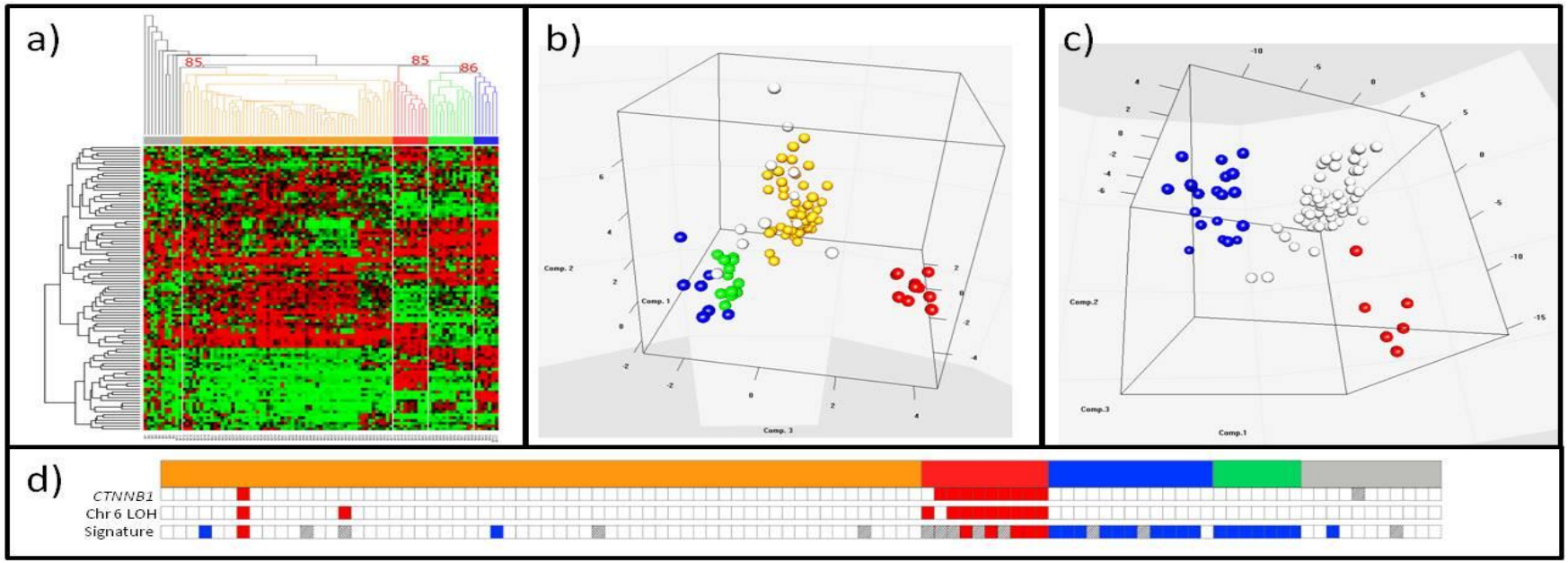

Figure 5.1. Identification of medulloblastoma subgroups using expression and methylomic analyses. (a) Bootstrapped cluster dendrogram of methylation patterns in 100 medulloblastoma samples. Numbers in red refer to bootstrap percentages of major dendrogram branches. Major subgroups are coloured (orange, red, green, blue), with outlying samples marked grey. Heatmap shows methylation scores, from green (hypomethylated) to red (fully-methylated). (b) Principal component analysis loadings plot of methylomic data confirming the four distinct subgroups identified in (a). (c) Principal component analysis loadings plot of WNT/SHH gene expression signature assay (Schwalbe, Lindsey et al. 2011): WNT signature expressing (red), SHH signature expressing (blue). (d) Molecular correlates and relation to methylomic subgroup assignment. Subgroups are coloured as in (a). Line 1: *CTNNB1* activating mutation, *CTNNB1* mutation (red); no mutation (white) (p=2.7 X 10^{-16}). Line 2: Chromosome 6 loss of heterozygosity (LOH), LOH detected (red); no LOH (white) (p=9.4 X 10^{-16}). Line 3: Signature - activation of WNT and SHH pathways by gene expression, WNT (red), SHH (blue) pathway activation; WNT/SHH independent (white) (p=2.1 X 10^{-26}). Grey hatching – DNA/ RNA unavailable. All p values derived using chi-squared tests. Adapted figures and data kindly supplied by Dr Ed Schwalbe, Northern Institute Cancer Research, UK.

5.1.4 Study Aims

To date understanding of the CNS-PNET DNA methylome is limited. A detailed description and understanding of the CNS-PNET methylome and its role in tumorigenesis is now required. This approach may afford the potential to develop a sub-classification within this heterogenous group of tumours, identify novel methylation events for further investigation and investigate the relationship with other highly malignant paediatric brain tumours including medulloblastomas and high-grade gliomas.

The specific aims of this study were:

1. To determine the global methylation patterns in CNS-PNET primary tumours in comparison with those observed within the normal brain.

2. To identify tumour-specific markers in CNS-PNET and to develop a model to enable the identification of CNS-PNET tumour from normal brain using methylation markers.

3. To correlate methylation events observed with known clinical, pathological and genetic features in CNS-PNET and discover possible sub-groups within this disease.

4. To compare and contrast the methylation profiles of CNS-PNET with other aggressive paediatric brain tumours and examine any molecular interrelationships that may exist between the different tumour groups.

5.2 Materials and methods

5.2.1 CNS-PNET primary tumour cohort

Thirty-nine primary CNS-PNET samples were available for inclusion in the methylation array study. The clinical characteristics of these samples have been previously given in Table 2.1. DNA was extracted from the tumour samples and processed using the Illumina Goldengate Methylation array, using methods previously described (Section 2.3.1 and section 2.13.1).

5.2.2 Control brain cohort

The methylation profiles of normal control brain samples were established from two sources. DNA was extracted from normal brain samples from the Northern Institute for Cancer Research (Table 2.3) and processed using the Illumina Goldengate methylation array, as has been previously described (Section 2.3.1 and section 2.13.1). The methylation results from a published series of normal cerebellar and cerebral samples was also included (Ladd-Acosta, Pevsner et al. 2007). Additional clinical information shown in Table 5.2 pertaining to this published series was kindly made available by Dr Potash (Research Director, Mood Disorders Center Meyer, Baltimore, USA) in a personal communication. In total 43% of the samples (16/37) were derived from the cerebrum and 57% (21/37) from the cerebellum. Samples were obtained from a wide range of cases of different ages incorporating both infant cases under the age of 3 years (9/37, 27%), and adult cases (27/37, 73%). The age of the patient was not available for one of the samples (3%). The clinical features of the normal brain cohort are summarised in Table 5.3.

Array ID	Site	Age (years)	Sex	Source
cbll1	cerebellum	25	female	Ladd-Acosta
cbm1	cerebrum	25	female	Ladd-Acosta
cbll2	cerebellum	24	male	Ladd-Acosta
cbm2	cerebrum	24	male	Ladd-Acosta
cbll3	cerebellum	28	male	Ladd-Acosta
cbm3	cerebrum	28	male	Ladd-Acosta
cbll4	cerebellum	2	female	Ladd-Acosta
cbm4	cerebrum	2	female	Ladd-Acosta
cbll5	cerebellum	21	male	Ladd-Acosta
cbm5	cerebrum	21	male	Ladd-Acosta
cbm6	cerebrum	26	male	Ladd-Acosta
cbll6	cerebellum	26	male	Ladd-Acosta
cbm7	cerebrum	21	male	Ladd-Acosta
cbll7	cerebellum	21	male	Ladd-Acosta
cbm8	cerebrum	19	male	Ladd-Acosta
cbll8	cerebellum	19	male	Ladd-Acosta
cbm9	cerebrum	30	male	Ladd-Acosta
cbll9	cerebellum	30	male	Ladd-Acosta
cbm10	cerebrum	30	-	Ladd-Acosta
cbll10	cerebellum	30	-	Ladd-Acosta
cbm11	cerebrum	22	male	Ladd-Acosta
cbll11	cerebellum	22	male	Ladd-Acosta
cbm12	cerebrum	2	female	Ladd-Acosta
cbll12	cerebellum	2	female	Ladd-Acosta
cbm13	cerebrum	20	male	Ladd-Acosta
cbll13	cerebellum	20	male	Ladd-Acosta
cbm14	cerebrum	42	male	Ladd-Acosta
cbm15	cerebrum	72	male	Ladd-Acosta
cbm16	cerebrum	67	male	Ladd-Acosta
cbll17	cerebellum	prenatal*	male	Newcastle
cbll18	cerebellum	prenatal*	male	Newcastle
cbll19	cerebellum	-	-	Newcastle
cbll20	cerebellum	67	male	Newcastle
cbll21	cerebellum	newborn	female	Newcastle
cbll22	cerebellum	60	male	Newcastle
cbll23	cerebellum	prenatal*	female	Newcastle
cbll24	cerebellum	prenatal*	male	Newcastle

Table 5.2. Normal brain control samples used in methylation array. Newcastle samples were derived from the Northern Institute for Cancer Research archive. The Ladd-Acosta samples describe those used in their published series (Ladd-Acosta, Pevsner et al. 2007). Clinical details for the Ladd-Acosta samples were kindly provided by Dr Potash (personal communication). * prenatal samples from foetuses at 18-22 weeks gestation.

Criteria	Category	n (%)
Site	Cerebrum	16 (43%)
	Cerebellum	21 (57%)
Age	<3 years	9 (24%)
	3-18 years	0 (0%)
	>18 years	27 (73%)
	Unknown	1 (3%)
Sex	Male	26 (70%)
	Female	8 (22%)
	Unknown	3 (8%)

Table 5.3. Methylation array normal brain control samples clinical characteristics summary.

5.2.3 Malignant brain tumour comparator cohorts

5.2.3.1 Pineoblastoma

Four pineoblastomas confirmed on central pathological review using the current WHO classification system (Louis, Ohgaki et al. 2007) were included in the study. DNA was extracted from the cases, as has been previously described (Section 2.3.1). The clinical features of the four pineoblastoma cases used in the study are given in Table 5.4.

Array ID	Sex	Age (months)	Metastasis (Chang stage)	Follow-up (months)	Status
PB1	F	300	M3	Unknown	Unknown
PB4	F	45	Unknown	35	DOD
SP2	F	73	M0	124	ADF
SP114	F	13	M3	10	DOD

Table 5.4. Clinical characteristics of methylation array pineoblastoma cohort. DOD, died of disease; ADF, alive and disease free.

5.2.3.2 Medulloblastoma

The methylation profiles of 100 medulloblastomas processed concurrently with the CNS-PNET study using the Illumina GoldenGate platform, confirmed on central histopathological review according to the current WHO classification by Prof David Ellison (St Judes Research hospital, Memphis, Tennessee, USA), was kindly made available for use in this study by Dr Ed Schwalbe from the Northern Institute for Cancer Research, Newcastle University, UK. A summary of the pathological subgroup and clinical features of these tumour samples is given in Table 5.5.

Medulloblastoma characteristic	Category	No
Classification subgroup	Classic Nodular desmoplastic Large cell / anaplastic MBEN	72 17 10 1
Sex	Male Female	63 37
Age (years)	<3 3-16 >16	15 78 7
Metastasis (Chang score)	M0 M0/1 M1 M2 M3 M4 Unknown	47 8 7 8 12 0 18
Status	Alive, disease free Alive, with disease Died of disease Died of other cause Unknown	60 5 30 2 3
Molecular features*	Wnt/ Wingless SHH Non-Wnt/ Wingless & Non-SHH Unknown	10 20 59 11

Table 5.5. Clinical and molecular characteristics of the medulloblastoma primary tumour cohort. 100 primary medulloblastoma tumour samples in the cohort. MBEN, medulloblastoma with extended nodularity; SHH, sonic hedgheohog pathway; *data kindly supplied by Dr Ed Schwalbe, Northern Institute for Cancer Research at Newcastle University.

5.2.3.3 High grade glioma

The methylation profiles, processed using the Illumina GoldenGate platform, of 29 high grade gliomas (HGG), confirmed on pathological review, were very kindly made available for use in this study by Dr Martyna Adamowicz and Professor Richard Grundy from the Children's Brain Tumour Research Centre (CBTRC), University of Nottingham, UK. Further clinical details for these samples are not available.

5.2.4 Array sample preparation

Control and tumour samples to be investigated using the Illumina GoldenGate Methylation array platform were prepared and processed as has been previously described in section 2.13.2.

5.2.5 Quality control assessment

The data produced by the Wellcome Trust Centre for Human Genetics (Oxford, UK) from processing the Illumina GoldenGate microarrays were subjected to a quality control assessment. Firstly, the data was analysed in the BeadStudio Methylation Module (version 3.0 (Illumina)) as has been described in section 2.13.3.1. The data was also subjected to a further quality control assessment using the BeadArray Subversion of Harshlight (BASH) programme within the BeadArray package, as has been described in section 2.13.3.2. The methylation data from samples that successfully passed both quality control assessments were used in subsequent analyses.

5.2.6 Methylation array platform validation

The methylation values obtained using the Illumina methylation array platform were validated by comparing the methylation scores obtained for 18 tumour samples on the

array at a number of differentially methylated loci with the methylation status identified by direct bisulphite sequencing. A panel of loci of seven genes were analysed comprising *ASCL2, CCKAR, COL1A2, HFE, MSH2, NOS2A* and *SPDEF.* PCR primers to amplify regions containing the relevant methylation array probe loci were designed using methods previously described (section 2.12.3) and are given in Table 5.6. Standard PCR reactions were performed as described in section 2.4.3, and the resultant PCR product purified and sequenced using Sanger sequencing (see sections 2.4.5 and 2.6). Anonymised traces for each sample were scored using direct visual inspection and the percentage methylation ranging from 0% (unmethylated) to 100% (fully methylated) at each CpG locus under investigation estimated. The validation study was performed with Dr Janet Lindsey at the Northern Institute for Cancer Research at Newcastle University.

Gene	Array probe ID	Forward primer (5'-3')	Reverse primer (5'-3')
HFE	HFE_E273_R	GGTAATAGTTGTAGGGTGATTTTTG	CAAATCCTCCAAAATTAACAAACTC
ASCL2	ASCL2_P360_F	GGGAATTTGAATTTTTTATTT	AAACTAAATTCCTACTAAACCCC
NOS2A	NOS2A_E117_R	AAAAATAATTTTTTGGATGGTATGG	TTACAACTAACTACACTACCTCCCC
CCKAR	CCKAR_P270_F	ATTGTTTTTTTATAAGGAGGTAGAATATA	CTAAATACAAACAACCTAACTACCC
SPDEF	SPDEF_P6_R	TTGTTTGTGGTTTGAGGTAAGTAAG	CCCTCAAAAAATAACCCTCTAAAAT
MSH2	MSH2_P1008_F	GGTAGAAGATTTTTTGGGTTTAAA	CACCATCCTAAACAACATAATAAAAC
COL1A2	COL1A2_E299_F	AGGTATTTTAGGGTTAGGGAAATTTT	ATTACTACAAACAACAACAAAATCC

Table 5.6. PCR primers used in the array validation study.

5.2.7 Methylation status classification ascertainment

β-values provided by the Illumina GoldenGate microarray were used to determine the methylation status of a sample for a probe at a given locus. The reported β-values ranged from 0 (fully unmethylated) to 1 (fully methylated). β-values greater than 0.67 were classified as being methylated, less than 0.34 as unmethylated and between these values (0.34-0.67) as showing partial methylation at a given locus. Differentially methylated probes were categorised as those in which the methylation scores across the cohort varied in a range of more than 0.34 (Δβ>0.34).

5.2.8 Comparison of the methylation profiles of the normal brain and CNS-PNET

5.2.8.1 Methylation profile ascertainment in the normal brain

The methylation profile of the normal brain was established using methylation scores derived from the Illumina Goldengate methylation platform (see section 2.13) in the normal brain cohort (section 5.2.2). The data were processed using unsupervised techniques (section 2.13.4) to establish any patterns of methylation within this cohort.

5.2.8.2 Methylation profile ascertainment in CNS-PNET

The methylation profile of the CNS-PNET cohort was established using methylation scores derived from the Illumina Goldengate methylation platform (see section 2.13) in the CNS-PNET cohort (section 5.2.1). The data was processed using unsupervised techniques (section 2.13.4) to establish any patterns of methylation within this cohort.

5.2.8.3 Methylation profile comparison

Comparison of the methylation profiles of the 37 cerebellar and cerebral normal brain samples (section 5.2.2) was made with the 31 CNS-PNET cohort (section 5.2.1) using unsupervised approaches previously described (section 2.13.4). Comparison of the methylation status in different sample groups of probes situated within and outside of CpG islands was made using the probe location data supplied by Illumina (data not shown).

5.2.9 Assessment of aberrant methylation in CNS-PNET

5.2.9.1 Identification of aberrantly methylated genes in CNS-PNET

To identify aberrant methylation in CNS-PNET, the methylation profile of the control cohort was firstly analysed and the probes found in all samples to be consistently either methylated ($\beta>0.67$) or hypomethylated ($\beta<0.34$) recorded. Probes that were found to be consistently methylated or hypomethylated in all samples were designated as "invariant". The methylation values of the invariant probes were then investigated in the CNS-PNET cohort. A probe was shown to exhibit an aberrant methylation profile if the average β value of the CNS-PNET cohort differed significantly from that observed in the normal brain. Assessment of significant difference was made using the Mann-Whitney test, and a multi-test Benjamini-Hochberg false discovery rate correction applied.

The most significant aberrantly methylated probes in CNS-PNET were determined by requiring the difference in the average β-values between the tumour and normal brain cohorts to be greater than the reported limit of detection on the Illumina Goldengate Methylation array platform ($\Delta\beta>0.17$) (Bibikova, Lin et al. 2006), as has been previously used in published reports by separate groups (Archer, Mas et al. 2010).

5.2.9.2 Ontological analysis of aberrantly methylated genes in CNS-PNET

To determine whether CNS-PNET development is associated with the involvement of particular functional pathways, processes or cellular mechanisms, an ontological analysis was performed. The functional classification tool (FCT) within the web-based database for annotation, visualisation and integrated discovery (DAVID) ontological analysis tool, was used (http://david.abcc.ncifcrf.gov/gene2gene.jsp). The DAVID FCT uses an algorithm which classifies highly related genes into functionally related groups. Each gene may be represented in a number of different biological pathways or processes and is compared with the DAVID FCT tool to reduce the list of genes to be investigated into organised classes of related genes or biology (Reviewed in (Huang, Sherman et al. 2009b; Huang, Sherman et al. 2009)). A list of most differentially methylated genes in CNS-PNET was generated, as has been previously described (section 5.2.9.1), and compared using the DAVID FCT with the list of 807 genes represented on the methylation array as a background panel.

5.2.9.3 Investigating associations between aberrant methylation in CNS-PNET and clinical features

A young age at diagnosis (<3 years) and the presence of metastatic disease are the only two clinical variables known to influence survival in CNS-PNET. To determine whether aberrant methylation of specific genes is associated with either of these 2 clinical features the most aberrantly methylated genes in CNS-PNET (see section 5.2.9.1) were investigated. A Mann-Whitney test was performed and the Benjamini-Hochberg correction applied to ascertain any significant differences in the methylation of the aberrantly methylated genes in those patients diagnosed before or after 3 years of age, and in those with (M1-M4) and without (M0 or M0/1) metastatic disease at diagnosis. Analyses were performed using the "R" statistical computer package, as has been previously described (section 2.13.4).

5.2.9.4 Investigating associations between aberrant methylation in CNS-PNET and survival

To determine whether any aberrantly methylated genes are associated with survival outcomes, the list of most aberrantly methylated genes (see section 5.2.9.1), were analysed for associations with outcome using the 'R' statistical package (see section 2.13.4). Univariate analysis was performed and the most significant genes ($p<0.05$) from this analysis were entered into a multivariate Cox-model analysis to determine whether any of these probes were independently prognostically significant.

5.2.10 Comparison of the methylation profiles of CNS-PNET with other malignant brain tumours

The methylation profile of CNS-PNETs was compared with that observed in other malignant brain tumours using unsupervised approaches previously described (section 2.13.4). Comparison of the methylation profiles of the 37 normal brain samples (section 5.2.2) and the 31 CNS-PNETs (section 5.2.1) was made with 4 pineoblastomas (section 5.2.3.1), 100 medulloblastomas (section 5.2.3.2) and 29 high-grade gliomas (section 5.2.3.3). Comparisons were made in triplicate utilising firstly the methylation scores of all 1505 probes on the array, secondly using only differentially methylated probes (see section 5.2.7), and thirdly using the methylation scores arising from 1421 probes targeting genes not located on the X-chromosome.

5.3 Results

5.3.1 Array quality control

Thirty-nine primary CNS-PNET cases that had undergone central pathological review were included in the CNS-PNET cohort. As outlined in Figure 5.2, tumour material was available in 34 of these to be included on the methylation array. The data obtained from the methylation array was subjected to a quality control assessment. Beadstudio quality control assessment found that SP42, SP49 and SP55 were quality control failures (Figure 5.3). In all 3 cases, abnormal signals were detected in the negative control analysis and significant levels of contamination were observed in the analysis of both SP42 and SP49. Bisulphite conversion was found to be borderline in SP42, and SP55 failed this quality control requirement. In addition SP55 failed tests on both the first and secondary hybridisation steps, and SP49 failed the quality control analysis on the secondary hybridisation and allele-specific extension steps. The quality control process findings were confirmed using a second technique. On BASH assessment SP42, SP49 and SP55 failed the analysis (Figure 5.4), and these 3 samples were subsequently removed from the analysis. The clinical features of the final cohort of 31 primary CNS-PNET tumour samples that passed the quality control assessment and were used in the subsequent methylation analyses are given in Table 5.7. DNA had been extracted from frozen material in 20 of these cases (20/31, 65%), and formalin fixed paraffin embedded (FFPE) material in 11 cases (11/31, 35%). In the three cases that failed the quality control analysis, DNA had been extracted from frozen material in one (SP55) and from FFPE in 2 cases (SP42 and SP49).

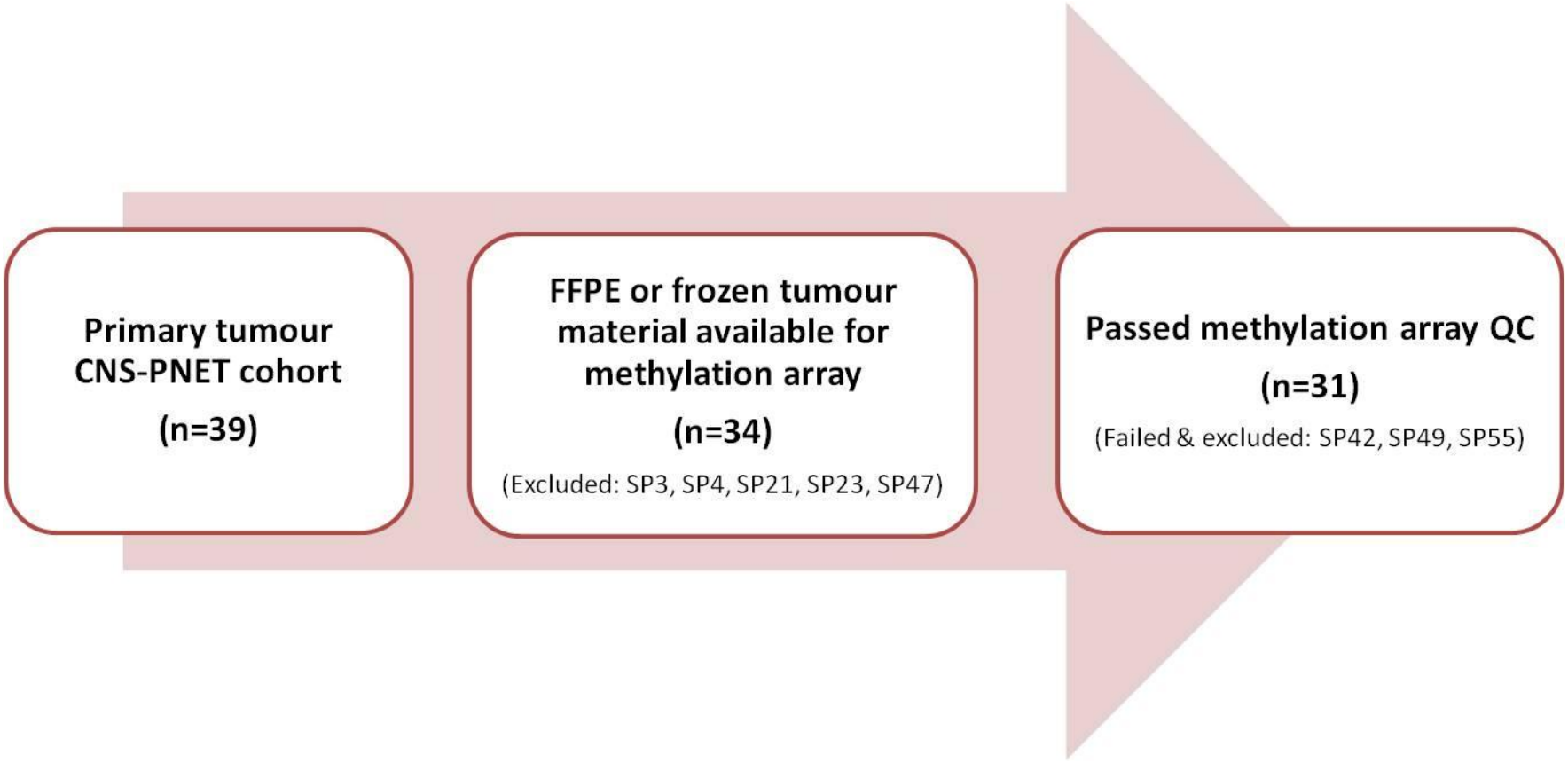

Figure 5.2. CNS-PNET cohort ascertainment. FFPE, Formalin fixed paraffin embedded material; QC, Quality control.

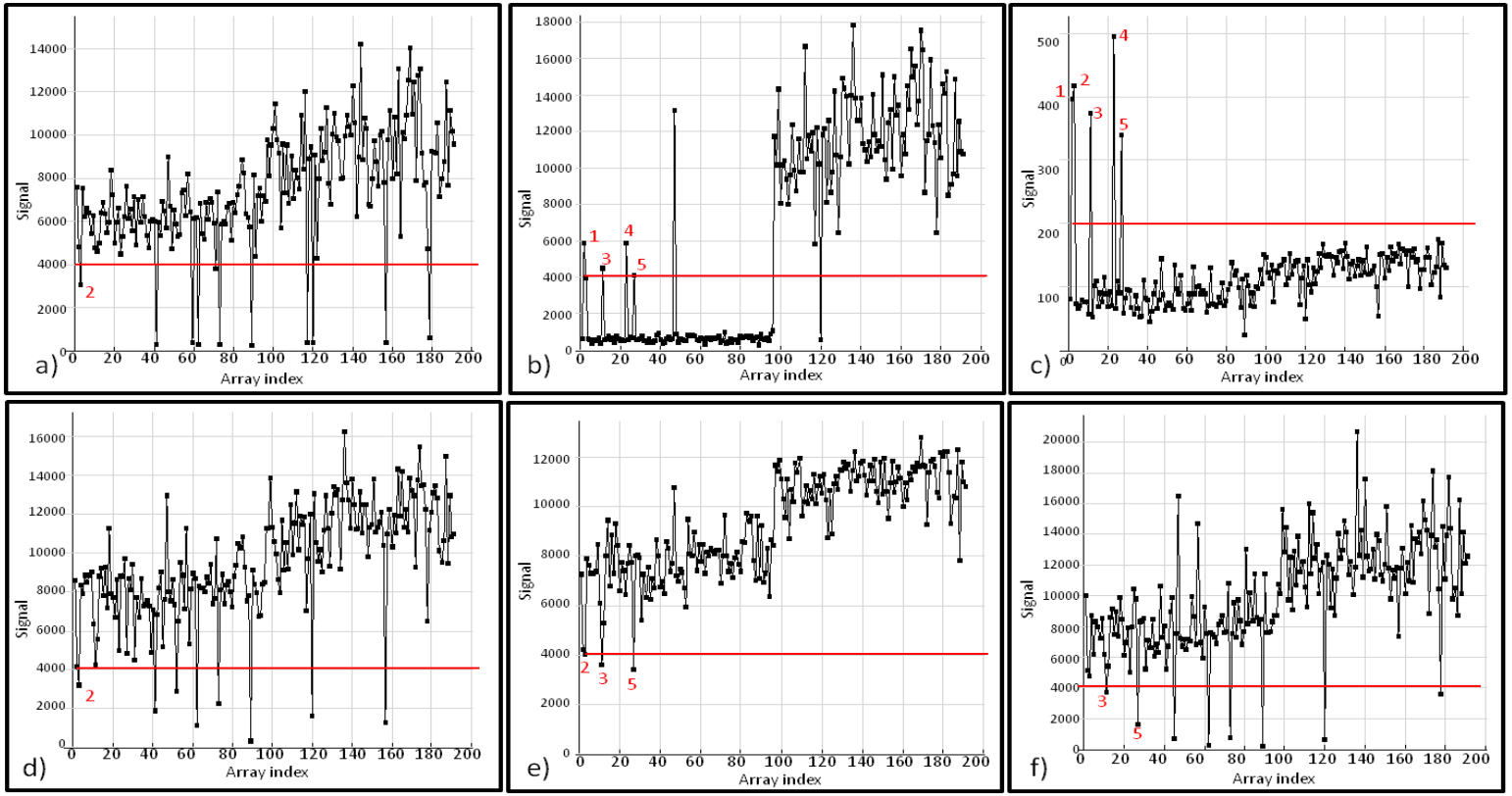

Figure 5.3 Beadstudio quality control analysis. Data shown includes the combined results of two methylation array plates (Array index 1-96 (plate 1), 97-192 (plate 2)). CNS-PNET cohort: array index cases 1-36 (excluding 11 and 22). Red line indicates cut-off for quality control (QC) pass. Red numbers indicate samples failing the QC analysis for the different QC parameters (1) SP42 (CNS-PNET), (2) SP55 (CNS-PNET), (3) index case 11 (medulloblastoma), (4) index case 22 (medulloblastoma) (5) SP49 (CNS-PNET): a) First hybridisation; b) Contamination (note failures are below red line for 2nd plate); c) Negative control; d) Bisulphite conversion; e) Second hybridisation; f) Allele specific extension.

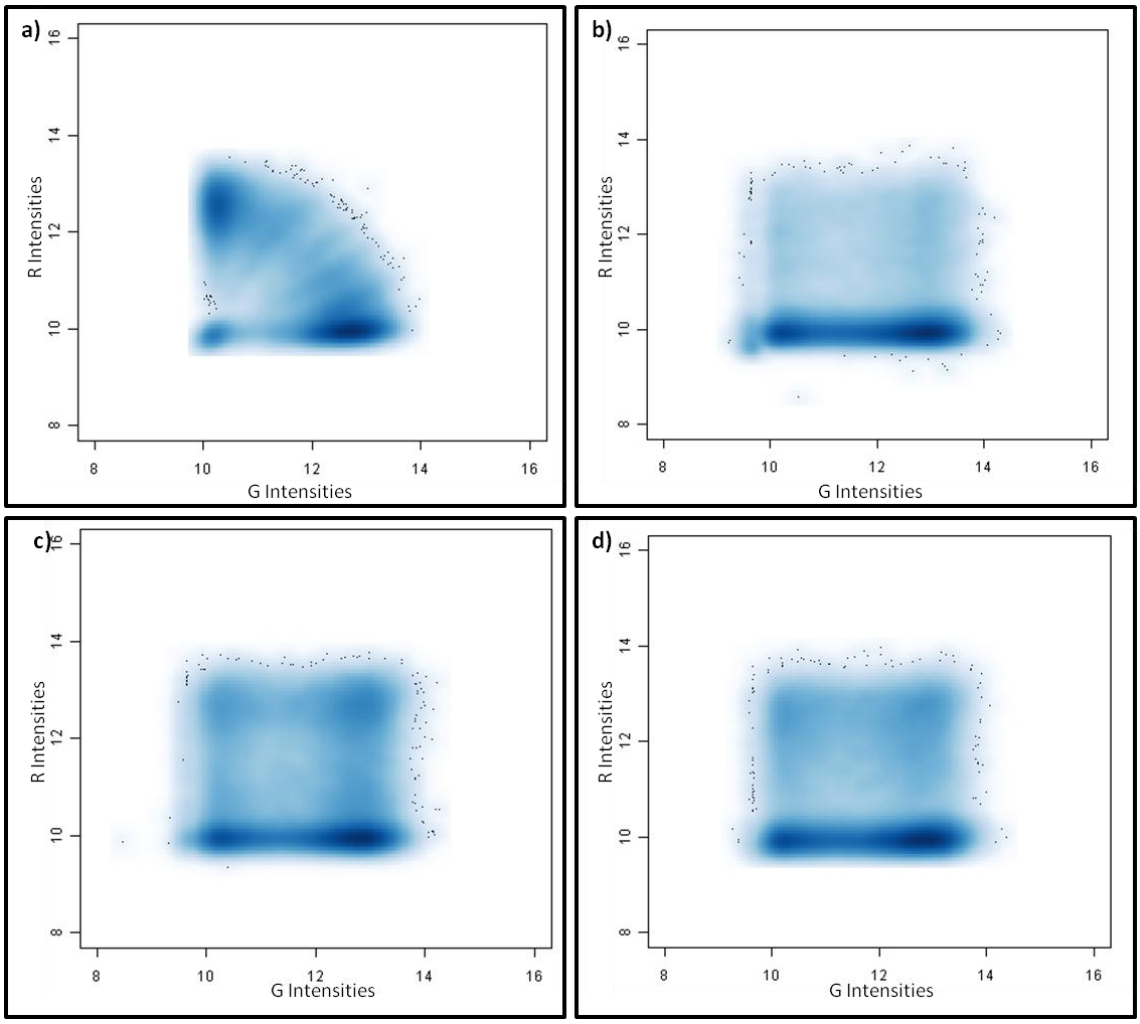

Figure 5.4. BASH analysis plots. Methylated (R, red) and unmethylated (G, Green) intensities across all 1505 CpG probes for individual tumour samples are shown. a) A normal plot passing the quality control process showing a bimodal distribution (consistent with most loci being either methylated or unmethylated with partial methylation at only a few loci. Three samples were excluded from the study as the red (methylated) channel failed to detect signals in b) SP42, c) SP55 and d) SP49.

Clinical characteristic		Number (Frequency %)	
Sex	Male	15	(48%)
	Female	16	(52%)
Age at diagnosis	Infant (<3 years)	8	(26%)
	Child (3-16 years)	18	(58%)
	Adult (>16 years)	4	(13%)
	Unknown	1	(3%)
Metastasis (Chang score)	M0/1	21	(68%)
	M1	1	(3%)
	M2	4	(13%)
	M3	1	(3%)
	M4	1	(3%)
	Unknown	3	(10%)
Survival	Alive	9	(29%)
	Died	19	(61%)
	Unknown	3	(10%)

Table 5.7. Clinical characteristics of the quality control approved CNS-PNET methylation array cohort. In total 31 CNS-PNET primary tumour samples passed the methylation array quality control requirements and the methylation data from these tumours were used in the subsequent studies.

5.3.2 Validation for methylation array results

The methylation values obtained on the Illumina Goldengate methylation array were validated by direct bisulphite sequencing, using a panel of 18 tumour samples to assess 7 differentially methylated loci which were present on the array. The direct bisulphite sequencing traces were inspected, and a numerical score between 0 (fully unmethylated) and 1 (fully methylated) recorded by measuring the peak heights of the methylated (a) and unmethylated (b) traces at each locus and calculating the proportion of methylation present (a/a+b). The results, shown in Figure 5.5, revealed a high concordance between the two approaches. The mean difference was 0.006, and standard deviation of 0.167. In only 10/126 (7.9%) of cases did a difference greater than 2 standard deviations (>0.34) between the methylation array and direct bisulphite sequencing occur.

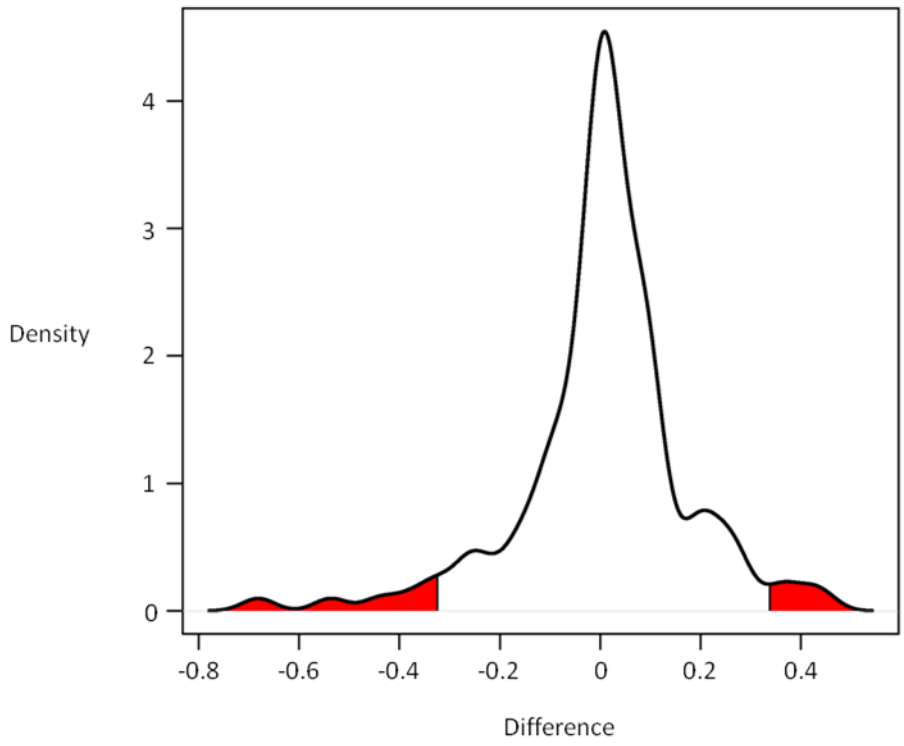

Figure 5.5. Validation of methylation array β values. For 18 tumour samples at 7 differentially methylated loci (*ASCL2, CCKAR, COL1A2, HFE, MSH2, NOS2A, SPDEF*), the methylation status of the interrogated CpG dinucleotide reported from the methylation array was compared against estimates from bisulfite sequencing. The distribution of differences between array and bisulfite values across all 7 loci, for all 18 samples, is summarised in the density plot. The mean difference was 0.006, and standard deviation was 0.167. Samples lying more than 2 standard deviations from the mean (10/126, 7.9%) are shaded red.

5.3.3 Methylation patterns in the normal brain

The methylation pattern across 1505 probes associated with 807 genes implicated in cancer development using the Illumina Goldengate cancer panel I was assessed in 37 control normal brain samples. 28.1% of the genes are represented by 1 probe, 57.3% by 2 probes and 14.1% of the genes have 3 or more probes on the array. The mean methylation for each probe across the control cohort was calculated and 64.2% (966/1505) of probes were hypomethylated, 28% (422/1505) were fully methylated and 7.8% (117/1505) were partially methylated. Overall, the methylation values in the normal brain control group cohort exhibited a bimodal distribution, as shown in Figure 5.6. The normal brain samples were shown to exhibit variable methylation (β range > 0.34) with 28% (421/1505) of the probes on the array, but the majority (72%, 1084/1505) of probes were therefore invariantly methylated (β range < 0.34).

The normal brain cohort comprised a diverse range samples from the cerebellum and cerebrum, including samples from across the age spectrum (prenatal, paediatric and adult) as well as from both male and female patients. Unsupervised hierarchical clustering of the normal brain cohort (Figure 5.6c) showed two main branches associated with the site of origin of the sample ($p= 0.0005$, Fisher's exact test). Clustering was not found to be statistically significantly associated with age at biopsy ($p=0.47$, Fisher's exact test).

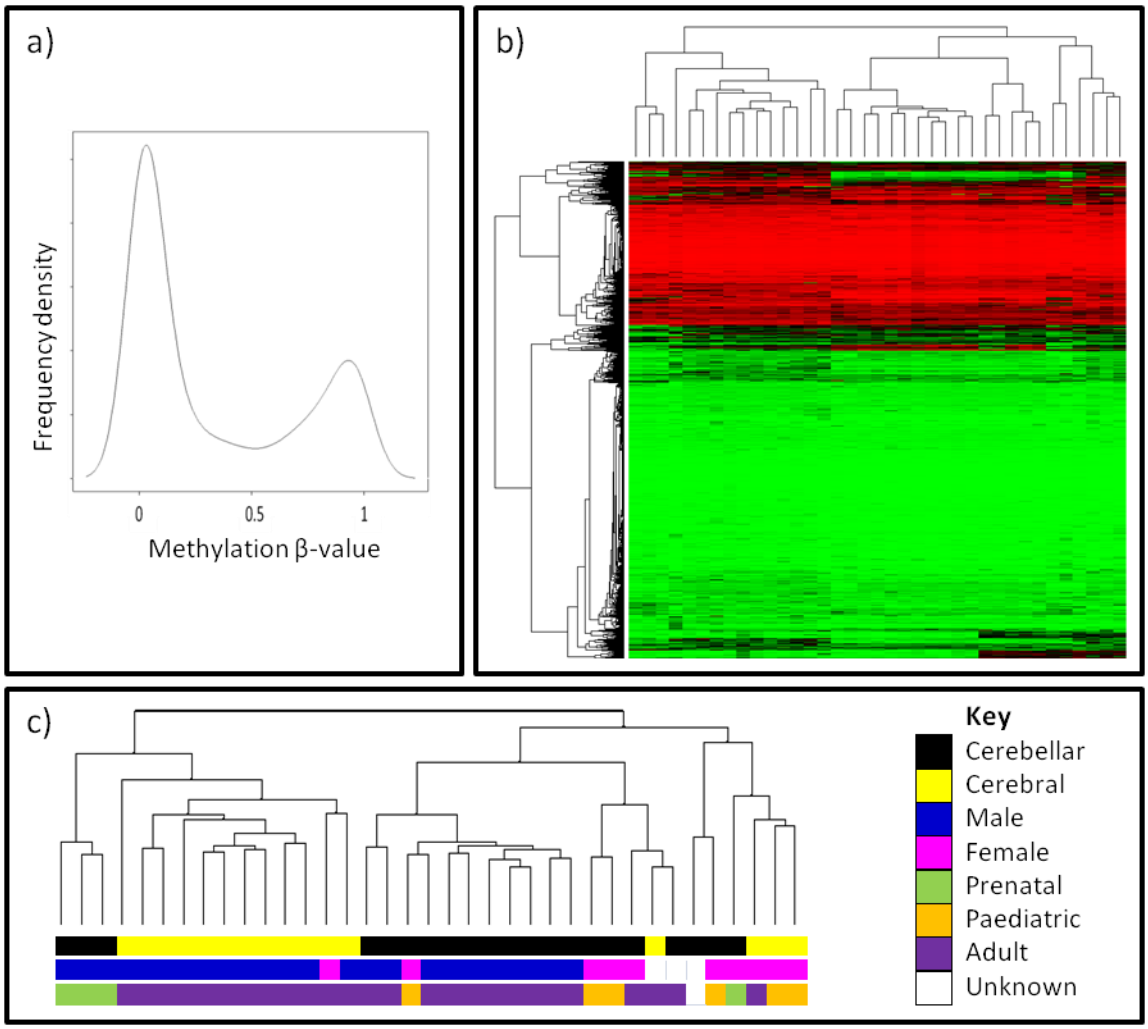

Figure 5.6. Methylation patterns in the normal brain. Assessment of the methylation patterns using 1505 probes on the methylation array of 37 normal brain samples. (a) Density plot showing the bimodal distribution of average methylation β-values in the normal brain. (b) Unsupervised hierarchical clustering heatmap. Green, hypomethylated; black, partially methylated and red, fully methylated. (c) clinical characteristics of the normal brain samples. Top bar, sample site; middle bar, sex; bottom bar, age at biopsy.

5.3.4 Methylation patterns in CNS-PNET

The methylation patterns of 31 CNS-PNET primary tumour samples were next investigated using the Illumina Goldengate Cancer panel I. The methylation or β-values at each locus for the 1505 probes on the array are graphically represented in Figure 5.7. The experiment was repeated using only the 1065 probes that exhibited variable methylation (β range > 0.34) in CNS-PNET and also repeated excluding those probes on the X chromosome, with similar results obtained (data not shown).

Four of the CNS-PNET samples were shown to be outliers (SP54, SP126, SP40 and SP24) and did not cluster with other CNS-PNETs. In contrast to the normal brain (Figure 5.6) the unsupervised hierarchical clustering of the remaining samples did not yield discrete clusters or sub-groups from which associations with clinical characteristics could be determined, but demonstrated methylation heterogeneity within the CNS-PNET cohort.

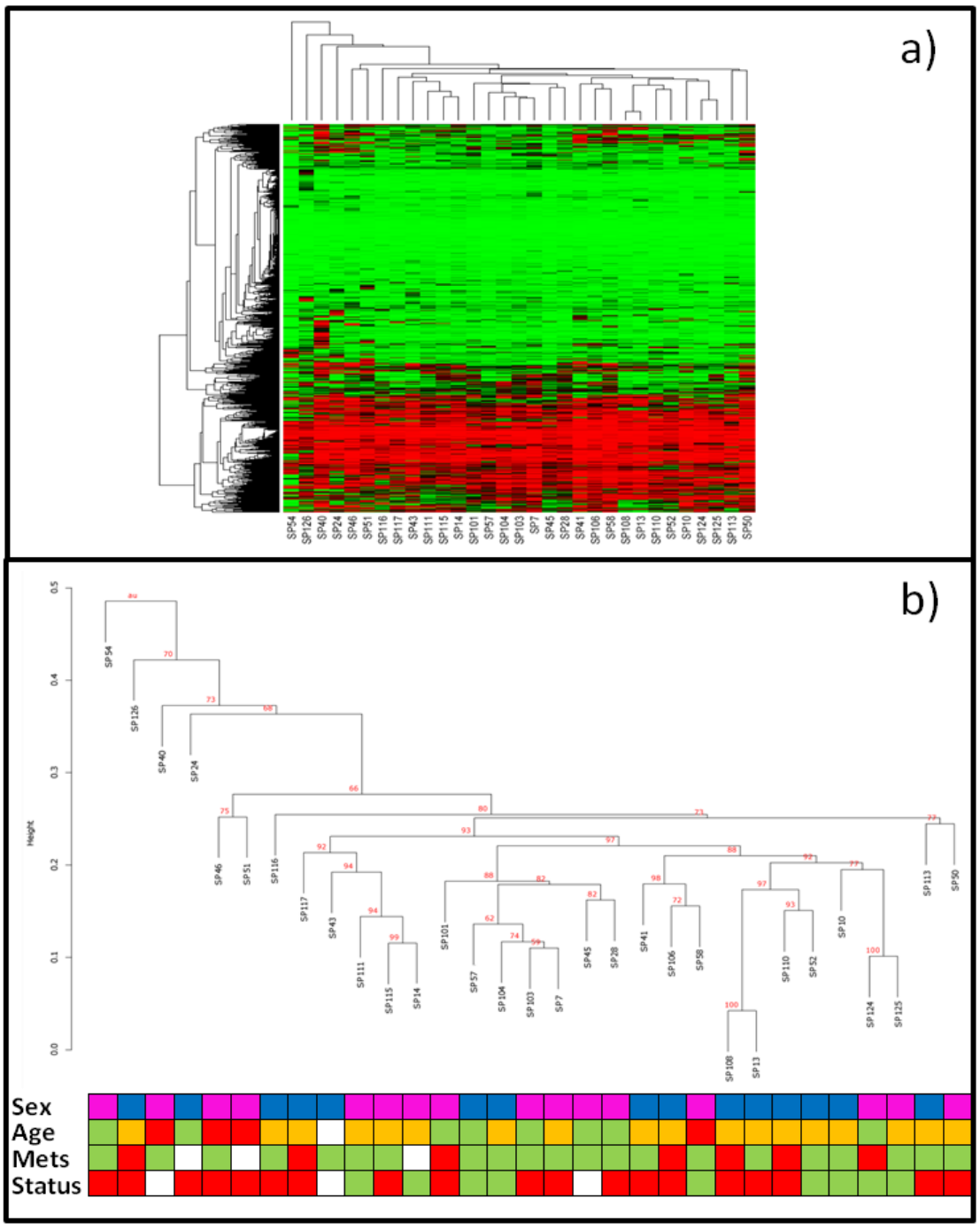

Figure 5.7. Methylation profile of 31 CNS-PNET primary tumour samples using the Illumina Goldengate methylation array. (a) Heatmap showing the methylation profiles of the CNS-PNET cohort across 1505 probes. Fully methylated (red), partially methylated (black) and unmethylated (green). (b) Unsupervised hierarchal clustering dendrogram of the bootstrapped methylation profiles of 31 CNS-PNETs. Numbers in red indicate the percentage frequency at which individual branches occur. CNS-PNET clinical characteristics. Sex: male (blue), female (pink); Age at diagnosis: Infant (green), child (amber), adult (red); metastatic disease: present (red), absent (green); status: died of disease (red), alive (green). No result available (blank).

5.3.5 Comparison of CNS-PNET methylation patterns with normal brain

Comparison was next made between the CNS-PNET samples and the methylation profile of the normal brain. In total, 1044 of the 1505 probes (69%) on the Cancer I panel used with the methylation array were located within CpG islands, defined according to the criteria described by Takai and Jones (Takai and Jones 2002). An additional 461 probes (31%) hybridised to CpG dinucleotides outside of CpG islands. As shown in Figure 5.8, methylation of the 1044 probes within CpG islands was significantly greater in the CNS-PNET tumours compared with the normal brain (interquartile range 100-151 and median 120 probes in CNS-PNET vs interquartile range 96-106 and median of 101 probes in the control samples; $p=0.002$). In contrast methylation of the 461 probes located outside of CpG islands was greater in the control sample cohort (interquartile range 235-303 and median 269 probes in CNS-PNET vs interquartile range 325-335 and median of 330 probes in the control samples ($p<0.0001$). The variability amongst samples also differed. In the tumour cohort the standard deviation of methylated probes inside and outside of CpG islands was 46.5 and 44.9 respectively, compared to only 8.2 and 8.9 in the normal brain cohort. Taken together these data show that methylation profiles of primary CNS-PNET differ significantly to those observed in normal brains both with respect the frequency and variablity of methylation. Tumour-specific methylation is therefore a feature of CNS-PNET, although the methylation profiles of a minority of tumours may more closely resemble those observed in the normal brain (Figure 5.9).

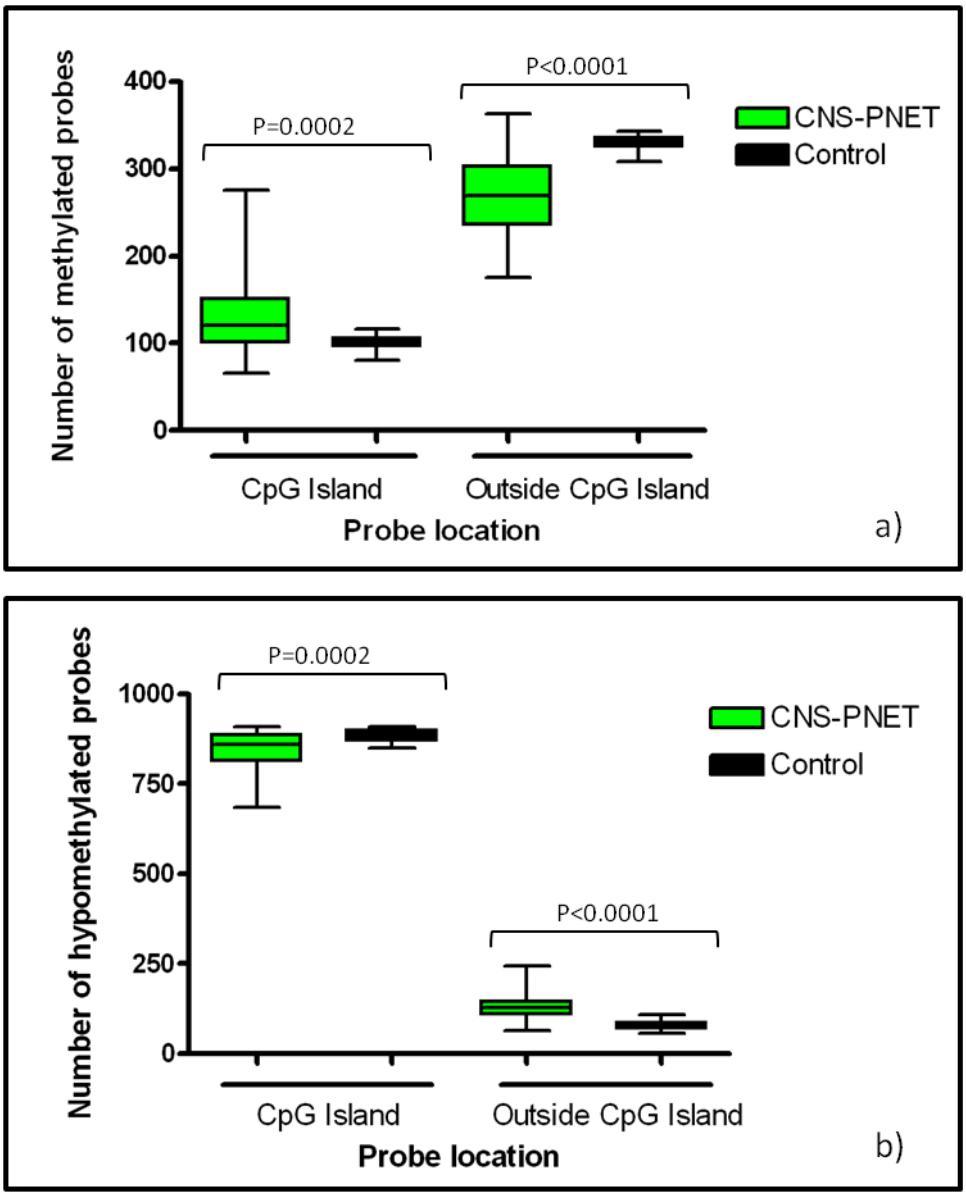

Figure 5.8. Box and whisker plots comparing methylation patterns at and outside of CpG island sites in normal brain tissue and in CNS-PNET. (a) methylated, and (b) hypomethylated probe comparison.

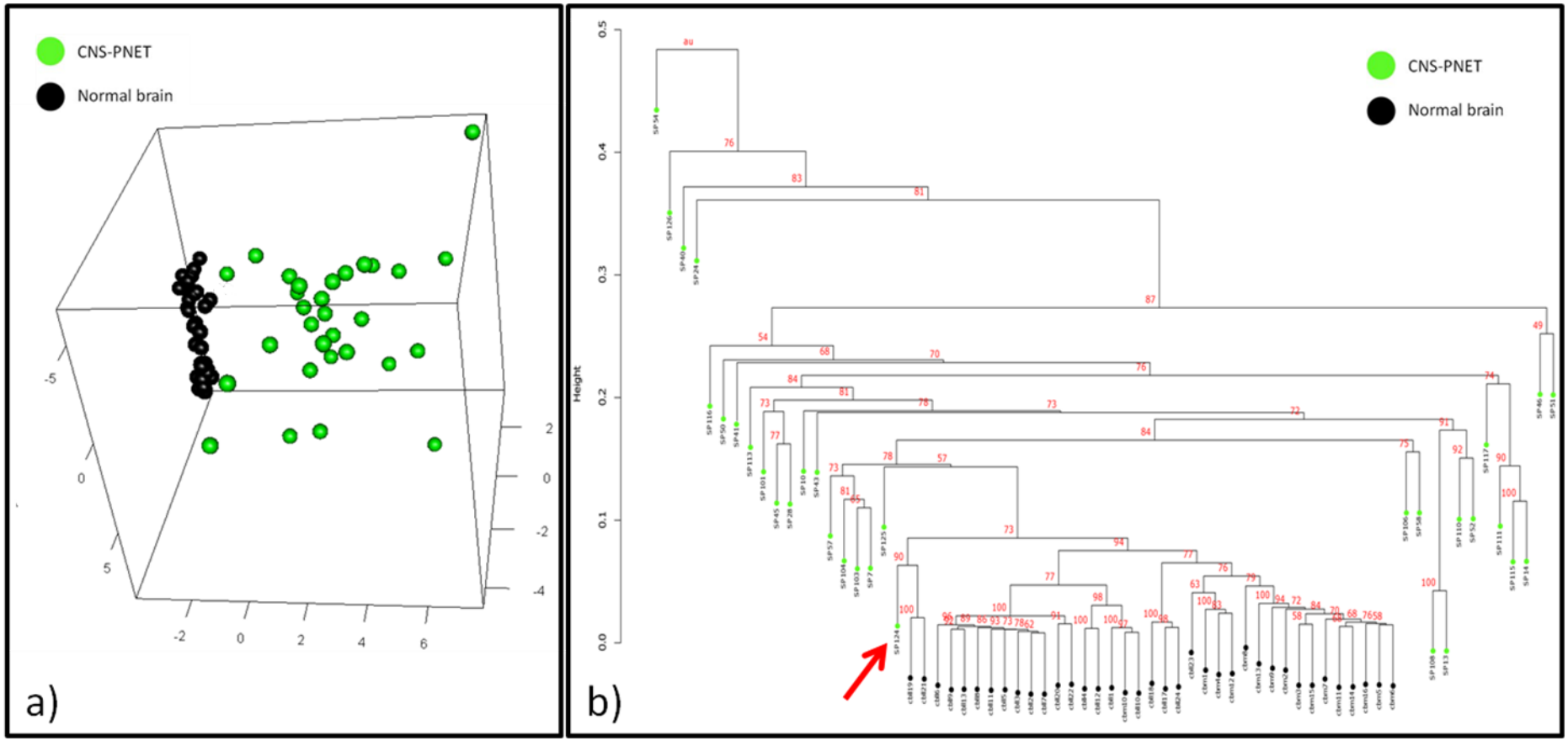

Figure 5.9. Comparison of CNS-PNET methylation profiles with normal brain. (a) Principal component analysis showing the co-clustering of normal brain samples and CNS-PNET heterogeneity. (b) Unsupervised hierarchical clustering bootstrapped dendrogram. SP124 (red arrow) is shown to have a methylation profile closely related to the normal brain samples.

5.3.6 Identification of tumour-specific methylation events in CNS-PNET

The identification of probes that are significantly aberrantly methylated in CNS-PNETs was derived as has been detailed in section 5.2.9.1, and the process summarised in Figure 5.10. In the normal brain, 52.1% (784/1505) of probes were found to be invariantly hypomethylated and 17.4% (262/1505) of probes were found to be invariantly fully methylated. Of the invariantly fully methylated and hypomethylated probes 138 and 418 probes respectively were found to exhibit significantly different methylation in the CNS-PNET cohort. In total 76 probes were identified that exhibited the most significantly aberrant methylation, 24 of which have an invariantly hypomethylated profile and 52 of which have an invariantly fully methylated profile in the normal brain (Figure 5.11). These significant aberrantly methylated probes in CNS-PNET target in total 63 different genes as summarised in Table 5.8 and Table 5.9.

In these 76 probes, aberrant methylation occurs in 16-77% (5/31 – 24/31) of CNS-PNET cases (Figure 5.12). The KLK11_P103_R and HLADPB1_E2_R probes are the two most frequently aberrantly hypo-methylated probes in CNS-PNET that are fully methylated in the normal brain (aberrantly methylated in 77% and 74% of CNS-PNETs respectively). The two most frequently aberrantly hyper-methylated probes in CNS-PNET which are hypomethylated in the normal brain are RASSF1_E116_F and FZD9_E458_F (aberrantly methylated in 68% and 61% of CNS-PNETs respectively).

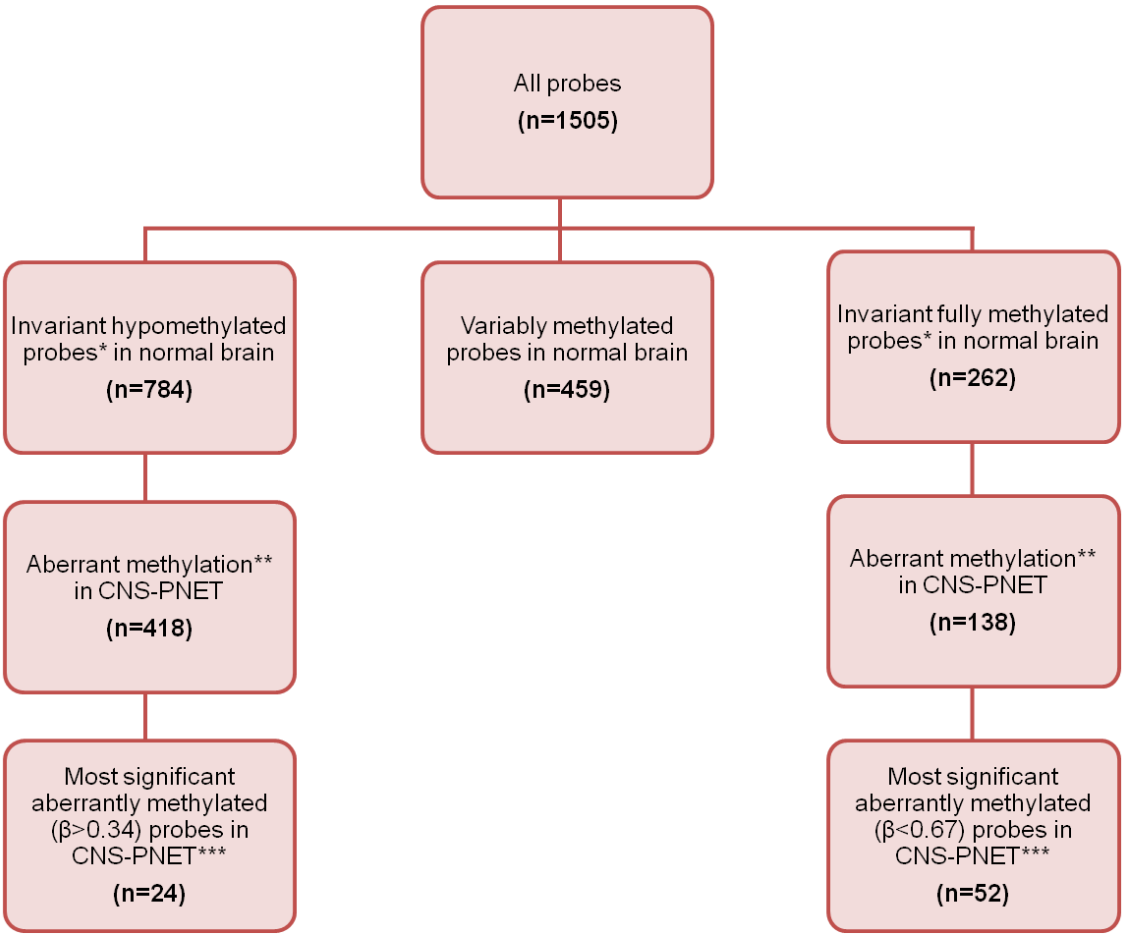

Figure 5.10. Ascertainment of aberrantly methylated probes in CNS-PNET.
*Invariantly fully methylated (β>0.67) and hypomethylated (β<0.34) probes showed consistent values in all normal brain samples. **The average methylation in the normal brain and CNS-PNET samples differed significantly ($p<0.05$, Mann-Whitney testing after multi-test correction), and ***magnitude of difference exceeded the limit of detectability on the methylation array platform ($\Delta\beta>0.17$).

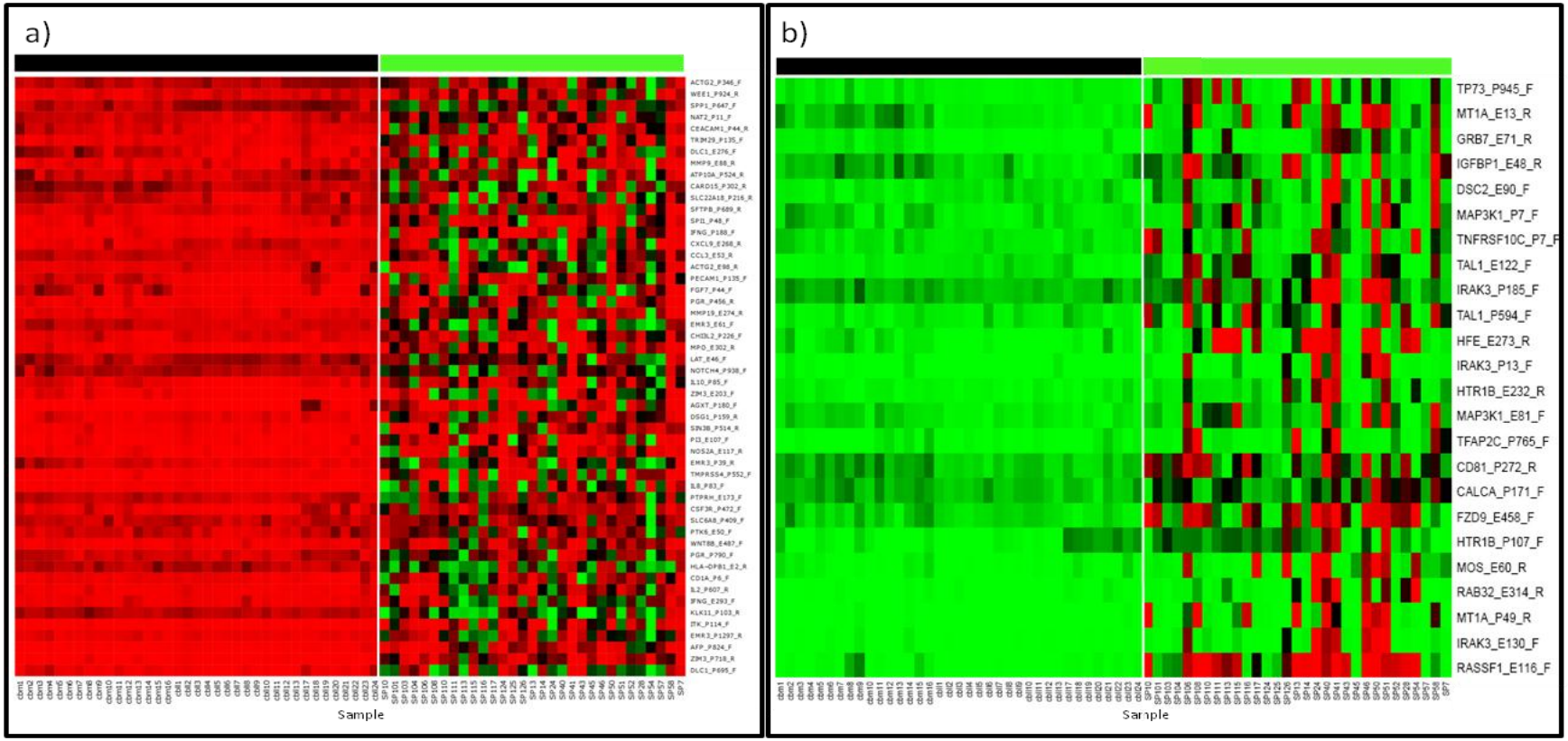

Figure 5.11. Heatmaps of gene probes significantly differentially methylated between CNS-PNETs and the normal brain. (a) Consistently methylated probes (β > 0.66) in all normal brain samples with a significant variation in CNS-PNET samples. (b) Consistently hypomethylated probes (β < 0.34) in all normal brain samples with a significant variation in CNS-PNET samples. In (a) and (b), median β in CNS-PNET is significantly different ($p<0.05$, Mann-Whitney test and Benjamin-Hochberg correction. Methylation β values shown: Green, hypomethylated; black, partially methylated; red, fully methylated. Black bar, normal brain; Green bar, CNS-PNET.

Probe	Methylation		Gene	Chr	Function(s)
	Aberrant No (%)	Hypo No (%)			
ACTG2_E98_R	15 (48%)	8 (26%)			
ACTG2_P346_F	14 (45%)	6 (19%)	*ACTG2*	2	actin-like protein, structural constituent of cytoskeleton
AFP_P824_F	5 (16%)	2 (6%)	*AFP*	4	transfer/ carrier protein, mesoderm development
AGXT_P180_F	7 (23%)	4 (13%)	*AGXT*	2	transaminase, cellular amin aocid and derivative metabolism
ATP10A_P524_R	13 (42%)	9 (29%)	*ATP10A*	15	cation transporter, hydrolase activity, cation transmebrane transporter activity
CARD15_P302_R	13 (42%)	8 (26%)	*CARD15*	16	intracellular receptor, immune system process, apoptosis induction
CCL3_E53_R	14 (45%)	5 (16%)	*CCL3*	17	chemokine, immune response, cell-cell signaling, cell surface receptor linked signal transduction
CD1A_P6_F	12 (39%)	7 (23%)	*CD1A*	1	immunoglobulin receptor, B cell mediated immunity
CEACAM1_P44_R	10 (32%)	5 (16%)	*CEACAM1*	19	cell adhesion molecule, signal transduction, cell-cell adhesion
CHI3L2_P226_F	10 (32%)	4 (13%)	*CHI3L2*	1	glycosidease, hydrolase activity, hydrolysing N-glycosyl compounds
CSF3R_P472_F	5 (16%)	3 (10%)	*CSF3R*	1	signaling molecule, B cell mediated immunity, cell surface receptor linked signal transduction, ectoderm/ mesoderm & nervous system development, haemopoiesis
CXCL9_E268_R	17 (55%)	12 (39%)	*CXCL9*	4	chemokine, cellular defence response, IFNγ response, angiogenesis, mesoderm development, cell-cell signaling, signal transduction, macrophage activation
DLC1_E276_F	11 (35%)	8 (26%)			
DLC1_P695_F	18 (58%)	14 (45%)	*DLC1*	8	G-protein modulator, PDGF signaling pathway
DSG1_P159_R	11 (35%)	3 (10%)	*DSG1*	18	cell junction protein, cell-cell adhesion, signal transduction, calcium ion binding
EMR3_E61_F	21 (68%)	14 (45%)			
EMR3_P1297_R	15 (48%)	8 (26%)			
EMR3_P39_R	18 (58%)	11 (35%)	*EMR3*	19	G-protein coupled receptor, synaptic transmission, B cell mediated immunity, mesoderm & heart development, angiogenesis, signal transduction
FGF7_P44_F	15 (48%)	10 (32%)	*FGF7*	15	FGF signaling pathway receptor, ectoderm & nervous system development, cell cycle, cell-cell signaling, intracellular signaling cascade
HLA-DPB1_E2_R	23 (74%)	17 (55%)	*HLA-DPB1*	6	major histocompatibility complex antigen, antigen processing & presentation, cellular defense response
IFNG_E293_F	15 (48%)	8 (26%)			
IFNG_P188_F	12 (39%)	4 (13%)	*IFNG*	12	interferon glycoprotein, interferon gamma signaling pathway, cellular defense response, cell-cell signaling, natural killer cell activation, apoptosis regulation

IL10_P85_F	12 (39%)	4 (13%)	*IL10*	1	interleukin cytokine, cellular defense response, modulate inflammation and immunity by regulating growth, mobility and differentiation of lymphoid cells
IL2_P607_R	11 (35%)	5 (16%)	*IL2*	4	interleukin cytokine, cellular defense response, modulate inflammation and immunity by regulating growth, mobility and differentiation of lymphoid cells
IL8_P83_F	17 (55%)	12 (39%)	*IL8*	4	chemokine, cellular defense response, inflamation mediated by chemokine & cytokine signaling pathway, , IFNγ response, angiogenesis, mesoderm development
ITK_P114_F	10 (32%)	4 (13%)	*ITK*	5	transmembrane receptor protein kinase, ectoderm/ mesoderm & nervous system development, cell cycle & apoptosis, cell-cell signaling & adhesion
KLK11_P103_R	24 (77%)	16 (52%)	*KLK11*	19	serine protease, blood coagulation, immune system processing, ectoderm & nervous system development, cell cycle
LAT_E46_F	14 (45%)	6 (19%)	*LAT*	16	adapter protein, T-cell activation pathway
MMP19_E274_R	8 (26%)	2 (6%)	*MMP19*	12	metalloprotease, protein metabolism processing
MMP9_E88_R	8 (26%)	4 (13%)	*MMP9*	20	metalloprotease, protein metabolism processing
MPO_E302_R	9 (29%)	3 (10%)	*MPO*	17	peroxidase, immune response, oxygen species metabolic process
NAT2_P11_F	14 (45%)	2 (6%)	*NAT2*	8	acetyltransferase, metabolism
NOS2A_E117_R	8 (26%)	3 (10%)	*NOS2A*	17	nitric oxide synthase
NOTCH4_P938_F	19 (61%)	6 (19%)	*NOTCH4*	6	transcription factor, ectoderm & nervous system development, cell-cell signaling & adhesion, signal transduction
PECAM1_P135_F	10 (32%)	5 (16%)	*PECAM1*	17	immunoglobulin receptor, B cell mediated immunity, natural killer cell & macrophage activation, cell adhesion, signal transduction
PGR_P456_R	9 (29%)	4 (13%)			
PGR_P790_F	15 (48%)	5 (16%)	*PGR*	11	nuclear hormone receptor, neuronal action potential propagation, neurotransmitter secretion, sensory perception
PI3_E107_F	8 (26%)	5 (16%)	*PI3*	20	serine protease inhibitor, protein metabolism
PTK6_E50_F	11 (35%)	3 (10%)	*PTK6*	20	transmembrane receptor protein kinase, ectoderm/ mesoderm & nervous system development, cell cycle & apoptosis, cell-cell signaling & adhesion
PTPRH_E173_F	14 (45%)	7 (23%)	*PTPRH*	19	receptor, hydrolase & phosphatase activity, ectoderm & nervous system development, cellular glucose homeostasis, mitosis, immune system process, cell-cell & cell-matrix adhesion
SFTPB_P689_R	9 (29%)	6 (19%)	*SFTPB*	2	surfactant, lipid metabolism and transport, blood circulation
SIN3B_P514_R	6 (19%)	3 (10%)	*SIN3B*	19	transcription factor, deacetylase activity, DNA & chromatin binding
SLC22A18_P216_R	17 (55%)	9 (29%)	*SLC22A18*	11	transmembrane transporter

SLC6A8_P409_F	11 (35%)	3 (10%)	*SLC6A8*	X	amino acid transporter, nicotinic & muscarinic receptor signaling pathways, neuronal action potential propagation, neurotransmitter secretion, sensory perception.
SPI1_P48_F	8 (26%)	3 (10%)	*SPI1*	11	transcription factor, interleukin signaling pathway, B cell mediated immunity, macrophage activation, cell cycle, mesoderm & endoderm development, hemopoiesis
SPP1_P647_F	16 (52%)	7 (23%)	*SPP1*	4	extracellular matrix cytokine, cell adhesion, immune system processing
TMPRSS4_P552_F	10 (32%)	8 (26%)	*TMPRSS4*	11	serine protease, blood coagulation, immune system processing
TRIM29_P135_F	8 (26%)	3 (10%)	*TRIM29*	11	nucleic acid binding protein, nervous system & ectoderm development, cell cycle
WEE1_P924_R	6 (19%)	3 (10%)	*WEE1*	11	mitosis protein kinase
WNT8B_E487_F	6 (19%)	4 (13%)	*WNT8B*	10	signaling molecule, Wnt & cadherin signaling pathway
ZIM3_E203_F	15 (48%)	10 (32%)	*ZIM3*	19	KRAB box transcription factor, spermatogenesis, nucleic acid metabolic process
ZIM3_P718_R	6 (19%)	1 (3%)			

Table 5.8. Most significant differentially hypomethylated gene probes in CNS-PNET. Aberrantly methylated (aberrant): β<0.67, and hypomethylated (hypo): β<0.34.

Probe	Methylation		Gene	Chr	Function(s)
	Aberrant No (%)	Fully No (%)			
CALCA_P171_F	16 (52%)	2 (6%)	*CALCA*	11	peptide hormone, skeletal & mesoderm development, phosphate metabolism
CD81_P272_R	18 (58%)	8 (26%)	*CD81*	11	membrane bound signaling molecule, neuronal action potential propagation, neurotransmitter secretion, sensory perception, B cell mediated immunity
DSC2_E90_F	7 (23%)	7 (23%)	*DSC2*	18	cell junction protein, cell-cell adhesion, signal transduction
FZD9_E458_F	19 (61%)	17 (55%)	*FZD9*	7	signaling molecule, cadherin & wnt signaling pathway
GRB7_E71_R	7 (23%)	2 (6%)	*GRB7*	17	transmembrane receptor adaptorv protein, signal transduction
HFE_E273_R	14 (45%)	12 (39%)	*HFE*	6	immunoglobulin receptor, B cell mediated immunity, antigen processing & presentation
HTR1B_E232_R	7 (23%)	5 (16%)			
HTR1B_P107_F	7 (23%)	4 (13%)	*HTR1B*	6	G-protein coupled receptor, neuronal action potential propagation, neurotransmitter secretion, sensory perception
IGFBP1_E48_R	9 (29%)	7 (23%)	*IGFBP1*	7	binding protein, PI3 kinase pathway, cell matrix adhesion
IRAK3_E130_F	8 (26%)	7 (23%)			
IRAK3_P13_F	7 (23%)	5 (16%)			
IRAK3_P185_F	13 (42%)	8 (26%)	*IRAK3*	12	protein kinase, Toll receptor signaling pathway, immune system process, protein metabolism
MAP3K1_E81_F	9 (29%)	6 (19%)			
MAP3K1_P7_F	9 (29%)	6 (19%)	*MAP3K1*	5	protein kinase, signaling pathways: Toll receptor, Ras, EGF receptor, integrin, FGF & apoptosis
MOS_E60_R	9 (29%)	9 (29%)	*MOS*	8	protein kinase, signal transduction, apoptosis regulation, cell cycle, immune system process
MT1A_E13_R	12 (39%)	10 (32%)			
MT1A_P49_R	10 (32%)	8 (26%)	*MT1A*	16	metallothionein protein
RAB32_E314_R	8 (26%)	6 (19%)	*RAB32*	6	GTPase, signal transduction, neurotransmitter secretion, cell cycle, endocytosis, exocytosis
RASSF1_E116_F	21 (68%)	19 (61%)	*RASSF1*	3	G-protein modulator, signal transduction, apoptosis
TAL1_E122_F	13 (42%)	6 (19%)			
TAL1_P594_F	13 (42%)	7 (23%)	*TAL1*	1	transcription factor, DNA binding, nucleic acid metabolism
TFAP2C_P765_F	7 (23%)	5 (16%)	*TFAP2C*	20	transcription factor, ectoderm development, nucleic acid metabolism
TNFRSF10C_P7_F	9 (29%)	7 (23%)	*TNFRSF10C*	8	tumour necrosis factor receptor, p53 & apoptosis signaling pathways, B cell mediated immunity, macrophage activation, ectoderm & nervous system development
TP73_P945_F	11 (35%)	7 (23%)	*TP73*	1	transcription factor, p53 pathway, apoptosis induction, cell cycle regulation

Table 5.9. Most significant differentially fully methylated gene probes in CNS-PNET. Aberrantly methylated (aberrant): β>0.34, and fully methylated (fully): β>0.67.

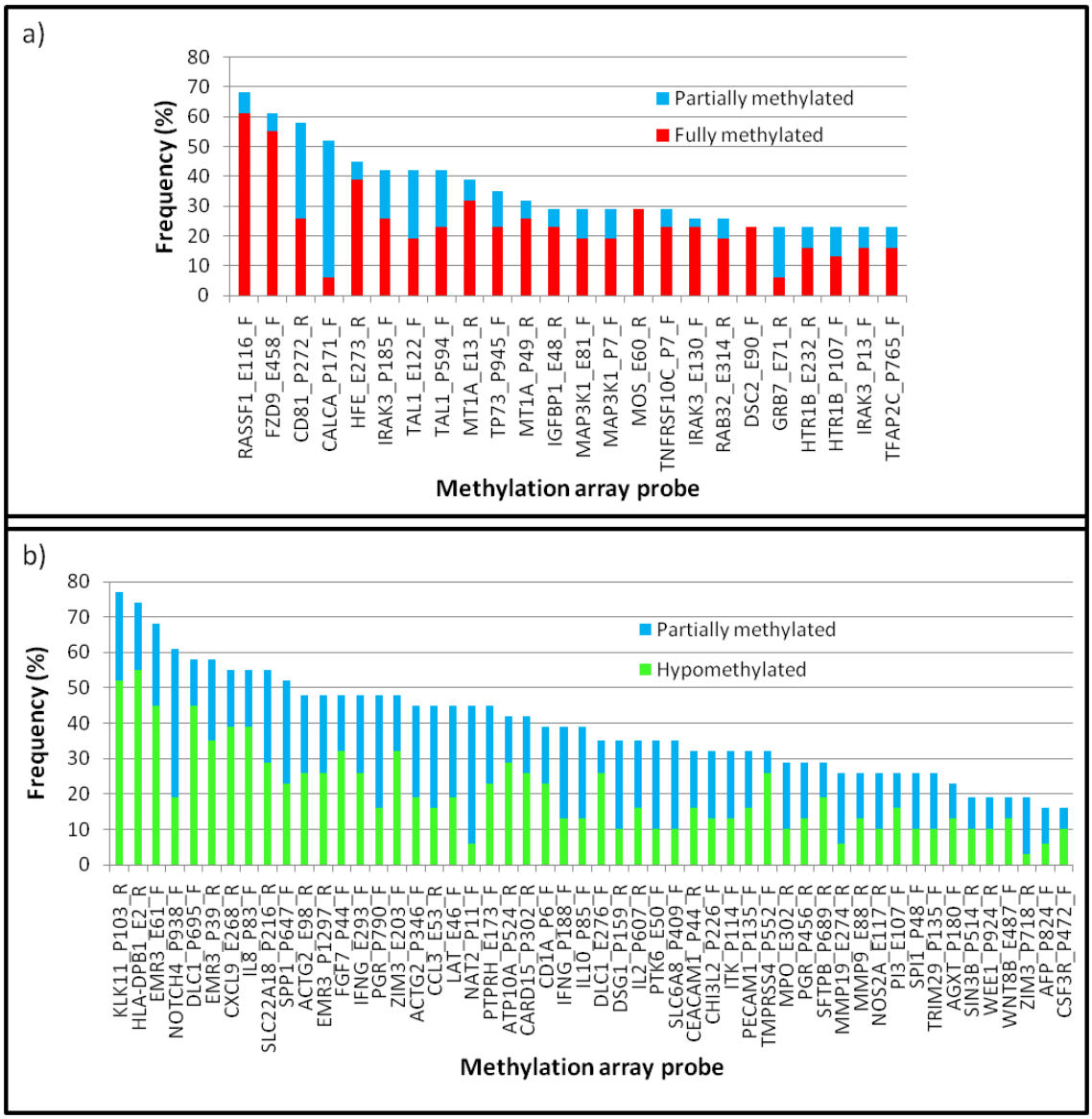

Figure 5.12. Frequency of the most significant aberrantly methylated probes in CNS-PNET. (a) Probes hypomethylated in normal brain that exhibit aberrant methylation in CNS-PNET. Partially methylated (β= 0.34-0.67); fully methylated (β>0.67). (b) Probes fully methylated in the normal brain that exhibit aberrant methylation in CNS-PNET. Partially methylated (β= 0.34-0.67); hypomethylated (β<0.34).

5.3.7 CNS-PNET methylation ontological analysis

An ontological analysis using the DAVID Functional Classification Tool of the identified most significantly differentially methylated genes (section 5.3.6) was performed as described in section 5.2.9.2. The list of CNS-PNET aberrantly methylated genes was not found to be statistically significantly enriched for any biological pathway or process.

5.3.8 Correlation with CNS-PNET clinical characteristics

5.3.8.1 Identification of age-specific methylation markers

The age at diagnosis of patients with a CNS-PNET was known for 30 samples. In 8 cases (27%) the samples originated from infants, under the age of 3 years (36 months). In 22/30 (73%) cases patients were aged 36 months or older at diagnosis. Analysis of the 76 CNS-PNET specific probes determined in section 5.3.6, as using methods described in section 5.2.9.2, identified the probes TAL1_E122_F, MAP3K1_E81_F and IGFBP1_E48_R to be statistically significantly associated with age at diagnosis (Figure 5.13) following false discovery rate correction. For all 3 probes, the methylation profile, in common with that observed in the normal brain, was consistently hypomethylated in children under the age of 3, but showed variation in older patients. This suggests that age-specific methylation events occur in the development of CNS-PNET in infants.

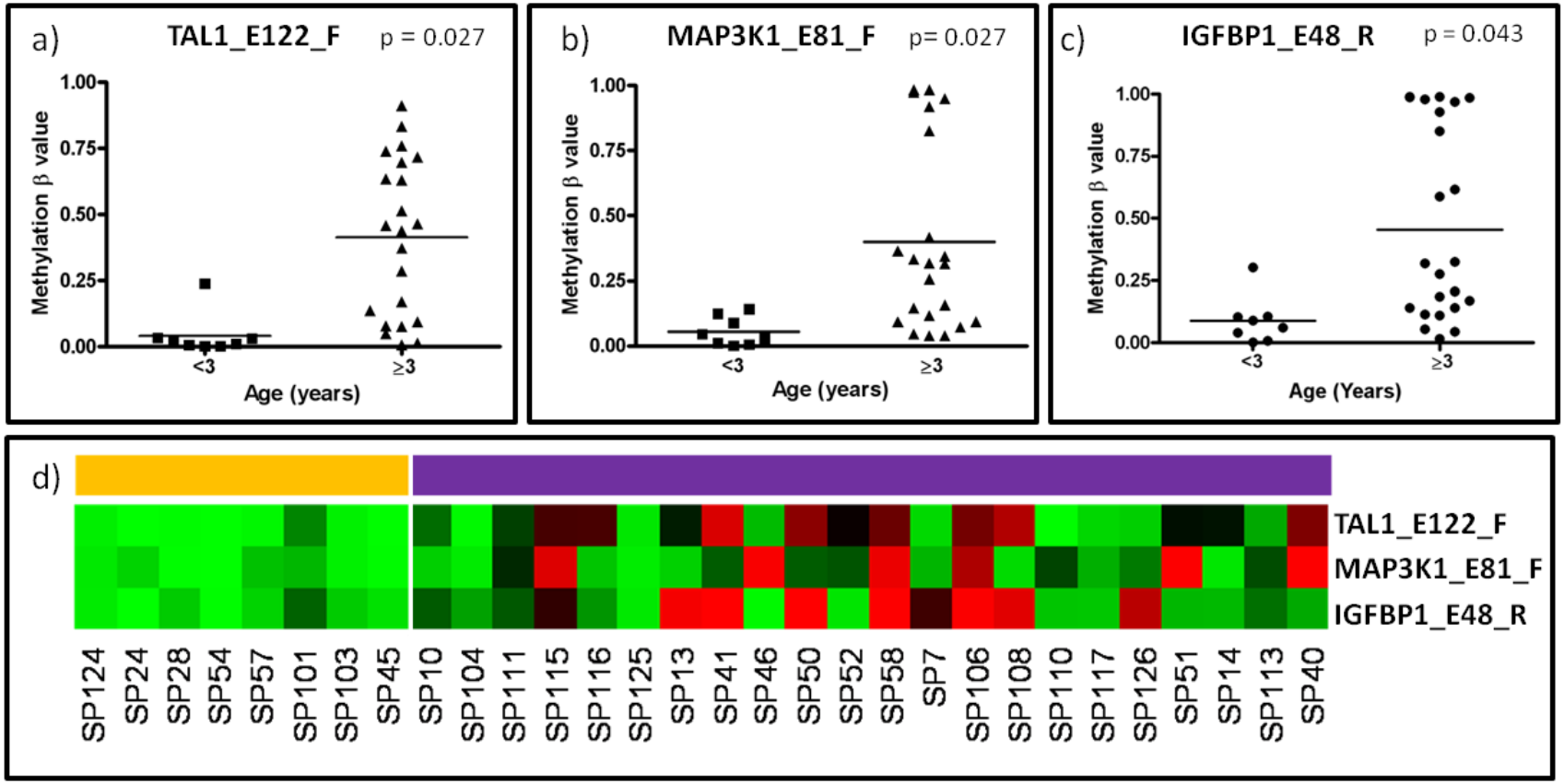

Figure 5.13. Methylation probes associated with CNS-PNET age at diagnosis. Methylation scores in individual tumours for three probes significantly associated with age at diagnosis (a) TAL1_E122_F, (b) MAP3K1_E81_F and (c) IGFBP1_E48_R. (d) Significant probes heatmap: Yellow bar, infant cases; purple bar, children and adults >3 years old. Hypomethylated (green); partially methylated (black); fully methylated (red)

5.3.8.2 Identification of methylation markers associated with metastatic disease

Metastatic status at diagnosis was known in 29 cases. Metastatic disease (Chang stage M1-M4) was identified in 7 (24%) of cases, and 21 (68%) cases classified as non-metastatic according to the criteria outlined in section 2.1.1 (Chang stage M0 or M0/1). The development of metastatic disease was not found to be correlated with aberrant methylation in any of the disease specific probes, following analysis, as described in section 5.2.9.3.

5.3.9 Survival analysis

5.3.9.1 Overall CNS-PNET methylation cohort survival analysis

Survival data was not available for SP40, SP43 and SP45. SP103 and SP113 died within 7 days from surgery, at day 0 and day 4 post-operatively respectively, and were therefore excluded from the survival analysis. The survival analysis therefore comprised 26 cases, 9 (35%) of whom are alive and 17 (65%) have died of their disease (Figure 5.14). The duration of follow up ranged from 1 – 112 months (median: 24 months) in the cohort and ranged from 3 – 112 months (median: 41 months) in the survivor group. The overall cohort survival was 72.2% at 1 year (56.7-92%, 95% CI), 46.2% at 3 years (30-71.5%, 95% CI), and 32.3% at 5 years (16.5-63%, 95% CI).

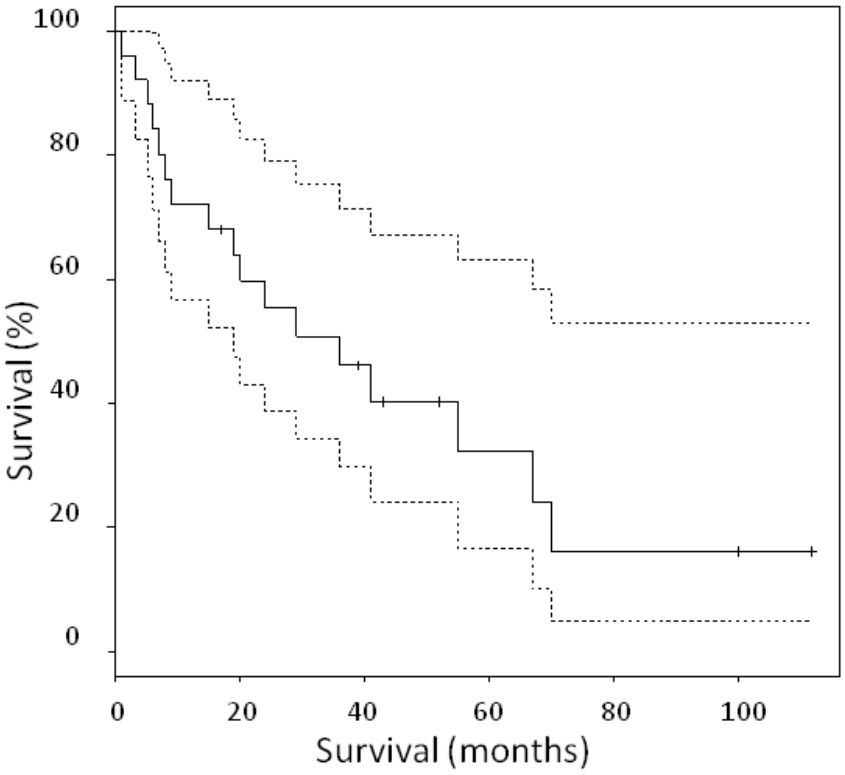

Figure 5.14. Kaplan-Meier plot of survival of patients with CNS-PNET used in the methylation array. Graph based on data from 26 cases. Survival (solid line) and 95% confidence interval (broken lines) are shown.

5.3.9.2 Identification of methylation markers associated with survival

Analysis to identify markers associated with survival in CNS-PNET was undertaken using the 76 most differentially methylated probes identified in section 5.2.9.4 as described in section 5.2.9.1. Shown in Figure 5.15, nine probes (HTR1B_E232_R, ITK_P114_F, MMP9_ E88_R, MOS_E60_R, PGR_P456_R, SIN3B_P514_R, SLC6A8_P409_F, TRIM29_P135_F and WEE1_P924_R) were found to have a p-value <0.05 on univariate analysis, but none of the probes were significant following Bonferroni-Hochberg correction for multiple testing. For two probes, (SIN3B_P514_R and TRIM29_P135_F) a change in methylation from being hypermethylated in the normal brain to becoming hypomethylated in the tumour was associated with a survival advantage (p= 0.007 and p= 0.038 respectively). For the other 7 probes,

hypermethylation relative to the normal brain was associated with an adverse outcome.

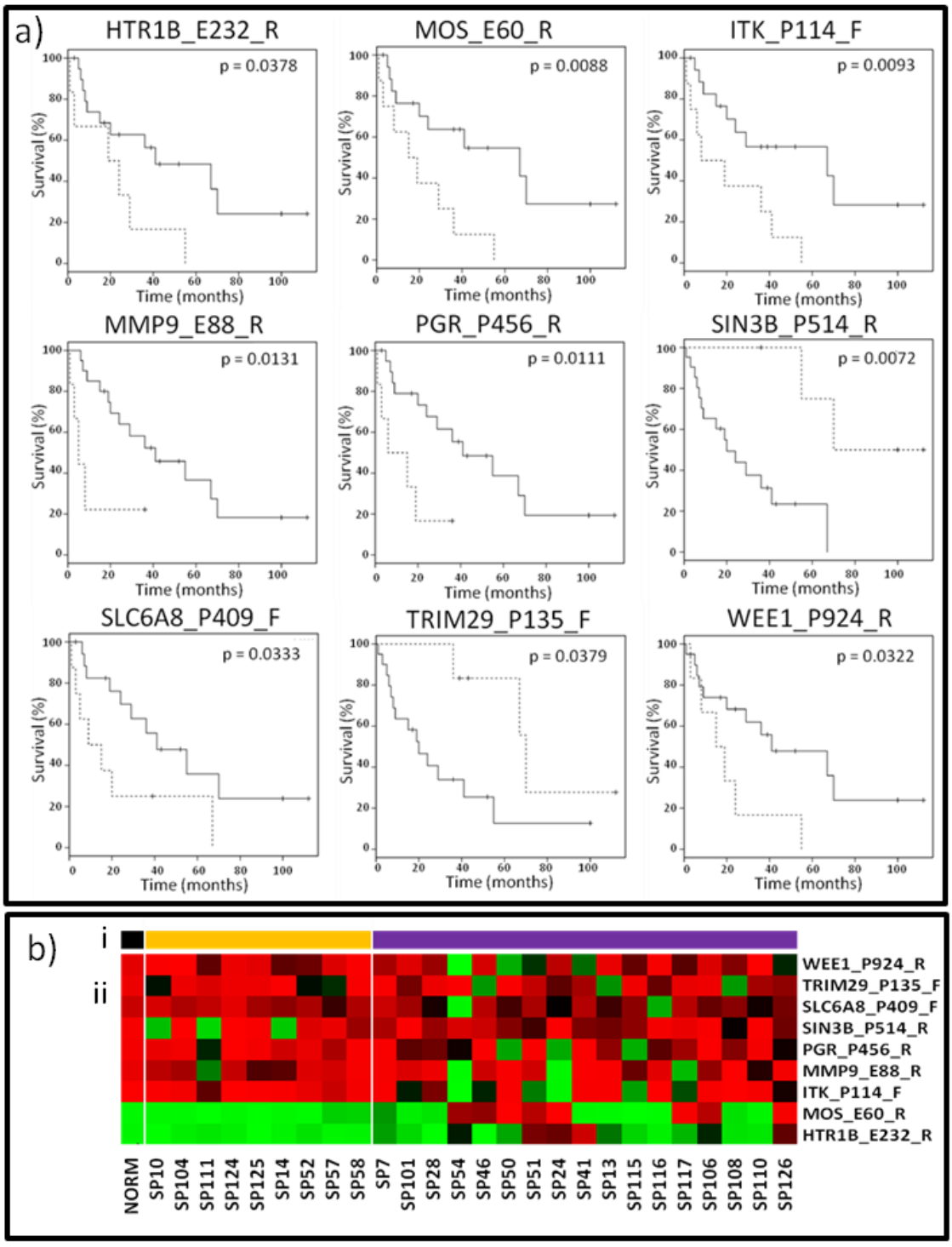

Figure 5.15. CNS-PNET tumour-specific methylation events associated with survival. (a) Kaplan-Meier plots; normally methylated (solid line); aberrantly methylated (hatched line). (b) Survival probe features; i) Status, normal brain (black); alive (orange); died (purple), ii) Heatmap: Hypomethylated (green); partially methylated (black); fully methylated (red). Norm: Normal brain (cohort mean β-value).

5.3.10 Development of a model to discern CNS-PNET from normal brain

A model to discern normal brain from CNS-PNET was constructed using the list of 76 most differentially methylated probes identified in section 5.3.6. Linear discriminant analysis identified two of these probes which, when the β-values for these 2 probes were used in conjunction, were able to delineate normal brain from CNS-PNET. Control normal brain samples were shown in all cases to exhibit hypomethylation (β<0.34) of RASSF1_E116_F and for the HLA_DPB1_E2_R probe to be fully methylated (β>0.67). With this model a change from hypomethylation of RASSF1_E116_F or from fully methylated in HLA_DPB1_E2_R to either RASSF1_E116_F becoming fully methylated (β>0.67) or HLA_DPB1_E2_R becoming hypomethylated (β<0.34) signified that a sample was a CNS-PNET rather than normal brain Figure 5.16. The system correctly identifies all control samples (37/37), and 87% (27/31) of CNS-PNETs. In one case (SP103) the sample is found to be indeterminate as the β-value for HLA_DPB1_E2_R (β=0.612) lies between the cut-off for a CNS-PNET (β<0.34) and that for a normal brain sample (β>0.67). For both SP124 and SP125 (2/31, 6%) the classifier system incorrectly determines that CNS-PNET samples are normal brain.

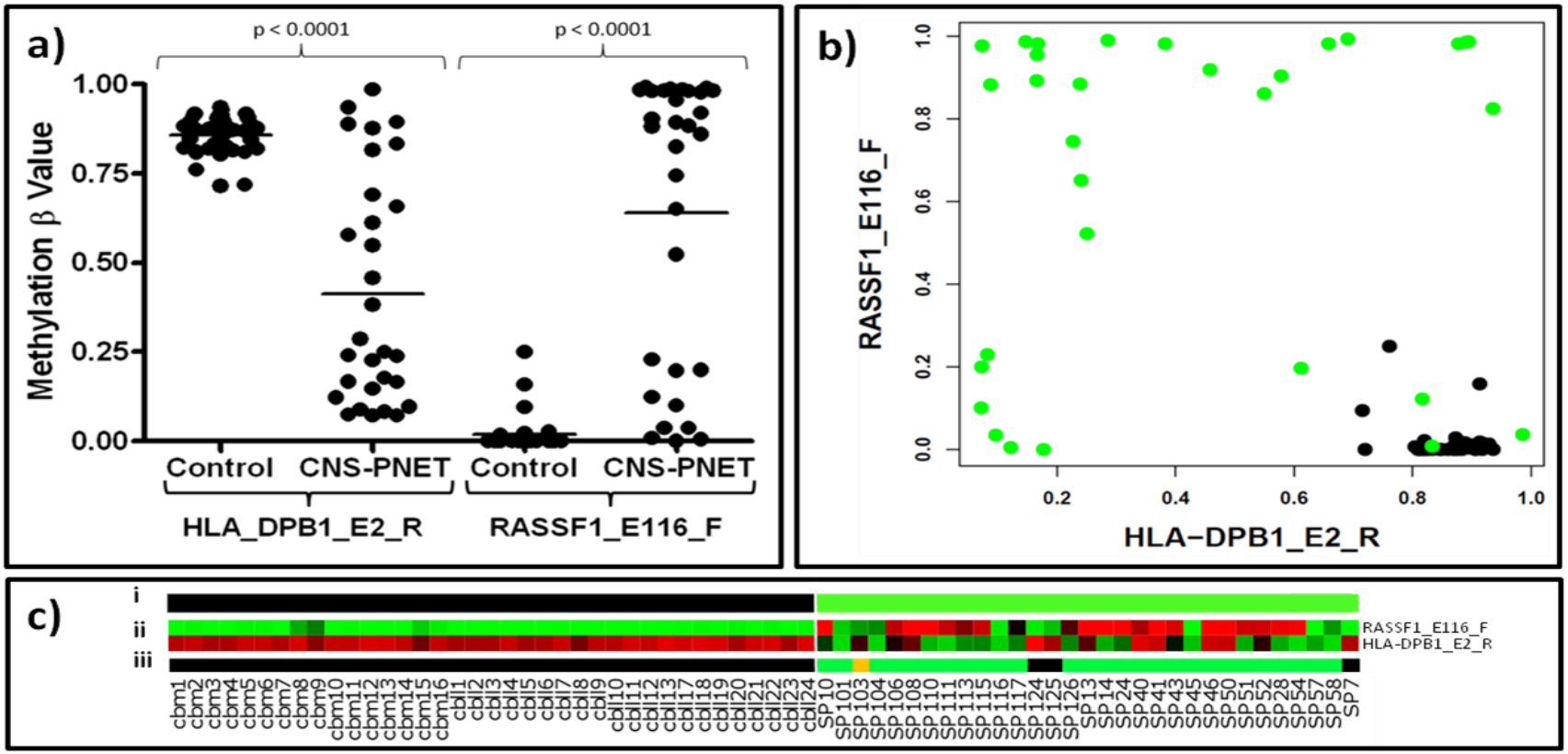

Figure 5.16. CNS-PNET classifier system. Normal brain can be distinguished from CNS-PNET using the methylation β values of 2 probes: HLA-DPB1_E2_R and RASSF1_E116_F. (a) Scatter plot showing the statistically significant difference β values between CNS-PNET and control brain, which when combined (b) the control normal brain (black) co-cluster separately from the CNS-PNET (green). (c) i) Normal brain (black) and CNS-PNET (green) ii) heatmap showing the methylation values (hypomethylated, green; partially methylated, black; fully methylated, red) of the samples. iii) Designation using the classifier system: normal brain (black), indeterminate (amber), CNS-PNET (green).

5.3.11 Comparison of CNS-PNET with the methylation profiles other CNS tumours

5.3.11.1 CNS-PNET vs pineoblastomas

The methylation profile of 4 pineoblastomas was compared with that observed in CNS-PNETs (Figure 5.17). The analysis was repeated with the 1085 differentially methylated probes and also with the 1421 probes not located on the x-chromosome, and identical results obtained (see Appendix). With the exception of SP113, an atypical CNS-PNET with supratentorial and infratentorial components, the pineoblastomas co-cluster separate from the CNS-PNETs.

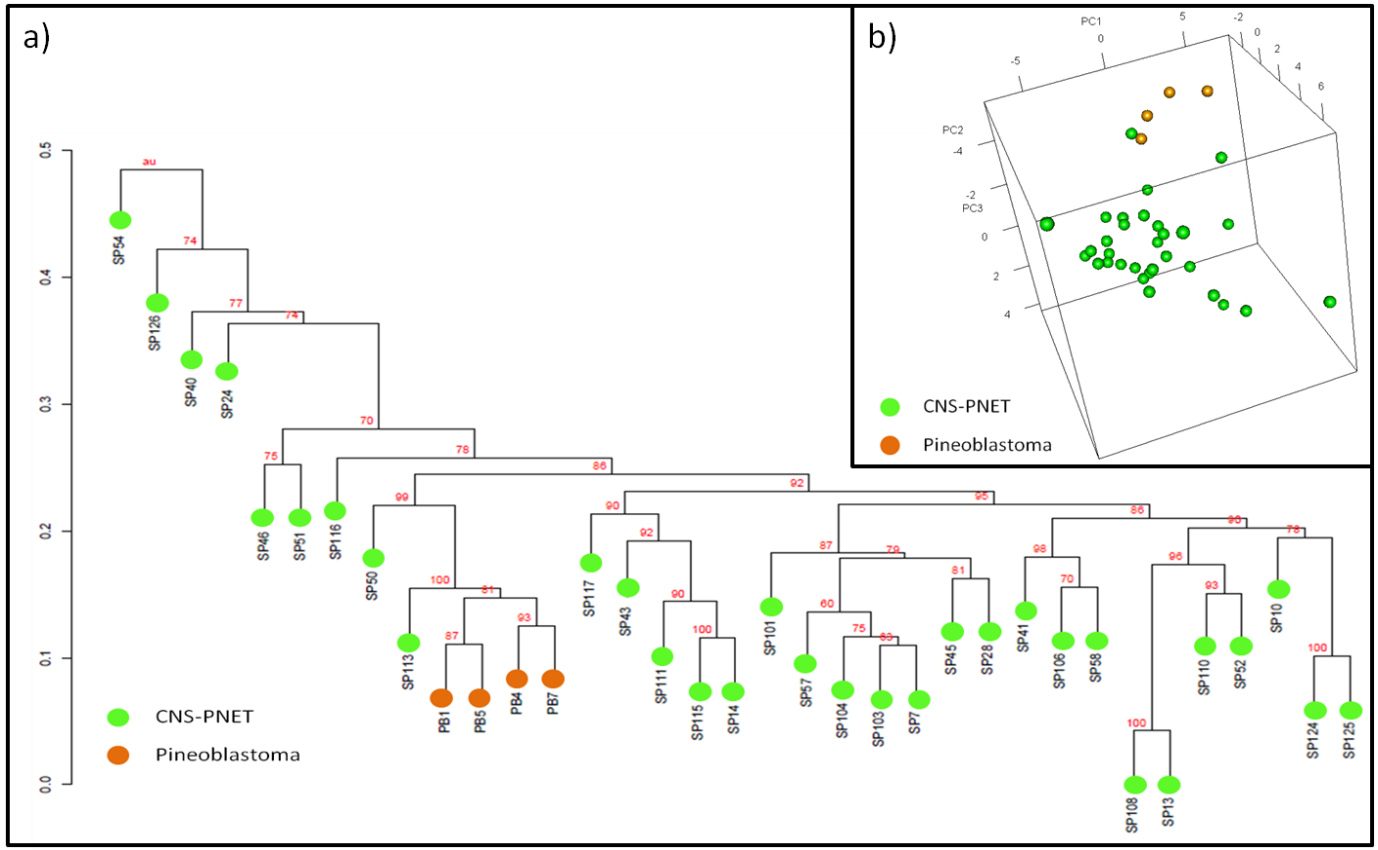

Figure 5.17. Unsupervised analysis of the relationship between the CNS-PNET and pineoblastoma methylome. (a) Principal component analysis, (b) Hierarchical clustering bootstrapped dendrograms.

5.3.11.2 CNS-PNET vs medulloblastoma

The methylation profile of CNS-PNETs was next compared with that of 100 medulloblastomas. As illustrated in Figure 5.18a, both the infratentorial (MB) and supratentorial (CNS-PNET) tumours clustered separately from the normal brain. The relationships between the methylation profiles of the MB and CNS-PNET groups were further interrogated by including medulloblastoma molecular sub-classification details (section 5.2.3.2). This detailed study was performed in triplicate with consistent results in each analysis. The triplicate analysis included an unsupervised approach utilising all of the 1505 probes on the array (data shown in Figure 5.18 and Figure 5.19), clustering using the 1421 probes not located on the X-chromosome, and also using only the 1178 differentially methylated probes (see section 5.2.9.1) across the study cohort (see Appendix 8.2).

The medulloblastoma and CNS-PNET tumours clustered into 6 groups, with the exclusion of 9 medulloblastoma and 10 CNS-PNET outlier samples (Figure 5.19, Group A). Two predominant clusters of CNS-PNETs were observed (Figure 5.19, Groups B and D). With the exception of NMB161, NMB250 and NMB252, all of the designated group 1 non-wnt and non-SHH medulloblastoma tumours (59/100) formed a discreet cluster separate from both the CNS-PNETs and medulloblastoma Wnt and SHH subgroups (Figure 5.19, Group G). NMB161 and NMB250 co-clustered with the Group D CNS-PNETs, and NMB252 with the SHH cluster (Figure 5.19, Group F).

Three of the CNS-PNET samples clustered with the medulloblastoma molecular subgroups. SP10 clustered within the dysregulated Wnt pathway group (Figure 5.19, Group E), and both SP124 and SP125 clustered amongst the medulloblastomas with aberrant SHH signalling (Figure 5.19, Group F). All three of these patients with CNS-PNETs in medulloblastoma subgroups are alive.

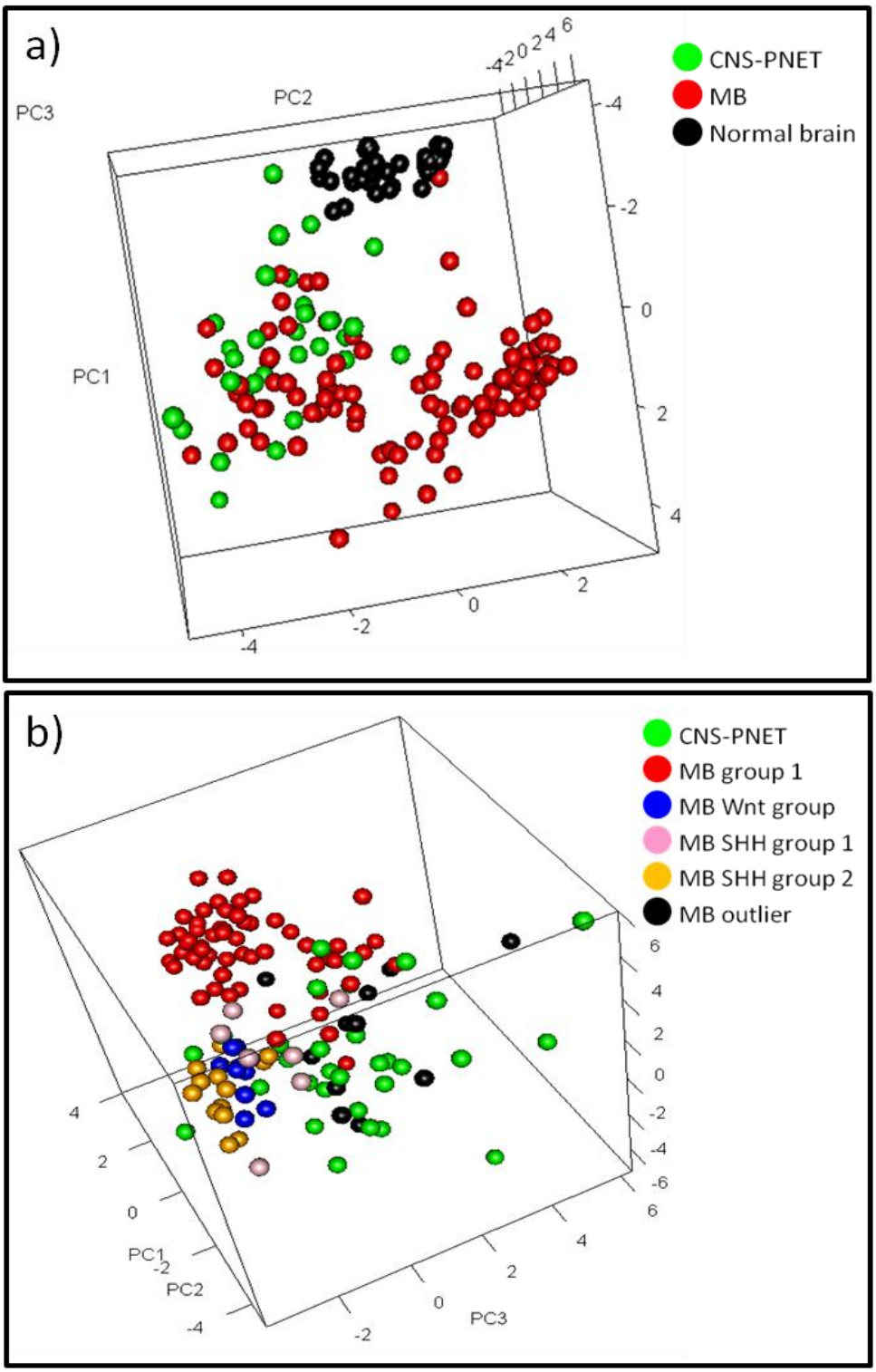

Figure 5.18. Principal component analysis (PCA) comparison of the methylomes of CNS-PNET and medulloblastoma. (a) PCA plot comparing the CNS-PNET and medulloblastoma with the normal brain. (b) PCA plot comparison of CNS-PNET with medulloblastoma sub groups. Wnt, Aberrant Wnt/ Wingless pathway signalling; SHH, Aberrant sonic hedgehog pathway signalling.

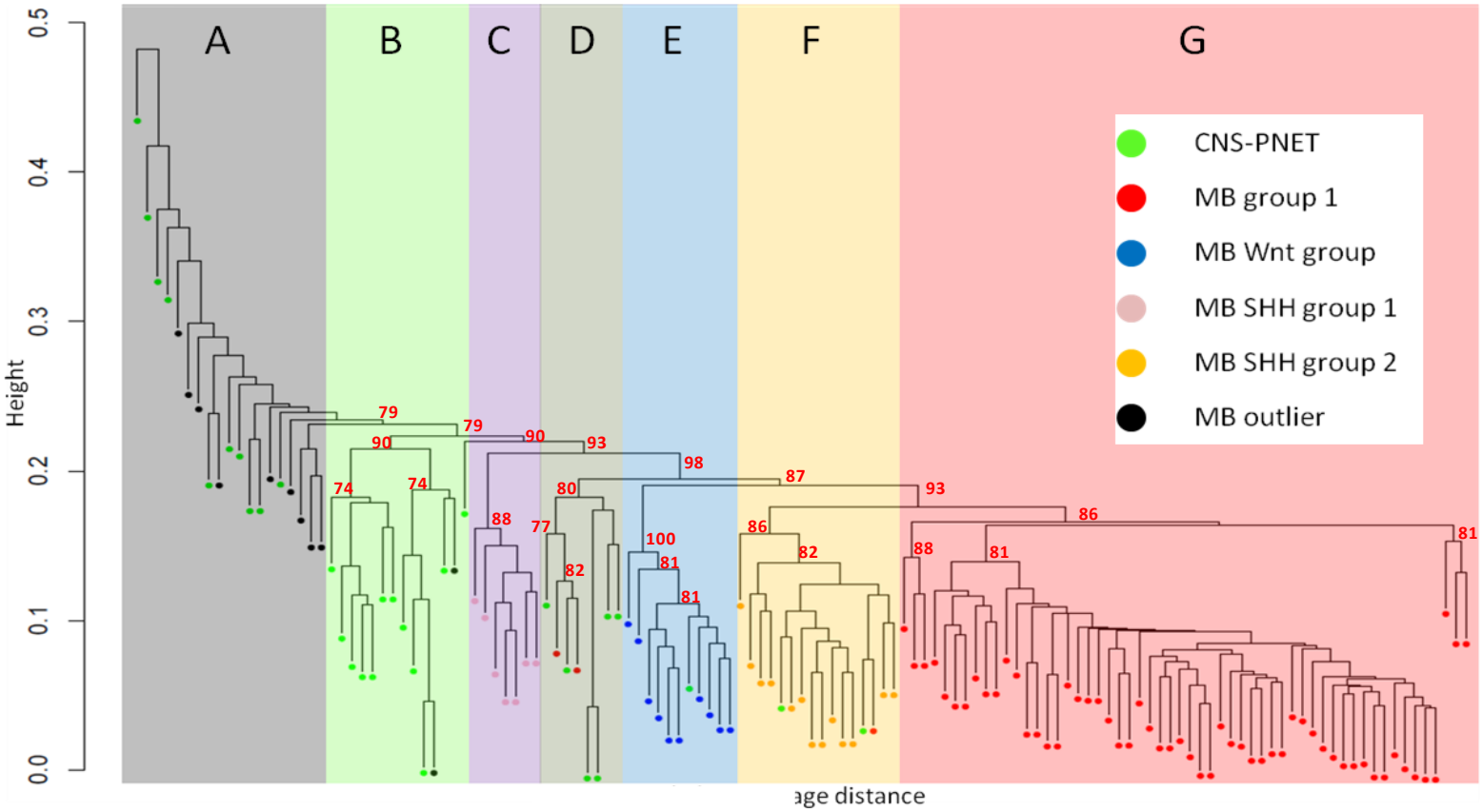

Figure 5.19. Dendrogram showing relationship between CNS-PNET methylation profiles and subgroups of medulloblastoma tumours. MB, medulloblastoma; SHH, sonic hedgehog pathway dysregulation; Wnt, Wnt/ wingless pathway dysregulation. A: Outliers, B: CNS-PNET group 1, C: SHH group1, D: CNS-PNET group 2, E: Wnt group, F: SHH group 2, G: MB group 1.

5.3.11.3 CNS-PNET vs high-grade gliomas

The methylation profile of 29 paediatric high-grade gliomas was compared with those observed in the normal brain and in CNS-PNET. Unsupervised clustering showed the high-grade gliomas to have a different methylation profile to the normal brain, but was not found to cluster as a distinct entity separately from the CNS-PNETs (Figure 5.20). This overlap occurred in contrast to the predominant separation observed between CNS-PNETs and medulloblastomas (see section 5.3.11.2) indicating that CNS-PNET may share a greater homology to high-grade gliomas than to medulloblastomas at the epigenetic level. Some subgroups of high grade gliomas were however demonstrated including one containing 5 cases (HGG_03_0480, HGG_02_1107, HGG_06_20918, HGG_18_71 and HGG_99_14974), and another of 4 (HGG_08_18756, HGG_18_407, HGG_18_72 and HGG_01_10325). Consistent results were obtained in two further analyses using firstly only the 1134 differentially methylated probes and secondly a probe set that excluded the 84 probes located on the X–chromosome.

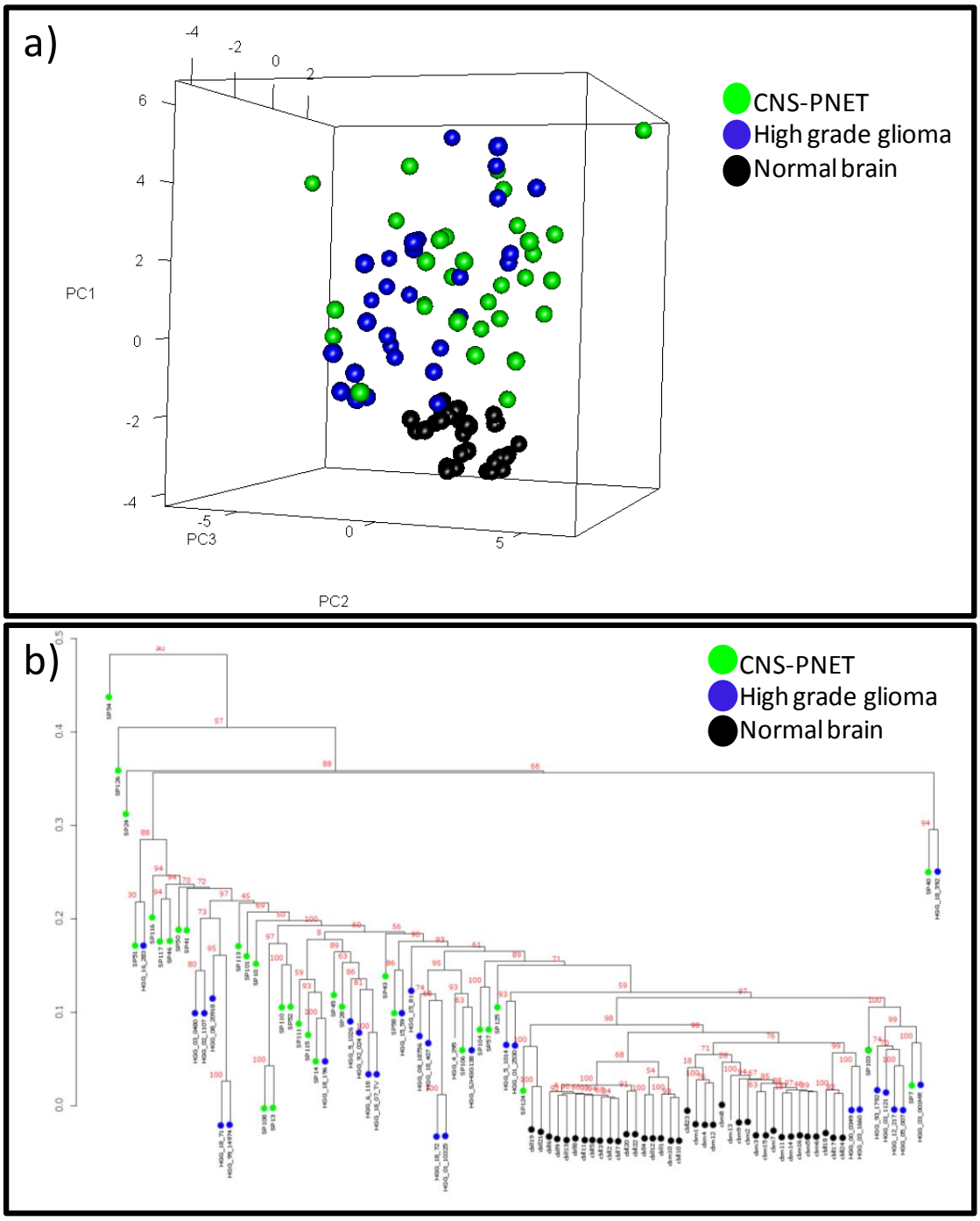

Figure 5.20. Unsupervised analysis of the relationship between the CNS-PNET, normal brain and high-grade glioma methylomes. (a) Principal component analysis, (b) Hierarchical clustering bootstrapped dendrograms.

5.3.11.4 Comparison of CNS-PNET methylation with a panel of primary malignant brain tumour and normal brain samples

The methylation profile of 31 CNS-PNETs was finally compared with that of a panel of 170 normal brain and malignant primary brain tumour samples (Figure 5.21). In this summary analysis, the observations identified from investigation of the methylation profiles of CNS-PNET with the normal brain, pineoblastoma, medulloblastoma, and high grade gliomas (detailed in sections 5.3.5, 5.3.11.1, 5.3.11.2 and 5.3.11.3 respectively) are maintained.

The methylation profile of the normal brain is distinct from that observed in primary brain tumours. Medulloblastomas are revealed to exhibit a variant methylation profile to that observed in the majority of CNS-PNETs, although as has previously been described in isolated cases similar patterns and co-clustering may occur. Pineoblastomas are shown to have a similar methylation pattern and co-cluster. A similar finding is not observed in assessment of high grade gliomas which do not form a discrete group, but can exhibit a similar methylation pattern to CNS-PNETs.

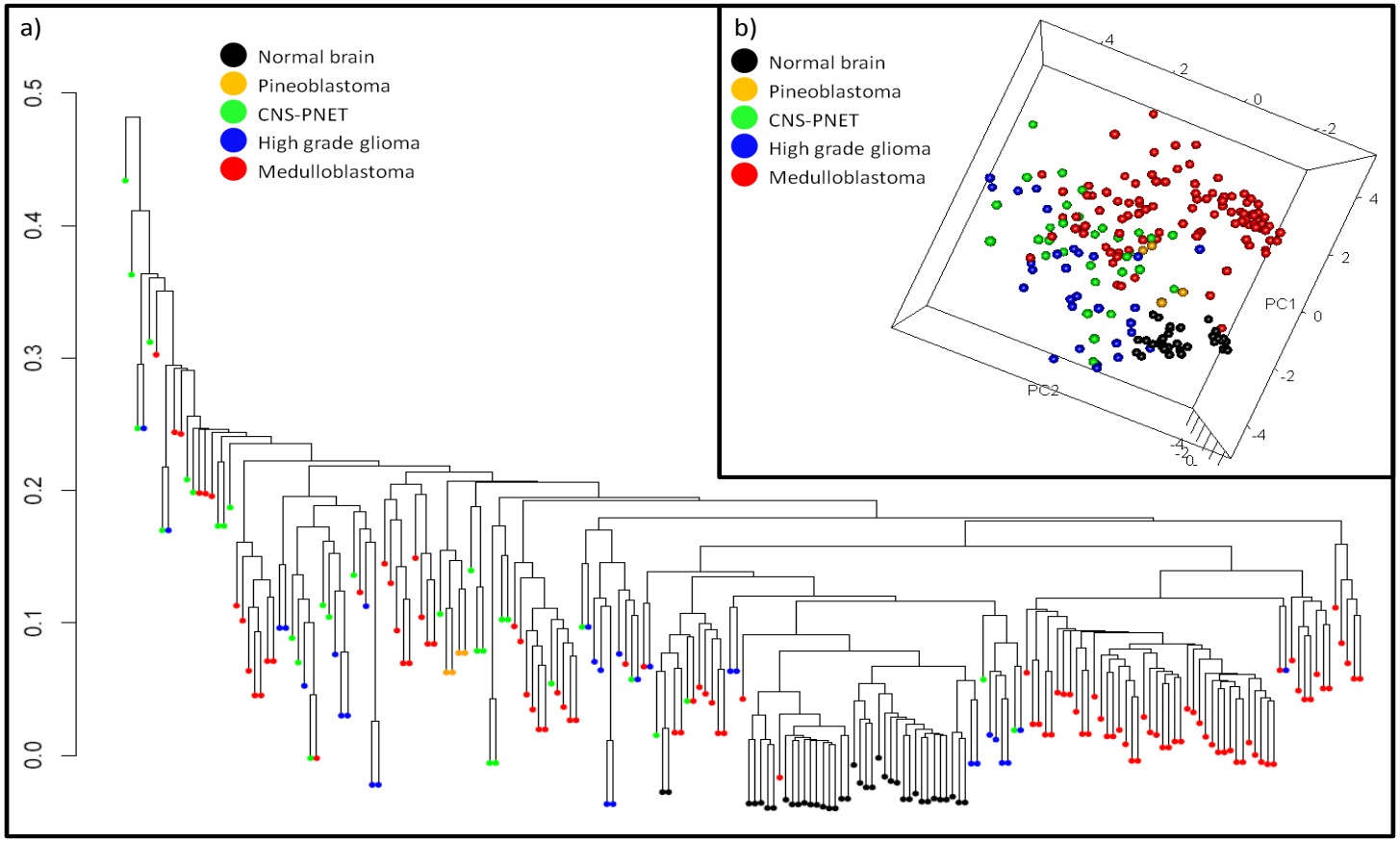

Figure 5.21 Comparison of methylation in CNS-PNET and a panel of normal brain and primary malignant brain tumour samples. The methylation profile of 31 CNS-PNET samples compared with samples taken from the normal brain (n=37), paediatric high grade gliomas (n=29), medulloblastomas (n=100), and pineoblastoma (n=4).

5.4 Discussion

5.4.1 Epigenetic modification by methylation can be assessed using an array based approach in CNS-PNET

In this study the Illumina Goldengate platform was used for the first time to assess the methylation in CNS-PNETs. A high correlation of methylation scores was recorded between the Illumina Goldengate method and bisulphite sequencing, with a mean difference 0.006, and standard deviation 0.167. This finding is in concordance with the previously reported reliability and reproducibility of this method (Martin-Subero, Kreuz et al. 2009).

The cohort included samples derived from both frozen and formalin fixed paraffin embedded (FFPE) archival material. In total 3 samples failed the quality control (QC) requirements and were accordingly removed from the study. Overall, 95.2% (20/31) of the cases where DNA had been derived from frozen material, and 84.6% (11/13) of cases where DNA had been extracted from FFPE passed the QC and were included in the study. In the case of SP24, DNA was successfully extracted, used in the methylation array and passed the QC assessment from a 12 year old FFPE block. These findings confirm that epigenetic analyses may successfully be performed in archival material including archival FFPE, as has been previously reported (Killian, Bilke et al. 2009). Importantly this means that a large scale assessment of epigenetic diversity incorporating hundreds of genes may be made using this methylation platform where expression or CGH approaches requiring high quality DNA or RNA extracted from frozen material is not feasible. In the context of rare tumours such as CNS-PNETs for which studies necessitating material derived from frozen material may take over a decade to collate, crucially the successful application of this technology to FFPE archival material permits further contemporary large studies, with international collaboration, utilising libraries of archival FFPE material.

5.4.2 Genome-wide methylation changes in CNS-PNET are consistent with those reported in other cancers

Alterations in methylation patterns have been identified in most human cancers (Baylin and Herman 2000). It has been shown that genome-wide hypomethylation outside of CpG islands occurs during cancer development (Feinberg and Vogelstein 1983) and occurs across multiple tumour types (Kim, Jen et al. 1994; Cravo, Pinto et al. 1996; Soares, Pinto et al. 1999). In contrast, aberrant hypermethylation occurs particularly at CpG islands (Costello, Fruhwald et al. 2000; Jones and Baylin 2007). It has been estimated that on average 400 CpG islands are aberrantly methylated in tumours (Costello and Plass 2001). In this current study genome-wide methylation patterns in CNS-PNET were shown to be consistent with findings reported in other tumour groups. A statistically significant difference ($p<0.0001$) was observed when comparing the number of hypomethylated probes outside of CpG islands in CNS-PNETs (median 129, IQR 109-144) compared with the normal brain (median 79, IQR 67.5-84.5). Consistent with other studies, within CpG islands a statistically significant ($p=0.002$) increase in methylation of probes was observed in CNS-PNET compared with the normal brain (median 120, IQR 100-151 in CNS-PNET compared with median 101, IQR 96-106 I the normal brain). Methylation of genes within CpG islands may inactivate tumour suppressor genes or inactivate DNA repair genes which both may result in tumour development (Strathdee and Brown 2002) and therefore the findings in this current study in CNS-PNET support the hypothesis that hypermethylation at CpG islands is implicated in CNS-PNET tumorigenesis.

5.4.3 CNS-PNETs are a heterogenous group of tumours

CNS-PNETs are commonly regarded as a heterogenous group of tumours (Eberhart 2011) for which no accepted classification of subgroups exists. The investigation of the methylation profiles of CNS-PNETs afforded the opportunity to ascertain whether distinct subgroups do exist in relation to this tumour. As outlined in section 5.1.2, the

Goldengate methylation array has been used to identify altered methylation patterns in a spectrum of tumours and more detailed examination of the methylation profiles in some tumours, including breast, colorectal, AML and testicular, have also revealed distinct subgroups (Ang, Loh et al. 2010; Cheung, Lee et al. 2010; Figueroa, Lugthart et al. 2010). Investigation of the methylation patterns in CNS-PNET using unsupervised clustering methods (principal component analysis and bootstrapping) in this study did not however identify distinct subgroups. This study was however limited by the availability of tumour material, and therefore distinct subgroups may exist but the study failed to identify them as there were insufficient cases. Additional studies analysing CNS-PNETs with other brain tumours did however provide critical insights into the heterogeneity in this disease (see section 5.4.8).

5.4.4 Age related methylation patterns in CNS-PNET

Infants, under the age of 3 years, with a CNS-PNET are treated differently to older children and adults, but have an inferior prognosis (reviewed in section 1.4.4 and 1.4.5). Infant protocols limit the use of radiotherapy to avoid the devastating neurological consequences that arise following delivery of cranial irradiation to the developing brain (reviewed in section 1.4.5.3). CNS-PNETs are however radio-sensitive tumours and therefore it could be hypothesised that the poor outcome seen in young children may result from the inability to deliver effective treatment, rather than because of biological differences in the disease at different ages.

In this study however, it has been shown that whilst the methylation profiles of CNS-PNETs overall do not differ at different ages, isolated age-specific methylation events do occur. Using the 76 CNS-PNET specific probes (identified in section 5.3.6), probes for three genes were found to be statistically significantly associated with age at diagnosis. Hypomethylation of TAL1_E122_F, MAP3K1_E81_F and IGFBP1_E48_R were found to occur in infant tumours, whilst in CNS-PNETs arising in older children and adults these probes were typically methylated (p=0.027, p=0.027, p=0.043 respectively). In the normal brain cohort, comprising both infant and adult cases (24%

(9/27) < 3 years and 73% (27/37) > 3 years), the probes are universally hypomethylated. The hypomethylation of probes *TAL1*, *MAP3K1* and *IGFBP1* in infant CNS-PNET cases indicates methylation occurring in older patients is a tumour-specific aberration and not a normal feature of age in brain tissues.

The identification of variable patterns of methylation correlated with age of onset supports the hypothesis that differences in the clinical outcomes of patients with CNS-PNETs at different ages reflects fundamental differences at the genetic level. Investigation of the role that *TAL1*, *MAP3K1* and *IGFB1* have in CNS-PNET tumorigeneisis in older children did not form part of the current study, but is work that should now be undertaken.

5.4.5 Methylation patterns associated with metastatic disease in CNS-PNET

A number of genes have been identified that inhibit cell growth and tumour invasion which may act as metastasis suppressor genes (Reviewed in (Esteller 2005)). Methylation of tissue inhibitors of proteases (TIMPs), cadherin genes or laminin genes have all previously been identified in a number of cancers including gastric, colorectal, breast, lung, prostate bladder, pancreatic and gliomas and have been associated with advanced disease (Konduri, Srivenugopal et al. 2003; Sathyanarayana, Padar et al. 2003; Miotto, Sabbioni et al. 2004; Sato, Parker et al. 2005).

In this study no aberrant methylation events were found to be significantly associated with metastatic disease. An involvement of epigenetic modification by DNA methylation in the metastatic potential of this disease, cannot however be excluded. The CNS-PNET cohort in this study comprised 31 cases for which a Chang score was assigned in 90% (28/31). A significant finding may not have been obtained because the study was relatively underpowered. It is also possible that a significant result was not identified because the cohort contained archival material. In this study material was obtained prior to the introduction of the routine cytological examination of CSF to

determine microscopic metastatic disease, and accordingly in 68% of cases an M0/1 status was assigned. Cases with an M0/1 Chang score were categorized as being non-metastatic, in accordance with convention when analysing historical samples in this disease (Pizer, Weston et al. 2006). Regrettably it is plausible however that in some of these cases, had a CSF sample undergone a cytological examination, that evidence of metastatic disease would have been identified, the tumour classified as M1 and analysed with other known metastatic cases. The non-metastatic group may therefore have been contaminated with metastatic cases reducing the likelihood of identifying a difference between these 2 groups. In summary, it is conceivable that a falsely negative result (type II error) has been obtained in this study, and that it may be possible to determine methylation markers associated with metastatic disease in future larger, precisely clinically characterised cohorts.

5.4.6 Identification of genes that may be implicated in CNS-PNET survival

In this study, epigenetic modification by methylation in CNS-PNET was investigated across 1505 probes incorporating 807 genes known to be implicated in tumorigenesis. This has enabled the most extensive investigation to date, of the effect of methylation on survival in this disease. Clinical data were available on 26 CNS-PNET cases to perform a survival analysis. The subsequent survival analysis was therefore constrained by the cohort size and therefore permitted a relatively underpowered study. In addition the cohort contained both archival material as well as samples from current cases (range 1-112 months, median 24 months) resulting in early censorship in a proportion of cases which further limited the capacity of the study to identify survival characteristics.

Nonetheless, univariate analysis identified 9 genes that may be associated with survival. These included *TRIM29*, *HTR1B*, *MOS*, *ITK*, *MMP9*, *PGR*, *SIN3B*, *SLC6AE* and *WEE1*. After correction for multiple testing and calculation of the false discovery rate,

none of these probes remained significant at the 5% level. It can therefore only be concluded that these genes may be associated with survival in CNS-PNET, but require further study in larger series to substantiate any survival effect.

5.4.7 Using methylation as a diagnostic tool

Alterations in the methylation status for specific genes are currently being evaluated for use in diagnosis and screening disease in a range of cancers including breast, lung, prostate, gliomas and colorectal oral cancers (Goldenberg, Harden et al. 2004; Tokumaru, Harden et al. 2004; Sunami, Shinozaki et al. 2009; Al-Moghrabi, Al-Qasem et al. 2011; Hinoue, Weisenberger et al. 2011; Radhakrishnan, Kabekkodu et al. 2011).To date, the assessment of specific genetic features does not form part of the diagnostic protocol for investigating suspected CNS-PNETs. The findings from this study suggest that a targeted methylation analysis of 2 genes may be of clinical diagnostic value. Specifically, probes for the *RASSF1* and *HLA-DPB1* genes were found to be aberrantly methylated in CNS-PNET. Hypomethylation of RASSF1_E116_F and hypermethylation of HLA_DPB1_E2_R was found to occur in all normal brain samples (37/37). In CNS-PNET samples, RASSF1_E116_F became hypemethylated or HLA_DPB1_E2_R became hypomethylated in 87% (27/31). In total the determination of methylation status of RASSF1_E116_F and HLA_DPB1_E2_R correctly identified 94% (64/68) of samples as either normal brain tissue or CNS-PNET. Unfortunately however, a second panel of tumours and normal brain samples was not available to perform a validation study which is required to confirm that these findings are reproducible in different cohorts, work which now needs to be undertaken.

Aberrant methylation of the *RASSF1* and *HLA-DPB1* genes is not CNS-PNET specific. As has been discussed previously (section 1.5.6 and section 3.4.2) hypermethylation of the *RASSF1A* promoter is a feature observed in many paediatric and adult tumours, and in the context of CNS embryonal tumours has been shown to be a frequent event in both CNS-PNET and medulloblastoma (section 3.4.1). Increased expression of HLA-DPB1 has been associated with cervical cancers and pilocytic astrocytomas (Huang,

Hara et al. 2005; Liang, Xu et al. 2008), and aberrant methylation observed to be a feature of renal tumours (McRonald, Morris et al. 2009). Whilst identification of aberrant methylation of RASSF1_E116_F or HLA_DPB1_E2_R may therefore signify deviation from the normal tissue and the presence of disease, they cannot be employed to determine specifically whether the disease process is a CNS-PNET.

Should aberrant methylation of *RASSF1* and *HLA-DPB1*, following further validation studies, be confirmed to be tumour-specific events in CNS-PNET, then these findings will represent the most frequent genetic abnormalities identified to date in this disease. The high frequency (87%) in which aberrant methylation of *RASSF1* or *HLA-DPB1* occurs in CNS-PNET suggests that the probes on these 2 genes are potentially significant novel disease markers which may have clinical applicability and warrants further investigation. This study has identified aberrant methylation of RASSF1_E116_F or HLA_DPB1_E2_R in tumour tissue but, as will be discussed further in section 5.4.9, this should be investigated in blood and CSF samples. If aberrant methylation was identified in circulating DNA either in the blood or CSF in patients with CNS-PNETs, then analysing the methylation of these probes may have a considerable clinical utility in monitoring treatment response and diagnosing progression or relapse.

5.4.8 Pineoblastomas and CNS-PNETs are distinct entities

Reviewed in section 1.3.4, following the review of CNS tumours by Hart and Earle in 1973 and the development of the PNET concept, pineoblastomas and CNS-PNETs arising at other supratentorial non-pineal sites were co-classified as suprtatentorial PNETs (SPNETs) (Hart and Earle 1973; Becker and Hinton 1983). In the second WHO CNS tumour classification system, and maintained in subsequent revisions, pineoblastomas were removed from the PNET group and reclassified as pineal parenchymal tumours along with other pineal tumours (Kleihues, Burger et al. 1993). These tumours have however continued to be both investigated and treated alongside CNS-PNETs.

In this study the methylation profiles of 31 primary CNS-PNETs was compared with that of 4 primary pineoblastomas. The four pineoblastomas, using either PCA or hierarchical clustering unsupervised analyses, were shown to co-cluster (Figure 5.17). The methylation profiles of these tumours were thus shown to have more in common with each other than with CNS-PNETs. The CNS-PNET with a profile that was most similar to that observed in pineoblastomas was SP113. SP113 originated from an 11 year old boy with non-metastatic disease at diagnosis who subsequently died from his disease. Unusually, the tumour had both infratentorial and supratentorial components occurring in the posterior 3rd ventricle and subthalamic region of the left lateral ventricle.

Despite the pineoblastoma comparator group containing a restricted number of tumours, the findings of this study suggest that pineoblastomas are a separate group of tumours. In addition, this study has shown that pineoblastomas may be distinguished from other supratentorial aggressive brain tumours by investigation of their methylome. Finally, this study provides new evidence to support the classification change and distinction between CNS-PNETs and pineoblastomas.

5.4.9 CNS-PNET and medulloblastoma exhibit divergent methylation profiles

The methylation profiles of 100 primary medulloblastomas were compared with those from 31 primary CNS-PNETs. This study showed a predominantly divergent pattern in methylation between the 2 groups of embryonal tumours. As shown in Figure 5.19, after removal of the outliers (9/100, group A) in total only 4 medulloblastomas (4/91, 4.4%) co-located in the CNS-PNET groups, and three CNS-PNETs (3/31, 10%) with medulloblastomas. The methylation profiles of these 2 groups of tumours in this study have therefore been shown to differ significantly. This finding of divergent methylation profiles corroborates similar conclusions made in previous smaller studies supporting separate classification and treatments. Differences in epigenetic modifications

between medulloblastomas and CNS-PNETs were highlighted in a study investigating a microRNA cluster. Amplification of the C19MC microRNA cluster on chromosome 19q13.41 was identified in 24% (11/45) of CNS-PNETs but not in other paediatric brain tumours, including 118 medulloblastomas, 34 high grade gliomas and 111 ependymomas (p=0.0001) (Li, Lee et al. 2009). Aberrant methylation of the $p14^{ARF}$ promoter has been shown to be a feature in CNS-PNETs, but not in medulloblastomas (Inda, Munoz et al. 2006). In addition, a number of other studies have previously identified aberrant methylation of particular genes (see section 1.5.6) in CNS-PNETs, but these have been in small cohorts which have impaired the capacity of such studies to make significant comparisons with other tumour groups, and in particular medulloblastomas.

5.4.10 Co-clustering with medulloblastomas in isolated cases is significant

Whilst, as described in section 5.4.9, predominantly divergent methylation patterns were observed between CNS-PNET and medulloblastomas, in a few isolated cases similar profiles were derived. The identification of tumours which have similar profiles may have significant implications for both understanding the biology and improving treatments for these tumours.

SP10 was found to co-cluster with the group of medulloblastomas with aberrant Wnt signalling. This sample was taken from a 13 year old male with a 3rd ventricular CNS-PNET with non-metastatic disease and who is alive 9 years following diagnosis. In chapter 3 molecular analysis of SP10 also revealed evidence of aberrant Wnt signalling, with the nuclear accumulation of β-catenin. Unfortunately this was an isolated case, and therefore it cannot be determined whether aberrant Wnt signalling and clustering within the Wnt group confers a significantly different prognosis and a superior outcome as has been demonstrated in medulloblastoma (Cho, Tsherniak et al. 2010; Northcott, Korshunov et al. 2010).

Two cases (SP124 and SP125) clustered with the aberrant SHH signalling group of medulloblastomas. Both of these tumours originated in the suprasellar region of females aged 14 months and 12 years of age respectively, who are both alive but with limited follow up (24 and 3 months respectively). In medulloblastoma this group of tumours has been shown to have an outcome that is intermediate between the Wnt group and other medulloblastomas (80%, 10 year overall survival) (Northcott, Fernandez et al. 2009) but the significance in CNS-PNET has not been established.

The co-clustering of isolated CNS-PNET cases with SHH and Wnt MB tumours are novel findings which require further investigation. This result suggests that in a small proportion of cases CNS-PNETs and medulloblastomas may share similar genetic features. It is thus conceivable that these cases may continue to benefit from similar treatments to those used and being developed to treat medulloblastoma. Furthermore this study provides a rationale to extend the ascertainment of Wnt status, determined immunohistochemically by screening for the presence of nuclear β-catenin, which is now routinely performed in the management of children with medulloblastomas, to include CNS-PNETs. When similar methods have been evaluated and validated to assess the SHH pathway in medulloblastomas, it would be potentially advantageous for these to be applied in addition to CNS-PNETs.

5.4.11 Methylation analysis identifies overlap with high-grade gliomas

High-grade gliomas (HGGs) account for 8-12% of all brain tumours arising in childhood (Bondy, Scheurer et al. 2008) and arise throughout the brain but most commonly at supratentorial sites. Histologically the most frequently HGGs are either anaplastic astrocytomas (AA) (WHO grade 3) or glioblastoma multiforme (GBM) (WHO grade 4) (Fangusaro 2009). The survival from these tumours is dismal with overall survival rates of 20-40% and 5-15% at 5 years for AAs and GBMs respectively (Tamber and Rutka 2003), although in a recently report superior outcomes have been described in a

subgroup of infants (Sanders, Kocak et al. 2007). Clinically, high grade gliomas and CNS-PNETs can be difficult to discern (Burger 2006). The clinical course and management of these tumours however differ significantly. The methylation profiles of 31 CNS-PNETs and 29 paediatric high grade gliomas were therefore assessed to investigate the relationship between these two tumour groups and the results given in section 5.3.11.3.

The methylomes of HGGs and CNS-PNETs, as shown in Figure 5.20, were found not be mutually exclusive, but exhibited substantial overlap. In contrast to the study with medulloblastomas (discussed in section 5.4.9) it is not possible to distinguish CNS-PNETs from high grade gliomas by analysis of their global methylation patterns using the Illumina Goldengate methylation array cancer panel I. To further elucidate and validate this phenomenon the methylation profiles of the HGGs and CNS-PNETs were also compared with a normal brain panel and with medulloblastomas. When investigated alongside the panel of 100 medulloblastoma samples (described in section 5.2.3.2) in contrast to the relationship observed with CNS-PNETs, the HGGs and medulloblastomas form distinct and mutually exclusive clusters (Figure 5.22). Comparison with the normal brain cohort (Figure 5.20), which includes samples taken from diverse CNS locations including from both the supratentorial and infratentorial compartments (further details given in section 5.2.2), showed the normal brain samples to form a separate cluster. This in turn suggests that the differential methylation patterns observed therefore between the normal brain and CNS-PNETs, high-grade gliomas or medulloblastomas, reflect a fundamental difference in methylation due to the cancerous process rather than a discrepancy attributable to the site of origin.

The co-clustering between HGGs and CNS-PNETs observed in this study is also supported by the hypothesis that brain tumours may arise from neural stem cells. In a study by Singh et al, CD133 and nestin (neural stem cell surface markers) were identified in gliomas, suggesting that both neuronal and glial neoplastic cells may arise from a common neural stem cell (Singh, Clarke et al. 2003) and from this a multi-potent brain tumour stem cell (BTSC) may arise (Singh, Clarke et al. 2004). These

findings are also consistent with the “cancer stem cell hypothesis”, in which tumours are considered to arise from such stem cells capable of self-renewal, differentiaition along multiple lines, and possess an ability to migrate throughout the brain parenchyma (Wicha, Liu et al. 2006). It has recently also been shown that PNET or glial tumours may arise from the same stem cell following different combinations of genetic events (Jacques, Swales et al. 2010). In this study recombination of PTEN/p53 was shown to give rise to gliomas whilst deletion of Rb/p53 resulted in PNETs. It is therefore conceivable that the co-clustering between CNS-PNETs and HGGs may reflect a similar origin, which requires further investigation.

In addition to the histopathological similarities that occur in some cases between HGGs and CNS-PNET resulting in the diagnostic challenge illustrated by Burger (Burger 2006), there is evidence that this overlap may have clinical significance. Glial differentiation has been shown previously to be associated with an adverse outcome in CNS-PNET (Janss, Yachnis et al. 1996). In their investigation of 86 PNET tumours (11 CNS-PNETs and 75 MBs), GFAP immunohistochemical staining, a feature of glial differentiation, was identified in 52 (52/86, 60%) and associated in a Cox model with a 6.7 fold increased risk of relapse and an adverse outcome. Furthermore, in a series of predominantly case reports tumours with combined features of HGGs and CNS-PNET have been described (Wharton, Whittle et al. 2001; Ishizawa, Kan-nuki et al. 2002; Kepes 2002; McLendon and Provenzale 2002; Dulai, Bosanko et al. 2004; Kaplan and Perry 2007; Kandemir, Bahadir et al. 2009). Recently a review of 53 such cases, predominantly arising in adults (range: 12-84 years, median: 54 years) of HGGs with CNS-PNET components has been reported, and such tumours were found to be highly aggressive and conferring a median survival of only 9 months (Perry, Miller et al. 2009). In contrast to HGGs where only 1.1% are reported to be metastatic at diagnosis (Stark, Nabavi et al. 2005), but in common with CNS-PNETs, 40% of these tumours were metastatic at diagnosis. In this report the authors also commented that in three patients who failed to respond to HGG therapy with radiation and temozolamide, a response was recorded when their treatment was changed to included platinum-based chemotherapy, as is routinely used in CNS-PNET management. This study therefore

highlights the potential that the combination of histopathological features and tumour behaviour characteristics in this group of tumours can have on clinical management.

Evidence for an inter-relationship between HGGs and CNS-PNETs has been demonstrated in this study, which now requires further investigation. Crucially, the relationship between HGG and CNS-PNET tumours may provide novel opportunities for the development of an enhanced classification but also in the management of patients with these tumours. These concepts will be explored in further detail in chapter 6.

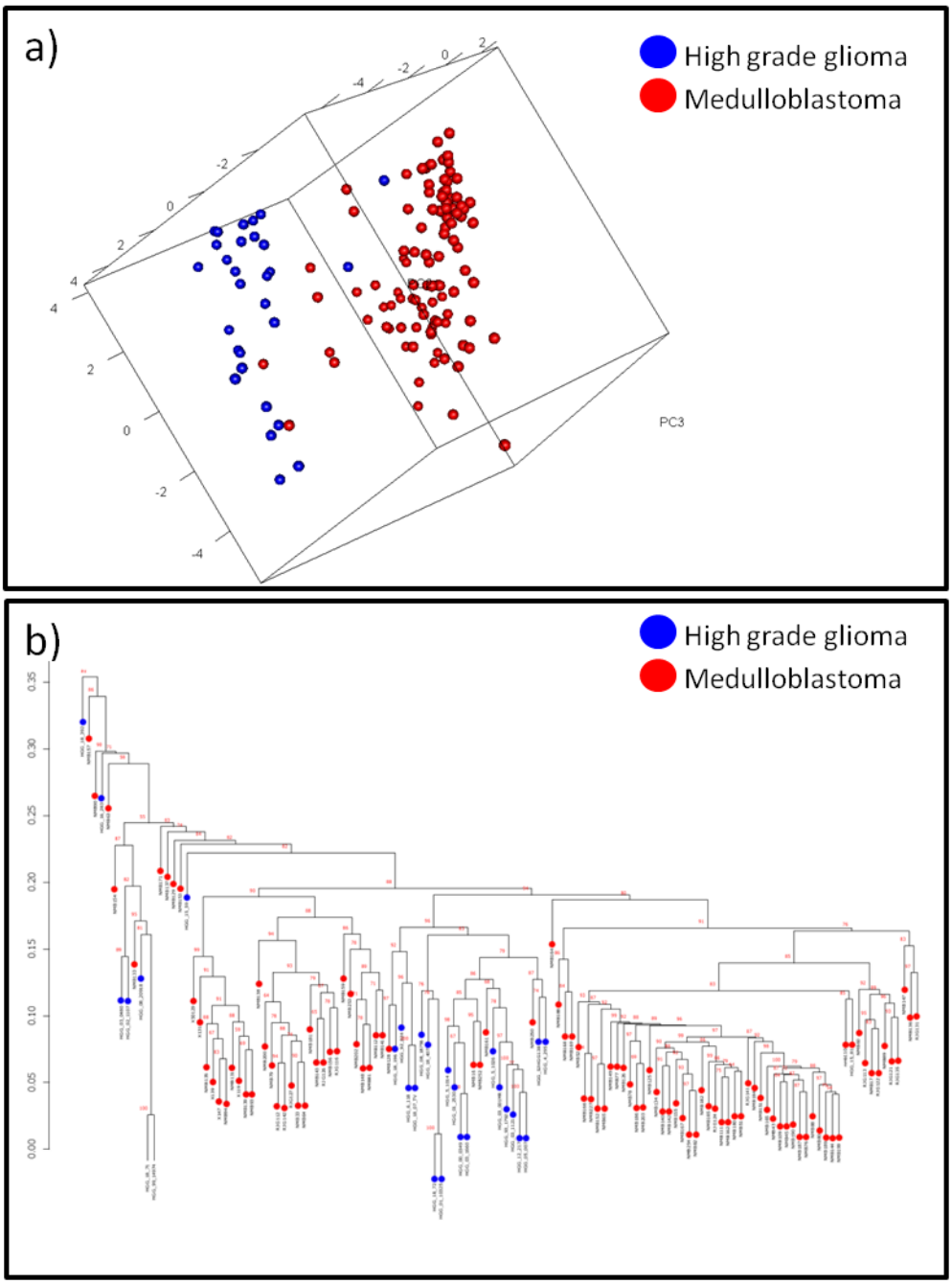

Figure 5.22. Unsupervised analysis showing distinct methylation profiles of high grade gliomas, and medulloblastoma. (a) Principal component analysis, (b) Hierarchical clustering bootstrapped dendrograms.

5.4.12 The future role of methylation in CNS-PNET research

This study has provided the most extensive and detailed investigation into the methylome of CNS-PNETs to date. In common with other cancers, alterations in DNA methylation appear to be frequent events in CNS-PNET. These investigations have afforded a number of critical insights into this disease which warrant further investigation and may have clinical utility.

As part of this study a list of the most frequently aberrantly methylated genes has been generated (section 5.3.6, Table 5.8 and Table 5.9), which has provided evidence for a wider range of genes being epigentically modified in this disease than had previously been described. Investigating the potential role these candidate genes may have in the tumorigenesis of CNS-PNETs was beyond the scope of this study, but could form the basis for important further work.

In this study, two of the most frequently aberrantly methylated genes, *RASSF1* and *HLA-DPB1*, were found in combination to be able to discern normal brain tissue from CNS-PNET (section 5.3.10 and discussed in section 5.4.7). One of the potential future roles for such methylation markers in CNS-PNET would be to detect the presence of residual disease or disease progression. Tumour specific methylation markers as well as being found in the tumour tissue may also be present in other samples including sputum, urine, plasma, stool and saliva (Miyamoto and Ushijima 2005). These may be obtained less invasively making them more suitable for follow up screening. Recently however it has also been shown that cell free tumour DNA can be obtained from sampling of cerebrospinal fluid in patients with brain tumours (Liu, Cheng et al. 2010). In a study of 66 high grade gliomas the methylation profiles of 4 candidate genes (*MGMT*, $p16^{INK4A}$, *TIMP3* and *THBS1*) were analysed in the tumour, DNA and CSF (Liu, Cheng et al. 2010). No aberrant methylation was observed in a panel of 20 normal samples. Hypermethylation of CSF DNA was accompanied with hypermethylation in the corresponding tumour with 100% specificity, and hypermethylation of *MGMT* and *THBS1* in the CSF were found to be independent prognostic markers. In the context of CNS-PNET management, the presence of hypomethylation of the *HLA-DPB1* marker

(HLA_DPB1_E2_R) or methylation of the *RASSF1* marker (RASSF1_E116_F) in CSF derived DNA could provide useful information in determining response to therapy and re-emergence of these markers could be used in predicting recurrence. Studies to determine whether tumour DNA is present in the CSF in patients with CNS-PNETs and specifically whether these markers are evident would form an important extension of this current work.

Methylation markers may also be used to identify high risk tumours and to monitor response to treatment. In breast, bladder and lung cancers for example, DNA methylation profiling has been used to predict prognosis (Silva, Dominguez et al. 1999; Palmisano, Divine et al. 2000; Hoque, Begum et al. 2006; Belinsky, Schiller et al. 2008; Levenson 2010; Wen, Fu et al. 2011; Yamamoto, Nakayama et al. 2011). Furthermore, therapeutically DNA methylation patterns have been shown to predict response to chemotherapy agents. In the management of high grade gliomas for example, methylation of the *MGMT* promoter is associated with an improved response to alkylating agents such as temozolamide (Hegi, Diserens et al. 2004; Stupp, van den Bent et al. 2005). The prognostic impact *MGMT* methylation status has in this disease has resulted in a treatment stratification being proposed to reduce the exposure of alkylating drugs to those with a hypomethylated MGMT status (Stupp, Hegi et al. 2010). In other tumour groups including ovarian, breast, oesophageal and gastric, aberrant methylation of different genes have also been shown to predict response to treatment (Wei, Brown et al. 2003; Suzuki, Yoshida et al. 2007; Brabender, Arbab et al. 2009; Chaudhry, Srinivasan et al. 2009; Hartmann, Spyratos et al. 2009). The current study has provided a precedent for using methylation markers to predict survival in CNS-PNET. Further evaluation of the aberrantly methylated genes identified in this current study may therefore yield clinically significant methylation markers which can be used in CNS-PNET management.

In contrast to genetic events, epigenetic modifications are potentially reversible which renders aberrant methylation a highly desirable exploitable chemotherapeutic target. In two recent reviews the progress in targeting DNA methylation to develop novel anticancer therapies is described (Yang, Lay et al. 2010; Ren, Singh et al. 2011).

Following experiments which showed that genetic silencing by DNA hypermethylation can be reversed using the DNA methyltransferase inhibitor (DNMTi) azacytidine (or 5-Aza-CR) (Plumb, Strathdee et al. 2000), a series of drugs have now been developed and are currently being evaluated (Yang, Lay et al. 2010; Ren, Singh et al. 2011). 5-Aza-CR and the deoxy analogue deoxycytidine (5-Aza-CdR) for example, have been shown to be effective in acute myeloid leukaemia and myelodysplastic syndromes (Kornblith, Herndon et al. 2002; Bots and Johnstone 2009). Such agents may have a role to play in the management of patients with CNS-PNET to impair growth and restore normal cellular functions by demethylating genes that have become hypermethyalted in the cancer process. However, as has been illustrated in a study in pancreatic cancer where the use of Aza-CR resulted in stimulation of the metastatic potential through activation of genes promoting tumour invasion, these drugs are not without potentially significant side effects (Sato, Maehara et al. 2003). In the context of CNS-PNET, a disease of early childhood with two-thirds of such tumours occurring before the age of 5 (Jakacki, Zeltzer et al. 1995; Louis, Ohgaki et al. 2007), such side effects may also arise from alterations to pathways essential for normal development.

Finally this research, as has been discussed in sections 5.4.8, 5.4.9, 5.4.10 and 5.4.11 has provided critical insights into the relationship between CNS-PNETs and other highly malignant brain tumours. This work has shown that CNS-PNETs are predominantly a distinct group of tumours to medulloblastomas, that share a similar to methylome to HGGs, but that in isolated cases may be indistinguishable from some of the recently identified medulloblastoma subgroups. These findings have applicability not only to disease classification, but may also provide rationales for divergent treatment regimens within the same tumour group based on their genetic features. Further research that seeks to investigate and advance our understanding of these inter-relationships may therefore also yield evidence for future clinical exploitation.

Chapter 6

Discussion

Table of contents

Chapter 6

6.1 Background and project summary

CNS-PNETs are the second most common CNS embryonal tumour, which occur predominantly in early childhood and account for 2-3% of all paediatric brain tumours (Bruno, Rorke et al. 1981; Gaffney, Sloane et al. 1985; Jakacki, Zeltzer et al. 1995). Whilst the overall five year survival rate for children with cancer continues to improve and is now 75% (ONS 2010), the prognosis for children with CNS-PNETs remains dismal. Despite aggressive multi-modal therapy in children over the age of 3 years, the 3 year progression free survival remains only 34-54% (Timmermann, Kortmann et al. 2002; Massimino, Gandola et al. 2006; Pizer, Weston et al. 2006), whilst for infants under the age of 3 years survival rates are consistently under 20% (Duffner, Horowitz et al. 1993; Marec-Berard, Jouvet et al. 2002; Timmermann, Kortmann et al. 2006; Grundy, Wilne et al. 2010). New therapies are urgently required to improve the outcome of children who develop this catastrophic disease.

Following the review of CNS tumours by Hart and Earle in 1973 (Hart and Earle 1973), and the origination of the term "primitive neuroectodermal tumour" (PNET), CNS-PNETs have been treated along similar lines to other brain "PNETs" (medulloblastomas) in view of their similar histopathological features. Contemporary treatment protocols now cure over 70% of children with medulloblastoma, but such improvements have not been realised using the same treatments in those with a CNS-PNET (Taylor, Bailey et al. 2003; Pizer, Weston et al. 2006; Pizer and Clifford 2008). Clinically therefore, these tumours, despite sharing common histopathological features and a classification system that suggests a unifying origin, appear to be separate entities requiring distinct therapeutic strategies. The "PNET hypothesis" which has been at the heart of how these tumours are investigated and managed for the last three decades, therefore may be invalid.

To date, research into the molecular basis for CNS-PNET development and their relationship with medulloblastomas and other brain tumours has been limited. Loss of chromosome 17p, which is seen in up to 40% of medulloblastomas (McDonald, Daneshvar et al. 1994; Burnett, White et al. 1997), has only rarely been observed in

CNS-PNET (Roberts, Chumas et al. 2001; Bayani, Pandita et al. 2005). *MYC* family gene amplification, which occurs in 15-25% of medulloblastomas and is associated with the large cell / anaplastic subtype and a poor prognosis (Leonard, Cai et al. 2001; Lamont, McManamy et al. 2004; Vita and Henriksson 2006; Pfister, Remke et al. 2009), has only been investigated in a few small studies and found to occur in CNS-PNET in approximately 5% of cases (Fruhwald, O'Dorisio et al. 2000; Pfister, Remke et al. 2007; Behdad and Perry 2010). Conversely, aberrant Wnt signalling is associated with a favourable prognosis in medulloblastoma disruption (Ellison, Onilude et al. 2005; Gajjar, Chintagumpala et al. 2006; Fattet, Haberler et al. 2009; Ellison, Kocat et al. 2011) but the role in CNS-PNET is unclear (Koch, Waha et al. 2001; Rogers, Miller et al. 2009). Finally, in 2005 Eberhart et al discovered a significant difference between p53 pathway dysregulation in medulloblastomas and CNS-PNETs (Eberhart, Chaudhry et al. 2005). Dysregulation of the p53 pathway was suggested in 88% of CNS-PNETs, compared with 18% of classic medulloblastomas, but only 8 CNS-PNET cases were investigated (Eberhart, Chaudhry et al. 2005).

Epigenetic as well as genetic mechanisms have been shown to be implicated in the development of CNS-PNETs. In three small studies epigenetic modification by aberrant DNA methylation has revealed *RASSF1A* hypermethylation to occur in between 67 – 83% of cases (Chang, Pang et al. 2005; Muhlisch, Schwering et al. 2006; Inda and Castresana 2007). Whilst *RASSF1A* hypermethylation is the most frequent epigenetic event reported in CNS-PNET, previous studies have only investigated a small number of candidate genes (see table 1.12), and a detailed study of the DNA methylome in CNS-PNET disease has, however, never previously been undertaken.

The aim of this study was to investigate the molecular mechanisms involved in CNS-PNET development and determine their clinical and histopathological significance by; (i) investigating in CNS-PNETs the common genetic features associated with medulloblastomas, (ii) considering in CNS-PNETs novel genetic events determined through genome-wide studies in other brain tumours and, (iii) examining the DNA methylome in CNS-PNETs.

A panel of confirmed CNS-PNETs that had undergone a central pathological review were investigated in this study for a series of common medulloblastoma defects. Multiplex ligation-dependent probe amplification (MLPA) was used to determine the copy number of *MYCC* and *MYCN* in a cohort of 25 primary CNS-PNETs. An elevated copy number of *MYCC* was not identified in any case, but *MYCN* amplification was identified in 12% (3/25) and confirmed by quantitative real-time PCR and fluorescent in situ hybridisation (FISH). Nuclear β-catenin accumulation was assessed immunohistochemically to identify cases with aberrant Wnt pathway signalling. Direct sequencing of *CTNNB1* was also performed to detect the presence of characteristic mutations associated with aberrant Wnt signalling. Intense nuclear β-catenin accumulation suggesting aberrant Wnt signalling was identified in 2 cases (2/22, 9%) which was associated, in one of these cases, with a *CTNNB1* mutation providing evidence that aberrant Wnt signalling occurs in a small subset of CNS-PNETs. p53 pathway activation or disruption was determined immunohistochemically and observed in 91% (20/22). Additionally, direct sequencing of DNA identified *TP53* mutations in 18% (4/22) and, using MLPA, a copy number gain of *MDM2* in a further case, but no evidence of homozygous *CDKN2A* loss was found. Whilst limited by the study cohort size and treatment heterogeneity, neither Wnt or p53 pathway disruption was found to be correlated with survival, age at diagnosis or the presence of metastatic disease. Loss of chromosome 17p was assessed using the homozygous mapping of deletions (HOMOD) technique to identify loss of heterozygosity in 25 CNS-PNETs. In 2 cases a segmental loss was suggested by the presence of an extended region of heterozygosity, which was associated with a homozygous mutation of *TP53* (located at 17p13.1) in both cases. The final common feature in medulloblastoma investigated was *RASSF1A* DNA methylation. Direct sequencing of bisulphite converted DNA showed that *RASSF1A* hypermethylation in CNS-PNETs occurred at a similarly high frequency (82%, 18/22) to that which has previously been observed in medulloblastoma (Lusher, Lindsey et al. 2002; Lindsey, Lusher et al. 2004).

A genome-wide study by Balss et al (Balss, Meyer et al. 2008) which included 9 CNS-PNET cases suggested that mutations in *IDH1*, a novel tumour suppressor gene which

occur frequently in glioblastomas whilst do not appear to occur in medulloblastomas, may be a feature in CNS-PNET. Direct sequencing in this current study discovered *IDH1* mutations in 8% (2/25) of cases. Mutant cases were found to be associated with disease in adults but not CNS-PNETs arising in childhood (p=0.003), suggesting that the tumorigenesis of CNS-PNET arising at different ages differ (Hayden, Fruhwald et al. 2009).

Hypermethylation of *RASSF1A* was identified as the most frequent molecular event identified in CNS-PNET and therefore the CNS-PNET DNA methylome was investigated in detail in chapter 5 using the Illumina Goldengate methylation array platform. A series of 76 tumour-specific methylation events were identified including *RASSF1* hypermethylation and *HLA-DPB1* hypomethylation which in combination can be used to distinguish tumour from normal brain in 94% (64/68) of cases. Age-specific methylation patterns were also observed with aberrant methylation of *TAL1*, *MAP3K1* and *IGFBP1* being observed in CNS-PNETs arising in older children and adults (>3 years old). Unsupervised hierarchical clustering approaches using the methylation data showed CNS-PNETs to be a heterogenous group of tumours, which are predominantly distinct from medulloblastomas, but exhibit some overlap with high-grade gliomas. In isolated cases however, co-clustering with medulloblastomas occurs associated with known molecular subgroups (Wnt pathway and sonic hedgehog pathway activated tumours).

In summary, this project has provided support for the assertion that CNS-PNETs are a heterogenous group of tumours that are distinct from medulloblastomas, and has shown that they may possess a range of different genetic and epigenetic features that may differ in infant, childhood and adult disease.

6.2 The challenge of investigating CNS-PNET

The prognosis for patients diagnosed with a CNS-PNET is poor. New treatments are urgently required to resolve this problem but currently there is a paucity of biological information available on which to base the development of such therapies. These new therapies could potentially include stratified therapies based on molecular classification or targeted drugs. Unfortunately, as has been encountered in this study and described below, the investigation of CNS-PNETs is challenged by a number of factors.

Investigation of CNS-PNETs is firstly limited by their incidence. CNS-PNETs are rare tumours accounting for only 2-3% of all paediatric brain tumours (Bruno, Rorke et al. 1981; Gaffney, Sloane et al. 1985; Dai, Backstrom et al. 2003) and therefore accruing an adequately sized cohort requires sustained national and international collaboration. Such an undertaking was realised in this study and the CNS-PNET cohort was populated with cases from a 16 year period (1992 – 2008) from multiple centres across the UK and overseas (see section 2.1.1). Unfortunately this means that cases included have not been treated uniformly, but instead have been managed using a variety protocols from within and outside the clinical trial setting. The variation in treatment approaches may be a significant confounding factor and therefore results obtained in this study subsequently require validation in a clinical trial cohort.

The second challenging factor in CNS-PNET research results from changes in diagnostic practice and the frequent difficulties or uncertainty in confidently diagnosing this tumour. CNS-PNETs do not exhibit characteristic pathognomic features that permit the assured assignment to this disease category. On the contrary, CNS-PNETs are recognised to be a heterogenous group of tumours which may display a plethora of features attributable to their divergent differentiation, which may also be observed in other tumour groups and therefore creates diagnostic uncertainty (Burger 2006; Louis, Ohgaki et al. 2007). In the SIOP PNET3 study, for example, in 12% of cases the central pathological review did not confirm the tumour to be a CNS-PNET (Pizer, Weston et al. 2006). One of the tumour categories that have been misclassified as CNS-PNETs

previously are ATRTs (Haberler, Laggner et al. 2006). In accordance with current diagnostic practice, in the current study tumours were immunohistochemically screened for nuclear INI1 expression and excluded if this was absent, but misclassification of ATRTs as CNS-PNETs is possible in historical cases that have not undergone a pathological review.

Changes in disease risk stratification assignment, creates a third challenge. Over the 16 year period from which the cases in this study were collated the requirements for determining metastatic disease status changed. Presently, a CSF sample is taken 2 weeks after surgery and examined to detect the presence of malignant cells. In the absence of radiological evidence of metastasis, the presence of malignant cells in the CSF is classified as M1 disease using the modified Chang staging system (Zeltzer, Boyett et al. 1999) (see section 1.4.4). However, the cohort in this study contained cases collected prior to the routine assessment of CSF, and therefore in 68% (21/31) no radiological evidence of metastatic disease only could be reported (M0/1). Whilst conventionally in CNS-PNET the M0, M0/1 and M1 cases are analysed together as a non-metastatic group (Pizer, Weston et al. 2006), it has been shown in medulloblastoma that M1 compared with M0 disease is associated with a poorer outcome and should be considered high risk (Sanders, Onar et al. 2008). It is possible therefore that the capacity for the study to detect differences between non-metastatic and metastatic cases was impaired by contamination of the former group with cases that should have been assigned to the latter group if CSF analysis had been undertaken.

In summary, the future of CNS-PNET research requires that consented material is preferably obtained from within large international clinical trials based on a specified treatment regimen and includes a central pathological review as part of their entry criteria, to advance scientific discovery and improve outcomes.

6.3 CNS-PNETs are a heterogenous group of tumours

CNS-PNET are a group of aggressive tumours that may be poorly differentiated, or show divergent differentiation along neuronal, astrocytic and ependymal lines, and are accordingly defined as a heterogenous group of tumours based on these histopathological features (Louis, Ohgaki et al. 2007). This study has demonstrated that the histopathological heterogeneity observed is also reflected in their genetic and epigenetic composition.

In chapters 3 and 4, a series of molecular events were shown to occur in a proportion of CNS-PNETs. *MYCN* gene amplification was found to be present in 12.5% (3/24), *TP53* mutation in 17% (4/24), aberrant Wnt pathway activation in 2/21 (9.5%), and mutation of *IDH1* was identified in 8% (2/25) of cases. These findings suggest that a range of different pathways and molecular events are implicated in the tumorigenesis of different CNS-PNET.

Genome-wide study of the DNA methylome in CNS-PNET (chapter 5) confirmed the heterogeneity of this disease. Whereas in medulloblastoma, DNA methylation profiling results in 89% of tumours being assigned to one of 4 defined groups (see figure 5.1), unsupervised hierarchical clustering analyses of the DNA methylome in CNS-PNET did not reveal comparable discrete disease sub-clusters (see figure 5.7). Whilst CNS-PNETs were shown to have a different methylation profile to the normal brain, and were predominantly distinct from medulloblastomas comparison with high-grade gliomas revealed that, even after exclusion of outlier cases, a number of CNS-PNETs (SP14, SP58 and SP106) showed greater homology with this different tumour group than with other CNS-PNETs (Figure 5.20). However, the study cohort included only 31 CNS-PNETs and therefore it is feasible that the disease is not as heterogenous as this study suggests, and that distinct clusters and sub-groups do occur but that this study lacked sufficient power for this to be revealed. Further large-scale studies are therefore required to establish precisely the heterogeneity of this disease.

6.4 CNS-PNET genetic features vary at different ages

A significant disparity exists between the outcomes of infants and young children under the age of 3 years with CNS-PNET and older children and adults. In infants and young children, the 3 year even free survival (EFS) is dismal at 0-19% (Duffner, Horowitz et al. 1993; Timmermann, Kortmann et al. 2006; Grundy, Wilne et al. 2010) whereas the 3 year EFS in older children is 33-54% (Yang, Nam et al. 1999; Reddy, Janss et al. 2000; Timmermann, Kortmann et al. 2002; Paulino, Cha et al. 2004; Fangusaro, Finlay et al. 2008) and indeed an EFS of 78 ± 14% has been reported in this group in one study (Chintagumpala, Hassall et al. 2009). Whilst, as is discussed in section 1.4.5.3, the desirability of delivering effective radiotherapy to infants and young children may be a factor in the prognostic disparity, any biological reasons for this difference have not yet been fully elucidated.

It has recently been shown that CNS-PNETs arising in patients of different ages may possess different genetic abnormalities. Amplification of 19q13.42 was first shown in 2009 by Pfister et al, in a 2 year old girl with a CNS-PNET (Pfister, Remke et al. 2009). This abnormality has subsequently been found in an additional 48 cases, occurring in infants and young children under the age of 6 years (median age 2 years) (Li, Lee et al. 2009; Korshunov, Remke et al. 2010). In Chapter 3, genetic features frequently associated with medulloblastomas were investigated in the CNS-PNET cohort. None of these, including *RASSF1A* hypermethylation, *MYCN* gene amplification, p53 pathway defects, aberrant Wnt signalling, and chromosome 17p loss were found to be associated with age. However, whilst this was a comparatively large CNS-PNET study, the overall number of tumours investigated and those possessing an abnormality were often small, and therefore significant associations with age may exist, but the power of this study was insufficient to detect them.

In chapter 4, a novel study investigating *IDH1* mutations in CNS-PNET, found that mutations of *IDH1* occurred exclusively in adults cases. R132H mutations were observed in 2 of the 5 adult cases (26 and 29 years old), and not in any of the 19 paediatric (<16 years) cases (p=0.04, Fisher's exact test). When these data were

combined with the results of a previously published report including 9 CNS-PNETs (Balss, Meyer et al. 2008), this association was confirmed and *IDH1* mutations identified in 42% (5/12) of adult cases, but not in any paediatric cases (0/22)(p=0.003, Fisher's exact test). This study has therefore provided further evidence to support the hypothesis that the molecular mechanisms underlying tumour development differ at different ages. It has also shown for the first time, a significant difference in CNS-PNET biology between adult and paediatric disease.

Finally, the study investigating the CNS-PNET DNA methylome provided further evidence for age-specific features. Overall, tumours were not found to cluster based on age of onset (Figure 5.7), but an analysis of tumour-specific methylation events revealed statistically significant age-specific methylation of three genes. *TAL1*, *MAP3K1* and *IGFBP1* were all found to be consistently hypomethylated in infants under the age of 3 years, but exhibited variable methylation in older patients (p=0.027, p=0.027, p=0.043 respectively).

Overall, the biology of CNS-PNETs, including both genetic and epigenetic features has been shown to vary at different ages. Specifically, disease in infancy (< 3 years), older children (3-16 years) and adults (>16 years) have been shown to exhibit different biological features. That the biology of infant tumours differs from that in older children could explain in part the significant difference in clinical outcome that is observed between these two groups, and supports the need for developing distinct treatment strategies. The observation in this study that a distinction between adult and paediatric disease may also be determined is novel. This requires further investigation, but ultimately may suggest that CNS-PNETs in adults are a separate group of tumours that would benefit from a distinctive therapeutic strategy.

6.5 Methylation profiling in CNS-PNET

In this study, the Illumina Goldengate platform was used to assess the CNS-PNET DNA methylome in detail for the first time. The tumour cohort included samples derived

from both frozen and formalin fixed paraffin embedded (FFPE) archival material and data from both sources was successfully obtained. Large scale assessment of epigenetic diversity incorporating hundreds of genes using this platform is therefore feasible and, crucially, may provide information where expression or CGH approaches requiring high quality DNA or RNA extracted from frozen material are not possible.

Using this approach a series of genes have been discovered not previously known to be implicated in CNS-PNET development (see section 5.3.6), three of which appear to be age-specific (*TAL1*, *MAP3K1* and *IGFBP1*, see section 5.3.8.1). Similarly, this method has also identified two genes (*RASSF1* and *HLA-DPB1*, see section 5.3.10) which may have clinical utility as markers of disease. These now all require further analysis in follow up studies to validate these findings and substantiate any future clinical role.

Methylation profiling has also afforded an opportunity to examine the relationship between CNS-PNETs and other highly malignant brain tumours. CNS-PNETs have been shown to exhibit a methylation signature which, with few exceptions, is distinct from medulloblastomas, but more closely aligned to the HGG methylome. Discussed in section 6.6, this supports the assertion that the "PNET" concept does not adequately reflect the underlying properties of this group of tumours. Moreover, the histopathological similarities between HGGs and CNS-PNET, which create significant diagnostic challenges for the neuropathologist (Burger 2006), may occur as the these two tumour groups are indeed more closely related than is traditionally recognised.

6.6 PNET: A historical concept

The classification of embryonal brain tumours has always been both complicated and controversial which the WHO classification system sought to rectify and produce clarity but the difficulties persist. The term PNET, first applied in 1973 by Hart and Earle and later modified by others (Becker and Hinton 1983; Rorke 1983) was used to co-classify aggressive embryonal tumours based on their similar histopathological features, suggesting a common origin, and enabled unified treatment. Unfortunately,

the outcomes for patients managed with the same treatment with cerebellar and non-cerebellar disease, and in particular between what are now classified as medulloblastomas and CNS-PNETs (see section 1.3.3), have been shown to differ significantly. In the PNET3 study for example, the EFS at 5 years for patients with CNS-PNET was only 41%, compared with 74% for those with medulloblastomas (Taylor, Bailey et al. 2003; Pizer, Weston et al. 2006). This clinical outcome disparity suggests that the biological nature of these tumours may be fundamentally different, and that the concept of a PNET entity that may simply arise in different parts of the brain, may be false.

In chapter 3, genetic and epigenetic defects frequently observed in medulloblastoma were investigated in CNS-PNETs, to determine whether the differences seen in the clinical outcome between these tumour groups were also observed in their biology. In common with medulloblastomas where *RASSF1A* promoter hypermethylation has been shown to occur in 87% of cases (Lindsey, Lusher et al. 2004), *RASSF1A* promoter hypermethylation was found to be a frequent event CNS-PNET (18/22, 82%). Similarly *MYC* gene amplification which occurs in under 7% of medulloblastomas (Ryan 2009) occurred in a subgroup (*MYCN*: 3/25 (12%), *MYCC*: 0/25 (0%)). Both *RASSF1A* promoter hypermethylation and *MYC* gene amplification are however both events which occur in a spectrum of cancers (see sections 1.5.6.1 and 1.5.4.1 respectively), and therefore their discovery in CNS-PNET disease does not imply that these tumours are necessarily related. The results of the study of chromosome 17p loss and p53 pathway activation in CNS-PNET on the contrary support the assertion that medulloblastomas and CNS-PNETs are genetically different tumours. Loss of chromosome 17p was observed in only 2 of the 23 CNS-PNET investigated, compared with 25% of medulloblastomas (Ellison, Kocat et al. 2011). Conversely, p53 nuclear accumulation, which occurs infrequently in medulloblastomas (Eberhart, Chaudhry et al. 2005; Tabori, Baskin et al. 2010), occurred significantly more frequently in CNS-PNET (91%, 20/22, p= 0.0001 Fisher's exact test).

The investigation of *IDH1* mutations in CNS-PNET provided further evidence to support this fundamental difference between CNS-PNETs and medulloblastomas. In total, in 2

published studies, 113 medulloblastomas have been investigated for a mutation in *IDH1* (Balss, Meyer et al. 2008; Yan, Parsons et al. 2009) and no mutant case identified. In contrast, by combining the data from the current study and that reported by Balss et al (Balss, Meyer et al. 2008), 13.5% (5/37) of CNS-PNETs are found to harbour an *IDH1* mutation, which is statistically significantly more prevalent than in medulloblastoma (p=0.0007, Fisher's exact test).

Comparison of the DNA methylome using unsupervised clustering analyses in CNS-PNET with other brain tumours revealed not only that CNS-PNETs were predominantly distinct from medulloblastomas, but that they in fact shared greater commonality with high-grade gliomas. This finding suggests therefore that the PNET concept is not only incorrect but that it is a different relationship, the relationship between CNS-PNET and high-grade gliomas, which requires further exploration.

In summary, this thesis supports, through an extensive investigation and characterisation of the genetic and epigenetic features of these tumours, the rejection of the PNET hypothesis, and its place merely as a historical concept. The relevance of this finding is found however not only in respect to precise nomenclature and classification but also in the clinical management of patients with this disease. By determining that CNS-PNETs and medulloblastomas are different tumours and vary at the genetic and epigenetic levels, further support is provided for the expansion of disease specific research and the development of potentially divergent treatment strategies to advance and optimise outcome for both tumour groups.

6.7 Towards an improved classification of CNS-PNETS

Classification plays a vital and fundamental central role in both the study and clinical management of cancer. The WHO classification system was indeed originally established in 1979 to harmonize the plethora of systems and terms used to generate a consensus which would facilitate the study of tumours between different institutions internationally (Zulch 1979). The original WHO classification was based on

histopathological features, but now findings from additional techniques including immunohistochemical and molecular genetic analyses may be used to inform classification. Immunohistochemical lack of INI1 nuclear expression, for example, can be used to distinguish CNS-PNETs from ATRTs, which have an inferior prognosis and are treated differently, and therefore now forms part of the recommended routine diagnostic work up of these tumours (Haberler, Laggner et al. 2006). Sub-classification based on the results of genetic findings may also be used to improve outcomes by developing targeted or risk-adapted therapeutic approaches. In the management of childhood acute lymphoblastic leukaemia (ALL) for example, sub-classification based on genetic findings is used to identify cases that would benefit from molecular targeted therapies and those where a risk-adapted therapeutic approach is taken to improve outcome (Schrappe 2008; Harrison 2009; Moorman, Ensor et al. 2010).

In the current 4th Edition of the WHO classification of brain tumours CNS-PNETs are a designated as a group of embryonal tumours based on their histopathological features (Louis, Ohgaki et al. 2007). No subcategory of CNS-PNET to inform risk and treatment stratification currently exists, although a separate group of tumours, often classified as CNS-PNETs, with distinct pathological and genetic features has recently been proposed (see section 1.3.3). This study has identified a number of genetic and epigenetic events that suggest that CNS-PNETs sub-classification may be possible and could be used to aid in the development and delivery of improved therapeutic strategies.

Aberrant Wnt signalling, associated with a superior prognosis in medulloblastoma, has been shown in this study to occur in a minority (2/22, 9%) of CNS-PNETs. Whether aberrant Wnt signalling in CNS-PNET similarly confers a superior outcome which may, as has been proposed for medulloblastoma (Pizer and Clifford 2009), direct treatment strategy is unknown and requires further study. Unsupervised hierarchical clustering of DNA methylomic array data in this study also potentially identified a further sub-group of CNS-PNETs with aberrant SHH signalling. SP124 and SP125 (2/31, 6%) were found to co-cluster with a group of medulloblastomas with aberrant SHH signalling. This finding however requires further investigation including a detailed study of SHH pathway components and association with clinical features in larger cohorts. If validated,

molecular sub-classification could be adopted to direct alternative stratified therapies for the standard and higher risk tumours. Overall however, confirmatory studies in larger and, preferably, clinical trial based cohorts are now needed, to explore the utility of the genetic and epigenetic events discussed in determining future classification and treatment stratification.

6.8 Development of targeted therapies for CNS-PNET

Discussed in section 1.4.5.7, for over 50% of those who develop a CNS-PNET, this diagnosis is fatal, whilst in survivors the diagnosis is commonly associated with a syndrome of chronic morbidity attributable to the detrimental long-term effects of the curative treatment. New strategies are therefore urgently required in the management of this disease to improve survival whilst minimising treatment toxicities and late effects – the current *cost of cure* (Marder 2010). In this study, a series of biological pathways, genetic and epigenetic events have been shown to be involved in the development of CNS-PNETs. These findings not only contribute to enhance our understanding of the disparate biology in this disease, but may also be exploited clinically to aid in the clinical management and improve the prognosis for patients with CNS-PNETs.

Comparison with genetic features associated with medulloblastoma development identified a number of findings that may benefit CNS-PNET management in the future. Firstly, 91% of CNS-PNETs in this study were shown to exhibit nuclear accumulation of p53. Mutant p53 protein is known to confer resistance to vincristine and cisplatin (Hamada, Fujiwara et al. 1996; Shelling 1997; Giannakakou, Sackett et al. 2000), and as both of these drugs are currently used in the management of this disease, aberrant p53 may be a contributing factor in the dismal prognosis. In the future however, disruption of the p53 pathway may be exploited positively with the introduction of one of the p53 pathway targeted new agents that are currently under development (Lu and El-Deiry 2009). Disruption of the canonical Wnt signalling pathway as identified with

nuclear accumulation of β-catenin was determined in 2/22 (9%) primary CNS-PNET cases. In medulloblastoma such disruption is associated with a favourable prognostic phenotype and has directed the development of a stratified therapeutic strategy (Ellison, Onilude et al. 2005; Gajjar, Chintagumpala et al. 2006; Fattet, Haberler et al. 2009; Ellison, Kocat et al. 2011). Small molecule inhibitors such as OSU03012, which targets Wnt signalling (Baryawno, Sveinbjornsson et al. 2010), may also therefore provide a therapeutic option in CNS-PNET although further investigation of the role of Wnt signalling in this subgroup of CNS-PNETs is required.

Clinical opportunities may also be derived from studies of CNS-PNETs with other tumour groups. *IDH1* mutations do not appear to occur in medulloblastomas, but occur in a third of gliomas (307/917) and associated with an improved survival (Parsons, Jones et al. 2008; Bleeker, Lamba et al. 2009; Nobusawa, Watanabe et al. 2009; Watanabe, Nobusawa et al. 2009; Yan, Parsons et al. 2009). The investigation of *IDH1* mutations in CNS-PNET in this study (chapter 4) identified *IDH1* mutations as a potentially novel therapeutic target in adult disease. Agents currently under development which inhibit mIDH1 expression or downstream effectors (Semenza 2003; Sonoda and Tominaga 2010) may therefore also have a role in CNS-PNET management in the treatment of a subgroup with this genetic feature.

Methylation profiling in CNS-PNET (chapter 5) has yielded a number of findings that may have clinical utility. Firstly a number of tumour-specific events were identified that, following successful validation, could be used in clinical diagnostic practice. The combination of aberrant methylation of *RASSF1* and *HLA-DPB1* was shown to be able to discern normal brain from CNS-PNET in 94% of cases (64/68). In a recent study methylation markers were investigated in gliomas and identified in both CSF and serum (Liu, Cheng et al. 2010). If in CNS-PNET it is also possible to detect tumour DNA in CSF or serum then the presence of aberrantly methylated *RASSF1* and *HLA-DPB1* DNA could potentially be used to monitor treatment response or identify cases of relapse. In breast cancer, for example, the persistence or resolution of *RASSF1A* methylation in blood sera following treatment with Tamoxifen® indicates treatment resistance or a good response respectively (Fiegl, Millinger et al. 2005). Finally, this

study also genes that may be associated with survival in CNS-PNET (see section 5.3.9). Methylation markers have been shown to predict survival in a range of cancers including brain tumours (Silva, Dominguez et al. 1999; Palmisano, Divine et al. 2000; Hoque, Begum et al. 2006; Belinsky, Schiller et al. 2008; Levenson 2010; Liu, Cheng et al. 2010; Wen, Fu et al. 2011; Yamamoto, Nakayama et al. 2011) and therefore the potential for methylation markers to determine prognosis in CNS-PNET needs further evaluation.

Further work is also required to determine the role the tumour-specific genes identified in this study may have in CNS-PNET tumorigenesis. Functional studies initially using CNS-PNET cell lines including PFSK and CHP707m (see section 2.12) in *in-vitro* work could be used to study the effect aberrant methylation has on RNA expression and tumour growth. Candidate genes that exhibit *in-vitro* a demonstrable tumourigenic effect may then be studied in CNS-PNET murine models (Tong, Ohgaki et al. 2003). As has been discussed previously (see section 5.4.9), this approach has led the development of a number of early phase clinical trials in other cancers in which a range of agents that affect DNA methylation are being studied, and could provide novel therapeutic opportunities in CNS-PNET management.

6.9 Summary

To date, research investigating CNS-PNET biology has been limited. This study is one of the largest undertaken in this disease and has provided a series of critical insights into their pathogenesis. In particular, this study has demonstrated that CNS-PNETs are a heterogenous group of tumours that differ from medulloblastomas at the genetic level. In a minority of cases however, processes involved in the development of medulloblastomas are also implicated in CNS-PNET disease including aberrant Wnt signalling and *MYCN* amplification. The future development of targeted therapies for medulloblastoma molecular subgroups may therefore have clinical applicability in the management of individual cases of CNS-PNET. In contrast, dysregulation of the p53

pathways is a common finding in CNS-PNET which may enable advancements in the therapeutic targeting of this pathway to play a significant role in this disease. Whilst classified separately, a close relationship with high grade gliomas was however also observed in a proportion of cases. Research into, and clinical advancements in the management of, high grade gliomas may therefore have applicability in a subgroup of CNS-PNETs. Finally, this work has identified a number of developmental pathways, genetic aberrations and epigenetic events that are associated with CNS-PNET development. The associations between the identified findings and clinical features, and their functional roles in disease development, warrant further investigation to establish their translational capacity in aiding future classification and treatment advancements.

Chapter 7

References

(2004). Human Tissue Act. UK.
(2009). "Human Tissue Authority, Code of Practice 9: Research." Retrieved 10th July 2010, from http://www.hta.gov.uk/legislationpoliciesandcodesofpractice/codesofpractice/code9research.cfm.
Adams, M. J., S. E. Lipshultz, et al. (2003). "Radiation-associated cardiovascular disease: manifestations and management." Semin Radiat Oncol **13**(3): 346-356.
Adhikary, S. and M. Eilers (2005). "Transcriptional regulation and transformation by Myc proteins." Nat Rev Mol Cell Biol **6**(8): 635-645.
Agathanggelou, A., W. N. Cooper, et al. (2005). "Role of the Ras-association domain family 1 tumor suppressor gene in human cancers." Cancer Res **65**(9): 3497-3508.
Aghili, M., F. Zahedi, et al. (2009). "Hydroxyglutaric aciduria and malignant brain tumor: a case report and literature review." J Neurooncol **91**(2): 233-236.
Agrawal, M., R. J. Garg, et al. (2010). "Chronic myeloid leukemia in the tyrosine kinase inhibitor era: what is the "best" therapy?" Curr Oncol Rep **12**(5): 302-313.
Ahmadian, A., M. Ehn, et al. (2006). "Pyrosequencing: History, biochemistry and future." Clinica Chimica Acta **363**(1-2): 83-94.
Ahmed, H. (2010). "Promoter Methylation in Prostate Cancer and its Application for the Early Detection of Prostate Cancer Using Serum and Urine Samples." Biomark Cancer **2010**(2): 17-33.
Aik Choon, T., J. Antonio, et al. (2009). "Characterizing DNA methylation patterns in pancreatic cancer genome." Mol Oncol **3**(5): 425-438.
Al-Moghrabi, N., A. J. Al-Qasem, et al. (2011). "Methylation-related mutations in the BRCA1 promoter in peripheral blood cells from cancer-free women." Int J Oncol **39**(1): 129-135.
Alberts, B., A. Johnson, et al. (2002). Molecular Biology of the Cell, Garland Science Taylor and Francis Group.
Albright, A. L., J. H. Wisoff, et al. (1995). "Prognostic factors in children with supratentorial (nonpineal) primitive neuroectodermal tumors. A neurosurgical perspective from the Children's Cancer Group." Pediatr Neurosurg **22**(1): 1-7.
Allegrucci, C. (2007). "Restriction landmark genome scanning identifies culture-induced DNA methylation instability in the human embryonic stem cell epigenome." Hum. Mol. Genet. **16**: 1253-1268.
Allenspach, E. J., I. Maillard, et al. (2002). "Notch signaling in cancer." Cancer Biol Ther **1**(5): 466-476.
Alvarez, S., J. Suela, et al. (2010). "DNA Methylation Profiles and Their Relationship with Cytogenetic Status in Adult Acute Myeloid Leukemia." PLoS ONE **5**(8): e12197.
Ambros, I. M., J. Benard, et al. (2003). "Quality assessment of genetic markers used for therapy stratification." J Clin Oncol **21**(11): 2077-2084.
Amlashi, S. F., L. Riffaud, et al. (2003). "Nevoid basal cell carcinoma syndrome: relation with desmoplastic medulloblastoma in infancy. A population-based study and review of the literature." Cancer **98**(3): 618-624.

Ang, P. W., M. Loh, et al. (2010). "Comprehensive profiling of DNA methylation in colorectal cancer reveals subgroups with distinct clinicopathological and molecular features." BMC Cancer **10**: 227.
Antequera, F. and A. Bird (1993). "Number of CpG islands and genes in human and mouse." Proc Natl Acad Sci U S A **90**(24): 11995-11999.
Archer, K. J., V. R. Mas, et al. (2010). "High-throughput assessment of CpG site methylation for distinguishing between HCV-cirrhosis and HCV-associated hepatocellular carcinoma." Mol Genet Genomics **283**(4): 341-349.
Armstrong, G. T., N. Jain, et al. (2010). "Region-specific radiotherapy and neuropsychological outcomes in adult survivors of childhood CNS malignancies." Neuro Oncol **(epub ahead of print)**.
Ashwal, S., D. B. Hinshaw, et al. (1984). "CNS primitive neuroectodermal tumors of childhood." Med Pediatr Oncol **12**(3): 180-188.
Astuti, D., A. Agathanggelou, et al. (2001). "RASSF1A promoter region CpG island hypermethylation in phaeochromocytomas and neuroblastoma tumours." Oncogene **20**(51): 7573-7577.
Ausio, J., D. B. Levin, et al. (2003). "Syndromes of disordered chromatin remodeling." Clin Genet **64**(2): 83-95.
Avet-Loiseau, H., A. M. Venuat, et al. (1999). "Comparative genomic hybridization detects many recurrent imbalances in central nervous system primitive neuroectodermal tumours in children." Br J Cancer **79**(11-12): 1843-1847.
Baccarani, M., M. Dreyling, et al. (2009). "Chronic myelogenous leukemia: ESMO Clinical Recommendations for diagnosis, treatment and follow-up." Annals of oncology **20**(suppl 4): iv105-iv107.
Baker, D. L., U. R. Reddy, et al. (1990). "Human central nervous system primitive neuroectodermal tumor expressing nerve growth factor receptors: CHP707m." Ann Neurol **28**(2): 136-145.
Balss, J., J. Meyer, et al. (2008). "Analysis of the IDH1 codon 132 mutation in brain tumors." Acta Neuropathol **116**(6): 597-602.
Banelli, B., I. Gelvi, et al. (2005). "Distinct CpG methylation profiles characterize different clinical groups of neuroblastic tumors." Oncogene **24**(36): 5619-5628.
Barak, Y., T. Juven, et al. (1993). "mdm2 expression is induced by wild type p53 activity." EMBO J **12**(2): 461-468.
Barker, N. and H. Clevers (2006). "Mining the Wnt pathway for cancer therapeutics." Nat rev Drug Discov **5**(12): 997-1014.
Barnes, L. D., G. D. Kuehn, et al. (1971). "Yeast diphosphopyridine nucleotide specific isocitrate dehydrogenase. Purification and some properties." Biochem **10**(21): 3939-3944.
Baryawno, N., B. Sveinbjornsson, et al. (2010). "Small-molecule inhibitors of phosphatidylinositol 3-kinase/Akt signaling inhibit Wnt/beta-catenin pathway cross-talk and suppress medulloblastoma growth." Cancer Res **70**(1): 266-276.
Battagli, C., R. G. Uzzo, et al. (2003). "Promoter hypermethylation of tumor suppressor genes in urine from kidney cancer patients." Cancer Res **63**(24): 8695-8699.
Bayani, J., A. Pandita, et al. (2005). "Molecular cytogenetic analysis in the study of brain tumors: findings and applications." Neurosurg Focus **19**(5): E1.

Bayani, J., M. Zielenska, et al. (2000). "Molecular cytogenetic analysis of medulloblastomas and supratentorial primitive neuroectodermal tumors by using conventional banding, comparative genomic hybridization, and spectral karyotyping." J Neurosurg **93**(3): 437-448.

Baylin, S. B. and J. G. Herman (2000). "DNA hypermethylation in tumorigenesis: epigenetics joins genetics." Trends Genet **16**(4): 168-174.

Baylin, S. B. and J. G. Herman (2000). "DNA hypermethylation in tumorigenesis: epigenetics joins genetics." Trends in genetics : TIG **16**(4): 168-174.

Becker, L. E. and D. Hinton (1983). "Primitive neuroectodermal tumors of the central nervous system." Hum Pathol **14**(6): 538-550.

Behdad, A. and A. Perry (2010). "Central nervous system primitive neuroectodermal tumors: a clinicopathologic and genetic study of 33 cases." Brain Pathol **20**(2): 441-450.

Belinsky, S. A., J. H. Schiller, et al. (2008). "DNA Methylation biomarkers to assess therapy and chemoprevention for non-small cell lung cancer." Nutr Rev **66**: S24-S26.

Berman, B. P., D. J. Weisenberger, et al. (2009). "Locking in on the human methylome." Nature Biotechnol **27**(4): 341-342.

Bestor, T. H. (2000). "The DNA methyltransferases of mammals." Hum Mol Genet **9**(16): 2395-2402.

Bhattacharjee, M. B., D. D. Armstrong, et al. (1997). "Cytogenetic analysis of 120 primary pediatric brain tumors and literature review." Cancer Genet Cytogenet **97**(1): 39-53.

Bibikova, M., J. Le, et al. (2009). "Genome-wide DNA methylation profiling using Infinium assay." Epigenomics **1**: 177-200.

Bibikova, M., Z. Lin, et al. (2006). "High-throughput DNA methylation profiling using universal bead arrays." Genome Res **16**(3): 383-393.

Biegel, J. A., C. D. Burk, et al. (1992). "Evidence for a 17p tumor related locus distinct from p53 in pediatric primitive neuroectodermal tumors." Cancer Res **52**(12): 3391-3395.

Biegel, J. A., A. J. Janss, et al. (1997). "Prognostic significance of chromosome 17p deletions in childhood primitive neuroectodermal tumors (medulloblastomas) of the central nervous system." Clin Cancer Res **3**(3): 473-478.

Bieri, S., C. Sklar, et al. (1997). "Late effects of radiotherapy on the neuroendocrine system." Cancer Radiother **1**(6): 706-716.

Bigner, S. H., H. S. Friedman, et al. (1990). "Amplification of the c-myc Gene in Human Medulloblastoma Cell Lines and Xenografts." Cancer Res **50**(8): 2347-2350.

Bigner, S. H., R. E. McLendon, et al. (1997). "Chromosomal characteristics of childhood brain tumors." Cancer Genet Cytogenet **97**(2): 125-134.

Birch, J. M., R. D. Alston, et al. (2001). "Relative frequency and morphology of cancers in carriers of germline TP53 mutations." Oncogene **20**(34): 4621-4628.

Birren, B., E. D. Green, et al. (1999). Cloning Systems, Cold Spring Harbor Laboratory Press.

Biswas, S., A. Burke, et al. (2009). "Non-pineal supratentorial primitive neuro-ectodermal tumors (sPNET) in teenagers and young adults: Time to reconsider

cisplatin based chemotherapy after cranio-spinal irradiation?" Pediatr Blood Cancer **52**(7): 796-803.
Bleeker, F. E., N. A. Atai, et al. (2010). "The prognostic IDH1(R132) mutation is associated with reduced NADP+-dependent IDH activity in glioblastoma." Acta Neuropathol **119**(4): 487-494.
Bleeker, F. E., S. Lamba, et al. (2009). "IDH1 mutations at residue p.R132 (IDH1(R132)) occur frequently in high-grade gliomas but not in other solid tumors." Hum Mutat **30**(1): 7-11.
Bondy, M. L., M. E. Scheurer, et al. (2008). "Brain tumor epidemiology: consensus from the Brain Tumor Epidemiology Consortium." Cancer **113**(7 Suppl): 1953-1968.
Bots, M. and R. W. Johnstone (2009). "Rational Combinations Using HDAC Inhibitors." Clin Cancer Res **15**(12): 3970-3977.
Bouyon-Monteau, A., J. L. Habrand, et al. (2010). "Is proton beam therapy the future of radiotherapy? Part I: Clinical aspects." Cancer Radiother.
Bown, N. (2001). "Neuroblastoma tumour genetics: clinical and biological aspects." J Clin Pathol **54**(12): 897-910.
Brabender, J., D. Arbab, et al. (2009). "Death-associated protein kinase (DAPK) promoter methylation and response to neoadjuvant radiochemotherapy in esophageal cancer." Ann Surg Oncol **16**(5): 1378-1383.
Broman, K. W., J. C. Murray, et al. (1998). "Comprehensive human genetic maps: individual and sex-specific variation in recombination." Am J Hum Genet **63**(3): 861-869.
Broniscer, A., T. P. Nicolaides, et al. (2004). "High-dose chemotherapy with autologous stem-cell rescue in the treatment of patients with recurrent non-cerebellar primitive neuroectodermal tumors." Pediatr Blood Cancer **42**(3): 261-267.
Brooks, J. D., P. Cairns, et al. (2010). "DNA methylation in pre-diagnostic serum samples of breast cancer cases: Results of a nested case-control study." Cancer Epidemiol.
Brown, S. W. (1966). "Heterochromatin." Science **151**(709): 417-425.
Brown, W. D., C. J. Tavare, et al. (1995). "The applicability of Collins' Law to childhood brain tumors and its usefulness as a predictor of survival." Neurosurgery **36**(6): 1093-1096.
Brunner, A. L., D. S. Johnson, et al. (2009). "Distinct DNA methylation patterns characterize differentiated human embryonic stem cells and developing human fetal liver." Genome Res **19**(6): 1044-1056.
Bruno, L. A., L. B. Rorke, et al. (1981). Primitive neuroectodermal tumours of infancy and childhood. Paediatric Oncology. G. B. Humphrey, L. P. Dehner, G. B. Grindey and R. T. Acton. Nijhoff, Boston. **1:** 265-267.
Burbee, D. G., E. Forgacs, et al. (2001). "Epigenetic inactivation of RASSF1A in lung and breast cancers and malignant phenotype suppression." J Natl Cancer Inst **93**(9): 691-699.
Burger, P. C. (2006). "Supratentorial Primitive Neuroectodermal Tumor (sPNET)." Brain Pathol **16**(1): 86-86.
Burnett, M. E., E. C. White, et al. (1997). "Chromosome arm 17p deletion analysis reveals molecular genetic heterogeneity in supratentorial and infratentorial

primitive neuroectodermal tumors of the central nervous system." Cancer Genet Cytogenet **97**(1): 25-31.
Bustin, S. A. (2000). "Absolute quantification of mRNA using real-time reverse transcription polymerase chain reaction assays." J Mol Endocrinol **25**(2): 169-193.
Cairns, J. M., M. J. Dunning, et al. (2008). "BASH: a tool for managing BeadArray spatial artefacts." Bioinformatics **24**(24): 2921-2922.
Calin, G. A., C. D. Dumitru, et al. (2002). "Frequent deletions and down-regulation of micro- RNA genes miR15 and miR16 at 13q14 in chronic lymphocytic leukemia." Proc Natl Acad Sci U S A **99**(24): 15524-15529.
Capper, D., H. Zentgraf, et al. (2009). "Monoclonal antibody specific for IDH1 R132H mutation." Acta Neuropathol **118**(5): 599-601.
Capra, M., D. Hargrave, et al. (2003). "Central nervous system tumours in adolescents." Eur J Cancer **39**(18): 2643-2650.
Carr, J., E. Bell, et al. (2006). "Increased frequency of aberrations in the p53/MDM2/p14(ARF) pathway in neuroblastoma cell lines established at relapse." Cancer Res **66**(4): 2138-2145.
Carr, J., N. P. Bown, et al. (2007). "High-resolution analysis of allelic imbalance in neuroblastoma cell lines by single nucleotide polymorphism arrays." Cancer Genet Cytogenet **172**(2): 127-138.
Casali, P. G., A. Messina, et al. (2004). "Imatinib mesylate in chordoma." Cancer **101**(9): 2086-2097.
CCLG (2010). Children's Cancer and Leukaemia Group Scientific report: 2010.
Chadduck, W. M., F. A. Boop, et al. (1991). "Cytogenetic Studies of Pediatric Brain and Spinal Cord Tumors." Pediatr Neurosurg **17**(2): 57-65.
Chan, J. A., A. M. Krichevsky, et al. (2005). "MicroRNA-21 is an antiapoptotic factor in human glioblastoma cells." Cancer Res **65**(14): 6029-6033.
Chan, M. W., L. W. Chan, et al. (2003). "Frequent hypermethylation of promoter region of RASSF1A in tumor tissues and voided urine of urinary bladder cancer patients." Int J Cancer **104**(5): 611-616.
Chang, Q., J. C. Pang, et al. (2005). "Promoter hypermethylation profile of RASSF1A, FHIT, and sFRP1 in intracranial primitive neuroectodermal tumors." Hum Pathol **36**(12): 1265-1272.
Charron, J., B. A. Malynn, et al. (1992). "Embryonic lethality in mice homozygous for a targeted disruption of the N-myc gene." Genes Dev **6**(12A): 2248-2257.
Chaudhry, P., R. Srinivasan, et al. (2009). "Utility of gene promoter methylation in prediction of response to platinum-based chemotherapy in epithelial ovarian cancer (EOC)." Cancer Invest **27**(8): 877-884.
Chawla, A., J. V. Emmanuel, et al. (2007). "Paediatric PNET: pre-surgical MRI features." Clin Radiol **62**(1): 43-52.
Cheung, H. H., T. L. Lee, et al. (2010). "Genome-wide DNA methylation profiling reveals novel epigenetically regulated genes and non-coding RNAs in human testicular cancer." Br J Cancer **102**(2): 419-427.
Chintagumpala, M., T. Hassall, et al. (2009). "A pilot study of risk-adapted radiotherapy and chemotherapy in patients with supratentorial PNET." Neuro Oncol **11**(1): 33-40.

Cho, Y. J., A. Tsherniak, et al. (2010). "Integrative Genomic Analysis of Medulloblastoma Identifies a Molecular Subgroup That Drives Poor Clinical Outcome." J Clin Oncol.

Chou, W. C., H. A. Hou, et al. (2010). "Distinct clinical and biologic characteristics in adult acute myeloid leukemia bearing the isocitrate dehydrogenase 1 mutation." Blood **115**(14): 2749-2754.

Choudry, Q., H. C. Patel, et al. (2007). "Radiation-induced brain tumours in nevoid basal cell carcinoma syndrome: implications for treatment and surveillance." Childs Nerv Syst **23**(1): 133-136.

Christensen, B. C., E. A. Houseman, et al. (2010). "Integrated profiling reveals a global correlation between epigenetic and genetic alterations in mesothelioma." Cancer Res **70**(14): 5686-5694.

Christensen, B. C., K. T. Kelsey, et al. (2010). "Breast cancer DNA methylation profiles are associated with tumor size and alcohol and folate intake." PLoS Genet **6**(7): e1001043.

Ciafrè, S. A., S. Galardi, et al. (2005). "Extensive modulation of a set of microRNAs in primary glioblastoma." Biochem Biophys Res Commun **334**(4): 1351-1358.

Clark, S. J., A. Statham, et al. (2006). "DNA methylation: bisulphite modification and analysis." Nature Protoc **1**(5): 2353-2364.

Clifford, S. C., M. E. Lusher, et al. (2006). "Wnt/Wingless pathway activation and chromosome 6 loss characterize a distinct molecular sub-group of medulloblastomas associated with a favorable prognosis." Cell Cycle **5**(22): 2666-2670.

Cohen, B. H., P. M. Zeltzer, et al. (1995). "Prognostic factors and treatment results for supratentorial primitive neuroectodermal tumors in children using radiation and chemotherapy: a Childrens Cancer Group randomized trial." J Clin Oncol **13**(7): 1687-1696.

Cohen, N., D. R. Betts, et al. (2004). "Karyotypic evolution pathways in medulloblastoma/primitive neuroectodermal tumor determined with a combination of spectral karyotyping, G-banding, and fluorescence in situ hybridization." Cancer Genet Cytogenet **149**(1): 44-52.

Collins, V. P., R. K. Loeffler, et al. (1956). "Observations on growth rates of human tumors." Am J Roentgenol **76**(5): 988-1000.

Constine, L. S., P. D. Woolf, et al. (1993). "Hypothalamic-pituitary dysfunction after radiation for brain tumors." N Engl J Med **328**(2): 87-94.

Coolen, M. W., A. L. Statham, et al. (2007). "Genomic profiling of CpG methylation and allelic specificity using quantitative high-throughput mass spectrometry: critical evaluation and improvements." Nucleic Acids Res **35**(18): e119.

Coons, A. H., H. J. Creech, et al. (1941). "Immunological properties of an antibody containing a fluorescent group." Proc Soc Exp Biol Med **47**: 200-202.

Costello, J. F., M. C. Fruhwald, et al. (2000). "Aberrant CpG-island methylation has non-random and tumour-type-specific patterns." Nat Genet **24**(2): 132-138.

Costello, J. F. and C. Plass (2001). "Methylation matters." J Med Genet **38**(5): 285-303.

Cravo, M., R. Pinto, et al. (1996). "Global DNA hypomethylation occurs in the early stages of intestinal type gastric carcinoma." Gut **39**(3): 434-438.

Croce, C. M. (2008). "Oncogenes and Cancer." N Engl J Med **358**(5): 502-511.

Dahmane, N., P. Sanchez, et al. (2001). "The Sonic Hedgehog-Gli pathway regulates dorsal brain growth and tumorigenesis." Development **128**(24): 5201-5212.
Dai, A. I., J. W. Backstrom, et al. (2003). "Supratentorial primitive neuroectodermal tumors of infancy: clinical and radiologic findings." Pediatr Neurol **29**(5): 430-434.
Dang, L., D. W. White, et al. (2010). "Cancer-associated IDH1 mutations produce 2-hydroxyglutarate." Nature **465**(7300): 966.
Danoff, B. F., F. S. Cowchock, et al. (1982). "Assessment of the long-term effects of primary radiation therapy for brain tumors in children." Cancer **49**(8): 1580-1586.
Davis, A. C., M. Wims, et al. (1993). "A null c-myc mutation causes lethality before 10.5 days of gestation in homozygotes and reduced fertility in heterozygous female mice." Genes Dev **7**(4): 671-682.
Davis, P. K. and R. K. Brackmann (2003). "Chromatin remodeling and cancer." Cancer Biol Ther **2**(1): 22-29.
De Vos, M., B. E. Hayward, et al. (2006). "PMS2 mutations in childhood cancer." J Natl Cancer Inst **98**(5): 358-361.
Dedeurwaerdere, F., C. Giannini, et al. (2002). "Primary Peripheral PNET//Ewing's Sarcoma of the Dura: a Clinicopathologic Entity Distinct from Central PNET." Mod Pathol **15**(6): 673-678.
di Magliano, M. P. and M. Hebrok (2003). "Hedgehog signalling in cancer formation and maintenance." Nat Rev Cancer **3**(12): 903-911.
Donehower, L. A., M. Harvey, et al. (1992). "Mice deficient for p53 are developmentally normal but susceptible to spontaneous tumours." Nature **356**(6366): 215-221.
Down, T. A., V. K. Rakyan, et al. (2008). "A Bayesian deconvolution strategy for immunoprecipitation-based DNA methylome analysis." Nature Biotechnol **26**(7): 779-785.
Duffner, P. K., M. E. Horowitz, et al. (1993). "Postoperative chemotherapy and delayed radiation in children less than three years of age with malignant brain tumors." N Engl J Med **328**(24): 1725-1731.
Duffner, P. K., M. E. Horowitz, et al. (1993). "Postoperative chemotherapy and delayed radiation in children less than three years of age with malignant brain tumors." The New England journal of medicine **328**(24): 1725-1731.
Dulai, M. S., C. M. Bosanko, et al. (2004). "Mixed cystic gliosarcoma and primitive neuroectodermal tumor: a case report." Clin Neuropathol **23**(5): 218-222.
Dulaimi, E., R. G. Uzzo, et al. (2004). "Detection of bladder cancer in urine by a tumor suppressor gene hypermethylation panel." Clin Cancer Res **10**(6): 1887-1893.
Dunham, C., E. Sugo, et al. (2007). "Embryonal tumor with abundant neuropil and true rosettes (ETANTR): report of a case with prominent neurocytic differentiation." J Neurooncol **84**(1): 91-98.
Dunning, M. J., M. L. Smith, et al. (2007). "beadarray: R classes and methods for Illumina bead-based data." Bioinformatics **23**(16): 2183-2184.
Eads, C. A., K. D. Danenberg, et al. (2000). "MethyLight: a high-throughput assay to measure DNA methylation." Nucleic Acids Res **28**(8): E32.
Eberhart, C. G. (2011). "Molecular diagnostics in embryonal brain tumors." Brain Pathol **21**(1): 96-104.

Eberhart, C. G., D. J. Brat, et al. (2000). "Pediatric neuroblastic brain tumors containing abundant neuropil and true rosettes." Pediatr Dev Pathol **3**: 346-352.
Eberhart, C. G., A. Chaudhry, et al. (2005). "Increased p53 immunopositivity in anaplastic medulloblastoma and supratentorial PNET is not caused by JC virus." BMC Cancer **5**: 19.
Eberhart, C. G., J. E. Kratz, et al. (2002). "Comparative genomic hybridization detects an increased number of chromosomal alterations in large cell/anaplastic medulloblastomas." Brain Pathol **12**(1): 36-44.
Eldering, E., C. A. Spek, et al. (2003). "Expression profiling via novel multiplex assay allows rapid assessment of gene regulation in defined signalling pathways." Nucleic Acids Res **31**(23): e153.
Ellison, D. (2002). "Classifying the medulloblastoma: insights from morphology and molecular genetics." Neuropathol Appl Neurobiol **28**(4): 257-282.
Ellison, D. W., M. Kocat, et al. (2011). "Definition of disease-risk stratification groups in childhood medulloblastma using combined clinical, pathological and molecular variables." J Clin Oncol **29**(11): 1400-1407.
Ellison, D. W., O. E. Onilude, et al. (2005). "beta-Catenin status predicts a favorable outcome in childhood medulloblastoma: the United Kingdom Children's Cancer Study Group Brain Tumour Committee." J Clin Oncol **23**(31): 7951-7957.
Esteller, M. (2005). How CPG island methylation leads to cancer dissemination: The sound of silence of tumors and metastasis suppressor genes. DNA methylation, epigenetics and metastasis. M. Esteller. Dordrecht, Netherlands, Springer**:** 1-8.
Esteller, M. (2006). "Epigenetics provides a new generation of oncogenes and tumour-suppressor genes." Br J Cancer **94**(2): 179-183.
Evans, D. G., J. M. Birch, et al. (2006). "Malignant transformation and new primary tumours after therapeutic radiation for benign disease: substantial risks in certain tumour prone syndromes." J Med Genet **43**(4): 289-294.
Evans, D. G., E. J. Ladusans, et al. (1993). "Complications of the naevoid basal cell carcinoma syndrome: results of a population based study." J Med Genet **30**(6): 460-464.
Fan, J. B., K. L. Gunderson, et al. (2006). "Illumina universal bead arrays." Meth Enymol **410**: 57-73.
Fan, X., I. Mikolaenko, et al. (2004). "Notch1 and notch2 have opposite effects on embryonal brain tumor growth." Cancer Res **64**(21): 7787-7793.
Fan, Y. S. (2002). Molecular Cytogenetics: Protocols and Applications, Humana Press.
Fangusaro, J. (2009). "Pediatric high-grade gliomas and diffuse intrinsic pontine gliomas." J child neurol **24**(11): 1409-1417.
Fangusaro, J., J. Finlay, et al. (2008). "Intensive chemotherapy followed by consolidative myeloablative chemotherapy with autologous hematopoietic cell rescue (AuHCR) in young children with newly diagnosed supratentorial primitive neuroectodermal tumors (sPNETs): report of the Head Start I and II experience." Pediatr Blood Cancer **50**(2): 312-318.
Farndon, P. A., R. G. Del Mastro, et al. (1992). "Location of gene for Gorlin syndrome." Lancet **339**(8793): 581-582.
Fattet, S., C. Haberler, et al. (2009). "Beta-catenin status in paediatric medulloblastomas: correlation of immunohistochemical expression with

mutational status, genetic profiles, and clinical characteristics." J Pathol **218**(1): 86-94.
Feig, L. A. and R. J. Buchsbaum (2002). "Cell signaling: life or death decisions of ras proteins." Current Biol **12**(7): R259-261.
Feinberg, A. P. and B. Vogelstein (1983). "Hypomethylation distinguishes genes of some human cancers from their normal counterparts." Nature **301**(5895): 89-92.
Fiegl, H., S. Millinger, et al. (2005). "Circulating tumor-specific DNA: a marker for monitoring efficacy of adjuvant therapy in cancer patients." Cancer Res **65**(4): 1141-1145.
Figueroa, M. E., S. Lugthart, et al. (2010). "DNA methylation signatures identify biologically distinct subtypes in acute myeloid leukemia." Cancer Cell **17**(1): 13-27.
Ford, D., D. F. Easton, et al. (1998). "Genetic heterogeneity and penetrance analysis of the BRCA1 and BRCA2 genes in breast cancer families. The Breast Cancer Linkage Consortium." Am J Hum Genet **62**(3): 676-689.
Fraga, M. F., E. Ballestar, et al. (2005). "Loss of acetylation at Lys16 and trimethylation at Lys20 of histone H4 is a common hallmark of human cancer." Nat Genet **37**(4): 391-400.
Frank, A. J., R. Hernan, et al. (2004). "The TP53-ARF tumor suppressor pathway is frequently disrupted in large/cell anaplastic medulloblastoma." Brain Res Mol Brain Res **121**(1-2): 137-140.
Franks, L. M. and N. M. Teich (1997). Introduction to the Cellular and Molecular Biology of Cancer, Oxford University Press.
Freshney, R. I. (2000) "Culture of animal cells. A manual of basic technique.".
Friedman, H., P. Burger, et al. (1988). "Phenotypic and genotypic analysis of a human medulloblastoma cell line and transplantable xenograft (D341 Med) demonstrating amplification of c-myc." Am J Pathol **130**(3): 472-484.
Friend, S. H., R. Bernards, et al. (1986). "A human DNA segment with properties of the gene that predisposes to retinoblastoma and osteosarcoma." Nature **323**(6089): 643-646.
Frigola, J., M. Ribas, et al. (2002). "Methylome profiling of cancer cells by amplification of inter-methylated sites (AIMS)." Nucleic Acids Res. **30**: e28.
Frommer, M., L. E. McDonald, et al. (1992). "A genomic sequencing protocol that yields a positive display of 5-methylcytosine residues in individual DNA strands." Proc Natl Acad Sci U S A **89**(5): 1827-1831.
Fruhwald, M. C., M. S. O'Dorisio, et al. (2001). "Aberrant promoter methylation of previously unidentified target genes is a common abnormality in medulloblastomas--implications for tumor biology and potential clinical utility." Oncogene **20**(36): 5033-5042.
Fruhwald, M. C., M. S. O'Dorisio, et al. (2000). "Gene amplification in PNETs/medulloblastomas: mapping of a novel amplified gene within the MYCN amplicon." J Med Genet **37**(7): 501-509.
Fujii, Y., T. Hongo, et al. (1994). "Chromosome analysis of brain tumors in childhood." Genes Chromosomes Cancer **11**(4): 205-215.

Fults, D., C. A. Pedone, et al. (1992). "Establishment and characterization of a human primitive neuroectodermal tumor cell line from the cerebral hemisphere." J Neuropathol Exp Neurol **51**(3): 272-280.
Gaffney, C. C., J. P. Sloane, et al. (1985). "Primitive neuroectodermal tumours of the cerebrum. Pathology and treatment." J Neurooncol **3**(1): 23-33.
Gaiano, N. and G. Fishell (2002). "The role of notch in promoting glial and neural stem cell fates." Annu Rev Neurosci **25**: 471-490.
Gajjar, A., M. Chintagumpala, et al. (2006). "Risk-adapted craniospinal radiotherapy followed by high-dose chemotherapy and stem-cell rescue in children with newly diagnosed medulloblastoma (St Jude Medulloblastoma-96): long-term results from a prospective, multicentre trial." Lancet Oncol **7**(10): 813-820.
Gajjar, A. and B. Pizer (2010). "Role of high-dose chemotherapy for recurrent medulloblastoma and other CNS primitive neuroectodermal tumors." Pediatr Blood Cancer **54**(4): 649-651.
Gao, J., X. Liu, et al. (2005). "Nitric oxide-donating aspirin induces apoptosis in human colon cancer cells through induction of oxidative stress." Proc Natl Acad Sci USA **102**: 17207-17212.
Gao, Y., M. Guan, et al. (2004). "Hypermethylation of the RASSF1A gene in gliomas." Clinica Chimica Acta **349**(1-2): 173-179.
Garre, M. L., A. Cama, et al. (2009). "Medulloblastoma variants: age-dependent occurrence and relation to Gorlin syndrome--a new clinical perspective." Clin Cancer Res **15**(7): 2463-2471.
Garzon, R., G. A. Calin, et al. (2009). "MicroRNAs in Cancer." Ann Rev Med **60**: 167-179.
Gayther, S. A., S. J. Batley, et al. (2000). "Mutations truncating the EP300 acetylase in human cancers." Nat Genet **24**(3): 300-303.
Geisbrecht, B. V. and S. J. Gould (1999). "The human PICD gene encodes a cytoplasmic and peroxisomal NADP(+)-dependent isocitrate dehydrogenase." J Biol Chem **274**(43): 30527-30533.
Geyer, J. R., R. Sposto, et al. (2005). "Multiagent chemotherapy and deferred radiotherapy in infants with malignant brain tumors: a report from the Children's Cancer Group." J Clin Oncol **23**(30): 7621-7631.
Giangaspero, F., S. H. Bigner, et al. (2000). Medulloblastoma. Tumours of the Nervous System. P. Kleihues and W. K. Cavenee. Lyon, IARC Press**:** 129–139.
Giannakakou, P., D. L. Sackett, et al. (2000). "p53 is associated with cellular microtubules and is transported to the nucleus by dynein." Nature Cell Biol **2**(10): 709-717.
Giardiello, F. M. (1993). "Treatment of colonic and rectal adenomas with sulindac in familial adenomatous polyposis." N Engl J Med. **328**: 1313-1316.
Gilbertson, R. J. (2004). "Medulloblastoma: signalling a change in treatment." Lancet Oncol **5**(4): 209-218.
Gleeson, H. K. and S. M. Shalet (2004). "The impact of cancer therapy on the endocrine system in survivors of childhood brain tumours." Endocr Relat Cancer **11**(4): 589-602.
Goker, E., M. Waltham, et al. (1995). "Amplification of the dihydrofolate reductase gene is a mechanism of acquired resistance to methotrexate in patients with

acute lymphoblastic leukemia and is correlated with p53 gene mutations." Blood **86**(2): 677-684.
Goldberg, E. K., J. M. Glendening, et al. (2000). "Localization of multiple melanoma tumor-suppressor genes on chromosome 11 by use of homozygosity mapping-of-deletions analysis." Am J Hum Genet **67**(2): 417-431.
Goldenberg, D., S. Harden, et al. (2004). "Intraoperative molecular margin analysis in head and neck cancer." Arch Otolaryngol **130**(1): 39-44.
Goldman, J. M. and J. V. Melo (2001). "Targeting the BCR-ABL Tyrosine Kinase in Chronic Myeloid Leukemia." N Engl J Med **344**(14): 1084-1086.
Gonzalez, K. D., K. A. Noltner, et al. (2009). "Beyond Li Fraumeni Syndrome: clinical characteristics of families with p53 germline mutations." J Clin Oncol **27**(8): 1250-1256.
Gonzalgo, M. L. and P. A. Jones (1997). "Rapid quantitation of methylation differences at specific sites using methylation-sensitive single nucleotide primer extension (Ms-SNuPE)." Nucleic Acids Res **25**(12): 2529-2531.
Goodrich, L. V., L. Milenkovic, et al. (1997). "Altered Neural Cell Fates and Medulloblastoma in Mouse *patched* Mutants." Science **277**: 1109-1113.
Gopalakrishnan, S., B. O. Van Emburgh, et al. (2008). "DNA methylation in development and human disease." Mutat Res **647**(1-2): 30-38.
Gorczyca, W. (2008). Cytogenetics, FISH and Molecular Testing in Hematologic Malignancies. London, Informa Healthcare.
Gordon, M. D. and R. Nusse (2006). "Wnt signaling: multiple pathways, multiple receptors, and multiple transcription factors." J Biol Chem **281**(32): 22429-22433.
Gravendeel, L. A., N. K. Kloosterhof, et al. (2010). "Segregation of non-p.R132H mutations in IDH1 in distinct molecular subtypes of glioma." Hum Mutat **31**(3): E1186-1199.
Greco, C. and S. Wolden (2007). "Current status of radiotherapy with proton and light ion beams." Cancer **109**(7): 1227-1238.
Greenblatt, M. S., W. P. Bennett, et al. (1994). "Mutations in the p53 tumor suppressor gene: clues to cancer etiology and molecular pathogenesis." Cancer Res **54**(18): 4855-4878.
Grote, H. J., V. Schmiemann, et al. (2006). "Methylation of RAS association domain family protein 1A as a biomarker of lung cancer." Cancer **108**(2): 129-134.
Grundy, R. G., S. H. Wilne, et al. (2010). "Primary postoperative chemotherapy without radiotherapy for treatment of brain tumours other than ependymoma in children under 3 years: results of the first UKCCSG/SIOP CNS 9204 trial." Eur J Cancer **46**(1): 120-133.
Haberler, C., U. Laggner, et al. (2006). "Immunohistochemical analysis of INI1 protein in malignant pediatric CNS tumors: Lack of INI1 in atypical teratoid/rhabdoid tumors and in a fraction of primitive neuroectodermal tumors without rhabdoid phenotype." Am J Surg Pathol **30**(11): 1462-1468.
Hahn, C. A., R. H. Dunn, et al. (2003). "Prospective study of neuropsychologic testing and quality-of-life assessment of adults with primary malignant brain tumors." Int J Radiat Oncol Biol Phys **55**(4): 992-999.

Hallahan, A. R., J. I. Pritchard, et al. (2004). "The SmoA1 mouse model reveals that notch signaling is critical for the growth and survival of sonic hedgehog-induced medulloblastomas." Cancer Res **64**(21): 7794-7800.
Hamada, M., T. Fujiwara, et al. (1996). "The p53 gene is a potent determinant of chemosensitivity and radiosensitivity in gastric and colorectal cancers." J Cancer Res Clin Oncol **122**: 360-365.
Hamilton, D. W., M. E. Lusher, et al. (2005). "Epigenetic inactivation of the RASSF1A tumour suppressor gene in ependymoma." Cancer Lett **227**(1): 75-81.
Hamilton, S. R., B. Liu, et al. (1995). "The molecular basis of Turcot's syndrome." N Engl J Med **332**(13): 839-847.
Hanahan, D. and R. A. Weinberg (2000). "The hallmarks of cancer." Cell **100**(1): 57-70.
Harada, K., S. Toyooka, et al. (2002). "Aberrant promoter methylation and silencing of the RASSF1A gene in pediatric tumors and cell lines." Oncogene **21**(27): 4345-4349.
Harrison, C. J. (2009). "Cytogenetics of paediatric and adolescent acute lymphoblastic leukaemia." Br J Haematol **144**(2): 147-156.
Hart, M. N. and K. M. Earle (1973). "Primitive neuroectodermal tumors of the brain in children." Cancer **32**(4): 890-897.
Hartmann, C., J. Meyer, et al. (2009). "Type and frequency of IDH1 and IDH2 mutations are related to astrocytic and oligodendroglial differentiation and age: a study of 1,010 diffuse gliomas." Acta Neuropathol **118**(4): 469-474.
Hartmann, O., F. Spyratos, et al. (2009). "DNA methylation markers predict outcome in node-positive, estrogen receptor-positive breast cancer with adjuvant anthracycline-based chemotherapy." Clin Cancer Res **15**(1): 315-323.
Hauser, S., T. Zahalka, et al. (2010). "Cell-free circulating DNA: Diagnostic value in patients with renal cell cancer." Anticancer Res **30**(7): 2785-2789.
Hayden, J. T., M. C. Fruhwald, et al. (2009). "Frequent IDH1 mutations in supratentorial primitive neuroectodermal tumors (sPNET) of adults but not children." Cell Cycle **8**(11): 1806-1807.
He, T. C., A. B. Sparks, et al. (1998). "Identification of c-MYC as a target of the APC pathway." Science **281**(5382): 1509-1512.
Hegi, M. E., A. C. Diserens, et al. (2004). "Clinical trial substantiates the predictive value of O-6-methylguanine-DNA methyltransferase promoter methylation in glioblastoma patients treated with temozolomide." Clin Cancer Res **10**(6): 1871-1874.
Heinrich, M. C., C. D. Blanke, et al. (2002). "Inhibition of KIT Tyrosine Kinase Activity: A Novel Molecular Approach to the Treatment of KIT-Positive Malignancies." J Clin Oncol **20**(6): 1692-1703.
Hesson, L. B., D. Krex, et al. (2008). "Epigenetic markers in human gliomas: prospects for therapeutic intervention." Expert Rev Neurother **8**(10): 1475-1496.
Higuchi, R., G. Dollinger, et al. (1992). "Simultaneous amplification and detection of specific DNA sequences." Biotechnology **10**(4): 413-417.
Hinoue, T., D. J. Weisenberger, et al. (2011). "Genome-scale analysis of aberrant DNA methylation in colorectal cancer." Genome Res.

Hinoue, T., D. J. Weisenberger, et al. (2009). "Analysis of the association between CIMP and BRAF in colorectal cancer by DNA methylation profiling." PLoS ONE **4**(12): e8357.
Hjortsberg L, Rubio-Nevado J.M, et al. (2010). The p53 Mutation handbook.
Ho, Y. S., L. L. Hsieh, et al. (1996). "p53 gene mutation in cerebral primitive neuroectodermal tumor in Taiwan." Cancer Lett **104**(1): 103-113.
Holcombe, R. F., J. L. Marsh, et al. (2002). "Expression of Wnt ligands and Frizzled receptors in colonic mucosa and in colon carcinoma." Mol Pathol **55**(4): 220-226.
Holdhoff, M., D. W. Parsons, et al. (2009). "Mutations of IDH1 and IDH2 are not detected in brain metastases of colorectal cancer." J Neurooncol **94**(2): 297.
Hollstein, M., D. Sidransky, et al. (1991). "p53 mutations in human cancers." Science **253**(5015): 49-53.
Holm, L. E. (1990). "Cancer occurring after radiotherapy and chemotherapy." Int J Radiat Oncol Biol Phys **19**(5): 1303-1308.
Hong, T. S., M. P. Mehta, et al. (2004). "Patterns of failure in supratentorial primitive neuroectodermal tumors treated in Children's Cancer Group Study 921, a phase III combined modality study." Int J Radiat Oncol Biol Phys **60**(1): 204-213.
Hong, T. S., M. P. Mehta, et al. (2005). "Patterns of treatment failure in infants with primitive neuroectodermal tumors who were treated on CCG-921: a phase III combined modality study." Pediatr Blood Cancer **45**(5): 676-682.
Honorio, S., A. Agathanggelou, et al. (2003). "Detection of RASSF1A aberrant promoter hypermethylation in sputum from chronic smokers and ductal carcinoma in situ from breast cancer patients." Oncogene **22**(1): 147-150.
Hoque, M. O., S. Begum, et al. (2006). "Quantitation of promoter methylation of multiple genes in urine DNA and bladder cancer detection." J Natl Cancer Inst **98**(14): 996-1004.
Horiguchi, K., Y. Tomizawa, et al. (2003). "Epigenetic inactivation of RASSF1A candidate tumor suppressor gene at 3p21.3 in brain tumors." Oncogene **22**(49): 7862-7865.
Horiuchi, H., H. Kawamata, et al. (2004). "Negative immunohistochemical staining of p53 protein does not always reflect wild-type <i>p53</i> gene in cancer cells." J Gastroenterol **39**(8): 801-803.
Hottinger, A. F. and Y. Khakoo (2009). "Neurooncology of familial cancer syndromes." J Child Neurol **24**(12): 1526-1535.
Houshdaran, S., S. Hawley, et al. (2010). "DNA methylation profiles of ovarian epithelial carcinoma tumors and cell lines." PLoS ONE **5**(2): e9359.
Huang, d. W., B. T. Sherman, et al. (2009). "Bioinformatics enrichment tools: paths toward the comprehensive functional analysis of large gene lists." Nucleic Acids Res **37**(1): 1-13.
Huang, d. W., B. T. Sherman, et al. (2009). "Systematic and integrative analysis of large gene lists using DAVID bioinformatics resources." Nature Protoc **4**(1): 44-57.
Huang, H., A. Hara, et al. (2005). "Altered expression of immune defense genes in pilocytic astrocytomas." J Neuropathol Exp Neurol **64**(10): 891-901.
Hughes, J. M., A. J. Groot, et al. (2010). "Active HIF-1 in the normal human retina." J Histochem Cytochem **58**(3): 247-254.

Ichimura, K., D. M. Pearson, et al. (2009). "IDH1 mutations are present in the majority of common adult gliomas but rare in primary glioblastomas." Neuro Oncol **11**(4): 341-347.

Inda, M. M. and J. S. Castresana (2007). "RASSF1A promoter is highly methylated in primitive neuroectodermal tumors of the central nervous system." Neuropathology **27**(4): 341-346.

Inda, M. M., J. Munoz, et al. (2006). "High promoter hypermethylation frequency of p14/ARF in supratentorial PNET but not in medulloblastoma." Histopathology **48**(5): 579-587.

Inda, M. M., C. Perot, et al. (2005). "Genetic heterogeneity in supratentorial and infratentorial primitive neuroectodermal tumours of the central nervous system." Histopathology **47**(6): 631-637.

Irizarry, R. A., C. Ladd-Acosta, et al. (2009). "The human colon cancer methylome shows similar hypo- and hypermethylation at conserved tissue-specific CpG island shores." Nat Genet **41**(2): 178-186.

Ishibashi, M., S. L. Ang, et al. (1995). "Targeted disruption of mammalian hairy and Enhancer of split homolog-1 (HES-1) leads to up-regulation of neural helix-loop-helix factors, premature neurogenesis, and severe neural tube defects." Genes Dev **9**(24): 3136-3148.

Ishizawa, K., S. Kan-nuki, et al. (2002). "Lipomatous primitive neuroectodermal tumor with a glioblastoma component: a case report." Acta Neuropathol **103**(2): 193-198.

Jacques, T. S., A. Swales, et al. (2010). "Combinations of genetic mutations in the adult neural stem cell compartment determine brain tumour phenotypes." EMBO J **29**(1): 222-235.

Jakacki, R. I. (1999). "Pineal and nonpineal supratentorial primitive neuroectodermal tumors." Childs Nerv Syst **15**(10): 586-591.

Jakacki, R. I. (2005). "Treatment strategies for high-risk medulloblastoma and supratentorial primitive neuroectodermal tumors. Review of the literature." J Neurosurg **102**(1 Suppl): 44-52.

Jakacki, R. I., P. M. Zeltzer, et al. (1995). "Survival and prognostic factors following radiation and/or chemotherapy for primitive neuroectodermal tumors of the pineal region in infants and children: a report of the Childrens Cancer Group." J Clin Oncol **13**(6): 1377-1383.

Jannoun, L. and H. J. Bloom (1990). "Long-term psychological effects in children treated for intracranial tumors." Int J Radiat Oncol Biol Phys **18**(4): 747-753.

Janss, A. J., A. T. Yachnis, et al. (1996). "Glial differentiation predicts poor clinical outcome in primitive neuroectodermal brain tumors." Ann Neurol **39**(4): 481-489.

Jaros, E., J. Lunec, et al. (1993). "p53 protein overexpression identifies a group of central primitive neuroectodermal tumours with poor prognosis." Br J Cancer **68**(4): 801-807.

Jeans, A. F., I. Frayling, et al. (2009). "Cerebral primitive neuroectodermal tumor in an adult with a heterozygous MSH2 mutation." Nat Rev Clin Oncol **6**(5): 295-299.

Jesse Chung-Sean, P., C. Qing, et al. (2005). "Epigenetic inactivation of DLC-1 in supratentorial primitive neuroectodermal tumor." Hum Pathol **36**(1): 36-43.

Jho, E.-h., T. Zhang, et al. (2002). "Wnt/{beta}-Catenin/Tcf Signaling Induces the Transcription of Axin2, a Negative Regulator of the Signaling Pathway." Mol Cell Biol. **22**(4): 1172-1183.
Jimenez, G. S., S. H. Khan, et al. (1999). "p53 regulation by post-translational modification and nuclear retention in response to diverse stresses." Oncogene **18**(53): 7656-7665.
Jing, F., W. Yuping, et al. (2010). "CpG island methylator phenotype of multigene in serum of sporadic breast carcinoma." Tumour Biol **31**(4): 321-331.
Jones, H. W., V. A. McKusick, et al. (1971). "George Otto Gey. (1899-1970). The HeLa cell and a reappraisal of its origin." Obstet Gynecol **38**(6): 945-949.
Jones, P. A. and S. B. Baylin (2007). "The epigenomics of cancer." Cell **128**(4): 683-692.
Jones, T. D., M. D. Carr, et al. (2005). "Clonal origin of lymph node metastases in bladder carcinoma." Cancer **104**(9): 1901-1910.
Kaatsch, P., E. Steliarova-Foucher, et al. (2006). "Time trends of cancer incidence in European children (1978-1997): report from the Automated Childhood Cancer Information System project." Eur J Cancer **42**(13): 1961-1971.
Kagawa, N., M. Maruno, et al. (2006). "Detection of genetic and chromosomal aberrations in medulloblastomas and primitive neuroectodermal tumors with DNA microarrays." Brain Tumor Pathol **23**(1): 41-47.
Kalderon, D. (2002). "Similarities between the Hedgehog and Wnt signaling pathways." Trends Cell Biol **12**(11): 523-531.
Kallioniemi, A., O. P. Kallioniemi, et al. (1992). "Comparative genomic hybridization for molecular cytogenetic analysis of solid tumors." Science **258**(5083): 818-821.
Kandemir, N. O., B. Bahadir, et al. (2009). "Glioblastoma with primitive neuroectodermal tumor-like features: case report." Turk Neurosurg **19**(3): 260-264.
Kang, M. R., M. S. Kim, et al. (2009). "Mutational analysis of IDH1 codon 132 in glioblastomas and other common cancers." Int J Cancer **125**(2): 353-355.
Kapetonovik IM, R. S., Izmirilian G (2004). "Overview of Commonly used Bioinformatics Methods and Their Applications." Ann. N.Y. Acad. Sci **1020**: 10-21.
Kaplan, K. J. and A. Perry (2007). "Gliosarcoma with primitive neuroectodermal differentiation: case report and review of the literature." J Neurooncol **83**(3): 313-318.
Kaput, J. and T. W. Sneider (1979). "Methylation of somatic vs germ cell DNAs analyzed by restriction endonuclease digestions." Nucleic Acids Res. **7**: 2303-2322.
Kato, H., S. Kato, et al. (2000). "Functional evaluation of p53 and PTEN gene mutations in gliomas." Clin Cancer Res **6**(10): 3937-3943.
Katoh, M., H. Kirikoshi, et al. (2001). "WNT2B2 mRNA, up-regulated in primary gastric cancer, is a positive regulator of the WNT-[beta]-catenin-TCF signaling pathway." Biochem Biophys Res Commun **289**: 1093-1098.
Kepes, J. J. (2002). "Gliosarcoma with areas of primitive neuroepithelial differentiation and extracranial metastasis." Clin Neuropathol **21**(4): 193-195; author reply 195-196.
Keshet, I., Y. Schlesinger, et al. (2006). "Evidence for an instructive mechanism of de novo methylation in cancer cells." Nature Genet **38**(2): 149-153.

Kiehna, E. N., R. K. Mulhern, et al. (2006). "Changes in attentional performance of children and young adults with localized primary brain tumors after conformal radiation therapy." J Clin Oncol **24**(33): 5283-5290.
Killian, J. K., S. Bilke, et al. (2009). "Large-scale profiling of archival lymph nodes reveals pervasive remodeling of the follicular lymphoma methylome." Cancer Res **69**(3): 758-764.
Kim, H., J. Jen, et al. (1994). "Clinical and pathological characteristics of sporadic colorectal carcinomas with DNA replication errors in microsatellite sequences." Am J Pathol **145**(1): 148-156.
Kleihues, P., P. C. Burger, et al., Eds. (1993). Histological typing of tumours of the central nervous system. World Health Organization international histological classifcation of tumours. Heidelberg, Springer.
Kleihues, P. and W. K. Cavenee, Eds. (2000). Tumours of the Nervous System. World Health Organization Classification of Tumours—Pathology and Genetics. Lyon, IARC Press.
Kleihues, P., B. Schauble, et al. (1997). "Tumors associated with p53 germline mutations: a synopsis of 91 families." Am J Pathol **150**(1): 1-13.
Knudson, A. G., Jr. (1971). "Mutation and cancer: statistical study of retinoblastoma." Proc Natl Acad Sci U S A **68**(4): 820-823.
Koch, A., A. Waha, et al. (2001). "Somatic mutations of WNT/wingless signaling pathway components in primitive neuroectodermal tumors." Int J Cancer **93**(3): 445-449.
Koehne, C. H. and R. N. Dubois (2004). "COX-2 inhibition and colorectal cancer." Semin Oncol **31**: 12-21.
Koga, Y., M. Pelizzola, et al. (2009). "Genome-wide screen of promoter methylation identifies novel markers in melanoma." Genome Res **19**(8): 1462-1470.
Kohler, G. and C. Milstein (1975). "Continuous cultures of fused cells secreting antibody of predefined specificity." Nature **256**(5517): 495-497.
Kolker, S., E. Mayatepek, et al. (2002). "White matter disease in cerebral organic acid disorders: clinical implications and suggested pathomechanisms." Neuropediatrics **33**(5): 225-231.
Kolker, S., V. Pawlak, et al. (2002). "NMDA receptor activation and respiratory chain complex V inhibition contribute to neurodegeneration in d-2-hydroxyglutaric aciduria." Eur J Neurosci **16**(1): 21-28.
Konduri, S. D., K. S. Srivenugopal, et al. (2003). "Promoter methylation and silencing of the tissue factor pathway inhibitor-2 (TFPI-2), a gene encoding an inhibitor of matrix metalloproteinases in human glioma cells." Oncogene **22**(29): 4509-4516.
Kool, M., J. Koster, et al. (2008). "Integrated genomics identifies five medulloblastoma subtypes with distinct genetic profiles, pathway signatures and clinicopathological features." PLoS ONE **3**(8): e3088.
Korinek, V. (1997). "Constitutive transcriptional activation by a [beta]-catenin-Tcf complex in APC-/- colon carcinoma." Science **275**: 1784-1787.
Kornblith, A. B., J. E. Herndon, et al. (2002). "Impact of azacytidine on the quality of life of patients with myelodysplastic syndrome treated in a randomized phase III trial: a Cancer and Leukemia Group B study." J Clin Oncol **20**(10): 2441-2452.

Korshunov, A., M. Remke, et al. (2010). "Focal genomic amplification at 19q13.42 comprises a powerful diagnostic marker for embryonal tumors with ependymoblastic rosettes." Acta Neuropathologica **120**(2): 253-260.
Krassenstein, R., E. Sauter, et al. (2004). "Detection of breast cancer in nipple aspirate fluid by CpG island hypermethylation." Clin Cancer Res **10**(1 Pt 1): 28-32.
Kraus, J. A., J. Felsberg, et al. (2002). "Molecular genetic analysis of the TP53, PTEN, CDKN2A, EGFR, CDK4 and MDM2 tumour-associated genes in supratentorial primitive neuroectodermal tumours and glioblastomas of childhood." Neuropatholo Appl Neurobiol **28**(4): 325-333.
Kressner, U., M. Inganas, et al. (1999). "Prognostic value of p53 genetic changes in colorectal cancer." J Clin Oncol **17**(2): 593-599.
Kubista, M., J. M. Andrade, et al. (2006). "The real-time polymerase chain reaction." Mol Aspects Med **27**(2-3): 95-125.
Kume, T. (2009). "Novel insights into the differential functions of Notch ligands in vascular formation." J Angiogenesis Res **1**(1): 8.
La Spina, M., S. Pizzolitto, et al. (2006). "Embryonal tumor with abundant neuropil and true rosettes. A new entity or only variations of a parent neoplasms (PNETs)? This is the dilemma." J Neurooncol **78**(3): 317-320.
Ladd-Acosta, C., J. Pevsner, et al. (2007). "DNA methylation signatures within the human brain." Am J Hum Genet **81**(6): 1304-1315.
Laird, P. W. (2010). "Principles and challenges of genome-wide DNA methylation analysis." Nat Rev Genet **11**(3): 191-203.
Lalloo, F., J. Varley, et al. (2006). "BRCA1, BRCA2 and TP53 mutations in very early-onset breast cancer with associated risks to relatives." Eur J Cancer **42**(8): 1143-1150.
Lamont, J. M., C. S. McManamy, et al. (2004). "Combined histopathological and molecular cytogenetic stratification of medulloblastoma patients." Clin Cancer Res **10**(16): 5482-5493.
Lane, D. P. (1992). "Cancer. p53, guardian of the genome." Nature **358**(6381): 15-16.
Lang, G. A., T. Iwakuma, et al. (2004). "Gain of function of a p53 hot spot mutation in a mouse model of Li-Fraumeni syndrome." Cell **119**(6): 861-872.
Langdon, J. A., J. M. Lamont, et al. (2006). "Combined genome-wide allelotyping and copy number analysis identify frequent genetic losses without copy number reduction in medulloblastoma." Genes Chromosomes Cancer **45**(1): 47-60.
Lannering, B. and R. D. Kortmann (2004). SIOP-PNET 4: A prospective randomised controlled trial of hyperfractionated versus conventionally fractionated radiotherapy in standard risk medulloblastoma. United Kingdom Children's Cancer Study Group. Leicester, UK.
Latini, A., K. Scussiato, et al. (2003). "D-2-hydroxyglutaric acid induces oxidative stress in cerebral cortex of young rats." Eur J Neurosci **17**(10): 2017-2022.
Lee, R. C., R. L. Feinbaum, et al. (1993). "The C. elegans heterochronic gene lin-4 encodes small RNAs with antisense complementarity to lin-14." Cell **75**(5): 843-854.
Lee, S. M., H. J. Koh, et al. (2002). "Cytosolic NADP(+)-dependent isocitrate dehydrogenase status modulates oxidative damage to cells." Free Radic Biol Med **32**(11): 1185-1196.

Leon, S. A., B. Shapiro, et al. (1977). "Free DNA in the serum of cancer patients and the effect of therapy." Cancer Res **37**(3): 646-650.
Leonard, J. R., D. X. Cai, et al. (2001). "Large cell/anaplastic medulloblastomas and medullomyoblastomas: clinicopathological and genetic features." J Neurosurg **95**(1): 82-88.
Levenson, V. V. (2010). "DNA methylation as a universal biomarker." Exp Rev Mol Diagn **10**(4): 481-488.
Levine, A. J. (1997). "p53, the cellular gatekeeper for growth and division." Cell **88**(3): 323-331.
Li, F. P., J. F. Fraumeni, et al. (1988). "A cancer family syndrome in twenty-four kindreds." Cancer Res **48**(18): 5358-5362.
Li, M., K. F. Lee, et al. (2009). "Frequent amplification of a chr19q13.41 microRNA polycistron in aggressive primitive neuroectodermal brain tumors." Cancer Cell **16**(6): 533-546.
Li, M. H., E. Bouffet, et al. (2005). "Molecular genetics of supratentorial primitive neuroectodermal tumors and pineoblastoma." Neurosurg Focus **19**(5): E3.
Liang, G., M. L. Gonzalgo, et al. (2002). "Identification of DNA methylation differences during tumorigenesis by methylation-sensitive arbitrarily primed polymerase chain reaction." Methods **27**: 150-155.
Liang, J., A. Xu, et al. (2008). "Some but not all of HLA-II alleles are associated with cervical cancer in Chinese women." Cancer Genet Cytogenet **187**(2): 95-100.
Linabery, A. M. and J. A. Ross (2008). "Trends in childhood cancer incidence in the U.S. (1992-2004)." Cancer **112**(2): 416-432.
Lindsey, J. C., J. A. Anderton, et al. (2005). "Epigenetic events in medulloblastoma development." Neurosurg Focus **19**(5): E10.
Lindsey, J. C., M. E. Lusher, et al. (2004). "Identification of tumour-specific epigenetic events in medulloblastoma development by hypermethylation profiling." Carcinogenesis **25**(5): 661-668.
Linzer, D. I. and A. J. Levine (1979). "Characterization of a 54K dalton cellular SV40 tumor antigen present in SV40-transformed cells and uninfected embryonal carcinoma cells." Cell **17**(1): 43-52.
Liu, B. L., J. X. Cheng, et al. (2010). "Quantitative detection of multiple gene promoter hypermethylation in tumor tissue, serum, and cerebrospinal fluid predicts prognosis of malignant gliomas." Neuro Oncol **12**(6): 540-548.
Liu, L., S. Tommasi, et al. (2003). "Control of microtubule stability by the RASSF1A tumor suppressor." Oncogene **22**(50): 8125-8136.
Lo Muzio, L. (2008). "Nevoid basal cell carcinoma syndrome (Gorlin syndrome)." Orphanet J Rare Dis **3**(1): 32.
Logan, C. Y. and R. Nusse (2004). "The Wnt signaling pathway in development and disease." Ann Rev Cell Dev Biol **20**: 781-810.
Loh, M., N. Liem, et al. (2010). "Impact of Sample Heterogeneity on Methylation Analysis." Diagn Mol Pathol **19**(4): 243-247 210.1097/PDM.1090b1013e3181de4396.
Louis, D. N., H. Ohgaki, et al., Eds. (2007). WHO Classifcation of tumours of the central nervous system. Lyon, IARC.

Louis, D. N., H. Ohgaki, et al. (2007). "The 2007 WHO classification of tumours of the central nervous system." Acta Neuropathol **114**(2): 97-109.
Lu, C. and W. S. El-Deiry (2009). "Targeting p53 for enhanced radio- and chemo-sensitivity." Apoptosis **14**(4): 597-606.
Lu, W., H. N. Tinsley, et al. (2009). "Suppression of Wnt/beta-catenin signaling inhibits prostate cancer cell proliferation." Eur J Pharmacol **602**(1): 8-14.
Lu, X., A. Pearson, et al. (2003). "The MYCN oncoprotein as a drug development target." Cancer Lett **197**(1-2): 125-130.
Lusher, M. E., J. C. Lindsey, et al. (2002). "Biallelic epigenetic inactivation of the RASSF1A tumor suppressor gene in medulloblastoma development." Cancer Res **62**(20): 5906-5911.
Lustig, B., B. Jerchow, et al. (2002). "Negative Feedback Loop of Wnt Signaling through Upregulation of Conductin/Axin2 in Colorectal and Liver Tumors." Mol Cell Biol **22**(4): 1184-1193.
Mai, S., J. Hanley-Hyde, et al. (1996). "c-Myc overexpression associated DHFR gene amplification in hamster, rat, mouse and human cell lines." Oncogene **12**(2): 277-288.
Malkin, D., F. P. Li, et al. (1990). "Germ line p53 mutations in a familial syndrome of breast cancer, sarcomas, and other neoplasms." Science **250**(4985): 1233-1238.
Marder, J. (2010). "Cancer research. Childhood's cures haunted by adulthood's 'late effects'." Science **328**(5985): 1474-1475.
Mardis, E. R., L. Ding, et al. (2009). "Recurring mutations found by sequencing an acute myeloid leukemia genome." N Engl J Med **361**(11): 1058-1066.
Marec-Berard, P., A. Jouvet, et al. (2002). "Supratentorial embryonal tumors in children under 5 years of age: An SFOP study of treatment with postoperative chemotherapy alone." Med Pediatr Oncol **38**(2): 83-90.
Margittai, E. and G. Banhegyi (2008). "Isocitrate dehydrogenase: A NADPH-generating enzyme in the lumen of the endoplasmic reticulum." Arch Biochem Biophys **471**(2): 184-190.
Marine, J. C., S. Francoz, et al. (2006). "Keeping p53 in check: essential and synergistic functions of Mdm2 and Mdm4." Cell Death Differ **13**(6): 927-934.
Marino, S., M. Vooijs, et al. (2000). "Induction of medulloblastomas in p53-null mutant mice by somatic inactivation of Rb in the external granular layer cells of the cerebellum." Genes Dev **14**(8): 994-1004.
Martin-Subero, J. I., M. Kreuz, et al. (2009). "New insights into the biology and origin of mature aggressive B-cell lymphomas by combined epigenomic, genomic, and transcriptional profiling." Blood **113**(11): 2488-2497.
Martin, V., L. Mazzucchelli, et al. (2009). "An overview of the epidermal growth factor receptor fluorescence in situ hybridisation challenge in tumour pathology." J Clin Pathol **62**(4): 314-324.
Mason, W. P., A. Grovas, et al. (1998). "Intensive chemotherapy and bone marrow rescue for young children with newly diagnosed malignant brain tumors." J Clin Oncol **16**(1): 210-221.
Massimino, M., L. Gandola, et al. (2006). "Supratentorial primitive neuroectodermal tumors (S-PNET) in children: A prospective experience with adjuvant intensive

chemotherapy and hyperfractionated accelerated radiotherapy." Int J Radiat Oncol Biol Phys **64**(4): 1031-1037.
Masumoto, H., D. Hawke, et al. (2005). "A role for cell-cycle-regulated histone H3 lysine 56 acetylation in the DNA damage response." Nature **436**(7048): 294-298.
Mathew, P., M. B. Valentine, et al. (2001). "Detection of MYCN gene amplification in neuroblastoma by fluorescence in situ hybridization: a pediatric oncology group study." Neoplasia **3**(2): 105-109.
McCabe, M. G., K. Ichimura, et al. (2006). "High-resolution array-based comparative genomic hybridization of medulloblastomas and supratentorial primitive neuroectodermal tumors." J Neuropathol Exp Neurol **65**(6): 549-561.
McDonald, J. D., L. Daneshvar, et al. (1994). "Physical mapping of chromosome 17p13.3 in the region of a putative tumor suppressor gene important in medulloblastoma." Genomics **23**(1): 229-232.
McLendon, R. E., H. S. Friedman, et al. (1999). "Diagnostic markers in paediatric medulloblastoma: a Paediatric Oncology Group Study." Histopathology **34**(2): 154-162.
McLendon, R. E. and J. Provenzale (2002). "Glioneuronal tumors of the central nervous system." Brain Tumor Pathol **19**(2): 51-58.
McManamy, C. S., J. M. Lamont, et al. (2003). "Morphophenotypic variation predicts clinical behavior in childhood non-desmoplastic medulloblastomas." J Neuropathol Exp Neurol **62**(6): 627-632.
McRonald, F., M. Morris, et al. (2009). "CpG methylation profiling in VHL related and VHL unrelated renal cell carcinoma." Mol Cancer **8**(1): 31.
McRonald, F. E., M. R. Morris, et al. (2009). "CpG methylation profiling in VHL related and VHL unrelated renal cell carcinoma." Mol Cancer **8**: 31.
Megahed, H. (2010). Wnt/Wg pathway activation in medulloblastoma and disease risk stratification, Newcastle University.
Meyer, N. and L. Z. Penn (2008). "Reflecting on 25 years with MYC." Nat Rev Cancer **8**(12): 976-990.
Michael, D. and M. Oren (2002). "The p53 and Mdm2 families in cancer." Curr Opin Genet Dev **12**(1): 53-59.
Michalowski, M. B., F. de Fraipont, et al. (2006). "Methylation of RASSF1A and TRAIL pathway-related genes is frequent in childhood intracranial ependymomas and benign choroid plexus papilloma." Cancer Genet Cytogenet **166**(1): 74-81.
Michalowski, M. B., F. de Fraipont, et al. (2008). "Methylation of tumor-suppressor genes in neuroblastoma: The RASSF1A gene is almost always methylated in primary tumors." Pediatr Blood Cancer **50**(1): 29-32.
Milani, L., A. Lundmark, et al. (2010). "DNA methylation for subtype classification and prediction of treatment outcome in patients with childhood acute lymphoblastic leukemia." Blood **115**(6): 1214-1225.
Milovanovic, T. (2004). "Expression of Wnt genes and frizzled 1 and 2 receptors in normal breast epithelium and infiltrating breast carcinoma." Int J Oncol. **25**: 1337-1342.
Miotto, E., S. Sabbioni, et al. (2004). "Frequent aberrant methylation of the CDH4 gene promoter in human colorectal and gastric cancer." Cancer Res **64**(22): 8156-8159.

Mitelman, F., Ed. (1995). ISCN1995: An international system for human cytogenetic nomenclature (1995). Memphis, Tennessee, USA, Karger.
Miyaki, M. (1994). "Characteristics of somatic mutation of the adenomatous polyposis coli gene in colorectal tumors." Cancer Res. **54**: 3011-3020.
Miyamoto, K. and T. Ushijima (2005). "Diagnostic and therapeutic applications of epigenetics." Jpn J Clin Oncol **35**(6): 293-301.
Mizzen, C. A. and C. D. Allis (2000). "Transcription. New insights into an old modification." Science **289**(5488): 2290-2291.
Mohammadi-Asl, J., B. Larijani, et al. (2010). "Qualitative and quantitative promoter hypermethylation patterns of the P16, TSHR, RASSF1A and RARbeta2 genes in papillary thyroid carcinoma." Med Oncol.
Momand, J., D. Jung, et al. (1998). "The MDM2 gene amplification database." Nucleic Acids Res **26**(15): 3453-3459.
Momota, H., A. H. Shih, et al. (2008). "c-Myc and beta-catenin cooperate with loss of p53 to generate multiple members of the primitive neuroectodermal tumor family in mice." Oncogene **27**(32): 4392-4401.
Moorman, A. V., H. M. Ensor, et al. (2010). "Prognostic effect of chromosomal abnormalities in childhood B-cell precursor acute lymphoblastic leukaemia: results from the UK Medical Research Council ALL97/99 randomised trial." Lancet Oncol **11**(5): 429-438.
Morin, P. J. (1997). "Activation of [beta]-catenin-Tcf signaling in colon cancer by mutations in [beta]-catenin or APC." Science **275**: 1787-1790.
Moriuchi, S., K. Shimizu, et al. (1996). "An immunohistochemical analysis of medulloblastoma and PNET with emphasis on N-myc protein expression." Anticancer Res **16**(5A): 2687-2692.
Mostow, E. N., J. Byrne, et al. (1991). "Quality of life in long-term survivors of CNS tumors of childhood and adolescence." J Clin Oncol **9**(4): 592-599.
MRC-Holland (2009) "Designing syntheic MLPA probes." 1-18.
Muhlisch, J., T. Bajanowski, et al. (2007). "Frequent but borderline methylation of p16 (INK4a) and TIMP3 in medulloblastoma and sPNET revealed by quantitative analyses." J Neurooncol **83**(1): 17-29.
Muhlisch, J., A. Schwering, et al. (2006). "Epigenetic repression of RASSF1A but not CASP8 in supratentorial PNET (sPNET) and atypical teratoid/rhabdoid tumors (AT/RT) of childhood." Oncogene **25**(7): 1111-1117.
Mulhern, R. K., J. L. Kepner, et al. (1998). "Neuropsychologic functioning of survivors of childhood medulloblastoma randomized to receive conventional or reduced-dose craniospinal irradiation: a Pediatric Oncology Group study." J Clin Oncol **16**(5): 1723-1728.
Mulhern, R. K., S. L. Palmer, et al. (2001). "Risks of young age for selected neurocognitive deficits in medulloblastoma are associated with white matter loss." J Clin Oncol **19**(2): 472-479.
Muller, H. M., H. Fiegl, et al. (2004). "Prognostic DNA methylation marker in serum of cancer patients." Ann N Y Acad Sci **1022**: 44-49.
Mullis, K. B. and F. A. Faloona (1987). "Specific synthesis of DNA in vitro via a polymerase-catalyzed chain reaction." Methods Enzymol **155**: 335-350.

Mutskov, V. and G. Felsenfeld (2004). "Silencing of transgene transcription precedes methylation of promoter DNA and histone H3 lysine 9." EMBO J **23**(1): 138-149.
Nagao, K., H. Ito, et al. (1997). "Chromosomal rearrangement t(11;22) in extraskeletal Ewing's sarcoma and primitive neuroectodermal tumour analysed by fluorescence in situ hybridization using paraffin-embedded tissue." The Journal of pathology **181**(1): 62-66.
Nakane, P. K. and G. B. Pierce (1966). "Enzyme-labeled antibodies: preparation and application for the localization of antigens." J Histochem Cytochem **14**(12): 929-931.
Nath, N., R. Vassell, et al. (2009). "Nitro-aspirin inhibits MCF-7 breast cancer cell growth: effects on COX-2 expression and Wnt/beta-catenin/TCF-4 signaling." Biochem Pharmacol **78**(10): 1298-1304.
Nesbit, C. E., J. M. Tersak, et al. (1999). "MYC oncogenes and human neoplastic disease." Oncogene **18**(19): 3004-3016.
Newcomb, E. W., M. Alonso, et al. (2000). "Incidence of p14ARF gene deletion in high-grade adult and pediatric astrocytomas." Hum Pathol **31**(1): 115-119.
Ng, H. K., S. Y. Lo, et al. (1994). "Paraffin section p53 protein immunohistochemistry in neuroectodermal tumors." Pathology **26**(1): 1 - 5.
Ngo, C. V., M. Gee, et al. (2000). "An in vivo function for the transforming Myc protein: elicitation of the angiogenic phenotype." Cell Growth Differ **11**(4): 201-210.
Nicholls, R. D. and J. L. Knepper (2001). "Genome organization, function, and imprinting in Prader-Willi and Angelman syndromes." Annu Rev Genomics Hum Genet **2**: 153-175.
Nicholson, J., C. Wickramasinghe, et al. (2000). "Imbalances of chromosome 17 in medulloblastomas determined by comparative genomic hybridisation and fluorescence in situ hybridisation." Mol Pathol **53**(6): 313-319.
Nobusawa, S., T. Watanabe, et al. (2009). "IDH1 mutations as molecular signature and predictive factor of secondary glioblastomas." Clin Cancer Res **15**(19): 6002-6007.
Noguera, R., A. Canete, et al. (2003). "MYCN gain and MYCN amplification in a stage 4S neuroblastoma." Cancer Genet Cytogenet **140**(2): 157-161.
Northcott, P. A., L. A. Fernandez, et al. (2009). "The miR-17/92 polycistron is up-regulated in sonic hedgehog-driven medulloblastomas and induced by N-myc in sonic hedgehog-treated cerebellar neural precursors." Cancer Res **69**(8): 3249-3255.
Northcott, P. A., A. Korshunov, et al. (2010). "Medulloblastoma Comprises Four Distinct Molecular Variants." J Clin Oncol.
Noushmehr, H., D. J. Weisenberger, et al. (2010). "Identification of a CpG island methylator phenotype that defines a distinct subgroup of glioma." Cancer Cell **17**(5): 510-522.
Nowell, P. C. and D. A. Hungerford (1960). "Chromosome studies on normal and leukemic human leukocytes." Journal of the National Cancer Institute **25**: 85-109.
O'Riain, C., D. M. O'Shea, et al. (2009). "Array-based DNA methylation profiling in follicular lymphoma." Leukemia **23**(10): 1858-1866.

Oda, M., J. L. Glass, et al. (2009). "High-resolution genome-wide cytosine methylation profiling with simultaneous copy number analysis and optimization for limited cell numbers." Nucl Acids Res **37**(12): 3829-3839.
Ohba, S., K. Yoshida, et al. (2008). "A supratentorial primitive neuroectodermal tumor in an adult: a case report and review of the literature." J Clin Oncol **86**(2): 217-224.
Ohtani-Fujita, N., T. Fujita, et al. (1993). "CpG methylation inactivates the promoter activity of the human retinoblastoma tumor-suppressor gene." Oncogene **8**(4): 1063-1067.
Olive, K. P., D. A. Tuveson, et al. (2004). "Mutant p53 gain of function in two mouse models of Li-Fraumeni syndrome." Cell **119**(6): 847-860.
Olivier, M., D. E. Goldgar, et al. (2003). "Li-Fraumeni and related syndromes: correlation between tumor type, family structure, and TP53 genotype." Cancer Res **63**(20): 6643-6650.
Onel, K. and C. Cordon-Cardo (2004). "MDM2 and prognosis." Mol Cancer Res **2**(1): 1-8.
ONS (2010). Cancer statistics - Registrations, England, 2007, Office for National statistics. **MB1**.
ONS (2010). Statistical Bulletin: Childhood, infant and perinatal mortality in England and Wales: 2008., Office for National Statistics.
Oppenheim, R. W. (1991). "Cell death during development of the nervous system." Ann Rev Neurosci **14**: 453-501.
Orellana, C., F. Martinez, et al. (1998). "A novel TP53 germ-line mutation identified in a girl with a primitive neuroectodermal tumor and her father." Cancer Genet Cytogenet **105**(2): 103-108.
Packer, R. J., L. N. Sutton, et al. (1994). "Outcome for children with medulloblastoma treated with radiation and cisplatin, CCNU, and vincristine chemotherapy." J Neurosurg **81**(5): 690-698.
Palmisano, W. A., K. K. Divine, et al. (2000). "Predicting lung cancer by detecting aberrant promoter methylation in sputum." Cancer Res **60**(21): 5954-5958.
Pardanani, A., T. L. Lasho, et al. (2010). "IDH1 and IDH2 mutation analysis in chronic- and blast-phase myeloproliferative neoplasms." Leukemia **24**(6): 1146-1151.
Parsons, B. L. (2008). "Many different tumor types have polyclonal tumor origin: evidence and implications." Mutat Res **659**(3): 232-247.
Parsons, D. W., S. Jones, et al. (2008). "An integrated genomic analysis of human glioblastoma multiforme." Science **321**(5897): 1807-1812.
Patnaik, M. M., T. L. Lasho, et al. (2010). "WHO-defined 'myelodysplastic syndrome with isolated del(5q)' in 88 consecutive patients: survival data, leukemic transformation rates and prevalence of JAK2, MPL and IDH mutations." Leukemia.
Paulino, A. C., D. T. Cha, et al. (2004). "Patterns of failure in relation to radiotherapy fields in supratentorial primitive neuroectodermal tumor." Int J Radiat Oncol Biol Phys **58**(4): 1171-1176.
Paulino, A. C. and E. Melian (1999). "Medulloblastoma and supratentorial primitive neuroectodermal tumors." Cancer **86**(1): 142-148.
Paulus, W. (2009). "GFAP, Ki67 and IDH1: perhaps the golden triad of glioma immunohistochemistry." Acta Neuropathol **118**(5): 603-604.

Paulus, W. and P. Kleihues (2010). "Genetic profiling of CNS tumors extends histological classification." Acta Neuropathol **120**(2): 269-270.
Pelengaris, S., M. Khan, et al. (2002). "c-MYC: more than just a matter of life and death." Nat Rev Cancer **2**(10): 764-776.
Peris-Bonet, R., C. Martinez-Garcia, et al. (2006). "Childhood central nervous system tumours--incidence and survival in Europe (1978-1997): report from Automated Childhood Cancer Information System project." Eur J Cancer **42**(13): 2064-2080.
Peris-Bonet, R., D. Salmeron, et al. (2010). "Childhood cancer incidence and survival in Spain." Ann Oncol **21 Suppl 3**: iii103-110.
Perry, A., C. R. Miller, et al. (2009). "Malignant Gliomas with Primitive Neuroectodermal Tumor-like Components: A Clinicopathologic and Genetic Study of 53 Cases." Brain Pathology **19**(1): 81-90.
Petitjean, A., E. Mathe, et al. (2007). "Impact of mutant p53 functional properties on TP53 mutation patterns and tumor phenotype: lessons from recent developments in the IARC TP53 database." Hum Mut **28**(6): 622-629.
Pfaff, E., M. Remke, et al. (2010). "TP53 Mutation Is Frequently Associated With CTNNB1 Mutation or MYCN Amplification and Is Compatible With Long-Term Survival in Medulloblastoma." Journal of Clinical Oncology.
Pfeifer, G. P. and R. Dammann (2005). "Methylation of the tumor suppressor gene RASSF1A in human tumors." Biochem **70**(5): 576-583.
Pfister, S., M. Remke, et al. (2009). "Outcome Prediction in Pediatric Medulloblastoma Based on DNA Copy-Number Aberrations of Chromosomes 6q and 17q and the MYC and MYCN Loci." J Clin Oncol **27**(10): 1627-1636.
Pfister, S., M. Remke, et al. (2009). "Novel genomic amplification targeting the microRNA cluster at 19q13.42 in a pediatric embryonal tumor with abundant neuropil and true rosettes." Acta Neuropathol **117**(4): 457-464.
Pfister, S., M. Remke, et al. (2007). "Supratentorial primitive neuroectodermal tumors of the central nervous system frequently harbor deletions of the CDKN2A locus and other genomic aberrations distinct from medulloblastomas." Genes Chromosomes Cancer **46**(9): 839-851.
Phillips, R. K. (2002). "A randomised, double blind, placebo controlled study of celecoxib, a selective cyclooxygenase 2 inhibitor, on duodenal polyposis in familial adenomatous polyposis." Gut **50**: 857-860.
Pietsch, T., T. Scharmann, et al. (1994). "Characterization of Five New Cell Lines Derived from Human Primitive Neuroectodermal Tumors of the Central Nervous System." Cancer Res **54**(12): 3278-3287.
Piperi, C., M. S. Themistocleous, et al. (2010). "High incidence of MGMT and RARbeta promoter methylation in primary glioblastomas: association with histopathological characteristics, inflammatory mediators and clinical outcome." Mol Med **16**: 1-9.
Pizer, B. and S. Clifford (2008). "Medulloblastoma: new insights into biology and treatment." Arch Dis Child Educ Pract Ed **93**(5): 137-144.
Pizer, B. L. and S. C. Clifford (2009). "The potential impact of tumour biology on improved clinical practice for medulloblastoma: progress towards biologically driven clinical trials." Br J Neurosurg **23**(4): 364-375.

Pizer, B. L., C. L. Weston, et al. (2006). "Analysis of patients with supratentorial primitive neuro-ectodermal tumours entered into the SIOP/UKCCSG PNET 3 study." Eur J Cancer **42**(8): 1120-1128.
Plumb, J. A., G. Strathdee, et al. (2000). "Reversal of drug resistance in human tumor xenografts by 2'-deoxy-5-azacytidine-induced demethylation of the hMLH1 gene promoter." Cancer Res **60**(21): 6039-6044.
Polakis, P. (2000). "Wnt signaling and cancer." Genes Dev **14**(15): 1837-1851.
Pollard, K. S., H. N. Gilbert, et al. (2010) "Resampling-based multiple hypothesis testing. Package 'multtest'."
Pomeroy, S. L., P. Tamayo, et al. (2002). "Prediction of central nervous system embryonal tumour outcome based on gene expression." Nature **415**(6870): 436-442.
Press, M. F., R. S. Finn, et al. (2008). "HER-2 gene amplification, HER-2 and epidermal growth factor receptor mRNA and protein expression, and lapatinib efficacy in women with metastatic breast cancer." Clin Cancer Res **14**(23): 7861-7870.
Prochownik, E. V. and Y. Li (2007). "The ever expanding role for c-Myc in promoting genomic instability." Cell Cycle **6**(9): 1024-1029.
Quackenbush, J. (2001). "Computational analysis of microarray data." Nat Rev Genet **2**(6): 418-427.
Radhakrishnan, R., S. Kabekkodu, et al. (2011). "DNA hypermethylation as an epigenetic mark for oral cancer diagnosis." J Oral Pathol Med.
Rauch, T. and G. P. Pfeifer (2005). "Methylated-CpG island recovery assay: a new technique for the rapid detection of methylated-CpG islands in cancer." Lab Invest **85**(9): 1172-1180.
Ray, A., M. Ho, et al. (2004). "A clinicobiological model predicting survival in medulloblastoma." Clin Cancer Res **10**(22): 7613-7620.
Reddy, A. T., A. J. Janss, et al. (2000). "Outcome for children with supratentorial primitive neuroectodermal tumors treated with surgery, radiation, and chemotherapy." Cancer **88**(9): 2189-2193.
Reifenberger, J., G. Janssen, et al. (1998). "Primitive neuroectodermal tumors of the cerebral hemispheres in two siblings with TP53 germline mutation." J Neuropathol Exp Neurol **57**(2): 179-187.
Reinders, J., C. Delucinge Vivier, et al. (2008). "Genome-wide, high-resolution DNA methylation profiling using bisulfite-mediated cytosine conversion." Genome Res **18**(3): 469-476.
Ren, J., B. N. Singh, et al. (2011). "DNA hypermethylation as a chemotherapy target." Cell Signal **23**(7): 1082-1093.
Reynolds, T. C., S. D. Smith, et al. (1987). "Analysis of DNA surrounding the breakpoints of chromosomal translocations involving the beta T cell receptor gene in human lymphoblastic neoplasms." Cell **50**(1): 107-117.
Rhee, C. S., M. Sen, et al. (2002). "Wnt and frizzled receptors as potential targets for immunotherapy in head and neck squamous cell carcinomas." Oncogene **21**(43): 6598-6605.
Rigas, B. (2007). "Novel agents for cancer prevention based on nitric oxide." Biochem Soc Trans **35**(Pt 5): 1364-1368.

Rigas, B. and J. L. Williams (2002). "NO-releasing NSAIDs and colon cancer chemoprevention: a promising novel approach (Review)." Int J Oncol **20**: 885-890.

Roberts, P., P. D. Chumas, et al. (2001). "A review of the cytogenetics of 58 pediatric brain tumors." Cancer Genet Cytogenet **131**(1): 1-12.

Robertson, K. D. (2005). "DNA methylation and human disease." Nat Rev Genet **6**(8): 597-610.

Rogers, H. A., S. Miller, et al. (2009). "An investigation of WNT pathway activation and association with survival in central nervous system primitive neuroectodermal tumours (CNS PNET)." Br J Cancer **100**(8): 1292-1302.

Rorke, L. B. (1983). "The cerebellar medulloblastoma and its relationship to primitive neuroectodermal tumors." J Neuropathol Exp Neurol **42**(1): 1-15.

Rorke, L. B., J. Q. Trojanowski, et al. (1997). "Primitive neuroectodermal tumors of the central nervous system." Brain Pathol **7**(2): 765-784.

Rosenbaum, E., M. O. Hoque, et al. (2005). "Promoter hypermethylation as an independent prognostic factor for relapse in patients with prostate cancer following radical prostatectomy." Clin Cancer Res **11**(23): 8321-8325.

Rossi, M. R., J. Conroy, et al. (2006). "Array CGH analysis of pediatric medulloblastomas." Genes Chromosomes Cancer **45**(3): 290-303.

Rostomily, R. C., O. Bermingham-McDonogh, et al. (1997). "Expression of neurogenic basic helix-loop-helix genes in primitive neuroectodermal tumors." Cancer Res **57**(16): 3526-3531.

Roupret, M., V. Hupertan, et al. (2007). "Molecular detection of localized prostate cancer using quantitative methylation-specific PCR on urinary cells obtained following prostate massage." Clin Cancer Res **13**(6): 1720-1725.

Russo, C., M. Pellarin, et al. (1999). "Comparative genomic hybridization in patients with supratentorial and infratentorial primitive neuroectodermal tumors." Cancer **86**(2): 331-339.

Ryan, K. M. and G. D. Birnie (1996). "Myc oncogenes: the enigmatic family." Biochem J **314 (Pt 3)**: 713-721.

Ryan, S. (2009). The clinical and biological roles of MYC gene family amplification in childhood medulloblastoma, Newcastle University.

Sambrook, J. and D. W. Russell (2001). Molecular Cloning: A Laboratory Manual. New York, Cold Spring Harbor Laboratory Press.

Sanders, R. P., M. Kocak, et al. (2007). "High-grade astrocytoma in very young children." Pediatr Blood Cancer **49**(7): 888-893.

Sanders, R. P., A. Onar, et al. (2008). "M1 Medulloblastoma: high risk at any age." J Neurooncol **90**(3): 351-355.

Sanger, F., S. Nicklen, et al. (1977). "DNA sequencing with chain-terminating inhibitors." Proc Natl Acad Sci U S A **74**(12): 5463-5467.

Sanson, M., Y. Marie, et al. (2009). "Isocitrate dehydrogenase 1 codon 132 mutation is an important prognostic biomarker in gliomas." J Clin Oncol **27**(25): 4150-4154.

Saran, F. (2004). "New technology for radiotherapy in paediatric oncology." Eur J Cancer **40**(14): 2091-2105.

Saran, F., R. E. Taylor, et al. (2004). Hyperfractionated accelerated radiotherapy (HART) with chemotherapy (cisplatin, CCNU, vincristine) for non-pineal supratentorial

primitive neuroectodermal tumours. United Kingdom Children's Cancer Study Group. Leicester, UK.
Sarkar, C., P. Deb, et al. (2005). "Recent advances in embryonal tumours of the central nervous system." Childs Nerv Syst **21**(4): 272-293.
Sathyanarayana, U. G., A. Padar, et al. (2003). "Aberrant promoter methylation of laminin-5-encoding genes in prostate cancers and its relationship to clinicopathological features." Clin Cancer Res **9**(17): 6395-6400.
Sato, N., N. Maehara, et al. (2003). "Effects of 5-aza-2'-deoxycytidine on matrix metalloproteinase expression and pancreatic cancer cell invasiveness." J Natl Cancer Inst **95**(4): 327-330.
Sato, N., A. R. Parker, et al. (2005). "Epigenetic inactivation of TFPI-2 as a common mechanism associated with growth and invasion of pancreatic ductal adenocarcinoma." Oncogene **24**(5): 850-858.
Scheithauer, B. W. (2009). "Development of the WHO Classification of Tumors of the Central Nervous System: A Historical Perspective." Brain Pathol **19**(4): 551-564.
Schell, M. J., V. A. McHaney, et al. (1989). "Hearing loss in children and young adults receiving cisplatin with or without prior cranial irradiation." J Clin Oncol **7**(6): 754-760.
Scheurlen, W. G., G. C. Schwabe, et al. (1998). "Molecular analysis of childhood primitive neuroectodermal tumors defines markers associated with poor outcome." J Clin Oncol **16**(7): 2478-2485.
Scheurlen, W. G., P. Seranski, et al. (1997). "High-resolution deletion mapping of chromosome arm 17p in childhood primitive neuroectodermal tumors reveals a common chromosomal disruption within the Smith-Magenis region, an unstable region in chromosome band 17p11.2." Genes Chromosomes Cancer **18**(1): 50-58.
Schmidt, E. E., K. Ichimura, et al. (1994). "CDKN2 (p16/MTS1) gene deletion or CDK4 amplification occurs in the majority of glioblastomas." Cancer Res **54**(24): 6321-6324.
Schouten, J. P., C. J. McElgunn, et al. (2002). "Relative quantification of 40 nucleic acid sequences by multiplex ligation-dependent probe amplification." Nucleic Acids Res **30**(12): e57.
Schrappe, M. (2008). "Risk-adapted stratification and treatment of childhood acute lymphoblastic leukaemia." Radiat Prot Dosim **132**(2): 130-133.
Schwalbe, E. C., J. C. Lindsey, et al. (2011). "Rapid diagnosis of medulloblastoma molecular subgroups." Clin Cancer Res.
Semenza, G. L. (2003). "Targeting HIF-1 for cancer therapy." Nat Rev Cancer **3**(10): 721-732.
Shariat, S. F., J. Kim, et al. (2003). "Association of p53 and p21 expression with clinical outcome in patients with carcinoma in situ of the urinary bladder." Urology **61**(6): 1140-1145.
Shaulsky, G., N. Goldfinger, et al. (1990). "Nuclear accumulation of p53 protein is mediated by several nuclear localization signals and plays a role in tumorigenesis." Mol Cell Biol **10**(12): 6565-6577.
Shaw, D. W., E. Weinberger, et al. (1996). "Spinal subdural enhancement after suboccipital craniectomy." Am J Neuroradiol **17**(7): 1373-1377.

Shelling, A. N. (1997). "Role of p53 in drug resistance in ovarian cancer." Lancet **349**(9054): 744-745.
Shen, L., Y. Kondo, et al. (2007). "Drug sensitivity prediction by CpG island methylation profile in the NCI-60 cancer cell line panel." Cancer Res **67**(23): 11335-11343.
Shin, S. H., B. H. Kim, et al. (2010). "Identification of novel methylation markers in hepatocellular carcinoma using a methylation array." J Korean Med Sci **25**(8): 1152-1159.
Shtutman, M., J. Zhurinsky, et al. (1999). "The cyclin D1 gene is a target of the β-catenin/LEF-1 pathway." Proc Natl Acad Sci U S A **96**(10): 5522-5527.
Silber, J. H., P. S. Littman, et al. (1990). "Stature loss following skeletal irradiation for childhood cancer." J Clin Oncol **8**(2): 304-312.
Silva, J. M., G. Dominguez, et al. (1999). "Aberrant DNA methylation of the p16INK4a gene in plasma DNA of breast cancer patients." Br J Cancer **80**(8): 1262-1264.
Singh, S. K., I. D. Clarke, et al. (2004). "Cancer stem cells in nervous system tumors." Oncogene **23**(43): 7267-7273.
Singh, S. K., I. D. Clarke, et al. (2003). "Identification of a cancer stem cell in human brain tumors." Cancer Res **63**(18): 5821-5828.
Sionov, R. V., S. Coen, et al. (2001). "c-Abl regulates p53 levels under normal and stress conditions by preventing its nuclear export and ubiquitination." Mol Cell Biol **21**(17): 5869-5878.
Skinner, R., W. Wallace, et al., Eds. (2005). Therapy based long term follow up: Practice statement. Leicester, UKCCSG.
Smith, A. J., J. Xian, et al. (2002). "Cre-loxP chromosome engineering of a targeted deletion in the mouse corresponding to the 3p21.3 region of homozygous loss in human tumours." Oncogene **21**(29): 4521-4529.
Smith, M. A., B. Freidlin, et al. (1998). "Trends in reported incidence of primary malignant brain tumors in children in the United States." J Natl Cancer Inst **90**(17): 1269-1277.
Smith, M. A., N. L. Seibel, et al. (2010). "Outcomes for children and adolescents with cancer: challenges for the twenty-first century." J Clin Oncol **28**(15): 2625-2634.
Soares, J., A. E. Pinto, et al. (1999). "Global DNA hypomethylation in breast carcinoma: correlation with prognostic factors and tumor progression." Cancer **85**(1): 112-118.
Sonoda, Y., T. Kumabe, et al. (2009). "Analysis of IDH1 and IDH2 mutations in Japanese glioma patients." Cancer Sci **100**(10): 1996-1998.
Sonoda, Y. and T. Tominaga (2010). "2-hydroxyglutarate accumulation caused by IDH mutation is involved in the formation of malignant gliomas." Expert Rev Neurother **10**(4): 487-489.
Soussi, T. and G. Lozano (2005). "p53 mutation heterogeneity in cancer." Biochem Biophys Res Commun **331**(3): 834-842.
Spunberg, J. J., C. H. Chang, et al. (1981). "Quality of long-term survival following irradiation for intracranial tumors in children under the age of two." Int J Radiat Oncol Biol Phys **7**(6): 727-736.
St Clair, W. H., J. A. Adams, et al. (2004). "Advantage of protons compared to conventional X-ray or IMRT in the treatment of a pediatric patient with medulloblastoma." Int J Radiat Oncol Biol Phys **58**(3): 727-734.

Stark, A. M., A. Nabavi, et al. (2005). "Glioblastoma multiforme-report of 267 cases treated at a single institution." Surg Neurol **63**(2): 162-169; discussion 169.
Stavrou, T., E. C. Dubovsky, et al. (2000). "Intracranial calcifications in childhood medulloblastoma: relation to nevoid basal cell carcinoma syndrome." Am J Neuroradiol **21**(4): 790-794.
Steenman, M. J., S. Rainier, et al. (1994). "Loss of imprinting of IGF2 is linked to reduced expression and abnormal methylation of H19 in Wilms' tumour." Nat Genet **7**(3): 433-439.
Stiller, C. A. (2004). "Epidemiology and genetics of childhood cancer." Oncogene **23**(38): 6429-6444.
Stiller, C. A. (2007). Childhood Cancer in Britain. Incidence, survival, mortality. Oxford, Oxford University Press.
Storlazzi, C. T., T. Fioretos, et al. (2004). "Identification of a commonly amplified 4.3 Mb region with overexpression of C8FW, but not MYC in MYC-containing double minutes in myeloid malignancies." Hum Mol Genet **13**(14): 1479-1485.
Strachan, T. and A. P. Read (2004). Human Molecular Genetics. London, Garland Science Publishers Limited.
Strahl, B. D. and C. D. Allis (2000). "The language of covalent histone modifications." Nature **403**(6765): 41-45.
Strathdee, G. and R. Brown (2002). "Aberrant DNA methylation in cancer: potential clinical interventions." Expert Reviews In Molecular Medicine **4**(4): 1-17.
Stroun, M., P. Anker, et al. (1989). "Neoplastic characteristics of the DNA found in the plasma of cancer patients." Oncology **46**(5): 318-322.
Struys, E. A., G. S. Salomons, et al. (2005). "Mutations in the D-2-hydroxyglutarate dehydrogenase gene cause D-2-hydroxyglutaric aciduria." Am J Hum Genet **76**(2): 358-360.
Stupp, R., M. Hegi, et al. (2010). "Neuro-oncology, a decade of temozolomide and beyond." Exp Rev Anticanc **10**(11): 1675-1677.
Stupp, R., M. J. van den Bent, et al. (2005). "Optimal role of temozolomide in the treatment of malignant gliomas." Curr Neurol Neurosci **5**(3): 198-206.
Su, X., V. Gopalakrishnan, et al. (2006). "Abnormal expression of REST/NRSF and Myc in neural stem/progenitor cells causes cerebellar tumors by blocking neuronal differentiation." Mol Cell Biol **26**(5): 1666-1678.
Sunami, E., M. Shinozaki, et al. (2009). "Multimarker Circulating DNA Assay for Assessing Blood of Prostate Cancer Patients." Clin Chem **55**(3): 559-567.
Suzuki, T., K. Yoshida, et al. (2007). "Melanoma-associated antigen-A1 expression predicts resistance to docetaxel and paclitaxel in advanced and recurrent gastric cancer." Oncol Rep **18**(2): 329-336.
Syndikus, I., D. Tait, et al. (1994). "Long-term follow-up of young children with brain tumors after irradiation." Int J Radiat Oncol Biol Phys **30**(4): 781-787.
Tabori, U., B. Baskin, et al. (2010). "Universal poor survival in children with medulloblastoma harboring somatic TP53 mutations." J Clin Oncol **28**(8): 1345-1350.
Takai, D. and P. A. Jones (2002). "Comprehensive analysis of CpG islands in human chromosomes 21 and 22." Proc Natl Acad Sci U S A **99**(6): 3740-3745.

Takei, H., Y. Nguyen, et al. (2009). "Low-level copy gain versus amplification of myc oncogenes in medulloblastoma: utility in predicting prognosis and survival. Laboratory investigation." J Neurosurg Pediatr **3**(1): 61-65.
Tamber, M. S. and J. T. Rutka (2003). "Pediatric supratentorial high-grade gliomas." Neurosurg Focus **14**(2): e1.
Taylor, M. D., L. Liu, et al. (2002). "Mutations in SUFU predispose to medulloblastoma." Nat Genet **31**(3): 306-310.
Taylor, M. D., T. G. Mainprize, et al. (2000). "Molecular insight into medulloblastoma and central nervous system primitive neuroectodermal tumor biology from hereditary syndromes: a review." Neurosurgery **47**(4): 888-901.
Taylor, R. E., C. C. Bailey, et al. (2003). "Results of a randomized study of preradiation chemotherapy versus radiotherapy alone for nonmetastatic medulloblastoma: The International Society of Paediatric Oncology/United Kingdom Children's Cancer Study Group PNET-3 Study." J Clin Oncol **21**(8): 1581-1591.
Tefferi, A., T. L. Lasho, et al. (2010). "IDH1 and IDH2 mutation studies in 1473 patients with chronic-, fibrotic- or blast-phase essential thrombocythemia, polycythemia vera or myelofibrosis." Leukemia.
Terheggen, F., D. Troost, et al. (2007). "Local recurrence and distant metastasis of supratentorial primitive neuro-ectodermal tumor in an adult patient successfully treated with intensive induction chemotherapy and maintenance temozolomide." J Neurooncol **82**(1): 113-116.
Tetsu, O. and F. McCormick (1999). "[beta]-Catenin regulates expression of cyclin D1 in colon carcinoma cells." Nature **398**(6726): 422-426.
Teyssier, J. R. (1989). "The chromosomal analysis of human solid tumors. A triple challenge." Cancer Genet Cytogenet **37**(1): 103-125.
Theissen, J., M. Boensch, et al. (2009). "Heterogeneity of the MYCN oncogene in neuroblastoma." Clin Cancer Res **15**(6): 2085-2090.
Thirlwell, C., M. Eymard, et al. (2010). "Genome-wide DNA methylation analysis of archival formalin-fixed paraffin-embedded tissue using the Illumina Infinium HumanMethylation27 BeadChip." Methods **52**(3): 248-254.
Thol, F., E. M. Weissinger, et al. (2010). "IDH1 mutations in patients with myelodysplastic syndromes are associated with an unfavorable prognosis." Haematologica.
Thomas, G. A. and C. Raffel (1991). "Loss of heterozygosity on 6q, 16q, and 17p in human central nervous system primitive neuroectodermal tumors." Cancer Res **51**(2): 639-643.
Thompson, M. C., C. Fuller, et al. (2006). "Genomics identifies medulloblastoma subgroups that are enriched for specific genetic alterations." J Clin Oncol **24**(12): 1924-1931.
Thun, M. J. (1997). "Aspirin and gastrointestinal cancer." Adv Exp Med Biol **400A**: 395-402.
Thun, M. J., S. J. Henley, et al. (2002). "Nonsteroidal anti-inflammatory drugs as anticancer agents: mechanistic, pharmacologic, and clinical issues." J Natl Cancer Inst **94**: 252-266.
Timmermann, B., R. D. Kortmann, et al. (2002). "Role of radiotherapy in the treatment of supratentorial primitive neuroectodermal tumors in childhood: results of the

prospective German brain tumor trials HIT 88/89 and 91." J Clin Oncol **20**(3): 842-849.
Timmermann, B., R. D. Kortmann, et al. (2006). "Role of radiotherapy in supratentorial primitive neuroectodermal tumor in young children: results of the German HIT-SKK87 and HIT-SKK92 trials." J Clin Oncol **24**(10): 1554-1560.
Tokumaru, Y., S. V. Harden, et al. (2004). "Optimal use of a panel of methylation markers with GSTP1 hypermethylation in the diagnosis of prostate adenocarcinoma." Clin Cancer Res **10**(16): 5518-5522.
Tola, J. S. (1951). "The histopathological and biological characteristics of the primary neoplasms of the cerebellum and the fourth ventricle, with some aspects of their clinical picture, diagnosis, and treatment on the basis of 71 verified cases." Acta Chir Scand Suppl **164**: 1-112.
Tomizawa, Y., H. Iijima, et al. (2004). "Clinicopathological significance of aberrant methylation of RARbeta2 at 3p24, RASSF1A at 3p21.3, and FHIT at 3p14.2 in patients with non-small cell lung cancer." Lung Cancer **46**(3): 305-312.
Tommasi, S., R. Dammann, et al. (2005). "Tumor susceptibility of Rassf1a knockout mice." Cancer Res **65**(1): 92-98.
Tong, W. M., H. Ohgaki, et al. (2003). "Null mutation of DNA strand break-binding molecule poly(ADP-ribose) polymerase causes medulloblastomas in p53(-/-) mice." Am J Pathol **162**(1): 343-352.
Topaloglu, O., M. O. Hoque, et al. (2004). "Detection of promoter hypermethylation of multiple genes in the tumor and bronchoalveolar lavage of patients with lung cancer." Clin Cancer Res **10**(7): 2284-2288.
Trask, B. J. and J. L. Hamlin (1989). "Early dihydrofolate reductase gene amplification events in CHO cells usually occur on the same chromosome arm as the original locus." Genes Dev **3**(12A): 1913-1925.
Tsacopoulos, M. (2002). "Metabolic signaling between neurons and glial cells: a short review."
Tumilowicz, J. J., W. W. Nichols, et al. (1970). "Definition of a continuous human cell line derived from neuroblastoma." Cancer Res **30**(8): 2110-2118.
Uematsu, K. (2003). "Activation of the Wnt pathway in non small cell lung cancer: evidence of dishevelled overexpression." Oncogene **22**: 7218-7221.
Uematsu, Y., R. Takehara, et al. (2002). "Pleomorphic primitive neuroectodermal tumor with glial and neuronal differentiation: clinical, pathological, cultural, and chromosomal analysis of a case." J Neurooncol **59**(1): 71-79.
Valasek, M. A. and J. J. Repa (2005). "The power of real-time PCR." Adv Physiol Educ **29**(3): 151-159.
van Bokhoven, H., J. Celli, et al. (2005). "MYCN haploinsufficiency is associated with reduced brain size and intestinal atresias in Feingold syndrome." Nat Genet **37**(5): 465-467.
Vasudevan, S. A., J. G. Nuchtern, et al. (2005). "Gene profiling of high risk neuroblastoma." World J Surg **29**(3): 317-324.
Versteege, I., N. Sevenet, et al. (1998). "Truncating mutations of hSNF5/INI1 in aggressive paediatric cancer." Nature **394**(6689): 203-206.
Vita, M. and M. Henriksson (2006). "The Myc oncoprotein as a therapeutic target for human cancer." Semin Cancer Biol **16**(4): 318-330.

Vogelstein, B., D. Lane, et al. (2000). "Surfing the p53 network." Nature **408**(6810): 307-310.
Vousden, K. H. and X. Lu (2002). "Live or let die: the cell's response to p53." Nat Rev Cancer **2**(8): 594-604.
Wajner, M., A. Latini, et al. "The role of oxidative damage in the neuropathology of organic acidurias: insights from animal studies."
Wang, X., M. Wang, et al. (2009). "Evidence for common clonal origin of multifocal lung cancers." J Natl Cancer Inst **101**(8): 560-570.
Wang, Y. and F. C. Leung (2004). "An evaluation of new criteria for CpG islands in the human genome as gene markers." Bioinformatics **20**(7): 1170-1177.
Watanabe, T., S. Nobusawa, et al. (2009). "IDH1 mutations are early events in the development of astrocytomas and oligodendrogliomas." Am J Pathol **174**(4): 1149-1153.
Weber, M., J. J. Davies, et al. (2005). "Chromosome-wide and promoter-specific analyses identify sites of differential DNA methylation in normal and transformed human cells." Nat Genet **37**(8): 853-862.
Wei, S. H., R. Brown, et al. (2003). "Aberrant DNA methylation in ovarian cancer: is there an epigenetic predisposition to drug response?" Ann N Y Acad Sci **983**: 243-250.
Wen, J., J. Fu, et al. (2011). "Genetic and epigenetic changes in lung carcinoma and their clinical implications." Mod Pathol.
Wharton, S. B., I. R. Whittle, et al. (2001). "Gliosarcoma with areas of primitive neuroepithelial differentiation and extracranial metastasis." Clin Neuropathol **20**(5): 212-218.
WHO (2009). Cancer. W. H. Organsisation, World Health Organsisation.
Wicha, M. S., S. Liu, et al. (2006). "Cancer Stem Cells: An Old Idea—A Paradigm Shift." Cancer Research **66**(4): 1883-1890.
Widschwendter, A., C. Gattringer, et al. (2004). "Analysis of aberrant DNA methylation and human papillomavirus DNA in cervicovaginal specimens to detect invasive cervical cancer and its precursors." Clin Cancer Res **10**(10): 3396-3400.
Wiener, M. D., O. B. Boyko, et al. (1990). "False-positive spinal MR findings for subarachnoid spread of primary CNS tumor in postoperative pediatric patients." Am J Neuroradiol **11**: 1100-1103.
Willert, K., J. D. Brown, et al. (2003). "Wnt proteins are lipid-modified and can act as stem cell growth factors." Nature **423**(6938): 448-452.
Williamson, D., Y. J. Lu, et al. (2005). "Relationship between MYCN copy number and expression in rhabdomyosarcomas and correlation with adverse prognosis in the alveolar subtype." J Clin Oncol **23**(4): 880-888.
Wilne, S., J. Collier, et al. (2007). "Presentation of childhood CNS tumours: a systematic review and meta-analysis." Lancet Oncol **8**(8): 685-695.
Wolff, E. M., Y. Chihara, et al. (2010). "Unique DNA methylation patterns distinguish noninvasive and invasive urothelial cancers and establish an epigenetic field defect in premalignant tissue." Cancer Res **70**(20): 8169-8178.
Wolffe, A. P. and D. Guschin (2000). "Review: chromatin structural features and targets that regulate transcription." J Struct Biol **129**(2-3): 102-122.

Wong, I. H., J. Chan, et al. (2004). "Ubiquitous aberrant RASSF1A promoter methylation in childhood neoplasia." Clin Cancer Res **10**(3): 994-1002.
Workman, P. (2001). "Scoring a bull's-eye against cancer genome targets." Curr Opin Pharmacol **1**(4): 342-352.
Xie, J., M. Murone, et al. (1998). "Activating *Smoothened* mutations in sporadic basal-cell carcinoma." Nature **391**: 90-92.
Yamamoto, N., T. Nakayama, et al. (2011). "Detection of aberrant promoter methylation of GSTP1, RASSF1A, and RARβ2 in serum DNA of patients with breast cancer by a newly established one-step methylation-specific PCR assay." Breast Cancer Res Tr.
Yan, H., D. W. Parsons, et al. (2009). "IDH1 and IDH2 mutations in gliomas." N Engl J Med **360**(8): 765-773.
Yang, H. J., D. H. Nam, et al. (1999). "Supratentorial primitive neuroectodermal tumor in children: clinical features, treatment outcome and prognostic factors." Childs Nerv Syst **15**(8): 377-383.
Yang, Q., P. Zage, et al. (2004). "Association of epigenetic inactivation of RASSF1A with poor outcome in human neuroblastoma." Clin Cancer Res **10**(24): 8493-8500.
Yang, X., F. Lay, et al. (2010). "Targeting DNA methylation for epigenetic therapy." Trends Pharmacol Sci **31**(11): 536-546.
Yang, Y. and L. M. Fu (2003). "TSGDB: a database system for tumor suppressor genes." Bioinformatics **19**(17): 2311-2312.
Yoshimoto, M., J. Bayani, et al. (2006). "Metaphase and array comparative genomic hybridization: unique copy number changes and gene amplification of medulloblastomas in South America." Cancer Genet Cytogenet **170**(1): 40-47.
You, L., B. He, et al. (2004a). "An Anti-Wnt-2 Monoclonal Antibody Induces Apoptosis in Malignant Melanoma Cells and Inhibits Tumor Growth." Cancer Res **64**(15): 5385-5389.
You, L., B. He, et al. (2004). "Inhibition of Wnt-2-mediated signaling induces programmed cell death in non-small-cell lung cancer cells." Oncogene **23**(36): 6170-6174.
Zagzag, D., D. C. Miller, et al. (2000). "Primitive neuroectodermal tumors of the brainstem: investigation of seven cases." Pediatrics **106**(5): 1045-1053.
Zakrzewska, M., P. Rieske, et al. (2004). "Molecular abnormalities in pediatric embryonal brain tumors--analysis of loss of heterozygosity on chromosomes 1, 5, 9, 10, 11, 16, 17 and 22." Clin Neuropathol **23**(5): 209-217.
Zeltzer, P. M., J. M. Boyett, et al. (1999). "Metastasis stage, adjuvant treatment, and residual tumor are prognostic factors for medulloblastoma in children: conclusions from the Children's Cancer Group 921 randomized phase III study." J Clin Oncol **17**(3): 832-845.
Zhan, Q., M. J. Antinore, et al. (1999). "Association with Cdc2 and inhibition of Cdc2/Cyclin B1 kinase activity by the p53-regulated protein Gadd45." Oncogene **18**(18): 2892-2900.
Zhang, X., J. Yazaki, et al. (2006). "Genome-wide high-resolution mapping and functional analysis of DNA methylation in arabidopsis." Cell **126**(6): 1189-1201.
Zhang, Y. and A. Jeltsch (2010). "The Application of Next Generation Sequencing in DNA Methylation Analysis." Genes **1**(1): 85-101.

Zhao, S., Y. Lin, et al. (2009). "Glioma-derived mutations in IDH1 dominantly inhibit IDH1 catalytic activity and induce HIF-1alpha." Science **324**(5924): 261-265.
Zulch, K. J., Ed. (1979). Histological Typing of Tumours of the Central Nervous System. Geneva. , World Health Organization.

Chapter 8

Appendices

Table of Contents

Chapter 8

Appendix 1

Preparation of chemical reagents

All buffers were prepared according to (Sambrook and Russell 2001), and were stored at room temperature, unless otherwise stated.

8.1.1 10x TBE:

Tris base	108g	(Sigma-Aldrich)
Boric acid	55g	(Sigma-Aldrich)
EDTA	9.3g	(Sigma-Aldrich)

Made up to 1000ml with deionised water

8.1.2 1x TE:

1M Tris-HCl (pH8.0)	10ml	(Sigma-Aldrich)
0.25M EDTA	400µl	(Sigma-Aldrich)

Make up to 1000ml with deionised water

8.1.3 Phosphate Buffered Saline (PBS):

NaCl	8g	(VWR)
KCl	0.2g	(Sigma-Aldrich)
Na_2HPO_4	1.44g	(Sigma-Aldrich)
KH_2PO_4	0.24g	(Sigma-Aldrich)

Make up to 800ml with deionised water and adjust pH to 7.4 using hydrochloric acid

Make up to final volume of 1000ml with deionised water and sterilise by autoclaving

8.1.4 0.01M Citrate Buffer:

To make 10 litres:

Citric Acid monohydrate	21g	(VWR)
Distilled water	10,000ml	

Final solution adjusted to pH6.0 by adding 2M sodium hydrochloride solution

8.1.5 Tris Buffered Saline (TBS) 0.05M:

To make 5000ml:

Trizma® Base	6.95g	(Sigma-Aldrich)
Trizma®Hydrochloride	30.3g	(Sigma-Aldrich)
NaCl	45.0g	(VWR)
Distilled water	5000ml	

Final solution adjusted with 2M sodium hydrochloride solution to pH7.6

8.1.6 Sodium Hydrochloride 2M:

Sodium Hydrochloride	32g	(Sigma-Aldrich)
Distilled water	400ml	

8.1.7 Dako High pH9.8 Target Retrieval buffer:

To make 1000ml:

High pH Target retrieval	100ml	(Dako)
Distilled Water	900ml	

8.1.8 Scott's Water

Sodium bicarbonate	7g	(Sigma-Aldrich)
Magnesium sulphate	40g	(Sigma-Aldrich)
Thymol crystals	3	(Sigma-Aldrich)
Water	2000ml	

8.1.9 Acid/Alcohol immunohistochemistry solution

100% Ethanol	1400ml	
Hydrochloric acid	20ml	(Sigma-Aldrich)
Deionised water	600ml	

8.1.10 10x TBS-Tween:

Sodium Chloride	45g	(Sigma-Aldrich)

Tris	30g	(Becton Dickinson)
Made up to 500ml with deionised water		
Adjust to pH7.5 using hydrochloric acid		(Sigma-Aldrich)
Tween-20	2.5ml	
Made up to final volume of 5000ml with deionised water		

8.1.11 Harris Haematoxylin solution

Potassium alum	100g	(Sigma-Aldrich)
Haematoxylin	5g	(Sigma-Aldrich)
Mercuric oxide	2.5g	(Sigma-Aldrich)
Acetic acid	40ml	(Sigma-Aldrich)
100% Ethanol	50ml	
Water	1000ml	

The potassium alum is first dissolved in water by gently warming and stirring. Haematoxylin is dissolved in 100% ethanol and then added to the potassium alum solution which is boiled and removed from the heat before the mecuric acid is added. Finally once cooled acetic acid is added and the solution filtered to remove any deposits.

8.1.12 FISH wash buffer (SSCTM):

Skimmed milk powder	1g	
Tween-20	250µl	(Sigma-Aldrich)
4xSSC	500ml	(Becton Dickinson)

Appendix 2

“R” programme scripts

8.2

8.2.1 To generate a table to include a subset of probes

```
setwd("T:/Data/Raw Data/Array/subfolder")
#### Read in two group files. Obviously can subset to define separate groups
probes<-read.table("filename_a.csv",sep=",",header=TRUE,row.names=1)
probes2<-as.vector(probes[,1])
data<-read.table("filename_b.csv",header=TRUE,row.name=1, as.is =TRUE,sep=",")
group1<-data[rownames(data) %in% probes2,]
write.table(group1, file="filename_c.csv", sep=",")
dev.off()
```

8.2.2 Principal component analysis script

```
# set working directory
setwd("T:/Data/Raw Data/Array/subfolder")
# load library for displaying 3D graphs
library(rgl)
# Read in data, using arguments header=TRUE - sets first row as column titles,
# row.names=1 sets row names as first column
meth<-read.table("filename.csv",sep=",",header=TRUE,row.names=1)
meth.pca<-prcomp(t(meth))
# Label sample types with different colours eg: MB -red, C Pineos-blue, SPNETs-green,
control, black,
colour<-c(rep("black",37),rep("green",31),rep("blue",4),rep("red",100))
# plot principal component loadings with plot3d
plot3d(meth.pca$x[,1:3], type="s",size=1.0,col=colour)
#now plot PCA again, but removing selected samples eg the controls
meth1<-meth[,-c(1:37)]
meth1.pca<-prcomp(t(meth1))
dim(meth1)
colour1<-colour[-c(1:37)]
plot3d(meth1.pca$x[,1:3], type="s",size=1.0,col=colour1)
```

8.2.3 Bootstrapped hierarchical clustering and dendrograms

```
setwd("T:/Data/Raw Data/Array/subfolder")
library(pvclust)
library(gplots)
meth<-read.table("filename.csv",sep=",",header=TRUE,row.names=1)
# Store output in pdf
pdf("pdf_filename.pdf",height=11.7,width=16.5)
# Carry out bootstrapped hierarchical clustering
```

```
# Make cluster for parallel clustering
cl<-makeCluster(4)
clust1<-parPvclust(cl,meth,method.hclust="average",method.dist="cor",nboot=10000)
# Plot with 'flattened' projection
plot(clust1, print.pv=TRUE, print.num = FALSE, hang=-
1,cex.pv=0.5,cex=0.7,col.pv=c("red","#0000ff00","#0000ff00"))
# Plot with height representing where cluster originates
plot(clust1, print.pv=TRUE, print.num = FALSE, cex=0.7,
col.pv=c("red","#0000ff00","#0000ff00"))
# Plot without (red) probability numbers
plot(clust1, print.pv=TRUE, print.num = FALSE, hang=-
1,cex.pv=0.5,cex=0.7,col.pv=c("#0000ff00","#0000ff00","#0000ff00"))
plot(clust1, print.pv=TRUE, print.num =
FALSE,cex.pv=0.5,cex=0.7,col.pv=c("#0000ff00","#0000ff00","#0000ff00"))
dev.off()
```

8.2.4 Heatmap of selected probes

```
setwd("T:/Data/Raw Data/Array/Array Summer 09")
# Probe list to be selected
probes<-read.table("filename_a.csv",sep=",",header=TRUE,row.names=1)
probes<-as.vector(probes[,1])
probes
# Load data file containing from which only selected probes will be used in heatmap
methData<-read.table("filename_b.csv",sep=",",header=TRUE,row.names=1)
methData.edit<-methData[rownames(methData) %in% probes,]
odd <- function(x) x!=as.integer(x/2)*2
even <- function(x) x==as.integer(x/2)*2
# To generate heatmap red/green colour profile using colorpanal function
colorpanel <- function(n,low='green',mid='black',high='red')
  {
    if(even(n)) warning("n is even: colors panel will not be symmetric")
    # convert to rgb
    low <- col2rgb(low)
    mid <- col2rgb(mid)
    high <- col2rgb(high)
    # determine length of each component
    lower <- floor(n/2)
    upper <- n - lower
    red  <- c(
            seq(low[1,1], mid [1,1], length=lower),
            seq(mid[1,1], high[1,1], length=upper)
            )/255
    green <- c(
             seq(low[3,1], mid [3,1], length=lower),
```

```
            seq(mid[3,1], high[3,1], length=upper)
            )/255
    blue <- c(
           seq(low[2,1], mid [2,1], length=lower),
            seq(mid[2,1], high[2,1], length=upper)
            )/255
    rgb(red,blue,green)
  }
# Generate green-black-red colourscale
greenred <- function(n) colorpanel(n, 'green', 'black', 'red' )

#draw heat map
#second code alters the label font size
heatmap(as.matrix(methData.edit),col=greenred(255),scale="none",Colv=TRUE,Rowv=
TRUE)
heatmap(as.matrix(methData.edit),col=greenred(255),scale="none",Colv=TRUE,Rowv=
TRUE,cexCol=0.3)
```

8.2.5 Comparison of 2 groups of data using Mann-Whitney test and correction for multiple tests

```
setwd("T:/Data/Raw Data/Array/subfolder")
library(multtest)
#### Read in two group files.
group1<-read.table("filename_a.csv",header=TRUE,row.name=1, as.is=TRUE,sep=",")
group2<-read.table("filename_b.csv",header=TRUE,row.name=1, as.is =TRUE,sep=",")
#### Transpose data tables to get samples as rows and probes as columns
tg1<-t(group1)
tg2<-t(group2)
#### Get row numbers
rowNo<-nrow(group1)
#### Get probe names from first data set
probeName<-rownames(group1)
#### Create matrix to store results
result<-matrix(nrow=nrow(group1), ncol=4)
i<-1
#### Carry out unpaired Mann-Whitney test
for (i in 1: rowNo)
        {
        test<-wilcox.test(as.numeric(tg1[,i]), as.numeric(tg2[,i]), paired = FALSE)
        result[i,1] <- probeName[i]
        result[i,2] <- test$p.value
        result[i,3] <- test$statistic
        i<-i+1
```

```
        }
write.table(result, file="filename.csv", sep=",")
### Correct for multi-testing (Bonferroni and Benjamini-Hochberg FDR)
procs<-c("Bonferroni","BH")
### Get p values from Mann-Whitney
rawp<-as.numeric(result[,2])

### Original data has probes with measurements of zero for all groups. This will cause NaNs when carrying out test. Need to replace NaN with 1(not sig) so the script does not fail.
rawp[is.nan(rawp)]<-1
#### Carry out multiple hypothesis testing
res2<-mt.rawp2adjp(rawp,procs)
### Sort res2 so that probe alphabetical order is maintained
res3<-res2$adjp[order(res2$index),]
### add in abs delta beta
mean<-matrix(nrow=nrow(group1),ncol=3)
mean[,1]<-rowMeans(group1)
mean[,2]<-rowMeans(group2)
mean[,3]<-abs(mean[,1]-mean[,2])
### Now write to final table
write.table(cbind(probeName,res3,mean), file="age_034_MW_with_fdr.csv", sep=",", col.names=c("probeName","rawp","Bonferroni","BH","grp1 beta","grp2 beta","abs delta beta"))
```

8.2.6 Classifier probe selection

```
setwd("T:/Data/Raw Data/Array/subfolder")
library(klaR)
setwd("T:/Data/Raw Data/Array/subfolder")
data<-read.csv("filename.csv",header=TRUE,row.names=1)
probes<-read.table("test1.csv",sep=",",header=TRUE,row.names=1)
probes2<-as.vector(probes[,1])
data<-data[rownames(data) %in% probes2,]
data<-t(data)
case<-ifelse(substr(row.names(data),start=1,stop=1)=="c",1,2)
wpval<-matrix(data=NA,nrow=dim(data)[2],ncol=2)
wpval[,1]<-apply(data,2, function(x) wilcox.test(x~case,exact=FALSE)$p.value)
plimit<-0.05
sum(wpval[,1]<plimit)
nprobes<-12
d3<-data[,order(wpval[,1],decreasing=FALSE)[1:nprobes]]
set.seed(1234)
pdf("pdf_filename.pdf",height=11.7,width=16.5)
#1st
```

```
s3<-stepclass(d3,case,"qda",direction="both",improvement = 0.0005)
list(s3$model$name)
l1<-list(s3$model$name)
pairs(d3[,s3$model$nr],pch=21,bg=c("red", "green3")[unclass(case)])
partimat(as.factor(case)~d3[,s3$model$nr],method="qda")
#Run  last 5 lines of code 10 times, change “l1” in line 3: to “l2” – “l10” in successive
runs
dev.off()
```

8.2.7 Survival analysis

```
setwd("T:/Data/Raw Data/Array/subfolder")
library(survival)
library(multtest)

## Read in table
data<-read.table("filename.csv",sep=",",header=T,row.names=1)
data <- t(data)
data<-as.data.frame(data)
###  To plot Kaplan Meier curves
pval<-c()
# If 76 probes under investigation
for(i in 1:76)
        {
        KM <- survdiff(Surv(Survival,Status) ~ data[,i+2], data=data)
        temp <- 1-pchisq(KM$chisq,df=1)
        pval<-c(pval,temp)
        }
names(pval) <- colnames(data)[-c(1:2)]
names(pval)[pval<0.05]
data2<-cbind(data[,1:2],data[,colnames(data) %in% names(pval)[pval<0.05]])
# Make and store plots for the most significant probes
pdf("KM_sig_Plots.pdf")
# For the top 9 significant probes
for (i in 1:9)
        {
        plot(main=colnames(data2)[i+2], lty=1:2, xlab="Months",
ylab="Proportion",survfit(Surv(Survival,Status) ~ data2[,i+2], data=data2))
        legend(bty="n","bottomright",lty=1:2,c("Normally methylated","Aberrantly
methylated"))
        KM <- survdiff(Surv(Survival,Status) ~ data2[,i+2], data=data2)
        temp <- 1-pchisq(KM$chisq,df=1)
        temp <- round(temp,4)
        temp <- paste("p =",temp)
        legend("topright",bty="n",temp)
```

```
        }
procs<-"BH"
pvals_corrected <- mt.rawp2adjp(pval,procs) # none significant
pval_order <- pval[order(pval)]
rownames(pvals_corrected$adjp) <- names(pval_order)
write.table(pvals_corrected$adjp,file="adjusted_logrank_pval.csv",sep=",")
```

8.2.8 Survival univariate Cox model

```
setwd("T:/Data/Raw Data/Array/subfolder")
library(survival)
## read in data
cox <-
read.table("km_surv_raw_combsignifprobe_apr2011.csv",sep=",",header=T,row.name
s=1)
cox<-t(cox)
# Functions
tableWrite<-function(results, x, columnNames)
{
temp<-paste(x,".csv")
write.table(results,file=temp,sep=",",col.names=columnNames)
}
coxAnalyseUnivariateEFS<-function(methData, filename)
        {
        colNumber<-dim(methData)[[2]]
        i<-1
        results<-matrix(nrow=(colNumber-2),ncol=3)
        probeNames<-colnames(methData)[3:colNumber]
        pvals<-vector()
        while(i<(colNumber-1))
                {
                try(temp<-coxph(Surv(methData[,2],methData[,1])
                ~methData[,i+2]),TRUE)
                pval<-summary(temp)$coefficients[1,5]
                pvals[i]<-pval

                results[i,1]<-probeNames[i]
                i<-i+1
                }
        pvals2<-mt.rawp2adjp(pvals,proc="BH")
        pvals2<-pvals2$adjp[order(pvals2$index),]
        results[,2:3]<-pvals2
        tableWrite(results, filename, c("ProbeID","Raw Probe p","BH Probe p"))
        }
coxAnalyseUnivariateEFS(cox,"univariateCox")
```

8.2.9 Multivariate analysis

```
setwd("T:/Data/Raw Data/Array/subfolder")
library(multtest)
library(survival)
data<-read.table("filename.csv",sep=",",header=T,row.names=1)
LR_Fn2<-
function(data,baseVar,covariates){
data<-as.data.frame(data)
 results<-vector(length=length(covariates))
names(results) <- colnames(data)[covariates]
# For 9 most significant probes found on univariate analysis
i<-1
while (i <=length(covariates))
{
 if(length(baseVar)==1){
 base <- coxph(Surv(EFS_Time,EFS_Status)~data[,baseVar],data=data)
lr1<- -2*base$loglik[2]
 extend<-coxph(Surv(EFS_Time,EFS_Status)~ data[,baseVar] +
data[,covariates[i]],data=data)
  lr2<- -2*extend$loglik[2]
} else if(length(baseVar)==2) {
base <- coxph(Surv(EFS_Time,EFS_Status) ~ data[,baseVar[1]] +
data[,baseVar[2]],data=data)
lr1<- -2*base$loglik[2]
extend<-coxph(Surv(EFS_Time,EFS_Status)~ data[,baseVar[1]] + data[,baseVar[2]] +
data[,covariates[i]],data=data)
 lr2<- -2*extend$loglik[2]
} else if(length(baseVar)==3) {
base <- coxph(Surv(EFS_Time,EFS_Status) ~ data[,baseVar[1]] + data[,baseVar[2]] +
data[,baseVar[3]] ,data=data)
lr1<- -2*base$loglik[2]
extend<-coxph(Surv(EFS_Time,EFS_Status) ~ data[,baseVar[1]] + data[,baseVar[2]] +
data[,baseVar[3]] + data[,covariates[i]],data=data)
 lr2<- -2*extend$loglik[2]
} else if(length(baseVar)==4) {
base <- coxph(Surv(EFS_Time,EFS_Status) ~ data[,baseVar[1]] +  data[,baseVar[2]] +
data[,baseVar[3]] + data[,baseVar[4]] ,data=data)
lr1<- -2*base$loglik[2]
extend<-coxph(Surv(EFS_Time,EFS_Status) ~ data[,baseVar[1]] + data[,baseVar[2]] +
data[,baseVar[3]] + data[,baseVar[4]] + data[,covariates[i]],data=data)
lr2<- -2*extend$loglik[2]
} else if(length(baseVar)==5) {
```

```
base <- coxph(Surv(EFS_Time,EFS_Status) ~ data[,baseVar[1]] + data[,baseVar[2]] +
data[,baseVar[3]] + data[,baseVar[4]] + data[,baseVar[5]],data=data)
 lr1<- -2*base$loglik[2]
extend<-coxph(Surv(EFS_Time,EFS_Status) ~ data[,baseVar[1]] + data[,baseVar[2]] +
data[,baseVar[3]] + data[,baseVar[4]] + data[,baseVar[5]] +
data[,covariates[i]],data=data)
lr2<- -2*extend$loglik[2]
} else if(length(baseVar)==6) {
base <- coxph(Surv(EFS_Time,EFS_Status) ~ data[,baseVar[1]] + data[,baseVar[2]] +
data[,baseVar[3]] + data[,baseVar[4]] + data[,baseVar[5]] +
data[,baseVar[6]],data=data)
 lr1<- -2*base$loglik[2]
extend<-coxph(Surv(EFS_Time,EFS_Status) ~ data[,baseVar[1]] + data[,baseVar[2]] +
data[,baseVar[3]] + data[,baseVar[4]] + data[,baseVar[5]] + data[,baseVar[6]] +
data[,covariates[i]],data=data)
lr2<- -2*extend$loglik[2]
 } else if(length(baseVar)==7) {

base <- coxph(Surv(EFS_Time,EFS_Status) ~ data[,baseVar[1]] + data[,baseVar[2]] +
data[,baseVar[3]] + data[,baseVar[4]] + data[,baseVar[5]] +
data[,baseVar[6]]+data[,baseVar[7]],data=data)
 lr1<- -2*base$loglik[2]
 extend<-coxph(Surv(EFS_Time,EFS_Status) ~ data[,baseVar[1]] + data[,baseVar[2]] +
data[,baseVar[3]] + data[,baseVar[4]] + data[,baseVar[5]] + data[,baseVar[6]] +
data[,baseVar[7]] + data[,covariates[i]],data=data)
lr2<- -2*extend$loglik[2]
 } else if(length(baseVar)==8) {
 base <- coxph(Surv(EFS_Time,EFS_Status) ~ data[,baseVar[1]] + data[,baseVar[2]] +
data[,baseVar[3]] + data[,baseVar[4]] + data[,baseVar[5]] +
data[,baseVar[6]]+data[,baseVar[7]] + data[,baseVar[8]],data=data)
 lr1<- -2*base$loglik[2]
 extend<-coxph(Surv(EFS_Time,EFS_Status) ~ data[,baseVar[1]] + data[,baseVar[2]] +
data[,baseVar[3]] + data[,baseVar[4]] + data[,baseVar[5]] + data[,baseVar[6]] +
data[,baseVar[7]] + data[,baseVar[8]] + data[,covariates[i]],data=data)
 lr2<- -2*extend$loglik[2]
}
results[i] <- pchisq(q=lr1-lr2, df=1, lower.tail = FALSE)
print(paste("i",i,"p val",results[i],covariates[i]))
 i<-i+1
 }
results
 }
data<-read.table("filename.csv",sep=",",header=T,row.names=1)
data <- t(data)
colnames(data)[1:2] <-c("EFS_Status","EFS_Time")
colnames(data)
```

```
rownames(data)
# Include  most significant probe sequentially in model
extend_LR<-LR_Fn2(data,baseVar=c(11), covariates=c(5,6,7,8,9,10,12,13,14))
extend_LR[order(extend_LR)]
extend_LR<-LR_Fn2(data,baseVar=c(11,14), covariates=c(5,6,7,8,9,10,12,13))
extend_LR[order(extend_LR)]
extend_LR<-LR_Fn2(data,baseVar=c(11,14,6), covariates=c(5,7,8,9,10,12,13))
extend_LR[order(extend_LR)]
extend_LR<-LR_Fn2(data,baseVar=c(11,14,6,12), covariates=c(5,7,8,9,10,13))
extend_LR[order(extend_LR)]
extend_LR<-LR_Fn2(data,baseVar=c(11,14,6,12,13), covariates=c(5,7,8,9,10))
extend_LR[order(extend_LR)]
data<-as.data.frame(data)
finalModel <- coxph(Surv(EFS_Time,EFS_Status) ~ SIN3B_P514_R + WEE1_P924_R +
ITK_P114_F + SLC6A8_P409_F
+ TRIM29_P135_F,data=data);summary(finalModel)
```

Appendix 3

CNS-PNET methylation study

supplementary data

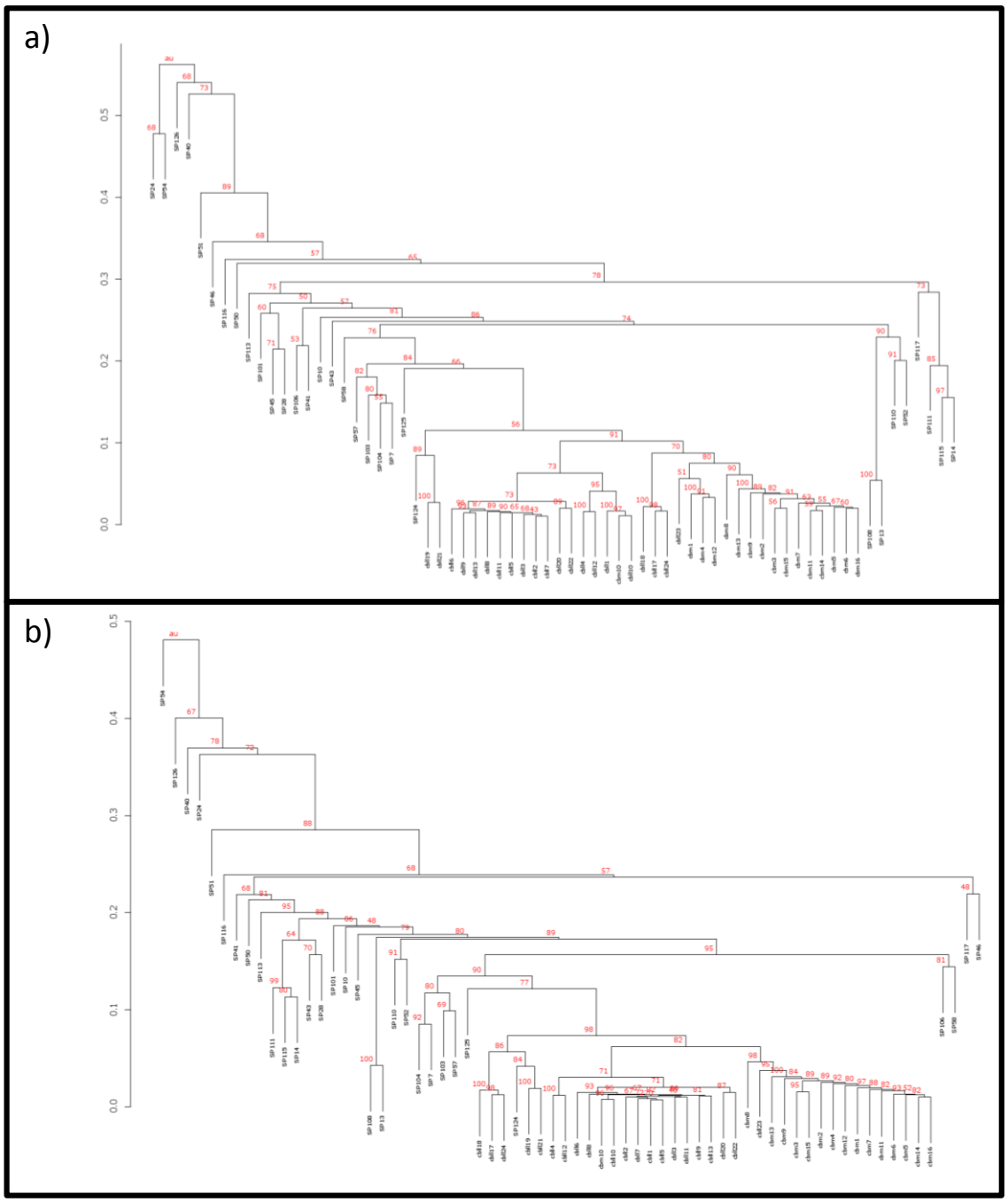

Figure 8.1. Bootstrapped hierarchical clustering dendrogram of the methylation profiles of CNS-PNET and normal brain samples. (a) Clustering using variantly methylated probes, and (b) clustering excluding the chromosome X probes. Samples: SPx, CNS-PNET; Cbx, normal brain.

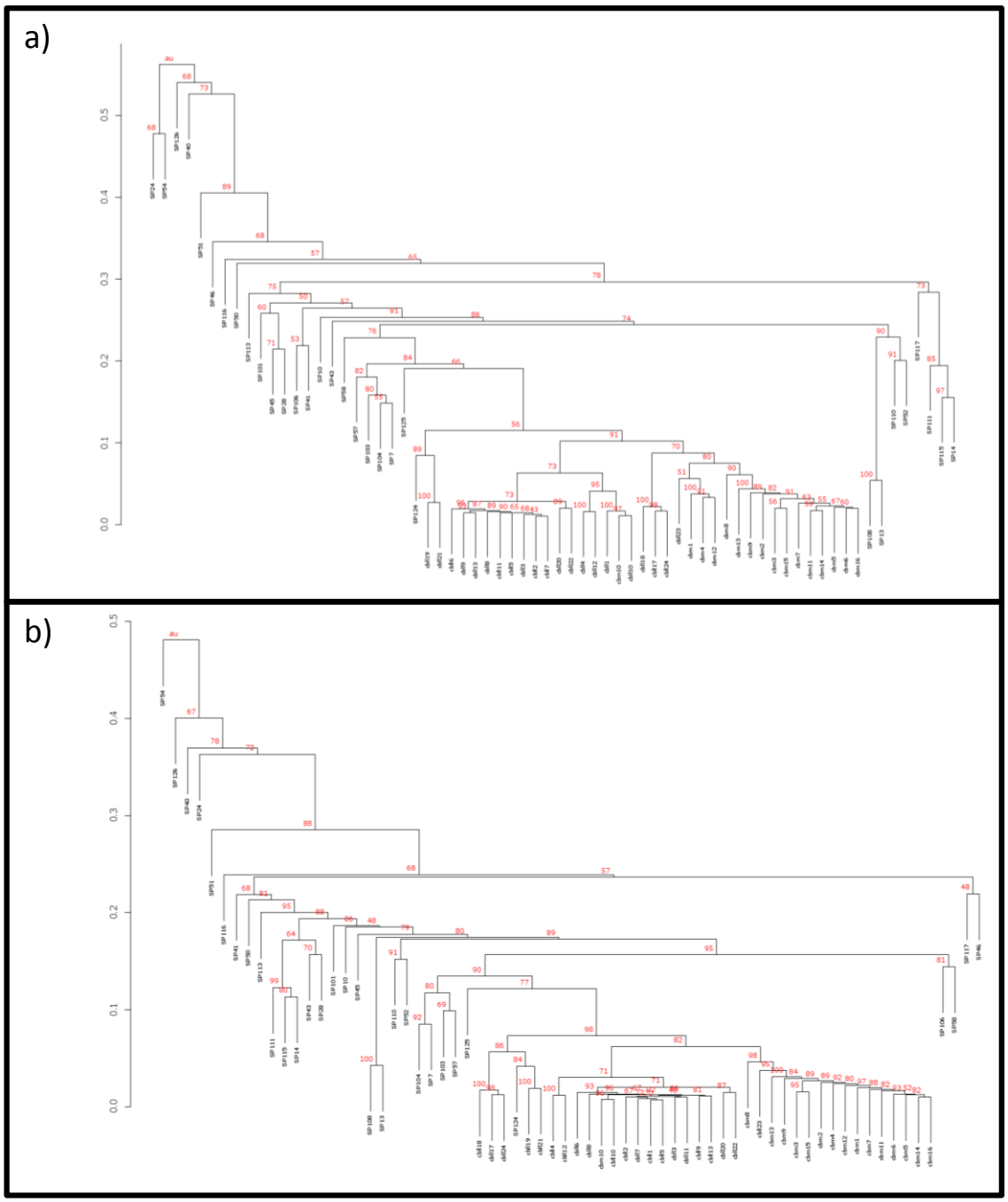

Figure 8.2. Bootstrapped hierarchical clustering dendrogram of the methylation profiles of CNS-PNET and pineoblastoma tumours. (a) Clustering using variantly methylated probes, and (b) clustering excluding the chromosome X probes. Samples: SPx, CNS-PNET; PB, pineoblastoma

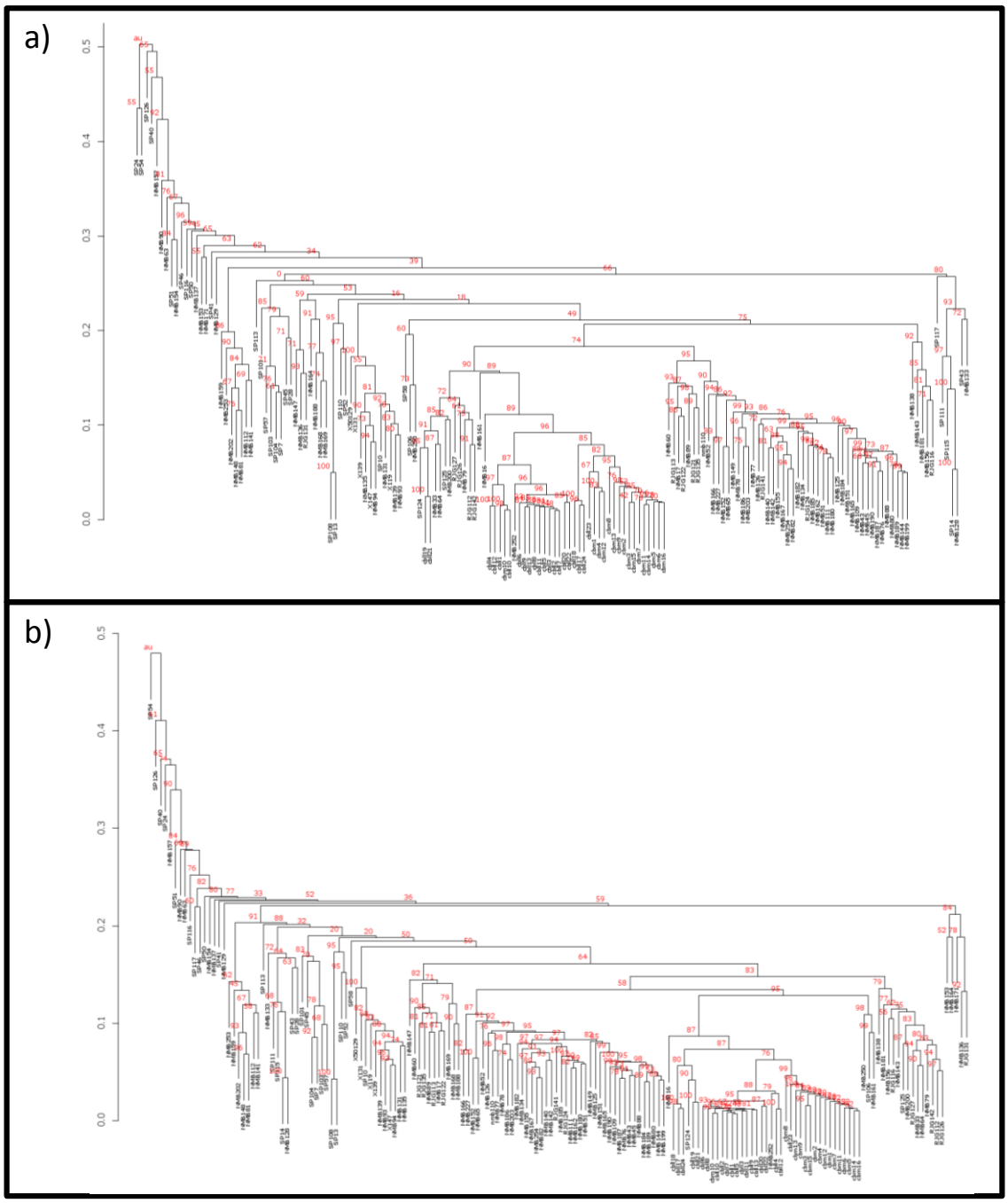

Figure 8.3. Bootstrapped hierarchical clustering dendrogram of the methylation profiles of CNS-PNET, medulloblastomas and normal brain samples. (a) Clustering using variantly methylated probes, and (b) clustering excluding the chromosome X probes. Samples: SP*, CNS-PNET; Cb*, normal brain; RJG*, NMB* or X*, medulloblastoma.

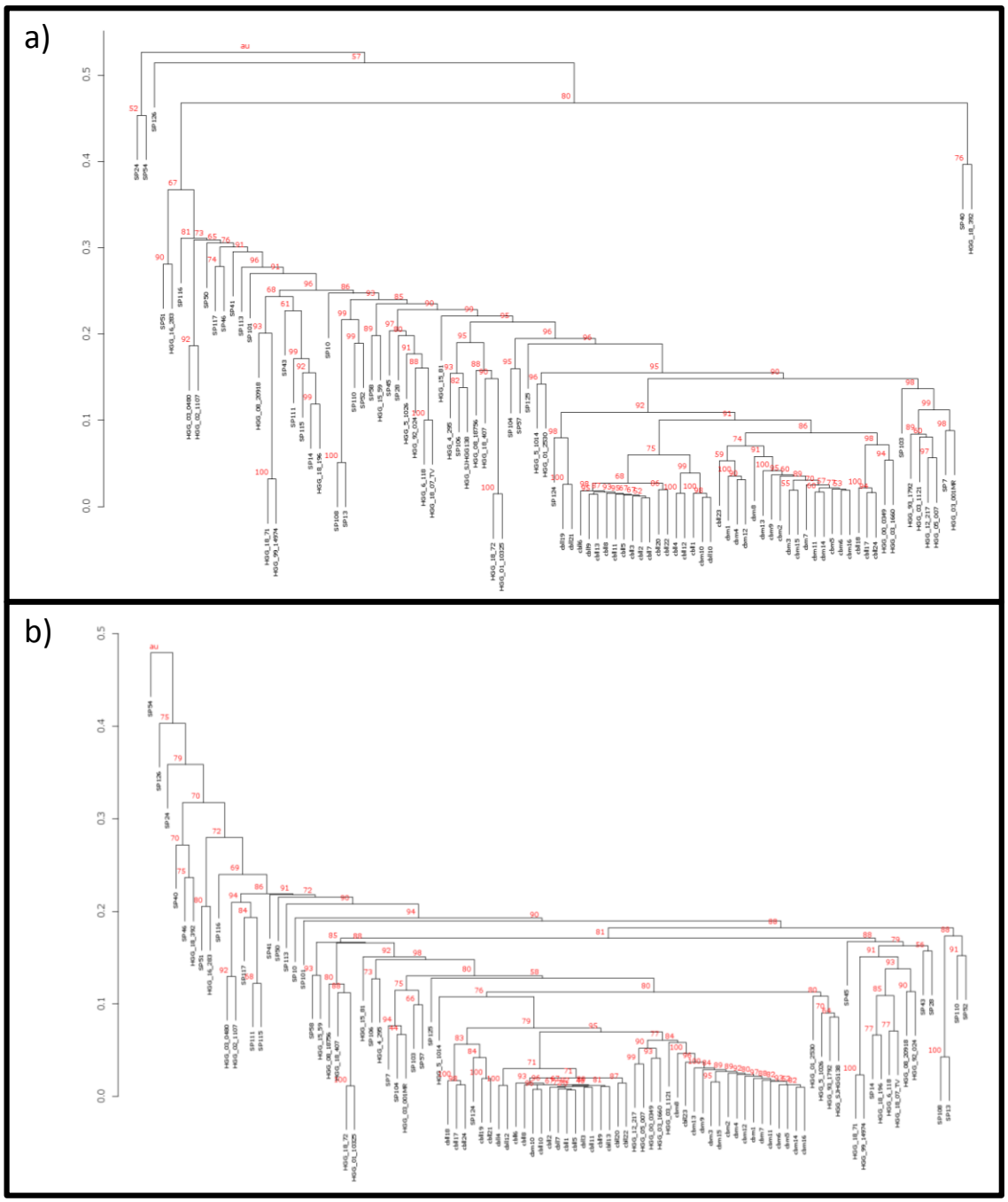

Figure 8.4. Bootstrapped hierarchical clustering dendrogram of the methylation profiles of CNS-PNET, high grade gliomas and normal brain samples. (a) Clustering using variantly methylated probes, and (b) clustering excluding the chromosome X probes. Samples: SPx, CNS-PNET; Cbx, normal brain; HGG*, high grade glioma.

Published papers

[Cell Cycle 8:11, 1806-1807; 1 June 2009]; ©2009 Landes Bioscience

Letter to the Editor

Frequent *IDH1* mutations in supratentorial primitive neuroectodermal tumors (sPNET) of adults but not children

James T. Hayden,[1] Michael C. Frühwald,[2] Martin Hasselblatt,[3] David W. Ellison,[4] Simon Bailey[1] and Steven C. Clifford[1,*]

[1]Northern Institute for Cancer Research; The Medical School; Newcastle University; Newcastle upon Tyne, UK; [2]Department of Pediatric Hematology; Oncology; University Children's Hospital; Münster, Germany; [3]Institute of Neuropathology; University Hospital Münster; Münster, Germany; and [4]Department of Pathology; St. Jude Children's Research Hospital; Memphis, TN USA

Key words: *IDH1*, mutation, supratentorial, PNET, sPNET

Supratentorial primitive neuroectodermal tumors (sPNET) are rare aggressive embryonal tumors of the cerebral hemispheres, which predominantly occur in childhood but also arise in adults. Despite multi-modal therapy, less than half of affected patients will survive 5 years post-diagnosis, and late effects associated with current treatment protocols are a significant complication in survivors.[1] Advances in our understanding of the molecular basis of sPNET development will be critical to improve outcome. The biological mechanisms underlying sPNET pathogenesis, however, remain poorly understood and afford few opportunities for the application of novel or targeted therapeutic approaches to achieve this objective.

In a recently published systematic screen of 22 glioblastoma tumor samples for evidence of genetic mutation in 20,661 protein coding genes, the most frequently mutated novel candidate cancer gene was *IDH1*, which encodes cytoplasmic isocitrate dehydrogenase, involved in the control of cellular oxidative damage.[2] Subsequent mutation analysis in an extensive panel identified *IDH1* mutations in 12% (18/149) of glioblastomas.

A series of studies have now investigated *IDH1* mutations in human malignancies,[2-6] the combined results of which are summarised in Table 1. Analysis of central nervous system (CNS) tumors identified *IDH1* mutations in 37% of cases (590 mutations, 1,603 cases), all affecting codon 132. *IDH1* mutations appear to occur predominantly in neuroepithelial tumors of glial origin. In embryonal brain tumors, no evidence of *IDH1* mutation has been found in the infratentorial PNET, medulloblastoma (0/113), however mutations were identified in a third (3/9) of sPNET. In contrast, no *IDH1* mutations were detected in a panel of 1,053 extracranial tumors. Taken together, these data indicate that *IDH1* mutations are a common and specific feature of glioblastomas and other brain tumors of neuroepithelial and in particular glial origin, and suggest a potential role in the pathogenesis of sPNET.

Table 1 **Reported isocitrate dehydrogenase (IDH1) mutations in clinically classified human tumor biopsies**

	Number of tumors analyzed	Number of mutations	Mutation Frequency (%)	Reference
Central nervous system (CNS)				
Astrocytic Tumors	917	307	33	2–6
Oligodendroglial Tumors	241	182	76	3–6
Oligoastrocytic Tumors	124	101	81	4–6
Embryonal Tumors				
sPNET	9	3	33	5
Medulloblastoma	113	0	0	5, 6
Ependymal Tumors	87	0	0	4–6
Sellar Region Tumor	23	0	0	5
Cranial & Paraspinal Nerves Tumors	17	0	0	5
Meningothelial Cell Tumors	72	0	0	5
Non-CNS				
Leukamia	63	0	0	6
Bladder	34	0	0	3
Breast	223	0	0	3, 6
Gastric	57	0	0	6
Colorectal	267	0	0	3, 6
Lung	142	0	0	3, 6
Melanoma	23	0	0	3
Thyroid	42	0	0	3
Ovary	73	0	0	3, 6
Pancreas	118	0	0	3, 6
Prostate	11	0	0	3, 6

We therefore investigated the prevalence of *IDH1* mutations in an extensive cohort of sPNET, which included 34 primary tumors (mean age 9.4 years; range 2 months to 30 years; 8 infant cases <3 years, 20 childhood cases ≥3 years to 17 years, 6 adult cases ≥18 years). Polymerase chain reaction (PCR) was employed to amplify exon 4 of *IDH1*, using previously described primers and methods.[5] PCR products were subsequently purified (PureLink™ PCR Purification kit, Invitrogen, Paisley, UK) and directly sequenced in forward and reverse directions using an Applied Biosystems 3730 DNA Analyser (DBS Genomics, Durham University, UK).

Mutations in *IDH1* were identified in 2/34 (6%) primary sPNET. In both cases, a missense mutation in codon 132 was observed (G395A; R132H). Interestingly, both mutations were detected in sPNET from adult cases (2/6; ≥18 years at diagnosis), while no mutations were observed in paediatric sPNET (0/28; 0–17 years) ($p = 0.027$; Fisher's exact test). This overall rate of *IDH1* mutation in sPNET is lower than previously reported (33% (3/9) of cases; Balss et al.[5]). However, detailed examination of the ages at diagnosis of cases in this previous study revealed the two datasets are in close agreement; *IDH1*

*Correspondence to: Steven C. Clifford; Northern Institute for Cancer Research; The Medical School; Framlington Place; Newcastle University; Newcastle-upon-Tyne NE2 4HH UK; Tel.: +44.191.2464422; Fax: +44.191.2464301; Email: s.c.clifford@ncl.ac.uk

Submitted: 03/23/09; Accepted: 03/30/09

Previously published online as a *Cell Cycle* E-publication: http://www.landesbioscience.com/journals/cc/article/8594

mutations also occurred exclusively in adult sPNET in the study by Balss et al.[5] (3/6 ≥18 years; 0/3 <18 years) (Prof. A. von Deimling, Personal communication). Taken together, these data clearly demonstrate that mutations in *IDH1* are amongst the most frequent mutational events identified in sPNET to date, and characterize a significant proportion of adult cases (42% (5/12), based on the combined datasets), but do not appear to play a major role in paediatric cases (0/31 in combination; p = 0.0008, Fisher's exact test).

It is notable that, in studies to date, *IDH1* mutations occur specifically in CNS malignancies and, within these, have only been detected in astrocytic, oligodendroglial, oligoastrocytic and adult sPNET, suggesting IDH1 plays a role in the development of these tumors, but not in other brain tumor types including medulloblastomas. Moreover, our findings are consistent with the arguments that (i) PNET arising in the infratentorial (i.e., medulloblastoma) and supratentorial (i.e., sPNET) compartments display distinct mechanisms of molecular pathogenesis, despite their histopathological similarities, and (ii) sPNET arising in adults and children differ at the molecular level. However, whilst the identification of *IDH1* mutations in sPNET and other neuroepithelial tumors suggests these tumor types may share common mechanisms of molecular pathogenesis, it must also be considered that the observation of *IDH1* mutations in both may reflect the recognized challenge that can exist in establishing the histopathological differential diagnosis of these different supratentorial tumor types.[7]

In conclusion, these data identify *IDH1* mutations as a feature of a significant subset of adult sPNET. The significance of *IDH1* mutations in this group, and any functional contribution they make to tumor development is, however, currently unclear. Further studies are now required to investigate the role of *IDH1* mutations in tumorigenesis, their relationship to disease histopathology, and to discover whether these findings may be exploited to aid the development of improved therapeutic approaches for patients with sPNET.

Acknowledgements

This work was supported by grants from the Samantha Dickson Brain Tumor Trust (SDBTT), the North of England Children's Cancer Research Fund (NECCR), and Cancer and Leukaemia in Children (CLIC).

References

1. Pizer BL, et al. Eur J Cancer 2006; 42:1120-8.
2. Parsons DW, et al. Science 2008; 321:1807-12.
3. Bleeker FE, et al. Hum Mutat 2009; 30:7-11.
4. Watanabe T, et al. Am J Path 2009; 174:(epub).
5. Balss J, et al. Acta Neuropathol 2008; 116:597-602.
6. Yan H, et al. New Eng J Med 2009; 360:765-73.
7. Armstrong DD, et al. Brain Pathol 2003; 13:373-5.